frontiers | Research Topics

The adaptation strategies of plants to alleviate important environmental stresses

Edited by
Walid Soufan, Oksana Sytar, Ashwani Kumar, Akihiro Ueda and Muhammad Ali Raza

Published in
Frontiers in Plant Science

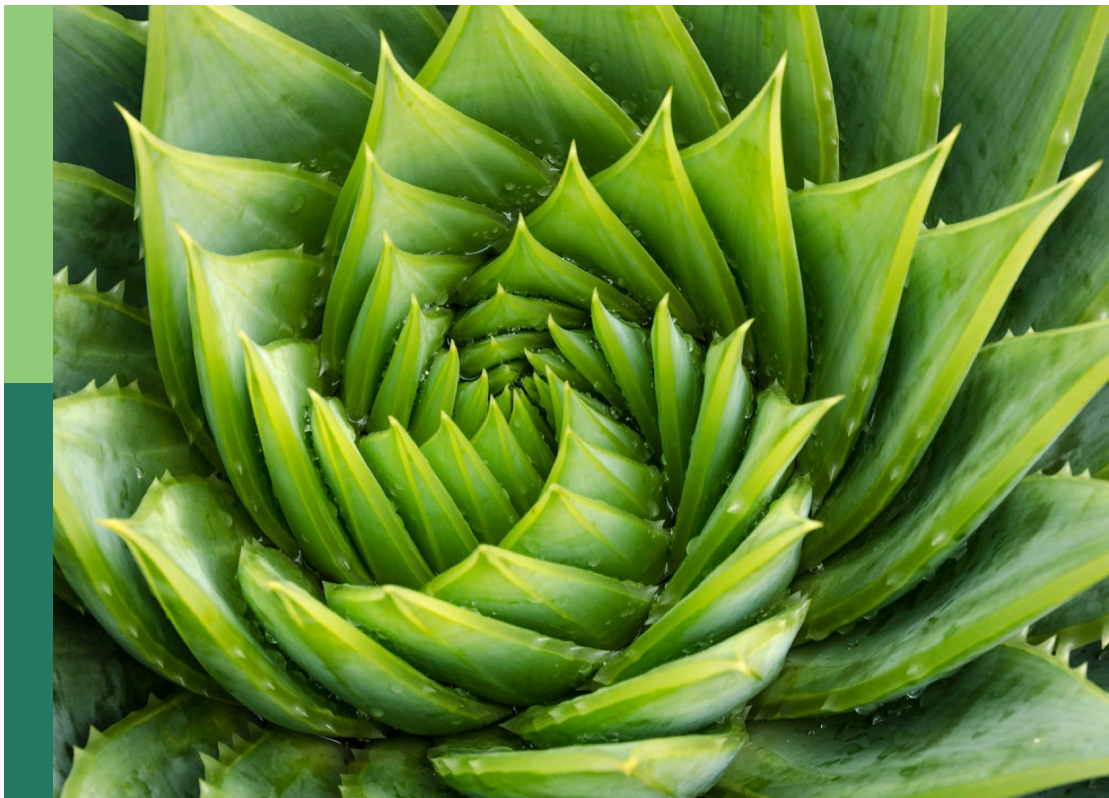

ISSN 1664-8714
ISBN 978-2-8325-3816-6
DOI 10.3389/978-2-8325-3816-6

About Frontiers

Frontiers is more than just an open access publisher of scholarly articles: it is a pioneering approach to the world of academia, radically improving the way scholarly research is managed. The grand vision of Frontiers is a world where all people have an equal opportunity to seek, share and generate knowledge. Frontiers provides immediate and permanent online open access to all its publications, but this alone is not enough to realize our grand goals.

Frontiers journal series

The Frontiers journal series is a multi-tier and interdisciplinary set of open-access, online journals, promising a paradigm shift from the current review, selection and dissemination processes in academic publishing. All Frontiers journals are driven by researchers for researchers; therefore, they constitute a service to the scholarly community. At the same time, the *Frontiers journal series* operates on a revolutionary invention, the tiered publishing system, initially addressing specific communities of scholars, and gradually climbing up to broader public understanding, thus serving the interests of the lay society, too.

Dedication to quality

Each Frontiers article is a landmark of the highest quality, thanks to genuinely collaborative interactions between authors and review editors, who include some of the world's best academicians. Research must be certified by peers before entering a stream of knowledge that may eventually reach the public - and shape society; therefore, Frontiers only applies the most rigorous and unbiased reviews. Frontiers revolutionizes research publishing by freely delivering the most outstanding research, evaluated with no bias from both the academic and social point of view. By applying the most advanced information technologies, Frontiers is catapulting scholarly publishing into a new generation.

What are Frontiers Research Topics?

Frontiers Research Topics are very popular trademarks of the *Frontiers journals series*: they are collections of at least ten articles, all centered on a particular subject. With their unique mix of varied contributions from Original Research to Review Articles, Frontiers Research Topics unify the most influential researchers, the latest key findings and historical advances in a hot research area.

Find out more on how to host your own Frontiers Research Topic or contribute to one as an author by contacting the Frontiers editorial office: frontiersin.org/about/contact

The adaptation strategies of plants to alleviate important environmental stresses

Topic editors

Walid Soufan — King Saud University, Saudi Arabia
Oksana Sytar — Taras Shevchenko National University of Kyiv, Ukraine
Ashwani Kumar — University of Allahabad, India
Akihiro Ueda — Hiroshima University, Japan
Muhammad Ali Raza — Islamia University of Bahawalpur, Pakistan

Citation

Soufan, W., Sytar, O., Kumar, A., Ueda, A., Raza, M. A., eds. (2023). *The adaptation strategies of plants to alleviate important environmental stresses*. Lausanne: Frontiers Media SA. doi: 10.3389/978-2-8325-3816-6

Table of contents

frontiers | Frontiers in Plant Science

TYPE Editorial
PUBLISHED 12 October 2023
DOI 10.3389/fpls.2023.1307399

OPEN ACCESS

EDITED AND REVIEWED BY
Simone Landi,
University of Naples Federico II, Italy

*CORRESPONDENCE
Ashwani Kumar
ashwaniiitd@hotmail.com;
ashwanikumar@allduniv.ac.in

RECEIVED 04 October 2023
ACCEPTED 09 October 2023
PUBLISHED 12 October 2023

CITATION
Sytar O and Kumar A (2023) Editorial: The adaptation strategies of plants to alleviate important environmental stresses.
Front. Plant Sci. 14:1307399.
doi: 10.3389/fpls.2023.1307399

Editorial: The adaptation strategies of plants to alleviate important environmental stresses

Oksana Sytar [1] and Ashwani Kumar [2*]

[1]Institute of Plant and Environmental Sciences, Slovak University of Agriculture, Nitra, Slovakia, [2]Metagenomics and Secretomics Research Laboratory, Department of Botany, University of Allahabad (A Central University), Prayagraj, Uttar Pradesh, India

KEYWORDS

adaptation, stresses, abiotic, plant health, crop growth

Editorial on the Research Topic
The adaptation strategies of plants to alleviate important environmental stresses

Agriculture, the backbone of global food security, is constantly challenged by various environmental stresses such as drought, temperature fluctuations, soil pollution, and changing rainfall patterns. Researchers have been exploring innovative strategies and technologies to address these challenges and ensure sustainable crop production (Kumar and Dubey, 2020). Over the years, complex arrays of plant responses to various environmental pressures have been documented. However, a clear mechanistic foundation is often missing from these studies, making it difficult to consider them as the basis for plant development and tolerance pathways (Figure 1). Our Research topic comprises 13 original research articles contributed by more than 80 authors (total downloads: 3272; total views: 15k). With this Research topic, we aimed to covers various stress responses, precipitation variability, biochar applications, metal toxicity, alleviation of terminal drought stress and various agricultural practices that help the plants to adapt and mitigate different environmental stresses.

Drought stress severely impacts cereal crop growth and yields, making it a top concern for farmers worldwide. The paper titled "*Foliar application of putrescine alleviates terminal drought stress in wheat*" by Wasaya et al. explores the use of putrescine as a potential solution. The research reveals that foliar application of putrescine at a concentration of 1.0 PPM significantly improved wheat's water status, membrane stability, and yield-related traits under terminal drought stress. This finding offers a promising approach to mitigate drought-related yield losses in wheat cultivation. In water-scarce regions, efficient irrigation methods are essential for cotton cultivation. A study of Singh et al. compares sub-surface drip fertigation (SSDF) with traditional irrigation methods in India. The research highlights the potential of SSDF to save irrigation water, enhance cotton productivity, and improve farmers' returns, offering a water-savvy concept for sustainable cotton production.

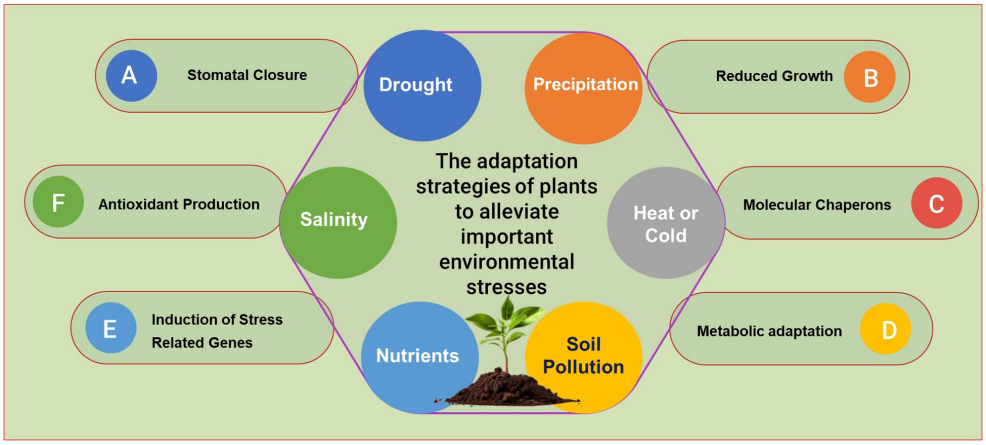

FIGURE 1
Common plant adaptation strategies against environmental stresses.

Understanding historical precipitation patterns is crucial for crop management in regions with variable precipitation. The work conducted by Fang et al. on characteristics of historical precipitation for winter wheat cropping analyzes two decades of climate data in a semi-arid and semi-humid area of China. The study characterizes rainfall distribution during key growth stages of winter wheat, providing valuable insights for managing waterlogging and drought risks. In their group, Qin et al. investigated the water use strategies of *Ferula bungeana* in the Badain Jaran Desert. The study reveals that the plant adapts to extreme drought conditions by adjusting its water absorption sources, water potential, hydraulic conductivity, and water use efficiency. Water availability plays a significant role in regulating these strategies. The investigation of Veenstra et al. explores the role of tillering in stabilizing corn yield components under sub-optimal plant densities. It suggests that optimizing plant density to maximize the main stalk primary ears is desirable for maximizing yields. However, tiller expression offers an avenue to reduce dependence on variable optimum plant densities. It suggests that optimizing plant density to maximize the main stalk primary ears is desirable for maximizing yields, but tiller expression offers an avenue to reduce dependence on variable optimum plant densities.

Among environmental stresses, heavy metals are of significant interest in the research related to the impact on plant growth, quality and mitigation of the hard impact of this stress together with the adaptation potential of plants. For example, Wang et al. investigate low-level cadmium exposure in peppermint, this research identifies genes and pathways associated with hormetic responses. Low-level cadmium exposure consistently enhances antioxidant activity in peppermint plants, aiding in their resistance to oxidative damage. This hormetic effect could have implications for peppermint cultivation in contaminated environments.

The study by Abeed et al. titled "*Mitigating cadmium stress in sunflower with microorganisms*" explores the use of *Trichoderma harzianum* and plant growth-promoting bacteria to alleviate cadmium (Cd) stress in sunflower plants. These microorganisms play a vital role in helping sunflower plants adapt to Cd stress by regulating various physiological and biochemical processes, reducing stress markers, and improving water use efficiency. This approach holds promise for enhancing sunflower resilience against Cd-induced damage. Research by Chen into how zinc (Zn) alleviates cadmium (Cd) toxicity in mangrove plants reveals that low-dose Zn treatment positively influences biomass, phenolic acid metabolism-related enzymes, antioxidant capacity, and chlorophyll content. These effects help mitigate Cd toxicity in mangrove plants, indicating a potential strategy for managing heavy metal stress.

Biochar, derived from biomass, has attracted attention for its potential to enhance soil fertility and crop productivity. The study by Wan et al. explores the impact of biochar, specifically wheat-straw biochar, on maize plants under reduced irrigation. Biochar addition significantly increases root parameters, soil nutrient availability, and plant biomass. It suggests combining wheat-straw biochar with partial root-zone drying can improve maize growth and nutrient uptake, particularly in water-limited conditions. Another biochar study by Farhangi-Abriz and Ghasemmi-Golezani examines the impact of chemically modified biochars on mint plants exposed to fluoride and cadmium toxicities. Modified biochars effectively reduce fluoride and cadmium levels in plant leaves, improve soil properties, and enhance plant growth and nutrient uptake. They are more efficient at protecting plants from soil pollutants than solid biochar.

Soybean, widely used in intercropping systems, must adapt to varying light conditions. Wu et al. explore how soybean seedlings adjust to shade. The study reveals that soybean seedlings adapt by altering morphological and physiological traits, highlighting the plant's plasticity in response to environmental stressors.

The research findings reported in this Research Topic offer promising solutions for mitigating issues such as drought, heavy metal exposure, and variable precipitation patterns. Strategies

include the uses of putrescine for drought-tolerant wheat, water-efficient cotton cultivation methods, and optimizing plant density for corn yields. Additionally, studies highlight plant adaptability in response to environmental stressors and the potential of microorganisms and biochar to combat heavy metal stress and enhance soil fertility. These findings hold significant promise for sustainable and resilient agriculture.

Author contributions

OS: Writing – original draft. AK: Writing – original draft, Writing – review & editing.

Funding

The author(s) declare financial support was received for the research, authorship, and/or publication of this article. AK gratefully acknowledges DST-SERB for financial support obtained through the project grant of (CRG/2021/003696), New Delhi Govt of India.

Reference

Kumar, A., and Dubey, A. (2020). Rhizosphere microbiome: engineering bacterial competitiveness for enhancing crop production. *J. Advanced Res.* 24, 337–352. doi: 10.1016/j.jare.2020.04.014

Acknowledgments

The authors wish to thank the editor for proofreading the manuscript.

Conflict of interest

The authors declare that the research was conducted in the absence of any commercial or financial relationships that could be construed as a potential conflict of interest.

The author(s) declared that they were an editorial board member of Frontiers, at the time of submission. This had no impact on the peer review process and the final decision.

Publisher's note

frontiers | Frontiers in Plant Science

TYPE Original Research
PUBLISHED 06 October 2022
DOI 10.3389/fpls.2022.1015414

OPEN ACCESS

EDITED BY
Muhammad Ali Raza,
Islamia University of Bahawalpur, Pakistan

REVIEWED BY
Sabin Saurav Pokharel,
Nanjing Agricultural University, China
Ting Peng,
Henan Agricultural University, China

*CORRESPONDENCE
Wenyu Yang
mssiyangwy@sicau.edu.cn

†These authors have contributed equally to this work and share first authorship

SPECIALTY SECTION
This article was submitted to Plant Abiotic Stress, a section of the journal Frontiers in Plant Science

RECEIVED 09 August 2022
ACCEPTED 26 August 2022
PUBLISHED 06 October 2022

CITATION
Wu Y, Chen P, Gong W, Gul H, Zhu J, Yang F, Wang X, Yong T, Liu J, Pu T, Yan Y and Yang W (2022) Morphological and physiological variation of soybean seedlings in response to shade.
Front. Plant Sci. 13:1015414.
doi: 10.3389/fpls.2022.1015414

Morphological and physiological variation of soybean seedlings in response to shade

Yushan Wu[1,2†], Ping Chen[1,2†], Wanzhuo Gong[3†], Hina Gul[4], Junqi Zhu[5], Feng Yang[1,2], Xiaochun Wang[1,2], Taiwen Yong[1,2], Jiang Liu[2,6], Tian Pu[1,2], Yanhong Yan[7] and Wenyu Yang[1,2*]

[1]College of Agronomy, Sichuan Agricultural University, Chengdu, China, [2]Key Laboratory of Crop Eco-Physiology and Farming System, Sichuan Engineering Research Center for Crop Strip Intercropping System, Chengdu, China, [3]Crop Research Institute, Chengdu Academy of Agricultural and Forestry Sciences, Chengdu, China, [4]National Center of Industrial Biotechnology (NCIB), PMAS Arid Agriculture University, Rawalpindi, Pakistan, [5]Plant and Food Research, Blenheim, New Zealand, [6]College of Life Science, Sichuan Agricultural University, Chengdu, China, [7]College of Grassland Science and Technology, Sichuan Agricultural University, Chengdu, China

Soybean (*Glycine max*) is a legume species that is widely used in intercropping. Quantitative analyses of plasticity and genetic differences in soybean would improve the selection and breeding of soybean in intercropping. Here, we used data of 20 varieties from one year artificial shading experiment and one year intercropping experiment to characterize the morphological and physiological traits of soybean seedlings grown under shade and full sun light conditions. Our results showed that shade significantly decreased biomass, leaf area, stem diameter, fraction of dry mass in petiole, leaf mass per unit area, chlorophyll a/b ratio, net photosynthetic rate per unit area at PAR of 500 μmol m^{-2} s^{-1} and 1,200 μmol m^{-2} s^{-1} of soybean seedling, but significantly increased plant height, fraction of dry mass in stem and chlorophyll content. Light × variety interaction was significant for all measured traits, light effect contributed more than variety effect. The biomass of soybean seedlings was positively correlated with leaf area and stem diameter under both shade and full sunlight conditions, but not correlated with plant height and net photosynthetic rate. The top five (62.75% variation explained) most important explanatory variables of plasticity of biomass were that the plasticity of leaf area, leaf area ratio, leaflet area, plant height and chlorophyll content, whose total weight were 1, 0.9, 0.3, 0.2, 0.19, respectively. The plasticity of biomass was positively correlated with plasticity of leaf area and leaflet area but significant negative correlated with plasticity of plant height. The principal component one account for 42.45% variation explain. A cluster analysis further indicated that soybean cultivars were classified into three groups and cultivars; *Jiandebaimaodou*, *Gongdou 2*, and *Guixia 3* with the maximum plasticity of biomass. These results suggest that for soybean seedlings grown under shade increasing the capacity for light interception by larger leaf area is more vital than light searching (plant height) and light conversion (photosynthetic rate).

KEYWORDS

shade, soybean, plasticity, morphological, physiological

Introduction

Intercropping, defined as the cultivation of two or more crop species simultaneously in the same field (Willey, 1979; Francis, 1989), is widely practiced by smallholder farmers across the world, and is attracting attention in the context of ecological intensification of agriculture (Vandermeer, 2011; Brooker et al., 2015; Tanveer et al., 2017). Compared with sole cropping, intercropping often leads to higher yield because of the full use of time, space, and resources (Willey, 1990; Keating and Carberry, 1993; Szumigalski and Van Acker, 2006; Malézieux et al., 2009; Raza et al., 2021). Adaptive plant morphological and physiological responses to intercropping environments are likely to contribute to the yield advantage (Li et al., 2021; Wang et al., 2021). It has been shown that plasticity of the shoot traits of wheat contribute significantly to the enhanced light capture in wheat-maize intercropping systems (Zhu et al., 2015, 2016). This suggests that phenotypic plasticity, which is defined as the ability of a genotype to alter its expressed trait values in response to environmental conditions (Bradshaw, 1965; Valladares et al., 2007; Sultan, 2010), may improve crop performance in intercropping systems. However, detailed information about the genetic differences in phenotypic plasticity in the context of intercropping is still lacking. Such information can be used as a guide in variety selection and breeding to optimize the benefits of intercropping systems (Zhu et al., 2016).

The cereal-legume system is one of the most common types of intercropping systems (Yu et al., 2015), and soybean is one of the most widely used legumes in these systems, which include maize–soybean (Wu et al., 2021) and sorghum–soybean (Ghosh et al., 2009). Due to the shorter plant height and late sowing time than maize and sorghum, soybean plants are often grown under shade conditions in these intercropping systems (Wu et al., 2022). Plants adapt to shade through either shade tolerance (Yang et al., 2018) or shade avoidance mechanisms (Valladares et al., 2007; Valladares and Niinemets, 2008; Niinemets, 2010). Shade tolerance mechanisms, which can help plants survive under low light conditions, increase light harvesting or light use efficiency. These mechanisms include increasing chlorophyll (Chl) content, increasing specific leaf area, and reducing the Chl *a/b* ratio (Givnish, 1988; Valladares and Niinemets, 2008; Niinemets, 2010). Shade avoidance mechanisms, which can help plants escape from shade and likely increase light capture, include responses such as enhanced stem and petiole elongation, higher dry mass allocation to the stem than to the leaf and root, and develop a small leaf angles (Ballaré, 1999; Smith, 2000; Franklin and Whitelam, 2005; Vandenbussche et al., 2005; Casal, 2012; de Wit et al., 2012).

Phenotypic plasticity plays a remarkable role in the ecological distribution and evolutionary diversification of plants (Enbody et al., 2021). The degrees of plasticity differ among species or populations from contrasting habitats. It has been reported that shade-grown *Impatiens capensis* possesses longer stems and internodes than its counterparts grown under full sunshine and that *I. capensis* populations originating from open habitats are more sensitive to shade than those from shade habitats (Dudley and Schmitt, 1995; Anten et al., 2009). Other studies comparing the plasticity of morphological and physiological variables in different species found that shade-intolerant species from light habitats are more sensitive to light and exhibit a greater degree of plasticity than shade-tolerant species from shade habitats (Valladares et al., 2000a,b; Portsmuth and Niinemets, 2007). Comparisons of the plasticity of different functional traits revealed that shade-intolerant species have relatively higher plasticity for physiological traits, but lower plasticity for morphological traits than shade-tolerant species (Valladares et al., 2000b; Li et al., 2012; Naseer et al., 2022). It has been pointed out that light-favoring plants have enhanced physiological plasticity for variables related to photosynthesis, while shade tolerant species rely on enhanced plasticity in light-harvesting traits (Valladares et al., 2002; Poorter et al., 2019).

It has been shown that soybean plants display a suite of shade-avoidance responses when co-grown with maize; these responses result in a lower photosynthetic capacity, an elongated stem, reduced branching, a higher lodging rate and lower yield (Yan et al., 2010; Su et al., 2014; Yang et al., 2014; Wu et al., 2022). Previously, we showed that there are genetic differences in the shade responses of two soybean varieties (Gong et al., 2015). However, it remains unclear how these responses reflect the inherent strategies for coping with shade, and which traits should be displayed in the ideotype for breeding soybean varieties with better performance in intercropping. The aim of this study was: (1) to characterize the phenotypic variation in morphological and physiological traits of soybean grown under both shade and full-light conditions; (2) to quantify the relationship between the biomass of soybean and morphological and physiological traits under the different light conditions; and (3) to develop approaches to establish an ideotype contributing to higher biomass accumulation under shade based on plasticity in morphological and physiological traits.

Materials and methods

Experimental design and field management

Experiment 1: Experiment 1 was conducted in 2014 under field conditions at the Teaching and Experimental Farm of Sichuan Agricultural University in Ya'an (29°59'N, 103°00'E), which is located at the western border of the Sichuan Basin. The soil of the experimental field is a purple clay loam (pH 7.5). On June 19th, the seeds of 20 soybean varieties (names refer to **Supplementary Table 1**) were sown, each varieties were sown in one plot with a row spacing of 0.5 m and a row length of 2.5 m, and three rows of each variety were planted for each condition.

The shade and full sun light treatments were started immediately after sowing. The shade treatment was achieved by installing green shading nets above the experimental field at a height of 2 m, ∼40% transmittance, PAR was around 500 μmol m^{-2} s^{-1}, average daily temperature was 30.7 ℃, average daily humidity was 71.9%. The average daily temperature and humidity of full sun light treatment was 32.9 ℃ and 64.5% (Yang et al., 2014; Wu et al., 2017b; **Figures 1A,B**). After the first trifoliolate leaves expanded, soybean seedlings were thinned to 0.1 m between plants in each row.

Experiment 2: In order to further verify the shade response of soybean and variety performance of 2014 in a real intercropping shade environment, we conducted Experiment 2 in 2015 at the same field of 2014, so the soil of the experimental field is a purple clay loam (pH 7.5). It was conducted by a split-plot experiment design with three replications. The planting pattern was set as main plot with two levels: maize-soybean relay strip intercropping (shade) and soybean monoculture (full sun light) (**Figures 1C,D**). 14 soybean varieties (in order to reduce the field work, we only selected 14 varieties with large difference in growth in shade) were used in sub plot based on the results of 2014 (**Supplementary Table 1**). The field arrangement of relay intercropping was carried out as follows. Briefly, For the full sun light treatment in sole cropping, soybeans were planted as solid rows with a 0.5-m row spacing. For the shade treatment in intercropping, soybean and maize were planted as alternating strips, and every soybean strip was relay intercropped between the maize strips. Each plot contained two maize and two soybean strips, and each soybean strip and maize strip consisted of two soybean and two maize rows. The strip spacing (distance between maize and soybean rows), soybean row spacing and maize row spacing were all 0.5 m (Wu et al., 2017b). Each plot was 6 m long. The maize cultivar, *Zhenghong 505*, was sown on 9 April and harvested on 9 August, the soybeans were sown on 20 June and harvested on 23 October. When soybean was planted, maize was 2.5 meters high and reduced the light interception rate of soybean by 66%, the average daily temperature and humidity of intercropping treatment was 30.1 ℃ and 68.6%. The weather condition (rainfall and temperature) of two years are shown in **Supplementary Figure 1**.

Measurements

In Experiment 1, three individual plants grown in the middle section of the middle row were tagged on August 5th, 2014 (47 days after sowing); these plants were used for all measurements and each individual plant was a biological replicate. Photosynthetic indexes were mearsured on on the 47 days after sowing, and the middle leaflets of the latest fully expanded trifoliolate leaves were used for measurements. Photosynthesis was measured using a portable photosynthesis system (LI-6400XT, Li-Cor Inc., USA) equipped with an LED Light Source (6400-02B). Net photosynthetic rate per unit area was measured under light intensities of 500 (P_{N500}) and 1,200 (P_{N1200}) μmol m^{-2} s^{-1}, a CO_2 concentration of 380 μmol mol^{-1} sample, an air flow rate of 500 ml min^{-1}, 60–75% relative humidity and a temperature of 30°C. The net photosynthetic rate value was taken when the range is between 0.1 and 0.2 after 1–2 min. After the measurement of photosynthesis, the same trifoliolate leaves were collected in white ziplock bag, and put in a ice box and brought to the laboratory no more than 30 min. First, leaves were scanned using a flatbed scanner (CanoScan LiDE 200, Canon Inc., Japan), and the captured images were used for later analysis of the leaflet area in ImageJ 1.45s. Second, two leaf discs (diameter = 1 cm) from the middle leaflet were punched out, and extracted in a centrifuge tube with 80% aqueous acetone solvent for 24 h in a dark environment with 20 ℃ indoor temperature, and then used spectrophotometer to determine the total Chl concentration and the Chl *a*/*b* ratio (Lichtenthaler, 1987). The remaining leaves were oven-dried and weighed to calculate the leaf mass per unit area and the Chl concentration per unit dry mass. Dried leaves were finally ground into a fine powder for the measurement of nitrogen (N) and carbon (C) concentration using an elemental analyzer (CE-440 Elemental Analyzer, Exeter Analytical Inc., USA). N concentrations were expressed based on unit content per unit area.

On August 6th, 2014 (48 days after sowing), the aboveground parts of the tagged plants were sampled and brought back to the laboratory to measure biomass and morphological traits. Plants were divided into three parts: stem, lamina and petiole. Laminas were scanned, and then the total leaf area per plant was determined using ImageJ. Plant height and stem diameter (measured at the middle point of the first internode) were also measured. The separate parts of the leaf were oven-dried at 70°C to a constant weight (∼72 h). Biomass, fraction of dry mass in the stem, fraction of dry mass in the lamina, and fraction of dry mass in the petiole were then calculated.

In Experiment 2, all sampling and measurement were conducted on July 27th, 2015 (37 days after sowing). First, P_{N1200} was measured on five newly expanded leaves in five individual plants grown in the middle section of the middle row per plot, other parameters were maintained as described in experiment 1. Second, the measured plant for photosynthetic rates were sampled and brought to laboratory, leaf area, plant height, stem diameter, biomass were measured as described in experiment 1. The mean value per plot were calculated and used for statistics.

Data processing and analysis

The plasticity of plants in response to shade was calculated as the dimensionless slope of norm of reaction as previously

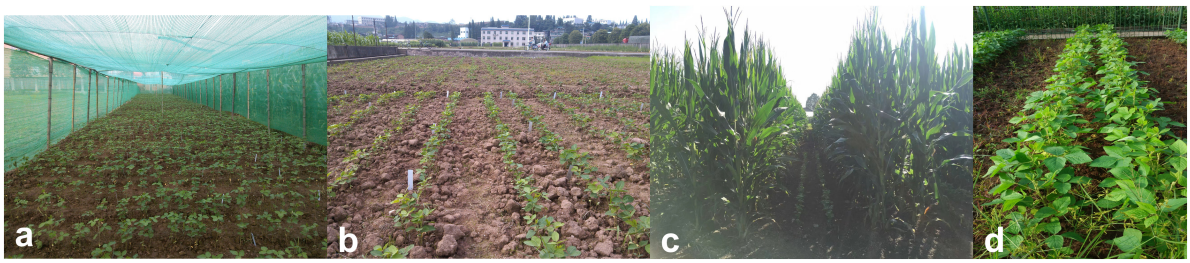

FIGURE 1
Photographes of the experiment. **(a)** Shade treatment in 2014; **(b)** full sun light treatment in 2014; **(c)** maize-soybean relay strip intercropping in 2015; **(d)** soybean monoculture in 2015.

reported (Sadras et al., 2009). Briefly, Plasticity = (T_{i_shade}-$T_{i\_fulllight}$)/($_{shade}$-$_{fulllight}$), where T_i is the value of one trait (e.g., biomass) of the ith variety, and is the mean value of the trait across all varieties. Thus, slope = 1 indicates average plasticity over the two light environments, slope > 1 indicates above-average plasticity, and slope < 1 indicates below-average plasticity (Sadras et al., 2009).

Two-way ANOVA was used to test for the effects of light and variety on the measured traits. Light was set as a fixed factor, and variety was set as a random factor. Before analysis, trait values were transformed by taking the natural logarithm. Correlation and regression analysis were used to explore associations between traits and plasticity (**Supplementary Tables 2, 3** and **Supplementary Figures 3**, **4**). Analyses were performed using *SPSS 19.0* software (*SPSS*, Chicago, USA).

R version 4.0.5 was used to reveal the quantitative relationships between the plasticity of biomass and the plasticity of morphological and physiological traits. Features selection was performed with the *train* function in R package *caret* v6.0-91. Then, features importance was obtained with *varImp* function in R package *caret* v6.0-91 (**Figure 2**). The critical features ($p < 0.05$) were selected, and correlation analysis was performed with *ggpairs* function in R package *GGally* v2.1.2 (**Figure 3**). Similarly, the critical features were performed with principle component analysis with the *PCA* function in R package *FactoMineR* package v1.34. The results of PCA were visualized with the *fviz_pca_biplot* function in R *factoextra* package v1.0.7 (**Figure 6A**). Meanwhile, hierarchical cluster analysis (**Figure 6B**) was performed with the *hclust* function and visualized with the *fviz_dend* function in R package *factoextra*.

Results

Plant biomass and biomass allocation

In 2014, shade significantly reduced biomass, the mean biomass of soybean seedlings grown under shade across all varieties was 6.6 g per plant, which was 37.8% less than that of seedlings grown under full light (10.6 g per plant) (**Figure 2A**). Similar variations trend were observed in 2015 when soybean plants grown under shade in intercropping and under full light in sole cropping. The mean biomass of soybean seedling was 1.5 g per plant, the corresponding grown under full light was 7.6 g per plant (**Figure 2A**). Significant interactions between light and variety were found for biomass. Partitioning of total sum of squares (SS) indicated that the light effect was the major contributor (**Table 1**).

In 2014, the mean fraction of dry mass in stem increased from 31.7% under full light to 36.4% under shade. Meanwhile, the mean fraction of dry mass in petiole decreased from 18.3% under full light to 12.5% under shade (**Figure 2B**). There was no difference in fraction of dry mass in leaf between plants grown under the two treatments. Significant varietal differences and interactions between light and variety were found in fraction of dry mass. The total SS indicated that the variety effect was the major contributor for stem and leaf, while petiole variation was caused by light (**Table 1**). In 2015, Similar variations trend of fraction of dry mass in stem and petiole were observed. While the mean fraction of dry mass in leaf decreased from 58% under full light to 45% under shade.

Morphological traits

In 2014, plant height greatly increased under shade conditions, while stem diameter decreased. The mean plant height of soybean seedlings grown under shade across all varieties was 79 cm, which was 71.5% higher than that for seedlings grown under full light (46 cm), while the mean stem diameter reduced from 6.1 mm in full light to 4.5 mm in shade (**Figures 2D,E**). leaf area was significantly reduced in shade. The mean value of leaf area across all varieties grown under shade was 1,171.1 cm^2, which was 33.3% less than that under full light (1,755.4 cm^2) (**Figure 2F**). In 2015, when grown under shade in intercropping, morphological traits significantly varied. Mean plant height of soybean seedling was 71.3 cm, but the value of seedlings grown under full light was 33.3 cm (**Figure 2D**).

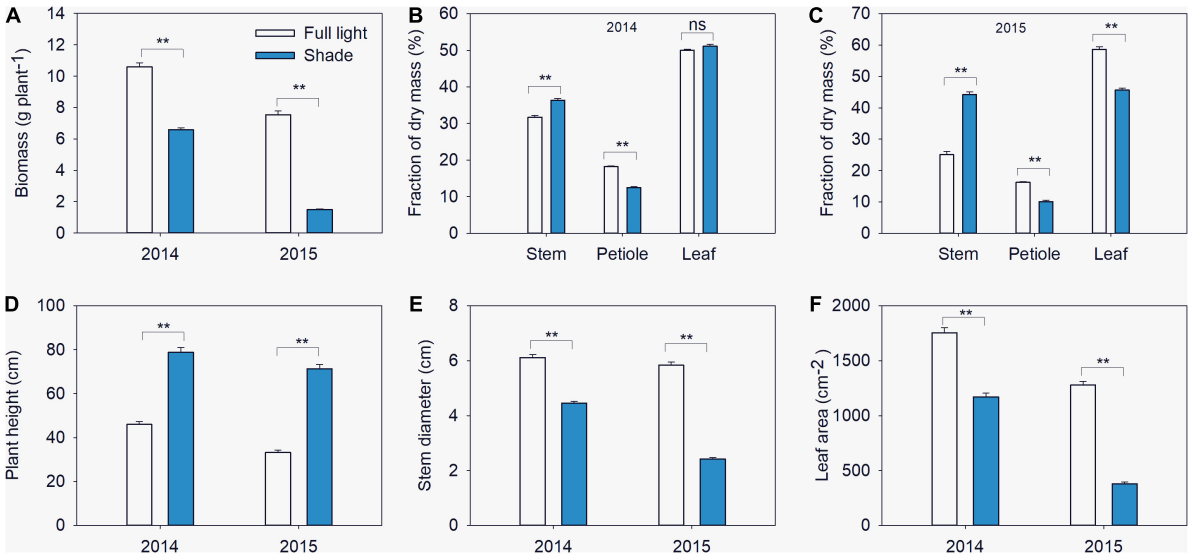

FIGURE 2
Biomass **(A)**, fractions of dry mass in stem, petiole and leaf **(B,C)**, plant height **(D)**, stem diameter **(E)** and leaf area **(F)** of different soybean varieties grown under shade and the control conditions in 2014–2015. Traits were expressed as mean ± standard errors from 20 cultivars in 2014 and 14 cultivars in 2015. ** represent significant difference at 0.01 level.

TABLE 1 The sum of squares (SS) and mean squares (MS) of two-way ANOVAs of the effects of light and variety on morphological traits.

Year	ANOVA	d.f.	BMS		f_s		f_p		f_l		LA		PHT		DMT	
			SS	MS	SS	MS	SS	MS	SS	MS	SS	MS	SS	MS	SS	MS
2014	Light	1	6.57	6.57**	0.56	0.56**	4.45	4.45**	0.01	0.01	4.93	4.93**	9.01	9.01**	3.00	3.00**
	Variety	19	2.75	0.14**	0.91	0.05**	0.90	0.05**	0.36	0.02**	3.39	0.18*	4.47	0.24**	0.05*	0.05*
	Light*Variety	19	0.92	0.05**	0.11	0.01**	0.15	0.01*	0.06	0.00**	1.23	0.06**	0.7	0.04**	0.02**	0.02**
2015	Light	1	56.93	56.93**	~	~	~	~	~	~	32.42	32.42**	12.31	12.31**	16.42	16.42**
	Variety	13	1.84	0.14	~	~	~	~	~	~	1.69	0.13	1.947	0.15*	0.61	0.04
	Light*Variety	13	1.68	0.12**	~	~	~	~	~	~	1.47	0.11**	0.56	0.04**	0.39	0.03**

*, ** represent significant difference at 0.05 and 0.01 levels, respectively. BMS, biomass; f_s, fraction of dry mass in stem; f_p, fraction of dry mass in petiole; f_l, fraction of dry mass in lamina; LA, leaf area per plant; PHT, plant height; DMT, diameter of the first node.

Meanwhile, the leaf area of soybean seedlings reduced from 1,278.4 cm^2 in full light to 379.9 cm^2 in shade, and the stem diameter reduced from 5.84 mm in full light to 2.42 mm in shade (Figures 2E,F). Significant interaction between light and variety were found for those traits in both two years, the partition of the total SS revealed that the major percentage was attributable to light (Table 1). The yields of the 14 soybean varieties in two treatments are also shown in Supplementary Table 4.

Physiological traits

Leaf physiological traits related to light use efficiency were affected by shade. Leaf mass per unit area, P_{N500}, P_{N1200} and the Chl *a/b* ratio decreased under the shade condition, while Chl content increased (Figure 3). Leaf mass per unit area and Chl content differed between varieties, while P_{N500}, P_{N1200} and leaf nitrogen content did not. The interactions between light and variety for leaf mass per unit area, P_{N500}, P_{N1200}, Chl content, Chl a/b ratio and N content were significant. ANOVA results revealed that light effect was the major contributor for Leaf mass per unit area, P_{N500}, P_{N1200}, Chl a/b ratio and nitrogen content, while Chl content variation was caused by variety (Table 2).

Relationships between the biomass and the morphological and physiological traits

In 2014, the biomass of soybean seedlings was positively correlated with leaf area (Supplementary Figure 3A), as well as with the stem diameter under both shade and full light

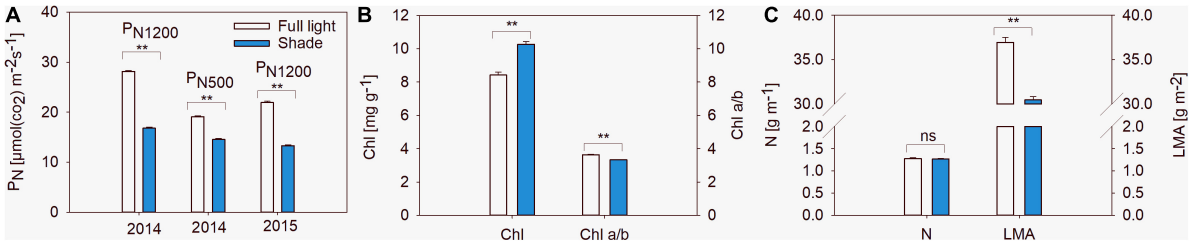

FIGURE 3
Net photosynthetic rates at 500 μmol m^{-2} s^{-1} (P_{N500}) and 1,200 μmol m^{-2} s^{-1} (P_{N1200}) **(A)**, chlorophyll concentration (Chl) and Chl a/b ratio (Chl a/b) **(B)**, nitrogen (N) concentration and leaf mass per unit area (LMA) **(C)** of 20 soybean varieties grown under shade and the control conditions in 2014. Traits were expressed as mean ± standard errors from 20 cultivars in 2014 and 14 cultivars in 2015. ** represent significant difference at 0.01 level.

TABLE 2 The sum of squares (SS) and mean squares (MS) of two-way ANOVAs of the effects of light and variety on physiological traits.

Year	ANOVA	d.f.	LMA		Pn500		Pn1200		Chl		Chl a/b		N	
			SS	MS	SS	MS	SS	MS	SS	MS	SS	MS	SS	MS
2014	Light	1	1.10	1.10**	2.29	2.29**	8.09	8.09**	1.23	1.23**	0.23	0.23**	0.00	0.00
	Variety	19	0.73	0.04*	0.54	0.03	0.33	0.02	1.59	0.08*	0.14	0.01**	0.39	0.02
	Light*Variety	19	0.32	0.02**	0.28	0.01	0.26	0.01**	0.58	0.03**	0.03	0.00*	0.33	0.02**

*, ** represent significant difference at 0.05 and 0.01 levels, respectively. LMA, leaf mass per unit area; Pn_{500}, net photosynthetic rate per unit area at 500 μmol m^{--2} s^{--1}; Pn_{1200}, net photosynthetic rate per unit area at 1,200 μmol m^{--2} s^{--1}; Chl, chlorophyll content per unit dry mass; Chl a/b, chlorophyll a/b ratio; N, nitrogen content per unit area.

conditions (Supplementary Figure 3B). But biomass was not correlated with plant height (Supplementary Figure 3C), P_{N500} (Supplementary Figure 3E) and P_{N1200} (Supplementary Figure 3F). Plant height was positively correlated with f_S under both shade and full light conditions (Supplementary Table 2). Interestingly, leaf mass per unit area was negatively correlated with biomass only under the shade condition (Supplementary Figure 3D).

In 2015, for the variation between shade in intercropping and full light in sole cropping, biomass of soybean seedlings positively correlated with leaf area (Supplementary Figure 4A). For the relationship between biomass and plant height, negative correlations were found only in shade conditions (Supplementary Figure 4B).

Quantitative relationships between the plasticity of biomass and the plasticity of morphological and physiological traits

A multi-variable analysis and features selection were conducted to evaluate the relative importance of plasticity variables of biomass. Results indicated that the plasticity of leaf area, leaf area ratio, leaflet area, plant height, and Chl content were the top five explanatory variables, which significantly affected the plasticity of biomass (Figure 4). A further pearson correlations between the plasticity of biomass and the plasticity of the top five explanatory variables indicated that only leaf area, leaflet area, and plant height were significantly positively correlated with biomass (Figure 5). However, leaf area and leaflet area were significant positive correlated with biomass, plant height was significant negative correlated with the biomass (Figure 5). Results of principal component analysis (PCA) showed that the relationships between soybean cultivars' biomass and explanatory variables, i.e., leaf area, leaflet area, Chl content, leaf area ratio, and plant height. A total of 62.7% variation explained by the explanatory variables and the principal component one account for 42.5% variation explain (Figure 6A), this was constant with the results of features selection (Figure 4) and correlation analysis (Figure 5). On the basis of the top five explanatory variables, cluster analysis indicated that soybean cultivars were classified into three groups (Figure 6B). Cluster one, including cultivars 3 (*Jiandebaimaodou*), 13 (*Gongdou 2*), and 20 (*Guixia*), with the maximum plasticity of biomass.

Discussion

Soybean seedling responses to shade

Compared with seedlings grown in full light, shade-grown soybean seedlings showed increased plant height, internode length and fraction of dry mass in stem and reduced leaf area, leaflet area and leaflet number (Figure 2).

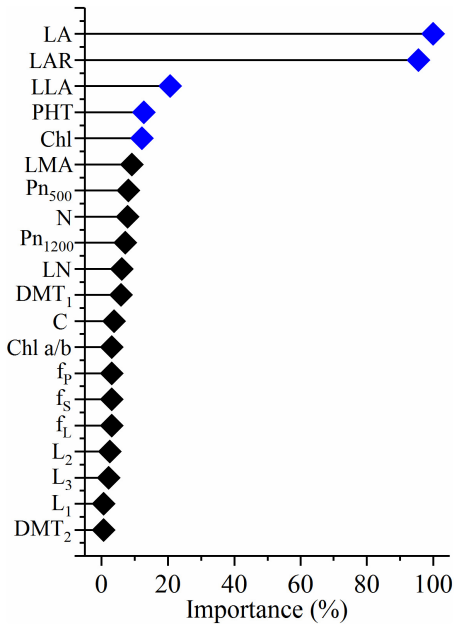

FIGURE 4
Relative importance of the plasticity of morphological and physiological variables that affect the plasticity of biomass in shade. LA, leaf area per plant; LAR, leaf area ratio; LLA, leaflet area; LN, leaflet number; PHT, plant height; Chl, chlorophyll content per unit dry mass; Chl a/b, chlorophyll a/b ratio; LMA, leaf mass per unit area; Pn_{500}, net photosynthetic rate per unit area at 500 μmol m^{-2} s^{-1}; Pn_{1200}, net photosynthetic rate per unit area at 1,200 μmol m^{-2} s^{-1}; N, nitrogen content per unit area; LN, leaflet number; C, carbon content per unit area; DMT_1, diameter of the first node; DMT_2, diameter of the second node; f_S, fraction of dry mass in stem; f_P, fraction of dry mass in petiole; f_{Lr}, fraction of dry mass in lamina; L_1, first internode length; L_2, second internode length; L_3, third internode length.

These phenotypes are typical shade avoidance symptoms that allow plants to search for light and escape from shade (Franklin, 2008). The presence of these symptoms indicates that soybean seedlings escape from shade by increasing stem elongation at the cost of reduced leaf expansion (Valladares et al., 2011). We also found that plant height was positively correlated with fraction of dry mass in stem under both light treatments and that fraction of dry mass in stem was inversely related to fraction of dry mass in lamina (**Supplementary Table 2**). These results indicate a trade-off between increased plant height which allows plants to search for light, and leaf expansion which increases light capture and utilization. Under shading this trade-off was balanced toward light searching.

Other findings in this study were that biomass was positively correlated with stem diameter under both light conditions (**Supplementary Figures 3B** and **Supplementary Table 2**) and that the plasticity of biomass was correlated with the plasticity of stem diameter under shading net (**Supplementary Table 3**). In addition, the stem diameter was positively correlated with leaf area under both light conditions, but it was negatively correlated with the length of the first internode under shade. Because the measurement of stem diameter was taken at the middle point of the first internode, these results indicate that the growth in the horizontal direction led to an increase in internode length in seedling development, which was consistent with Zhang et al. (2020). As the trifoliolate leaves of soybean develop at the apex of stem, a wider stem might lead to bigger leaf primordia due to the presence of more cells produced by cell division (Reinhardt et al., 2005; Wu et al., 2017a). Whether the thicker stem could produce larger leaf and the stem diameter of seedling grown under shade could be used to predict the leaf area still need to be testified in future studies.

Besides avoiding shade via stem elongation, plants often cope with shade by increasing light use efficiency via a shade tolerance strategy (Gong et al., 2015). We found that a reduced Chl *a*/*b*, a lower leaf mass per unit area and a higher Chl concentration were beneficial for photosynthesis under low light conditions, consistent with previous studies (Hussain et al., 2020; Tan et al., 2022). A higher Chl concentration indicates that there are more pigment-binding proteins for photons captured by photosystem II per unit N content. As the light-harvesting complex of photosystem II contains mostly Chl *b*, increased accumulation of the light-harvesting complex under shade causes a decline in the Chl *a*/*b* ratio (Boardman, 1977; Anderson, 1986; Evans, 1989).

Leaf mass per unit area reflects the trade-off between the functions of the leaf lamina in light radiation interception and conversion. A decline in leaf mass per unit area is beneficial for receiving more light per unit of leaf mass; however, low leaf mass per unit area negatively affects carboxylation because the reduced thickness of the palisade mesophyll resulting in less area for CO_2 exchange (Terashima et al., 2001, 2006, 2011). Leaf mass per unit area is also strongly correlated with leaf thickness (especially palisade thickness) and the chemical composition of the leaf (i.e., N content and Chl concentration) (Poorter et al., 2009). In this study, leaf mass per unit area was positively correlated with P_{N1200} (r = 0.572**) under full light, indicating that a thicker leaf mesophyll layer leads to increased CO_2 exchange as discussed above. But, we did not find a relationship between leaf mass per unit area and P_{N500} when soybean was grown under the shade treatment, which suggesting that when leaf mass per unit area was reduced, photosynthetic rate of all soybean genotypes declined to the similar levels. It is notable that the biomass of shade-grown soybean was negatively correlated with leaf mass per unit area (**Supplementary Figure 3D**), suggesting that soybean seedlings respond to shade by increasing leaf mass per unit area, which increases light interception at the cost of light conversion.

Although the plasticity of plant morphological and leaf physiological traits were helpful for acclimating to shade, the

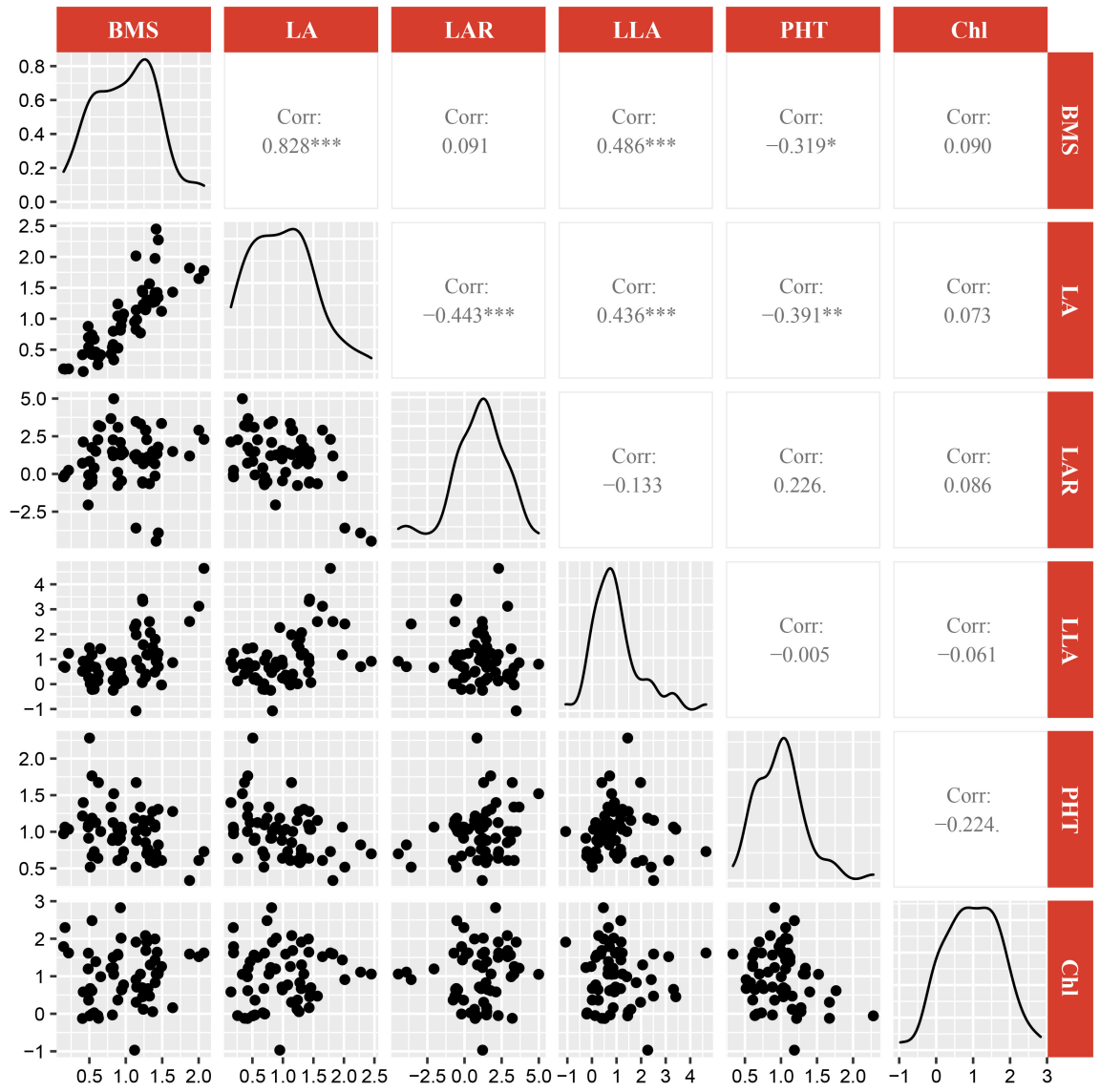

FIGURE 5
Correlations between the plasticity of biomass and the plasticity of top five most important explanatory variables. BMS, biomass;LA, leaf area; LAR, leaf area ratio; LLA, leaflet area; PHT, plant height; Chl, Chl content. *, **, *** represent significant difference at 0.05, 0.01, and 0.001 levels, respectively.

biomass of soybean seedlings was still severely reduced under the shade treatment (**Figure 2A**). The plasticity of biomass was positively correlated with the plasticity in leaf area and stem diameter under both light treatments (**Supplementary Table 3**), although leaf area and stem diameter were significantly reduced under the shade condition (**Figures 2E,F**). However, the plasticity of biomass was not correlated with plant height, P_{N500}, P_{N1200}, or Chl concentration in the present study. Thus, the increase in plant height and Chl concentration, as well as the decrease in Chl *a*/*b* ratio could not offset the light deficit. Based on these findings, we speculate that the formation of a canopy that increases light interception is more important than increasing light conversion for soybean seedlings that cannot escape from shade.

Phenotypic plasticity in response to light is the remarkable ability of plants to adjust morphology and physiology under different light conditions (Delagrange et al., 2004; Valladares and Niinemets, 2008). Previous studies have found that mean plasticity in morphological traits in response to light (e.g., elongation of the stem and internodes) is lower for shade-tolerant plants than for shade-intolerant plants (Dudley and Schmitt, 1995; Valladares et al., 2000b; Sánchez-Gómez et al., 2006; Portsmuth and Niinemets, 2007). Most plants from open habitats show shade avoidance responses, such as searching for

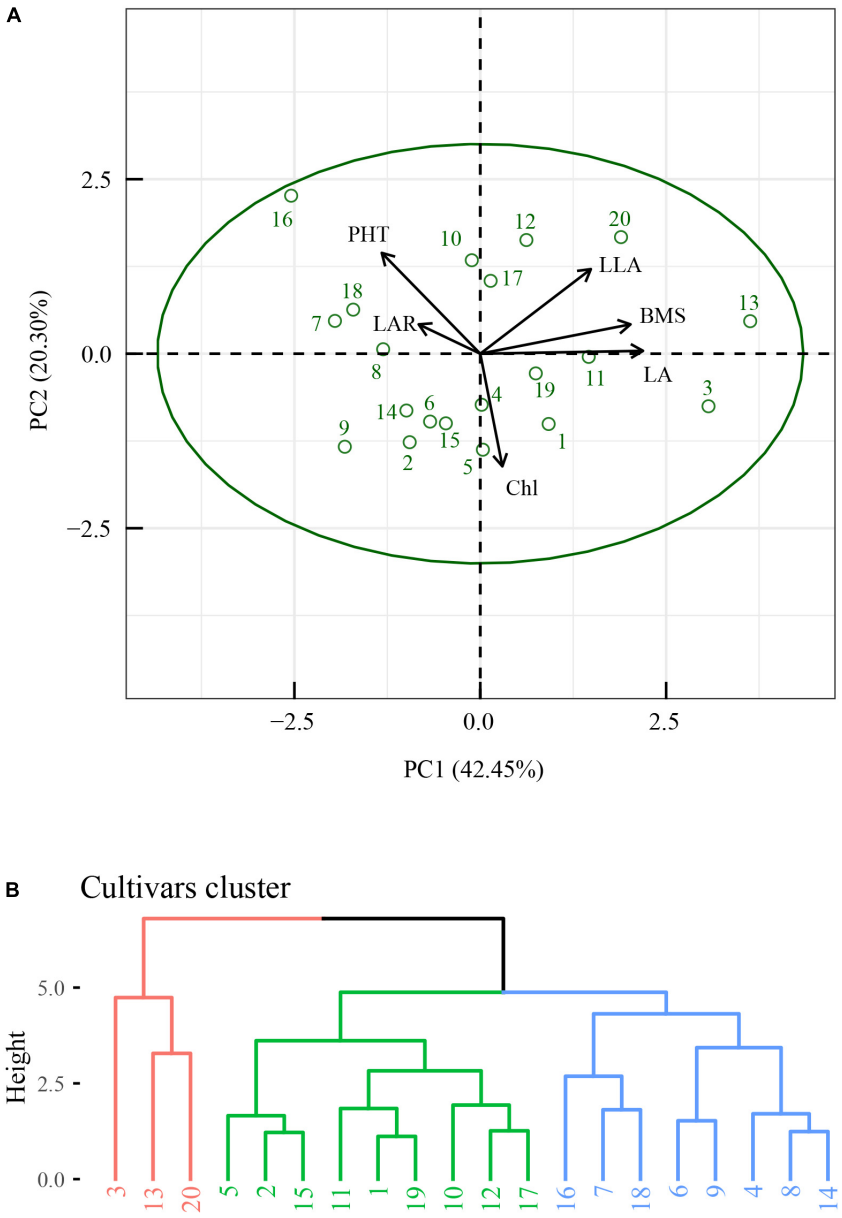

FIGURE 6
Principal component analysis (PCA) of the plasticity of biomass and the plasticity of top five most important explanatory variables **(A)**, and clustering analysis of the soybean cultivars **(B)**. BMS, biomass; LA, leaf area; LAR, leaf area ratio; LLA, leaflet area; PHT, plant height; Chl, Chl content. The numbers in panel **(B)** represent cultivars.

light and escaping shade, when grown under shade (Gommers et al., 2013). Therefore, plasticity in plant height and internode length could be explained as the capacity for light searching. In this study, all soybean varieties showed the capacity for light searching via stem elongation. However, the plasticity of biomass was negative correlated to the plasticity of plant height (**Supplementary Table 3**). This is probably because soybean seedlings could not escape from shade in our shading net treatment or intercropping. Thus, the elongation of the stem could not enhance light interception. It can be inferred that under intercropping conditions where there is a large companion crop, e.g., maize, a strategy that enhances leaf area and allows more light to be captured, would be more beneficial than escaping shade through stem elongation.

Leaves are involved in both shade avoidance and tolerance strategies, as the leaf lamina directly captures light and converts the light into carbohydrates. Leaf area as the most important factor that affect plasticity of biomass and has strong positive relationship between plasticity of biomass, suggesting that light capture by the leaf determines light utilization, rather than the

light search by elongating the stem. The abundance of climbing plants in deep shade was found to be directly related to their ability to intercept light efficiently but not to their ability to increase carbon fixation by increasing leaf area (Valladares et al., 2011). Hence, these findings suggest that capacity for light capture and absorption by the leaf is different from the ability to search for light by elongating the stem under deep shade, although both strategies might help increase light capture.

Phenotypic plasticity of light searching, capturing, and conversion and their relationships to agronomic practices

Soybean is a light-favoring crop and is usually grown in a sole cropping system without shade from other plants. Soybean seedlings display a suite of architectural and physiological changes in response to shade, and there are genetic differences in these responses as shown in this study. In the maize-soybean relay strip intercropping system, soybean grew under shade environment during the seedling stages and the morphological traits were more plastic. Our previous study pointed out that most of the genetic differences in morphological traits are only expressed during the seedling stages (Hussain et al., 2020). So, we infer that plant seedlings have higher plasticity in architectural and morphological traits than in leaf physiological traits. It has been reported that plasticity in architectural traits leads to increased light interception and a yield advantage in intercropping systems (Zhu et al., 2015, 2016; Li et al., 2021),but it depends on the planting configurations (Li et al., 2020). This previous finding, combined with our results, indicates that the performance of component crops in intercropping systems might be based on light capture rather than photosynthesis and that increasing light capture might be a more feasible approach for increasing the total light intercepted in field production.

Plasticity in leaf physiological traits, such as photosynthetic rates and Chl concentration, is associated with changes in the capacity for photosynthesis in the leaf mesophyll. However, the plasticity of leaf physiological traits were not correlated with plasticity of biomass. Among the 20 varieties that we investigated in experiment 1, there was less variation in photosynthetic rate, Chl content and Chl *a*/*b* ratio compared with morphological traits, consistent with the findings of our previous study on two soybean varieties (Gong et al., 2015; Wu et al., 2022). These findings suggest that the capacity to adjust photosynthetic rate seems to be a conserved resource use strategy (Valladares et al., 2000a); thus, the soybean genotypes with contrasting capacities for light conversion in the mesophyll did not differ in their ability to accumulate biomass. Therefore, the selection of soybean varieties possessing higher photosynthesis rates might have little effect on improving shade tolerance.

The evolution of crops is not only driven by natural forces but also by selection by humans to meet the demand for food; crops became less shade tolerant over the past few thousands of years when grown in sole cropping systems, and fewer studies have focused on the genotypic differences in the shade tolerance of crops. It had been reported that shade reduced tillering in maize (Rotili et al., 2021), leaf size and morphology in tomato (Chitwood et al., 2015) and also negatively affected biomass in grasses (Warnasooriya and Brutnell, 2014). Many shade avoidance on crops focused on discovery and validation of molecular function. Cultivated soybean was domesticated from its wild progenitor *Glycine soja*, which is a typical climbing species that usually grows in shade environments. It is obvious that cultivated soybean was domesticated by humans to grow in high-light conditions. However, the capacities for light searching, light capture and light conversion were maintained in soybean. When modern soybean is grown under shade conditions such as those found in intercropping systems, elongation of the main stem seems to be an atavism.

The responses of the investigated traits in this study can be classified into three functional strategies: light searching, light capture and light conversion. Among these strategies, increasing light searching via elongation of the stem easily led to lodging (Liu et al., 2016), and increasing light conversion by increasing Chl content and photosynthesis in the mesophyll could not offset the light limitation and seems to be a conserved response among genotypes (Gong et al., 2015). The strategy of searching for light via stem elongation might increase the opportunity to escape from shade or to intercept more light; however, this trait is probably not acceptable in agriculture for several reasons. Firstly, it is hard for soybean plants to escape from shading in intercropping systems due to the presence of a tall companion crop, e.g., maize (Fan et al., 2018). Thus, enhanced stem elongation will not contribute to biomass accumulation. Secondly, over-elongated plants have increased rates of lodging (Liu et al., 2015, 2016). Soybean varieties with less stem elongation have a lower capacity to search for light. As we found negative correlation between the plasticity of biomass and plasticity of plant height, soybean varieties with low stem elongation plasticity might perform better in intercropping systems. A previous study of climbing plants grown under deep shade found that those plants with a higher capacity to intercept light were more abundant (Valladares et al., 2011), consistent with our finding that light capture contributed more to growth when soybeans could not escape from shade. In wheat/maize and wheat/cotton intercropping, although the leaf area of intercropped wheat and maize was lower compared with that of wheat and maize grown as single crops, the productivity of the intercrops was still increased by increased light interception (Zhang et al., 2008; Gou et al., 2017). In short, when selecting soybean varieties for intercropping, the focus should be on those traits related to light capture, such as leaf area per plant and leaflet area.

Conclusion

A suite of shade responses for soybean varieties was documented. The biomass of soybean seedlings was positively correlated with leaf area per plant and stem diameter under both shade and full-light conditions. Although plant height increased significantly under shade, it was unrelated to the changes of biomass in this study. The top three most important explanatory variables of plasticity of biomass were leaf area, leaf area ratio and leaflet area. Plasticity of biomass was positively correlated with plasticity of leaf area and leaflet area and negatively correlated with plasticity of plant height, but it was not associated with plasticity of photosynthetic rate. These results suggest that increasing the capacity to capture light by increasing leaf area, rather than increasing the capacity to search for light by elongating the stem or by increasing light conversion in the leaf mesophyll, was more vital for light utilization by soybean seedlings grown under shade. Increasing light capture via the production of larger leaves gave rise to higher biomass accumulation in seedlings under shade. Therefore, selection and breeding of soybean varieties for future intercropping systems should focus on traits contributing to light capture, such as the production of more and larger leaves.

Data availability statement

The original contributions presented in this study are included in the article/**Supplementary material**, further inquiries can be directed to the corresponding author.

Author contributions

YW, WG, and WY designed the experiments. YW performed the experiments and data collection and wrote the manuscript. All authors contributed to the article and approved the submitted version.

Funding

This study was supported by Sichuan Science and Technology Program (No. 2021YJ0496) and National Natural Science Foundation of China (No. 32001416).

Conflict of interest

The authors declare that the research was conducted in the absence of any commercial or financial relationships that could be construed as a potential conflict of interest.

Publisher's note

All claims expressed in this article are solely those of the authors and do not necessarily represent those of their affiliated organizations, or those of the publisher, the editors and the reviewers. Any product that may be evaluated in this article, or claim that may be made by its manufacturer, is not guaranteed or endorsed by the publisher.

Supplementary material

The Supplementary Material for this article can be found online at: https://www.frontiersin.org/articles/10.3389/fpls.2022.1015414/full#supplementary-material

References

Anderson, J. M. (1986). Photoregulation of the composition, function, and structure of thylakoid membranes. *Annu. Rev. Plant Physiol.* 37, 93–136. doi: 10.1146/annurev.pp.37.060186.000521

Anten, N. P., von Wettberg, E. J., Pawlowski, M., and Huber, H. (2009). Interactive effects of spectral shading and mechanical stress on the expression and costs of shade avoidance. *Am. Nat.* 173, 241–255. doi: 10.1086/595761

Ballaré, C. L. (1999). Keeping up with the neighbours: Phytochrome sensing and other signalling mechanisms. *Trends Plant Sci.* 4, 97–102. doi: 10.1016/S1360-1385(99)01383-7

Boardman, N. K. (1977). Comparative photosynthesis of sun and shade plants. *Annu. Rev. Plant Physiol.* 28, 355–377. doi: 10.1146/annurev.pp.28.060177.002035

Bradshaw, A. D. (1965). Evolutionary significance of phenotypic plasticity in plants. *Adv. Genet.* 13, 115–155. doi: 10.1016/S0065-2660(08)60048-6

Brooker, R. W., Bennett, A. E., Cong, W.-F., Daniell, T. J., George, T. S., Hallett, P. D., et al. (2015). Improving intercropping: A synthesis of research in agronomy, plant physiology and ecology. *N. Phytol.* 206, 107–117. doi: 10.1111/nph.13132

Casal, J. J. (2012). Shade avoidance. *Arabidopsis Book* 10:e0157. doi: 10.1199/tab.0157

Chitwood, D. H., Kumar, R., Ranjan, A., Pelletier, J. M., Townsley, B., Ichihashi, Y., et al. (2015). Light-induced indeterminacy alters shade avoiding tomato leaf morphology. *Plant Physiol.* 169, 2030–2047. doi: 10.1104/pp.15.01229

de Wit, M., Kegge, W., Evers, J. B., Vergeer-van Eijk, M. H., Gankema, P., Voesenek, L. A. C. J., et al. (2012). Plant neighbor detection through touching leaf tips precedes phytochrome signals. *Proc. Natl. Acad. Sci. U.S.A.* 109, 14705–14710. doi: 10.1073/pnas.1205437109

Delagrange, S., Messier, C., Lechowicz, M. J., and Dizengremel, P. (2004). Physiological, morphological and allocational plasticity in understory deciduous

trees: Importance of plant size and light availability. *Tree Physiol.* 24, 775–784. doi: 10.1093/treephys/24.7.775

Dudley, S. A., and Schmitt, J. (1995). Genetic differentiation in morphological responses to simulated foliage shade between populations of impatiens capensis from open and woodland sites. *Funct. Ecol.* 9, 655–666. doi: 10.2307/2390158

Enbody, E. D., Pettersson, M. E., Sprehn, C. G., Palm, S., Wickström, H., and Andersson, L. (2021). Ecological adaptation in European eels is based on phenotypic plasticity. *Proc. Natl. Acad. Sci. U.S.A.* 118:e2022620118. doi: 10.1073/pnas.2022620118

Evans, J. R. (1989). Photosynthesis and nitrogen relationships in leaves of C3 plants. *Oecologia* 78, 9–19. doi: 10.1007/BF00377192

Fan, Y., Chen, J., Cheng, Y., Raza, M. A., Wu, X., Wang, Z., et al. (2018). Effect of shading and light recovery on the growth, leaf structure, and photosynthetic performance of soybean in a maize-soybean relay-strip intercropping system. *PLoS One* 13:e0198159. doi: 10.1371/journal.pone.0198159

Francis, C. A. (1989). Biological efficiencies in multiple-cropping systems. *Adv. Agron.* 42, 1–42. doi: 10.1016/S0065-2113(08)60522-2

Franklin, K. A. (2008). Shade avoidance. *N. Phytol.* 179, 930–944. doi: 10.1111/j.1469-8137.2008.02507.x

Franklin, K. A., and Whitelam, G. C. (2005). Phytochromes and shade-avoidance responses in plants. *Ann. Bot.* 96, 169–175. doi: 10.1093/aob/mci165

Ghosh, P. K., Tripathi, A. K., Bandyopadhyay, K. K., and Manna, M. C. (2009). Assessment of nutrient competition and nutrient requirement in soybean/sorghum intercropping system. *Eur. J. Agron.* 31, 43–50. doi: 10.1016/j.eja.2009.03.002

Givnish, T. J. (1988). Adaptation to sun and shade: A whole-plant perspective. *Funct. Plant Biol.* 15, 63–92. doi: 10.1071/PP9880063

Gommers, C. M. M., Visser, E. J. W., Onge, K. R. S., Voesenek, L. A. C. J., and Pierik, R. (2013). Shade tolerance: When growing tall is not an option. *Trends Plant Sci.* 18, 65–71. doi: 10.1016/j.tplants.2012.09.008

Gong, W. Z., Jiang, C. D., Wu, Y. S., Chen, H. H., Liu, W. Y., and Yang, W. Y. (2015). Tolerance vs. avoidance: Two strategies of soybean (Glycine max) seedlings in response to shade in intercropping. *Photosynthetica* 53, 259–268. doi: 10.1007/s11099-015-0103-8

Gou, F., van Ittersum, M. K., Simon, E., Leffelaar, P. A., van der Putten, P. E. L., Zhang, L., et al. (2017). Intercropping wheat and maize increases total radiation interception and wheat RUE but lowers maize RUE. *Eur. J. Agron.* 84, 125–139. doi: 10.1016/j.eja.2016.10.014

Hussain, S., Pang, T., Iqbal, N., Shafiq, I., Skalicky, M., Brestic, M., et al. (2020). Acclimation strategy and plasticity of different soybean genotypes in intercropping. *Funct. Plant Biol.* 47, 592–610. doi: 10.1071/FP19161

Keating, B. A., and Carberry, P. S. (1993). Resource capture and use in intercropping: Solar radiation. *Field Crops Res.* 34, 273–301. doi: 10.3389/fpls.2022.848893

Li, S., Evers, J. B., van der Werf, W., Wang, R., Xu, Z., Guo, Y., et al. (2020). Plant architectural responses in simultaneous maize/soybean strip intercropping do not lead to a yield advantage. *Ann. Appl. Biol.* 177, 195–210. doi: 10.1111/aab.12610

Li, S., van der Werf, W., Zhu, J., Guo, Y., Li, B., Ma, Y., et al. (2021). Estimating the contribution of plant traits to light partitioning in simultaneous maize/soybean intercropping. *J. Exp. Bot.* 72, 3630–3646. doi: 10.1093/jxb/erab077

Li, X., Cai, J., Li, H., Bo, Y., Liu, F., Jiang, D., et al. (2012). Effect of shading from jointing to maturity on high molecular weight glutenin subunit accumulation and glutenin macropolymer concentration in grain of winter wheat. *J. Agron. Crop Sci.* 198, 68–79. doi: 10.1111/j.1439-037X.2011.00484.x

Lichtenthaler, H. K. (1987). Chlorophylls and carotenoids: Pigments of photosynthetic biomembranes. *Methods Enzymol.* 148, 350–382. doi: 10.1515/znc-2001-11-1225

Liu, W., Deng, Y., Hussain, S., Zou, J., Yuan, J., Luo, L., et al. (2016). Relationship between cellulose accumulation and lodging resistance in the stem of relay intercropped soybean [Glycine max (L.) Merr.]. *Field Crops Res.* 196, 261–267. doi: 10.1016/j.fcr.2016.07.008

Liu, W., Zou, J., Zhang, J., Yang, F., Wan, Y., and Yang, W. (2015). Evaluation of soybean (Glycine max) stem vining in maize-soybean relay strip intercropping system. *Plant Prod. Sci.* 18, 69–75. doi: 10.1626/pps.18.69

Malézieux, E., Crozat, Y., Dupraz, C., Laurans, M., Makowski, D., Ozier-Lafontaine, H., et al. (2009). Mixing plant species in cropping systems: Concepts, tools and models. A review. *Agron. Sustain. Dev.* 29, 43–62. doi: 10.1051/agro:2007057

Naseer, M. A., Hussain, S., Nengyan, Z., Ejaz, I., Ahmad, S., Farooq, M., et al. (2022). Shading under drought stress during grain filling attenuates photosynthesis, grain yield and quality of winter wheat in the Loess Plateau of China. *J. Agron. Crop Sci.* 208, 255–263. doi: 10.1111/jac.12563

Niinemets, Ü (2010). A review of light interception in plant stands from leaf to canopy in different plant functional types and in species with varying shade tolerance. *Ecol. Res.* 25, 693–714. doi: 10.1007/s11284-010-0712-4

Poorter, H., Niinemets, Ü, Ntagkas, N., Siebenkäs, A., Mäenpää, M., Matsubara, S., et al. (2019). A meta-analysis of plant responses to light intensity for 70 traits ranging from molecules to whole plant performance. *N. Phytol.* 223, 1073–1105. doi: 10.1111/nph.15754

Poorter, H., Niinemets, Ü, Poorter, L., Wright, I. J., and Villar, R. (2009). Causes and consequences of variation in leaf mass per area (LMA): A meta-analysis. *N. Phytol.* 182, 565–588. doi: 10.1111/j.1469-8137.2009.02830.x

Portsmuth, A., and Niinemets, Ü (2007). Structural and physiological plasticity in response to light and nutrients in five temperate deciduous woody species of contrasting shade tolerance. *Funct. Ecol.* 21, 61–77. doi: 10.1111/j.1365-2435.2006.01208.x

Raza, M. A., Gul, H., Wang, J., Yasin, H. S., Qin, R., Bin Khalid, M. H., et al. (2021). Land productivity and water use efficiency of maize-soybean strip intercropping systems in semi-arid areas: A case study in Punjab Province, Pakistan. *J. Clean Prod.* 308:127282. doi: 10.1016/j.jclepro.2021.127282

Reinhardt, D., Frenz, M., Mandel, T., and Kuhlemeier, C. (2005). Microsurgical and laser ablation analysis of leaf positioning and dorsoventral patterning in tomato. *Development* 132, 15–26. doi: 10.1242/dev.01544

Rotili, D. H., Sadras, V. O., Abeledo, L. G., Ferreyra, J. M., Micheloud, J. R., Duarte, G., et al. (2021). Impacts of vegetative and reproductive plasticity associated with tillering in maize crops in low-yielding environments: A physiological framework. *Field Crops Res.* 265:108107. doi: 10.1016/j.fcr.2021.108107

Sánchez-Gómez, D., Valladares, F., and Zavala, M. A. (2006). Functional traits and plasticity in response to light in seedlings of four Iberian forest tree species. *Tree Physiol.* 26, 1425–1433. doi: 10.1093/treephys/26.11.1425

Sadras, V. O., Reynolds, M. P., de la Vega, A. J., Petrie, P. R., and Robinson, R. (2009). Phenotypic plasticity of yield and phenology in wheat, sunflower and grapevine. *Field Crops Res.* 110, 242–250. doi: 10.1016/j.fcr.2008.09.004

Smith, H. (2000). Phytochromes and light signal perception by plants—an emerging synthesis. *Nature* 407, 585–591. doi: 10.1038/35036500

Su, B. Y., Song, Y. X., Song, C., Cui, L., Yong, T. W., and Yang, W. Y. (2014). Growth and photosynthetic responses of soybean seedlings to maize shading in relay intercropping system in Southwest China. *Photosynthetica* 52, 332–340. doi: 10.1007/s11099-014-0036-7

Sultan, S. E. (2010). Plant developmental responses to the environment: Eco-devo insights. *Curr. Opin. Plant Biol.* 13, 96–101. doi: 10.1016/j.pbi.2009.09.021

Szumigalski, A. R., and Van Acker, R. C. (2006). Nitrogen yield and land use efficiency in annual sole crops and intercrops. *Agron. J.* 98, 1030–1040. doi: 10.2134/agronj2005.0277

Tan, T., Li, S., Fan, Y., Wang, Z., Ali Raza, M., Shafiq, I., et al. (2022). Far-red light: A regulator of plant morphology and photosynthetic capacity. *Crop J.* 10, 300–309. doi: 10.1016/j.cj.2021.06.007

Tanveer, M., Anjum, S. A., Hussain, S., Cerdà, A., and Ashraf, U. (2017). Relay cropping as a sustainable approach: Problems and opportunities for sustainable crop production. *Environ. Sci. Pollut. Res.* 24, 6973–6988. doi: 10.1007/s11356-017-8371-4

Terashima, I., Hanba, Y. T., Tazoe, Y., Vyas, P., and Yano, S. (2006). Irradiance and phenotype: Comparative eco-development of sun and shade leaves in relation to photosynthetic CO2 diffusion. *J. Exp. Bot.* 57, 343–354. doi: 10.1093/jxb/erj014

Terashima, I., Hanba, Y. T., Tholen, D., and Niinemets, U. (2011). Leaf functional anatomy in relation to photosynthesis. *Plant Physiol.* 155, 108–116. doi: 10.1104/pp.110.165472

Terashima, I., Miyazawa, S.-I., and Hanba, Y. T. (2001). Why are sun leaves thicker than shade leaves? — Consideration based on analyses of CO2 diffusion in the leaf. *J. Plant Res.* 114, 93–105. doi: 10.1007/PL00013972

Valladares, F., Chico, J., Aranda, I., Balaguer, L., Dizengremel, P., Manrique, E., et al. (2002). The greater seedling high-light tolerance of Quercus robur over Fagus sylvatica is linked to a greater physiological plasticity. *Trees* 16, 395–403. doi: 10.1007/s00468-002-0184-4

Valladares, F., Gianoli, E., and Gómez, J. M. (2007). Ecological limits to plant phenotypic plasticity. *N. Phytol.* 176, 749–763. doi: 10.1111/j.1469-8137.2007.02275.x

Valladares, F., Gianoli, E., and Saldaña, A. (2011). Climbing plants in a temperate rainforest understorey: Searching for high light or coping with deep shade? *Ann. Bot.* 108, 231–239. doi: 10.1093/aob/mcr132

Valladares, F., Martinez-Ferri, E., Balaguer, L., Perez-Corona, E., and Manrique, E. (2000a). Low leaf-level response to light and nutrients in Mediterranean evergreen oaks: A conservative resource-use strategy? *N. Phytol.* 148, 79–91.

Valladares, F., and Niinemets, Ü (2008). Shade tolerance, a key plant feature of complex nature and consequences. *Annu. Rev. Ecol. Evol. Syst.* 39, 237–257.

Valladares, F., Wright, S. J., Lasso, E., Kitajima, K., and Pearcy, R. W. (2000b). Plastic phenotypic response to light of 16 congeneric shrubs from a panamanian rainforest. *Ecology* 81, 1925–1936. doi: 10.1890/0012-9658(2000)081[1925:PPRTLO]2.0.CO;2

Vandenbussche, F., Pierik, R., Millenaar, F. F., Voesenek, L. A. C. J., and Van Der Straeten, D. (2005). Reaching out of the shade. *Curr. Opin. Plant Biol.* 8, 462–468. doi: 10.1016/j.pbi.2005.07.007

Vandermeer, J. H. (2011). *The Ecology of Agroecosystems*. Boston, MA: Jones and Bartlett Publishers.

Wang, R., Sun, Z., Bai, W., Wang, E., Wang, Q., Zhang, D., et al. (2021). Canopy heterogeneity with border-row proportion affects light interception and use efficiency in maize/peanut strip intercropping. *Field Crops Res.* 271:108239. doi: 10.1016/j.fcr.2021.108239

Warnasooriya, S. N., and Brutnell, T. P. (2014). Enhancing the productivity of grasses under high-density planting by engineering light responses: From model systems to feedstocks. *J. Exp. Bot.* 65, 2825–2834. doi: 10.1093/jxb/eru221

Willey, R. W. (1979). Intercropping: Its importance and research needs. I. Competition and yield advantages. *Field Crop Abstr.* 32, 1–10. doi: 10.2307/1941795

Willey, R. W. (1990). Resource use in intercropping systems. *Agric. Water Manag.* 17, 215–231. doi: 10.1016/0378-3774(90)90069-B

Wu, Y., Gong, W., Yang, F., Wang, X., Yong, T., Liu, J., et al. (2022). Dynamic of recovery growth of intercropped soybean after maize harvest in maize–soybean relay strip intercropping system. *Food Energ. Secur.* 11:e350. doi: 10.1002/fes3.350

Wu, Y., Gong, W., and Yang, W. (2017a). Shade inhibits leaf size by controlling cell proliferation and enlargement in soybean. *Sci. Rep.* 7:9259. doi: 10.1038/s41598-017-10026-5

Wu, Y., He, D., Wang, E., Liu, X., Huth, N. I., Zhao, Z., et al. (2021). Modelling soybean and maize growth and grain yield in strip intercropping systems with different row configurations. *Field Crops Res.* 265:108122. doi: 10.1016/j.fcr.2021.108122

Wu, Y., Yang, F., Gong, W., Ahmed, S., Fan, Y., Wu, X., et al. (2017b). Shade adaptive response and yield analysis of different soybean genotypes in relay intercropping systems. *J. Integr. Agricult.* 16, 1331–1340. doi: 10.1016/S2095-3119(16)61525-3

Yan, Y., Gong, W., Yang, W., Wan, Y., Chen, X., Chen, Z., et al. (2010). Seed treatment with uniconazole powder improves soybean seedling growth under shading by corn in relay strip intercropping system. *Plant Prod. Sci.* 13, 367–374. doi: 10.1626/pps.13.367

Yang, F., Feng, L., Liu, Q., Wu, X., Fan, Y., Raza, M. A., et al. (2018). Effect of interactions between light intensity and red-to-far-red ratio on the photosynthesis of soybean leaves under shade condition. *Environ. Exp. Bot.* 150, 79–87. doi: 10.1016/j.envexpbot.2018.03.008

Yang, F., Huang, S., Gao, R., Liu, W., Yong, T., Wang, X., et al. (2014). Growth of soybean seedlings in relay strip intercropping systems in relation to light quantity and red:far-red ratio. *Field Crops Res.* 155, 245–253. doi: 10.1016/j.fcr.2013.08.011

Yu, Y., Stomph, T.-J., Makowski, D., and van der Werf, W. (2015). Temporal niche differentiation increases the land equivalent ratio of annual intercrops: A meta-analysis. *Field Crops Res.* 184, 133–144. doi: 10.1016/j.fcr.2015.09.010

Zhang, L., van der Werf, W., Bastiaans, L., Zhang, S., Li, B., and Spiertz, J. H. J. (2008). Light interception and utilization in relay intercrops of wheat and cotton. *Field Crops Res.* 107, 29–42. doi: 10.1016/j.fcr.2007.12.014

Zhang, R., Shan, F., Wang, C., Yan, C., Dong, S., Xu, Y., et al. (2020). Internode elongation pattern, internode diameter and hormone changes in soybean (Glycine max) under different shading conditions. *Crop Pasture Sci.* 71, 679–688. doi: 10.1071/CP20071

Zhu, J., van der Werf, W., Anten, N. P. R., Vos, J., and Evers, J. B. (2015). The contribution of phenotypic plasticity to complementary light capture in plant mixtures. *N. Phytol.* 207, 1213–1222. doi: 10.1111/nph.13416

Zhu, J., van der Werf, W., Vos, J., Anten, N. P. R., van der Putten, P. E. L., and Evers, J. B. (2016). High productivity of wheat intercropped with maize is associated with plant architectural responses. *Ann. Appl. Biol.* 168, 357–372. doi: 10.1111/aab.12268

frontiers | Frontiers in Plant Science

TYPE Original Research
PUBLISHED 20 October 2022
DOI 10.3389/fpls.2022.1004173

OPEN ACCESS

EDITED BY
Ashwani Kumar,
Dr. Harisingh Gour Central University, India

REVIEWED BY
Mohammad Saidur Rhaman,
Bangladesh Agricultural University, Bangladesh
Mieke Rochimi Setiawati,
Universitas Padjadjaran, Indonesia

*CORRESPONDENCE
Amany H. A. Abeed
dramany2015@aun.edu.eg
Rasha E. Mahdy
rasha.mahdy@aun.edu.eg
Arafat Abdel Hamed Abdel Latef
moawad76@gmail.com

†These authors have contributed equally to this work and share senior authorship

SPECIALTY SECTION
This article was submitted to Plant Abiotic Stress, a section of the journal Frontiers in Plant Science

RECEIVED 27 July 2022
ACCEPTED 23 September 2022
PUBLISHED 20 October 2022

CITATION
Abeed AHA, Mahdy RE, Alshehri D, Hammami I, Eissa MA, Abdel Latef AAH and Mahmoud GA (2022) Induction of resilience strategies against biochemical deteriorations prompted by severe cadmium stress in sunflower plant when *Trichoderma* and bacterial inoculation were used as biofertilizers. *Front. Plant Sci.* 13:1004173. doi: 10.3389/fpls.2022.1004173

Induction of resilience strategies against biochemical deteriorations prompted by severe cadmium stress in sunflower plant when *Trichoderma* and bacterial inoculation were used as biofertilizers

Amany H. A. Abeed[1*†], Rasha E. Mahdy[2*], Dikhnah Alshehri[3], Inès Hammami[4], Mamdouh A. Eissa[5], Arafat Abdel Hamed Abdel Latef[6*] and Ghada Abd-Elmonsef Mahmoud[1†]

[1]Botany and Microbiology Department, Faculty of Science, Assiut University, Assiut, Egypt, [2]Agronomy Department, Faculty of Agriculture, Assiut University, Assiut, Egypt, [3]Department of Biology, Faculty of Science, Tabuk University, Tabuk, Saudi Arabia, [4]Department of Biology, College of Science, Imam Abdulrahman Bin Faisal University, Dammam, Saudi Arabia, [5]Department of Soils and Water, Faculty of Agriculture, Assiut University, Assiut, Egypt, [6]Department of Botany and Microbiology, Faculty of Science, South Valley University, Qena, Egypt

Background: Cadmium (Cd) is a highly toxic heavy metal. Its emission is suspected to be further increased due to the dramatic application of ash to agricultural soils and newly reclaimed ones. Thereby, Cd stress encountered by plants will exacerbate. Acute and chronic exposure to Cd can upset plant growth and development and ultimately causes plant death. Microorganisms as agriculturally important biofertilizers have constantly been arising as eco-friendly practices owing to their ability to built-in durability and adaptability mechanisms of plants. However, applying microbes as a biofertilizer agent necessitates the elucidation of the different mechanisms of microbe protection and stabilization of plants against toxic elements in the soil. A greenhouse experiment was performed using *Trichoderma harzianum* and plant growth-promoting (PGP) bacteria (*Azotobacter chroococcum* and *Bacillus subtilis*) individually and integrally to differentiate their potentiality in underpinning various resilience mechanisms versus various Cd levels (0, 50, 100, and 150 mg/kg of soil). Microorganisms were analyzed for Cd tolerance and biosorption capacity, indoleacetic acid production, and phosphate and potassium solubilization *in vitro*. Plant growth parameters, water relations, physiological and biochemical analysis, stress markers and membrane damage traits, and nutritional composition were estimated.

10.3389/fpls.2022.1004173

Results: Unequivocal inversion from a state of downregulation to upregulation was distinct under microbial inoculations. Inoculating soil with *T. harzianum* and PGPB markedly enhanced the plant parameters under Cd stress (150 mg/kg) compared with control plants by 4.9% and 13.9%, 5.6% and 11.1%, 55.6% and 5.7%, and 9.1% and 4.6% for plant fresh weight, dry weight, net assimilation rate, and transpiration rate, respectively; by 2.3% and 34.9%, 26.3% and 69.0%, 26.3% and 232.4%, 135.3% and 446.2%, 500% and 95.6%, and 60% and 300% for some metabolites such as starch, amino acids, phenolics, flavonoids, anthocyanin, and proline, respectively; by 134.0% and 604.6% for antioxidants including reduced glutathione; and by 64.8% and 91.2%, 21.9% and 72.7%, and 76.7% and 166.7% for enzymes activity including ascorbate peroxidase, glutathione peroxidase, and phenylalanine ammonia-lyase, respectively. Whereas a hampering effect mediated by PGP bacterial inoculation was registered on levels of superoxide anion, hydroxyl radical, electrolyte leakage, and polyphenol oxidase activity, with a decrease of 0.53%, 14.12%, 2.70%, and 5.70%, respectively, under a highest Cd level (150 mg/kg) compared with control plants. The available soil and plant Cd concentrations were decreased by 11.5% and 47.5%, and 3.8% and 45.0% with *T. harzianum* and PGP bacterial inoculation, respectively, compared with non-inoculated Cd-stressed plants. Whereas, non-significant alternation in antioxidant capacity of sunflower mediated by *T. harzianum* action even with elevated soil Cd concentrations indicates stable oxidative status. The uptake of nutrients, *viz*., K, Ca, Mg, Fe, nitrate, and phosphorus, was interestingly increased (34.0, 4.4, 3.3, 9.2, 30.0, and 1.0 mg/g dry weight, respectively) owing to the synergic inoculation in the presence of 150 mg of Cd/kg.

Conclusions: However, strategies of microbe-induced resilience are largely exclusive and divergent. Biofertilizing potential of *T. harzianum* showed that, owing to its Cd biosorption capability, a resilience strategy was induced *via* reducing Cd bioavailability to be in the range that turned its effect from toxicity to essentiality posing well-known low-dose stimulation phenomena (hormetic effect), whereas using *Azotobacter chroococcum* and *Bacillus subtilis*, owing to their PGP traits, manifested a resilience strategy by neutralizing the potential side effects of Cd toxicity. The synergistic use of fungi and bacteria proved the highest efficiency in imparting sunflower adaptability under Cd stress.

KEYWORDS

adaptability, biofertilizers, growth-promoting bacteria, *Trichoderma harzianum*, *Bacillus subtilis*

Abbreviations: PGP, plant growth promoting; HMT, heavy metal tolerant; IAA, indole-3-acetic acid; Fwt, fresh weight; Dwt, dry weight; PH, plant height; LSA, specific leaf area; NAR, net assimilation rate; Sc, stomatal conductance; Tr, transpiration rate; WUE, water use efficiency; RWC, relative water content; TN, total nitrogen content; NR, nitrate reductase; MDA, malondialdehyde; LOX, lipoxygenase; EL, electrolyte leakage; ROS, reactive oxygen species; H_2O_2, hydrogen peroxide; $^{\bullet}OH$, hydroxyl radical; O_2^-, superoxide anion; PCs, phytochelatin; GSH, reduced glutathione; ASA, ascorbic acid; CAT, catalase; SOD, superoxide dismutase; POD, guaiacol peroxidase; APX, ascorbate peroxidase; GPX, glutathione peroxide; GST, glutathione-*S*-transferase; PAL, phenylalanine ammonia-lyase; PPO, polyphenol oxidase.

Introduction

The exceptional change in the environmental conditions due to population explosion, amplified air and soil pollution, ecosystem heavy metal (HM) contamination, depletion of soil quality, and global climate change has considerably impacted the capability of plants to adapt to changing climactic conditions (Dimkpa et al., 2009). These changes make agricultural production systems liable to altering environmental conditions. Such suboptimal environmental conditions can prompt damaging the physiological changes which occur within the plants, called stresses (Raza et al., 2020). Abiotic stresses such as high temperature, metal toxicity, drought, salinity, and nutrient imbalance are those environmental stresses that restrict crop growth and production below the threshold level.

The sunflower (*Helianthus annuus* L.) ranks the fourth most important oilseed crop, following soybean, palm seeds, and canola seeds as a significant source of oil used in various food products worldwide (USDA, FAO, 2008). It is a protein source of great interest for human nutrition, especially due to its sensory, nutritional, and functional properties (Zorzi et al., 2020). In Egypt, the shortage of edible oil represents a huge problem due to the rise in human growth rate with limited oilseed cultivated area at the same time. Therefore, the government is earnestly seeking to increase oilseed crop production, which could be achieved in two ways: horizontal expansion through the cultivation of large newly reclaimed areas or vertical expansion by increasing plant growth rates and production by plant regulators and antioxidants (Hayat et al., 2020). Newly reclaimed soil is likely to explore numerous environmental stress situations, such as nutrient deprivation, low water availability, temperature fluctuations, saline water and soil, high irradiances, and HM contamination.

Available information on the contamination of urban agricultural areas and newly reclaimed ones in Egypt by metals is now widespread (Naggar et al., 2014). According to Lu et al. (2019) and Singh and Steinnes (2020), the maximum allowable concentration for Cd is 0.3 mg/kg, and the toxic soil for plants contains 3–8 mg/kg. However, Naggar et al. (2014) have shown that many agricultural soils in Egypt exceeded the maximum Cd allowable concentrations and reached about 30 mg/kg of soil. This was suspected to be further increased due to the dramatic application of ash to agricultural soils and newly reclaimed ones. Using these agricultural soil types for cultivation will exacerbate the Cd stress encountered by plants; thus, the yield of crops decreases and the quality of field products gets degraded (Abdel Latef, 2013; Hakla et al., 2021; Yaashikaa et al., 2022). Acute and chronic exposure to Cd can induce more damage including severe disturbance and downregulation in the physiological processes of plants, such as increased reactive oxygen and nitrogen species in the cells, which, in turn, act as deleterious molecules mediating an oxidative/nitrosative burst that could cause growth inhibition, accelerated senescence, and mostly cause plant death (Noor et al., 2022). To survive severe Cd stress, the built-in durability and adaptability mechanisms of plants to withstand metal stress conditions are used to improve plant resistance against metal stress, furthermore enhancing the natural role of microorganisms as biofertilizers that will be beneficial in improving soil health and plant productivity (Ortiz and Sansinenea, 2022).

Toward a sustainable agricultural vision and fulfilling HM stress tolerance and better nutritional value, agricultural practitioners are looking increasingly for environmentally friendly inputs such as biofertilizers to manage their crops and cropping systems. Biofertilizers are defined as substances containing living organisms that, when applied to seeds, plant surfaces, or soil, colonize the rhizosphere or the interior of the plant and promote growth by increasing the supply or availability of primary nutrients to the host (Dimkpa et al., 2009). Biofertilizer also refers to the different inoculations of agriculturally beneficial microorganisms (bacteria/fungi) with certain desirable physiological and behavioral characteristics that are utilized for crop nutrition management programs (Zainab et al., 2021). Rhizosphere microorganisms have been used to underpin resilience strategies against abiotic stress in many plants, such as *Solanum nigrum*, *Brassica napus*, tomato, and maize (Dell'Amico et al., 2008; Sheng et al., 2008; Chen et al., 2010; Dourado et al., 2013) mainly achieved by increasing the bioavailability of phosphorus (P) and nitrogen (N) and other soil trace elements essential to plant growth. Moreover, the presence of the symbiotic association also helps to increase plant water uptake; encompasses the adverse effects of phytopathogens; modifies plant growth hormone production; and diminishes the impact of abiotic stresses like drought, salinity, and HM toxicity (Ortiz and Sansinenea, 2022). Their significant role in HM stress management is substantially by eliminating the negative effects of metal on yield quantity and quality (Basu et al., 2017; Ding et al., 2021). They can also accumulate, transform, or detoxify HM.

Consequently, the use of microorganisms that primarily colonizes the rhizosphere/endorhizosphere of plants and hence favors growth directly or indirectly is gaining priority in stress management (Ding et al., 2021). Adaptation and acclimatization of plants for survival under stress conditions due to microorganism inoculations induced physical and chemical changes, wherein the term Induced Systemic Tolerance (IST) has been coined (Basu et al., 2017). This matter catapults them as natural biofertilizers and bioprotection agents (Ortiz and Sansinenea, 2022). However, the underlying strategies of microbe-induced resilience are not well understood, and the modes of action largely remain elusive and microbe species-dependent.

Plant growth-promoting bacteria (PGPB) represent a group of significant microorganisms characterized by plant growth promotion by secreting important compounds such as

phytohormones (Gupta et al., 2022) or by increasing nutrient availability of plants (mineralization) (Etesami and Adl, 2020). There is great potential for use of PGPB as biofertilizer agents for a wide variety of crop plants in a wide range of climatic and edaphic conditions. Currently, an array of bacterial inoculates are commercially available for use as biofertilizers or bioprotection against abiotic/biotic stresses (Dasgupta et al., 2021; Kumar et al., 2022). Substantial progress has been exerted in exploring the molecular, physiological, and morphological mechanisms underlying bacterially mediated tolerance to abiotic stresses (Dimkpa et al., 2009; Khan et al., 2021). *Azotobacter and Bacillus* species were common plant growth-promoting (PGP) bacteria (Sheng and Xia, 2006; Abdel-Hakeem et al., 2019). A single PGP bacterium often has multiple uses and modes of action (Rojas-Solis et al., 2020). They impart plant stress tolerance by facilitating the needing resources like fixing N, P, calcium (Ca), potassium (K), and other essential mineral solubilizations and altering plant hormone uptake. Their presence can contribute to the reduction in metal stress on plants when applied to them as single bioinoculants (Wani and Khan, 2010).

The free-living N-fixing bacterium *Azotobacter* secretes biologically active compounds that promote plant growth, such as pantothenic acid, nicotinic acid, B vitamins, biotin, and gibberellin (Patil et al., 2020). *Azotobacter* could promote the growth of plant roots, accelerate the intake of minerals, and compete with other pathogenic microbes (Aasfar et al., 2021). In addition, these are effective phosphate- and K-solubilizing bacteria (Diep and Hieu, 2013); according to Hafez et al. (2016), *Azotobacter* solubilized up to 43% of Egyptian phosphate rock. Singh et al. (2010) stated that *Azotobacter* species can enhance K uptake by plants. Another PGP characteristic of *Azotobacter* is auxin production, which helps the plants for longer roots and increases root hair number and lateral roots, cell division, elongation, and fruit development (Grossmann, 2010; Phillips et al., 2011). In addition, *Bacillus subtilis* has the capacity to solubilize soil P, improve N fixation, and create siderophores that support its growth while inhibiting that of pathogens (Kuan et al., 2016). By promoting the expression of stress-response genes, phytohormones, and stress-related metabolites in their plant hosts, *Bacillus subtilis* improves the tolerance of those hosts to stress (Hashem et al., 2019). According to Kang et al. (2015), *Bacillus* species secrete phosphatases and organic acids that help turn inorganic phosphate into free phosphate by acidifying the environment. *Bacillus* spp. produce chemicals that encourage plant growth, such as indole-3-acetic acid (IAA), gibberellins, cytokinins, and spermidines, and these compounds enhance root and shoot cell division and elongation (Radhakrishnan and Lee, 2016). *Bacillus* species can be introduced to soil that has been contaminated with HMs to lessen the metals' detrimental effects on plant development and help plants grow by boosting water absorption and lowering electrolyte leaks to lessen Cd stress (Ahmad et al., 2014).

Trichoderma has been proven as a potential biofertilization agent to enhance rice plant growth, physiological traits, nutrient uptake, and yield under controlled greenhouse conditions (Doni et al., 2018) when used in the form of a suspension of fungal cells applied to rice seeds or seedlings. They are presently marketed as biopesticides, biofertilizers, growth and yield enhancers, nutrient solubilizers, and organic matter decomposers as well as phytohormones producers, such as IAA, cytokinin, zeatin, and gibberellin. *Trichoderma* species tolerate or detoxify various HMs, especially those microbes from metal-contaminated sites (Zafar et al., 2007). Moreover, it has a high aggregation capability of numerous metals simultaneously, giving it the advantage in use during the bioremediation of soil contaminated with metals (Errasquin and Vazquez, 2003).

Researchers have determined that *Trichoderma* species are important fungi in the reduction of Cd ions. Bazrafshan et al. (2016) and Nongmaithem et al. (2016) confirmed that *Trichoderma* fungus biosorption of Cd (II) ions was spontaneous and endothermic in nature, and *Trichoderma* isolates IBT-I and UBT-18 can tolerant up to 200 ppm. *Trichoderma asperellum* demonstrated a 76.17% effectiveness in removing Cd as recorded by Mohsenzade and Shahrokhi (2014). Cd translocation, tolerance, and absorption in barley have all been linked *to T. harzianum*. It lessens the detrimental effects of Cd pollution and decreases Cd uptake in plants that have received an inoculation of *T. harzianum* (Ghasemkheili et al., 2022). Herliana et al. (2018) found that the highest dry weight of spinach under Cd contamination was recorded in *Trichoderma*-treated plants. According to Marchel et al. (2018), *Trichoderma* inoculation enhanced plant biomass. In addition, Li et al. (2019) stated that plant inoculation with *Trichoderma* improved loofah roots dry weight to 67% comparing with control plants.

Trichoderma harzianum represents the most common species of *Trichoderma* that is genetically special, establishes many rhizosphere soils, and could survive in stress conditions for several months (Kubicek et al., 2003). It represents a strong antagonist genus with high soil colonization on the target site and suppresses the other population of pathogenic microorganisms as a biocontrol agent (Hermosa et al., 2012).

This study applied the aspects and mechanisms of HM action of HM-tolerant (HMT) and PGP microbes in ensuring sunflower plant survival and growth in highly Cd-contaminated soils. Using these microbes and studying their interaction with plants in reducing accumulated Cd in plants grown in heavily HM-loaded soil can be the approach for a healthy future. We ascertain the effectiveness of PGPB (*Azotobacter chroococcum* and *Bacillus subtilis*), HMT fungus *Trichoderma harzianum*, and consortium (Mix) treatment on sunflower resurrection, growth, and mitigation of severe Cd stress in agricultural soil. In addition, we assessed the physiological and biochemical sunflower plant responses to the interaction between severe toxic Cd levels and microbe inoculation on accumulated Cd

and the performances of a sensitive sunflower cultivar. Thus, knowledge generated from studies on resilience strategies against Cd stress will be very useful in decoding signaling cascades induced by microbial fertilizing agents, resulting in enhanced tolerance and combat versus HM stress.

Materials and methods

Plant growth-promoting bacteria

Two bacterial microbes were used in this study. *Azotobacter chroococcum* 14346 and *Bacillus subtilis* 642 were kindly supplemented from Agriculture Research Center, Egypt. The cultures were maintained on nutrient agar (NA) medium (Atlas, 1993) aerobically, stored at 4°C ± 1°C, and subcultured every 4 weeks. The microbes were tested for antagonistic effect on NA plates before use (no antagonistic effect was detected). Prior to the experiments, the bacteria were grown on NA medium at 28° C ± 1°C for 24 h with rotary shaking (200 rpm) until OD660. After that, the bacterial mass was harvested, centrifuged at 6,000×g for 15 min, washed, and suspended in new sterilized water saline with 1×10^6 colony-forming units (CFU)/ml.

In vitro tests for plant growth-promoting bacteria

IAA production was estimated in a mineral broth medium fortified with L-tryptophan (0.2 g/L; Mahmoud and Mostafa, 2017). The sterilized medium was inoculated with bacterial inoculum and incubated for 120 h at 28°C ± 1°C in a rotary shaking incubator at 200 rpm. After that, bacterial cultures were harvested and centrifuged at 6,000×g for 15 min; 1.5 ml of bacterial culture supernatant was mixed with 1 ml of Salkowski reagent pink to red color, which will appear after 30 min according to the IAA concentration (Chrastil, 1976). The developed color was measured using a T60UV split-beam spectrophotometer with wavelength (190–1,100 nm) at 535 nm against free blank and calculated in micrograms per milliliter through the standard curve of pure IAA (1–100 μg/ml). For testing the bacterial ability for phosphate solubilization, Pikovskaya's agar medium in sterilized petri dishes was inoculated with the microbes and incubated for 120 h at 28°C ± 1°C (Pande et al., 2017). Phosphate solubilization was calculated as the formation of the clear zone (mm) around the bacterial colony, and this diameter was measured every 12 h. For testing the bacterial ability for K solubilization, Aleksandrov's agar medium in sterilized petri dishes was inoculated with the microbes and incubated for 120 h at 28°C ± 1°C. K solubilization was calculated as the formation of the clear zone (millimeters) around the bacterial colony, and this diameter was measured every 12 h. (Khanghahi et al., 2018). *Azotobacter chroococcum* N-fixing ability was tested on a N-free medium. The microbe was grown on N-free medium plates for 1 week at 28°C ± 1°C incubation temperature; the growth indicated N-fixation capacity (Doroshenko et al., 2007).

In vitro tests for cadmium-resistant fungi

Trichoderma harzianum was isolated from HM-contaminated soil on Czapek's dextrose agar medium supplemented with 50 ppm Cd chloride, identified according to its macroscopic and microscopic properties, preserved aerobically on Czapek's dextrose agar medium in low temperature at 4°C ± 1°C until use, and subcultured every 3 weeks. For screening the ability of *T. harzianum* to grow on different concentrations of Cd, the agar dilution plate method was used (Ibrahim et al., 2020). Different concentrations of Cd chloride including 0, 50, 100, 150, 200, 250, and 300 ppm were mixed with Czapek's dextrose agar medium in sterilized petri dishes and left to solidify. *Trichoderma harzianum* 6-mm disc of 3 days growing fungus inoculated on the medium center of the plate and incubated at the moderate temperature at 28°C ± 1°C for a week, and the growth area of the fungus was detected by measuring the colony diameter in millimeters with three replicates. For biosorption activity, *T. harzianum* was grown on Czapek's dextrose agar medium for 3 days at moderate temperature (28°C ± 1°C); the spores were harvested from the plate surface, mixed with sterilized 0.1% Triton X-100, and diluted to 3×10^6 CFU/ml. Czapek's dextrose broth medium supplemented with the same Cd concentrations was inoculated with 1% of the fungal spores and incubated at 28°C ± 1°C for 1 week after the fungal broth was used to measure the Cd concentration *via* the Atomic Absorption Spectrophotometer (Buck model 210 VGP, USA) (Mahmoud et al., 2020).

Experimental design

A greenhouse experiment was performed through a completely randomized design (CRD) with a 6 × 4 factorial plan. Six sunflower plant treatments [with or without PGPB, *T. harzianum*, and consortium (Mix) inoculation] and four Cd soil concentrations with a range of 0–150 mg/kg of soil were used. Four replicates were assessed through each treatment. Each replicate included four plants. Plants exposed to Cd concentrations (50, 100, and 150 mg of Cd/kg of soil) without microbe inoculation underwent severe toxic Cd symptoms ultimately death occurring within 3 days after Cd treatments. Thus, the experiment was completed with plants introduced to interaction between microbe inoculation and the various Cd levels (0, 50, 100, and 150 mg of Cd/kg of soil) only.

Plant and the microbial treatments

Sunflower (*Helianthus annuus* L) seeds were supplied from the Agronomy Department, Faculty of Agriculture, Assiut University, Egypt. The seeds were sterilized as follows: they were put in 70% ethanol for 2 min and then in 1% NaClO for 10 min, then washed three times with sterilized distilled water, and transferred for germination on sterilized wet filter paper at low temperature (4°C) for 48 h for the synchronized germination; 1-week-old seedlings were further transplanted for the investigation. Microbial inoculums were prepared as s follows: 2-day-old bacterial cells were cultivated in nutrient broth medium, collected by centrifugation at 6,000×g for 15 min, and washed and suspended in new sterilized water saline with 2×10^8 CFU/ml for use. Four-day-old *T. harzianum* cultivated in Czapek's agar medium was scratched and suspended in sterilized water saline with 3×10^6 CFU/ml inoculum for use. PGPB (*Azotobacter chroococcum* and *Bacillus subtilis*) treatment, *T. harzianum* treatment, and the consortium (Mix) were used for enhancing the growth rate of the sunflower plant under different concentrations of Cd stress (0, 50, 100, and 150 mg of Cd/kg of soil).

Soil accommodation

Mixed soil samples from 0- to 25-cm depth of sandy loam type were prepared from the surface soil horizon of Assiut University farm; then, the physicochemical properties of the soil were assessed, as shown in Table 1. The collected soil was dried in the open air, sieved through 2-mm sieve pores for removing inconstant particles, and autoclaved three times at 121°C for 20 min for 3 consecutive days to remove the native microorganisms. Four Cd concentrations (0, 50, 100, and 150 mg/kg of soil) as Cd dichloride ($CdCl_2$) were mixed into the soil as a water solution, and samples were incubated at 20°C for 30 days for Cd distribution and stabilization through the soil layers.

Planting and growth conditions

Pots were then transferred into a greenhouse at 28°C ± 2°C/18°C ± 2°C day/night cycle, 60%–70% relative humidity, and a photoperiod of 14 h. The experimental pots were watered using deionized water once every 3 days to near-field capacity. After 35 days of transplanting, the sunflower plants (42 days old) were harvested by cutting the shoots at the soil surface, and the roots were carefully separated from the soil. The shoots and roots were rinsed with distilled water and wiped with tissue paper.

Plant growth parameters

Shoot and root length, fresh shoot, and root weight were estimated. For dry shoot and root values, harvested plants were oven-dried at 60°C for 2 days. The leaf area and the net assimilation values were estimated using the adopted methods (Dawood et al., 2019).

Water relations

Relative water content (RWC) was calculated following the equation adopted by Silveira et al. (2009): RWC = [(FW − DW)/(TW − DW)] × 100, where FW is the fresh weight, TW is the turgid weight measured after 24 h of saturation on deionized water at 4°C in the dark, and DW is the dry weight. The transpiration rate was measured as specified by Bozcuk (1975). Leaf stomatal conductance was estimated by adopting the equation recommended by Dawood and Abeed (2020), in which stomatal conductance is expressed as the reverse of the stomatal resistance. The stomatal resistance was measured from the equation displayed by Holmgren et al. (1965) and as modified by Slatyer and Markus (1968). The water use efficiency (WUE) according to Larcher (2003) was determined as follows: WUE (g/kg) = biomass (g/plant)/water use rate (kg/plant).

Physiological and biochemical analysis

Chlorophyll a, chlorophyll b, and carotenoids were estimated at 663, 644, and 452 nm following the method by Lichtenthaler (1987). Carbon metabolism is evaluated through the detection of glucose and fructose (mg/g DW) as described by Halhoul and Kleinberg (1972), sucrose (mg/g DW) by Van Handel (1968), and starch quantification (mg/g DW) by Fales (1951) and Schlegel (1956). N metabolism was detected by measuring total N, nitrate reductase (NR) activity, amino acids, and proteins following Moore and Stein (1948); Lang (1958); Downs et al. (1993), and Lowry et al. (1951), respectively. Other metabolic molecules were measured as phenolics, flavonoids, anthocyanin, and proline following the methods by Krizek et al. (1993); Kofalvi and Nassuth (1995); Khyade and Vaikos (2009), and Bates et al. (1973), respectively.

Stress markers and membrane damage traits

Oxidative stress was monitored by determining stress markers such as superoxide anion (μg/g FW, O_2^-), hydroxyl

radical (μmol/g FW, $^{\bullet}OH$), and hydrogen peroxide (μmol/g FW, H_2O_2) level in sunflowers leaves, which was quantified as reported by Mukherjee and Choudhuri (1983). Lipid peroxidation was assessed as malondialdehyde (MDA) (μmol/g FW) using the method by Madhava Rao and Sresty (2000). Lipoxygenase (LOX) activity (LOX/EC.1.13.11.1) was assessed at 234 nm according to the method by Minguez-Mosquera et al. (1993). Electrolyte leakage (EL) was estimated by conduct meter (YSI model 35 Yellow Springs, OH, USA) as described by Silveira et al. (2009).

Non-enzymatic and enzymatic antioxidant capacities

Non-enzymatic antioxidants such as ascorbic acid (ASA) and reduced glutathione (GSH) were assessed following the methods applied by Jagota and Dani (1982) and Ellman (1959), respectively. Phytochelatins (PCs) are determined by the protocols by Ellman (1959) and Nahar et al. (2016). The enzymatic potential of leaves was detected by screening the activities of superoxide dismutase (SOD/EC.1.15.1.1), catalase (CAT/EC 1.11.1.6), ascorbate peroxidase (APX/EC1.11.1.11), glutathione peroxidase (GPX/EC.1.11.1.9), polyphenol oxidase (PPO/EC 1.10.3.1), guaiacol peroxidase (POD/EC 1.11.1.7), phenylalanine ammonia-lyase (PAL/EC 4.3.1.5), and glutathione-S-transferase (GST/EC 2.5.1.18) using the adopted methods by Misra and Fridovich (1972); Nakano and Asada (1981); Kumar and Khan (1983); Aebi (1984); Flohé and Günzler (1984); Tatiana et al. (1999); Sykłowska-Baranek et al. (2012), and Ghelfi et al. (2011), respectively.

Element composition of the plants

Sodium and K were determined by the flame emission technique (Carl-Zeiss DR LANGE M7D flame photometer) (Havre, 1961). The contents of Ca, Mg, Fe, and Cd were determined with atomic absorption (Shimadzu, model AA-630-02). Nitrate content was quantified by the protocol by Cataldo et al. (1975). P content was estimated spectrophotometrically following the methods by Fogg and Wilkinson (1958).

Statistical analysis

A CRD was utilized for the pot experiments. Obtained data were expressed as means ± SE. SPSS 10.0 software program was used for performing the statistical analysis. Comparisons between control and treatments were assessed by one-way ANOVA using the least significant difference (LSD) test. Difference from control was counted significant at the probability levels of 0.05 or very significant at the probability levels of 0.01.

Experimental results

Plant growth-promoting bacteria

Both bacterial strains (*Azotobacter chroococcum* and *Bacillus subtilis*) showed no antagonistic properties with plant growth promotion capabilities through the production of IAA, phosphate, and K solubilization (Figures 1, 2). IAA production starts after 12 h in low quantities for both bacteria and then increased. By increasing the bacterial growth time, IAA production increased in harmony until 96 h and then decreased for both bacteria, giving 78.8 ± 0.98 μg/ml for *A. chroococcum* and 84.27 ± 2.7 μg/ml for *B. subtilis*. However, the maximum CFU for them was 4.79 ± 0.1 × 10^7 CFU for *A. chroococcum* and 4.36 ± 0.03 ×10^7 CFU for *B. subtilis* after 96 and 84 h, respectively (Figures 1A, B). Both bacterial strains showed high phosphate-solubilizing activities after 24 h of growth and reached their highest values after 120 h with phosphate-solubilizing clear zone of 17.33 ± 0.46 mm for *A. chroococcum* and of 23.3 ± 1.24 mm for *B. subtilis* (Figure 2A). K solubilization also takes the same direction as phosphate solubilization, reaching its highest values after 120 h with K solubilizing clear zone of 13.7 ± 0.5 mm for *A. chroococcum* and of 20 ± 0.82 mm for *B. subtilis* (Figure 2B). *A. chroococcum* was confirmed as N-fixing bacteria through its growth on a specific N-free medium; both microbes showed no antagonistic properties between each other on NA.

Cadmium-resistant *Trichoderma*

Trichoderma harzianum showed the ability to grow on different Cd concentrations in the range of 0–300 ppm as high resistance (Figures 3A, B). The growth of *T. harzianum* on Czapek's agar plates with different Cd concentrations showed that the fungus is slightly affected after 50 ppm and highly affected after 200 ppm. At 50 ppm, the fungus showed complete growth, such as at 0 ppm (90 mm); at 100 ppm, the fungus was

TABLE 1 Physical and chemical characteristics of the used soil.

pH (1:1)	ECdS/m (1:1)	Soluble cations (ppm)				Soluble anions (meq/L)		Particle size distribution (%)		
		Ca^{++}	Mg^{++}	Na^{+}	K^{+}	$CO_3^{-} + HCO_3^{-}$	Cl^{-}			
7.1	2.25	574	344	186	47	1525	887	Sand 12.4%	Silt 30.9%	Clay 56.7%

slightly affected (89 ± 1.4 mm), and at 200 ppm, it had a growth of 80 ± 0.82 mm. The highest Cd concentration (300 ppm) decreased the growth to 67.3 ± 1.2 mm (Figure 3A). The biosorption pattern of *T. harzianum* is indicated in Figure 3B; at 50 ppm, the biosorption percentage was 90.32% ± 0.1%, at 100 ppm was 89.54% ± 0.44%, at 150 ppm was 81.35% ± 0.28%, and at 300 ppm was 32.17% ± 1.1%.

Plant growth and leaf biochemical characteristics derived from cadmium treatments and microbe–soil inoculations interactions

Influence of Cd and microbe–soil interaction on morphological and growth attributes of sunflower plant

All Cd concentrations exposure caused fatal damage to plants accompanied by toxic symptoms appearance, including yellowing, chlorosis, stem necrosis, stunting, and wilting. Chlorosis started to appear on leaves after 3 days of Cd exposure and progressed until the end of the treatment, resulting in plant death rather than growth or metabolic retardation, suggesting that plant detoxification processes are insufficient to cope with these lethal concentrations; thus, plants failed to survive the exposure duration. Therefore, the physiological data were obtained from survivor plants in the remaining 13 treatments. Soil microbe inoculations presented a successful approach to reverted plants from distressing to aliveness, thus performing comparably to unstressed plants even at elevated soil Cd levels (up to 150 mg/kg of soil). An initial characterization of the effect of inoculation with microbes was attempted by measuring growth parameters. The resultant plant death due to Cd exposure can effectively be held up by microbe inoculation. Data in Table 2 showed that the stimulatory effect on plant growth parameters in terms of plant fresh and dry weights (Fwt and Dwt), plant height (PH), and leaf-specific area (LSA) induced by PGPB was more pronounced in non–Cd-stressed plants. Cd stress reduces the beneficial effect of PGPB; however, values of growth parameters registered slight percentages of increase amounted as by 13.9% and 11.1% for plant fresh and dry weights compared with the levels determined for the non-inoculated plants grown on Cd-unpolluted soils. Soil inoculation with *T. harzianum* did not show a stimulatory impact on of non–Cd-stressed plants; however, all detected growth parameters in terms of Fwt, Dwt, PH, and LSA were significantly stimulated by the interaction between *T. harzianum* inoculation and Cd soil existence, particularly in the initial Cd concentration (50 mg/kg of soil). The elevated Cd concentration slightly reduced growth parameters levels compared with those of 50 mg/kg of soil contaminated plants; however, they were still in an acceptable range compared with the control and by percentages of increase amounted as by 4.9% and 5.6% for plant fresh and dry weights. The beneficial effect of soil microbe inoculation was maximized when microbes were in consortium; hence, the highest growth parameters were recorded in the absence or presence of Cd.

Influence of Cd and microbe–soil interaction on water relations attributes of sunflower plant

Alleviated Cd toxicity along with soil inoculations can be assessed by analyzing plant–water relation–related factors (Table 2). The exhibited trend among the various treatments regarding net assimilation rate (NAR) was increased in food factory units (LSAs). NAR was stimulated by soil inoculated with PGPB in non–Cd-stressed conditions, whereas soil inoculation with *T. harzianum* exhibited stimulatory impact when only Cd existed. Whatever elevated Cd levels were encountered by plants, NAR values were maintained near the levels determined for the non-inoculated plants grown on Cd-unpolluted soils by soil inoculation. The synergistic use of fungi and bacteria in a consortium proved the highest efficiency in enhancing NAR of sunflower plants. Visual toxic appearance including severe wilting resulted in plant death indicated lethal doses encountered by non-inoculated plants. Inoculated soil with PGPB, *T. harzianum*, or in consortium markedly re-stabilized cell water status in terms of RWC (RWC%) that was accompanied by normal transpiration rate and stomatal conductance; thus, efficient water economy in terms of WUE even under elevated Cd levels in the soil indicated effectiveness action of the used microbes under severe Cd stress condition.

Influence of Cd and microbe–soil interaction on pigment content and primary and secondary metabolites of sunflower plant

Cd-induced inhibitory effect on photosynthetic machinery *via* depletion of chlorophyll synthesis advocated by apparent chlorosis was significantly ameliorated by the microbe's inoculation. Microbes' inoculations reverted chlorophyll contents to those measured for the non-inoculated control even under elevated Cd concentrations (Table 3). PGPB-inoculated plants exhibited significant photosynthetic pigment increase under non-Cd stress conditions, whereas the stimulatory effect of *T. harzianum*–inoculated soil was attained by the interaction between *T. harzianum* inoculation and Cd soil existence. Inoculated soil with microbes in consortium posed the highest increase in the level of the photosynthetic pigment in both Cd absence and existence. Carbon metabolism analyzed by quantification of glucose, fructose, and starch was significantly prompted by soil inoculation with PGPB and microbe consortium by increasing the foliar content of glucose, fructose, and starch in both Cd-stressed or non-stressed plants compared with non-inoculated control plants (Table 3). Whereas *T. harzianum*–inoculated soil was able to maintain the levels comparable to those determined for non-inoculated

10.3389/fpls.2022.1004173

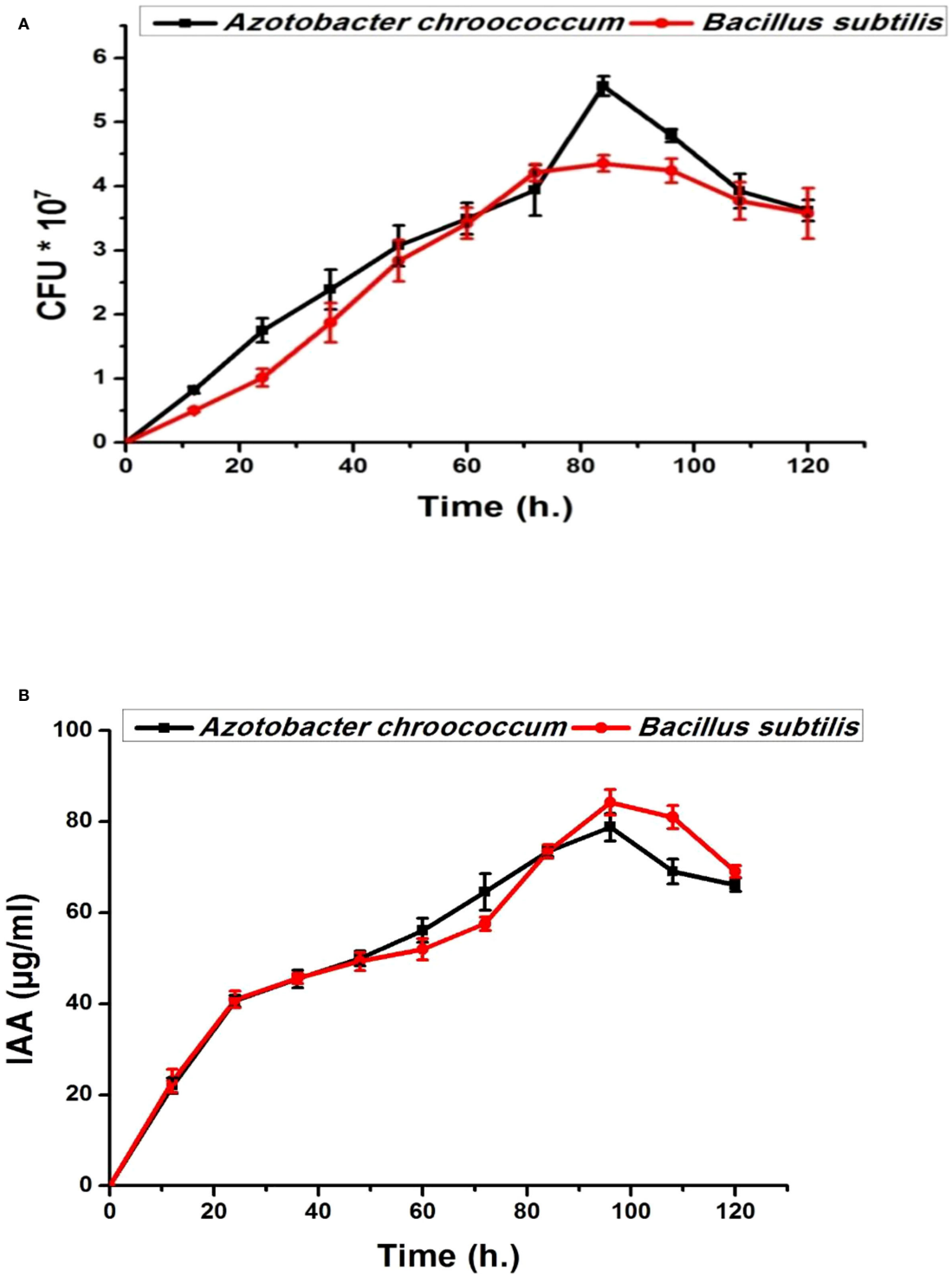

FIGURE 1
Bacterial growth curve (CFU × 10^7) **(A)** and indoleacetic acid (IAA) time course production (µg/ml) **(B)** of plant growth-promoting *Azotobacter chroococcum* and *Bacillus subtilis* on nutrient broth medium.

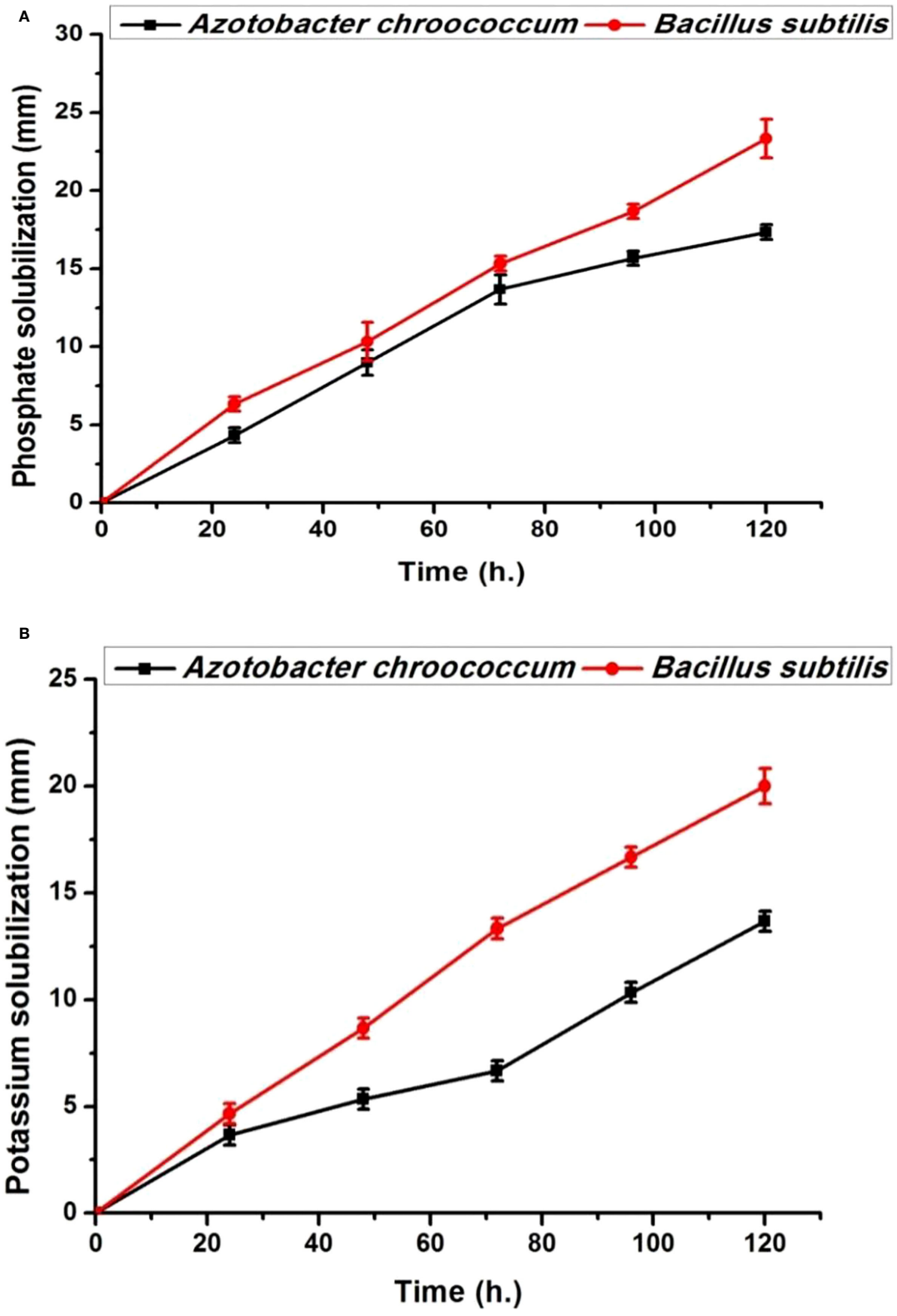

FIGURE 2
Phosphate solubilization time course as growth diameter (mm) on Pikovskaya's agar **(A)** and K solubilization on Aleksandrov's agar **(B)** mediums by the plant growth-promoting (PGP bacteria) *Azotobacter chroococcum* and *Bacillus subtilis*.

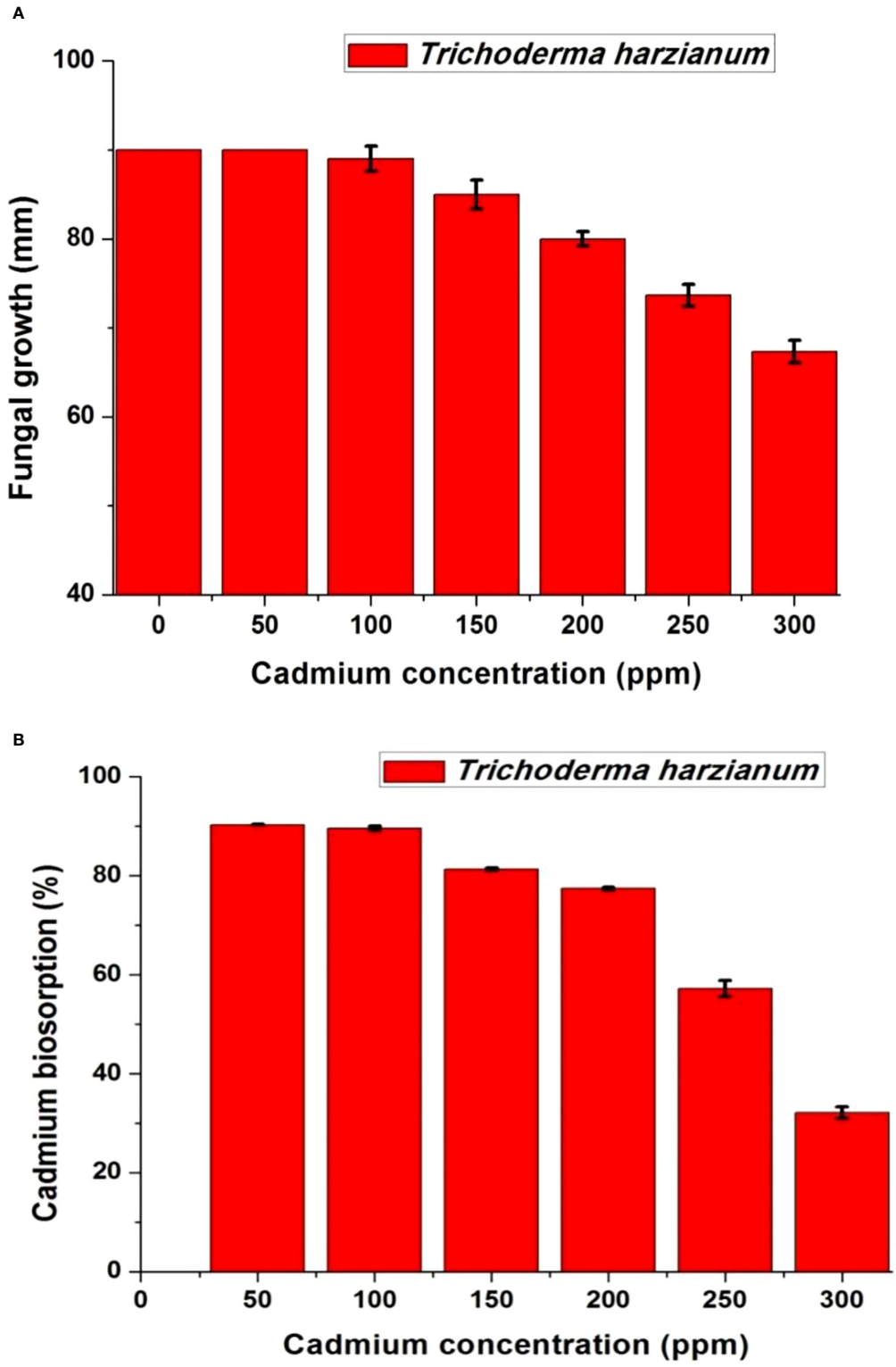

FIGURE 3
Growth (mm) **(A)** and biosorption percentage (%) **(B)** of cadmium resistance *Trichoderma harzianum* on different concentrations of Czapek's cadmium medium with cadmium concentrations range from 0 to 300 ppm.

control whatever elevated Cd concentrations. Visual Cd toxic symptoms such as necrosis are due to depletion in N uptake in non-inoculated Cd-stressed plants. Plants inoculated with PGPB and consortium registered well-furnished metabolizable N to their body in terms of augmented levels of protein and amino acid as well as enhanced NR activity. However, plants inoculated with *T. harzianum* kept these parameters near the levels of control under Cd-stressed or non-stressed conditions. Low–molecular weight molecules, ***viz.***, phenolics, flavonoids, anthocyanin, and proline, were significantly increased by the interaction between Cd stress and microbe inoculation individually or in consortium indicating their role in cellular damage restriction under Cd stress (Table 3). The percent of increase accounted as 26.3% and 232.4%, 135.3% and 446.2%, 500% and 95.6%, and 60% and 300%, in the levels of phenolics, flavonoids, anthocyanin, and proline for *T. harzianum* and PGPB, respectively.

Influence of Cd and microbe–soil interaction on oxidative injury and non-enzymatic and enzymatic antioxidants of sunflower plant

The data of reactive oxygen species (ROS) denoted in Table 4 revealed a decline in superoxide anion and hydroxyl radical by soil microbe inoculation individually or in the consortium, whereas hydrogen peroxide (H_2O_2) quietly prompted whatever the dose of Cd applied by PGPB or in the consortium. For example, the decrese is approximately 0.53%, 14.12%, 2.70%, and 5.70% for the levels of superoxide anion (O_2^-), hydroxyl radical ($^{\bullet}OH$), EL, and PPO activities, respectively, by the action of PGPB. Non-significant alternation in H2O2 level was mediated by *T. harzianum* action even with elevated soil Cd concentrations. The oxidative burst of ROS to cellular membranes was assessed *via* lipid peroxidation in terms of MDA content and LOX, as well as membrane leakage assay of microbe-inoculated Cd-stressed plants, which were found to be similar to the control plants and within the range ensured healthy growth. The upregulation effect of microbe inoculation against Cd stress appeared from low–molecular weight antioxidant metabolism as represented in Table 4, where the exacerbation of PCs, ASA, and GSH along with elevated Cd levels in addition to activation of secondary metabolites pathway is illustrated by the overproduction of phenolics, flavonoids, and anthocyanin contents, owing to microbes application. The maintenance of cell oxidative status by enzymatic antioxidants may be due to the increase of superoxide radical dismutation enzyme and SOD, in addition to the prompting of hydrogen peroxide quenching enzymes such as CAT, POD, GPX, APX, and GST, where the maximal activity of these antioxidant enzymes was manifested for plants inoculated with PGPB and in the consortium (Table 4). Whereas all antioxidant enzyme activities in leaves of Cd-exposed plants and inoculated with *T. harzianum* exhibited a similar pattern in response to Cd stress and generally showed no significant difference versus the control at 50 and 100 mg/kg, they were slightly stimulated by the highest Cd level (150 mg/kg) in the soil. Plants vastly elicited secondary metabolite-activating enzyme and PAL with microbe inoculation individually or in the consortium by percent increase of 76.7% and 166.7% for *T. harzianum* and PGPB, respectively (Table 4). On the other hand, PPO was highly significantly reduced (Table 4) for PGPB and in consortium-inoculated plants and non-significantly for *T. harzianum*–inoculated plants relative to non-inoculated control plants.

Influence of Cd and microbe–soil interaction on leaf nutrient content of sunflower plant

Cd in the nutrient medium was deleterious to nutrient uptake, ***viz.***, K, Ca, Mg, Fe, nitrate, and P; however, data illustrated in Table 5 showed that microbe inoculation, even in the presence of Cd, increased all of these parameters to be more than or very close to those of the control.

Influence of Cd and microbe–soil interaction on Cd concentrations in soil and sunflower plant

Data depicted in Table 6 showed that, by increasing the Cd concentration, the available soil and plant Cd increase. However, microbial fortification decreases the Cd soil and plant availability compared with control samples (free from applied microorganisms) by 11.5% and 47.5%, and 3.8% and 45.0% with *T. harzianum* and PGP bacterial inoculation, respectively, compared with non-inoculated Cd-stressed plants. The microbial consortium was the most efficient treatment that decreases Cd availability in soil.

Discussion

The potential of PGPB (*Azotobacter chroococcum* and *Bacillus subtilis*) and *Trichoderma harzianum* was investigated individually or synergistically for the first time regarding their capability to impart tolerance in sunflower plant for withstanding and survival to severe Cd dose up to 150 mg of Cd/kg of soil. Excessive concentrations of HMs upset various biochemical pathways in plants, such as inhibition of chlorophyll synthesis, photosynthesis, respiration, transpiration rates, N metabolism, uptake of nutrient elements, cell elongation, changes in photoassimilates translocation, hormone balance *via* a diminution of the endogenous level of growth-promoting hormone auxin, which happened due to boosted activity of the auxin-degrading enzyme, and alteration of water relations, which further enhance the metal-induced growth reduction; consequently, plant death was the result (Kumar and Trivedi, 2016; Eissa and Abeed, 2019; Zhu et al., 2020). Evidence indicates the fatal stress imposed by the applied doses upon sunflower plant resulted in plant death rather than limited growth or even reduced cell performance. Pretreatment

TABLE 2 Average values of Fwt, g/plant; Dwt, g/plant; PH, cm; LSA, cm^2; NAR, $\mu g/cm^2/d$; Sc, $mol/m^2/s$; Tr, water loss/leaf area; WUE, g DW/kg H_2O; RWC, % of sunflower inoculated and non-inoculated with PGP bacteria, *T. harzianum*, and Consortium and affected by different levels of Cd (0, 50, 100, and 150 mg/kg dry soil).

Cd dose (mg/kg)	Inoculation with microbes	Fwt	Dwt	PH	LSA	NAR	Sc	Tr	WUE	RWC
0	Non-inoculated	1.44 ± 0.03	0.36 ± 0.001	29.5 ± 1.1	93.33 ± 3.1	0.018 ± 0.002	1.1 ± 0.02	0.022 ± 0.003	3.4 ± 0.4	84 ± 2.1
	PGP bacteria	2.7 ± 0.04d**	0.58 ± 0.001c**	39 ± 1.5c**	110.1 ± 9.1c**	0.032 ± 0.002c**	1.8 ± 0.01c*	0.034 ± 0.002c**	4.5 ± 0.3c**	89 ± 1.9b**
	T. harzianum	1.38 ± 0.02a	0.38 ± 0.003a	31.5 ± 2.3a	95.21 ± 5.5a	0.016 ± 0.002a	1.2 ± 0.02a	0.021 ± 0.004a	3.1 ± 0.2a	84 ± 3.1a
	Consortium	2.04 ± 0.03c**	0.46 ± 0.004b*	37 ± 3.3cb**	101.03 ± 11b*	0.044 ± 0.003d**	1.6 ± 0.02b*	0.027 ± 0.005b*	4 ± 0.3b*	90 ± 2.2b**
50	Non-inoculated	—	—	—	—	—	—	—	—	—
	PGP bacteria	2.17 ± 0.02c**	0.49 ± 0.001b**	37 ± 1.5cb**	98.67 ± 7.5ab*	0.025 ± 0.001b*	1.6 ± 0.02b*	0.027 ± 0.004b*	4.2 ± 0.2b*	87 ± 5.1ab*
	T. harzianum	1.86 ± 0.02b*	0.46 ± 0.003b*	35 ± 1.4b*	100.91 ± 10.5b*	0.030 ± 0.003c**	1.7 ± 0.02bc*	0.031 ± 0.006cb*	4.1 ± 0.3b*	86 ± 3.4ab*
	Consortium	2.50 ± 0.01d**	0.51 ± 0.002cb**	39 ± 2.1c*	107.11 ± 11c**	0.041 ± 0.004d**	2.0 ± 0.03d**	0.034 ± 0.005c**	4.6 ± 0.2c**	90 ± 4.3b**
100	Non-inoculated	—	—	—	—	—	—	—	—	—
	PGP bacteria	1.95 ± 0.01b*	0.48 ± 0.001b*	36 ± 1.5b**	95.66 ± 8.7a	0.022 ± 0.002b*	1.4 ± 0.01ab*	0.027 ± 0.003b*	3.9 ± 0.4b*	86 ± 1.7ab*
	T. harzianum	1.82 ± 0.01b*	0.42 ± 0.002ab*	31 ± 1.3a	99.03 ± 10.4ab*	0.027 ± 0.003b*	1.5 ± 0.01b*	0.028 ± 0.004b*	3.8 ± 0.3b*	86 ± 2.5ab*
	Consortium	2.24 ± 0.03c**	0.50 ± 0.003cb**	37.5 ± 2.2cb**	100.12 ± 10.3b*	0.037 ± 0.004c**	1.8 ± 0.02c*	0.03 ± 0.005cb*	4.4 ± 0.1cb*	89 ± 2.3b**
150	Non-inoculated	—	—	—	—	—	—	—	—	—
	PGP bacteria	1.64 ± 0.02ab	0.40 ± 0.005a	29.5 ± 2.5a	93.11 ± 6.4a	0.019 ± 0.001a	1.1 ± 0.00a	0.023 ± 0.005a	3.2 ± 0.1a	85 ± 3.7a
	T. harzianum	1.51 ± 0.03ab	0.38 ± 0.004a	29.7 ± 0.9a	94.56 ± 7.7a	0.028 ± 0.002b*	1.3 ± 0.01ab*	0.024 ± 0.003a	3.3 ± 0.1a	84 ± 4.2a
	Consortium	1.95 ± 0.01b*	0.47 ± 0.002b*	34 ± 3.0b*	97.84 ± 6.6a*	0.025 ± 0.004b*	1.5 ± 0.01b*	0.026 ± 0.003b*	4.2 ± 0.2b*	86 ± 1.1ab*

Fwt,fresh weight; Dwt:dry weight; PH,plant height; LSA,specific leaf area; NAR,net assimilation; Sc,stomatal conductance; Tr,transpiration rate; WUE,water use efficiency rate; RWC, relative water content. Each value represents an average value of three replicates ± SE and averages were compared by LSD at $p \leq 0.05$. * and ** denote the difference significantly from the control (0 Cd and non-inoculated) at the probability levels of 0.05 and 0.01,respectively. abc,different letters within columns denote significant differences ($P \leq 0.05$) between inoculations with PGP bacteria,T. harzianum, or Consortium in each external Cd level.

of soil with microbes lessen the applied dose toxicity and enables sunflower plant to adjust its metabolism to overcome the fatal stress, manifesting evident plant liveliness, and prompted safely leaf characteristics (e.g., aliveness, greenness, and moisture profile) and also neutralized all growth and physiological parameters, leading to values comparable with those of the control. A trend of *Azotobacter chroococcum*– and *Bacillus subtilis*–inoculated soil submitted higher improving impact on sunflower plant than *Trichoderma harzianum*–inoculated soil under Cd-stressed or non-stressed conditions, whereas consortium treatment assures the highest improving impact along with elevated Cd doses. However, the imparted tolerance mechanism mediated by the two different inoculations (PGPB and HMT fungus) was distinct from each other according to their PGR traits and Cd biosorption capacities, whereas the consortium exhibited dual benefits.

The current findings revealed that the tolerance mechanism mediated by *Azotobacter chroococcum* and *Bacillus subtilis* was due to PGR traits. PGR traits regarding growth hormone (IAA) production and their high ability to solubilize P and K, displaying growth enrichment and intensified 1ry and 2ry metabolite production that was pronounced in the presence and absence of Cd. The high production level of IAA was actively maintained during Cd exposure as a responded hormone in *Azotobacter chroococcum* and *Bacillus subtilis*. This accomplished a continuous supply of IAA to sunflower along with elevated Cd doses that promoted photosynthetic pigments and plant biomass acquisition in terms of dry/fresh weights, PH, LSA, and NAR in sunflower plants under Cd stress. Consistent with our findings, *Azotobacter* and *Bacillus* species proved their ability to enhance plant growth by producing significant compounds such as IAA (Ahmad et al., 2008).

TABLE 3 Average values of photosynthetic pigments (Chl a, Chl b, and carotenoids; mg/g FW); sugar metabolism (glucose, sucrose, and starch; mg/g DW); nitrogen metabolism (TN, total nitrogen, mg/g DW; NR, nitrate reductase, μmolNO_2/g/h; amino acids, mg/g DW; and proteins, mg/g DW) and metabolic molecules (phenolics, mg/g; FW, flavonoids, mg/g FW; anthocyanin, mg/g FW; and proline, mg/g DW) of sunflower inoculated and non-inoculated with PGP bacteria, *T. harzianum*, and Consortium and affected by different levels of Cd (0, 50, 100, and 150 mg/kg dry soil).

Cd dose (mg/kg)	Inoculation with microbes	Photosynthetic pigments			Sugar metabolism			Nitrogen metabolism				Secondary metabolite molecules			
		Chl a	Chl b	Caro	Glucose	Sucrose	Starch	Total nitrogen	NR	Amino acids	Proteins	Phenolics	Flavonoids	Anthocyanin	Proline
0	Non-inoculated	0.54 ± 0.02	0.11 ± 0.007	0.66 ± 0.02	17 ± 1.3	51.12 ± 2.5	86 ± 6	30 ± 1.4	60 ± 2.2	22.86 ±	119 ± 7	3.4 ± 0.7	1.3 ± 0.06	0.45 ± 0.003	2.5 ± 0.3
	PGP bacteria	0.89 ± 0.03d**	0.28 ± 0.004d*	1.42 ± 0.1e**	25 ± 1.7b*	78.76 ± 4.5c*	130 ± 9b**	58 ± 1.5d*	110 ± 5.6e**	58.41 ± 2.1d**	134.02 ± 5b*	7.1 ± 0.9d*	2.5 ± 0.03b*	0.55 ± 0.005b*	4 ± 0.3c*
	T. harzianum	0.50 ± 0.02a	0.13 ± 0.008a	0.76 ± 0.03b	15 ± 1.1a	55.09 ± 3.3a	89 ± 7.7a	31 ± 0.9a	67.09 ± 1.2a	25.02 ± 1.4a	122 ± 6a	3.6 ± 0.5a	1.7 ± 0.05a	0.43 ± 0.004a	2.1 ± 0.2a
	Consortium	0.71 ± 0.02cb*	0.24 ± 0.009c*	0.95 ± 0.05d*	20 ± 1.8ab*	69.65 ± 2.4b*	150 ± 11.1c**	46 ± 1.1c*	88 ± 1.6c*	42.33 ± 2.1c*	134.89 ± 8b*	4.7 ± 0.4b*	2.4 ± 0.08b*	0.51 ± 0.008b*	3.7 ± 0.2b*
50	Non-inoculated	—	—	—	—	—	—	—	—	—	—	—	—	—	—
	PGP bacteria	0.79 ± 0.01c*	0.28 ± 0.01d*	1.22 ± 0.2ed**	23 ± 2.1b*	74.23 ± 3.2c*	122 ± 10ab**	50 ± 0.9d*	86.77 ± 2.2c*	50.70 ± 2.2d*	139 ± 8b*	7.8 ± 0.6ed**	4.9 ± 0.1d*	0.57 ± 0.008b*	6 ± 0.3e**
	T. harzianum	0.65 ± 0.01b	0.19 ± 0.006b	0.95 ± 0.05d*	16.03 ± 2.1a	57.12 ± 2.6a	99 ± 6.6a*	40 ± 1.7c*	76.76 ± 1.8b*	33.46 ± 1.5b*	128 ± 5ab	5.6 ± 0.5c*	3.5 ± 0.08c*	0.870.009e**	2.5 ± 0.1a
	Consortium	0.87 ± 0.02d*	0.31 ± 0.008d*	0.99 ± 0.06d*	26 ± 2.2b*	77.33 ± 4.1c**	220 ± 12.6d**	66 ± 2.2e*	95 ± 1.7d*	47.12 ± 1.2c*	136 ± 3b*	5.1 ± 0.7c*	2.5 ± 0.07b*	0.61 ± 0.006c*	4.4 ± 0.1c*
100	Non-inoculated	—	—	—	—	—	—	—	—	—	—	—	—	—	—
	PGP bacteria	0.68 ± 0.02b	0.20 ± 0.009b*	0.86 ± 0.05c*	21 ± 1.5b*	70.21 ± 3.1c*	116 ± 10.6a*	44 ± 1.4c*	80 ± 3.2c*	44.09 ± 1.4c*	148 ± 7c**	9.31 ± 0.6f**	5.53 ± 0.07e*	0.67 ± 0.007c*	7.6 ± 0.2f**
	T. harzianum	0.55 ± 0.01a	0.16 ± 0.007ab	0.77 ± 0.04b	18 ± 1.1a	63.95 ± 2.6b**	132 ± 10.1b*	34 ± 0.8ab	72 ± 1.7b*	32.77 ± 1.7b*	130 ± 5b*	6.6 ± 0.4d**	3.9 ± 0.06c**	1.9 ± 0.06f**	2.9 ± 0.2a
	Consortium	0.79 ± 0.01c*	0.28 ± 0.008d*	0.89 ± 0.05c*	28 ± 2.2cb*	75.11 ± 2.5c	181 ± 11d*	52 ± 1.7d*	89 ± 1.7c*	48.05 ± 1.5c*	135 ± 3b*	5.5 ± 0.6c*	2.7 ± 0.05b*	0.68 ± 0.005c*	5.3 ± 0.1d*
150	Non-inoculated	—	—	—	—	—	—	—	—	—	—	—	—	—	—
	PGP bacteria	0.56 ± 0.005a	0.16 ± 0.009ab	0.73 ± 0.04b	18 ± 2.3ab	61 ± 4.4b*	96 ± 5.5a*	36 ± 0.7b	76 ± 2.1b*	38.64 ± 1.9b*	162 ± 8d**	11.3 ± 0.9g**	7.1 ± 0.2f**	0.88 ± 0.007e**	10.1 ± 0.5g**
	T. harzianum	0.51 ± 0.006a	0.12 ± 0.008a	0.65 ± 0.03a	16.76 ± 1.1a	50 ± 2.6a	88 ± 5.7a	31 ± 1.1a	64 ± 1.3a	28.87 ± 1.8a	118 ± 2a	8 ± 0.6e**	4.2 ± 0.05d**	2.7 ± 0.07g**	4 ± 0.2c*
	Consortium	0.74 ± 0.01c*	0.20 ± 0.001b*	0.81 ± 0.05c*	30 ± 3.4c**	66 ± 3.7b*	140 ± 7.5cb**	41 ± 0.8c*	81 ± 3.4c*	45.32 ± 1.5c*	130 ± 3b*	6.7 ± 0.5d**	3.6 ± 0.06c*	0.76 ± 0.006d*	6.1 ± 0.3e**

Each value represents an average value of three replicates ± SE,and averages were compared by LSD at $p \leq 0.05$. * and ** denote the difference significantly from the control (0 Cd and non-inoculated) at the probability levels of 0.05 and 0.01,respectively. abc, different letters within columns denote significant differences ($P \leq 0.05$) between inoculations with PGP bacteria, T. harzianum ,or Consortium in each external Cd level.

10.3389/fpls.2022.1004173

Khan et al. (2009) and Kumar et al. (2001) revealed that *Azotobacter chroococcum* can solubilize phosphate and produce phytohormones as kinetin, gibberellin, and IAA P solubilization. Zaidi et al. (2006) stated that *Bacillus subtilis* produces IAA in addition to its ability to mineralize the unavailable phosphate in the soil. Most ***Azotobacter*** species can convert the state of atmospheric N to plant-usable (ammonia) through biological N fixation (Kim and Rees, 1994). A marked increase in plant germination, length, and weight was achieved by applying phosphate-solubilizing and N-fixing *Azotobacter* species (Widawati, 2018). Soil application with *Azotobacter chroococcum* increased cotton seed yield by 21% and PH by 5% (Anjum et al., 2007), in addition to protecting *Brassica juncea* from HM toxicity by increasing plant growth (Wu et al., 2006). Fortification of soil by PGP *Bacillus* species significantly boosted chickpea plant growth, chlorophyll, and yield and reduced metal uptake (Wani and Khan, 2010). *Bacillus subtilis* increased tomato biomass by 31%, okra by 36%, and spinach by 83% (Adesemoye et al., 2008).

On the other hand, *Trichoderma harzianum* has the unequivocal capacity to bind Cd (efficient Cd biosorption) counted for about 81.35% ± 0.28% at the highest Cd soil existence (150 mg of Cd/kg of soil; Figure 3B). Metal bioavailability is an important factor for metal uptake in plants. Reducing Cd bioavailability percentage in the rooting portion *via* the retention of HMs by fungal mycelia involves adsorption to cell walls or immobilizing them by insoluble metal oxalate formation or chelation on melanin-like polymers (Khan et al., 2017). Consequently, a minor amount of exposed Cd will be encountered by the plant, thus minimizing metal root uptake and low translocation level to the shoots. This hypothesis was corroborated by Kapoor and Bhatnagar (2007), who demonstrated that fungal mycelia had a high metal sorption capacity. Mycelia attenuate the toxic effect of metals *via* retaining them in the fungal structure with the subsequent restriction of metal transfer to the plant (Joner et al., 2000). Biosorption includes surface adsorption, ion chelation, ion exchange, and micro-precipitation (Lim et al., 2008). Fungal cell surfaces contain functional groups like carboxyl, amino, hydroxyl, and phosphate, which play a critical role in Cd ion uptake (Lim et al., 2008). Mohsenzade and Shahrokhi (2014)found that *T. harzianum* could adsorb Cd from 1 to 100 mg/L. *T. harzianum* could grow on different Cd concentrations (0–300 ppm) with huge tolerance, especially in high concentrations; in addition, it can absorb high quantities of Cd to reach 90% removal efficiency. Consistent with our results, Lima et al. (2011) demonstrated the *T. harzianum* potentiality of Cd removal, which increased by increasing the Cd concentration from 1 to 3 mM. The tolerance of *Trichoderma* to HMs can be explained by biosorption or bioaccumulation processes (Mahmoud, 2021) and metal binding to microbial biomass (Nair et al., 2008). Hence, *T. harzianum* application alleviated the toxic effects of Cd by accumulating and/or immobilizing most Cd in their biomass extracellularly, resulting in developing trace soil Cd concentration that remains free and available for plant roots after *T. harzianum* action witnessed in our study by the reduced total amount of Cd accumulated per plant (Table 6). Therefore, the bioprotective effect of *T. harzianum* on sunflower growth was due to a reduced amount of Cd uptake owing to biosorption property rather than the PGP traits; hence, the promoter effect of *T. harzianum* was sounded only in the presence of Cd in soil medium. Here, the positive effect on plant growth could be due to the low bioavailable Cd concentration, posing well-known low-dose stimulation phenomena (hormetic effect). Documented promoted growth was shown because of 10 mg of Cd/kg of soil (Jia et al., 2012; Jia et al., 2015) and 125 mg of Cd/kg of soil (Liu et al., 2012) in *Lonicera japonica*. This significant stimulating effect on growth parameters regarding PH, fresh and dry weights, and the specific leaf area after *T. harzianum* action was realized up to 150 mg of Cd/kg of soil (Table 2), indicating the ability of *T. harzianum* to tolerate Cd and acting actively even at lethal doses for the plant (Nongmaithem et al., 2016; Hoseinzadeh et al., 2017). A positive effect on plant growth at low Cd concentration has also been registered in plants, such as barley (Wu et al., 2003), miscanthus (Arduini et al., 2004), soybean (Sobkowiak and Deckert, 2003), and rice (Aina et al., 2007).

In the presence of Cd, chlorosis symptom appearance indicating chlorophyll degradation and plant death was registered in our study. Moreover, necrosis might have been caused by ROS production and membrane dysfunction, which eventually results in programmed cell death. Moreover, the enhanced chlorophyll content and function in inoculated Cd-stressed plants witnessed by high photoassimilates content and subsequent Cd stress recovery indicated that Cd stress tolerance herein may be attained through chlorophyll restoration against elevated Cd supplementation, which could be a promising mechanism to trigger sunflower tolerance against severe Cd stress mediated by microbe inoculation, and the main sensitivity criterion of the current tested sunflower cultivar was photosynthetic depletion under Cd stress and enhanced chlorophyll function and composition linked with a reversed plant from distressed to aliveness. This might be attributed to adequate Mg uptake due to the link between chlorophyll content and Mg uptake as an important part of the chlorophyll molecule (Sheng et al., 2008). Thus, for enhanced Chl a and b contents in PGPB- and *T. harzianum*–inoculated plants, the subsequent recovery of Cd-stressed plants could be accounted for by the effect of these microbes on Mg uptake (Shahabivand et al., 2017). Jia et al. (2015) reported that the stimulating effect of Cd (10 mg/kg) on plant biomass could be ascribed to the increment recorded in photosynthetic carbon assimilation, and the low doses of Cd induced some beneficial effects on the photosynthetic system and increased pigment contents, demonstrating that low doses of Cd induced some beneficial effects on the photosynthetic apparatus. Moreover, Zhou and

TABLE 4 Average values of some biochemical indices of sunflower inoculated and non-inoculated with PGP bacteria, *T. harzianum*, and Consortium and affected by different levels of Cd (0, 50, 100, and 150 mg/kg of soil).

Cd dose (mg/kg)	Inoculation with microbes	Membrane integrity traits			Reactive oxygen species			Non- enzymatic antioxidant			Enzymatic antioxidant capacities							
		MDA	LOX	EL	H_2O_2	$^{\bullet}OH$	O_2^{-}	PCs	ASA	GSH	SOD	CAT	POD	APX	GPX	GST	PAL	PPO
0	Non-inoculated	53.97 ± 2.3	4.53 ± 0.2	32.91 ± 1.2	170.08 ± 10.1	10.98 ± 0.9	39.44 ± 2.2	20.06 ± 1.1	35 ± 1.1	9.4 ± 0.8	30 ± 0.9	66 ± 1.4	90 ± 4.4	91 ± 3.4	132 ± 10	110 ± 5.9	30 ± 2.1	35 ± 1.9
	PGP bacteria	40.54 ± 2.1*	1.89 ± 0.09**	20.75 ± 1.1*	115.13 ± 9.8*	6.51 ± 0.8*	22.12 ± 2.3*	18.67 ± 1.2	49 ± 2.1*	20 ± 1.7**	44 ± 1.8*	80 ± 3.1*	147 ± 7.7*	114 ± 4.4*	159 ± 10*	100 ± 6.5	55 ± 4.3*	20 ± 1.1*
	T. harzianum	51.33 ± 1.4	4.09 ± 0.1	30.23 ± 2.0	165.43 ± 12.2	9.56 ± 0.8	33.06 ± 3.3	23.12 ± 1.4	37 ± 2.4	10 ± 1.3	33 ± 1.1	67 ± 2.5	89 ± 4.3	88 ± 5.6	130 ± 11	108 ± 6.9	28 ± 1.4	32 ± 1.2
	Consortium	43.22 ± 1.1*	2.57 ± 0.2*	22.07 ± 1.2*	120.12 ± 13.1*	5.64 ± 0.4*	21.23 ± 1.3*	20.43 ± 1.1	43 ± 2.4*	22 ± 2.3**	40 ± 1.7*	85 ± 2.6*	100 ± 7.7*	94 ± 6.4	164 ± 9*	111 ± 10	46 ± 2.2*	18 ± 0.9*
50	Non-inoculated	—	—	—	—	—	—	—	—	—	—	—	—	—	—	—	—	—
	PGP bacteria	51.76 ± 1.2	2.66 ± 0.1*	29.11 ± 1.1	190 ± 13.1*	7.43 ± 0.5*	32.21 ± 1.4	40.56 ± 2.2*	56.77 ± 2.1*	46 ± 3.4**	48 ± 2.1*	89 ± 4.3*	160 ± 8.5*	133 ± 9.9*	179 ± 10*	170 ± 12.4**	59 ± 3.1*	23 ± 1.3*
	T. harzianum	41.21 ± 2.4*	2.01 ± 0.1*	21.43 ± 1.1*	173 ± 12.1	9.32 ± 0.6	37.65 ± 2.1	19.65 ± 1.3	44 ± 1.9*	15 ± 1.8	32 ± 1.7	66 ± 2.1	90 ± 5.5	87 ± 6.4	131 ± 9	100 ± 7.9	35 ± 2.1	25 ± 1.8*
	Consortium	40.43 ± 2.2*	4.04 ± 0.1	25.76 ± 1.3*	120 ± 9.3*	5.43 ± 0.3*	20.32 ± 1.1*	22.21 ± 1.5	49 ± 1.8*	30 ± 2.1**	50 ± 2.4*	87 ± 2.3*	102 ± 6.1*	96 ± 5.7	166 ± 11*	155 ± 9.4*	61 ± 4.3*	16 ± 0.9*
100	Non-inoculated	—	—	—	—	—	—	—	—	—	—	—	—	—	—	—	—	—
	PGP bacteria	53.32 ± 1.5	3.87 ± 0.1	30.09 ± 2.2	185 ± 13.1*	9.65 ± 0.8	37.65 ± 2.1	52.33 ± 2.1**	67.98 ± 3.2**	57.98 ± 2.3**	52 ± 2.3*	97 ± 4.3*	161 ± 5.4*	153 ± 10.9*	194 ± 11*	190 ± 11.1**	68 ± 4.1*	29 ± 1.7
	T. harzianum	47.65 ± 1.4	4.32 ± 0.8	22.65 ± 1.1	173 ± 11.1	9.98 ± 0.9	25.44 ± 1.5*	20.24 ± 1.1	46 ± 1.8*	18 ± 1.5	33 ± 1.1	67 ± 3.5	88 ± 3.3	80 ± 5.5	133 ± 9	117 ± 10.9	34 ± 3.0	28 ± 1.9
	Consortium	44.56 ± 1.1*	3.87 ± 0.2	27.33 ± 2.1	144 ± 9.7*	6.02 ± 0.7*	22.76 ± 1.1*	30.11 ±	55 ± 2.3*	32 ± 1.7**	54 ± 1.3*	92 ± 3.5*	100 ± 9.9*	99 ± 6.4	157 ± 10*	179 ± 12**	69 ± 4.0*	20 ± 1.1*
150	Non-inoculated	—	—	—	—	—	—	—	—	—	—	—	—	—	—	—	—	—
	PGP bacteria	54.45 ± 1.5	4.65 ± 0.9	32.01 ± 1.1	223 ± 17.9*	9.43 ± 0.6	39.23 ± 2.3	58.97 ± 1.9**	87.55 ± 4.3**	66.23 ± 2.4**	61 ± 2.8*	126 ± 5.3*	188 ± 12.2*	174 ± 11*	228 ± 12*	233 ± 14**	80 ± 5.0*	33 ± 2.1
	T. harzianum	58.22 ± 1.7	4.08 ± 0.8	34.98 ± 1.7	192 ± 11.4*	10.15 ± 0.8	41.05 ± 2.2	40.12 ± 2.1**	53 ± 2.5*	22 ± 1.2**	39 ± 1.3	78 ± 2.3*	100 ± 8.7*	150 ± 6.8*	161 ± 10*	140 ± 11*	53 ± 4.1*	34 ± 1.5
	Consortium	46.56 ± 1.3	3.77 ± 0.5	29.11 ± 2.1	166 ± 10.9	6.99 ± 0.4*	26.65 ± 1.1*	25.66 ± 1.1	50 ± 1.9*	36 ± 2.1**	59 ± 2.5*	90 ± 3.3*	123 ± 10.1*	110 ± 9.9	170 ± 11*	181 ± 12**	76 ± 5.0*	23 ± 1.2*

MDA,malondialdehyde; LOX,lipoxygenase; EL,electrolyte leakage; H2O2,hydrogen peroxide; OH,hydroxyl radical; O2,superoxide anion; PCs,phytochelatin; GSH,reduced glutathione; ASA,ascorbic acid; CAT,catalase; SOD,superoxide dismutase; POD, guaiacol peroxidase; APX,ascorbate peroxidase; GPX,glutathione peroxide; GST,glutathione-S-transferase; PAL,phenylalanine ammonia-lyase; PPO,polyphenol oxidase. Each value represents an average value of three replicates ± SE,and averages were compared by LSD at $p \leq 0.05$. * and ** denote the difference significantly from the control (0 Cd and non-inoculated) at the probability levels of 0.05 and 0.01,respectively. abc,different letters within columns denote significant differences ($P \leq 0.05$) between inoculations with PGP bacteria,T. harzianum,or Consortium in each external Cd levels.

10.3389/fpls.2022.1004173

10.3389/fpls.2022.1004173

TABLE 5 Average values of Leaf Nutrient content (K, Mg, Ca, Fe, nitrate, and phosphorus) of sunflower inoculated and non-inoculated with PGP bacteria, *T. harzianum*, and Consortium and affected by different levels of Cd (0, 50, 100, and 150 mg/kg dry soil).

Cd doses (mg/kg)	Inoculation with microbes	Leaf Nutrient content (mg/g DW)					
		K	Ca	Mg	Fe	Nitrate	Phosphorus
0	Non-inoculated	22 ± 1.9	4.0 ± 0.2	3.3 ± 0.1	9 ± 0.6	29 ± 2.5	0.81 ± 0.02
	PGP bacteria	45 ± 3.3d**	7.8 ± 0.5e**	4 ± 0.1b*	12 ± 0.8g*	34 ± 2.4f*	1.6 ± 0.08b**
	T. harzianum	33 ± 2.6b*	5.1 ± 0.4c	2.9 ± 0.1a	6 ± 0.5a*	28 ± 1.8a	0.95 ± 0.03a*
	Consortium	39 ± 1.5c**	5.9 ± 0.3c*	3.8 ± 0.3b	9.3 ± 0.5d	33 ± 3.5e*	2 ± 0.1c**
50	Non-inoculated	—	—	—	—	—	—
	PGP bacteria	41 ± 1.1cd**	5 ± 0.1c	4 ± 0.2b*	11 ± 0.8f*	32 ± 1.9d*	1.5 ± 0.08b**
	T. harzianum	34 ± 2.1b*	6.5 ± 0.2d**	3.5 ± 0.1ab	7.5 ± 0.6b*	33 ± 1.3e*	1.2 ± 0.06ab*
	Consortium	43± 1.7d**	5.5 ± 0.2c*	4.4 ± 0.2b*	10 ± 0.9e	32 ± 2.4d*	1.9 ± 0.09cb**
100	Non-inoculated	—	—	—	—	—	—
	PGP bacteria	39 ± 1.7c**	4 ± 0.1b	5 ± 0.3c**	9 ± 0.5d	29 ± 1.5a	1 ± 0.08a*
	T. harzianum	37 ± 1.3c**	6.8 ± 0.1d**	3.1 ± 0.1a	10 ± 0.6e	31 ± 1.7c*	0.92 ± 0.05a*
	Consortium	40 ± 2.3cd**	5 ± 0.1c	4 ± 0.1b*	9 ± 0.4d	30 ± 1.7b	2.2 ± 0.1c**
150	Non-inoculated	—	—	—	—	—	—
	PGP bacteria	40 ± 2.6cd**	3 ± 0.2a	3 ± 0.2a	8.2 ± 0.5c	31 ± 1.1c*	0.82 ± 0.04a
	T. harzianum	44 ± 2.7d**	7.2 ± 0.1 e**	5.3 ± 0.3 c**	12 ± 0.6 g*	34 ± 1.4 f*	1.2 ± 0.06 a*
	Consortium	34 ± 2.1b*	4.4 ± 0.2b	3.3 ± 0.2a	9.2 ± 0.5 d	30 ± 1.0 b	1. 0 ± 0.06 a*

Each value represents an average value of three replicates ± SE,and averages were compared by LSD at $p \leq 0.05$. * and ** denote the difference significantly from the control (0 Cd and non-inoculated) at the probability levels of 0.05 and 0.01,respectively. abc,different letters within columns denote significant differences ($P \leq 0.05$) between inoculations PGP bacteria, T. harzianum,or Consortium in each external Cd levels. * and ** denote the difference significantly from the control (0 Cd and non-inoculated) at the probability levels of 0.05 and 0.01, respectively. abc,different letters within columns indicate significant differences ($P \leq 0.05$) between inoculations PGP bacteria, T. harzianum,or Consortium in each external Cd levels.

Qiu (2005) manifested the main explanation of the increase in chlorophyll content at a low Cd level due to a Cd-induced increase in Fe uptake. The other mechanism that may be mediated by *T. harzianum* inoculation as a biofertilizer to confer metal stress tolerance herein is *via* an increase in nutrient uptake under Cd stress. On the other hand, Bashri and Prasad (2015) reported that IAA liberated by PGPB could prompt the downregulation of pigment degradation, causing substantial preservation of pigment content (Abeed et al., 2020; Li et al., 2021).

Stomatal conductance and transpiration rate displayed adequate levels and comparable values of control due to *T. harzianum* that has high Cd-binding capacity, resulting in low available soil Cd. Similar results were submitted for corn plants exposed to 25 mM Cd (Chaneva et al., 2010). Furthermore, the adequate NAR along with Cd treatments submitted by *T. harzianum* inoculation could be ascribed to a high net photosynthetic rate. Ying et al. (2010) cited that increased photosynthesis could be due to elevated Rubisco content at low levels of Cd treatment, evidencing the positive effect of Cd by *T. harzianum* interaction. Moreover, data from water relations indicated that the concentration of HMs in inoculated soil was efficiently lowered to reach a level that causes no osmotic disturbances in plants. Thus, adequate soil–water relation leads to improved water uptake and economic use of water evidenced by adequate water status of the cell regarding RWC and high value of WUE. In different way and apart from *T. harzianum*, the IAAproducing microbe, enhanced root systems, including root hairs, are the most common phenotypic phenomena observed related to the secretion of phytohormones by PGP microbes. Thus, IAA enhanced the capability of plants to exploit the water from the soil in the highest concentration of soil Cd. Consequently, enhanced root growth and performance lead to improved water uptake and economic water use evidenced by adequate water status of the cell regarding RWC and high value of WUE.

Carbon and N resource use and photoassimilate production can be assessed by adopting some carbon and N metabolites and their related enzymes. In the current study, microbe's soil inoculations manifested adequate carbon and N metabolism that was reflected in starch and protein contents. As sucrose is the famous exported form of organic carbon transport from the photosynthetic source to sink organ in turn, high accumulation of starch indicated high efficiency of using carbon resources and photoassimilate production in favor of plant architecture, and this process is crucial for survival and healthiness as submitted in current investigated plants (Koch, 2004). NR is one of the coordinative enzymes that regulated the level of N in plants. The activity of this enzyme is downregulated by the presence of Cd (Gouia et al., 2000) as evident herein by minimized inducible rate (Table 3), resulting in an alternation in protein metabolism that negatively affected plant architecture witnessed by stunted plants (Table 2). Inoculated with PGPB, *T. harzianum*, individually and in the consortium, can significantly increase N metabolism as evidenced by the increased total N in shoots

TABLE 6 Cadmium concentrations in soil and sunflower plants inoculated and non-inoculated with PGP bacteria, *T. harzianum*, and Consortium after being affected by different doses of Cd (0, 50, 100, and 150 mg/kg of soil).

Cd dose (mg/kg)	Inoculation with microbes	Available Cd concentration (mg/kg)	
		Soil	Plant
0	Non-inoculated	0.05 ± 0.001a	0.42 ± 0.01c
	PGP bacteria	0.06 ± 0.001a	0.32 ± 0.01b
	T. harzianum	0.03 ± 0.000a	0.24 ± 0.02a
	Consortium	0.04 ± 0.001a	0.20 ± 0.02a
50	Non-inoculated	4.5 ± 0.06c	20 ± 0.21d
	PGP bacteria	3.6 ± 0.08b	16 ± 0.22c
	T. harzianum	3.0 ± 0.07a	10 ± 0.12b
	Consortium	3.2 ± 0.08a	6 ± 0.16a
100	Non-inoculated	10.2 ± 0.21d	27 ± 0.62c
	PGP bacteria	8.4 ± 0.11b	18 ± 0.22b
	T. harzianum	7.4 ± 0.23a	14 ± 0.24a
	Consortium	9 ± 0.22c	13 ± 0.33a
150	Non-inoculated	13.3 ± 0.12c	40 ± 0.67c
	PGP bacteria	12.5 ± 0.13bc	22 ± 0.87b
	T. harzianum	11.5 ± 0.11b	21 ± 0.55b
	Consortium	10.2 ± 0.11a	13 ± 0.64a

Each value represents an average value of three replicates ± SE,and averages were compared by LSD at $p \leq 0.05$. abc,different letters within columns indicate significant differences ($P \leq 0.05$) between inoculations PGP bacteria, T. harzianum ,or Consortium in each external Cd level.

reflected in the total N yield of inoculated plants because all fixed N is incorporated into the plants, resulting in high protein content as N is an integral part of proteins in Cd-stressed and non-stressed plant. In well-adapted plants, enhanced primary metabolism goes along with secondary metabolism augmentation. In the current study, the activation of the secondary metabolite pathway, as proved by the exacerbation of phenolics, flavonoids, and anthocyanin, was a significant feature of tolerance mechanism and adaptation in sunflower plant attained by microbe inoculations, hence providing powerful free-radical quenching antioxidants and larger antioxidant defense pools to restraint ROS toxicity, thereby no membrane dysfunction. The upregulation of the main biosynthetic pathways of these antioxidants was joined with the enhanced activity of secondary metabolites, regulating enzymes and PAL, and this was vastly sounded by microbe inoculation rather than non-inoculated control plants.

The correlation of proline in Cd stress tolerance is a major biochemical adaptation, membrane stabilization, and ROS scavenging involved in the chelation of Cd (Ahmad et al., 2016). The mediation inoculation with microbes remarkably increased proline content in sunflowers. In the current study, the exacerbation of proline was accompanied by the increment of amino acids and soluble protein production. This obvious proline accumulation was certainly to be profitable, not due to a harmful impact. Thus, it could be concluded that proline accumulation was a plant response associated with conferring metal tolerance, not a reaction to high Cd exposure, confirming the protective effect of microbe inoculation in neutralizing toxic ROS, therefore contributing to better growth under Cd exposure. Similar to our results, Hui et al. (2015) also recorded an increase in proline accumulation in *Nicotiana tabacum* due to *P. indica* inoculation under Cd stress conditions.

One vital strategy of avoidance of Cd-induced oxidative stress is *via* Cd complexation either by glutathione or PCs. They dropped the free availability of Cd in the cytosol, causing significant tolerance against Cd toxicity (Yamazaki et al., 2018). This was efficiently mediated by IAA-producing microbes. IAA enhanced the level of PCs in the cytosol as reported by Khare et al. (2022). Moreover, the improved nutritional status that was registered by improving Fe uptake after bacterial inoculation indicates possible action of PGPB in Cd deposition out of important metabolic processes (in vacuoles), which may clarify the reduction of Cd phytotoxic impact despite the increased Cd accumulation; hence, the total amount of Cd accumulated per plant in PGPB-inoculated plants was significantly higher than that in *T. harzianum*–inoculated plants (Table 6); however, no phytotoxic appearance was recorded. The Fe-dependent transporters that are responsible for transporting PC-Cd-S complex to vacuoles (Hall and Williams, 2003) are adequately available herein owing to improving Fe uptake due to PGP bacteria application. Furthermore, the abundance in PC biosynthesis can be explained by abundant glutathione as registered in the current study because glutathione is the substrate for PC biosynthesis (Yamazaki et al., 2018).

The abatement of both ROS and their toxic byproducts (oxidized proteins and lipid hydroperoxides) is a prerequisite for the survival of plants in the existence of toxic metals. The produced IAA by PGPB was demonstrated to alleviate H_2O_2 and $O_2^{\bullet-}$ under Cd stress; hence, decreased lipid peroxidation (protection of cell membrane) was observed (Bashri and Prasad, 2015). This was postulated by elevated antioxidant enzyme activities joined with abatement of H_2O_2, $^{\bullet}OH$, and $O_2^{\bullet-}$ contents, indicating an IAA-induced ameliorating effect inducing the expression of stress-responsive genes and enhanced the antioxidant levels (Khare et al., 2022). The strong activation of GST in the case of PGPB-inoculated plants advocates the crucial role of PGPB in the Cd-induced stress response, in which IAA might play an important signaling role in participating in the activation of GST. Previously, it has been shown that the expression of many GSTs is strongly activated by IAA (Bočová et al., 2013). The increment of proteins and free amino acids due to PGPB-inoculated soil may be attributed to the activation of stress proteins that include several antioxidant enzymes (Lamhamdi et al., 2011) witnessed by elevated activity of ROS-metabolizing enzymes under either Cd-stressed or non-stressed plants; thus, stimulating the defense system machinery helped the plant to orchestrate itself from damage up to threshold; in addition, eliciting the expression of low–molecular weight proteins comprised the metal ion homeostasis that is assumed to shoulder role in their detoxification, ***viz.***, ASA, GSH (acting as a substrate of APX and GPX, respectively), and tocopherol (Patel et al., 2012). PPO is related to stress conditions and involves the cell wall cross-linking and lignification process resulting in a reduction in cell wall extensibility, which restricts cell growth, revealing exhausted plant tissues (Bruce and West, 1989; Abeed and Salama, 2022). PPO oxidatively breaks up phenolic compounds included in the synthesis of quinines and ROS; thus, the promotion of PPO activity exacerbates oxidative stress. In the current investigation, fortunately, the data for the PPO activity were divergent from the other antioxidant enzymes. PPO, an oxidizer of phenolic compounds (Queiroz et al., 2008; Abeed et al., 2021), is not induced by IAA-producing microbe inoculation but rather dropped in its content compared with non-inoculated control plants; thus, the upregulation of PPO due to soil inoculation under Cd stress diminishes PPO activity in sunflower plant that offered to promote resistance to abiotic stress (Sánchez-Rodríguez et al., 2011).

On the other hand, regarding *T. harzianum* action, much more sensitive parameters, such as biochemical parameters, should be analyzed to evaluate the stimulatory effect induced by the developed low Cd concentration by soil inoculation with *Trichoderma harzianum*. As no quantity or quality of toxic symptoms was noticed, what was the mechanism of the corresponding alterations in redox status in the inoculated plants? The stress causative agents (free radical components) were progressively decreased in the available soil Cd concentration by *T. harzianum* action (Table 4), indicating that no oxidative stress was imposed by the remaining concentrations of Cd in the soil (counted by about 14% reduction from non-inoculated control plant, Figure 3B) due to *T. harzianum* action that advocated by low MDA content and LOX activity that reflected on membrane stability and integrity evidenced by low electric leakage value. Similar findings were detected by Lin et al. (2007) and Maksymiec et al. (2007). Consequently, well-functional membranes with adequate integrity and tight controlled permeability can be maintained, thus efficiently reducing water loss and providing high turgidity and firmness and optimum water status for metabolic activities that are evidenced by values of WUE and RWC comparable with that of control (Table 2). Furthermore, no changes in ROS quenching enzymes activities, *viz.*, SOD, CAT, POD, APX, GPX, and GST activities under the developed low Cd concentrations, displayed similar responses to Cd treatments, probably due to their co-regulation, indicating no excess accumulation of ROS in sunflower plants inoculated by *T. harzianum* because their activity is mediated by generated ROS level. Somashekaraiah et al. (1992) documented that the SOD activity mediated by superoxide level exhibited a slight drop or no change linked with no excess accumulation of superoxide anion in mung bean seedlings under low levels of Cd stress. Wu et al. (2003) also found a slight decrease in antioxidant capacities accompanied by a decrement in barley lipid peroxidation products with a low-level Cd dose. The abatement of H_2O_2 and $^{\bullet}OH$ and stabilization of $O_2^{\bullet-}$ production in the Cd stress plant inoculated with *T. harzianum* reflected that the Cd levels remained in the soil owing to *T. harzianum* action are in an acceptable extent that harmfully impact plants. This may also suggest that the stimulatory effects of low concentrations of Cd on the growth of sunflower plants may be joined with a limited degree of free radical accumulation and restricted oxidative stress (Lin et al., 2007). However, when organisms are subjected to low Cd concentrations, their intrinsic GSH might be rapidly consumed because of a high cellular prerequisite for SH compounds to resist stress by prompting PC synthesis (Yamazaki et al., 2018), which may explain the increasing PCs content in our study owing to *T. harzianum* action. On the basis of the results of the current study regarding oxidative status corresponding to the available Cd concentration (mg/kg) in soil and plant, we propose that the toxic critical value of soil Cd in inducing oxidative stress in sunflower plant is 10.2 and 13 mg/kg for soil and plant (Table 6), respectively. This was efficiently achieved by soil supplementation with microbes. Similar results were registered for wheat seedlings by Lin et al. (2007).

The enhanced nutritional status of sunflower plant due to *T. harzianum* inoculation can be explained by the observation of Liu et al. (2011), who demonstrated that there is a synergistic interaction in accumulation and translocation between Cd and Fe, Zn, Mn, and Mg uptake in *L. japonica* plant. They have been improved at low Cd concentrations. The competition for the same

uptake systems between Cd and other divalent ions required for plant development is minimized in low Cd soil existence (Liu et al., 2011). However, the nourishment of the nutrient content of plant leaves due to PGP inoculation could be ascribed to the IAA generated by PGPB that modifies membrane permeability (Mir et al., 2022), which, in turn, might have facilitated the uptake of N, P, Mg, Zn, and Fe, resulting in the exacerbation of their levels, even in the plants exposed to Cd stress.

Conclusions

Applying microbes as a biofertilizer agent necessitates the elucidation of the different mechanisms of microbe protection and stabilization of plants against toxic elements in the soil that may be varied according to their PGR traits and/or Cd-binding capacities. Overall, our findings indicate that the two microbes have differentially established and maintained healthy physiological and biochemical properties of plants cultivated in severe Cd doses (divergent imparted upregulation mechanisms displayed by the two microbes used on sunflower plant adaptation). The high ability of PGPB to produce IAA, which was actively maintained during Cd exposure as a responded hormone, accomplished a continuous supply of IAA to sunflower along with elevated Cd doses (extended for 5 days giving values of 78.8 μg/ml for *Azotobacter chroococcum* and of 84.27 μg/ml for *Bacillus subtilis*) that subsequently promoted photosynthetic pigments and plant biomass acquisition in terms of dry/fresh weights, PH, LSA, and NAR as well as improved the other assessed physiological traits in sunflower plants under Cd stress. Thus, the resilience strategy mediated by PGPB was *via* recovering the potential side effects of Cd toxicity. Whereas, the highly Cd-tolerant *Trichoderma harzianum* with high Cd biosorption capacity (counted as 81.35% at the highest Cd soil existence) induced a resilience strategy *via* reducing Cd bioavailability to be in the range that turned its effect from toxicity to essentiality (the available soil and plant Cd concentrations were decreased by 11.5% and 47.5%, respectively), posing well-known low-dose stimulation phenomena (hormetic effect). However, the consortium exhibited dual benefits, achieving the highest efficiency in the resurrection of sunflower under severe Cd levels.

Data availability statement

The original contributions presented in the study are included in the article/supplementary material, further inquiries can be directed to the corresponding authors.

Author contributions

AA and GM: conceived the experiments; performed the experiments; analyzed and interpreted the data; contributed to reagents, materials, analysis tools, or data; and wrote the paper. AA, GM, ME, and RM: materials, experimental analysis, and experimental design. ME, RM, DA, IH, and AL: experimental analysis, writing, revising, and editing. All authors contributed to the article and approved the submitted version.

Acknowledgments

The authors would like to acknowledge the Department of Botany and Microbiology, Faculty of Science, Assiut University; and Soil and Water Department, Faculty of Agriculture, Assiut University, for supporting this work.

Conflict of interest

The authors declare that the research was conducted in the absence of any commercial or financial relationships that could be construed as a potential conflict of interest.

Publisher's note

References

Aasfar, A., Bargaz, A., Yaakoubi, K., Hilali, A., Bennis, I., Zeroual, Y., et al. (2021). Nitrogen fixing azotobacter species as potential soil biological enhancers for crop nutrition and yield stability. *Front. Microbiol.* 12. doi: 10.3389/fmicb.2021.628379

Abdel-Hakeem, S. S., Mahmoud, G. A.-E., and Abdel-Hafeez, H. H. (2019). Evaluation and microanalysis of parasitic and bacterial agents of Egyptian fresh sushi, salmo salar. *Microscopy Microanal.* 25, 1498–1508. doi: 10.1017/s143192761901506x

Abdel Latef, A. A. (2013). Growth and some physiological activities of pepper (Capsicum annuum l.) in response to cadmium stress and mycorrhizal symbiosis. *J. Agric. Sci. Technol.* 15, 1437–1448. Available at: http://jast.modares.ac.ir/article-23-11530-en.html

Abeed, A. H. A., Ali, M., Ali, E. F., Majrashi, A., and Eissa, M. A. (2021). Induction of catharanthus roseus secondary metabolites when calotropis procera was used as bio-stimulant. *Plants* 10, 1623. doi: 10.3390/plants10081623

Abeed, A. H. A., Eissa, M. A., and Abdel-Wahab, D. A. (2020). Effect of exogenously applied jasmonic acid and kinetin on drought tolerance of wheat cultivars based on morpho-physiological evaluation. *J. Soil Sci. Plant Nutr.* 21, 131–144. doi: 10.1007/s42729-020-00348-1

Abeed, A. H. A., and Salama, F. M. (2022). Attenuating effect of an extract of cd-hyperaccumulator solanum nigrum on the growth and physio-chemical changes of datura innoxia under cd stress. *J. Soil Sci. Plant Nutr* 22. doi: 10.1007/s42729-022-00966-x

Adesemoye, A. O., Obini, M., and Ugoji, E. O. (2008). Comparison of plant growth-promotion with pseudomonas aeruginosa and bacillus subtilis in three vegetables. *Braz. J. Microbiol.* 39, 423–426. doi: 10.1590/s1517-83822008000300003

Aebi, H. (1984). Catalase *in vitro*. *Method Enzymol.* 105, 121–126. doi: 10.1016/S0076-6879(84)05016-3

Ahmad, P., Abdel Latef, A. A., Abd_Allah, E. F., Hashem, A., Sarwat, M., Anjum, N. A., et al. (2016). Calcium and potassium supplementation enhanced growth, osmolyte secondary metabolite production, and enzymatic antioxidant machinery in cadmium-exposed chickpea (Cicer arietinum l.). *Front. Plant Sci.* 7. doi: 10.3389/fpls.2016.00513

Ahmad, F., Ahmad, I., and Khan, M. S. (2008). Screening of free-living rhizospheric bacteria for their multiple plant growth promoting activities. *Microbiol. Res.* 163, 173–181. doi: 10.1016/j.micres.2006.04.001

Ahmad, I., Akhtar, M. J., Zahir, Z. A., Naveed, M., Mitter, B., and Sessitsch, A. (2014). Cadmium-tolerant bacteria induce metal stress tolerance in cereals.Environ. *Sci. pollut. Res.* 21, 11054–11065. doi: 10.1007/s11356-014-3010-9

Aina, R., Labra, M., Fumagalli, P., Vannini, C., Marsoni, M., Cucchi, U., et al. (2007). Thiol-peptide level and proteomic changes in response to cadmium toxicity in oryza sativa l. roots. *Environ. Exp. botany.* 59, 381–392. doi: 10.1016/j.envexpbot.2006.04.010

Anjum, M. A., Sajjad, M. R., Akhtar, N., Qureshi, M. A., Iqbal, A., Rehman, J. A., et al. (2007). Response of cotton to plant growth promoting rhizobacteria (PGPR) inoculation under different levels of nitrogen. *J. Agric. Res.* 45, 135–143. doi: 10.1007/978-3-319-13401-7_1

Arduini, I., Masoni, A., Mariotti, M., and Ercoli, L. (2004). Low cadmium application increase miscanthus growth and cadmium translocation. *Environ. Exp. Botany.* 52, 89–100. doi: 10.1016/j.envexpbot.2004.01.001

Atlas, R. M. (1993). *Handbook of microbiological media* (Boca Raton, FL: CRC Press). doi: 10.1201/ebk1439804063

Bashri, G., and Prasad, S. M. (2015). Indole acetic acid modulates changes in growth, chlorophyll a fluorescence and antioxidant potential of trigonella foenum-graecum l. grown under cadmium stress. *Acta physiologiae plantarum.* 37, 49. doi: 10.1007/s11738-014-1745-z

Basu, S., Rabara, R., and Negi, S. (2017). Towards a better greener future-an alternative strategy using biofertilizers. I: Plant growth promoting bacteria. *Plant Gene.* 12, 43–49. doi: 10.1016/j.plgene.2017.07.004

Bates, L., Waldren, R., and Teare, I. (1973). Rapid determination of free proline for water-stress studies. *Plant Soil.* 39, 205–207. doi: 10.1007/BF00018060

Bazrafshan, E., Zarei, A. A., and Mostafapour, F. K. (2016). Biosorption of cadmium from aqueous solutions by trichoderma fungus: kinetic, thermodynamic, and equilibrium study. *Desalination Water Treat* 57, 14598–14608. doi: 10.1080/19443994.2015.1065764

Bočová, B., Huttová, J., Mistrík, I., and Tamás, L. (2013). Auxin signalling is involved in cadmium-induced glutathione-s-transferase activity in barley root. *Acta physiologiae plantarum.* 35, 2685–2690. doi: 10.1007/s11738-013-1300-3

Bozcuk, S. (1975). "Effect of sodium chloride upon growth and transpiration in statice sp. and pisum sativum l," in *Proceedings of the 3rd MPP meetings*, vol. 75. (Izmir, Turkey: Ege university, Izmir, Turkey), 37–42.

Bruce, R. J., and West, C. A. (1989). Elicitation of lignin biosynthesis and isoperoxidase activity by pectic fragments in suspension cultures of castor bean. *Plant Physiol.* 91, 889–897. doi: 10.1104/pp.91.3.889

Cataldo, D. A., Maroon, M., Schrader, L. E., and Youngs, V. L. (1975). Rapid colorimetric determination of nitrate in plant tissue by nitration of salicylic acid. *Commun. Soil Sci. Plant analysis.* 6, 71–80. doi: 10.1080/00103627509366547

Chaneva, G., Parvanova, P., Tzvetkova, N., and Uzunova, A. (2010). Photosynthetic response of maize plants against cadmium and paraquat impact. *Water Air Soil pollut.* 208, 287–293. doi: 10.1007/s11270-009-0166-x

Chen, L., Luo, S., Xiao, X., Guo, H., Chen, J., Wan, Y., et al. (2010). Application of plant growth-promoting endophytes (PGPE) isolated from solanum nigrum l. for phytoextraction of cd-polluted soils. *Appl. Soil Ecol.* 46, 383–389. doi: 10.1016/j.apsoil.2010.10.003

Chrastil, J. (1976). Colorimetric estimation of indole-3-acetic acid. *Anal. Biochem.* 72, 134–138. doi: 10.1016/0003-2697(76)90514-5

Dasgupta, D., Kumar, K., Miglani, R., Mishra, R., Panda, A. K., and Bisht, S. S. (2021). Microbial biofertilizers: Recent trends and future outlook. *Recent Adv. Microbial Biotechnol.*, 1–26. doi: 10.1016/B978-0-12-822098-6.00001-X

Dawood, M. F. A., and Abeed, A. H. A. (2020). Spermine-priming restrained water relations and biochemical deteriorations prompted by water deficit on two soybean cultivars. *Heliyon* 6, e04038. doi: 10.1016/j.heliyon.2020.e04038

Dawood, M. F. A., Abeed, A. H. A., and Aldaby, E. E. S. (2019). Titanium dioxide nanoparticles model growth kinetic traits of some wheat cultivars under different water regimes. *Plant Physiol. Rep.* 24, 129–140. doi: 10.1007/s40502-019-0437-5

Dell'Amico, E., Cavalca, L., and Andreoni, V. (2008). Improvement of brassica napus growth under cadmium stress by cadmium-resistant rhizobacteria. *Soil Biol. Biochem.* 40, 74–84. doi: 10.1016/j.soilbio.2007.06.024

Diep, C. N., and Hieu, T. N. (2013). Phosphate and potassium solubilizing bacteria from weathered materials of denatured rock mountain, ha tien, kiên giang province Vietnam. *Am. J. Life Sci.* 1, 88–92. doi: 10.11648/j.ajls.20130103.12

Dimkpa, C., Weinand, T., and Asch, F. (2009). Plant–rhizobacteria interactions alleviate abiotic stress conditions. *Plant Cell Env.* 32, 1682–1694. doi: 10.1111/j.1365-3040.2009.02028.x

Ding, Z., Ali, E. F., Almaroai, Y. A., Eissa, M. A., and Abeed, A. H. (2021). Effect of potassium solubilizing bacteria and humic acid on faba bean (Vicia faba l.) plants grown on sandy loam soils. *J. Soil Sci. Plant Nutr.* 21, 791–800. doi: 10.1007/s42729-020-00401-z

Doni, F., Zain, C. R. C. M., Isahak, A., Fathurrahman, F., Anhar, A., Mohamad, W. N. A. W., et al. (2018). A simple, efficient, and farmer-friendly trichoderma-based biofertilizer evaluated with the SRI rice management system. *Organ. Agricul.* 8, 207–223. doi: 10.1007/s13165-017-0185-7

Doroshenko, E. V., Boulygina, E. S., Spiridonova, E. M., Tourova, T. P., and Kravchenko, I. K. (2007). Isolation and characterization of nitrogen-fixing bacteria of the genus azospirillum from the soil of a sphagnum peat bog. *Microbiology* 76, 93–101. doi: 10.1134/S0026261707010134

Dourado, M. N., Martins, P. F., Quecine, M. C., Piotto, F. A., Souza, L. A., Franco, M. R., et al. (2013). Burkholderia sp. SCMS54 reduces cadmium toxicity and promotes growth in tomato. *Ann. Appl. Biol.* 163, 494–507. doi: 10.1111/aab.12066

Downs, M. R., Nadelhoffer, K., Melillo, J. J., and Aber, J. (1993). Foliar and fine root nitrate reductase activity in seedlings of four forest tree species in relation to nitrogen availability. *Trees* 7, 233–236. doi: 10.1007/bf00202079

Eissa, M. A., and Abeed, A. H. (2019). Growth and biochemical changes in quail bush (Atriplex lentiformis (Torr.) s. wats) under cd stress. *Environ. Sci. pollut. Res.* 26, 628–635. doi: 10.1007/s11356-018-3627-1

Ellman, G. L. (1959). Tissue sulfhydryl groups. *Arch. Biochem. Biophys.* 82, 70–77. doi: 10.1016/0003-9861(59)90090-6

Errasquin, E. L., and Vazquez, C. (2003). Tolerance and uptake of heavy metals by trichoderma atroviride isolated from sludge. *Chemosphere* 50, 137–143. doi: 10.1016/s0045-6535(02)00485-x

Etesami, H., and Adl, S. M. (2020). "Plant growth-promoting rhizobacteria (PGPR) and their action mechanisms in availability of nutrients to plants," in *Phyto-microbiome in stress regulation. environmental and microbial biotechnology*. Eds. M. Kumar, V. Kumar and R. Prasad (Singapore: Springer). doi: 10.1007/978-981-15-2576-6_9

Fales, F. (1951). The assimilation and degradation of carbohydrates by yeast cells. *J. Biol. Chem.* 193, 113–124. doi: 10.1016/s0021-9258(19)52433-4

Flohé, L., and Günzler, W. A. (1984). "Methods in enzymology," in *Assays of glutathione peroxidase*. Ed. L. Packer (New York: Academic Press), 114–121.

Fogg, D. N., and Wilkinson, N. T. (1958). The colorimetric determination of phosphorus. *Analyst.* 83, 406. doi: 10.1039/an9588300406

Ghasemkheili, T. F., Ekelund, F., Johansen, J. L., Pirdashti, H., Shiade, S. R.G., Fathi, A., et al. (2022). Ameliorative effects of trichoderma harzianum and rhizosphere soil microbes on cadmium biosorption of barley (Hordeum vulgare l.) in cd-polluted soil. *J. Soil Sci. Plant Nutr.* 22, 527–539. doi: 10.1007/s42729-021-00666-y

Ghelfi, A., Gaziola, S. A., Cia, M. C., Chabregas, S. M., Falco, M. C., Kuser-Falcão, P. R., et al. (2011). Cloning, expression, molecular modelling and docking analysis of glutathione transferase from saccharum officinarum. *Ann. Appl. Biol.* 159, 267–280. doi: 10.1111/j.1744-7348.2011.00491.x

Gouia, H., Ghorbal, M. H., and Meyer, C. (2000). Effects of cadmium on activity of nitrate reductase and on other enzymes of the nitrate assimilation pathway in bean. *Plant Physiol. Biochem.* 38, 629–638. doi: 10.1016/s0981-9428(00)00775-0

Grossmann, K. (2010). Auxin herbicides: current status of mechanism and mode of action. *Pest Manage. Sci.* 66, 113–120. doi: 10.1002/ps.1860

Gupta, A., Mishra, R., Rai, S., Bano, A., Pathak, N., Fujita, M., et al. (2022). Mechanistic insights of plant growth promoting bacteria mediated drought and salt stress tolerance in plants for sustainable agriculture. *Int. J. Mol. Sci.* 23, 3741. doi: 10.3390/ijms23073741

Hafez, M., Elbarbary, T. A., Ibrahim, I., and Abdel-Fatah, Y. (2016). Azotobacter vinelandii evaluation and optimization of Abu tartur Egyptian phosphate ore dissolution. *Saudi J. Pathol. Microbiol.* 1, 80–93. doi: 10.21276/sjpm.2016.1.3.2

Hakla, H. R., Sharma, S., Urfan, M., Yadav, N. S., Rajput, P., Kotwal, D., et al. (2021). Gibberellins target shoot-root growth, morpho-physiological and molecular pathways to induce cadmium tolerance in vigna radiata l. *Agronomy* 11, 896. doi: 10.3390/agronomy11050896

Halhoul, M. N., and Kleinberg, I. (1972). Differential determination of glucose and fructose, and glucose- and fructose-yielding substances with anthrone. *Anal. Biochem.* 50, 337–343. doi: 10.1016/0003-2697(72)90042-5

Hall, J. L., and Williams, L. E. (2003). Transition metal transporters in plants. *J. Exp. Bot.* 54, 2601–2613. doi: 10.1093/jxb/erg303

Hashem, A., Tabassum, B., and Abd Allah, E. F. (2019). Bacillus subtilis: A plant-growth promoting rhizobacterium that also impacts biotic stress. *Saudi J. Biol. Sci.* 26, 1291–1297. doi: 10.1016/j.sjbs.2019.05.004

Havre, G. N. (1961). The flame photometric determination of sodium, potassium and calcium in plant extracts with special reference to interference effects. *Analytica Chimica Acta* 25 (6), 557–6. doi: 10.1016/0003-2670(61)80134-7

Hayat, K., Bundschuh, J., Jan, F., Menhas, S., Hayat, S., Haq, F., et al. (2020). Combating soil salinity with combining saline agriculture and phytomanagement with salt-accumulating plants. *Crit. Rev. Environ. Sci. Technol.* 50, 1085–1115. doi: 10.1080/10643389.2019.1646087

Herliana, O., Soesanto, L., and Mawadah, E. (2018). Phytobioremediation of cadmium-contaminated soil using combination of ipomoea reptans poir and trichoderma sp. and its effect on spinach growth and yield. *J. Degraded Min. Lands Manag.* 6, 1519–1526. doi: 10.15243/jdmlm.2018.061.1519

Hermosa, R., Viterbo, A., Chet, I., and Monte, E. (2012). Plant-beneficial effects of trichoderma and of its genes. *Microbiology* 158, 17–25. doi: 10.1099/mic.0.052274-0

Holmgren, P., Jarvis, P. G., and Jarvis, M. S. (1965). Resistances to carbon dioxide and water vapour transfer in leaves of different plant species. *Physiol. Plant* 18, 527–573. doi: 10.1111/j.1399-3054.1965.tb06917.x

Hoseinzadeh, S., Shahabivand, S., and Aliloo, A. A. (2017). Toxic metals accumulation in trichoderma asperellum and t. harzianum. *Microbiology* 86, 728–736. doi: 10.1134/s0026261717060066

Hui, F., Liu, J., Gao, Q., and Lou, B. (2015). Piriformospora indica confers cadmium tolerance in nicotiana tabacum. *J. Environ. Sci.* 37, 184–191. doi: 10.1016/j.jes.2015.06.005

Ibrahim, A. B. M., Zidan, A. S. A., Aly, A. A. M., Mosbah, H. K., and Mahmoud, G. A.-E. (2020). Mesoporous cadmium sulfide nanoparticles derived from a new cadmium anthranilato complex: Characterization and induction of morphological abnormalities in pathogenic fungi. *Appl. Organometal Chem.* 34, e5391. doi: 10.1002/aoc.5391

Jagota, S. K., and Dani, H. M. (1982). A new colorimetric technique for the estimation of vitamin c using folin phenol reagent. *Anal. Biochem.* 127, 178–182. doi: 10.1016/0003-2697(82)90162-2

Jia, L., Liu, Z. L., Chen, W., and He, X. Y. (2012). Stimulative effect induced by low-concentration cadmium in lonicera japonica thunb. *Afr J. Microbiol. Res.* 6, 826–833. doi: 10.5897/AJMR11.1337

Jia, L., Liu, Z., Chen, W., Ye, Y., Yu, S., and He, X. (2015). Hormesis effects induced by cadmium on growth and photosynthetic performance in a hyperaccumulator, lonicera japonica thunb. *J. Plant Growth Regulat.* 34, 13–21. doi: 10.1007/s00344-014-9433-1

Joner, E. J., Briones, R., and Leyval, C. (2000). Metal-binding capacity of arbuscular mycorrhizal mycelium. *Plant Soil.* 226, 227–234. doi: 10.1023/A:1026565701391

Kang, S. M., Radhakrishnan, R., Lee, K. E., You, Y. H., Ko, J. H., Kim, J. H., et al. (2015). Mechanism of plant growth promotion elicited by bacillus sp.LKE15 in oriental melon. *Acta Agric. Scand. Sect. B Soil Plant Sci.* 65, 637–647. doi: 10.1080/09064710.2015.1040830

Kapoor, R., and Bhatnagar, A. K. (2007). Attenuation of cadmium toxicity in mycorrhizal celery (Apium graveolens l.). *World J. Microbiol. Biotechnol.* 23, 1083–1089. doi: 10.1007/s11274-006-9337-8

Khan, N., Ali, S., Shahid, M. A., Mustafa, A., Sayyed, R. Z., and Curá, J. A. (2021). Insights into the interactions among roots, rhizosphere, and rhizobacteria for improving plant growth and tolerance to abiotic stresses: A review. *Cells* 10, 1551. doi: 10.3390/cells10061551

Khanghahi, M. Y., Pirdashti, H., Rahimian, H., Nematzadeh, G., and Sepanlou, M. G. (2018). Potassium solubilising bacteria (KSB) microbed from rice paddy soil: from isolation, identification to K use efficiency. *Symbiosis* 76, 13e23. doi: 10.1007/s13199-017-0533-0

Khan, A. R., Ullah, I., Waqas, M., Park, G. S., Khan, A. L., Hong, S. J., et al. (2017). Host plant growth promotion and cadmium detoxification in solanum nigrum, mediated by endophytic fungi. *Ecotoxicol. Environ. safety.* 136, 180–188. doi: 10.1016/j.ecoenv.2016.03.014

Khan, M. S., Zaidi, A., Wani, P. A., and Oves, M. (2009). Role of plant growth promoting rhizobacteria in the remediation of metal contaminated soils. *Environ. Chem. Lett.* 7, 1–19. doi: 10.1007/s10311-008-0155-0

Khare, S., Singh, N. B., Singh, A., Amist, N., Azim, Z., and Yadav, R. K. (2022). Phytochemicals mitigation of brassica napus by IAA grown under cd and Pb toxicity and its impact on growth responses of anagallis arvensis. *J. Biotechnol.* 343, 83–95. doi: 10.1016/j.jbiotec.2021.12.001

Khyade, M. S., and Vaikos, N. P. (2009). Phytochemical and antibacterial properties of leaves of alstonia scholaris r. *Br. Afr. J. Biotechnol.* 8, 6434–6436. doi: 10.5897/AJB2009.000-9489

Kim, J., and Rees, D. C. (1994). Nitrogenase and biological nitrogen fixation. *Biochemistry* 33, 389–397. doi: 10.1021/bi00168a001

Koch, K. (2004). Sucrose metabolism: regulatory mechanisms and pivotal roles in sugar sensing and plant development. *Curr. Opin. Plant Biol.* 7, 235e246. doi: 10.1016/j.pbi.2004.03.014

Kofalvi, S. A., and Nassuth, A. (1995). Influence of wheat streak mosaic virus infection phenyl propanoid metabolism and the accumulation of phenolics and lignin in wheat. *Physiol. Mol. Plant Pathol.* 47, 365–377. doi: 10.1006/pmpp.1995.1065

Krizek, D. T., Kramer, G. F., Upadhyaya, A., and Mirecki, R. M. (1993). UV-B response to cucumber seedlings grown under metal halide and high pressure sodium/deluxe lamps. *Physiol. Plant* 88, 350–358. doi: 10.1111/j.1399-3054.1993.tb05509.x

Kuan, K. B., Othman, R., Rahim, K. A., and Shamsuddin, Z. H. (2016). Plant growth-promoting rhizobacteria inoculation to enhance vegetative growth, nitrogen fixation and nitrogen remobilisation of maize under greenhouse conditions. *PLoS One* 11, e0152478. doi: 10.1371/journal.pone.0152478

Kubicek, C. P., Bissett, J., Druzhinina, I., Kullnig-Gradinger, C., and Szakacs, G. (2003). Genetic and metabolic diversity of trichoderma: a case study on south-East Asian isolates. *Fungal Genet. Biol.* 38, 310–319. doi: 10.1016/S1087-1845(02)00583-2

Kumar, V., Behl, R. K., and Narula, N. (2001). Establishment of phosphate solubilizing strains of azotobacter chroococcum in the rhizosphere and their effect on wheat cultivars under greenhouse conditions. *Microbiol. Res.* 156, 87–93. doi: 10.1078/0944-5013-00081

Kumar, K., and Khan, P. (1983). Age-related changes in catalase and peroxidase activities in the excised leaves of Eleusine coracana Gaertn. cv PR 202 during senescence. *Experimental Gerontology* 18 (5), 409–417. doi: 10.1016/0531-5565(83)90019-0

Kumar, V., Srivastava, A., Jain, L., Chaudhary, S., Kaushal, P., and Soni, R. (2022). Harnessing the potential of genetically improved bioinoculants for sustainable agriculture: Recent advances and perspectives. *Trends Appl. Microbiol. Sustain. Economy*, 319–341. doi: 10.1016/B978-0-323-91595-3.00007-0

Kumar, S., and Trivedi, P. K. (2016). Heavy metal stress signaling in plants. *Plant Metal Interaction*, 585–603. doi: 10.1016/b978-0-12-803158-2.00025-4

Lamhamdi, M., Bakrim, A., Aarab, A., Lafont, R., and Sayah, F. (2011). Lead phytotoxicity on wheat (Triticum aestivum l.) seed germination and seedlings growth. *Comptes rendus biologies.* 334, 118–126. doi: 10.1016/j.crvi.2010.12.006

Lang, C. A. (1958). Simple microdetermination of kjeldahl nitrogen in biological materials. *Anal. Chem.* 30, 1692–1694. doi: 10.1021/ac60142a038

Larcher, W. (2003). *Physiological plant ecology: ecophysiology and stress physiology of functional groups* (Berlin, Germany: Springer-Verlag).

Li, J., Chang, Y., Al-Huqail, A. A., Ding, Z., Al-Harbi, M. S., Ali, E. F., et al. (2021). Effect of manure and compost on the phytostabilization potential of heavy metals by the halophytic plant wavy-leaved saltbush. *Plants* 10. doi: 10.3390/plants10102176

Lichtenthaler, H. K. (1987). Chlorophyll and carotenoids pigments of photosynthetic biomembranes. *Methods Enzymols.* 148, 350–382. doi: 10.1016/0076-6879(87)48036-1

Lim, M.-S., Yeo, I. W., Roh, Y., Lee, K.-K., and Jung, M. C. (2008). Arsenic reduction and precipitation by shewanella sp.: batch and column tests. *Geosci. J.* 12, 151–157. doi: 10.1007/s12303-008-0016-7

Lima, A.d.-F., Ferreira de Moura, G., Barbosa de Lima, M. A., Mendes de Souza, P., Alves da Silva, C. A., de Campos Takaki, G. M., et al. (2011). Role of the morphology and polyphosphate in trichoderma harzianum related to cadmium removal. *Molecules* 16, 2486–2500. doi: 10.3390/molecules16032486

Li, M., Ma, G.-s., Lian, H., Su, X.-l., Tian, Y., Huang, W.-k, et al. (2019). The effects of trichoderma on preventing cucumber fusarium wilt and regulating cucumber physiology. *J. Integr. Agric.* 18, 607–617. doi: 10.1016/S2095-3119(18)62057-X

Lin, R., Wang, X., Luo, Y., Du, W., Guo, H., and Yin, D. (2007). Effects of soil cadmium on growth, oxidative stress and antioxidant system in wheat seedlings (Triticum aestivum l.). *Chemosphere* 69, 89–98. doi: 10.1016/j.chemosphere.2007.04.041

Liu, Z. L., Chen, W., and He, X. Y. (2012). Cadmium-induced physiological response in lonicera japonica thunb. *CLEAN Soil Air Water.* 41, 478–484. doi: 10.1002/clen.201200183

Liu, Z., He, X., and Chen, W. (2011). Effects of cadmium hyperaccumulation on the concentrations of four trace elements in lonicera japonica thunb. *Ecotoxicology* 20, 698–705. doi: 10.1007/s10646-011-0609-1

Lowry, O. H., Rosebrough, N. J., Farr, A. L., and Randall, R. J. (1951). Protein measurement with the folin phenol reagent. *J. Biol. Chem.* 193, 291–297. doi: 10.1016/S0021-9258(19)52451-6

Lu, Q., Xu, Z., Xu, X., Liu, L., Liang, L., Chen, Z., et al. (2019). Cadmium contamination in a soil-rice system and the associated health risk: an addressing concern caused by barium mining. *Ecotoxicol. Environ. safety.* 183, 109590. doi: 10.1016/j.ecoenv.2019.109590

Madhava Rao, K. V., and Sresty, T. V. (2000). Antioxidative parameters in seedlings of pigeon pea (Cajanus cajan l. millspaugh) in response to zn and Ni stresses. *Plant Sci.* 157, 113–128. doi: 10.1016/s0168-9452(00)00273-9

Mahmoud, G. A.-E. (2021). "Microbial scavenging of heavy metals using bioremediation strategies," in *Rhizobiont in bioremediation of hazardous waste*. Eds. V. Kumar, R. Prasad and M. Kumar (Singapore: Springer). doi: 10.1007/978-981-16-0602-1_12

Mahmoud, G. A.-E., Ibrahim, A. B. M., and Mayer, P. (2020). Zn(II) and Cd(II) thiosemicarbazones for stimulation/inhibition of kojic acid biosynthesis from aspergillus flavus and the fungal defense behavior against the metal complexes' excesses. *JBIC J. Biol. Inorganic Chem* 25. doi: 10.1007/s00775-020-01802-2

Mahmoud, G. A.-E., and Mostafa, H. H. A. (2017). Statistical optimization as a powerful tool for indole acetic acid production by fusarium oxysporum. *Eur. J. Biol. Res.* 7, 315–323. doi: 10.5281/zenodo.1012348

Maksymiec, W., Wojcik, M., and Krupa, Z. (2007). Variation in oxidative stress and photochemical activity in arabidopsis thaliana leaves subjected to cadmium and excess copper in the presence or absence of jasmonate and ascorbate. *Chemosphere* 66, 421–427. doi: 10.1016/j.chemosphere.2006.06.025

Marchel, M., Kaniuczak, J., Hajduk, E., and Właśniewski, S. (2018). Response of oat (Avena sativa) to the addition cadmium to soil inoculationwith the genus trichoderma fungi. *J. Elem.* 23, 471–482. doi: 10.5601/jelem.2017.22.1.1391

Minguez-Mosquera, M., Jaren-Galan, M., and Garrido-Fernandez, J. (1993). Lipoxygenase activity during pepper ripening and processing of paprika. *Phytochemistry* 32, 1103–1108. doi: 10.1016/S0031-9422(00)95073-8

Misra, H. P., and Fridovich, I. (1972). The role of superoxide anion in the autoxidation of epinephrine and a simple assay for superoxide dismutase. *J. Biol. Chem.* 247, 1972–3170. doi: 10.1016/S0021-9258(19)45228-9

Mir, A. R., Alam, P., and Hayat, S. (2022). Auxin regulates growth, photosynthetic efficiency and mitigates copper induced toxicity via modulation of nutrient status, sugar metabolism and antioxidant potential in Brassica juncea. *Physiol. Biochem.* 185, 244–259. doi: 10.1016/j.plaphy.2022.06.006

Mohsenzade, F., and Shahrokhi, F. (2014). Biological removing of cadmium from contaminated media by fungal biomass of trichoderma species. *J. Environ. Health Sci. Eng.* 12, 102. doi: 10.1186/2052-336X-12-102

Moore, S., and Stein, W. H. (1948). Photometric ninhydrin method for use in the chromatography of amino acids. *J. Biol. Chem.* 176, 367–388. doi: 10.1016/S0021-9258(18)51034-6

Mukherjee, S. P., and Choudhuri, M. A. (1983). Implications of water stress-induced changes in the levels of endogenous ascorbic acid and hydrogen peroxide in vigna seedlings. *Physiologia plantarum* 58, 166–170. doi: 10.1111/j.1399-3054.1983.tb04162.x

Naggar, Y. A., Naiem, E., Mona, M., Giesy, J. P., and Seif, A. (2014). Metals in agricultural soils and plants in Egypt. *Toxicol. Environ. Chem.* 96, 730–742. doi: 10.1080/02772248.2014.984496

Nahar, K., Hasanuzzaman, M., Alam, M. M., Rahman, A., Suzuki, T., and Fujita, M. (2016). Polyamine and nitric oxide crosstalk: antagonistic effects on cadmium toxicity in mung bean plants through upregulating the metal detoxification, antioxidant defense and methylglyoxal detoxification systems. *Ecotoxicol. Environ. safety.* 126, 245–255. doi: 10.1016/j.ecoenv.2015.12.026

Nair, A., Juwarkar, A. A., and Devotta, S. (2008). Study of speciation of metals in an industrial sludge and evaluation of metal chelators for their removal. *J. Haz. Mater.* 52, 545–553. doi: 10.1016/j.jhazmat.2007.07.054

Nakano, Y., and Asada, K. (1981). Hydrogen peroxide is scavenged by ascorbate-specific peroxidase in spinach chloroplasts. *Plant Cell Physiol.* 22, 867–880. doi: 10.1093/oxfordjournals.pcp.a076232

Nongmaithem, N., Roy, A., and Bhattacharya, P. M. (2016). Screening of trichoderma isolates for their potential of biosorption of nickel and cadmium. *Braz. J. Microbiol.* 47, 305–313. doi: 10.1016/j.bjm.2016.01.008

Noor, I., Sohail, H., Sun, J., Nawaz, M. A., Li, G., Hasanuzzaman, M., et al. (2022). Heavy metal and metalloid toxicity in horticultural plants: Tolerance mechanism and remediation strategies. *Chemosphere* 303, 135196. doi: 10.1016/j.chemosphere.2022.135196

Ortiz, A., and Sansinenea, E. (2022). The role of beneficial microorganisms in soil quality and plant health. *Afr J. Biotechnol.* 14 (9), 5358.

Pande, A., Pandey, P., Mehra, S., Singh, M., and Kaushik, S. (2022). Phenotypic and genotypic characterization of phosphate solubilizing bacteria and their efficiency on the growth of maize. *J. Genetic Engineering Biotechnol.* 15 (2), 379–391. doi: 10.1016/j.jgeb.2017.06.005

Patel, J., Parmar, P., Dave, B., and Subramanian, R. B. (2012). Antioxidative and physiological studies on colocasia esculentum in response to arsenic stress. *Afr J. Biotechnol.* 11, 16241–16246. doi: 10.5897/AJB11.3263

Patil, S. V., Mohite, B. V., Patil, C. D., Koli, S. H., Borase, H. P., and Patil, V. S. (2020). Azotobacter. In beneficial microbes in agro-ecology: Bacteria and fungi. Elsevier. 397–426. doi: 10.1016/B978-0-12-823414-3.00019-8

Phillips, K. A., Skirpan, A. L., Liu, X., Christensen, A., Slewinski, T. L., Hudson, C., et al. (2011). Vanishing tassel encodes a grass-specific tryptophan aminotransferase required for vegetative and reproductive development in maize. *Plant Cell.* 23, 550–566. doi: 10.1105/tpc.110.075267

Queiroz, C., Mendes Lopes, M. L., Fialho, E., and Valente-Mesquita, V. L. (2008). Polyphenol oxidase: characteristics and mechanisms of browning control. *Food Rev. Int.* 24, 361–375. doi: 10.1080/87559120802089332

Radhakrishnan, R., and Lee, I. J. (2016). Gibberellins producing bacillus methylotrophicus KE2 supports plant growth and enhances nutritional metabolites and food values of lettuce. *Plant Physiol. Biochem.* 109, 181–189. doi: 10.1016/j.plaphy.2016.09.018

Raza, A., Ashraf, F., Zou, X., Zhang, X., and Tosif, H. (2020). "Plant adaptation and tolerance to environmental stresses: Mechanisms and perspectives," in *Plant ecophysiology and adaptation under climate change: Mechanisms and perspectives I*. Ed. M. Hasanuzzaman (Singapore: Springer). doi: 10.1007/978-981-15-2156-0_5

Rojas-Solis, D., Vences-Guzmán, M.Á., Sohlenkamp, C., and Santoyo, G. (2020). Antifungal and plant growth–promoting bacillus under saline stress modify their membrane composition. *J. Soil Sci. Plant Nutr.* 20, 1549–1559. doi: 10.1007/s42729-020-00246-6

Sánchez-Rodríguez, E., Moreno, D. A., Ferreres, F., Rubio-Wilhelmi, M. M., and Ruiz, J. M. (2011). Differential responses of five cherry tomato varieties to water stress: changes on phenolic metabolites and related enzymes. *Photochem* 72, 723–729. doi: 10.1016/j

Schlegel, H. G. (1956). Die verwertung organischer saurenduch chlorella in licht. *Planta (Berl).* 47, 510–526. doi: 10.1007/bf01935418

Shahabivand, S., Parvaneh, A., and Aliloo, A. A. (2017). Root endophytic fungus piriformospora indica affected growth, cadmium partitioning and chlorophyll fluorescence of sunflower under cadmium toxicity. *Ecotoxicol. Environ. safety.* 145, 496–502. doi: 10.1016/j.ecoenv.2017.07.064

Sheng, M., Tang, M., Chan, H., Yang, B., Zhang, F., and Huang, Y. (2008). Influence of arbuscular mycorrhizae on photosynthesis and water status of maize plants under salt stress. *Mycorrhiza* 18, 287–296. doi: 10.1007/s00572-008-0180-7

Sheng, X. F., and Xia, J. J. (2006). Improvement of rape (Brassica napus) plant growth and cadmium uptake by cadmium-resistant bacteria. *Chemosphere* 64, 1036–1042. doi: 10.1016/j.chemosphere.2006.01.051

Silveira, J. A. G., Araújo, S. A. M., Lima, J. P. M. S., and Viégas, R. A. (2009). Roots and leaves display contrasting osmotic adjustment mechanisms in response to NaCl-salinity in atriplex nummularia. *Environ. Exp. Botany.* 66, 1–8. doi: 10.1016/j.envexpbot.2008.12.015

Singh, G., Biswas, D. R., and Marwaha, T. S. (2010). Mobilization of potassium from waste mica by plant growth promoting rhizobacteria and its assimilation by maize (Zea mays) and wheat (Triticum aestivum): a hydroponics study under phytotron growth chamber. *J. Plant Nutr.* 33, 1236–1251. doi: 10.1080/01904161003765760

Singh, B. R., and Steinnes, E. (2020). Soil and water contamination by heavy metals. *Soil Sci.* (Boca Raton, Florida: CRC Press), 233–271. doi: 10.1201/9781003070184-6

Slatyer, R. O., and Markus, D. K. (1968). Plant-water relationships. soil science *Soil Sci.* 106, 478. doi: 10.1097/00010694-196812000-00020

Sobkowiak, R., and Deckert, J. (2003). Cadmium-induced changes in growth and cell cycle gene expression in suspension-culture cells of soybean. *Plant Physiol. Biochem.* 41, 767–772. doi: 10.1016/S0981-9428(03)00101-3

Somashekaraiah, B. V., Padmaja, K., and Prasad, A. R. K. (1992). Phytotoxicity of cadmium ions on germinating seedlings of mung bean (Phaseolus vulgaris): Involvement of lipid peroxides in chlorphyll degradation. *Physiologia Plantarum.* 85, 85–89. doi: 10.1111/j.1399-3054.1992.tb05267.x

Sykłowska-Baranek, K., Pietrosiuk, A., Naliwajski, M. R., Kawiak, A., Jeziorek, M., Wyderska, S., et al. (2012). Effect of l-phenylalanine on PAL activity and production of naphthoquinonepigments in suspension cultures of arnebia euchroma (Royle) johnst. *In Vitro Cell Dev. Biol. Plant* 48, 555–564. doi: 10.1007/s11627-012-9443-2

Tatiana, Z., Yamashita, K., and Matsumoto, H. (1999). Iron deficiency induced changes in ascorbate content and enzyme activities related to ascorbate metabolism in cucumber root. *Plant Cell Physiol.* 40, 273–280. doi: 10.1093/oxfordjournals.pcp.a029538

USDA, FAO (2008). *Oil seed situation and outlook.* (Washington, DC: USDA Crop Stat., Agric. Stat.)

Van Handel, E. (1968). Direct microdetermination of sucrose. *Anal. Biochem.* (Washington, DC: USDA Crop Stat., Agric. Stat.) 22, 280–283. doi: 10.1016/0003-2697(68)90317-5

Wani, P. A., and Khan, M. S. (2010). Bacillus species enhance growth parameters of chickpea (Cicer arietinum l.) in chromium stressed soils. *Food Chem. Toxicol.* 48, 3262–3267. doi: 10.1016/j.fct.2010.08.035

Widawati, S. (2018). The effect of plant growth promoting rhizobacteria (PGPR) on germination and seedling growth of sorghum bicolor l. *Moench. IOP Conf. Series: Earth Environ. Sci.* 166, 12022. doi: 10.1088/1755-1315/166/1/012022

Wu, C. H., Wood, T. K., Mulchandani, A., and Chen, W. (2006). Engineering plant-microbe symbiosis for rhizoremediation of heavy metals. *Appl. Environ. Microbiol.* 72, 1129–1134. doi: 10.1128/aem.72.2.1129-1134.2006

Wu, F., Zhang, G., and Dominy, P. (2003). Four barley genotypes respond differently to cadmium: lipid peroxidation and activities of antioxidant capacity. *Environ. Exp. botany.* 50, 67–78. doi: 10.1016/s0098-8472(02)00113-2

Yaashikaa, P. R., Kumar, P. S., Jeevanantham, S., and Saravanan, R. (2022). A review on bioremediation approach for heavy metal detoxification and accumulation in plants. *Environ. pollut.* 301, 119035. doi: 10.1016/j.envpol.2022.119035

Yamazaki, S., Ueda, Y., Mukai, A., Ochiai, K., and Matoh, T. (2018). Rice phytochelatin synthases os PCS 1 and os PCS 2 make different contributions to cadmium and arsenic tolerance. *Plant Direct.* 2, e00034. doi: 10.1002/pld3.34

Ying, R. R., Qiu, R. L., Tang, Y. T., Hu, P. J., Qiu, H., Chen, H. R., et al. (2010). Cadmium tolerance of carbon assimilation enzymes and chloroplast in Zn/Cd hyperaccumulator picris divaricata. *J. Plant Physiol.* 167, 81–87. doi: 10.1016/j.jplph.2009.07.005

Zafar, S., Aqil, F., and Ahmad, I. (2007). Metal tolerance and biosorption potential of filamentous fungi isolated from metal contaminated agricultural soil. *Biores. Technol.* 98, 2557–2561. doi: 10.1016/j.biortech.2006.09.051

Zaidi, S., Usmani, S., Singh, B. R., and Musarrat, J. (2006). Significance of bacillus subtilis strain SJ 101 as a bioinoculant for concurrent plant growth promotion and nickel accumulation in brassica juncea. *Chemosphere* 64, 991–997. doi: 10.1016/j.chemosphere.2005.12.057

Zainab, N., Amna,, Khan, A. A., Azeem, M. A., Ali, B., Wang, T., et al. (2021). PGPR-mediated plant growth attributes and metal extraction ability of sesbania sesban l. @ in industrially contaminated soils. *Agronomy* 11, 1820. doi: 10.3390/agronomy11091820

Zhou, W., and Qiu, B. (2005). Effects of cadmium hyperaccumulation on physiological characteristics of sedum alfredii hance (Crassulaceae). *Plant Sci.* 169, 737–745. doi: 10.1016/j.plantsci.2005.05.030

Zhu, T., Li, L., Duan, Q., Liu, X., and Chen, M. (2020). Progress in our understanding of plant responses to the stress of heavy metal cadmium. *Plant Signaling Behavior.* 16, 1836884. doi: 10.1080/15592324.2020.1836884

Zorzi, C. Z., Garske, R. P., Flôres, S. H., and Thys, R. C. S. (2020). Sunflower protein concentrate: A possible and beneficial ingredient for gluten-free bread. *Innovative Food Sci. Emerging Technologies.* 66, 102539. doi: 10.1016/j.ifset.2020.102539

frontiers | Frontiers in Plant Science

TYPE Original Research
PUBLISHED 24 November 2022
DOI 10.3389/fpls.2022.1038163

OPEN ACCESS

EDITED BY
Muhammad Ali Raza,
Gansu Academy of Agricultural Sciences (CAAS), China

REVIEWED BY
Shahbaz Khan,
National Agricultural Research Center, Pakistan
Visha Kumari Venugopalan,
Central Research Institute for Dryland Agriculture (ICAR), India

*CORRESPONDENCE
Kulvir Singh
kulvir@pau.edu
Ayman El Sabagh
aymanelsabagh@gmail.com

SPECIALTY SECTION
This article was submitted to Plant Abiotic Stress, a section of the journal Frontiers in Plant Science

RECEIVED 06 September 2022
ACCEPTED 27 October 2022
PUBLISHED 24 November 2022

CITATION
Singh K, Singh P, Singh M, Mishra SK, Iqbal R, Al-Ashkar I, Habib-ur-Rahman M and El Sabagh A (2022) Sub-surface drip fertigation improves seed cotton yield and monetary returns.
Front. Plant Sci. 13:1038163.
doi: 10.3389/fpls.2022.1038163

Sub-surface drip fertigation improves seed cotton yield and monetary returns

Kulvir Singh[1]*, Prabhsimran Singh[1], Manpreet Singh[2], Sudhir Kumar Mishra[1], Rashid Iqbal[3], Ibrahim Al-Ashkar[4], Muhammad Habib-ur-Rahman[5] and Ayman El Sabagh[6]*

[1]Regional Research Station, Punjab Agricultural University, Faridkot, Punjab, India, [2]Punjab Agricultural University, Regional Research Station, Abohar, Punjab, India, [3]Department of Agronomy, Faculty of Agriculture and Environment, The Islamia University of Bahawalpur, Bahawalpur, Pakistan, [4]Department of Plant Production, College of Food and Agriculture, King Saud University, Riyadh, Saudi Arabia, [5]Crop Science, Institute of Crop Science and Resource Conservation (INRES), University of Bonn, Bonn, Germany, [6]Department of Agronomy, Faculty of Agriculture, Kafrelsheikh University, Kafrelsheikh, Egypt

Surface flood (SF) method is used to irrigate cotton in India, which results in huge wastage of water besides leaching of nutrients. This necessitates the adoption of efficient management strategies to save scarce water without compromising the yield. Therefore, a 2-year field investigation was conducted under two climatic regimes (Faridkot and Abohar) to study the effect of sub-surface drip fertigation (SSDF) on seed cotton yield (SCY), water productivity, nitrogen use efficiency (NUE), and economic parameters in comparison with SF and surface drip fertigation (SDF). The field experiment had a total of eight treatments arranged in a randomized complete block design. Three levels of sub-surface drip irrigation [(SSDI); *i.e.*, 60%, 80%, and 100% of crop evapotranspiration (ETc)] and two N fertigation levels [100% recommended dose of nitrogen (RDN; *i.e.*, 112.5 kg N ha^{-1}) and 75% RDN] made up six treatments, while SF (Control 1) and SDF at 80% ETc (Control 2), both with 100% of RDN, served as the controls. Among irrigation regimes, the SSDI levels of 80% ETc and 100% ETc recorded 18.7% (3,240 kg ha^{-1}) and 21.1% (3,305 kg ha^{-1}) higher SCY compared with SF (2,728 kg ha^{-1}). Water use efficiency under SF (57.0%) was reduced by 34.2%, 40.8%, and 38.2% compared with SSDI's 60 (76.5%), 80 (80.3%), and 100% ETc (78.8%), respectively. Among fertigation levels, NUE was higher by 19.2% under 75% (34.1 kg SCY kg^{-1} N) over 100% RDN (28.6 kg SCY kg^{-1} N), but later it also registered 11.9% higher SCY, indicating such to be optimum for better productivity. SSDF at 80% ETc along with 112.5 kg N ha^{-1} recorded 26.6% better SCY (3455 kg ha^{-1}) and 18.5% higher NUE (30.7 kg SCY kg^{-1} N) over SF. These findings demonstrate that the application of

SSDF could save irrigation water, enhance SCY, and improve the farmers' returns compared with SF. Therefore, in northwestern India, SSDF at 80% ETc along with 112.5 kg N ha^{-1} could be a novel water-savvy concept which would be immensely helpful in enhancing cotton productivity.

KEYWORDS

bio-physical water productivity, drip fertigation, economic water productivity, nitrogen use efficiency, surface flood method, water use efficiency

Introduction

Cotton (*Gossypium hirsutum* L.) is among the most important cash crops being cultivated in India and sustains the nation's largest organized textile industry. However, India accounts for the greatest area (13.4 m ha) and highest production of cotton in the world (37.1 million bales of 170 kg each), but its mean productivity (487 kg lint ha^{-1}) is very low (Anonymous, 2021). More than 65% of Indian cotton is rainfed, with the exception of the northwestern cotton belt (constituted by Punjab, Haryana, and Rajasthan states), where irrigated cotton is cultivated. In Punjab, cotton is mainly grown in the southwestern districts which are characterized by lightly textured soils, brackish groundwater, and arid climate with limited availability of canal water for irrigation (Singh et al., 2018). Here cotton crop is traditionally irrigated through the surface flood (SF) method at four to six growth stages with 75 mm of water required for a single irrigation. Irrigation for agriculture has been the leading consumer of water on the earth, so the gradual decline of water resources is posing a serious concern on the agriculture sector and insisting upon how to operate in a sustainable manner under the ever-growing concern on water scarcity for agrarian usage (Sinha et al., 2017).

This necessitates the adoption of improved and efficient water application strategies to increase the crop productivity with better irrigation management (FernÃ¡ndez et al., 2020; Mishra et al., 2021). To achieve food and fiber security for the ever-increasing population, a globally irrigated agricultural area needs to be increased by 20%, with about 40% increase in irrigated crop yield by year 2025 (Hashem et al., 2018). Different irrigation systems such as surface drip irrigation (SDI), sub-surface drip irrigation (SSDI), and sprinkler irrigation have been found to improve the irrigation efficiency (Ines et al., 2006). Drip fertigation exposes the crop to a certain level of water stress during crop growth stages without sacrificing the crop yield (Pereira et al., 2012) besides enhancing the water use efficiency and uptake of nutrients (Kaur and Brar, 2016; Gondal et al., 2021). In cotton, drip irrigation (DI) resulted in 18%–42% saving of water over furrow irrigation (Ibragimov et al., 2007) and up to 62.1% saving over SF method (Singh et al., 2018).

Nowadays, SSDI is also gaining importance due to more efficient usage of water since there is minimum surface runoff and evaporation from the soil surface as laterals having drippers are buried under the soil surface at regular spacing (Mchugh et al., 2008). SSDI can play a greater role in water management throughout arid and semi-arid regions by applying water and nutrients more precisely to the field in both position and quantity. In SSDI, applied water and nutrients result in higher use efficiency as the topsoil layer is mostly dry and wetting occurs only beneath the soil surface while soil evaporation is controlled (Ben-Gal et al., 2004). SSDI resulted in 20% water saving in organic olive over the conventional method (Martinez and Reca, 2014; Rahim et al., 2020) and 10% higher water use efficiency (WUE) over SDI in cotton (Roopashree et al., 2016). SSDI reduces evaporation from the soil surface compared with SDI and SF because water is delivered directly to the roots as laterals are located within the root zone, thus minimizing water loss. Both SDI and SSDI could be exploited on a large scale especially in northwestern India because this region is constituted by arid and semi-arid areas with a limited supply of irrigation water. Moreover, the groundwater here is brackish and thus unfit for irrigation purposes, which makes this zone ideal for exploiting drip irrigation (Singh et al., 2020).

Fertilizer use efficiency in India can be specifically enhanced greatly over the prevalent but inefficient method of fertilizer application by broadcasting (Harish et al., 2017). Drip-fertigated cotton not only exhibits enhanced N uptake over furrow-irrigated crops but also curbs the energy and labor costs for nutrient application as no extra equipment, labor, and machinery are required (Sidhu et al., 2019). Thus, the SSDF technique can be exploited to realize more crops per drop of water without sacrificing the seed cotton yield SCY besides sustaining cotton productivity. Moreover, fertilizers are applied in split doses under the fertigation system, thus readily facilitating the absorption of nutrients by the crop plants with a minimal problem of nutrient fixation in the soil (Janat, 2008; Imran et al., 2021).

So far, the feasibility of SSDF in cotton agro-ecosystems has been less evaluated in India, and the present study offers an opportunity to fill this gap in the extant agricultural scenario. We hypothesize that SSDF would improve the cotton productivity and also save a huge quantity of water over the conventional practice (surface flood method of irrigation and urea broadcasting) prevalent in India.

Thus, the present study investigated the effects of SSDF at varying irrigation and nitrogen levels on SCY, fiber quality, and water productivity indices so as to evaluate study gaps with the following objectives: (1) to assess the effect of SSDI and N fertigation on the growth, yield parameters, and SCY of *Bt* cotton in comparison with the SDI/SF method, (2) to compare the bio-physical water productivity, water use efficiency, and NUE of *Bt* cotton grown under different irrigation regimes and N levels, and (3) to recommend the most efficient SSDF level to maximize the production of quality seed cotton based on monetary evaluation. The present investigation therefore implements an experimental approach to explore this enunciated research query and produce data-based information for its implementation on a large scale under arid climates. The focus was to optimize the SSDF for increasing the yield and water productivity so as to achieve a higher SCY with the additional saving of water and N fertilizer.

Materials and methods

Location and weather

A 2-year field trial was conducted at regional research stations (RRS) of Punjab Agricultural University located at Faridkot and Abohar during the summer seasons (April–November) of 2019 and 2020. These Research Stations are located, 96 km apart, in two distinct agro-climatic locations of the southwestern cotton belt of Punjab. The experimental site of RRS Faridkot lies in agro-climatic zone IV at an altitude of 211 m above mean sea level (AMSL) and latitude of 30°40′ N and longitude of 74°44′ E, whereas the experimental site of RRS Abohar lies in agro-climatic zone V at an altitude of 186 m AMSL and latitude of 30°08′ N and longitude of 74°12′ E. Both of the experimental locations fall in the Trans Gangetic plain zone of India with the climate characterized by sub-tropical and semi-arid conditions experiencing a dry and hot summer from mid-April to June and a cold winter season from November to January, thus truly representing the cotton belt of northwestern India. The average annual rainfall of both sites varies from 300 to 400 mm, with 75% of the total precipitation mainly occurring from July to September.

Design of the experiment

The experiment having eight treatments has been laid out in a randomized complete block design with three replications (Figure 1). It was comprised of six treatment combinations from three levels of SSDI [60% crop evapotranspiration (ETc), 80% ETc, and 100% ETc of PAN evapotranspiration] and two N fertigation levels [75% RDN (84.4 kg N ha-1) and 100% RDN (112.5 kg N ha-1)]. In addition, there were two extra absolute Control treatments, *i.e.*, SF method of irrigation with 100% RDN through broadcasting of urea (Control 1) and SDI at 0.8 ETc coupled with 112.5 kg N ha-1 (Control 2).

Various treatment combinations included the following: T_1—SSDI at 60% ETc with DF of 75% RDN, T_2—SSDI at 60% ETc with DF of 100% RDN; T_3—SSDI at 80% ETc with DF of

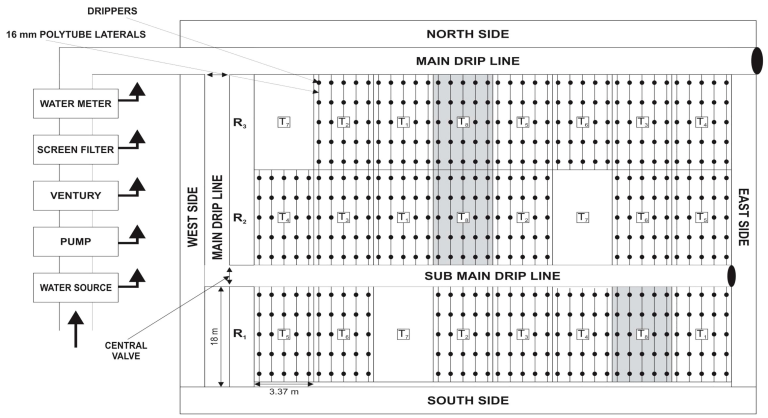

FIGURE 1
Layout of the experimental plots showing different treatments and drip line placement.

75% RDN; T_4—SSDI at 80% ETc with DF of 100% RDN; T_5—SSDI at 100% ETc with DF of 75% RDN; T_6—SSDI at 100% ETc with DF of 100% RDN; and T_7—SF irrigation with 100% RDN through broadcasting of urea–Control 1; and T_8—SDI at 80% ETc with DF of 100% RDN (Control 2).

Methodology and crop management

After harvesting of the wheat crop, the field was ploughed twice, and pre-sowing irrigation (*rauni*) was applied at both study locations. *Bt* cotton hybrid cultivar (RCH773 BGII) was sown in the first fortnight of May during both years (2018 and 2019) at Faridkot and Abohar. The sowing was done manually by hand dibbling method using two seeds per hill at a uniform depth of 5 cm. An inter-row spacing of 67.5 cm and intra-row spacing of 75 cm within plants was uniformly maintained. Each experimental plot (60.75 m^2) had a total of 125 plants in five rows, while each row length was 18 m.

The sub-surface laterals for SSDI were installed using a tractor-operated machine at a uniform depth of 20 cm, having an inter-row spacing of 67.5 cm with the emitter discharging 2.2 L of water per hour. However, for Control 2, SDI drip laterals with a similar discharge were manually laid out on the ground surface. The Control 1 plots receiving irrigation through SF were delivered with water through dedicated PVC pipes. All the experimental plots received regulated and measured water supply through a water meter and were surrounded by strong bunding all around, with a sufficient buffer area (2.0 m) so that variation owing to water application among different treatments could be minimized. The bulk density of soil has been measured by using the Core method (Black and Hartage, 1986), while soil moisture was determined by employing time domain refractometry (PR2/6 Profile Probe, Delta-T Devices Ltd. UK) after calibrating it with gravimetric methods (Richards and Weaver, 1943).

Growth- and yield-attributing characteristics and seed cotton yield

Growth- and yield-attributing parameters like plant height, sympodial branches per plant, bolls per plant, and boll weight have been recorded from 10 randomly selected plants per plot. Biomass accumulation was measured by cutting the whole aboveground portion of the plant after harvest and then weighing after thorough drying under the sun. SCY constituted the total weight of both the hand pickings and is expressed in kilograms per hectare (Mishra et al., 2021).

Irrigation, fertilizer application, and productivity indices

Irrigation under the SDI and SSDI method was applied at an interval of every 5 days. The total amount of applied irrigation water varied according to treatments, which were based on the amount of crop evapo-transpiration. In the SF method (conventional), water was applied by flood irrigation. A total of six and four SF irrigations were applied at the Faridkot and Abohar locations, respectively, during 2019, and the corresponding values were four and five during 2020. In SF plots, the first irrigation was given at 35 days after sowing (DAS) in mid-June at all locations and study years. The second, third, fourth, and fifth (last) SF irrigation, respectively, was applied during the end June, July, August, and September, respectively. The quantity of each irrigation was measured by using a water meter in all the treatment plots, and water applied under all irrigations was summed up to calculate the total irrigation water.

To work out the ETc, reference evapotranspiration (ETo) was calculated with a calculator developed by FAO from site-specific weather data for both locations. According to the user manual given by FAO, to calculate the daily crop evapotranspiration (ETc), the value of the crop coefficient (K_c) of cotton crop was 0.75 until the end of June, 1.15 during July and August, and 0.70 until boll picking. Fertilizer N in the form of urea (46% N) was applied for SDF and SSDF treatments starting from 35 DAS and delivered in 10 equal splits after every 5 days except for the SF, where 100% RDN was applied in two equal splits, *i.e.*, half dose at thinning and the remaining half at flowering. The application of phosphorous was skipped as the recommended dose of P was applied to the preceding wheat as recommended by Punjab Agricultural University (Anonymous, 2022). Actual crop evapotranspiration (ET_a) has been worked out with the help of the soil water balance equation (FernÃ¡ndez et al., 2020):

$$ET_a = IW + P - D - R \pm \Delta S \quad (1)$$

where IW is amount of irrigation water applied (mm), P represents precipitation in mm, R indicates surface runoff (mm), D is deep drainage (mm), and ΔS represents soil profile moisture change (mm). Runoff was nil as ridges/buffers surrounded all the plots. Deep drainage was assumed to be zero when moisture storage in the soil profile was lesser than the field capacity and when soil moisture storage (SMS) surpassed the field capacity storage either after a rain or due to irrigation. Thereafter, deep drainage has been developed as the gap between field capacity storage and SMS plus rain/irrigation. Since the water table at both study sites was below 3 m, an upward flux from the groundwater was not considered. Two-meter wide buffers were established between various plots to eliminate water fluxes in the vicinity of root zone laterals.

Bio-physical water productivity (BWP) and economic water productivity (EWP) were computed by using the following equations (Perry et al., 2017; FernÃ¡ndez et al., 2020):

$$BWP\ (kg\ m^{-3}) = SCY/ET_a \quad (2)$$

$$EWP\ (m^{-3}) = NR/ET_a \quad (3)$$

where SCY means seed cotton yield (kg ha^{-1}), ET_a is actual crop evapotranspiration (m^3 ha^{-1}), and NR indicates net returns ($ ha^{-1}).

WUE was calculated by using the following equations (Perry et al., 2009; Sahoo et al., 2018):

$$WUE = ET_a/IW + R \pm \Delta S \quad (4)$$

where IW is irrigation water applied (m^3 ha^{-1}), R represents rainfall (m^3 ha^{-1}), and ±ΔS was change in soil profile moisture (m^3 ha^{-1}), while ETa indicates actual crop evapotranspiration (m^3 ha^{-1}).

Nitrogen use efficiency (NUE) is calculated using the formula given below:

$$NUE = seed\ cotton\ yield/N\ applied \quad (5)$$

Fiber quality parameters

Lint samples were obtained by ginning the clean and dried weighed samples of seed cotton through a single-roller electric gin, and ginning turnout (GTO) was computed by using the following formula:

$$GTO\ (\%) = (weight\ of\ lint\ in\ grams/weight\ of\ seed\ cotton\ in\ grams) \times 100 \quad (6)$$

Fiber samples were sent to the laboratory of ICAR-Central Institute for Research on Cotton Technology (ICAR-CIRCOT), Mumbai, for measurement of various fiber parameters like halo length, fiber strength, uniformity index, micronaire, *etc.* A sample of 100-gram lint was taken to measure the micronaire value by using Prectitronic Digital Mic Tester at C, Mumbai.

Monetary evaluation

The total cost of cultivation incurred for raising cotton crop was calculated with the help of Enterprise budget (2021) of *Kharif* crops by the Department of Economics and Sociology, PAU, Ludhiana. Gross returns of different treatments were worked out by multiplying the SCY from respective treatments with the prevalent market price of $0.75 kg^{-1} of seed cotton. The benefit/cost ratio (B:C) was worked out to check the economic feasibility of treatments and is calculated by dividing the net returns by the total cost of cultivation (Singh et al., 2020).

Statistical analysis

Statistical analysis of various recorded parameters and calculated indices was performed to evaluate the effect of various treatments (SSDI regimes and N fertigation levels), in comparison with control treatments, using SAS Proc GLM (SAS software 9.3, SAS Institute Ltd., USA). Significant mean differences were compared using Fisher's least significant difference test at a probability level of 5%. The variance of data in both sites was homogeneous according to Bartlett's test ($p \leq 0.05$), so the data of both sites and years was pooled and analyzed.

Results and discussion

Weather and site characteristics

The data pertaining to weather-related parameters has been recorded from the agro-meteorological observatories of RRS, Faridkot, and RRS, Abohar and presented in Figures 2, 3.

Among the different treatments, the actual crop evapotranspiration (ET_a) ranged from 345.8 to 588.8 mm at both locations over the years. During 2019, except for the SF, negative soil moisture confirmed the necessity of underground water withdrawal for meeting irrigation demand that was substantially improved in the later year for each treatment at both experimental sites. The effects of the available moisture in the soil profile witnessed the heavy deep drainage during 2020 compared with the year 2019. Similarly, a huge surface runoff, *i.e.*, 86.4 and 88.2 mm at Faridkot and 92.3 and 93.3 mm at Abohar, was recorded for the surface flood method which was tremendously reduced under drip treatments. The data on the physio-chemical characteristics of soil at the experimental sites is given in Table 1. The layer-wise moisture retention capacity (at field capacity and permanent wilting point, PWP) of soil at both experimental sites for soil profile (0–150 cm) has been worked out and presented to work out various water indices (Table 2). Layer wise bulk density of both experimental sites is presented in Table 3. The detailed information on cultivar, planting geometry, sowing and harvesting dates, *etc.*, is summarized (Table 4).

Growth parameters and biomass accumulation by cotton

Different irrigation and fertigation treatments exerted a significant effect on growth parameters like plant height and

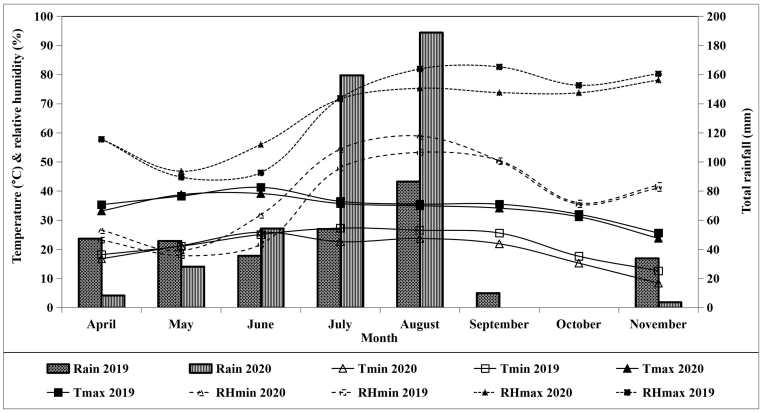

FIGURE 2
Weather data of the experimental site at Abohar during crop growth periods 2019 and 2020. RHm, maximum relative humidity; RHe, minimum relative humidity; Tmax, maximum temperature; Tmin, minimum temperature.

biomass accumulation (Table 5). Among the tested irrigation regimes, taller plants were recorded under SDI (170.0 cm), closely followed by a SSDI level of 80% ETc (164.3 cm) and 100% ETc (167.4 cm), while a significant reduction in plant height was observed under 60% ETc (148.1 cm) and SF (156.1 cm). Biomass accumulation has been highest under a SSDI level of 100% ETc (2,627 g m^{-2}) compared with 80% ETc (2439 g m^{-2}) and 60% ETc (1978 g m^{-2}). The reduced plant height and biomass accumulation under SSDI level of 60% ETc might be due to the fact that here least water was supplied, which, in turn, failed to maintain optimal crop growth. The better plant vigor under SDI over SF in the present findings is in close proximity with those of Yadav and Chauhan (2016), who observed taller plants under SDI over SF. Furthermore, SF not only recorded shorter plants in line with Prajapati and Subbaiah (2018) but also lesser biomass accumulation (2,138 g m^{-2}) in comparison with various SDF/SSDF treatments under 80%/100% ETc, elucidating that applied water and nitrogen could not be efficiently utilized (Table 5).

Among N fertigation schedules, higher plant height and biomass accumulation was evident under 100% RDN (2,420 g m^{-2}) over the 75% RDN (2276 g m^{-2}). Nevertheless, both SSDF levels of 75% RDN and 100% RDN revealed better plant height and biomass accumulation over the SF method (2,138 g m^{-2}), which could be attributed to the optimum availability of water and nitrogen to plants under SSDF, in agreement with Ayyadurai and Manickasundaram (2014) who recorded 36% higher biomass under DF of 100% RDN over soil

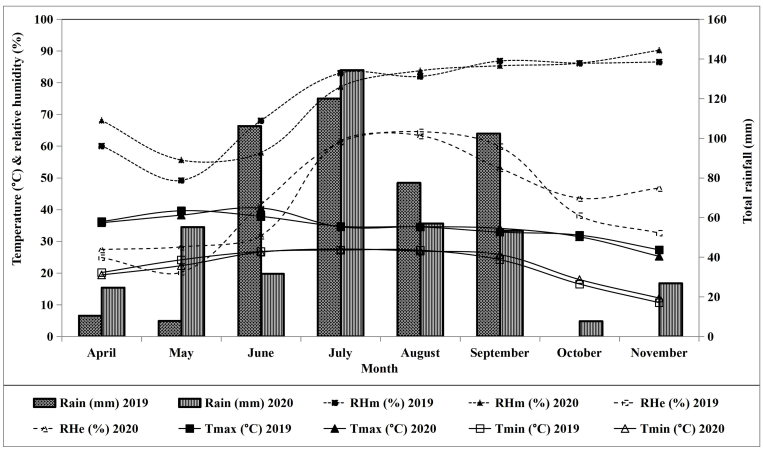

FIGURE 3
Weather data of the experimental site at Faridkot during crop growth periods 2019 and 2020. RHm, maximum relative humidity; RHe, minimum relative humidity; Tmax, maximum temperature; Tmin, minimum temperature.

10.3389/fpls.2022.1038163

TABLE 1 Chemical properties of soil at the experimental sites.

Soil properties	Faridkot		Abohar		Analytical method used
	Value	Rating	Value	Rating	
pH	8.3	Normal	8.3	Normal	Beckman's glass electrode pH meter (Jackson, 1967)
EC (dS m^{-1})	0.16	Normal	0.18	Normal	Solubridge conductivity meter (Jackson, 1967)
Organic carbon (%)	0.51	Medium	0.42	Medium	Rapid titration method (Walkley and Black, 1934)
Available nitrogen (kg ha^{-1})	188	Medium	192	Medium	Alkaline potassium permanganate method (Subbiah and Asija, 1956)
Available phosphorus (kg ha^{-1})	21.2	Medium	35	High	0.5 M sodium bicarbonate extractable P method (Olsen et al., 1954)
Available potassium (kg ha^{-1})	638	High	530	High	Ammonium acetate extractable K method (Merwin and Peech, 1950)
Soil texture	Sandy loam		Sandy loam		International pipette method (Piper, 1966)

TABLE 2 Layer-wise moisture retention capacity of soil at the experimental sites.

Soil depth (cm)	Volumetric moisture content (%) at field capacity		Volumetric moisture content (%) at permanent wilting point	
	Faridkot	Abohar	Faridkot	Abohar
0–10	21.2	19.9	12.3	8.6
11–20	16.9	14.5	9.9	9.9
20–30	16.1	15.1	9.6	10.1
30–40	18.0	16.2	10.7	9.8
40–60	17.8	16.5	10.2	8.1
60–100	16.1	14.9	9.8	9.0

TABLE 3 Layer wise bulk density of experimental sites.

Soil depth (cm)	Bulk density (g cm^{-3})	
	Faridkot	Abohar
0–15	1.56	1.58
15–30	1.54	1.68
30–60	1.66	1.72
60–90	1.61	1.59
90–120	1.60	1.63
120–150	1.58	1.65

application under SF. These findings established water and nitrogen to be among the essential growth factors as evident from better height and biomass accumulation under their increased supply (Brar et al., 2021). Higher biomass accumulation under SSDI over SF method is also supported by Sampthkumar et al. (2006) who recorded improved biomass accumulation under DI over border strip and SF irrigation.

Yield attributes and seed cotton yield

Sympodial branches, bolls per plant, boll weight, and SCY varied significantly under various irrigation regimes (Table 5). Higher sympodial branches per plant were recorded under SDI (24.2), closely followed by SSDI of 100% ETc (23.1), 80% ETc (22.2), and SF method (20.5), while the number was least under SSDI of 60% ETc (17.6). The observation on improved

10.3389/fpls.2022.1038163

TABLE 4 Details of crop, cultivars, planting geometry, and sowing and harvesting dates.

Crop	Cultivars	Planting geometry(cm)	Date of sowing		Date of harvesting			
			RRSA	RRSF	RRSA		RRSF	
Cotton	RCH 773 BGII	67.5 × 75	23.05.2019	09.05.2019	21.10.2019 (first picking)	6.11.2019 (second picking)	18.10.2019 (first picking)	6.11.2019 (second picking)
	RCH 773 BGII	67.5 × 75	05.05.2020	16.05.2020	17.10.2020 (first picking)	4.11.2020 (second picking)	19.10.2020 (first picking)	5.11.2020 (second picking)

A, RRSA (Abohar); F, RRSF (Faridkot).

sympodial branches per plant under SSDI is in conformity with that of Ali et al. (2017) who reported 15% higher sympodial branches under SDI over the furrow method. Higher bolls per plant was revealed under a SSDI of 100% ETc (60.2) and 80% ETc (57.2) over SSDI of 60% ETc (46.7) and SF method (46.5), which was in agreement with Prajapati and Subbaiah (2018) who recorded improved bolls per plant under SDI over the furrow method. A significant reduction by 23% and 29% for bolls per plant under the SF method over a SSDI of 80% ETc and 100% ETc was evident. Higher boll weight under SDI (4.11 g) was closely followed by SSDI at 100% ETc (4.04 g) and 80% ETc (3.95 g), while SSDI at 60% ETc recorded the significantly lowest

TABLE 5 Effect of various treatments on growth parameters, yield attributes, and seed cotton yield.

Nitrogen fertigation schedules (FS)	Irrigation regimes (IR)					
	60% ETc	80% ETc	100% ETc	Mean	Control 1	Control 2
Plant height (cm)						
75% RDN	144.4	162.2	166.1	157.6	156.1	170
100% RDN	151.9	166.3	168.8	162.3		
Mean	148.1	164.3	167.4			
LSD (p=0.05)	IR = 4.6 ; FS = 3.8; IR*FS = NS; IR*FS vs. Controls = 5.2					
Sympodial branches plant^{-1}						
75% RDN	16.8	21	22.2	20	20.5	24.2
100% RDN	18.4	23.3	24	21.9		
Mean	17.6	22.2	23.1			
LSD (p=0.05)	IR = 0.95 ; FS = 0.77; IR*FS =NS; IR*FS vs. Controls =1.10					
Bolls plant^{-1}						
75% RDN	44.5	54.1	58	52.2	46.5	56.9
100% RDN	48.9	60.4	62.5	57.2		
Mean	46.7	57.2	60.2			
LSD (p=0.05)	IR = 1.9 ; FS =1.5 ; IR*FS = NS; IR*FS vs. Controls =2.3					
Boll weight (g)						
75% RDN	3.58	3.9	4.01	3.83	3.81	4.11
100% RDN	3.7	4.01	4.07	3.92		
Mean	3.64	3.95	4.04			
LSD (p=0.05)	IR =0.11 ; FS =0.09; IR*FS = NS; IR*FS vs. Controls = 0.13					
Seed cotton yield (kg ha^{-1})						
75% RDN	2490	3024	3133	2882	2728	3300
100% RDN	2747	3455	3477	3226		
Mean	2619	3240	3305			
LSD (p=0.05)	IR = 120; FS = 98 ; IR*FS = NS; IR*FS vs. Controls = 143					
Biomass accumulation (g m^{-2})						
75% RDN	1867	2361	2601	2276	2138	2433
100% RDN	2090	2518	2652	2420		
Mean	1978	2439	2627			
LSD (p=0.05)	IR = 62 ; FS =50; IR*FS =NS; IR*FS vs. Controls = 83					

value (3.64 g) primarily due to reduced water supply (Singh et al., 2018).

Among SSDI levels, SCY was maximum at 100% ETc (3,305 kg ha^{-1}), closely followed by 80% ETc (3,240 kg ha^{-1}) and with the least value under 60% ETc (2619 kg ha^{-1}), where it was 26% and 23.7% lower compared with 80% ETc and 100% ETc, respectively. Nevertheless, SDI recorded statistically at par SCY (3,300 kg ha^{-1}) with SSDI of 80% ETc and 100% ETc. However, SSDI of 80% and 100% ETc resulted in 18.7% and 21% higher SCY over SF (2,728 kg ha^{-1}) due to better yield parameters (Aladakatti et al., 2012). This was primarily due to the improved boll count per plant which was 23% and 29.4% higher under SSDI level of 80% ETc and 100% ETc, respectively, over the SF method. Singh et al. (2018) also reported higher SCY by 19% and 23% over the conventional SF method under SDI of 100% ETc and 80% ETc, owing to the improved boll count. Better SCY and yield attributes such as higher bolls per plant under SSDI of 100% ETc and 80% ETc over SF irrigation are also supported by Neelakanth et al. (2019).

A fertigation level of 100% RDN elucidated better sympodial branches per plant (21.9), boll weight (3.92 g), and bolls per plant (57.2) over 75% RDN (20.0, 3.83 g, and 52.2, respectively) in conformity with Singh and Bhati (2018) who observed higher bolls per plant under SDI of 100% RDN (50.8) over the 75% RDN (46.2). Among N levels, 100% RDN revealed significantly higher SCY by 11.9% and 18.2% over the 75% RDN (2,882 kg ha^{-1}) and broadcasting method (2,728 kg ha^{-1}), respectively. Furthermore, the data elucidated that SSDF of 100% RDN either at 80% (3,455 kg ha^{-1}) or 100% ETc (3,477 kg ha^{-1}) improved SCY by 4.6% and 5.3%, respectively, over SDF.

Seed cotton yield revealed a positive and linear relationship (Figure 4) with crop evapotranspiration (ET_a), while its relationship with irrigation water applied (IWA) followed a second-order polynomial trend (Figure 5). Furthermore, the R^2 values for IWA and SCY for 2019 (Figure 5A), 2020 (Figure 5B), averaged over the years (Figure 5C), and averaged over the locations and years were significant (Figure 5D). The regression equations for individual year and location and also when averaged over the years and locations clearly elucidate SCY to be dependent upon ET_a (Figures 4A–D) and IWA (Figures 5A–D). A correlation heat map among various traits of cotton is given in Figure 6. This further signifies that efficient usage of water and nutrients can be made under SSDF as evident from better yield realization. These results clearly established that SSDF could play a pivotal role in improving the yield attributes and SCY compared with SF and the soil application of nutrients. Nevertheless, improved boll weight and bolls per plant under SSDF have remained as the primary reasons for the higher SCY. The boll count per plant was 12.2% and 23.0% higher under the SSDF of 75% RDN and 100% RDN, respectively, over broadcasting of 100% RDN in SF. These findings reveal that both water and nitrogen greatly govern the yield as envisaged from the fact that, by increasing the water and N fertigation level, crop yield tends to improve (Dar et al., 2017; Thanappan et al., 2020).

A significant reduction in yield attributes and SCY is evident under the least level of water and nitrogen (*i.e.*, SSDI of 60% ETc along with fertigation of 75% RDN), where the supply of both water and nitrogen was minimal (Table 5). SCY improved significantly by 23.7%, while the increasing irrigation level from 60% ETc to 80% ETc was in conformity with Singh et al. (2018). However, there was only a marginal increase of 2% while moving from 80% ETc to 100% ETc. The present data manifested that, under 100% RDN, SSDI—at either 80% ETc or 100% ETc—remained on par for SCY, though it increased by 708 and 730 kg ha^{-1}, respectively, over the SSDF at 60% ETc. This revealed that SCY exhibited a tendency to increase between the irrigation levels of 80% ETc and 100% ETc but was optimized at 80% ETc (Kumar et al., 2021).

Effect of different treatments on water productivity indices

The total irrigation water applied has been highest under SF (Control 1), *i.e.*, 550 and 400 mm during 2019, with a value of 400 and 475 mm during 2020 for Faridkot and Abohar, respectively (Tables 6, 7). However, actual crop evapotranspiration (ET_a) remained higher for SSDI at 100% ETc with 100% RDN (580.6 and 462.8 mm for 2019; 582.6 and 588.8 mm for 2020) for Faridkot and Abohar, respectively. A general reduction for ET_a was observed under SF (Control 1) compared with SSDI treatments across the locations. The ETa followed a linear relationship with SCY among the studied treatments over the locations during both study years (Figures 4A–D). During 2019, ETa was highest under T_6 (*i.e.*, 580.6 and 462.8 mm for Faridkot and Abohar, respectively), while during 2020, T_4 (584.8 $_{mm}$) and T_8 (590.2 mm) revealed higher ETa values for Faridkot and Abohar, respectively. These findings clearly elucidated a saving of 36–54.3% and 52.4-61.4% of irrigation water under SSDI for Faridkot and Abohar, respectively, during 2019 with increased ET_a over SF (Cetin and Kara, 2019). During 2020, the corresponding values ranged from 19.8–41.8% to 30.0–50.5%. The presented results on savings of water under SSDI are well supported by Patil et al. (2009) who observed 45.6% water saving under DI at 100% ETc over the SF method. Roopashree et al. (2016) also reported a saving of 21.7% irrigation water under SSDI over SF.

Among the studied irrigation regimes, improved BWP values (Table 8) were recorded under SSDI levels of 100% ETc (0.627 kg m^{-3}), 80% ETc (0.620 kg m^{-3}), and SDI (0.637 kg m^{-3}), while it was significantly reduced under 60% ETc (0.551 kg m^{-3}) and SF (0.601 kg m^{-3}). The reduced BWP by 12.5% under SSDI at 60% ETc compared with 80% ETc was clearly indicative of its poor efficiency (Brar et al., 2021). The SF method revealed least WUE (57%), while values were considerably improved under a

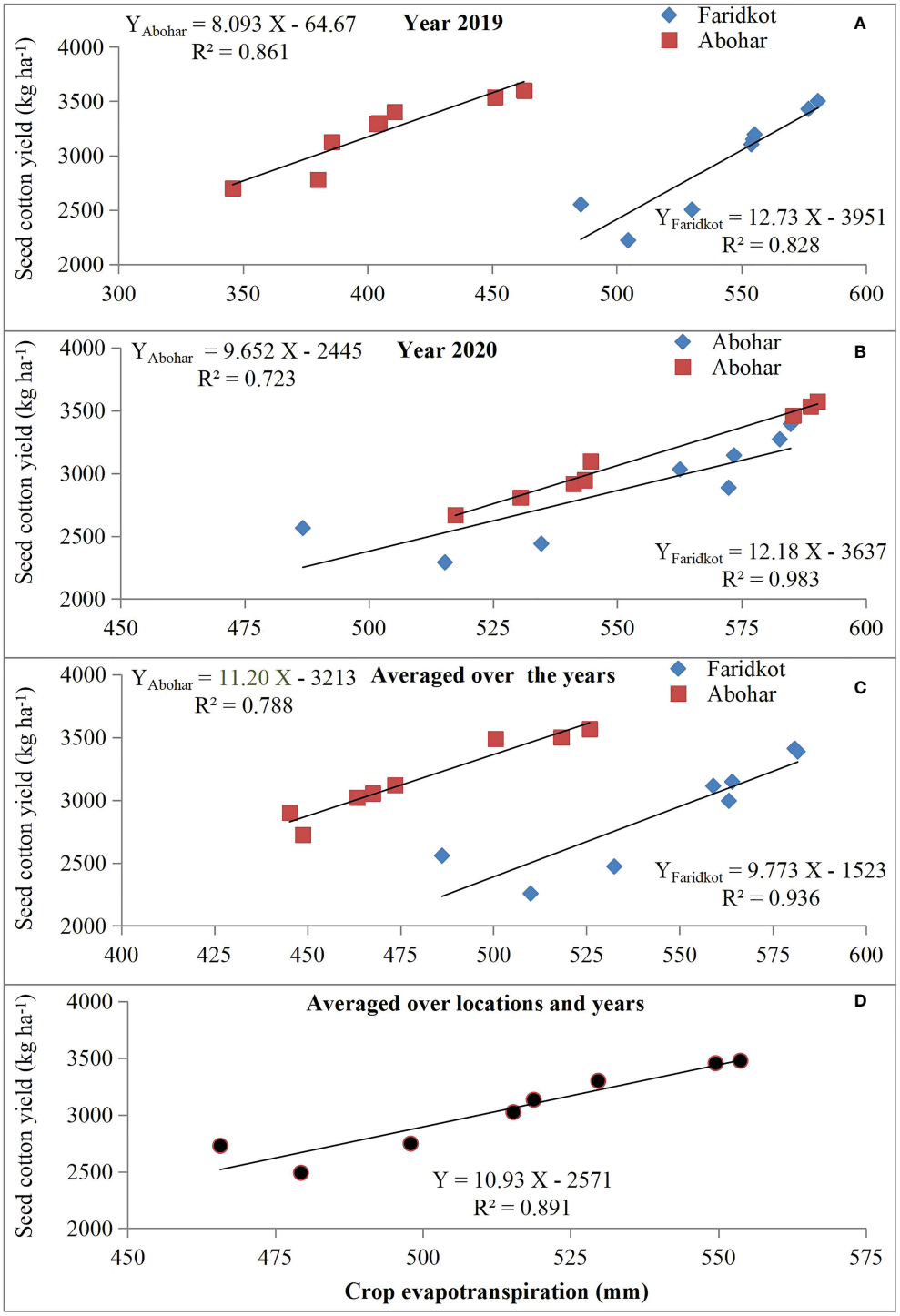

FIGURE 4
Seed cotton yield response to actual crop evapotranspiration during 2019 **(A)** and 2020 **(B)**, averaged over the years for each location **(C)** and averaged over the locations and years **(D)**.

SSDI level of 0.8 ETc (80.3%), closely followed by SDI (80.9%), SSDI level of 60% ETc (76.5%), and 100% ETc (78.8%). The better WUE under SDI/SSDI at 0.8 ETc was in conformity with Shruti and Aladakatti (2017), who elucidated higher values under DI applied at 80% ETc.

Among the fertigation levels, 100% RDN recorded a numerically higher BWP of 0.614 kg m^{-3} over 75% RDN and SF. However, SSDF of 75% and 100% RDN exhibited better WUE over broadcasting fertilizer (Jayakumar et al., 2015). These results clearly established that SSDF of either 80 or 100% ETc along

10.3389/fpls.2022.1038163

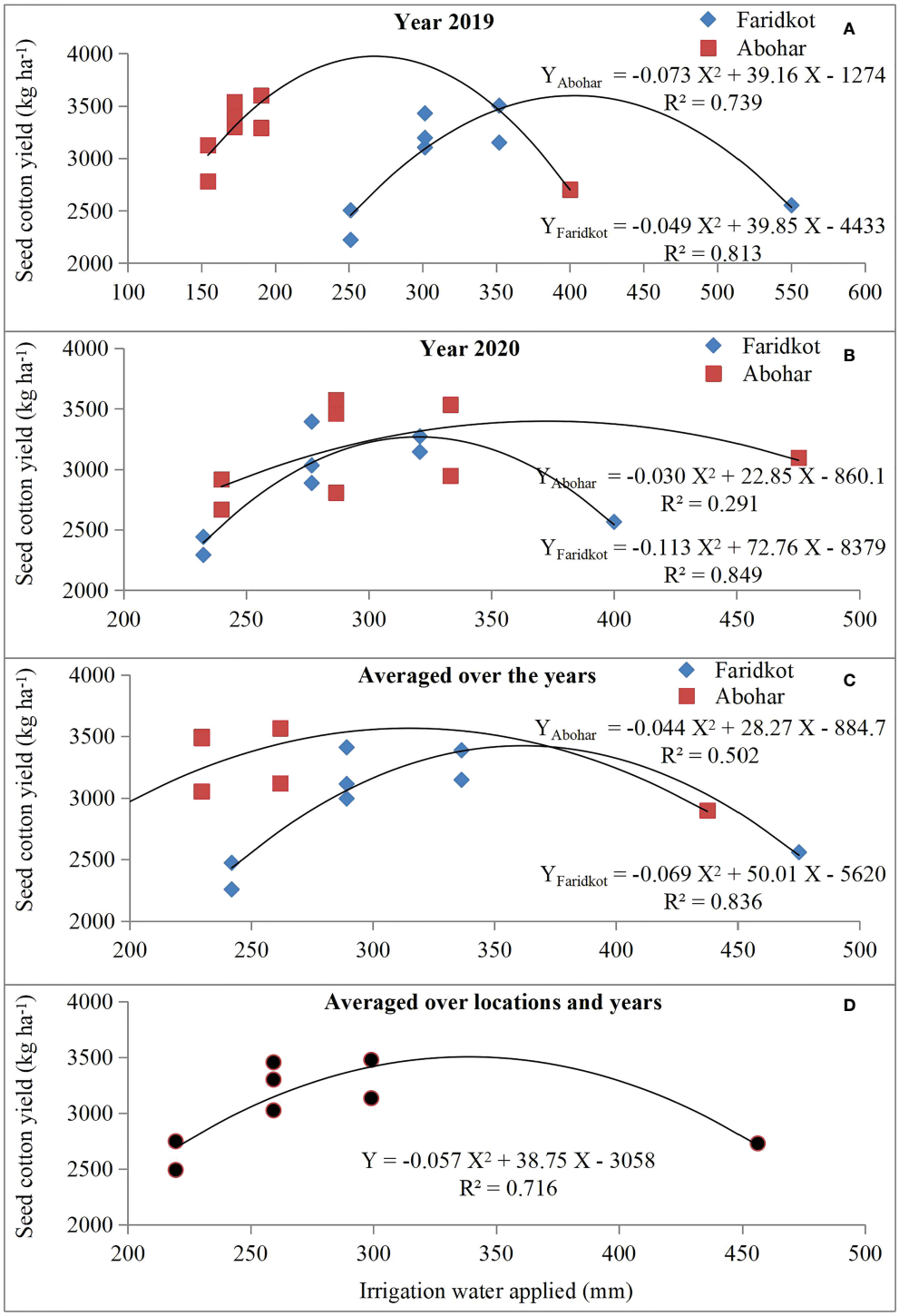

FIGURE 5
Seed cotton yield response to irrigation water applied (mm) during 2019 **(A)** and 2020 **(B)**, averaged over the years for each location **(C)** and averaged over the locations and years **(D)**.

	PH	SBP	BP	BW	SCY	BA	BPWP	WUE	NUE	GOT	HL	UI	FS	M	COC	GR	NR	B:C	EWP
PH	1	0.982	0.915	0.996	0.939	0.949	0.972	0.414	0.469	0.441	0.616	0.332	0.257	0.466	0.046	0.939	0.931	0.921	0.968
SBP	0.982	1	0.894	0.990	0.946	0.914	0.984	0.378	0.355	0.402	0.506	0.436	0.103	0.458	0.138	0.946	0.933	0.916	0.962
BP	0.915	0.894	1	0.905	0.977	0.964	0.874	0.653	0.516	0.735	0.583	0.240	0.300	0.401	-0.199	0.977	0.982	0.984	0.970
BW	0.996	0.990	0.905	1	0.935	0.937	0.970	0.404	0.447	0.429	0.560	0.361	0.198	0.441	0.063	0.935	0.926	0.915	0.961
SCY	0.939	0.946	0.977	0.935	1	0.933	0.929	0.609	0.391	0.649	0.524	0.382	0.221	0.501	-0.093	0.999	0.999	0.994	0.993
BA	0.949	0.914	0.964	0.937	0.933	1	0.914	0.454	0.579	0.569	0.660	0.199	0.278	0.339	-0.028	0.933	0.929	0.923	0.947
BPWP	0.972	0.984	0.874	0.970	0.929	0.914	1	0.301	0.326	0.333	0.528	0.477	0.115	0.512	0.218	0.929	0.912	0.892	0.952
WUE	0.414	0.378	0.653	0.404	0.609	0.454	0.301	1	0.297	0.941	0.231	0.059	0.481	0.341	-0.808	0.609	0.648	0.686	0.571
NUE	0.469	0.355	0.516	0.447	0.391	0.579	0.326	0.297	1	0.480	0.754	-0.583	0.674	0.189	-0.367	0.391	0.408	0.425	0.417
GOT	0.441	0.402	0.735	0.429	0.649	0.569	0.333	0.941	0.480	1	0.342	-0.089	0.454	0.234	-0.747	0.649	0.685	0.719	0.599
HL	0.616	0.506	0.583	0.560	0.524	0.660	0.528	0.231	0.754	0.342	1	-0.117	0.694	0.330	-0.113	0.524	0.527	0.530	0.563
UI	0.332	0.436	0.240	0.361	0.382	0.199	0.477	0.059	-0.583	-0.089	0.432	1	-0.463	0.352	0.357	0.382	0.361	0.338	0.382
FS	0.257	0.103	0.300	0.198	0.221	0.278	0.115	0.481	0.674	0.454	0.694	-0.463	1	0.505	-0.645	0.221	0.254	0.289	0.268
M	0.466	0.458	0.401	0.441	0.501	0.339	0.512	0.341	0.189	0.234	0.330	0.352	0.505	1	-0.122	0.501	0.505	0.505	0.528
COC	0.046	0.138	-0.199	0.063	-0.093	-0.028	0.218	-0.808	-0.367	-0.747	-0.113	0.357	-0.645	-0.122	1	-0.093	-0.145	-0.200	-0.073
GR	0.939	0.946	0.977	0.935	0.999	0.933	0.929	0.609	0.391	0.649	0.524	0.382	0.221	0.501	-0.093	1	0.999	0.994	0.993
NR	0.931	0.933	0.982	0.926	0.999	0.929	0.912	0.648	0.408	0.685	0.527	0.361	0.254	0.505	-0.145	0.999	1	0.998	0.991
B:C	0.921	0.916	0.984	0.915	0.994	0.923	0.892	0.686	0.425	0.719	0.530	0.338	0.289	0.505	-0.200	0.994	0.998	1	0.986
EWP	0.968	0.962	0.970	0.961	0.993	0.947	0.952	0.571	0.417	0.599	0.563	0.382	0.268	0.528	-0.073	0.993	0.991	0.986	1

FIGURE 6
Correlation heat map among various traits of cotton. PH, plant height (cm); SBP, sympodial branches plant^{-1}; BP, Bolls per plant; BW, Boll weight (g); SCY, seed cotton yield (kg ha^{-1}); BA, biomass accumulation (g m^{-2}); BPWP, bio-physical water productivity (kg m^{-3}); WUE, water use efficiency (%); NUE, nitrogen use efficiency (kg SCY kg^{-1} N); GOT, Ginning turnout (%); HL, halo length (mm); UI, uniformity index; FS, fiber strength (g tex^{-1}); M, micronaire; COC, cost of cultivation ($ ha^{-1}); GR, gross returns ($ ha^{-1}); NR, net returns ($ ha^{-1}); B:C, benefit/cost ratio; EWP, economic water productivity ($ m^{-3}).

with 100% RDN recorded better BWP and WUE over the SF method despite the limited application of water. Thus, SSDF can become an effective tool for increasing the cotton productivity as well as water use efficiency without sacrificing SCY (Singh et al., 2022). Further details are elaborated in the following subsections.

Actual crop evapotranspiration

Among the studied treatments, the mean evapotranspiration (Eta) at Faridkot during 2019 was 504.6, 530.2, 553.9, 576.8, 554.6, 580.6, 485.6, and 555.2 mm for T_1 to T_8, respectively. During 2020, the respective ETa values were 515.3, 534.7, 572.3, 584.8, 573.4, 582.6, 486.7, and 562.6 mm. At Abohar, the ETa values during 2019 were 380.1, 385.6, 404.6, 451.1, 403.7, 462.8, 345.8, and 410.8 mm for T_1 to T_8, respectively. The respective ETa value during 2020 was 517.4, 541.2, 530.5, 585.3, 543.4, 588.8, 544.6, and 590.2 mm. Reduction in ETa at Abohar during 2019 compared with a later year was observed, while at Faridkot the values were akin during both study years (Tables 6, 7). Higher ETa values for treatments receiving more water and fertilizer under drip fertigation resulted in vigorous cotton growth, which might have led to variability in the uptake of

TABLE 6 Irrigation water applied and actual crop evapotranspiration under various treatments (2019).

	Faridkot						Abohar					
	IWA (mm)	RF (mm)	Δ S (mm)	ET_a (mm)	D (mm)	R. (mm)	IWA (mm)	RF (mm)	Δ S (mm)	ET_a (mm)	D (mm)	R. (mm)
T_1: SSDI at 60% crop evapotranspiration (ETc) with DF of 75% RDN	232.5	486.3	38.3	515.3	114.6	50.6	239.9	457.8	33.3	517.4	94.3	52.7
T_2: SSDI at 60% ETc with DF of 100% RDN	232.5	486.3	34.8	534.7	102.1	47.2	239.9	457.8	22.5	541.2	83.4	50.6
T_3: SSDI at 80% ETc with DF of 75% RDN	276.7	486.3	40.7	572.3	109.9	40.1	286.6	457.8	58.7	530.5	99.6	55.6
T_4: SSDI at 80% ETc with DF of 100% RDN	276.7	486.3	35.9	584.8	97.5	44.8	286.6	457.8	26.2	585.3	84.6	48.3
T_5: SSDI at 100% ETc with DF of 75% RDN	320.8	486.3	51.5	573.4	129.4	52.8	333.2	457.8	79.1	543.4	110.1	58.4
T_6: SSDI at 100% ETc with DF of 100% RDN	320.8	486.3	48.6	582.6	125.8	50.1	333.2	457.8	68.2	588.8	86.7	47.3
T_7: surface flood with 100% RDN (Control 1)	400.0	486.3	62.8	486.7	248.6	88.2	475.0	457.8	95.8	544.6	200.1	92.3
T_8: surface drip at 80% ETc with 100% RDN (Control 2)	276.7	486.3	58.7	562.6	90.1	51.6	286.6	457.8	39.7	590.2	68.3	46.2

IWA, irrigation water applied; RF, rainfall; ΔS, change in soil profile moisture; ET_a, actual crop evapotranspiration; D, drainage; R, runoff; SSDI, subsurface drip irrigation; DF, drip fertigation; RDN, recommended dose of nitrogen.

TABLE 7 Irrigation water applied and actual crop evapotranspiration under various treatments (2020).

Treatment	Faridkot						Abohar					
	IWA (mm)	RF (mm)	ΔS (mm)	ET_a (mm)	D (mm)	R. (mm)	IWA (mm)	RF (mm)	ΔS (mm)	ET_a (mm)	D (mm)	R. (mm)
T_1: SSDI at 60% crop evapotranspiration (ETc) with DF of 75% RDN	251.2	366.1	-21.0	504.6	94.3	39.4	154.3	353.3	-18.2	380.1	89.6	56.1
T_2: SSDI at 60% ETc with DF of 100% RDN	251.2	366.1	-19.4	530.2	72.5	34.0	154.3	353.3	-16.5	385.6	92.3	46.2
T_3: SSDI at 80% ETc with DF of 75% RDN	301.6	366.1	-17.2	553.9	99.0	32.0	172.3	353.3	-12.8	404.6	98.2	35.6
T_4: SSDI at 80% ETc with DF of 100% RDN	301.6	366.1	-18.1	576.8	74.6	34.4	172.3	353.3	-10.1	451.1	69.2	15.4
T_5: SSDI at 100% ETc with DF of 75% RDN	352.0	366.1	-10.9	554.6	139.3	35.1	190.4	353.3	-4.8	403.7	99.2	45.6
T_6: SSDI at 100% ETc with DF of 100% RDN	352.0	366.1	-8.5	580.6	109.4	36.4	190.4	353.3	-2.1	462.8	70.4	12.6
T_7: surface flood with 100% RDN (Control 1)	550.0	366.1	45.0	485.6	299.1	86.4	400.0	353.3	32.8	345.8	281.4	93.3
T_8: surface drip at 80% ETc with 100% RDN (Control 2)	301.6	366.1	-6.7	555.2	73.9	45.3	172.3	353.3	-4.3	410.8	80.2	38.9

IWA, irrigation water applied; RF, rainfall; ΔS, change in soil profile moisture; ET_a, actual crop evapotranspiration; D, drainage; R, runoff; SSDI, subsurface drip irrigation; DF, drip fertigation; RDN, recommended dose of nitrogen.

water and its distribution. The higher ETa in 2020 might be owing to more rainfall which was primarily accountable for continuous soil wetting, thus leading to a higher evaporative loss (Dar et al., 2017). The variation in ETa over the seasons and locations was owing to the huge variation in the amount of rainfall and its distribution (Figure 2), which could have resulted into distinct effects on soil wetting followed by evaporative loss and crop water uptake. The variation among irrigation regimes is primarily owing to the variable quantity of IWA (Tables 6, 7). The higher ETa was observed under T_6, which received the maximum quantity of irrigation through SSDF, as a linear relationship has been observed between SCY and ETa (Figure 4) with the R^2 value ranging from 0.723 to 0.983 for individual and pooled data over the seasons and locations, respectively. The increase in ETa with IWA is in agreement with Irmak et al. (2016).

TABLE 8 Effect of various treatments on bio-physical water productivity, water use efficiency, and nitrogen use efficiency.

Nitrogen fertigation schedules (FS)	Irrigation regimes (IR)					
	60% crop evapotranspiration (ETc)	80% ETc	100% ETc	Mean	Control 1	Control 2
	Bio-physical water productivity (kg m^{-3})					
75% RDN	0.533	0.602	0.619	0.585		
100% RDN	0.570	0.638	0.636	0.614	0.601	0.637
Mean	0.551	0.620	0.627			
LSD (p = 0.05)	IR = 0.023; FS = 0.018; IR*FS = NS; IR*FS *vs.* controls = 0.017					
	Water use efficiency (%)					
75% RDN	75.4	77.1	74.9	75.8		
100% RDN	77.6	83.5	82.7	81.3	57.0	80.9
Mean	76.5	80.3	78.8			
	Nitrogen use efficiency (kg SCY kg^{-1} N)					
76.5	80.3	78.8	37.0	34.1	25.9	29.3
100% RDN	24.4	30.7	30.9	28.6		
Mean	26.9	33.2	33.9			
LSD (p = 0.05)	IR = 1.3; FS = 1.0; IR*FS = NS; IR*FS *vs.* controls = 1.4					

RDN, recommended dose of nitrogen; NS, non-significant; LSD, least significant difference; Control 1, surface flood irrigation and soil application of 100% RDN through urea broadcasting; Control 2, surface drip irrigation at 80% ETc with fertigation of 100% RDN.

Bio-physical water productivity, water use efficiency, and economic water productivity

The higher BWP was recorded in T_4 treatment (0.638 kg m^{-3}), while the lowest (0.533 kg m^{-3}) was observed in T_1 treatment (Table 8). The BWP declined owing to a huge reduction in SCY (Table 5) compared with the reduced crop ETa (Tables 6, 7). Among drip irrigation regimes, the BWP values were 0.551, 0.620, and 0.627 kg m^{-3} for 60% ETc, 80% ETc, and 100% ETc, respectively (Table 8). The improvement in BWP with any hike in irrigation level could be owing to the reason that IWA just fulfilled the required soil water deficit. This means that treatments which received more irrigation water experienced lesser water stress compared with treatments receiving lesser irrigation. As a result, the SCY was statistically better under 80% ETc and 100% ETc treatments having a high IWA compared with 60% ETc and resulted in higher BWP (Sun et al., 2006; Dar et al., 2017). When averaged over the years, a linear relationship between ETa and SCY was observed, with R^2 value of 0.723 at Abohar and 0.983 for Faridkot and R^2 of 0.936 (Figure 4C) and R^2 of 0.891 when averaged over the locations and years. This clearly elucidated that the efficient use of water by the cotton plants increased the SCY. Therefore, irrigating cotton with an adequate amount of water at regular intervals through drip might enhance the SCY and water productivity with additional saving of water compared with surface flood method.

Comparison of water use efficiency under SSDF treatments vs. surface flood

The WUE in SSDF treatments ranged from 75.4 to 83.5%, compared with SF (57.0%). The highest WUE of 83.5% was recorded in T_4 treatment, *i.e.*, drip irrigation at 80% ETc along with 100% RDN (Table 8), which elucidated that a huge water can be saved by adopting novel water-savvy techniques. During 2019, applied water under SF has been 56% and 110% higher compared with what was applied in SSDI at 100% ETc for Faridkot and Abohar, respectively. The corresponding values were higher by 24.6% and 42.5% during 2020, which was indicative of huge water saving.

Nitrogen use efficiency

Nitrogen is one of the most important limiting factors governing the growth and productivity of crop plants. The present findings clearly established a reduction in the NUE with each increase in N level. Within irrigation regimes, SSDI of 100% ETc recorded a higher NUE (33.9 kg SCY kg^{-1} N) which was closely followed by 80% ETc (33.2 kg SCY kg^{-1} N), while 60% ETc resulted in a significantly lowest value (26.9 kg SCY kg^{-1} N). Furthermore, NUE under SF (Control 1) has been 3.8%, 28.1%, and 30.8% lesser compared with SSDI of 60% ETc, 80% ETc, and 100% ETc, respectively (Table 8).

Among fertigation levels, SSDF of 75% RDN (34.1 kg SCY kg^{-1} N) recorded a statistically better NUE by 19.2% over 100% RDN (28.6 kg SCY kg^{-1} N), which was in agreement with Singh et al. (2018) who reported 27% higher NUE under 75% RDN over 100% RDN. However, both SSDF levels of 75% and 100% RDN exhibited increased NUE by 31.6% and 10.4%, respectively, over SF (25.9 kg SCY kg^{-1} N). The higher NUE under SSDF has been primarily due to the application of nitrogen directly to the root zone, which, in turn, minimized volatilization and leaching losses and consequently improved the yield (Brar et al., 2022). Moreover, the application of N in 10 equal splits under SSDF might have checked the N losses in the soil compared with only two splits under the broadcasting method, which further helped to enhance NUE, in agreement with Bharathraj et al. (2015) wherein 47% higher efficiency has been observed under fertigation compared with soil application.

Fiber quality parameters

Ginning turnout was significantly reduced under SF (31.9%) compared with all SDI/SSDF treatments (Table 9). However, fiber strength was significantly higher (30.5) under a SSDF combination of 80% ETc along with 100% of RDN, which was in conformity with Zhang et al. (2019). However, fertigation treatments could not differentiate much for either of the studied quality parameters (Magare et al., 2018; Zahid et al., 2021).

Monetary evaluation

A higher gross return ($2,572.9 ha^{-1}), net return ($1,648.9 ha^{-1}), and B:C ratio (1.78) have been recorded in the treatment receiving SSDF at 100% ETc with fertigation of 100% RDN. However, SSDI of 80% ETc with 100% RDN recorded much lesser net returns by $12.0 ha^{-1}, but with an additional saving of 20% irrigation water (Table 10). A statistically lowest gross return ($1,842.6 ha^{-1}), net return ($932.0 ha^{-1}), and B:C (1.02) was observed under SSDI at 0.6 ETc with 75% RDN, thus making it the least remunerative among the drip combinations studied. Nevertheless, SSDI at 0.8 ETc with 100% RDN recorded significantly higher net returns by 54.1% over the SF method. These findings get fair support from Aladakatti et al. (2012) and Pawar et al. (2015). Reduced B:C under the conventional practice of the SF method (1.11) further substantiated that fertilizer and water application through SSDF are more rewarding (Neelakanth et al., 2019).

Economic water productivity remained higher under the SSDI level of 100% ETc and SDI, closely followed by SSDI of

TABLE 9 Effect of various treatments on fiber quality parameters.

	Irrigation regimes (IR)					
Nitrogen fertigation schedules (FS)	**60% crop evapotranspiration (ETc)**	**80% ETc**	**100% ETc**	**Mean**	**Control 1**	**Control 2**
Ginning turnout (%)						
75% RDN	33.2	33.3	33.4	33.3	31.9	33.2
100% RDN	33.1	33.8	33.9	33.6		
Mean	33.1	33.5	33.7			
LSD (p = 0.05)	IR = NS; FS = NS; IR*FS = NS; IR*FS *vs.* controls = 0.99					
Halo length (mm)						
75% RDN	26.4	27.6	27.1	27.0	26.7	26.8
100% RDN	26.6	26.9	27.1	26.9		
Mean	26.5	27.3	27.1			
LSD (p = 0.05)	IR = NS; FS = NS; IR*FS = NS; IR*FS *vs.* controls = NS					
Uniformity index						
75% RDN	80.3	80.2	80.4	80.3	80.6	80.7
100% RDN	80.6	80.7	80.5	80.6		
Mean	80.4	80.5	80.4			
LSD (p = 0.05)	IR = NS; FS = NS; IR*FS = NS; IR*FS *vs.* controls = NS					
Fiber strength (g tex^{-1})						
75% RDN	29.9	30.8	30.3	30.3	29.5	30.1
100% RDN	30.1	30.2	29.8	30.0		
Mean	30.0	30.5	30.0			
LSD (p = 0.05)	IR = 0.44; FS = NS; IR*FS = NS; IR*FS *vs.* controls = 0.47					
Micronaire						
75% RDN	4.20	4.23	4.21	4.21	4.21	4.23
100% RDN	4.21	4.25	4.20	4.22		
Mean	4.21	4.24	4.20			
LSD (p = 0.05)	IR = NS; FS = NS; IR*FS = NS; IR*FS *vs.* controls = NS					

10.3389/fpls.2022.1038163

TABLE 10 Effect of various treatments on monetary parameters.

Nitrogen fertigation schedules (FS)	Irrigation regimes (IR)					
	60% ETc	80% ETc	100% ETc	Mean	Control 1	Control 2
Cost of cultivation ($ ha^{-1})						
75% RDN	910.5	914.8	919.1	914.8	956.7	919.8
100% RDN	915.4	919.7	924.0	919.7		
Mean	913.0	917.2	921.5			
Gross returns ($ ha^{-1})						
75% RDN	1842.6	2237.7	2318.4	2132.9	2018.7	2442.0
100% RDN	2032.7	2556.7	2572.9	2387.4		
Mean	1937.6	2397.2	2445.6			
Net Returns ($ ha^{-1})						
75% RDN	932.0	1322.9	1399.3	1218.1	1062.0	1522.2
100% RDN	1117.2	1636.9	1648.9	1467.7		
Mean	1024.6	1479.9	1524.1			
Benefit : Cost ratio						
75% RDN	1.02	1.44	1.52	1.33	1.11	1.65
100% RDN	1.22	1.77	1.78	1.59		
Mean	1.12	1.61	1.65			
Economic water productivity ($ m^{-3})						
75% RDN	0.201	0.265	0.277	0.248		
100% RDN	0.234	0.302	0.302	0.279	0.233	0.294
Mean	0.218	0.284	0.289			

80% ETc, while the least values were exhibited under 60% ETc ($0.218 m^{-3}) and the SF method ($0.233 m^{-3}). EWP under SF was lower by 17.9% and 20%, respectively, over the SSDI levels of 80% ETc and 100% ETc, which indicated it to be inferior compared with other treatments. Among fertigation levels, SSDF of 100% RDN recorded better EWP ($0.279 m^{-3}) over 75% RDN. However, both SSDF levels of 75% and 100% RDN exhibited increased EWP by 7% and 17%, respectively, over Control 1. The SSDF of 80% ETc with 100% RDN and 100% ETc with 100% RDN recorded 29.6% higher EWP over SF. These findings clearly elucidated the advantage of SSDF in increasing monetary advantage over SF.

Conclusion

The available freshwater for agrarian purposes in northwestern India is continuously declining due to reduced river flows, leading to sub-optimal canal water supply and changed levels of precipitation. Hence, effective irrigation strategies may help save water without sacrificing the crop productivity. Here we elucidated for the first time that, in northwestern India, the SSDF technique may result into significant savings of irrigation water due to lesser drainage loss compared with SF and is a potentially viable option for cotton cultivation. The highest WUE (83.5%) under SSDF of 80% ETc and 100% RDN, along with improvised BWP (0.638 kg m^{-3}) and better SCY (3,455 kg ha^{-1}), established it to be most efficient among the treatments tested. Furthermore, it also resulted in 26.6% higher SCY, 6.1% better BWP, and 29.6% higher EWP along with 18.5% higher NUE than surface flood. Therefore, implementation of SSDF in cotton would not only save a large quantity of irrigation water but also support more areas under micro-irrigation in sustaining a better yield. Therefore, growing cotton with optimized sub-surface drip fertigation would be an efficient and economically viable water-savvy strategy in northwestern India.

Data availability statement

The original contributions presented in the study are included in the article/supplementary material. Further inquiries can be directed to the corresponding authors.

Author contributions

Conceptualization: KS. Methodology: KS, PS, and MS. Investigation: KS, PS, MS, and SM. Resources: KS, MS, and

AS. Writing of the original draft: KS, PS, MS, and SM. Editing: KS, RI, IA-A, MH-u-R, and AS. All authors contributed to the article and approved the submitted version.

Funding

The authors gratefully acknowledge the funding received from the Punjab Agricultural University, Ludhiana, Punjab, India. This paper was funded by Researchers Supporting Project number (RSP-2021/298), King Saud University, Riyadh, Saudi Arabia.

Acknowledgments

The authors extend their appreciation to the Researchers Supporting Project number (RSP-2021/298), King Saud University, Riyadh, Saudi Arabia. The authors gratefully acknowledge the funding received from the Punjab Agricultural University, Ludhiana, Punjab, India.

Conflict of interest

The authors declare that the research was conducted in the absence of any commercial or financial relationships that could be construed as a potential conflict of interest.

The handling editor declared a past co-authorship with the authors KS and AS.

Publisher's note

All claims expressed in this article are solely those of the authors and do not necessarily represent those of their affiliated organizations, or those of the publisher, the editors and the reviewers. Any product that may be evaluated in this article, or claim that may be made by its manufacturer, is not guaranteed or endorsed by the publisher.

References

Aladakatti, Y. R., Hallikeri, S. S., Nand agavi, R. A., Shivamurthy, D., and Malik, R. (2012). "Precision irrigation and fertigation to enhance the productivity and economic returns of bt cotton in vertisols," in *Proc 3rd agro-informat precision agriculture*(Hyderabad, India: Agro-Informatics and Precision Agriculture), 341–343.

Ali, H., Arooj, M., Sarwar, N., Areeb, A., Shahzad, A. N., and Hussain, S. (2017). Sustainable weed management strategy in cotton crop. *Planta Daninha* 35, 1–12. doi: 10.1590/S0100-83582017350100052

Anonymous (2021). *All India coordinated research project on cotton, project co-ordinator. (PC) report., (2021)* (Nagpur, India: CICR). Available at: https://www.cicr.org.in/aicrp-2021/2_PC_Report.pdf.

Anonymous (2022). *Cotton package of practices for crops of punjab - kharif, (2022)* (Ludhiana, India: Punjab Agricultural University), Pp:37–Pp:51. Available at: https://www.pau.edu/content/ccil/pf/pp_kharif.pdf.

Ayyadurai, P., and Manickasundaram, P. (2014). Growth, nutrient uptake and seed cotton yield as influenced by foliar nutrition and drip fertigation in cotton hybrid. *Int. J. Agric. Sci.* 10 (1), 276–279. doi: 10.20546/ijcmas.2017.609.366

Ben-Gal, A., Lazorovitch, N., and Shani, U. (2004). Subsurface drip irrigation in gravel filled cavities. *Vadose Zone J3.* 4), 1407–1413. doi: 10.2136/vzj2004.1407

Bharathraj, H. R., Joshi, M., and Vishaka, G. V. (2015). Effect of surface fertigation on nutrient uptake, fertilizer use efficiency and economics of inter-specific hybrid *Bt* cotton. *Univ. J. Agric. Res.* 3, 46–48. doi: 10.13189/ujar.2015.030202

Black, G. R., and Hartage, K. H. (1986). Bulk density. in: Klute, a. (ed), methods of soil analysis. part i. physical and mineralogical methods. *Amer. Soc Agron. Soil Sci. Madison* WI pp, 363–375. doi: 10.2136/sssabookser5.1.2ed.c13

Brar, A. S., Buttar, G. S., Singh, M., Singh, S., and Vashist, K. K. (2021). Improving bio–physical and economic water productivity of menthol mint (*Mentha arvensis* l.) through drip fertigation. *Irrig. Sci* 39 (4), 505–516. doi: 10.1007/s00271-021-00722-6

Brar, A. S., Kaur, K., Sindhu, V. K., Tsolakis, N., and Srai, J.S. (2022). Sustainable water use through multiple cropping systems and precision irrigation. *J. Cleaner Prod.* 333, 130117. doi: 10.1016/Jjclepro.2021.130117

Cetin, O., and Kara, A. (2019). Assessment of water productivity using different drip irrigation systems for cotton. *Agric. Water Manage.* 223, 1–9. doi: 10.1016/j.agwat.2019.105693

Dar, E. A., Brar, A. S., and Singh, K. B. (2017). Water use and productivity of drip irrigated wheat under variable climatic and soil moisture regimes in north-West, India. *Agric. Ecosyst. Environ.* 248, 9–19. doi: 10.1016/Jagee.2017.07.019

FernÃ¡ndez, J. E., Alcon, F., Diaz-Espejo, A., Hernandez-Santana, V., and Cuevas, M. V. (2020). Water use indicators and economic analysis for on-farm irrigation decision: A case study of a super high density olive tree orchard. *Agric. Water Manage.* 237, 106074. doi: 10.1016/Jagwat.2020.106074

Gondal, M. R., Saleem, M. Y., Rizvi, S. A., Riaz, A., Naseem, W., Muhammad, G., et al. (2021). Assessment of drought tolerance in various cotton genotypes under simulated osmotic settings. *Asian J. Agric. Biol.* 2, 1–10. doi: 10.35495/ajab.2020.08.437

Harish, J., Rajkumar, B., Pawar, D. D., and Kale, K. D. (2017). Nutrient availability in *Bt*cotton by using drip fertigation under different phosphorous sources. *Int. J. Res. Sci. Tech.* 6, 406–410. doi: 10.17577/IJERTV6IS060233

Hashem, M. S., El-Abedin, T. Z., and Al-Ghobari, H. M. (2018). Assessing effects of deficit irrigation techniques on water productivity of tomato for subsurface drip irrigation system. *Int. j.* agric. *Biol. Eng.* 11 (4), 156–167. doi: 10.25165/j.ijabe.20181104.3846

Ibragimov, N., Evet, S. R., Esanbekov, Y., Kamilov, B., Mirzaev, L., and Lamers, J. P. A. (2007). Water use efficiency of irrigated cotton in Uzbekistan under drip and furrow irrigation. *Agric. Water Manage.* 90, 112–120. doi: 10.1016/j.agwat.2007.01.016

Imran, M., Ali, A., and Safdar, M. E. (2021). The impact of different levels of nitrogen fertilizer on maize hybrids performance under two different environments. *Asian J. Agric. Biol.* 4, 1–10. doi: 10.35495/ajab.2020.10.527

Ines, A. V. M., Honda, K., Das Gupta, A., Droogers, P., and Clemente, R. S. (2006). Combining remote sensing-simulation modeling and genetic algorithm optimization to explore water management options in irrigated agriculture. *Agric. Water Manage.* 83, 221–232. doi: 10.1016/j.agwat.2005.12.006

Irmak, S., Djaman., K., and Rudnick, D. R. (2016). Effect of full and limited irrigation amount and frequency on subsurface drip-irrigated maize evapotranspiration, yield, water use efficiency and yield response factors. *Irrig. Sci.* 34, 271–286. doi: 10.1007/s00271-016-0502-z

Jackson, M. L. (1967). *Soil chemical analysis. prentice hall of India, private limited* (New Delhi: Prentice Hall of India, Private Limited, New Delh). doi: 10.1002/jpln.19590850311

Janat., (2008). Response of cotton to irrigation methods and nitrogen fertilization: yield components, water use efficiency, nitrogen uptake and recovery. *Commun. Soil Sci. Plant Anal.* 39, 2282–2302. doi: 10.1080/00103620802292293

Jayakumar, M., Surendran, U., and Manicksundram, P. (2015). Drip fertigation program on growth, crop productivity, water and fertilizer use efficiency of *Bt*cotton in semi arid tropical region of India. *Commun. Soil Sci. Plant Anal.* 46, 293–300. doi: 10.1080/00103624.2014.969403

Kaur, A., and Brar, A. S. (2016). Influence of mulching and irrigation scheduling on productivity and water use of turmeric in north western India. *Irrig. Sci.* 34, 261–269. doi: 10.1007/s00271-016-0501-0

Kumar, D. S., Sharma, R., and Brar, A. S. (2021). Optimising drip irrigation and fertigation schedules for higher crop and water productivity of oilseed rape (*Brassica napus* l.). *Irrig. Sci* 39 (4), 535–548. doi: 10.1007/s00271-020-00714-y

Magare, P. N., Katkar, R. N., and Jadhao, S. D. (2018). Effect of fertigation on yield, quality and soil fertility status under cotton grown in vertisol. *Int. J. Chem. Stud.* 6 (2), 42–46.

Martinez, J., and Reca, J. (2014). Water use efficiency of surface drip irrigation versus an alternative sub-surface drip irrigation method. *J. Irrig. Drain. Eng.* 140, 1–9. doi: 10.1061/(ASCE)IR.1943-4774.0000745

Mchugh, A. D., Bhattarai, S., and Midmore, D. J. (2008). Effects of sub-surface drip irrigation rates and furrow irrigation for cotton grown on a vertisol on off-site movements of sediments, nutrients and pesticides. *Agric. Sustain. Dev.* 28, 507–519. doi: 10.1051/agro:2008034

Merwin, H. D., and Peech, M. (1950). Exchangeability of soil potassium in sand, silt and clay fractions as influenced by the nature of complementary exchangeable cations. *Proc. Soil America* 15, 125–128. doi: 10.2136/sssaj1951.036159950015000C0026x

Mishra, S. K., Kaur, V., and Singh, K. (2021). Evaluation of DSSAT-CROPGRO-cotton model to simulate phenology, growth and seed cotton yield in north-western India. *Agron. J.* 113, 3975–3990. doi: 10.1002/agj2.20788

Neelakanth, J. K., Rajkumar, S., Gundlur, S. S., and Dasar, G. V. (2019). Effect of surface and sub-surface drip irrigation system on seed cotton in *vertisols*of malaprabha command in northern karnataka. *J. Pharmacogn. Phytochem.* 8 (2), 956–958.

Olsen, S. R., Cole, C. V., Waternade, F. S., and Dean, L. A. (1954). Estimation of available phosphorous in soil by extraction with sodium bicarbonate. *USDA Circ.* 939, 1–19.

Patil, N. G., Ramamurthy, V., Venugopalan, M. V., and Challa, O. (2009). Effect of drip irrigation on productivity and water-use efficiency of hybrid cotton. (*Gossypium hirsutum*) in typic haplusterts. *Ind. J. Agric. Sci.* 79, 118–121.

Pawar, N., Bishnoi., D. K., Singh, M., and Dhillon, A. (2015). Comparative economic analysis of drip irrigation vis-a-vis flood irrigation system on productivity of *Bt* cotton in haryana. *Agric. Sci. Digest.* 35 (4), 300–303. doi: 10.18805/asd.v35i4.6863

Pereira, L. S., Cordery, I., and Lacovides, I. (2012). Improved indicators of water use performance and productivity for sustainable water conservation and saving. *Agric. Water Manage.* 108, 39–51. doi: 10.1016/j.agwat.2011.08.022

Perry, C., Pasquale, S., Allen, R. G., and Burt, C. M. (2009). Increasing productivity in irrigated agriculture: agronomic constraints and hydrological realities. *Agric. Water Manage.* 96, 1517–1524. doi: 10.1016/j.agwat.2009.05.005

Perry, C., Pasquale, S., Karajeh, F.Food and Agriculture Organization of the United Nations (2017). "Does improved irrigation technology save water," in *Discussion paper on irrigation and sustainable water resources management in the near East and north Africa*(Cairo: Food and Agriculture Organization of the United Nations, Cairo). Available at: https://www.fao.org/3/I7090EN/i7090en.pdf.

Piper, C. S. (1966). *Soil and plant analysis* (New York: International Science Publisher). doi: 10.1002/jps.3030350611

Prajapati, G. V., and Subbaiah, R. (2018). Combined response of irrigation system regimes and mulching on productivity of *Bt* cotton. *J. Agrometeorol.* 20, 47–51.

Rahim, H., Mian, I. A., Muhammad, A., Ahmad, S., and Khan, Z. (2020). Soil fertility status as influenced by the carryover effect of biochar and summer legumes. *Asian J. Agric.and Biol.* 8 (1), 11–16. doi: 10.35495/ajab.2019.05.198

Richards, L. A., and Weaver, L. R. (1943). Fifteen-atmosphere percentage as related to the permanent wilting percentage. *Soil Sci* 56, 331–39. doi: 10.1097/00010694-194311000-00002

Roopashree, M., Rajkumara, S., and Neelakanth, J. K. (2016). Effect of surface and sub-surface drip irrigation at different ETc levels on growth and yield of *Bt* cotton. (*Gossypium hirsutum*L.). *J. Farm Sci.* 29, 456–460.

Sahoo, P., Brar, A. S., and Sharma, S. (2018). Effect of methods of irrigation and sulphur nutrition on seed yield, economic and bio-physical water productivity of two sunflower (*Helianthus annus* l.) hybrids. *Agric. Water Manage.* 206, 158–164. doi: 10.1016/j.agwat.2018.05.009

Sampathkumar, T., Krishnasamy, S., Ramesh, S., Prabukumar, G., and Gobi, R. (2006). Growth, nutrient uptake and seed cotton yield of summer cotton as influenced by drip, surface irrigation methods and mulching practices. *Res. j. agric. Biol. Sci.* 2, 420–422.

Shruti, M. Y., and Aladakatti, Y. R. (2017). Effect of drip irrigation and fertigation on yield, economics and water use efficiency of intra-*hirsutumBt* cotton. *J. Farm Sci.* 30, 185–189.

Sidhu, H. S., Jat, M. L., Singh, Y., Sidhu, R. K., Gupta, N., Singh, P., et al. (2019). Sub-Surface drip fertigation with conservation agriculture in a rice-wheat system: A breakthrough for addressing water and nitrogen use efficiency. *Agric. Water Manage.* 216, 273–283. doi: 10.1016/j.agwat.2019.02.019

Singh, M., and Bhati, A. S. (2018). Nutrient use in cotton grown under drip irrigation system innorth-western India. *J. Crop Weed.* 14, 122–129.

Singh, K., Brar, A. S., and Singh, H. P. (2018). Drip fertigation improves water and nitrogen use efficiency of *Bt* cotton. *J. Soil Water Cons.* 73, 549–557. doi: 10.2489/jswc.73.5.549

Singh, K., Mishra, S. K., Singh, M., Singh, K., and Brar, A. S. (2022). Water footprint assessment of surface and subsurface drip fertigated cotton-wheat cropping system – a case study under semi-arid environments of Indian punjab. *J. Cleaner Prod.* 365, 132735. doi: 10.1016/Jjclepro.2022.132735

Singh, K., Singh, H. P., and Mishra, S. K. (2020). Irrigation module and sowing dates affect seed cotton yield, quality, productivity indices and economics of cotton in north-western india. *Commun. soil sci. Plant Annal.* 51 (7), 919–931. doi: 10.1080/00103624.2020.1744633

Sinha, I., Buttar, G. S., and Brar, A. S. (2017). Drip irrigation and fertigation improve economics, water and energy productivity of spring sunflower (*Helianthus annuus* L.) in Indian Punjab.. *Agric. Water Manage* 185, 58–64. doi: 10.1016/j.agwat.2017.02.008

Subbiah, B. V., and Asija, G. L. (1956). A rapid procedure for the estimation of available nitrogen in soils. *Curr. Sci.* 25, 259–260.

Sun, H. Y., Liu, C. M., Zhang, X. Y., Shen, Y. J., and Zhang, Y. Q. (2006). Effects of irrigation on water balance, yield and WUE of winter wheat in the north China plain. *Agric. Water Manage.* 85, 211–218. doi: 10.1016/j.agwat.2006.04.008

Thanappan, S., Hosamani, S. R., and Chandrappa, M. N. (2020). Rill treatments to enhance nutrient rich soil, a case study. *Asian J. Agric. Biol.* 8 (2), 186–193. doi: 10.35495/ajab.2019.06.242

Walkley, A., and Black, C. A. (1934). An examination of the digtjareff method for determination of soil organic matter and a proposed modification of chromic acid titration method. *Soil Sci.* 37, 29–38. doi: 10.1097/00010694-193401000-00003

Yadav, B. S., and Chauhan, R. P. S. (2016). Drip fertigation technology for enhancing water and nutrient use efficiency in arid agro-ecosystem of irrigated northwestern rajasthan. *Ann. Arid Zone.* 55, 139–145.

Zahid, N., Ahmed, M. J., Tahir, M. M., Maqbool, M., Shah, S. Z. A., Hussain, S. J., et al. (2021). Integrated effect of urea and poultry manure on growth, yield and postharvest quality of cucumber (*Cucumis sativus* l.). *Asian J. Agric. Biol.* 1, 1–9. doi: 10.35495/ajab.2020.07.381

Zhang, H., Liu, H., Wang, S., Guo, X., Ge, L., and Sun, J. (2019). Variations in growth, water consumption and economic benefit of transplanted cotton after winter wheat harvest subjected to different irrigation methods. *Sci. Rep.* 9, 1–11. doi: 10.1038/s41598-019-51391-7

frontiers | Frontiers in Plant Science

TYPE Original Research
PUBLISHED 06 December 2022
DOI 10.3389/fpls.2022.957421

OPEN ACCESS

EDITED BY
Muhammad Ali Raza,
Gansu Academy of Agricultural Sciences (CAAS), China

REVIEWED BY
Gabriela Woźniak,
University of Silesia in Katowice, Poland
Nilda Roma-Burgos,
University of Arkansas, United States

*CORRESPONDENCE
Jianhua Si
jianhuas@lzb.ac.cn

SPECIALTY SECTION
This article was submitted to Plant Abiotic Stress, a section of the journal Frontiers in Plant Science

RECEIVED 26 July 2022
ACCEPTED 16 November 2022
PUBLISHED 06 December 2022

CITATION
Qin J, Si J, Jia B, Zhao C, Zhou D, He X, Wang C and Zhu X (2022) Water use strategies of *Ferula bungeana* on mega-dunes in the Badain Jaran Desert.
Front. Plant Sci. 13:957421.
doi: 10.3389/fpls.2022.957421

Water use strategies of *Ferula bungeana* on mega-dunes in the Badain Jaran Desert

Jie Qin[1,2], Jianhua Si[1]*, Bing Jia[1,2], Chunyan Zhao[1], Dongmeng Zhou[1,2], Xiaohui He[1,2], Chunlin Wang[1,2] and Xinglin Zhu[1,2]

[1]Key Laboratory of Eco-Hydrology of Inland River Basin, Northwest Institute of Eco-Environment and Resources, Chinese Academy of Sciences, Lanzhou, China, [2]University of Chinese Academy of Sciences, Beijing, China

In desert ecosystems, ephemeral plants have developed specialized water use strategies in response to long-term natural water stress. To examine the water use strategies of desert ephemeral plants under natural extreme drought conditions, we investigated the water absorption sources, water potential, hydraulic conductivity, and water use efficiency of *Ferula bungeana* at different elevations on the slopes of mega-dunes in the Badain Jaran Desert, Inner Mongolia, during a period of extreme drought. We found that the water utilized by *F. bungeana* was mostly absorbed from the 0–60 cm soil layers (80.47 ± 4.28%). With progression of the growing season, the source of water changed from the 0–30 cm soil layer to the 30-60 cm layer. The water potentials of the leaves, stems, and roots of *F. bungeana* were found to be characterized by clear diurnal and monthly variation, which were restricted by water availability and the hydraulic conductivity of different parts of the plant. The root hydraulic conductivity of *F. bungeana* was found to be considerably greater than that of the canopy, both of which showed significant diurnal and monthly variation. The water use efficiency of *F. bungeana* under extreme drought conditions was relatively high, particularly during the early and late stages of the growing season. Variations in water availability led to the regulation of water uptake and an adjustment of internal water conduction, which modified plant water use efficiency. These observations tend to indicate that the water use strategies of *F. bungeana* are mainly associated with the growth stage of plants, whereas the distribution pattern of plants on mega-dunes appeared to have comparatively little influence. Our findings on the water use of ephemeral plants highlight the adaptive mechanisms of these plants in desert habitats and provide a theoretical basis for selecting plants suitable for the restoration and reconstruction of desert ecosystems.

KEYWORDS

stable isotope, water uptake, plant water potential, plant hydraulic conductivity, water use efficiency

Introduction

Desert ecosystems cover approximately 20% of global land area, and 43% of land is under threat of desertification. In recent years, global warming and increased human disturbances (IPCC, 2019) have markedly affected the accessibility of water resources in desert ecosystems. The sandy surface of the desert oasis transition zone has been activated, the vegetation protection system degraded, and the ecological environment has undegone a notable deterioration. In particular, during the 20th century, the Sahara Desert is estimated to have expanded by more than 10% (Thomas and Nigam, 2018). Similarly, the extent of the Badain Jaran Desert in Inner Mongolia increased by 363.24 km^2 in the 30 years between 1990 and 2018 (Wang, 2019). Given such trends, the restoration of desert ecosystems has emerged as an urgent problem in recent decades, and our efforts to control desertification have a long way to go. The most fundamental and effective measure for stemming the increase in desertification entails the control and fixation of drifting sand by establishing vegetation, and in this regard, it is of particular importance to select the most appropriate plant species for the ecological restoration or reconstruction of desert ecosystems. Unless such measures are taken, the extensive expansion of deserts and intensification of desertification will have severe repercussions for continued human subsistence.

When screening plant species for the suitability for use in ecosystem restoration or reconstruction, a primary consideration is their ability toadapt to water stress. In this regard, the water use strategy of plants can fully reflect the adaptability of plants to changing moisture environments (Dawson et al., 2002; Evaristo et al., 2016; Grossiord et al., 2017), and determine the mechanisms and extents of plant responses to hydrological change (Antunes et al., 2018a; Wu et al., 2019). Plants growing in arid regions adapt to water scarcity by modifying their physiological characteristics and reproductive stratgies, and respond to different water sources by adopting corresponding water use strategies. Whereas annuals are completely dependent on water obtained from summer precipitation, perennials can survive periods of long-term drought predominantly by the ability of their root systems to obtain the remaining soil moisture and the capacity of the above-ground organs to withstand water stress (Ehleringer et al., 1991). The efficiency with which plant roots obtain water is strongly dependent on the soil water availability, rooting depth, root distribution, and root hydraulic properties (Zencich et al., 2002; Warren et al., 2015; Phillips et al., 2016). Among these factors, the availabilityof soil water is a key determinant of plant growth and survival (Antunes et al., 2018b). During periods of drought, rooting depth primarily determines how much water plants can extract from the soil (Zencich et al., 2002), whereas during periods when the soil is occupied with water, the breadth of roots close to the soil surface is the principal determinant of water uptake. Root activity determines the process of root water uptake (Wu et al., 2014; Warren et al., 2015; Phillips et al., 2016; O'Keefe et al., 2019), and during "wet" periods, roots in the lateral root zone take up surface water, whereas when shallow water sources are insufficient, plants are dependent on the activity of penetrating taproots that gain access to deep soil water. Accordingly, differences in root morphology lead to different patterns of water uptake in plants (Wang et al., 2019; Wu et al., 2019), with shallow-rooted plants generally exploiting shallow soil water sources, and species with dimorphic root systems typically switching water uptake strategies, tapping either shallower or deeper soil layers, depending upon availability (Wang et al., 2019). In the process of transporting water from roots to leaves, the lower water conductivity of the canopy, branches, and leaves influences plant water status (Turner, 1982; Nissanka et al., 1997). When the amounts water absorbed by the root system are insufficient to maintain plant growth, plants may experience severe water shortages and succumb to physiological damage (Huang and Zhang, 2016). To mitigate such water deficit-induced damage, some plants can absorb condensate water through their leaves, thereby enhancing plant water potential (Hill et al., 2015; Dawson and Goldsmith, 2018; Berry et al., 2019; Hill et al., 2021).

Ephemeral plants are particularly important members of the arid desert flora (Goldblati, 1978; Ludwig et al., 1988; Brown, 2003) that have notable community significance (Qiu et al., 2007), playing key roles in ameliorating the effects of wind velocity, stabilizing the sandy landscape, conserving water and soil, and enhancing microhabitats (Wolfe and Nickling, 1993; Wiggs et al., 1995; Qiu et al., 2007). The long-term drought avoidance survival mode of ephemeral plants, based on structure, phenology, physiology, and biochemistry, has enabled these plants to adapt to extremely arid environments, and they typically occur as pioneer species in vegetation successions (Wang et al., 2005). Ephemeral plants, as their name suggests, are genrally short-lived species, with an average lifecycle of approximately 2.5 months. Preferentially exploiting early spring rains, they are characterized by rapid growth and development and contracted phenological stages. Moreover, their root systems tend to be shallow, generally distributed within the 10–30 cm soil layer, and rarely exceeding 40 cm.

Although early studies on ephemeral plants tended to focus primarily on flora and classification (Goldblati, 1978; Ludwig et al., 1988; Brown, 2003), more recently, authors have been turning their attention to the adaptation of ephemeral plants to specific habitats, including studies on the relationships between the physiological and ecological characteristics of these plants and environmental factors (Ehleringer, 1983; Wang et al., 2005; Qian et al., 2007; Qiu et al., 2007). To date, however, comparatively less research has been conducted on the systematic water use strategies of ephemeral plants. To enhance our understanding of the drought resistance mechanisms of ephemeral plants, it is necessary to investigate the water use strategies adopted for the absorption, transport,

and utilization of limited water resources. In addition, ephemeral plants may also modify their water use strategies at different stages of growth. For example, in the early stages of growth, the leaves of winter annual plants in the Sonoran Desert have a short-lived high vapor conductivity and water potential, which subsequently gradually decrease in the full bloom stage (Sawada et al., 2002), whereas in contrast, the vapor conductivity and diurnal water potential of the leaves of summer annual plants tend to remain almost constant throughout growth (Ehleringer, 1983). Moreover, different topographical factors may also affect the water use strategies of ephemeral plants, thereby leading to differences in biomass allocation (Zhang et al., 2021).

The Badain Jaran Desert is characterized by a series of mega-dunes with average heights of between 200 and 300 m. During field investigations conducted in the Badain Jaran Desert from June to July 2019, we discovered that many ephemeral plants typically grow in different parts of these mega-dunes. In this habitat, the roots of plants are distributed at some distance above the groundwater table, which lies at a depth of approximately 1.5-2 m in the main concentrated areas of the lake group (Huang, 2018). Precipitation in this region is sparse, with a multi-year average annual precipitation ranging from 50 to 100 mm, mainly falling in the months June to September, and over the past 50 years, the regional climate has shown a warm and dry trend (Hu, 2021); Given that the moisture content in the sand layer in this desert is extremely low (less than 3%) (Cui et al., 2017), it is remarkable that plants are able to grow in this exceptionally arid environment. It is thus of particular interest to determine the mechanisms whereby these plants efficiently utilize the limited water resources during different growth stages and also to established whether ephemeral plants growing at different sites in the dune system adopt different water use strategies. Clarifying the water use strategies of ephemeral plants in different parts of mega-dunes and gaining an understanding of their drought resistance mechanisms would contribute to predicting the future of desert plants under deteriorating moisture conditions, provide a theoretical basis for the screening of vegetation species in sandy areas, and yield scientific evidence that could be used to guide the rational allocation of water resources in sandy areas.

Over recent years, the hydrological cycle of the Badain Jaran Desert region has been a particularly active area of research (Chen et al., 2004; Zhao et al., 2011; Chen et al., 2014; Ma et al., 2016), and in this regard, the distribution of ephemeral plants can provide a good indication of the water content of the sand layer. Accordingly, the study of the plant–water relationships on mega-dunes may provide important insights with respect to the hydrological cycle in this region. In this context, *Ferula bungeana*, a perennial herb in the family Umbelliferae, which grows to heights of approximately 30 cm and has roots of approximately 40 cm in length and up to 8 mm in diameter, is generally distributed in sandy soils in most parts of North China, growing in dunes, sandy land, dry fields, roadsides, and gravel slopes. It is a typical ephemeral plant, with a growing season extending from May to July. It is also distributed among the mega-dunes in the southeastern part of the Badain Jaran Desert, but is rarely found in the flat terrain between mega-dunes. Consequently, we reasoned that by studying the water use strategies of this plant, we might gain important insights on the hydrological processes of mega-dunes. Furthermore, as a representative dune plant, studying the water use strategy of *F. bungeana* would be expected to enhance our understanding of the water use of ephemeral plants in general and contribute to elucidating the drought tolerance mechanisms of these plants.

In this study, we used the stable oxygen isotope technique (iso-source model) to analyze the sources of water used by the ephemeral plant *F. bungeana* on mega-dunes in the Badain Jaran Desert, including the contribution fraction of each soil layer and seasonal variations. Simultaneously, we analyzed the diurnal and seasonal variation characteristics of plant water potential, hydraulic conductivity, and water use efficiency to examine the adaptive mechanisms of *F. bungeana* under natural water stress conditions. Our comprehensive summary of the water use strategies of *F. bungeana* on these mega-dunes will provide a basis for the selection of appropriate species for use in desertification control and effective utilization of plant and water resources. The purposes of this study were to (1) quantify the proportion of soil water absorbed by *F. bungeana* in each soil layer and analyze the seasonal variation characteristics of water absorption; (2) analyze the temporal and spatial variation characteristics of soil water potential and the hydraulic properties of *F. bungeana*, and examine the mechanism of water acquisition by the roots of *F. bungeana*; and (3) determine the temporal and spatial variation characteristics of root, stem, and leaf water potentials and water use efficiency of *F. bungeana*, and summarize the adaptive mechanisms of *F. bungeana* under conditions of long-term water stress.

Materials and methods

Study sites

The study area is located near Lake Badain (39°43′19″N, 102°37′01″E) in the southeast of the Badain Jaran Desert (39°04′15″–42°12′23″N, 99°23′18″–104°34′02″E), which lies in the western part of the Alxa Plateau, Inner Mongolia, China. The landscape in this region is characterized by the coexistence of mega-dunes and lakes, the former of which account for more than half of the total desert area, and typically range in height from approximately 200 to 300 m, although can reach a maximum of close to 500 m. The lakes cover an area of 23 km^2, with a total of 144 lakes, 72 of which still contain water. The coverage and species diversity of the

vegetation in this area are generally low, and mainly comprises xerophytic and ultra-xerophytic shrubs and semi-shrubs and diverse herb species. The region is characterized by an extremely temperate continental arid climate, with dry and hot summers, cold and windy winters and springs, and an average annual temperature of around 7 to 8°C. The area receives very little precipitation (Figure 1), whereas the rate of evaporation is high, leading to water losses substantially greater than the amounts obtained from precipitation. The groundwater level fluctuates between 0.6 and 10.2 m (actual findings in the main concentrated areas of the lake group). The water content of the wet sand layer of mega-dunes is less than 3% (Cui et al., 2017), which limits plant survival, even though the water balance in this area is positive. These characteristics thus tend to indicate that there are certain cyclic transformation relationship among groundwater, lake water, sand layer water, and plant water in the Badain Jaran Desert and various water sources, and for a number of years, the mutual transformation relationships in this region have been a particularly active area of research.

The upper parts of the windward slopes of the mega-dunes are dominated by perennial herbs, whereas the central parts are dominated by shrubs and perennial herbs, and in the lower parts, semi-shrubs and perennial herbs predominate. In addition, annual herbs can be found growing across the entire elevation range. With regards to the leeward slopes, the upper parts are dominated by annual herbs, and perennial herbs predominate on the central and lower slopes. The dominant species of shrub and semi-shrub are *Zygophyllum xanthoxylum* and *Artemisia ordosica*, respectively, whereas *F. bungeana* and *Psammochloa villosa* predominate among the perennial herbs and *Agriophyllum squarrosum* is generally the most abundant species of annual herb.

Analysis of the $\delta^{18}O$ of plant water and water sources

Experiments were carried out from May to July 2020, during the observation days of which, samples were collected between 06:00 to 09:00 (typically a sunny day) in the middle of each month. The mega-dunes were divided into three sections, the upper, central, and lower sections, and *F. bungeana* growing on these mega-dunes was selected as the focal plant species (Figure 2). Within each area, three plants with uniform growth were selected, with three replicate analyses being performed for each sample. The complete root system (Figure 2C) was dug out of the sand with a shovel and the rhizosphere soil was removed using the "root shaking method". Subsequently, the fibrous roots and aerial parts were separated using scissors. The thick roots (the combined part of the rhizomes) were collected, rapidly placed into sampling bottles, sealed with Parafilm, placed in an ice box, brought back to the laboratory, and stored in an ultra-low temperature freezer at -20°C until used for water extraction.

Soil profiles were excavated from sample plots established in different parts of the mega-dunes, and soil samples were collected at different depths, starting from the appearance of the wet sand layer, with a sampling interval of 30 cm and a total sampling depth of 240 cm. Samples for isotopic analysis were collected in plastic vials and sealed with Parafilm, with three replicate samples being collected from each layer. These were rapidly placed in an ice box, and stored at -20°C in the laboratory until used for water extraction. Following sample collection, the excavated sand was backfilled.

For the purposes of isotopic analysis, we initially used a cryogenic vacuum distillation system (Ehleringer et al., 1991; Zhao et al., 2016) to extract water from plant and soil samples at the Key Laboratory of the Inland River Basin, Northwest

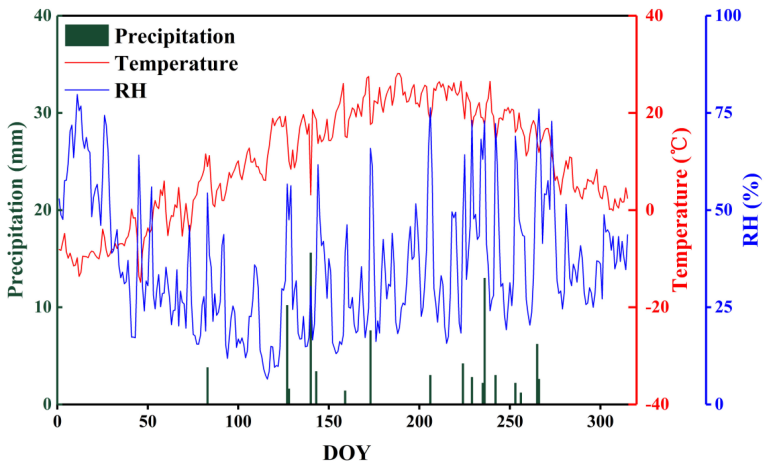

FIGURE 1
The distribution of monthly precipitation, temperature, and relative humidity during 2020 at the experimental site in the Badain Jaran Desert.

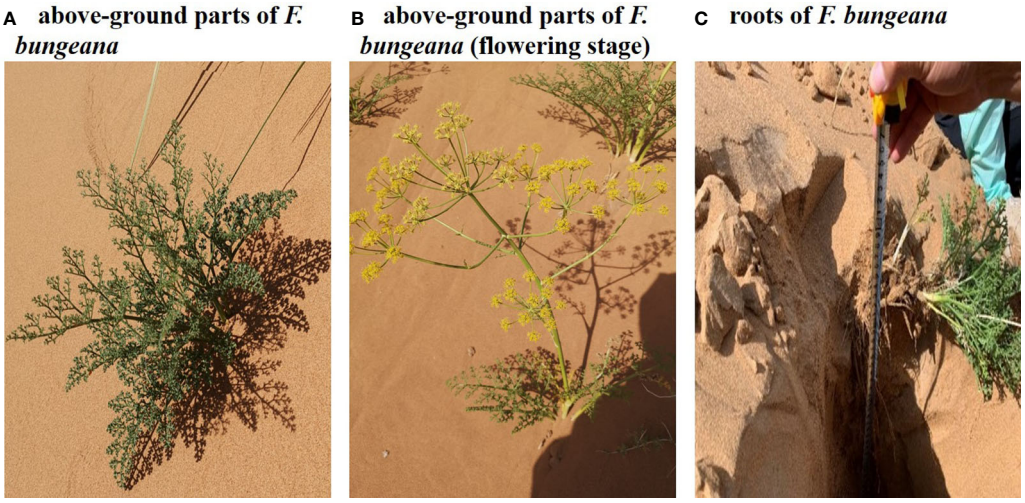

FIGURE 2
Photographs of *Ferula bungeana* growing on mega-dunes in the Badain Jaran Desert. **(A, B)** present the above-ground parts of Ferula bungeana and **(C)** present the root system of Ferula bungeana.

Institute of Eco-Environment and Resources, Chinese Academy of Sciences. Following extraction, the water samples were filtered through 0.22 μm pore size filters, transferred to 2 mL crimp cap vials, and stored at 4°C until used for isotopic analysis. The δ^2H and $\delta^{18}O$ values of the extracted water were determined using an isotope ratio infrared spectroscopy (IRIS) system, comprising a liquid water isotope analyzer (LWIA, 912-0008-1001; Los Gatos Research Inc., Mountain View, CA, USA). The isotopic composition of the water samples was expressed as follows:

$$\delta X(‰) = (R_{sample}/R_{standard} - 1) \times 1000 \quad (1)$$

where $R_{sample}$and $R_{standard}$ are the hydrogen and oxygen isotopic compositions ($^2H/^1H$ and $^{18}O/^{16}O$ ratios) of the sample and standard water (Vienna Standard Mean Ocean Water, V-SMOW), respectively.

Quantification of the water sources used by the plants

Taking into consideration the hydrogen isotope fractionation in some xerophytes (Ellsworth and Williams, 2007; Zhao et al., 2016), only $\delta^{18}O$ values were used for water source analysis and calculations. The iso-source model (Phillips and Gregg, 2003) was applied to estimate the proportional contributions of different water sources to the composition of plant water, with the source increment defined as 1% and the mass balance tolerance defined as 0.1‰. On the basis of the distribution of *F. bungeana* roots and the similarity of $\delta^{18}O$ values in each soil layer, the potential water sources were divided into the following four parts: soil water at depths of 0–30, 30–60, 60–90, and below 90 cm.

Soil water potential

Soil water potential was measured using a WP4 dew point potential meter (Decagon, Pullman, WA, USA). Given that the time for which soil has been exposed influences measurements, when excavating soil profiles, fresh soil was collected immediately each time a layer was excavated, and the water potential was measured and recorded.

Plant water potential

Plant water potential was measured using a pressure chamber water potential meter (Plant Moisture Stress; Corvallis, Oregon, USA). On each measurement day, three measurements were performed at predawn, midday, and during the evening. For measurements, we selected well-developed upper leaves from the middle and upper sections on the sunny side of sample plants, and simultaneously collected branches and uninjured roots from the same plant, and placed these into the pressure chamber to measure their water potentials, with each measurement being repeated three times. During each of the three periods, all measurements were completed within 1 h, and the times of measurement of predawn water potential were adjusted according to the time of sunrise, and was generally completed prior sunrise.

Plant hydraulic conductivity

Plant hydraulic conductivity was measured based on the water perfusion method using a high-pressure flow meter

(HPFM-GEN3; Dynamax Inc., Houston, USA), and was performed simultaneously with our measurements of plant water potential. Measurements of the hydraulic conductivity of the canopy were carried out using the flow meter in "steady mode" at a steady pressure of 350 kPa until attaining a stable water flow. Root hydraulic conductivity was measured using the flow meter in "transient mode", during which the pressure was rapidly increased from 0 to 500 kPa. On the basis of the pressure and flow, we performed linear regression analysis, with the slope obtained representing hydraulic conductivity. Each of the hydraulic conductivity measurements was performed *in situ* over a period of approximately 10 mins. The entire canopy of sample plants was cut from the main root at a distance of 3 cm above the sandy soil surface and rapidly placed into a water-filled bucket. To prevent air from entering the xylem, the base of the canopy was re-cut underwater, and the hydraulic conductivity of the entire canopy (Figures 2A, B) and the entire root system (Figure 2C) was measured.

Measurement of the $\delta^{13}C$ of plant leaves

Plant leaf samples collected in the field were placed in an oven, deactivated at 105°C for 25 min, and dried at 70°C for 48 h to a constant weight. Having dried, the leaves were ground to pass through a 100-mesh sieve, sealed, and stored in a dry place. The $\delta^{13}C$ values of plant leaves was determined using an isotope ratio mass spectrometer (IRMS) (DELTA V Advantage; Thermo Fisher Scientific, Bremen, Germany), with the isotopic composition expressed as in formula (1), with $R_{sample}$and $R_{standard}$ representing the carbon isotopic compositions ($^{13}C/^{12}C$ ratios) of the sample and standard (Vienna Pee Dee Belemnite, V-PDB), respectively.

Data analysis

Data analyses were performed using SPSS 21.0 software (SPSS Inc., Chicago, IL, USA), and figures were prepared using Origin 2017 software (OriginLab Corp., Northampton, MA, USA). One-way analysis of variance (ANOVA) was applied to determine differences in the contribution of the fractions of each layer of soil water to *F. bungeana*, soil water potential, and leaf $\delta^{13}C$ values across months and different sites on the mega-dunes. One-way ANOVA was also used to analyze differences in the soil water potential of different soil layers and to identify the differences in plant water potential, as well as the hydraulic conductivity of different parts of *F. bungeana*. Temporal differences in leaf, stem, and root water potentials, and canopy hydraulic conductivity were analyzed using one-way ANOVA combined with the *post hoc* Tukey's honestly significant difference (HSD) test. Two-way ANOVA combined with *post hoc* Tukey's HSD test was further conducted to analyze differences among the predawn, midday, and evening leaf, stem, and root water potentials, and predawn, midday, and evening canopy and root hydraulic conductivities of *F. bungeana*, among months and at different sites on the mega-dunes. The significance level for statistical analyses was set at 0.05. Pearson's correlation analysis was conducted to determine potential associations among the water uptake fraction, soil water potential, and root hydraulic conductivity (plant water potential, soil water potential, and hydraulic conductivity or water uptake fraction and water use efficiency).

Results

Temporal and spatial variation in water sources

The iso-source model revealed that *F. bungeana* can simultaneously extract water from four zones in the soil profile, although the relative amounts of water extracted from these four sources showed a monthly variation. As shown in Figure 3, a majority of the water absorbed by *F. bungeana* (80.47% ± 4.28%) was obtained from the 0–60 cm soil layer. Measurements obtained in May revealed that the major water source used by *F. bungeana* in this month was that in the 0–30 cm layer (87.27% ± 8.43%), although there was a significant reduction in the fraction absorbed from this layer in June (42.27% ± 5.40%) and July (50.03% ± 9.85%) ($P< 0.05$). In contrast, there was a significant increase in the proportional contribution of soil water from the 30–60 cm soil layer ($P< 0.05$) from May (5.23% ± 3.59%) to June (29.13% ± 5.13%), followed by a non-significant reduction in July (27.47% ± 8.67%) ($P > 0.05$). Similar temporal variation was detected with respect to the proportional contributions of soil water from the 60–90 cm soil layer (May, 3.6% ± 2.25%; June, 16.47% ± 4.31%; July, 11.30% ± 3.55%). However, we detected no distinct temporal differences in the percentage contribution of soil layers below 90 cm ($P > 0.05$). We also established that the proportion of soil water contributed by the 0–30 cm layer differed significantly from that derived from the other assessed layers ($P< 0.001$), whereas we detected no pronounced differences in the proportional contributions of different soil layers to *F. bungeana* growing at different sites on the mega-dunes ($P > 0.05$) (Figure 3).

The results of our analysis of the relationship between soil water potential and water source ratio indicated that the 0–30 cm fraction of soil water absorbed by *F. bungeana* was negatively correlated with the water potential of this layer (Figure 4A), whereas the absorption fraction of the 30–60 cm soil water was significantly positively correlated with the corresponding water potential ($P< 0.05$)(Figure 4B). However, we detected no pronounced association, either negative or positive, between the absorption percentage of the 60–90 cm soil water and the corresponding water potential (Figure 4C). Analysis of the relationships between the root hydraulic conductivity and

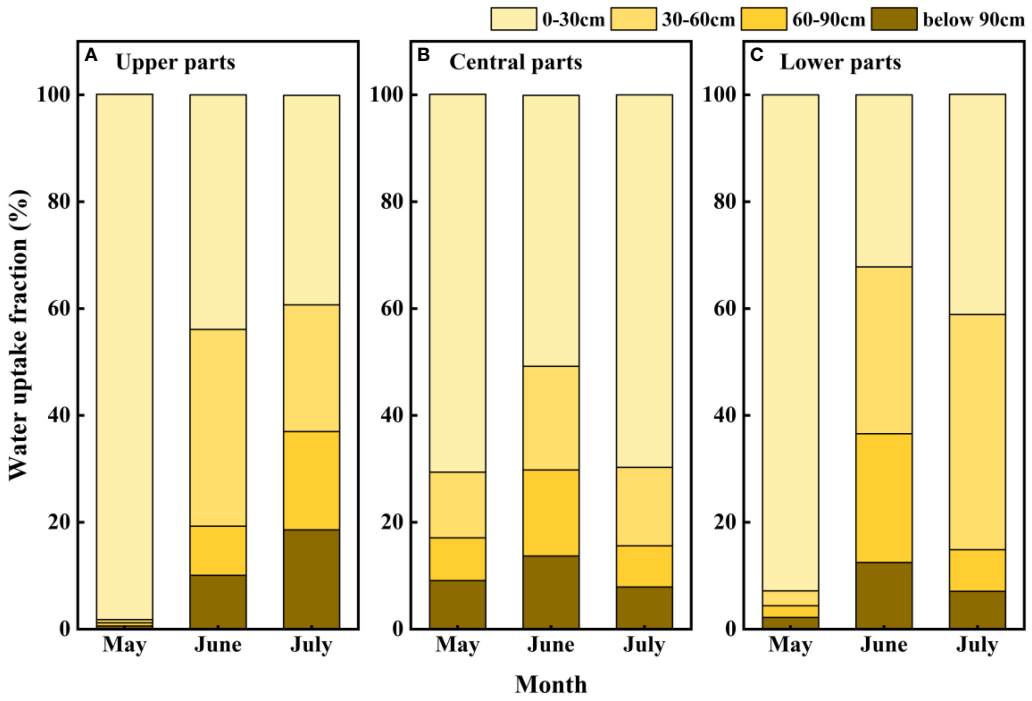

FIGURE 3
Seasonal variations in water uptake proportions from different soil layers for *Ferula bungeana* growing at different sites on mega-dunes. **(A–C)** present data for the upper, central parts, and lower parts of mega-dunes, respectively. The data were obtained using the iso-source model.

water source ratio of *F. bungeana* revealed that there were no significant correlations between the absorption fractions of the 0–30 cm and 60–90 cm soil water and root hydraulic conductivity (Figures 5A, C), whereas the percentage absorption from the 30–60 cm soil layer was positively correlated with root hydraulic conductivity, regardless of the time of day when measurements were obtained (predawn, midday, or evening) (Figure 5B).

Temporal and spatial variation in plant and soil water potentials

We detected distinct differences in the water potential of the different parts (root, stem, and leaf) of *F. bungeana* ($P< 0.05$), and established that water was transported upward along a water potential gradient from root to stem to leaf. Root, stem, and leaf water potentials showed the same diurnal and monthly fluctuations. For *F. bungeana* plants measured on the same sampling day at the same mega-dune sites, we detected significant differences in plant water potentials with time ($P< 0.05$), with the diurnal variations in plant water potentials showing a clear monthly variation. Significant monthly variations in the plant water potential at the same time were detected at all mega-dune sites ($P< 0.05$). Additionally, we found that the whole-plant water potentials of *F. bungeana* did not differ among the mega-dune sites ($P > 0.05$) (Figure 6).

At all assessed sites on mega-dunes in the Badain Jaran Desert, we detected significant temporal and spatial variation in soil water potential in different months ($P< 0.05$) and at different soil depths ($P< 0.05$). The soil water potential in the upper soil layers showed strong monthly differences, with lower values in May and higher values in June and July. Comparatively, the soil water potential in the deeper soil profile fluctuated minimally across months and the water potential values were higher than those close to the soil surface. However, no pronounced spatial differences were detected in soil water potential across the sites on mega-dunes ($P > 0.05$) (Figure 7).

Temporal and spatial variation in plant hydraulic conductivity

We detected significant differences between the canopy and root hydraulic conductivities of *F. bungeana* ($P< 0.001$), with values obtained for the hydraulic conductivity of roots generally being considerably greater than those obtained for the canopy. In addition, diurnal variations in hydraulic conductivity were significant in roots and canopies ($P<0.05$). Pronounced monthly differences were observed in plant hydraulic conductivity

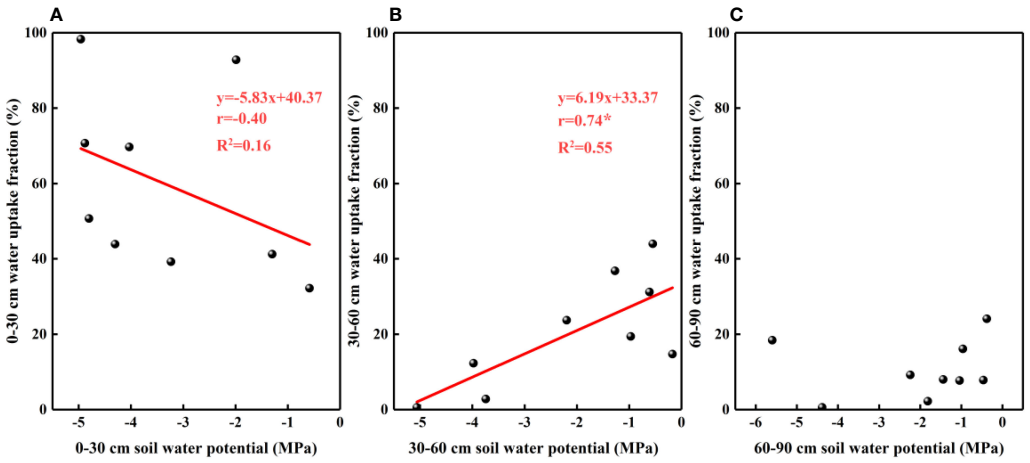

FIGURE 4
The relationship between soil water uptake fraction and soil water potential. **(A–C)** present data for the 0–30, 30–60, and 60–90 cm soil layers, respectively.

($P< 0.001$), with the largest overall values being recorded in June. Contrastingly, there appeared to be no significant differences in the hydraulic conductivity of *F. bungeana* growing at the different mega-dune sites ($P > 0.05$) (Figure 8).

Temporal and spatial variation in the plant water use efficiency

There were significant monthly differences in the leaf $\delta^{13}C$ values of *F. bungeana* growing at all mega-dune sampling sites ($P< 0.001$), with the largest value recorded in July (-25.59‰ ± 0.27‰), the smallest value in June (-28.19‰ ± 0.18‰), and an average value of -27.07‰ ± 0.20‰. However, whereas the differences detected in July were significant ($P< 0.001$), those measured in May and June were not significant ($P > 0.05$), and overall there were no distinct differences in the leaf $\delta^{13}C$ values of *F. bungeana* among the mega-dune sites ($P > 0.05$) (Figure 9).

Discussion

Variation in water sources

The fact that *F. bungeana* growing on the slopes of mega-dunes in the Badain Jaran Desert draws water primarily from the 0–60 cm soil layer (Figure 3) is consistent with the distribution of its root system, which extends to maximum depths of approximately 50 cm below the dry sand layer. This pattern of water usage is also comparable to that observed for the annual herb *Agriophyllum squarrosum* (Li et al., 2019). Interestingly, however, we also found that *F. bungeana* can utilize a certain proportion of soil water at depths below 90 cm. Given that its roots do not penetrate to these depths, we speculate that the water usage of this plant may be facilitated by the hydraulic lift mediated by *Zygophyllum xanthoxylum* growing in the same habitat (Wu, 2010). In this scenario, deep soil water absorbed by the roots of *Z. xanthoxylum* is released into the upper soil layers, wherein it can be utilized by the shallow branching roots of *F. bungeana*. In addition, *Artemisia ordosica*, which grows in the same dune habitat, utilizes soil water at depths down to 120 cm (Qin et al., 2022), thereby to a certain extent, drawing upon the water sources of *F. bungeana*. Consequently, there may exist a certain degree of competition between *F. bungeana* and *A. ordosica* for limited resources. During the dry season, however, these three species tend to be dependent on soil water sourced from different soil layers, which could be regarded as an effective strategy for hydrological niche segregation, the phenomenon whereby plants are able to coexist in the same habitat by utilizing different sources of water. This partitioning of resources thus serves an important mechanism facilitating plant coexistence in arid water-limited ecosystems (Moreno-Gutiérrez et al., 2012; Wu et al., 2014; Silvertown et al., 2015; Tiemuerbieke et al., 2018; Wu et al., 2019).

The iso-source model adopted in the present study indicated that the water sources exploited by *F. bungeana* show clear temporal variations. In May, *F. bungeana* mainly extracts water from the 0–30 cm soil layer, whereas in June and July, a significant increase was detected in the utilization of soil water at depths between 30 and 60 cm (Figure 3). Depending upon water availability, switching water utilization patterns between different soil layers is a necessary strategy enabling plants to

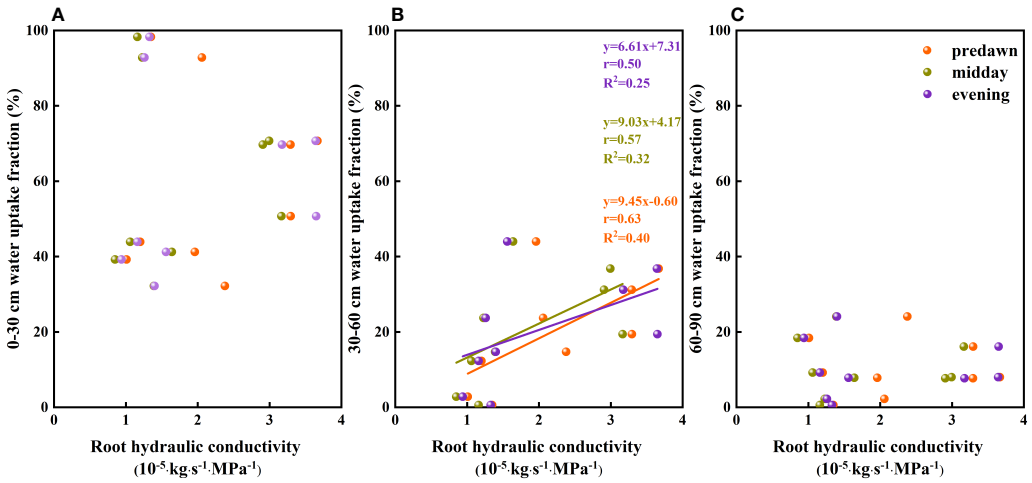

FIGURE 5
The relationship between the soil water uptake fraction and root hydraulic conductivity of Ferula bungeana. **(A–C)** present data for the 0–30 cm, 30–60 cm, and 60–90 cm soil layers, respectively.

tolerate drought conditions in water-deficient ecosystems (Hasselquist et al., 2010; Wang et al., 2019). Seasonal variations in plant water sources are associated with differences in multiple factors, notably soil water content, precipitation, transpiration, and competitive interactions at different growth stages (Zhao et al., 2019). In arid habitats, the upper soil water is predominantly replenished by precipitation, and plants can absorb water from these layers *via* aquaporins (Tan et al., 2018; Wu et al., 2019). With the progression of growing season, as the amounts of precipitation decline and temperatures begin to rise, there is a gradual depletion of soil moisture content, thereby resulting in the dehydration or death of fine roots distributed in the upper soil layer (Barbeta et al., 2015). Therefore, although soil water availability and root activity to a large extent determine the ability of plant roots to obtain water (Wu et al., 2014; Warren et al., 2015; Phillips et al., 2016; O'Keefe et al., 2019), the rooting depth determines the depth of soil from which plants can extract water (Zencich et al., 2002). In the present study, we established that the ratio of soil water absorbed by the roots of *F. bungeana* was largely determined by the water potential of the 30–60 cm soil layer.

However, we established that for *F. bungeana*, the percentage utilization of soil water was highest in the 0–30 cm soil layer, and was not restricted by either root hydraulic conductivity or the soil water potential of this layer, which consequently posed the question as to which absorption path is operational under these conditions. The findings of numerous studies have revealed that dew uptake by plants occurs in most deserts where water is limited by the scarcity of precipitation (Hill et al., 2015; Dawson and Goldsmith, 2018; Berry et al., 2019; Hill et al., 2021). For example, Hill et al. (2015) found that some dominant desert plants derive approximately 50% of their water requirements from dew (Hill et al., 2015), and several studies have provided evidence to indicate direct entry of dew water into leaves (Cavallaro et al., 2020), water uptake pathways into leaves through the cuticle (Gouvra and Grammatikopoulos, 2003; Goldsmith et al., 2017), and water uptake through stems (Breshears et al., 2008; Mason et al., 2016). Hill et al. (2021) also demonstrated that desert plants utilize dew on leaves (including direct absorption of dew by leaves and root absorption of dew falling onto the surface soil), transfer this water to the roots, and subsequent transport the water to the stems *via* different routes (Hill et al., 2021). It is thus conceivable that the input of dew with the same isotopic values as the upper soil causes a negative correlation between the proportion of water absorbed from the 0–30 cm soil layer and the soil potential of this layer, whereas the direct absorption of water *via* the leaves would account for the lack of correlation between the water source and hydraulic conductivity of the root system. However, more in-depth analysis will be necessary to clarify the underlying mechanisms.

Variations in plant and soil water potentials

Soil water potential fluctuates according to depth (Figure 7). The upper soil layers are strongly affected by precipitation and temperature, and the soil moisture content of these layers can undergo considerable fluctuation (Wu et al., 2019). Between May and July, precipitation in this region is typically low, with quantities insufficient to infiltrate downwards (Chen et al., 2014), whereas temperatures are high and there is a pronounced evaporative loss, thereby contributing to a substantial depletion of upper soil moisture. In recent years, studies have shown that air humidity, that is, the absorption of atmospheric water vapor, also has a

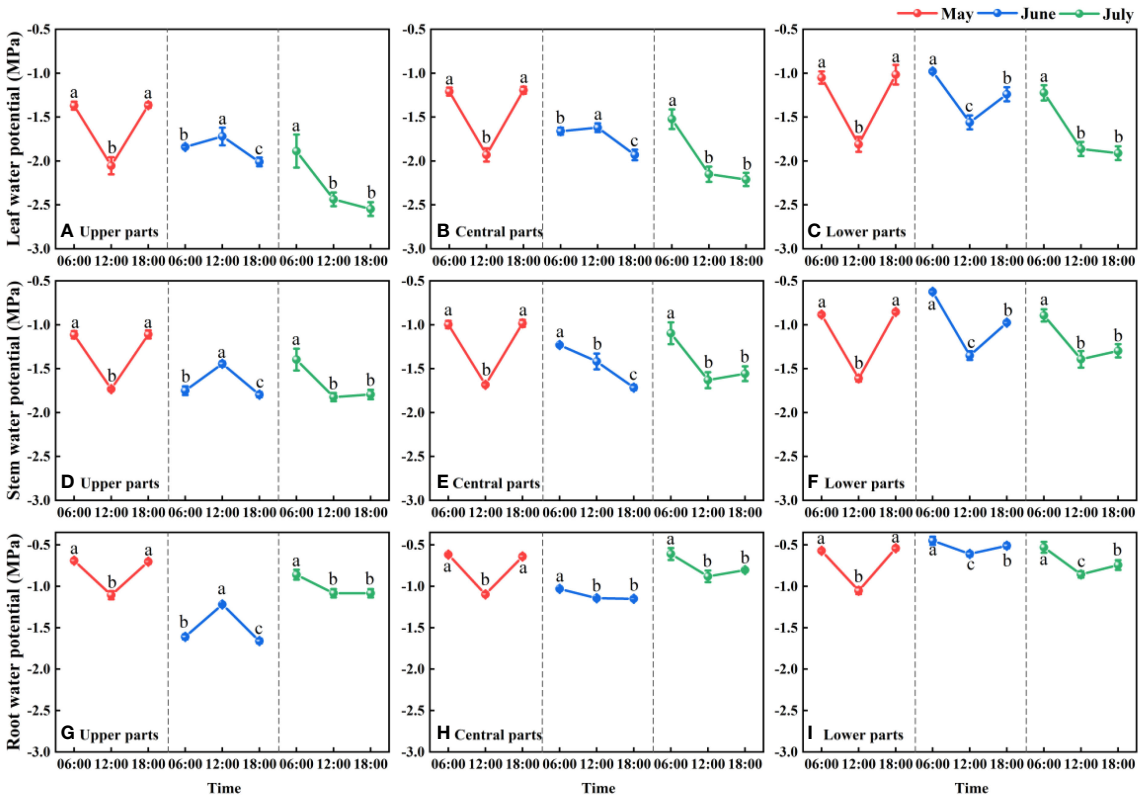

FIGURE 6
Daily and seasonal variations in the leaf **(A-C)**, stem **(D-F)**, and root **(G-I)** water potentials for Ferula bungeana growing on mega-dunes in the Badain Jaran Desert during the 2020 growth season. Data are presented as the means ± 1SE. Different lowercase letters indicate significant differences in water potential at different times within the same sampling day at the $P < 0.05$ level of significance.

notable influence on the upper soil moisture in dryland ecosystems (Kosmas et al., 1998; Kosmas et al., 2001; McHugh et al., 2015). Comparatively, deeper soil is influenced to a far lesser extent by environmental factors, and consequently, the levels of soil moisture in these deeper layers tend to be higher and less prone to fluctuate than those in shallower soils (Wang et al., 2017). From the perspective of the water potential gradient, we determined that water in the wet sand layers of mega-dunes is derived from groundwater, which migrates upward by evaporation as a thin film of water (Chen et al., 2004; Chen et al., 2014), thereby leading to a greater isotopic enrichment of the surface soil water (Qin et al., 2022). This process tends to run counter to the idea that local precipitation can infiltrate through mega-dunes to recharge lakes or groundwater (Zhao et al., 2011; Ma et al., 2016). Some experts also believe that the water in mega-dunes originates from the condensation of water vapor from the lakes (Zhao et al., 2011). Given these conflicting views, the hydrological cycle of the Badain Jaran Desert continues to be a subject of active debate.

Plant water potential can indirectly reflect the water status of plants, and its levels indicate the extent to which plants absorb water from the soil or adjacent cells to ensure normal physiological activities (Schütz et al., 2002). In the present study, monthly differences in the diurnal patterns of plant water potentials (Figure 6), might be associated with the regional monthly differences in diurnal temperature variation. Plants are dependent on the upward transport of water mediated by the transpiration pull along a water potential gradient (Kim et al., 2014; Zhang et al., 2017), the extent of which is influenced by temperature, thereby affecting the water potential of different parts of the plant. Theoretically, the temperature tends to be highest at midday, when the plant water potential should be lower than that predawn (González et al., 2004). A reduction in plant water potential at midday is beneficial to plants, in that it is conducive to the absorption of water from soil aquifers and reduces water loss to the atmosphere, thereby contributing to plant growth. Conversely, in this study, we found that the plant water potential at midday in June was higher than that recorded predawn (Figures 6A, B, D, G). We suspect that this counter-intuitive observation could be attributed to the fact that plants can enhance their water potential by absorbing condensed water (Boucher et al., 1995; Simonin et al., 2009; Eller et al., 2013; Berry et al., 2019; Cavallaro et al., 2020; Yokoyama et al., 2021), and it

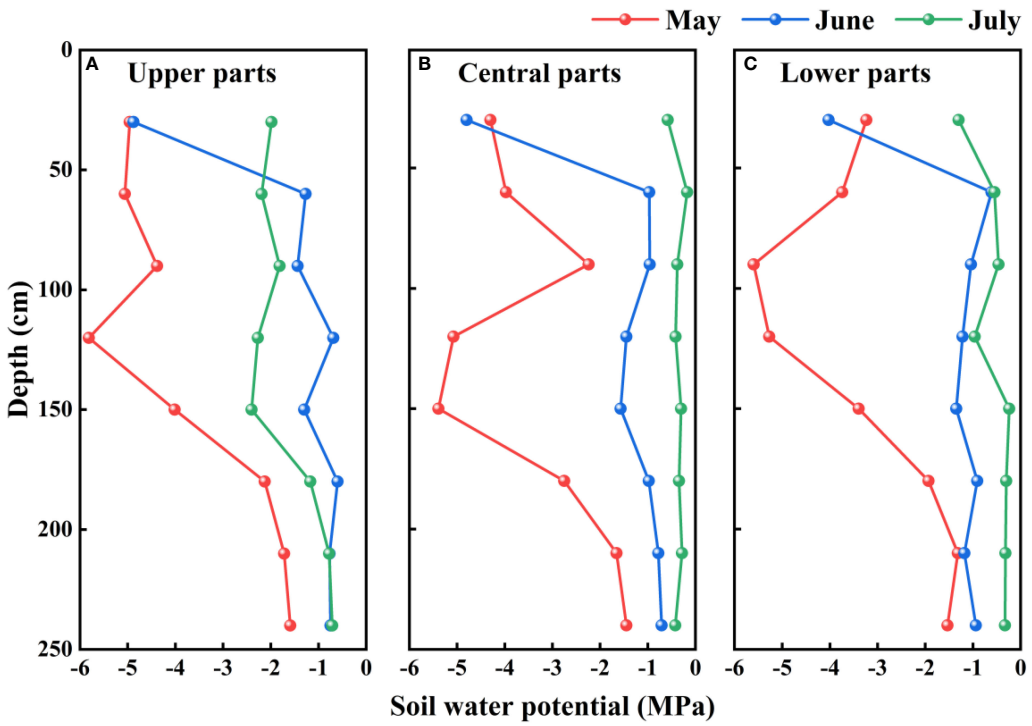

FIGURE 7
Vertical distribution of the soil water potentials on mega-dunes in the Badain Jaran Desert during the 2020 growth season. **(A–C)** present data for the upper, central, and lower parts of mega-dunes, respectively.

is conceivable that there might also be a certain hysteresis effect. In addition, foliar water uptake is markedly influenced by environmental conditions, such as wind speed, season, and terrain (Pan, 2001). Monthly differences in these environmental conditions may lead to monthly differences in the water potentials of plants growing at different sites on the mega-dunes surveyed in the present study.

Leaf water potential is considered to serve as an indicator of the water status of the entire plant (Sibounheuang et al., 2006), which is associated with drought resistance mechanisms (Jongdee et al., 2002; Pantuwan et al., 2002). Differences in water use patterns and water conductance from roots to leaf tips are important for maintaining the leaf water potential of plants (Sibounheuang et al., 2006), and in the present study, we detected different response relationships between leaf water potentials and the absorption fractions of different soil layers (Figure 10). These observations would tend to indicate that the water stress experienced by *F. bungeana* is alleviated by the utilization of deep soil water.

When water availability in the upper soil layer is reduced, the movement of water between the soil and roots is restricted by incomplete root–soil contact and an increase in hydraulic resistance, thereby hindering the absorption of water. To ensure uninterrupted water absorption, it is necessary for plants to continuously reduce their water potential. When the plant water potential reaches a certain threshold, plant water sources are gradually separated from shallow soil water and transferred to deep water sources (Wu et al., 2019), which to a certain extent contributes to relieving plant water stress. By extracting water from deep soil sources, plants can restore water potentials. In addition, temporal variation in plant water potential as soil water fluctuates in the same soil layer (Figure 10B) could be due to different factors restricting water absorption or the absorption ratio of condensed water or atmospheric water at different times. During the predawn and evening periods of day, leaf and stem water potentials are constrained by other conditions (Figure 11). We infer that during the predawn and evening periods of day, leaf and stem water potentials are restricted by canopy hydraulic conductivity, that is, canopy resistance tends to be greater at these times of day (Figure 12). If the stem presents a high resistance to water flow, the water uptake capacity of the root system has a limited effect on leaf water potential (Turner, 1982). Even in circumstances in which there is a high stem water potential, there may not be a high leaf water potential if the internal water conductivity of the leaf is low (Nissanka et al., 1997). Similarly, even if there is a high root water potential, if the stem water conductivity is low, there may not be a sufficiently high stem water potential, which in turn

10.3389/fpls.2022.957421

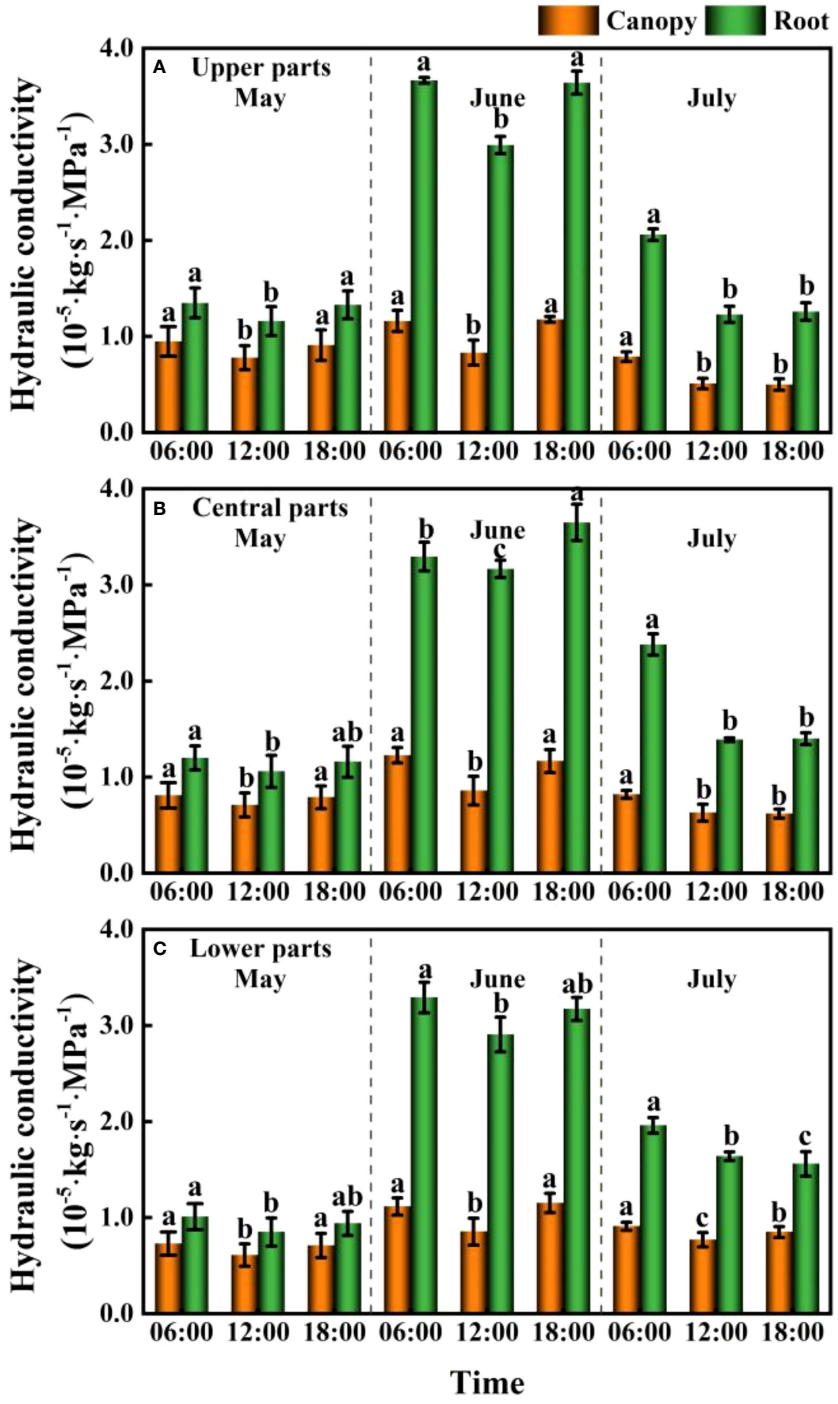

FIGURE 8
Daily and seasonal variations in the canopy and root hydraulic conductivity for Ferula bungeana growing on mega-dunes in the Badain Jaran Desert during the 2020 growth season. **(A–C)** present data for the upper, central, and lower parts of mega-dunes, respectively. Data are presented as the means ± 1SE. Different lowercase letters indicate significant differences in hydraulic conductivity at different times within a single sampling day at the $P < 0.05$ level of significance.

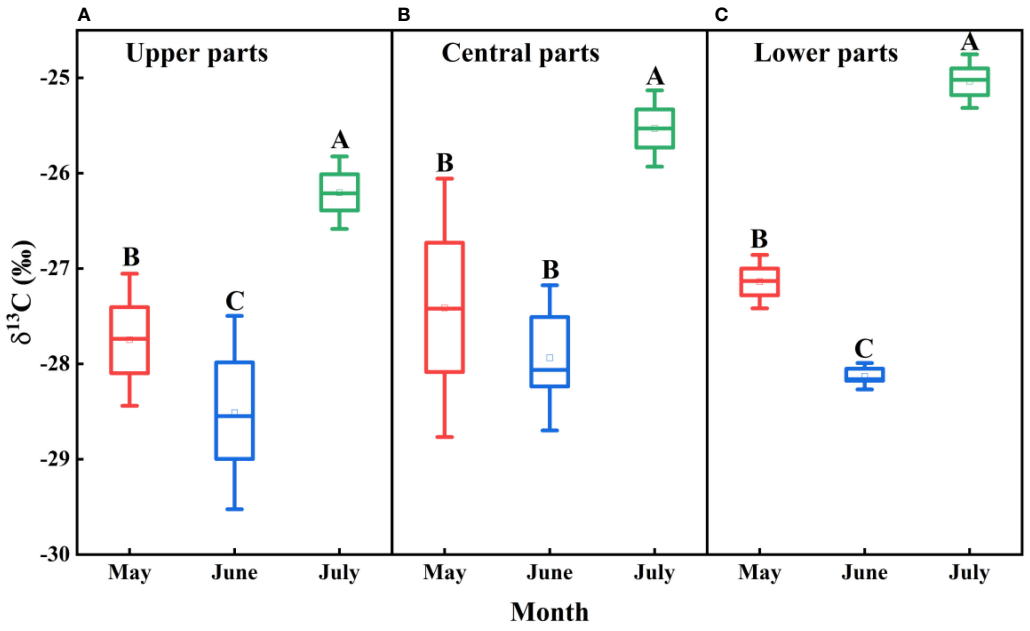

FIGURE 9
Spatio-temporal variations in d13C values for Ferula bungeana growing on mega-dunes in the Badain Jaran Desert during the 2020 growth season. **(A–C)** present data for the upper, central, and lower parts of mega-dunes, respectively. Data are presented as the means ± 2SD. Different uppercase letters indicate significant differences in d13C values among months at the P< 0.05 level of significance.

influences the leaf water potential. However, in the case of high root hydraulic conductivity, a reduction in root water potential might be attributable to poor soil water conditions and the radial movement of water absorbed by roots, the process whereby water enters the root xylem from the root surface.

Variations in plant hydraulic conductivity

Within plants, it is necessary for water to overcome a certain resistance to upward conductance. According to the main links of water entering plants from the soil and subsequently diffusing into the atmosphere, the resistance to water conduction can be divided into soil resistance, soil–root contact resistance, root absorption resistance, xylem conductive resistance within roots, internal conductive resistance of the above-ground parts of plants, and water vapor (stomatal) diffusion resistance. Among these, root absorption and stomatal diffusion resistances are the predominant sources of resistance in the below- and above-ground parts of plants, respectively (Shao et al., 1986). The reciprocal of the water flow resistance overcome by plants can be used as an index to characterize and evaluate the water conductivity of the different parts of plants (Yang et al., 2011), namely, plant hydraulic conductivity. The water absorption characteristics of plant roots and the water-conducting capacity of the aerial parts have been shown to have a decisive effect on the survival and growth of plants (Yang et al., 2011), and are also important indicators of the regulation of plant water balance. In the present study, the water transport capacity of the roots was substantially greater than that of the canopy (Figure 8), and this stronger water transport capacity of the root system directly influences the rate of water transport in the canopy and the entire plant. The root system is the source of plant water transport, the water absorption and conduction capacity of which play essential roles in determining the water status of the entire plant and the maintenance of plant water balance (Li et al., 2020). In general, the root system and leaves of plants are the parts most prone to embolism, resulting in an overall reduction in plant water conductivity. The most obvious manifestation of such impedance is a V-shaped diurnal variation in plant hydraulic conductivity (Figure 8). Monthly variations observed in the hydraulic conductivity of canopies and roots are plausibly associated with changes in growth stage, moisture conditions, and environmental conditions. The internal water transport structural features of plants determine the potential capacity of plant water transport, whereas the external soil moisture status determines the overall level of plant water transport, and environmental factors, such as light, determine instantaneous changes in plant water transport (Si et al., 2007).

As the main driving force for water conduction in plants, water potential is closely associated with plant hydraulic conductivity. Typically, in ecosystems characterized by poor water status, particularly desert ecosystems, the water consumption of plants exceeds the amount of water taken up by roots, thereby resulting in potentially serious deficits. Under

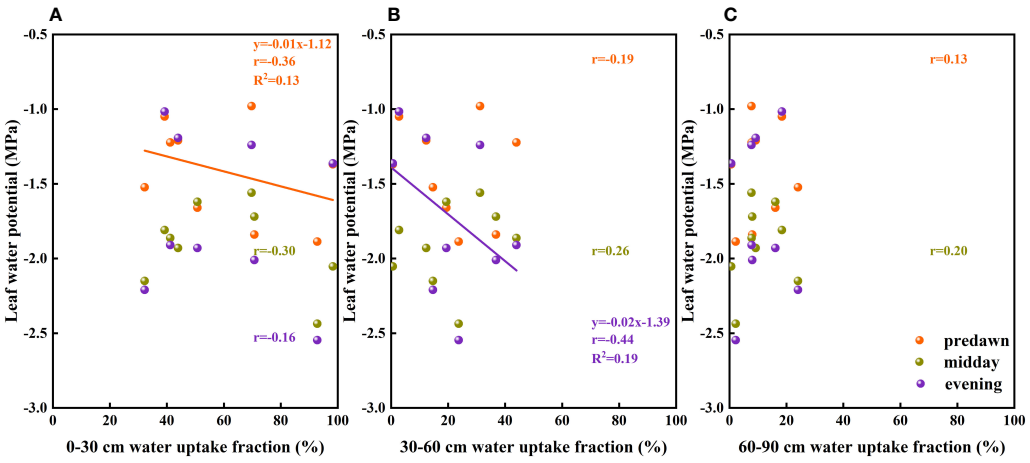

FIGURE 10
The relationship between leaf water potential and soil water uptake fraction. **(A–C)** present data for the 0–30, 30–60 cm, and 60–90 cm soil layers, respectively.

conditions of water deficiency, strong negative pressure develop at both ends of the xylem ducts, which exceed the cohesive and adhesive forces between water molecules within the ducts and between water molecules and the duct walls, thereby causing a rupture of the continuous water columns, and entry gas in the xylem ducts. The embolisms thus generated reduce hydraulic conductivity, resulting in a reduction of water potential necessary to maintain a sufficient water balance, which is characterized by the similar diurnal variations in plant water potential and hydraulic conductivity (Figures 6, 8). This can be seen an adaptive water transport strategy adopted by plants to maintain water homeostasis and life activities in specific habitats. However, it remains unclear as to whether a reduction in water potential contributes to a reduction in plant hydraulic conductivity or vice versa.

Variations in plant water use efficiency

Water use efficiency is an important indicator that can be used to characterize the effective water use capacity of plants. In

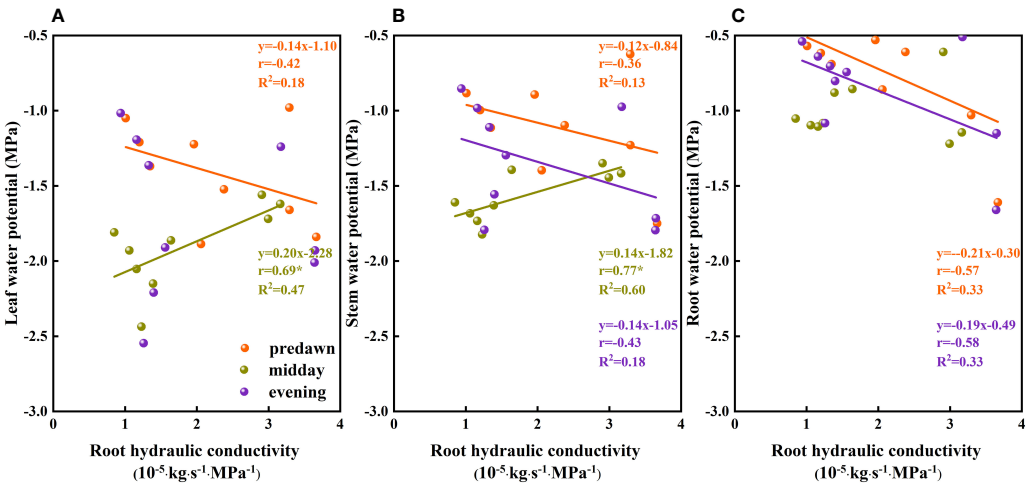

FIGURE 11
The relationship between the plant water potential and root hydraulic conductivity of *Ferula bungeana*. **(A–C)** present data for the relationships between leaf, stem, and root water potential and root hydraulic conductivity, respectively.

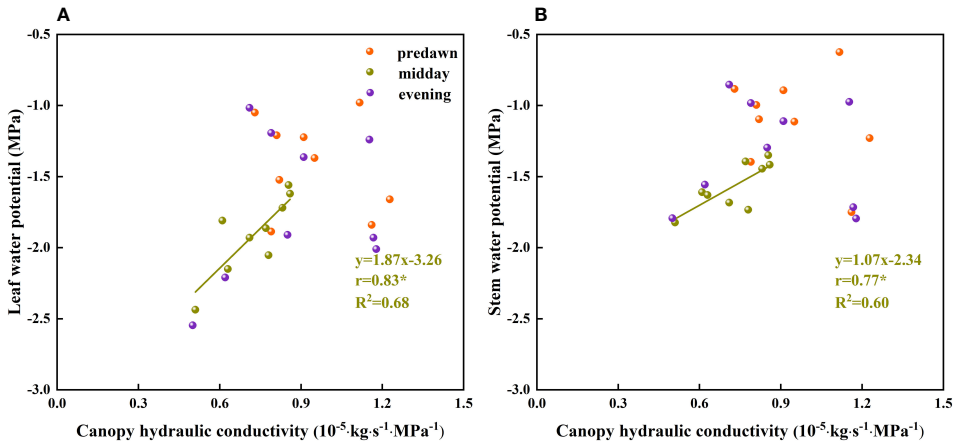

FIGURE 12
The relationship between the plant water potential and canopy hydraulic conductivity of *Ferula bungeana*. **(A, B)** present data for the relationships between leaf and stem water potentials and canopy hydraulic conductivity, respectively.

particular, long-term water use efficiency can fully reflect the long-term use of limited water sources and to a certain extent, the capacity of plants to adapt to water stress (Xing et al., 2019). Given that there is a significant positive correlation between the $\delta^{13}C$ values of plant leaves and water use efficiency, the $\delta^{13}C$ values are generally used to reflect the water use efficiency of plant leaves. In the present study, we established that the water use efficiency of *F. bungeana* was affected by water use pattern (Figure 13). To a large degree, water use efficiency reflects the difficulty plants experience in acquiring water. We found that in response to a reduction in the availability of water in the upper soil layers, plants switch to sourcing water from the deeper layers in the sand dune profile, which is comparatively more difficult. Consequently, plants can resist water stress by enhancing their water use efficiency.

The significant monthly variations in leaf water use efficiency of *F. bungeana* (Figure 9) could be associated with one or more of a number of factors, including growth stage, internal factors (e.g., leaf water potential and stomatal activity), and external environmental factors (e.g., light, water, and temperature). Generally, the water use efficiency of plants has been found be higher during the early growth stages than during the latter stages (Yan et al., 1998), which contrasts with our findings in the present study. We suspect that this discrepancy could be attributed to differences in the water use patterns of different plant species at different growth stages. In terms of

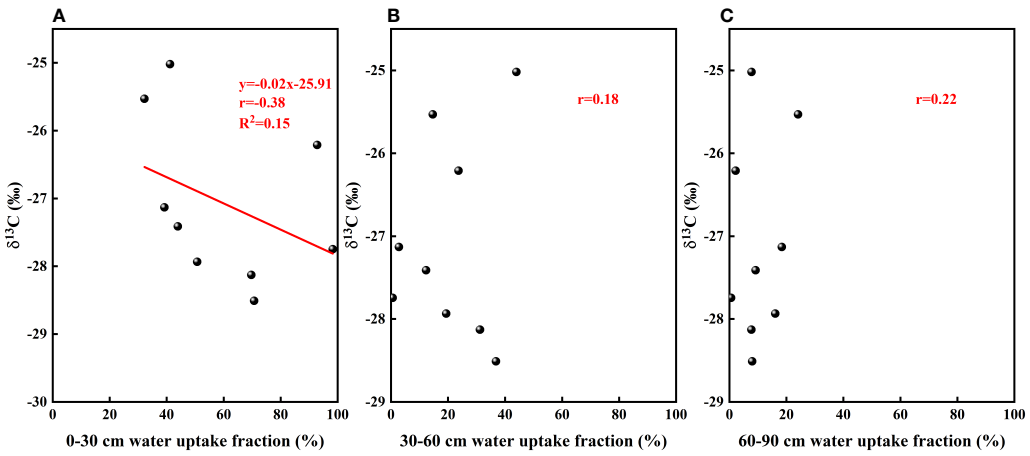

FIGURE 13
The relationship between leaf $\delta^{13}C$ values and soil water uptake fraction. **(A–C)** present data for the the relationships between leaf $\delta^{13}C$ values and the absorption ratio of the 0–30, 30–60, and 60–90cm soil layers, respectively.

intrinsic plant factors, plant water potential and stomatal activity both influence water use efficiency by affecting the rates of photosynthesis and transpiration; however, there tends to be a lack of consensus regarding the contribution of these effects. Among the external environmental factors influencing plant development, all factors that influence photosynthesis and transpiration would influence water use efficiency, although to differing extents. Within a certain range of light intensities, light enhancement can effectively improve water use efficiency, and in water-limited environments, plants have been found to be characterized by higher water use efficiency than those growing in water-sufficient environments (Yan et al., 1998). However, beyond a certain water threshold, water stress persists and the degree of water stress aggravation could lead to a reduction in water use efficiency. The water use efficiency of plants also increases in response to increases in atmospheric temperature (Liu et al., 2011). In the present study, we established that variations in the water use efficiency of *F. bungeana* growing at different sites on mega-dunes (Figure 9) are mainly associated with the grain size of sand and the depths to which plants are buried in sand in the different parts of the mega-dunes. The lower slopes of mega-dunes are characterized by coarser sand grains and thicker dry sand layers, and the stem sections of *F. bungeana* growing in these areas tend to be buried to a greater depth in the sand than at more elevated dune sites. Notably in this regard, the growth of buried stems supported by sand requires less carbon than that of upright plants of the same height growing above sand level (Pruyn et al., 2000). Consequently, under the same water conditions, the water use efficiency of *F. bungeana* in the lower parts of the mega-dunes was higher than that of plants growing in the more elevated parts of the dunes (Figure 9C). Moreover, the unfavorable water relationship in the upper slopes of mega-dunes has been shown to be associated with a lower carbon yield per unit leaf area (Gries et al., 2003), which would account for lower water use efficiency of *F. bungeana* in these upper parts compared with the plants growing at lower elevations (Figure 9A).

Variations in water use strategies

Under conditions of drought stress, plants generally adopt one of two opposing water use strategies: drought avoidance or drought tolerance. Drought avoidance indicates that plants do not encounter drought adversity throughout their growth and development, and thereby evade to detrimental effects of water deficits. Drought tolerance describes the measures adopted by plants to prevent, reduce, or repair the damage caused by water deficit based on metabolic reactions that contribute to maintaining a reasonably normal physiological state when encountering drought stress. A further strategy, drought resistance, refers to the ability of plants to defend themselves against drought and maintain normal physiological and biochemical processes under drought stress conditions. Examples of plants that adopt such strategies include *Lupinus arizonicus*, a drought-avoiding winter annual plant that reduces water loss through stomatal and morphological regulation, whereas the drought-tolerant *Malvastrum rotundifolium* can effectively utilize water, although its stomatal response, leaf movement, and osmotic regulation might contribute to water loss (Forseth and Ehleringer, 1983b). The *F. bungeana* plants examined in the present study were also assessed to be drought tolerant. Among other plants, the early spring ephemerals *Eremopyrum orientale* and *Schismus arabicus* adapt to drought based on higher water absorption and regulation capacities, whereas in *Plantago minuta* and *Senecio subdentatus*, the maintenance of sufficient water levels is achieved by high water-holding capacities and low transpiration intensities (Li and Wang, 1991). In general, ephemeral plants tend to be characterized by higher water use efficiency that can be maintained during the early growth period and when water is abundantly available (Ehleringer et al., 1979; Ehleringer and Forseth, 1980; Forseth and Ehleringer, 1983a), which is consistent with our findings in the present study.

The adaptation of plants to drought stress is a diverse and complex process, and the different water-use strategies adopted by plants at different developmental stages has rarely been reported. In this study, we characterized the water use strategies of *F. bungeana* in terms of water absorption, transport, and use efficiency, although we did not assess the processes associated with water consumption. Accordingly, in future studies, we should ideally focus on water consumption characteristics, including photosynthetic and transpiration rates, to gain a more in-depth understanding of the internal water status and intrinsic adaptation mechanisms of ephemeral plants, and comprehensively analyze their water use strategies.

Conclusions

The water use strategies of *F. bungeana* growing on the slopes of the mega-dunes in the Badain Jaran Desert are mainly associated with growth stage, and appear to be little influenced by the spatial distribution of plants on different parts of the mega-dunes. During the early stages of growth, *F. bungeana* mainly extracts water from the 0–30 cm soil layer, maintains high water potential and low hydraulic conductivity, and is characterized by high water use efficiency. During the mid-phase of the growth cycle, *F. bungeana* mainly utilizes water obtained from the 0–60 cm soil layer, and maintains moderate water potential and high hydraulic conductivity, although water use efficiency tends to be low. Water is still mainly sourced from the 0–60 cm soil layer during the latter stages of growth, with *F. bungeana* maintaining low water potential and low hydraulic conductivity, although has high water use

efficiency. The availability of soil water in the different layers of the mega-dunes is not only determined by precipitation and evaporation, but also by groundwater recharge, condensate recharge, and atmospheric water absorption, and we speculate that condensed water may also be an important source of water for *F. bungeana* in the study area. The proportion of water taken up by *F. bungeana* is limited by soil water availability and root hydraulic conductivity, which affect plant water potential, canopy hydraulic conductivity, and water use efficiency, the latter of which is also determined by carbon allocation.

Data availability statement

The raw data supporting the conclusions of this article will be made available by the authors, without undue reservation.

Author contributions

JQ: Conceptualization, Data curation, Investigation, Methodology, Formal analysis, Roles/Writing—original draft, Writing—review and editing. JS: Conceptualization, Data curation, Formal analysis, Funding acquisition, Methodology. BJ: Investigation. CZ: Conceptualization, Data curation, Formal analysis, Investigation. DZ: Investigation. XH: Investigation. CW: Investigation. XZ: Investigation. All authors read and approved the final manuscript. All authors have read and agreed to the published version of the manuscript.

Funding

This study was supported by the Major Science and Technology Project in Inner Mongolia Autonomous region of China (No. Zdzx2018057), the Innovation Cross Team Project of Chinese Academy of Sciences, CAS (No. JCTD-2019-19), Transformation Projects of Scientific and Technological Achievements in Inner Mongolia Autonomous region of China (No. 2021CG0046), the National Natural Science Foundation of China (No. 42001038), and the Open Project in the Key Laboratory of Conservation and Utilization of Biological Resources in Tarim Basin, Xinjiang Production and Construction Corps (No. BRZD2202).

Conflict of interest

The authors declare that the research was conducted in the absence of any commercial or financial relationships that could be construed as a potential conflict of interest.

Publisher's note

All claims expressed in this article are solely those of the authors and do not necessarily represent those of their affiliated organizations, or those of the publisher, the editors and the reviewers. Any product that may be evaluated in this article, or claim that may be made by its manufacturer, is not guaranteed or endorsed by the publisher.

References

Antunes, C., Chozas, S., West, J., Zunzunegui, M., Diaz Barradas, M. C., Vieira, S., et al. (2018a). Groundwater drawdown drives ecophysiological adjustments of woody vegetation in a semi-arid coastal ecosystem. *Glob. Change Biol.* 24, 4894–4908. doi: 10.1111/gcb.14403

Antunes, C., Díaz-Barradas, M. C., Zunzunegui, M., Vieira, S., and Máguas, C. (2018b). Water source partitioning among plant functional types in a semi-arid dune ecosystem. *J. Veg. Sci.* 29, 671–683. doi: 10.1111/jvs.12647

Barbeta, A., Mejía-Chang, M., Ogaya, R., Voltas, J., Dawson, T. E., and Peñuelas, J. (2015). The combined effects of a long-term experimental drought and an extreme drought on the use of plant-water sources in a Mediterranean forest. *Glob. Change Biol.* 21, 1213–1225. doi: 10.1111/gcb.12785

Berry, Z. C., Emery, N. C., Gotsch, S. G., and Goldsmith, G. R. (2019). Foliar water uptake: Processes, pathways, and integration into plant water budgets. *Plant Cell Environ.* 42, 410–423. doi: 10.1111/pce.13439

Boucher, J. F., Munson, A. D., and Bernier, P. Y. (1995). Foliar absorption of dew influences shoot water potential and root growth in pinus strobus seedlings. *Tree Physiol.* 15, 819–823. doi: 10.1093/treephys/15.12.819

Breshears, D. D., McDowell, N. G., Goddard, K. L., Dayem, K. E., Martens, S. N., Meyer, C. W., et al. (2008). Foliar absorption of intercepted rainfall improves woody plant water status most during drought. *Ecology* 89, 41–47. doi: 10.1890/07-0437.1

Brown, G. (2003). Species richness, diversity and biomass production of desert annuals in an ungrazed *Rhanterium epapposum* community over three growth seasons in Kuwait. *Plant Ecol.* 165, 53–68. doi: 10.1023/A:1021425308451

Cavallaro, A., Carbonell, S. L., Pereyra, D. A., Goldstein, G., Scholz, F. G., and Bucci, S. J. (2020). Foliar water uptake in arid ecosystems: seasonal variability and ecophysiological consequences. *Oecologia* 193, 337–348. doi: 10.1007/s00442-020-04673-1

Chen, J. S., Chen, X. X., and Wang, T. (2014). Isotopes tracer research of wet sand layer water sources in alax desert. *Adv. Water Sci.* 25, 196–206. doi: 10.14042/j.cnki.32.1309.2014.02.023

Chen, J. S., Li, L., Wang, J. Y., Barry, D. A., Sheng, X. F., Gu, W. Z., et al. (2004). Groundwater maintains dune landscape. *Nature* 432, 459–460. doi: 10.1038/432459a

Cui, X. J., Sun, H., Dong, Z. B., Luo, W. Y., Li, J. Y., Ma, Y. D., et al. (2017). Wet sand layer moisture of mega-dunes in the badain jaran sand Sea. *J. Desert Res.* 37, 214–221. doi: 10.7522/j.issn.1000-694X.2015.00242

Dawson, T. E., and Goldsmith, G. R. (2018). The value of wet leaves. *New Phytol.* 219, 1156–1169. doi: 10.1111/nph.15307

Dawson, T. E., Mambelli, S., Plamboeck, A. H., Templer, P. H., and Tu, K. P. (2002). Stable isotopes in plant ecology. *Annu. Rev. Ecol. Syst.* 33, 507–559. doi: 10.1146/annurev.ecolsys.33.020602.095451

Ehleringer, J. (1983). Ecophysiology of *Amaranthus palmeri*, a sonoran desert summer annual. *Oecologia* 57, 107–112. doi: 10.1007/BF00379568

Ehleringer, J., and Forseth, I. (1980). Solar tracking by plants. *Science* 210, 1094–1098. doi: 10.1126/science.210.4474.1094

Ehleringer, J., Mooney, H. A., and Berry, J. A. (1979). Photosynthesis and microclimate of *Camissonia claviformis*, a desert winter annual. *Ecology* 60, 280–286. doi: 10.2307/1937656

Ehleringer, J. R., Phillips, S. L., Schuster, W. S. F., and Sandquist, D. R. (1991). Differential utilization of summer rains by desert plants. *Oecologia* 88, 430–434. doi: 10.1007/BF00317589

Eller, C. B., Lima, A. L., and Oliveira, R. S. (2013). Foliar uptake of fog water and transport belowground alleviates drought effects in the cloud forest tree species, *Drimys brasiliensis* (Winteraceae). *New Phytol.* 199, 151–162. doi: 10.1111/nph.12248

Ellsworth, P. Z., and Williams, D. G. (2007). Hydrogen isotope fractionation during water uptake by woody xerophytes. *Plant Soil* 291, 93–107. doi: 10.1007/s11104-006-9177-1

Evaristo, J., McDonnell, J. J., Scholl, M. A., Bruijnzeel, L. A., and Chun, K. P. (2016). Insights into plant water uptake from xylem-water isotope measurements in two tropical catchments with contrasting moisture conditions. *Hydrol. Process.* 30, 3210–3227. doi: 10.1002/hyp.10841

Forseth, I. N., and Ehleringer, J. R. (1983a). Ecophysiology of two solar tracking desert winter annuals: III. gas exchange responses to light, CO_2 and VPD in relation to long-term drought. *Oecologia* 57, 344–351. doi: 10.1007/BF00377179

Forseth, I. N., and Ehleringer, J. R. (1983b). Ecophysiology of two solar tracking desert winter annuals: IV. effects of leaf orientation on calculated daily carbon gain and water use efficiency. *Oecologia* 58, 10–18. doi: 10.1007/BF00384536

Goldblati, P. (1978). An analysis of the flora of southern Africa: its characteristics, relationships, and orgins. *Ann. Mo. Bot. Gard.* 65, 369–436. doi: 10.2307/2398858

Goldsmith, G. R., Lehmann, M. M., Cernusak, L. A., Arend, M., and Siegwolf, R. T. W. (2017). Inferring foliar water uptake using stable isotopes of water. *Oecologia* 184, 763–766. doi: 10.1007/s00442-017-3917-1

González, R. H., Cantú, S. I., Gómez, M. M. V., and Ramírez, L. R. G. (2004). Plant water relations of thornscrub shrub species, north-eastern Mexico. *J. Arid. Environ.* 58, 483–503. doi: 10.1016/j.jaridenv.2003.12.001

Gouvra, E., and Grammatikopoulos, G. (2003). Beneficial effects of direct foliar water uptake on shoot water potential of five chasmophytes. *Can. J. Bot.-Rev. Can. Bot.* 81, 1278–1284. doi: 10.1139/b03-108

Gries, D., Zeng, F., Foetzki, A., Arndt, S. K., Bruelheide, H., Thomas, F. M., et al. (2003). Growth and water relations of *Tamarix ramosissima* and *Populus euphratica* on taklamakan desert dunes in relation to depth to a permanent water table. *Plant Cell Environ.* 26, 725–736. doi: 10.1046/j.1365-3040.2003.01009.x

Grossiord, C., Sevanto, S., Dawson, T. E., Adams, H. D., Collins, A. D., Dickman, L. T., et al. (2017). Warming combined with more extreme precipitation regimes modifies the water sources used by trees. *New Phytol.* 213, 584–596. doi: 10.1111/nph.14192

Hasselquist, N. J., Allen, M. F., and Santiago, L. S. (2010). Water relations of evergreen and drought-deciduous trees along a seasonally dry tropical forest chronosequence. *Oecologia* 164, 881–890. doi: 10.1007/s00442-010-1725-y

Hill, A. J., Dawson, T. E., Dody, A., and Rachmilevitch, S. (2021). Dew water-uptake pathways in Negev desert plants: a study using stable isotope tracers. *Oecologia* 196, 353–361. doi: 10.1007/s00442-021-04940-9

Hill, A. J., Dawson, T. E., Shelef, O., and Rachmilevitch, S. (2015). The role of dew in Negev desert plants. *Oecologia* 178, 317–327. doi: 10.1007/s00442-015-3287-5

Hu, M. J. (2021). *Mechanism of water vapor heat transport in vadose zone of badain jaran desert* (Zhengzhou: North China University of Hydraulic and Hydropower).

Huang, B. B. (2018). *Spatial-temporal variation of groundwater level in badain jaran desert* (Lanzhou: Lanzhou University).

Huang, L., and Zhang, Z. (2016). Effect of rainfall pulses on plant growth and transpiration of two xerophytic shrubs in a revegetated desert area: Tengger desert, China. *Catena* 137, 269–276. doi: 10.1016/j.catena.2015.09.020

IPCC (2019). *Climate change and land: an IPCC special report on climate change, desertification, land degradation, sustainable land management, food security, and greenhouse gas fluxes in interrestrial ecosystems* (UK: Cambridge University Press).

Jongdee, B., Fukai, S., and Cooper, M. (2002). Leaf water potential and osmotic adjustment as physiological traits to improve drought tolerance in rice. *Field Crop Res.* 76, 153–163. doi: 10.1016/S0378-4290(02)00036-9

Kim, H. K., Park, J., and Hwang, I. (2014). Investigating water transport through the xylem network in vascular plants. *J. Exp. Bot.* 65, 1895–1904. doi: 10.1093/jxb/eru075

Kosmas, C., Danalatos, N. G., Poesen, J., and van Wesemael, B. (1998). The effect of water vapour adsorption on soil moisture content under Mediterranean climatic conditions. *Agric. Water Manage.* 36, 157–168. doi: 10.1016/S0378-3774(97)00050-4

Kosmas, C., Marathianou, M., Gerontidis, S., Detsis, V., Tsara, M., and Poesen, J. (2001). Parameters affecting water vapor adsorption by the soil under semi-arid climatic conditions. *Agric. Water Manage.* 48, 61–78. doi: 10.1016/S0378-3774(00)00113-X

Li, Q. Y., Lai, L. M., Zhou, J. H., Zhou, L. H., Yang, L., Yi, S. G., et al. (2019). Water use characteristics of main species in different shrub encroachment stages on ordos plateau. *Chin. J. Ecol.* 38, 89–96. doi: 10.13292/j.1000-4890.201901.029

Li, D., Si, J. H., Zhang, X. Y., Gao, Y. Y., Luo, H., Qin, J., et al. (2020). Ecological adaptation of *Populus euphratica* to drought stress. *J. Desert Res.* 40, 17–23. doi: 1000-694X(2020)40:2<17:HYPEDG>2.0.TX;2-U

Liu, X. Z., Wang, G. A., Li, J. Z., Wang, W. W., Zhao, L. L., and Li, B. J. (2011). Relationship between temperature and $\delta^{13}C$ values of C_3 herbaceous plants and its implications of WUE in farming-pastoral zone in north China. *Acta Ecol. Sin.* 31, 123–136. 1000-0933(2011)31:1<123:ZGBFNM>2.0.TX;2-P

Li, Y. F., and Wang, Y. Z. (1991). *A study on water status of short-lived plants in early spring in xinjiang: anthology of xinjiang botany* (Beijing: Science Press).

Ludwig, J. A., Cunningham, G. L., and Whitson, P. D. (1988). Distribution of annual plants in north American deserts. *J. Arid. Environ.* 15, 221–227. doi: 10.1016/S0140-1963(18)31059-0

Mason, E. J., Sperling, O., Silva, L. C. R., McElrone, A. J., Brodersen, C. R., North, M. P., et al. (2016). Bark water uptake promotes localized hydraulic recovery in coastal redwood crown. *Plant Cell Environ.* 39, 320–328. doi: 10.1111/pce.12612

Ma, Y. D., Zhao, J. B., Luo, X. Q., Shao, T. J., Yue, D. P., and Zhou, Q. (2016). Runoff and groundwater rehcarge conditions in the megadune area of badain jaran desert. *Acta Geograph. Sin.* 71, 433–448. doi: 0375-5444(2016)71:3<433:BDJLSM>2.0.TX;2-M

McHugh, T. A., Morrissey, E. M., Reed, S. C., Hungate, B. A., and Schwartz, E. (2015). Water from air: an overlooked source of moisture in arid and semiarid regions. *Sci. Rep.* 5, 13767. doi: 10.1038/srep13767

Moreno-Gutiérrez, C., Dawson, T. E., Nicolás, E., and Querejeta, J. I. (2012). Isotopes reveal contrasting water use strategies among coexisting plant species in a Mediterranean ecosystem. *New Phytol.* 196, 489–496. doi: 10.1111/j.1469-8137.2012.04276.x

Nissanka, S. P., Dixon, M. A., and Tollenaar, M. (1997). Canopy gas exchange response to moisture stress in old and new maize hybrid. *Crop Sci.* 37, 172–181. doi: 10.2135/cropsci1997.0011183X003700010030x

O'Keefe, K., Nippert, J. B., and McCulloh, K. A. (2019). Plant water uptake along a diversity gradient provides evidence for complementarity in hydrological niches. *Oikos* 128, 1748–1760. doi: 10.1111/oik.06529

Pan, R. C. (2001). *Plant physiology* (Beijing: Higher Education Press).

Pantuwan, G., Fukai, S., Cooper, M., Rajatasereekul, S., and O'Toole, J. C. (2002). Yield response of rice (*Oryza sativa l.*) genotypes to different types of drought under rainfed lowlands - part 3. plant factors contributing to drought resistance. *Field Crop Res.* 73, 181–200. doi: 10.1016/S0378-4290(01)00194-0

Phillips, D. L., and Gregg, J. W. (2003). Source partitioning using stable isotopes: coping with too many sources. *Oecologia* 136, 261–269. doi: 10.1007/s00442-003-1218-3

Phillips, R. P., Ibáñez, I., D'Orangeville, L., Hanson, P. J., Ryan, M. G., and McDowell, N. G. (2016). A belowground perspective on the drought sensitivity of forests: Towards improved understanding and simulation. *For. Ecol. Manage.* 380, 309–320. doi: 10.1016/j.foreco.2016.08.043

Pruyn, M. L., Ewers, B. J., and Telewski, F. W. (2000). Thigmomorphogenesis: changes in the morphology and mechanical properties of two populus hybrids in response to mechanical perturbation. *Tree Physiol.* 20, 535–540. doi: 10.1093/treephys/20.8.535

Qian, Y. B., Wu, Z. N., Zhang, L. Y., Zhao, R. F., Wang, X. Y., and Li, Y. M. (2007). Spatial patterns of ephemeral plants in gurbantünggüt desert. *Chin. Sci. Bull.* 52, 3118–3127. doi: 10.1007/s11434-007-0465-9

Qin, J., Si, J. H., Jia, B., Zhao, C. Y., Zhou, D. M., He, X. H., et al. (2022). Water use characteristics of two dominant species in the mega-dunes of the badain jaran desert. *Water* 14, 53. doi: 10.3390/w14010053

Qiu, J., Tan, D. Y., and Fan, D. Y. (2007). Characteristics of photosynthesis and biomass allocation of spring ephemrals in the junggar desert. *Chin. J. Plant Ecol.* 31:883–891. doi: 10.17521/cjpe.2007.0111

Sawada, S., Kato, T., Sato, M., and Kasai, M. (2002). Characteristics of gas exchange and morphology of a spring ephemeral, *Erythronium japonicum*, in comparison with a sun plant, *Glycine max*. *Ecol. Res.* 17, 97–108. doi: 10.1046/j.1440-1703.2002.00465.x

Schütz, W., Milberg, P., and Lamont, B. B. (2002). Germination requirements and seedling responses to water availability and soil type in four eucalypt species. *Acta Oecol.-Int. J. Ecol.* 23, 23–30. doi: 10.1016/S1146-609X(01)01130-4

Shao, M. A., Yang, W. Z., and Li, Y. S. (1986). Hydraulic resistances and their relative importance in soil-plant-atmosphere continuum (SPAC). *J. Hydraul. Eng.* 8-14. doi: 10.3321/j.issn:0559-9350.1986.09.002

Sibounheuang, V., Basnayake, J., and Fukai, S. (2006). Genotypic consistency in the expression of leaf water potential in rice (*Oryza sativa l.*). *Field Crop Res.* 97, 142–154. doi: 10.1016/j.fcr.2005.09.006

Si, J. H., Feng, Q., Zhang, X. Y., Chang, Z. Q., Xi, H. Y., and Zhang, K. (2007). Sap flow of *Populus euphratica* in desert riparian forest in extreme arid region during the growing season. *J. Desert Res.* 27, 442–447. doi: 10.1111/j.1744-7909.2007.00388.x

Silvertown, J., Araya, Y., and Gowing, D. (2015). Hydrological niches in terrestrial plant communities: A review. *J. Ecol.* 103, 93–108. doi: 10.1111/1365-2745.12332

Simonin, K. A., Santiago, L. S., and Dawson, T. E. (2009). Fog interception by *Sequoia sempervirens* (D. don) crowns decouples physiology from soil water deficit. *Plant Cell Environ.* 32, 882–892. doi: 10.1111/j.1365-3040.2009.01967.x

Tan, X., Xu, H., Khan, S., Equiza, M. A., Lee, S. H., Vaziriyeganeh, M., et al. (2018). Plant water transport and aquaporins in oxygen-deprived environments. *J. Plant Physiol.* 227, 20–30. doi: 10.1016/j.jplph.2018.05.003

Thomas, N., and Nigam, S. (2018). Twentieth-century climate change over Africa: seasonal hydroclimate trends and Sahara desert expansion. *J. Clim.* 31, 3349–3370. doi: 10.1175/jcli-d-17-0187.1

Tiemuerbieke, B., Min, X. J., Zang, Y. X., Xing, P., Ma, J. Y., and Sun, W. (2018). Water use patterns of co-occurring C_3 and C_4 shrubs in the gurbantonggut desert in northwestern China. *Sci. Total Environ.* 634, 341–354. doi: 10.1016/j.scitotenv.2018.03.307

Turner, N. C. (1982). "The role of shoot characteristics in drought resistance of crop plants," in *Drought resistance in crops with emphasis on rice* (The Phillippines: IRRI, Los Banos), 115–134.

Wang, M. J. (2019). *Study on the changes of desert area, boundary and desert lake in western inner Mongolia in recent 30 years* (Hohhot: Inner Mongolia University).

Wang, J., Fu, B. J., Lu, N., Wang, S., and Zhang, L. (2019). Water use characteristics of native and exotic shrub species in the semi-arid loess plateau using an isotope technique. *Agric. Ecosyst. Environ.* 276, 55–63. doi: 10.1016/j.agee.2019.02.015

Wang, J., Fu, B. J., Lu, N., and Zhang, L. (2017). Seasonal variation in water uptake patterns of three plant species based on stable isotopes in the semi-arid loess plateau. *Sci. Total Environ.* 609, 27–37. doi: 10.1016/j.scitotenv.2017.07.133

Wang, X. Q., Wang, T., Jiang, J., and Zhao, C. J. (2005). On the sand surface stability in the southern part of gurbantünggüt desert. *Sci. China Ser. D-Earth Sci.* 48, 778–785. doi: 10.1360/03yd0340

Warren, J. M., Hanson, P. J., Iversen, C. M., Kumar, J., Walker, A. P., and Wullschleger, S. D. (2015). Root structural and functional dynamics in terrestrial biosphere models – evaluation and recommendations. *New Phytol.* 205, 59–78. doi: 10.1111/nph.13034

Wiggs, G. F. S., Thomas, D. S. G., Bullard, J. E., and Livingstone, I. (1995). Dune mobility and vegetation cover in the southwest Kalahari desert. *Earth Surf. Process. Landf.* 20, 515–529. doi: 10.1002/esp.3290200604

Wolfe, S. A., and Nickling, W. G. (1993). The protective role of sparse vegetation in wind erosion. *Prog. Phys. Geogr.* 17, 50–68. doi: 10.1177/030913339301700104

Wu, K. S. (2010). *Study of hydraulic lift in zygophyllum xanthoxylum of eremophytes* (Lanzhou: Lanzhou University).

Wu, X., Zheng, X. J., Yin, X. W., Yue, Y. M., Liu, R., Xu, G. Q., et al. (2019). Seasonal variation in the groundwater dependency of two dominant woody species in a desert region of central Asia. *Plant Soil* 444, 39–55. doi: 10.1007/s11104-019-04251-2

Wu, Y., Zhou, H., Zheng, X. J., Li, Y., and Tang, L. S. (2014). Seasonal changes in the water use strategies of three co-occurring desert shrubs. *Hydrol. Process.* 28, 6265–6275. doi: 10.1002/hyp.10114

Xing, P., Zang, Y. X., Min, X. J., Bahjayrarl, T., and Ma, J. Y. (2019). Photosynthetic characteristics and water use efficiency of *Tamarix ramosissima* in shelterbelt and natural communities in south fringe of taklamakan desert, China. *J. Appl. Ecol.* 30, 768–776. doi: 10.13287/j.1001-9332.201903.023

Yang, Q. L., Zhang, F. C., Liu, X. G., Wang, X., Zhang, N., and Ge, Z. Y. (2011). Research progress on regulation mechanism for the process of water transport in plants. *Acta Ecol. Sin.* 31, 4427–4436. doi: 1000-0933(2011)31:15<4427:ZWSFCS>2.0.TX;2-S

Yan, C. Y., Han, X. G., Chen, L. Z., Huang, J. H., and Su, B. (1998). Foliar $\delta^{13}C$ within temperate deciduous forest: its spatial change and interspecies variation. *Acta Botanica Sin.* 40, 853–859.

Yokoyama, G., Yasutake, D., Minami, K., Kimura, K., Marui, A., Yueru, W., et al. (2021). Evaluation of the physiological significance of leaf wetting by dew as a supplemental water resource in semi-arid crop production. *Agric. Water Manage.* 255, 106964. doi: 10.1016/j.agwat.2021.106964

Zencich, S. J., Froend, R. H., Turner, J. V., and Gailitis, V. (2002). Influence of groundwater depth on the seasonal sources of water accessed by banksia tree species on a shallow, sandy coastal aquifer. *Oecologia* 131, 8–19. doi: 10.1007/s00442-001-0855-7

Zhang, H. X., Yuan, F. H., Guan, D. X., Wang, A. Z., Wu, J. B., and Jin, C. J. (2017). A review on water transport in xylem of vascular plants and its affecting factors. *Chin. J. Ecol.* 36, 3281–3288. doi: 10.13292/j.1000-4890.201711.012

Zhang, C. X., Zhao, W. Q., Dang, H. L., Zhuang, L., and Sun, H. (2021). Effects of different slope aspect on biomass allocation and stoichiometry of ephemeral plants in the southern margin of junggar basin. *Acta Botanica Boreali-Occidentalia Sin.* 41, 151–158. doi: 1000-4025(2021)41:1<151:ZGEPDN>2.0.TX;2-N

Zhao, J. B., Shao, T. J., Hou, Y. L., Lv, X. H., and Dong, Z. B. (2011). Moisture content of sand layer and its origin in a mega-dune area in the badain jaran desert. *J. Natural Resour.* 26, 694–702. doi: 1000-3037(2011)26:4<694:BDJLSM>2.0.TX;2-S

Zhao, L. J., Wang, L. X., Cernusak, L. A., Liu, X. H., Xiao, H. L., Zhou, M. X., et al. (2016). Significant difference in hydrogen isotope composition between xylem and tissue water in *Populus euphratica*. *Plant Cell Environ.* 39, 1848–1857. doi: 10.1111/pce.12753

Zhao, L. J., Wang, X. G., Zhang, Y. C., Xie, C., Liu, Q. Y., and Meng, F. (2019). Plant water use strategies in the shapotou artificial sand-fixed vegetation of the southeastern margin of the tengger desert, northwestern China. *J. Mt. Sci.* 16, 898–908. doi: 10.1007/s11629-018-5028-9

frontiers | Frontiers in Plant Science

TYPE Original Research
PUBLISHED 12 December 2022
DOI 10.3389/fpls.2022.1064409

OPEN ACCESS

EDITED BY
Oksana Sytar,
Taras Shevchenko National University of Kyiv, Ukraine

REVIEWED BY
Atique ur Rehman,
Bahauddin Zakariya University, Pakistan
Shahbaz Khan,
National Agricultural Research Center (Pakistan), Pakistan

*CORRESPONDENCE
Kazem Ghassemi-Golezani
golezani@gmail.com

SPECIALTY SECTION
This article was submitted to Plant Abiotic Stress, a section of the journal Frontiers in Plant Science

RECEIVED 08 October 2022
ACCEPTED 29 November 2022
PUBLISHED 12 December 2022

CITATION
Farhangi-Abriz S and Ghassemi-Golezani K (2022) The modified biochars influence nutrient and osmotic statuses and hormonal signaling of mint plants under fluoride and cadmium toxicities.
Front. Plant Sci. 13:1064409.
doi: 10.3389/fpls.2022.1064409

The modified biochars influence nutrient and osmotic statuses and hormonal signaling of mint plants under fluoride and cadmium toxicities

Salar Farhangi-Abriz and Kazem Ghassemi-Golezani*

Department of Plant Eco-physiology, Faculty of Agriculture, University of Tabriz, Tabriz, Iran

Introduction: Chemically modified biochars are a new generation of biochars that have a great ability to absorb and stabilize environmental pollutants. In this research, the physiological performance of mint plants (*Mentha crispa* L.) under fluoride and cadmium toxicities and biochar treatments was evaluated.

Methods: Four levels of soil toxicities including non-toxic, 600 mg NaF kg^{-1} soil, 60 mg Cd kg^{-1} soil, and 600 mg NaF kg^{-1} soil + 60 mg Cd kg^{-1} soil were applied. The biochar addition to the soil was 25 g kg^{-1} (non-biochar, solid biochar, H_2O_2, KOH, and H_3PO_4-modified biochars).

Results: The results showed that the application of biochar and especially chemically modified biochars reduced fluoride (about 15-37%) and cadmium (30-52%) contents in mint leaves, while increased soil pH and cation exchange capacity (CEC), nitrogen (12-35%), phosphorus (16-59%), potassium (17-52%), calcium (19-47%), magnesium (28-77%), iron (37-114%), zinc (45-226%), photosynthetic pigments of leaves and plant biomass (about 10-25%) under toxic conditions.

Discussion: The biochar-related treatments reduced the osmotic stress and osmolytes content (proline, soluble proteins, and carbohydrates) in plant leaves. Plant leaf water content was increased by solid and modified biochar, up to 8% in toxic conditions. Furthermore, these treatments reduced the production of stress hormones [abscisic acid (27-55%), salicylic acid (31-50%), and jasmonic acid (6-12%)], but increased indole-3-acetic acid (14-31%) in plants under fluoride and cadmium stresses. Chemically modified biochars reduced fluoride and cadmium contents of plant leaves by about 20% and 22%, respectively, compared to solid biochar.

Conclusion: This result clearly shows the superiority of modified biochars in protecting plants from soil pollutants.

KEYWORDS

chlorophyll, nutrients, plant growth, pollutants, proline, salicylic acid

1 Introduction

Soil contamination with environmental pollutants reduces plant growth and productivity and causes many risks to food security and human health in the world (Alengebawy et al., 2021). Fluoride and cadmium are important pollutants that are increasing in nature due to human activities such as mining and application of chemical fertilizers in agriculture (Choudhary et al., 2019; Yotsova et al., 2020). Typically, these two environmental pollutants are present in the soil at the same time and cause various physiological and biochemical disorders in plants (Li et al., 2018). The accumulation of fluoride and cadmium ions in the plant cells increases oxidative stress in plant tissues and causes damage to the cells (Sharma and Kaur, 2018; Shen et al., 2022). Another harmful effect of cadmium and fluoride in the soil is the reduction of water absorption by plants. These environmental pollutants cause a decrease in water absorption by plants due to damage to the root and its transmission channels. Ghassemi-Golezani and Farhangi-Abriz (2019) have reported that fluoride reduces water absorption by safflower plants *via* decreasing root growth. Cadmium toxicity reduces water uptake by plants (Haider et al., 2021a). This toxicity decreases stomata conductivity and the constant flow of water from the rhizosphere to the plant (El Rasafi et al., 2022). In addition to reducing water absorption, the toxicity of fluoride and cadmium in plant cells causes a reduction in the absorption of numerous nutrients needed for plant growth, such as potassium (K), calcium (Ca), and magnesium (mg) (Ghassemi-Golezani and Farhangi-Abriz, 2019; Zulfiqar et al., 2022). Accumulation of environmental pollutants in plant organs can cause hormonal changes in tissues. For example, the accumulation of cadmium in plant tissues causes an increase in the concentration of abscisic acid (ABA) and a decrease in indole acetic acid (IAA) in plants (Hu et al., 2020; Rolon-Cardenas et al., 2022). The increment of ABA content, which is a stress hormone, causes a decrease in the growth of plants. Researchers have proposed various methods such as biochar application as an effective method to reduce the impacts of cadmium and fluoride toxicity in plants (Ali et al., 2019; Ghassemi-Golezani and Farhangi-Abriz, 2019).

Biochar is a carbon-rich material obtained through pyrolysis of natural materials such as agricultural waste (Ghassemi-Golezani and Farhangi-Abriz, 2022; Waqar et al., 2022). This natural substance has special electrochemical properties that act as a soil amender. Having alkaline nature (in most cases), a high level of cation exchange capacity, pollutant adsorption capacity, and being rich in nutrients are among the important characteristics of this organic matter (Boateng et al., 2015; Batool et al., 2015; Javeed et al., 2022). Application of the biochar under different environmental stresses has improved the growth and physiological efficiency of plants. For example, adding biochar to the soil has improved plant growth under salt (Ghassemi-Golezani et al., 2021), copper (Rehman et al., 2019) cadmium (Mehmood et al., 2018; Haider et al., 2021b), fluoride (Ghassemi-Golezani and Farhangi-Abriz, 2019) and arsenic (Alam et al., 2019) stresses. Ghassemi-Golezani and Farhangi-Abriz (2019) reported that biochar addition to the soil reduces fluoride availability in the rhizosphere and increases potassium uptake by plants under fluoride toxicity of soil. Abbas et al. (2017) showed that application of biochar noticeably enhances wheat growth and productivity under cadmium toxicity. Rizwan et al. (2018) stated that biochar enhances the physiological performance of rice plants by improving water retention between rhizosphere and plants under cadmium stress. In a recent study, Ren et al. (2021) showed that biochar addition to the soil increases tobacco growth *via* decreasing cadmium accumulation in plant tissues and increasing photosynthetic activities under contaminated soil with cadmium. Biochar can improve the growth of plants under environmental pollution in two direct and indirect ways. The direct effect is related to increasing the adsorption and retention of pollutants on the surface of biochar and reducing their transmission to rhizosphere and plants (Park et al., 2011). While the indirect effect is related to the improvement of rhizosphere conditions, such as increasing soil pH, microbial activity, cation exchange capacity, and availability of nutrients (Medyńska-Juraszek et al., 2020; Farhangi-Abriz et al., 2022).

Researchers have proposed different methods to increase the performance of biochar in decreasing the harmful effects of environmental stresses on plants and improving the physicochemical conditions of the rhizosphere. Improving the performance of biochar with chemical reagents is one of the easiest and most practical methods (Liu et al., 2022). Typically, biochars engineered by chemical reagents have a higher cation exchange capacity, absorbance ability of environmental pollutants, and specific surface area (Tan et al., 2016; Ghassemi-Golezani and Farhangi-Abriz, 2022). For example, modification of biochar by iron particles and application of this modified biochar under arsenic toxicity enhanced rice growth more than solid biochar (Wen et al., 2021). Farhangi-Abriz and Ghassemi-Golezani (2021) reported that modified biochars with magnesium and manganese ions have an excellent sodium sorption capacity, which noticeably improves safflower growth and productivity under salt stress. In another study, Ghassemi-Golezani and Farhangi-Abriz (2022) stated that modification of biochar with chemical regents such as H_2O_2, KOH, and H_3PO_4 increases field capacity and available water content of rhizosphere for plants, more than solid biochar. In a recent study, Rahimzadeh and Ghassemi-Golezani (2022) showed that biochar modifications with zinc and iron particles improved dill performance under salt stress *via* increasing nutrient availability in rhizosphere and decreasing sodium uptake by plants. The majority of the advantageous effects of chemically modified biochars in pollutant adsorption are related to modifications in functional groups on the surface area of the biochar. According to Xue et al. (2012), modification of biochar with H_2O_2 boosted lead sorption from 0.88 to 22.82 mg g^{-1}, compared to commercially activated carbon and increased oxygen-

containing functional groups on the surface of the biochar, particularly carboxyl groups. Based on a report by Jin et al. (2014), arsenic adsorption by KOH-modified biochar in comparison with solid biochar increased by more than 1.3 times.

Mint (*Mentha crispa* L.) is a medicinal and industrial plant that can be cultivated under contaminated soils with pollutants for the production of essential oil. Mints are economically significant, because they are employed as flavoring agents in the food, and used as medicine, fragrance, insect repellant, detergents, and cosmetics all over the world (Brahmi et al., 2017). Typically, environmental pollutants such as heavy metals are inorganic compounds that cannot enter the essential oil. However, the presence of environmental pollutants can cause growth reduction and various physiological disorders in plants. Considering the effectiveness of chemically modified biochars in adsorbing environmental pollutants and increasing plant growth, this research has been carried out to investigate the possible effects of chemically modified biochars by H_2O_2, KOH, and H_3PO_4 on the physiological efficiency of mint plants under fluoride and cadmium toxicities.

2 Materials and methods

2.1 Preparation of biochar and modified biochars

Solid biochar was obtained from a local company and then chemically modified by H_2O_2, KOH, and H_3PO_4, using standard methods. The method of Xue et al. (2012) was followed to prepare H_2O_2-modified biochar. In this method, 20 g of biochar were immersed in 200 ml of 30% hydrogen peroxide solution for 48 h at a temperature of 25°C. The method of Takaya et al. (2016) was applied to prepare KOH-modified biochar. About 20 g KOH were dissolved in 200 mL distilled water and 4 g biochar were added to the solution. The biochar was placed in the KOH solution for 24 hours at 25°C. To produce H_3PO_4-modified biochar, a 14% phosphoric acid solution was prepared. Subsequently, 200 g of biochar were added to 400 ml of H_3PO_4 solution. The biochar was kept in an H_3PO_4 solution for 24 hours at a temperature of 25°C. After mixing biochar with the chemical reagents, the pH of the modified biochar was adjusted to about the neutral pH (7-7.5). The various properties of solid and chemically modified biochars were determined by standard methods (White, 2010; Mohan et al., 2014; Xu et al., 2014; Graber et al., 2017; Lateef et al., 2019; Ghassemi-Golezani and Farhangi-Abriz, 2021) and presented in Table 1.

2.2 Experimental conditions

Three experimental soil samples (specifications are presented in Table 1) were contaminated with pollutants (600 mg NaF kg^{-1} soil, 60 mg Cd kg^{-1} soil, and 600 mg NaF kg^{-1} soil + 60 mg Cd kg^{-1} soil) and another soil sample was not contaminated (non-toxic). Then, non-biochar and biochar-related treatments (solid biochar, modified biochars with H_2O_2, KOH, and H_3PO_4) were applied. Contamination of soil with fluoride and cadmium ions was performed according Ghassemi-Golezani and Farhangi-Abriz (2019) and Cieśliński et al. (1996), respectively. Application rate of biochar was 25 g biochar per kg soil. About 3 kg of contaminated or non-contaminated soil was added to polyethylene pots (20 × 20 cm), using 60 pots in general. Thereafter, mint seeds were sown in each pot and irrigated with tap water up to 100% field capacity (FC) of growth media. The pots were kept in controlled greenhouse conditions for 45 days (day and night temperatures: 25 and 22°C, respectively; light intensity: 140 W m^{-2}; and photoperiod: about 13 h.). Total soluble fluoride and cadmium concentrations in each pot were determined by the methods of Larsen and Widdowson (1971) and Lindsay and Norvell (1978), respectively. The pH of the soil was measured using a pH meter (Model: HI 99121, Hanna Instrument, USA), and the cation exchange capacity of the soil was quantified using the ammonium acetate method (Chapman, 1965). All growth and physiological measurements were performed 45 days after sowing.

2.3 Fluoride and cadmium content in mint leaves

The leaves were dried in an oven at 80°C for 48 hours and then powdered. The powdered leaves were digested in 0.1 N HCl at 25°C for 24 hours and were kept at 120°C for an hour. The digested materials were centrifuged at 25°C for 15 minutes at 5000 rpm. The supernatant was combined with distilled water and TISAB buffer. Then, fluoride content was measured, using the ion selectivity method (Orion 9609, Thermo Scientific, USA). The NaF with a 99.99% purity level served as the reference material for calculating fluoride levels in plant tissue (Sigma-Aldrich, United States). The atomic absorption spectrophotometry technique was used to determine the amount of cadmium accumulation in plant tissues.

2.4 Photosynthetic pigments

Chlorophylls and carotenoid contents were measured by Arnon (1949) and Maclachlan and Zalik (1963) methods, respectively. After homogenizing each sample (approximately 1 g) in 4 mL of acetone (80%), the samples were centrifuged at 12,000 g for 20 min at 4°C. A sample of the supernatant was obtained, and a spectrophotometer (Dynamica, Halo DB-20-UV-Visible Spectrophotometer, United Kingdom) was used to measure the absorbance at 645 and 663 nm (for chlorophylls) and 480 and 510 nm (for carotenoids). The total flavonoid in plant tissues was calculated following the Zhishen et al. (1999) method.

TABLE 1 Some physicochemical properties of the experimental soil, solid biochar and chemically modified biochars.

Soil		Solid biochar		H_2O_2 Modified biochar		KOH Modified biochar		H_3PO_4 Modified biochar	
Texture	Silty loam	N (%)	0.52	N (%)	0.51	N (%)	0.48	N (%)	0.48
pH	6.2	C (%)	44.1	C (%)	38.23	C (%)	38.37	C (%)	40.31
EC (dSm^{-1})	1.32	H (%)	2.4	H (%)	3.51	H (%)	2.85	H (%)	2.96
OC ($g\ kg^{-1}$)	11.1	O (%)	27.40	O (%)	30.20	O (%)	31.89	O (%)	33.40
Total N (%)	0.09	P ($mg\ kg^{-1}$)	8250	P ($mg\ kg^{-1}$)	8120	P ($mg\ kg^{-1}$)	8212	P ($mg\ kg^{-1}$)	8940
P ($mg\ kg^{-1}$)	31.2	S ($mg\ kg^{-1}$)	5790	S ($mg\ kg^{-1}$)	4340	S ($mg\ kg^{-1}$)	4360	S ($mg\ kg^{-1}$)	5100
K ($mg\ kg^{-1}$)	187.1	Na ($mg\ kg^{-1}$)	2.30	Na ($mg\ kg^{-1}$)	1.34	Na ($mg\ kg^{-1}$)	1.12	Na ($mg\ kg^{-1}$)	1.35
Mg ($mg\ kg^{-1}$)	70.4	K ($mg\ kg^{-1}$)	4070	K ($mg\ kg^{-1}$)	3823	K ($mg\ kg^{-1}$)	4150	K ($mg\ kg^{-1}$)	3560
Mn ($mg\ kg^{-1}$)	10.80	Ca ($mg\ kg^{-1}$)	3750	Ca ($mg\ kg^{-1}$)	3021	Ca ($mg\ kg^{-1}$)	2980	Ca ($mg\ kg^{-1}$)	3090
SF ($mg\ kg^{-1}$)	8.30	Mg ($mg\ kg^{-1}$)	166.4	Mg ($mg\ kg^{-1}$)	102.7	Mg ($mg\ kg^{-1}$)	110.4	Mg ($mg\ kg^{-1}$)	105.3
Cd ($mg\ kg^{-1}$)	0.13	Mn ($mg\ kg^{-1}$)	37.30	Mn ($mg\ kg^{-1}$)	35.8	Mn ($mg\ kg^{-1}$)	32.2	Mn ($mg\ kg^{-1}$)	22.40
CEC ($cmol\ kg^{-1}$)	18.80	Cl ($mg\ kg^{-1}$)	N. A	Cl ($mg\ kg^{-1}$)	N. A	Cl ($mg\ kg^{-1}$)	N. A	Cl ($mg\ kg^{-1}$)	N. A
Bulk density ($g\ cm^{-3}$)	1.43	SF ($mg\ kg^{-1}$)	5.2	SF ($mg\ kg^{-1}$)	4.3	SF ($mg\ kg^{-1}$)	3.4	SF ($mg\ kg^{-1}$)	3.7
Moisture (%)	1	Cd ($mg\ kg^{-1}$)	0.06	Cd ($mg\ kg^{-1}$)	0.06	Cd ($mg\ kg^{-1}$)	0.06	Cd ($mg\ kg^{-1}$)	0.06
		CEC ($cmol\ kg^{-1}$)	20.21	CEC ($cmol\ kg^{-1}$)	24.60	CEC ($cmol\ kg^{-1}$)	25.20	CEC ($cmol\ kg^{-1}$)	26.10
		pH	7.1	pH	7.5	pH	7.5	pH	7.5
		S_{BET} ($m^2\ g^{-1}$)	14.2	S_{BET} ($m^2\ g^{-1}$)	48.1	S_{BET} ($m^2\ g^{-1}$)	69.3	S_{BET} ($m^2\ g^{-1}$)	77.3
		V_{tot} ($cm^3\ g^{-1}$)	0.024	V_{tot} ($cm^3\ g^{-1}$)	0.082	V_{tot} ($cm^3\ g^{-1}$)	0.063	V_{tot} ($cm^3\ g^{-1}$)	0.089
		AVP (nm)	3.43	AVP (nm)	3.57	AVP (nm)	3.22	AVP (nm)	3.24
		CA ($mmol\ g^{-1}$)	0.21	CA ($mmol\ g^{-1}$)	0.39	CA ($mmol\ g^{-1}$)	0.45	CA ($mmol\ g^{-1}$)	0.62
		LA ($mmol\ g^{-1}$)	0.11	LA ($mmol\ g^{-1}$)	0.19	LA ($mmol\ g^{-1}$)	0.26	LA ($mmol\ g^{-1}$)	0.18
		PA ($mmol\ g^{-1}$)	0.68	PA ($mmol\ g^{-1}$)	0.95	PA ($mmol\ g^{-1}$)	1.32	PA ($mmol\ g^{-1}$)	1.14
		F_{ab} ($mg\ g^{-1}$)	3.41	F_{ab} ($mg\ g^{-1}$)	4.59	F_{ab} ($mg\ g^{-1}$)	4.43	F_{ab} ($mg\ g^{-1}$)	5.17
		Cd_{ab} ($mg\ g^{-1}$)	16.76	Cd_{ab} ($mg\ g^{-1}$)	24.78	Cd_{ab} ($mg\ g^{-1}$)	29.54	Cd_{ab} ($mg\ g^{-1}$)	41.3
		Stability (∘C)	520	Stability (∘C)	505	Stability (∘C)	510	Stability (∘C)	505
		Moisture (%)	< 1	Moisture (%)	< 1	Moisture (%)	< 1	Moisture (%)	< 1

EC, Electrical conductivity; OC, Organic carbon; CEC, Cation exchange capacity; SF, Soluble fluoride; NA, Not available; F_{ab}, Fluoride absorbing capacity; Cd_{ab}, Cadmium absorbing capacity; S_{BET}, BET surface area; V_{tot}, Total pore volume; AVP, Average pore size, CA, Carboxylic acid groups; LA, Lactonic acid groups; PA, Phenolic acid groups.

2.5 Nutrients content in mint leaves

The Kjeldahl method was used to assess the nitrogen level (Jones, 1991), and the yellow method and spectrophotometric analysis at 430 nm were used to determine the phosphorus concentration in mint leaves (Tandon et al., 1968). The contents of potassium, calcium, magnesium, iron, and zinc were determined in dried leaves. After being dry-ashed at 550°C for 7 hours, the plant leaves were digested in 5 M HNO_3 and double-distilled water was added to achieve 50 mL. Then atomic absorption spectrophotometry was used to determine the cations ($mg\ g^{-1}$ DW).

2.6 Leaf water content and osmolytes production

A plant was taken out of each pot, its leaves were separated, and they were weighed (FW). The leaves were then reweighed after being dried at 80°C for 48 hours (DW). The leaf water content (LWC) was calculated using the formula shown below:

$$LWC = [(FW - DW)/DW] \times 100$$

The proline content of mint leaves was determined according to the method described by Bates et al. (1973). First, 5 ml of 3% sulfosalicylic acid was used to homogenize 500 mg of fresh leaves. A plastic tube containing 2 ml of the extracted material was then filled with this mixture, along with 2 ml of glacial acetic acid and 2 ml of ninhydrin. The prepared samples were heated in a Bain Marie (BM-15 Bain Marie, Magapor SL, Spain) for an hour at 100°C. The mixture was then extracted with toluene once the sample was cooled at room temperature, and then the upper phase absorbance was read at 520 nm. By using the calibration curve for pure proline, the proline content of leaves was determined and expressed as $mg\ g^{-1}$ fresh weight. The phenol-sulfuric acid and Bradford methods were applied to determine the contents of soluble sugars and proteins in mint leaves, respectively (Bradford, 1976; Kochert et al., 1978).

2.7 Hormones content in mint leaves

The ELISA method was applied to ascertain the endogenous concentrations of phytohormones including abscisic acid (ABA), indoleacetic acid (IAA), salicylic acid (SA), and jasmonic acid (JA). Initially, plant leaves were powdered and kept in the dark at 4°C for 24 hours. The powdered fresh samples (1 g each) were extracted in 80% cold methanol with butylated hydroxytoluene (BHT) as an antioxidant. Following the instructions provided in testing package, ELISA measurement was performed to assess the hormone content of leaves (Li and Meng, 1996; Wang et al., 2002).

2.8 Plant growth parameters

The plants of each pot were harvested separately and dried at 85°C for 48 hours to determine plant biomass. A portable leaf area meter (model ADCAM 300-United Kingdom) was used to measure the leaf area (LA) of the plants in each pot, and the results were reported as cm^2 $plant^{-1}$.

2.9 Statistical analysis

Using the MSTAT-C software from the East Lansing campus of Michigan State University in the United States, the data were analyzed on the basis of the experimental design (two-way ANOVA - factorial design based on randomized complete block arrangement with three repetitions). The Tukey HSD test was used to compare the means at $p \leq 0.05$. Due to the large difference in the amount of cadmium in the soil and mint leaves under normal and stressful conditions, the statistical analysis of these traits has been done separately in each of the stressful and normal conditions. Figures were drawn by Excel 2019 from Microsoft Corporation, USA.

3 Results

3.1 Chemically modified biochar specifications

Leaching during the creation of modified biochars reduced the amounts of some nutrients such as calcium and magnesium in the biochar structure, whereas treatments with H_3PO_4 and KOH increased the contents of phosphorous and potassium in the biochar matrix (Table 1). In addition, modified biochars had higher oxygen and hydrogen percentages than solid biochar. Chemical treatments slightly decreased the stability of biochar. Modified biochars in comparison to solid biochar had higher CEC, Brunauer-Emmett-Teller (BET) surface area, total pore volume, average pore size, functional groups on biochar surface area, and fluoride and cadmium absorption capabilities. Modification of biochar by H_3PO_4, H_2O_2, and KOH increased the levels of carboxyl groups on biochar structure by about 195%, 114%, and 85%, respectively, compared to solid biochar. The KOH-treated biochar also had the greatest lactonic acids (about 136% more than solid biochar) and phenolic groups. The H_3PO_4-modified biochar had the highest amount of Brunauer-Emmett-Teller (BET) surface area, sorption capacity, and CEC, compared to solid biochar and other forms of chemically modified biochars.

3.2 Soil parameters

Contamination of the soil with fluoride and cadmium decreased pH (about 5% and 3%, respectively) and CEC (about 8% and 12%, respectively), whereas application of biochar and chemically modified biochars in rhizosphere increased these parameters (Figure 1). Under fluoride and fluoride + cadmium toxicities, enhancing soil pH by chemically modified biochars in comparison with solid biochar was statistically similar. However, chemically modified biochars had a better effect on increasing soil pH under cadmium toxicity, compared to solid biochar (about 5% more than solid biochar). Chemically modified biochars showed a similar effect on rising soil CEC under non-toxic conditions, but in toxic conditions, the H_3PO_4-modified biochar largely enhanced the soil CEC. For example, the H_3PO_4-modified biochar increased soil CEC under the combined form of cadmium and fluoride toxicities by about 23%, compared to the non-biochar treatment. Improvements of soil CEC by H_3PO_4-modified biochar under individual forms of cadmium and fluoride were about 12% and 21%, respectively.

Fluoride and cadmium availability in rhizosphere was significantly decreased by the addition of solid and modified biochars under both individual and combined forms of toxicities The availability of fluoride and cadmium under non-toxic conditions was unaffected by biochar treatments. In response to H_3PO_4 and KOH-modified biochars, the availability of fluoride under fluoride toxicity of soil decreased by around 45% and 47%, respectively, compared to non-biochar treatment. The H_3PO_4 and KOH-modified biochars in comparison with non-biochar treatment reduced cadmium availability by about 37% and 35%, respectively, under cadmium toxicity. Under the combined form of toxicities, the reduction of cadmium availability in soil caused by H_3PO_4 and KOH-modified biochars was about 32%.

3.3 Fluoride and cadmium contents in plant leaves

The content of fluoride and cadmium in mint leaves increased under individual and combined toxicity of these environmental pollutants (Figure 1). Under toxic conditions,

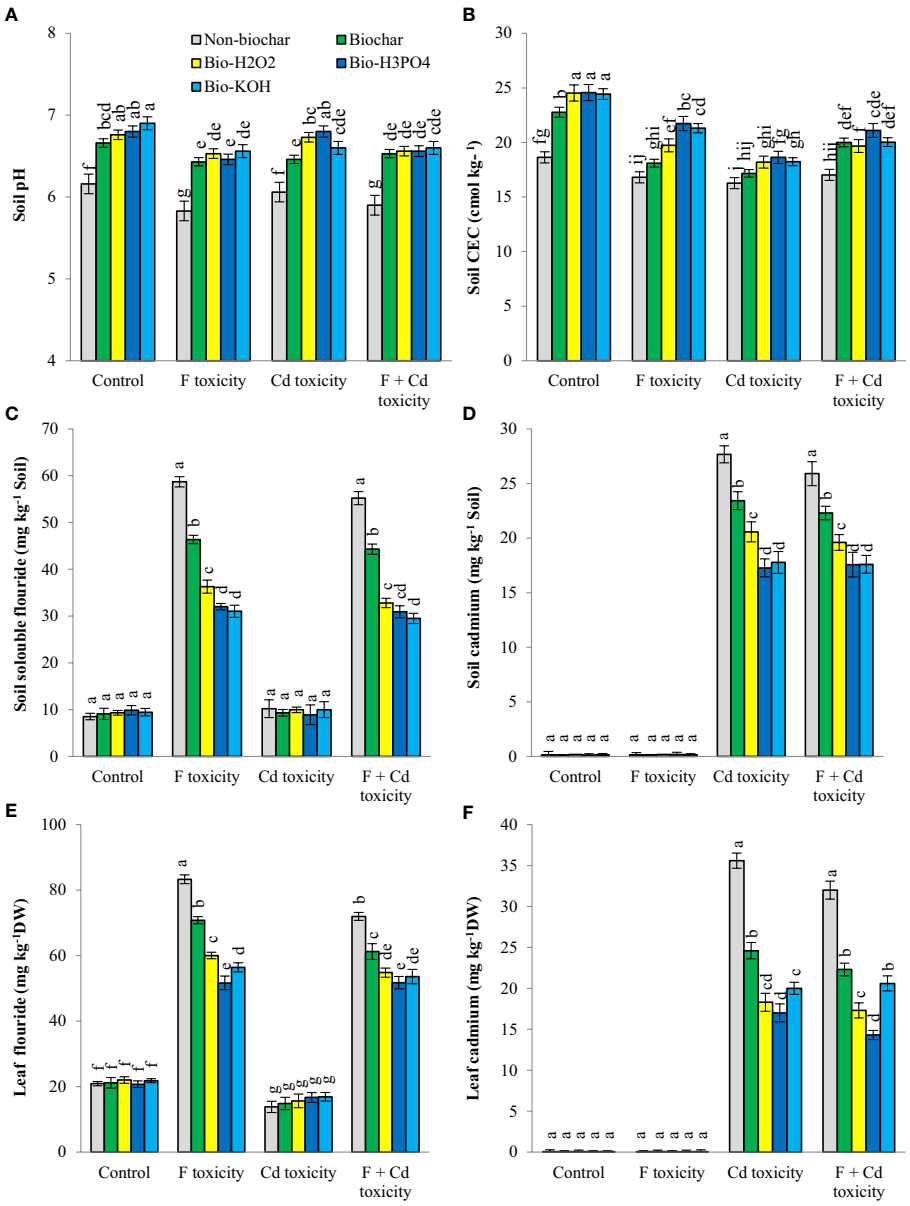

FIGURE 1
Changes in pH **(A)**, CEC **(B)**, fluoride **(C)** and cadmium **(D)** concentration of soil and fluoride **(E)** and cadmium **(F)** contents of leaves in response to biochar and chemically modified biochars under fluoride and cadmium toxicities. Data represent the average of three replicates (n = 3) ± standard error. Different letters indicate significant differences by Tukey HSD test at $p \leq 0.05$. CEC: Cation exchange capacity; DW: dry weight; F: Fluoride; Cd: Cadmium; Bio-H_2O_2: Modified biochar by H_2O_2; Bio-KOH: Modified biochar by KOH; Bio-H_3PO_4: Modified biochar by H_3PO_4.

the addition of solid and modified biochars to soil decreased the contents of fluoride and cadmium in mint leaves. However, biochar-related treatments did not change the fluoride and cadmium contents of leaves under non-toxic conditions. Chemically modified biochars were more successful than solid biochar in reducing fluoride (about 37%) and cadmium (about 27%) accumulation in plant leaves. Among the chemically modified biochars, The H_3PO_4 modified biochar was more successful in reducing the fluoride and cadmium in leaves. The reduction of fluoride in mint leaves by H_3PO_4-modified biochar under the individual and combined form of toxicities was about 38% and 28%, respectively. The decrement of cadmium toxicity by H_3PO_4-modified biochar under individual and combined forms of toxicities was about 41% and 55%, respectively.

3.4 Photosynthetic pigments

Fluoride and cadmium toxicities decreased the carotenoids (about 46% and 55%), flavonoids (about 57% and 64%), and chlorophylls contents (about 25% and 34%, respectively) in mint leaves (Table 2). The addition of solid and modified biochars significantly increased the photosynthetic pigments in mint plants under an individual and combined form of toxicities. However, biochar-related treatments did not have a tangible effect on photosynthetic pigments in non-toxic conditions. No significant difference was observed between different biochar treatments in increasing the content of photosynthetic pigments of mint leaves. The increment of total chlorophyll content in mint leaves by biochar-related treatments was about 17%, 27%, and 15%, under fluoride, cadmium, and fluoride + cadmium toxicities, respectively, compared to non-biochar treatment. Improvement of flavonoid and carotenoid contents of leaves by biochar treatments under combined form of cadmium and fluoride toxicities were about 58% and 32%, respectively.

3.5 Nutrient content of plants

Fluoride and cadmium toxicities decreased the N (about 35% and 45%, respectively), P (about 58% and 53%), K (about 44% and 54%), Ca (about 49% and 54%), Mg (about 51% and 55%), Fe (about 57%) and Zn (about 57% and 74%) contents in mint leaves (Table 3). Soil treatment with solid and modified biochars noticeably improved the nutrient content of mint plants under normal and stressful conditions. However, the increment of N and P nutrients in response to biochar-related treatments under normal conditions was not statistically significant. Chemically modified biochars had better effects than solid biochar in increasing the leaf nutrients. In most cases, KOH and H_3PO_4-modified biochars had better effects than other biochar-related treatments in increasing the nutrients of mint leaves. Under the individual form of fluoride toxicity, the H_3PO_4-modified biochar increased N, P, K, Ca, Mg, Fe, and Zn contents in mint leave by about 22, 59, 35, 50, 56, 91 and 88%, compared to non-biochar treatment. The H_3PO_4-modified biochar under cadmium toxicity enhanced N, P, K, Ca, Mg, Fe, and Zn contents by about 35, 35, 52, 37, 77, 108, and 226%, respectively. Under the combined form of toxicities, increments in N, P, K, Ca, Mg, Fe, and Zn contents of mint leaves by H_3PO_4 modified biochar were about 21, 32, 25, 23, 38, 70, and 105%.

3.6 Leaf water content and osmolytes

Leaf water content was decreased by fluoride (by about 19%) and cadmium (by about 25%) toxicities (Figure 2). However,

TABLE 2 Means of plant biomass, leaf area and photosynthetic pigments in mint plants affected by biochar and chemically modified biochars under fluoride and cadmium toxicities.

Toxicity	Soil treatments	Plant biomass g plant^{-1}	Leaf area cm^2 plant^{-1}	Chl a	Chl b	Chl Total mg g^{-1}DW	Carotenoid	Flavonoid
Non-toxic	Non-biochar	2.8 ± 0.09b	314.7 ± 2.90c	1.91 ± 0.08 a	0.93 ± 0.03 a	2.84 ± 0.07 a	0.63 ± 0.06 a	0.57 ± 0.05 ab
	Biochar	3.2 ± 0.08a	352.0 ± 4.27b	1.89 ± 0.05 a	0.96 ± 0.08 a	2.86 ± 0.11 a	0.58 ± 0.08 a	0.52 ± 0.03 b
	Biochar-H_2O_2	3.2 ± 0.06a	372.3 ± 3.68a	1.96 ± 0.09 a	0.95 ± 0.09 a	2.92 ± 0.08 a	0.60 ± 0.06 a	0.59 ± 0.04 a
	Biochar- H_3PO_4	3.3 ± 0.05a	383.7 ± 6.39a	1.97 ± 0.10 a	0.97 ± 0.04 a	2.95 ± 0.06 a	0.61 ± 0.05 a	0.53 ± 0.08 ab
	Biochar-KOH	3.2 ± 0.09a	384.0 ± 3.72a	2.01 ± 0.06 a	0.96 ± 0.02 a	2.94 ± 0.08 a	0.61 ± 0.04 a	0.54 ± 0.09 ab
Fluoride	Non-biochar	1.9 ± 0.06def	210.7 ± 5.81i	1.49 ± 0.05 e	0.62 ± 0.02 fg	2.11 ± 0.08 g	0.34 ± 0.07 d	0.24 ± 0.06 e
	Biochar	2.1 ± 0.09cd	241.7 ± 6.25efg	1.70 ± 0.11 bc	0.76 ± 0.08 bcd	2.46 ± 0.05 bcd	0.45 ± 0.09 bc	0.32 ± 0.04 cd
	Biochar-H_2O_2	2.1 ± 0.08cd	252.3 ± 7.31de	1.74 ± 0.06 bc	0.80 ± 0.08 b	2.53 ± 0.09 bc	0.46 ± 0.03 b	0.33 ± 0.03 cd
	Biochar- H_3PO_4	2.3 ± 0.11c	259.0 ± 3.93d	1.80 ± 0.09 b	0.78 ± 0.05 bc	2.57 ± 0.06 b	0.45 ± 0.09 bc	0.34 ± 0.05 cd
	Biochar-KOH	2.2 ± 0.08cd	251.0 ± 5.17def	1.76 ± 0.04 b	0.76 ± 0.09 bcd	2.52 ± 0.07 bc	0.44 ± 0.06 bc	0.33 ± 0.04 cd
Cadmium	Non-biochar	1.6 ± 0.04f	185.0 ± 2.88j	1.30 ± 0.06 f	0.55 ± 0.04 g	1.85 ± 0.05 h	0.28 ± 0.05 e	0.20 ± 0.04 e
	Biochar	1.8 ± 0.03def	222.3 ± 4.36hi	1.55 ± 0.09 de	0.72 ± 0.11 bcde	2.28 ± 0.05 ef	0.36 ± 0.06 d	0.32 ± 0.06 d
	Biochar-H_2O_2	1.9 ± 0.07cdef	241.3 ± 7.12efg	1.63 ± 0.05 cd	0.71 ± 0.05 cde	2.34 ± 0.09 de	0.36 ± 0.05 d	0.34 ± 0.09 cd
	Biochar- H_3PO_4	2.0 ± 0.09cde	245.0 ± 3.30def	1.66 ± 0.11 cd	0.72 ± 0.08 bcde	2.37 ± 0.12 cde	0.38 ± 0.08 d	0.33 ± 0.07 cd
	Biochar-KOH	1.9 ± 0.05cdef	245.0 ± 6.32def	1.65 ± 0.07 cd	0.69 ± 0.09 def	2.35 ± 0.07 de	0.40 ± 0.08 cd	0.34 ± 0.08 cd
Fluoride + Cadmium	Non-biochar	1.7 ± 0.07ef	192.0 ± 6.12j	1.48 ± 0.02 e	0.65 ± 0.04 ef	2.15 ± 0.06 fg	0.28 ± 0.04 e	0.24 ± 0.08 e
	Biochar	1.9 ± 0.07def	217.3 ± 4.32i	1.70 ± 0.08 bc	0.78 ± 0.02 bc	2.48 ± 0.05 bcd	0.35 ± 0.07 d	0.33 ± 0.09 cd
	Biochar-H_2O_2	2.1 ± 0.06cd	225.3 ± 7.39ghi	1.73 ± 0.04 bc	0.81 ± 0.05 b	2.52 ± 0.08 bc	0.37 ± 0.05 d	0.38 ± 0.08 c
	Biochar- H_3PO_4	1.8 ± 0.05def	234.3 ± 5.92fgh	1.74 ± 0.10 bc	0.80 ± 0.07 b	2.54 ± 0.09 bc	0.36 ± 0.07 d	0.34 ± 0.05 cd
	Biochar-KOH	2.1 ± 0.06cd	234.3 ± 4.38fgh	1.69 ± 0.07 bc	0.80 ± 0.08 b	2.52 ± 0.04 bc	0.36 ± 0.09 d	0.32 ± 0.09 cd

Data represents the average of three replicates (n=3) ± standard error. Different letters in each column indicate significant difference by Tukey HSD test at $p \leq 0.05$. DW, Dry weight; Chl, Chlorophyll.

soluble proteins, carbohydrates, and proline production in mint plants were increased under toxic conditions. The addition of solid and modified biochars to the soil significantly increased the leaf water content of mint plants under toxic conditions, with no tangible effect in non-toxic condition. These improvements in leaf water content by biochar-related treatments were up to 7.3%, 8.3%, and 7% at fluoride, cadmium, and fluoride + cadmium toxicities, respectively. Under toxic conditions, biochar-related treatments decreased osmolyte production in mint leaves. These treatments similarly reduced the production of osmotic regulators. Decrement of soluble proteins, carbohydrates, and proline by biochar-related treatments under both cadmium and fluoride toxicities was up to 27%, 26%, and 19%, respectively, compared to non-biochar conditions.

3.7 Phytohormones

Fluoride and cadmium toxicities increased ABA (about 462% and 578%, respectively), SA (about 173% and 231%), and JA (about 343% and 432%) in mint leaves (Figure 3). However, IAA content was reduced by individual fluoride (about 36%) and cadmium (about 44%) toxicities. The reduction of IAA in mint leaves under the combined form of toxicities was about 37%, Under fluoride and cadmium toxicities, soil treatment with solid and chemically modified biochars increased IAA content, but decreased ABA, SA, and JA productions in mint leaves. Biochar-related treatments did not affect the ABA, SA, and JA contents of plants under non-toxic conditions, but increased IAA content in this condition. Chemically modified biochars were more successful than solid biochar in decreasing the ABA content of mint leaves under different toxic conditions. No significant difference was observed between chemically modified biochars in reducing the abscisic acid content of plants under stressful conditions. Decrement of ABA content of mint leaves by H_3PO_4 modified biochar was about 47%, 43%, and 50%, under fluoride, cadmium, and fluoride + cadmium toxicities, respectively. In most cases, H_3PO_4 and H_2O_2 modified biochars caused the highest increment in IAA production in mint leaves under all toxic and non-toxic conditions. The H_3PO_4-modified biochar increased the IAA content of mint leaves by about 19, 30, 41, and 29%, under non-toxic, fluoride, cadmium, and combined forms of toxicities, respectively. All biochar-related treatments had similar effects in reducing jasmonic and salicylic acids under different stressful conditions.

3.8 Plant growth

The mint biomass was lowered by cadmium (about 42%) and fluoride (about 32%) toxicities (Table 2). In both toxic and non-toxic conditions, solid and modified biochars increased plant biomass. Under toxic and non-toxic conditions, chemically modified biochars enhanced dry matter

TABLE 3 Means of nutrients content in mint leaves affected by biochar and chemically modified biochars under fluoride and cadmium toxicities.

Toxicity	Soil treatments	Nitrogen	Phosphorous	Potassium	Calcium	Magnesium	Iron	Zinc
					mg g^{-1}DW			
Non-toxic	Non-biochar	33.9 ± 0.78 a	21.9 ± 0.27 a	34.6 ± 1.26 c	11.2 ± 0.22 b	8.1 ± 0.19 c	0.83 ± 0.03 c	0.59 ± 0.02 b
	Biochar	35.2 ± 0.51 a	22.4 ± 0.52 a	39.9 ± 0.66 b	12.9 ± 0.66 a	9.1 ± 0.18 b	0.98 ± 0.09 b	0.68 ± 0.04 a
	Biochar-H_2O_2	34.1 ± 1.23 a	22.4 ± 0.34 a	42.8 ± 0.89 a	13.4 ± 0.65 a	9.9 ± 0.22 a	1.10 ± 0.08 a	0.69 ± 0.05 a
	Biochar- H_3PO_4	34.0 ± 0.89 a	22.0 ± 0.61 a	43.2 ± 0.92 a	13.6 ± 0.78 a	9.8 ± 0.22 ab	1.10 ± 0.08 a	0.71 ± 0.04 a
	Biochar-KOH	34.1 ± 0.66 a	22.1 ± 0.22 a	41.5 ± 0.83 ab	13.3 ± 0.92 a	9.9 ± 0.20 a	0.95 ± 0.05 b	0.68 ± 0.04 a
Fluoride	Non-biochar	21.9 ± 0.45 f	9.1 ± 0.21 i	19.2 ± 1.11 hi	5.7 ± 0.30 hi	3.9 ± 0.16 h	0.36 ± 0.06 h	0.25 ± 0.05 hi
	Biochar	24.7 ± 0.88 cde	12.2 ± 0.26 fg	23.6 ± 1.05 defg	7.0 ± 0.21 f	5.0 ± 0.22 g	0.54 ± 0.07 g	0.34 ± 0.03 fg
	Biochar-H_2O_2	26.4 ± 0.98 bc	14.3 ± 0.33 cd	25.1 ± 0.83 de	7.9 ± 0.16 de	5.8 ± 0.21 def	0.57 ± 0.08 efg	0.44 ± 0.03 cd
	Biochar- H_3PO_4	26.9 ± 0.46 b	14.5 ± 0.37 bcd	26.0 ± 0.62 d	8.6 ± 0.35 cd	6.1 ± 0.19 de	0.69 ± 0.03 de	0.47 ± 0.02 c
	Biochar-KOH	25.2 ± 0.76 bcd	14.4 ± 0.27 bcd	23.8 ± 0.51 efg	8.1 ± 0.38 cde	5.8 ± 0.18 def	0.68 ± 0.08 de	0.49 ± 0.07 c
Cadmium	Non-biochar	18.6 ± 0.92 g	10.3 ± 0.16 h	15.7 ± 0.88 j	5.1 ± 0.23 i	3.6 ± 0.33 h	0.35 ± 0.08 h	0.15 ± 0.03 j
	Biochar	23.0 ± 0.72 ef	12.0 ± 0.28 fg	20.8 ± 1.07 gh	6.1 ± 0.36 h	5.7 ± 0.24 efg	0.59 ± 0.05 efg	0.37 ± 0.04 ef
	Biochar-H_2O_2	24.0 ± 0.82 de	13.0 ± 0.43 ef	22.9 ± 1.21 efg	6.2 ± 0.41 ghi	6.2 ± 0.27 de	0.68 ± 0.03 de	0.48 ± 0.05 c
	Biochar- H_3PO_4	25.1 ± 0.79 bcd	13.9 ± 0.57 cde	23.9 ± 1.12 def	7.0 ± 0.25 f	6.4 ± 0.23 d	0.75 ± 0.04 cd	0.49 ± 0.06 c
	Biochar-KOH	25.2 ± 0.80 bcd	13.7 ± 0.60 de	23.7 ± 1.22 defg	6.9 ± 0.17 fg	6.3 ± 0.24 de	0.73 ± 0.05 cd	0.40 ± 0.07 de
Fluoride + Cadmium	Non-biochar	21.3 ± 0.69 f	11.3 ± 0.25 gh	18.1 ± 0.63 ij	6.1 ± 0.18 h	3.8 ± 0.24 h	0.40 ± 0.03 h	0.20 ± 0.03 ij
	Biochar	24.4 ± 0.73 de	13.8 ± 0.28 cde	21.2 ± 0.89 fgh	7.7 ± 0.23 e	5.1 ± 0.12 fg	0.55 ± 0.04 fg	0.29 ± 0.03 gh
	Biochar-H_2O_2	25.0 ± 0.39 bcd	14.8 ± 0.37 bcd	23.5 ± 0.82 defg	8.7 ± 0.26 c	5.6 ± 0.23 efg	0.58 ± 0.05 efg	0.38 ± 0.04 ef
	Biochar- H_3PO_4	25.8 ± 0.46 bcd	15.0 ± 0.28 bc	22.8 ± 0.72 efg	8.0 ± 0.28 cde	6.2 ± 0.24 de	0.68 ± 0.05 de	0.41 ± 0.05 de
	Biochar-KOH	25.9 ± 0.67 bcd	15.3 ± 0.48 b	23.6 ± 0.59 defg	8.0 ± 0.19 cde	6.3 ± 0.28 de	0.66 ± 0.04 def	0.40 ± 0.03 de

Data represents the average of three replicates (n=3) ± standard error. Different letters in each column indicate significant difference by Tukey HSD test at $p \leq 0.05$. DW, Dry weight.

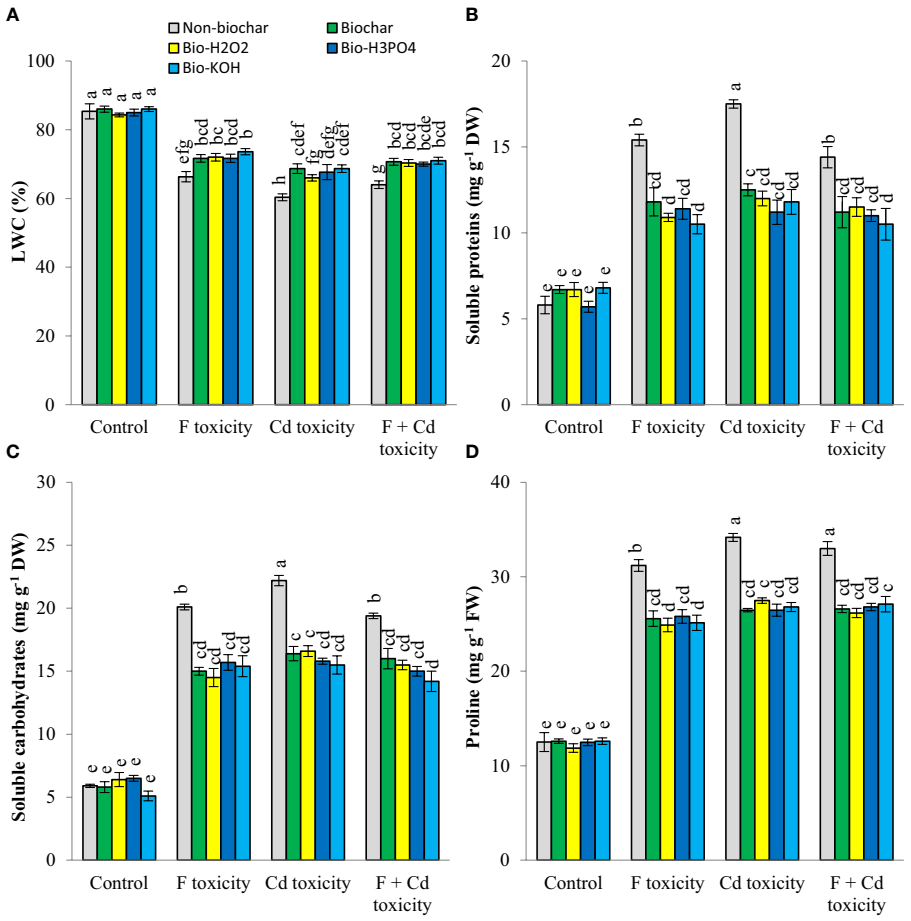

FIGURE 2
Changes in water content **(A)**, soluble proteins **(B)** carbohydrates **(C)** and proline **(D)** contents of mint leaves in response to biochar and chemically modified biochars under fluoride and cadmium toxicities. Data represent the average of three replicates (n = 3) ± standard error. Different letters indicate significant differences by Tukey HSD test at $p \leq 0.05$. LWC: Leaf water content; F: Fluoride; Cd: Cadmium; Bio-H2O2: Modified biochar by H_2O_2; Bio-KOH: Modified biochar by KOH; Bio-H_3PO_4: Modified biochar by H_3PO_4.

accumulation in mint plants, although in some cases this enhancement was not statistically significant, compared to solid biochar. Enhancement of dry mass production of mint plants by biochar-related treatments under fluoride, cadmium, and fluoride + cadmium toxicities was up to 21%, 25%, and 23%, respectively, compared to non-biochar treatment.

Mint leaf area was decreased by cadmium (by about 41%) and fluoride (by about 33%) toxicities, while soil treatment with biochar and modified biochars noticeably increased leaf expansion under both toxic and non-toxic conditions (Table 2). Chemically modified biochars were successful in developing the largest leaf area in plants. There was no statistically significant difference between the chemically modified biochars in terms of plant leaf area. Improvement of leaf area by the H_3PO_4 modified biochar was about 21%, 23%, 24%, and 17% under non-toxic, fluoride, cadmium, and fluoride + cadmium toxicities, respectively.

4 Discussion

The results of this research showed that the production and application of chemically modified biochars have a better effect than solid biochar in increasing the growth of plants under fluoride and cadmium toxicities. The biochar-related treatments improved the growth of plants by reducing fluoride and cadmium availabilities in the rhizosphere (Figure 1) and increasing the availability of water (Figure 2) and nutrients (Table 3) for plants. The pH and cation exchange capacity of the soil were raised by the biochar. The increment of soil pH by biochar is related to the alkaline nature of this organic matter. Typically, biochars have a more alkaline nature than soil, and their addition to soil increases soil pH. Improving the cation exchange capacity of the soil in response to biochar-related treatments is associated with increasing the injection of nutrients such as calcium and magnesium in the rhizosphere. Biochar is

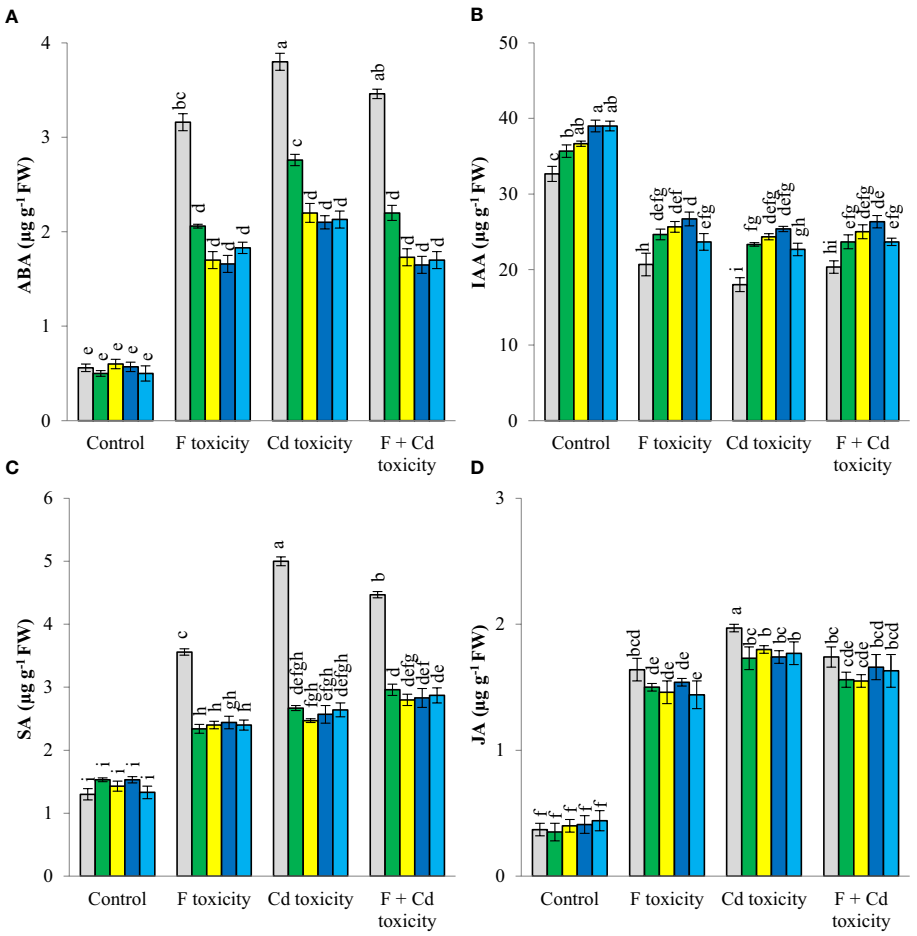

FIGURE 3
Changes in ABA **(A)**, IAA **(B)** SA **(C)** and JA **(D)** content of mint leaves in response to biochar and chemically modified biochars under fluoride and cadmium toxicities. Data represent the average of three replicates (n = 3) ± standard error. Different letters indicate significant differences by Tukey HSD test at $p \leq 0.05$. ABA: abscisic acid content; IAA: indole-3-acetic acid; SA: salicylic acid; JA: jasmonic acid F: Fluoride; Cd: Cadmium; Bio-H_2O_2: Modified biochar by H_2O_2; Bio-KOH: Modified biochar by KOH; Bio-H_3PO_4: Modified biochar by H_3PO_4.

rich in nutrients, that improves soil fertility. The effect of biochar in improving the cation exchange capacity of soil can be related to an increase in soil pH. Previous studies have shown that there is a positive correlation between the increment of pH and the cation exchange capacity of the soil (Chintala et al., 2014; Ghassemi-Golezani and Farhangi-Abriz, 2019). Hailegnaw et al. (2019) stated that the addition of 8% biochar to the soil noticeably increases soil pH, CEC, and exchangeable calcium content. The increment in cation exchange capacity of soil treated with chemically modified biochars was higher than solid biochar, which could be associated with the higher specific surface area and cation exchange capacity of chemically modified biochars (Table 1).

The availability of environmental pollutants such as fluoride and cadmium in the rhizosphere is controlled by different environmental parameters such as the organic matter of soil and pH. The addition of biochar, especially chemically modified biochars, reduced the availability of cadmium and fluoride in the rhizosphere, leading to a reduction of these pollutants in the leaves of the plants (Figure 1). Biochar could reduce the absorption of environmental pollutants such as cadmium and fluoride by plants through two mechanisms. First, increasing soil pH reduces the availability of cadmium and fluoride and their absorption by plants (Ghassemi-Golezani and Farhangi-Abriz, 2019; Jing et al., 2020). Second, biochars, especially chemically modified biochars, have different functional groups on their surface area (Liu et al., 2022) (Table 1), which increase the surface adsorption of cadmium and fluoride by biochar and ultimately reduce the absorption of these elements by the plant. Zong et al. (2021) proved that number of functional groups on biochar surface area is one of the main factors in controlling cadmium adsorption by this organic material. The reason for the

better performance of chemically modified biochars in reducing the availability of cadmium and fluoride in the soil (Figure 1) is related to their high adsorption capacity (Table 1), compared to solid biochar (Table 1). Modification of biochar by chemical reagents increases the number of functional groups on its surface area, which ultimately improves the adsorption capacity of this organic material (Li et al., 2020; Liu et al., 2022). In a recent study, Taqdees et al. (2022) showed that biochar modification with zinc particles improved radish growth under salt stress *via* decreasing sodium uptake by plants and enriching plant cells with zinc cations. In another study, Wen et al. (2021) reported that soil treatment by iron-modified biochar increases the cadmium sorption capacity of biochar, plant growth, and soil health in contaminated soils.

Destruction of photosynthetic pigments and reduction of their synthesis in plant leaves is one of the damaging effects of fluoride and cadmium stresses in plant leaves (Ghassemi-Golezani and Farhangi-Abriz, 2019; Chtouki et al., 2021). Cadmium and fluoride stresses in plant cells increase the activity of the chlorophyllase enzyme, which eventually destroys the chlorophyll structure (Sanjoy et al., 2011; Yadu et al., 2016). In addition, cadmium and fluoride toxicities increase reactive oxygen species, which have a high ability to destroy biological membranes. On the other hand, the decrease in chlorophyll synthesis in leaves under fluoride and cadmium stresses can be related to the reduction of some important nutrients such as iron and magnesium in leaves (Table 3). Magnesium is considered as a structural nutrient in the chlorophyll molecule, and iron is also a nutrient that plays a critical role in the synthesis of chlorophyll (Fageria, 2016). The decrease in the production of photosynthetic pigments under fluoride and cadmium toxicity has also been reported by other researchers (Lagriffoul et al., 1998; Ghassemi-Golezani and Farhangi-Abriz, 2019). Adding biochar to the soil improved the synthesis of photosynthetic pigments in mint leaves under fluoride and cadmium stress (Table 2). Solid and modified biochars reduced the harmful effects of these pollutants on the synthesis of chlorophyll by decreasing the absorption of fluoride and cadmium by plants. The biochar-related treatments may be also improved the synthesis of chlorophyll by increasing the absorption of various nutrients such as magnesium and iron. In addition, these treatments increased the nitrogen of leaves under fluoride and cadmium stress (Table 3), then can enhance chlorophyll synthesis. Researchers have reported a very strong correlation between leaf nitrogen content and chlorophyll synthesis (Ahanger et al., 2021). Another mechanism through which biochar can increase chlorophyll synthesis is the reduction of abscisic acid production under stress. Biochar treatments may also reduce chlorophyll destruction and helps its synthesis (Figure 3). An increase in the concentration of abscisic acid in the leaves engages the activation of enzymes such as chlorophyllase in the leaves, which ultimately causes a decrease in photosynthetic pigments of the leaves (Gupta et al., 2012). Zhu et al. (2020) reported that cadmium toxicity reduces chlorophyll content and photosynthetic activities in cotton leaves, but soil treatment with biochar mitigates the harmful effects of cadmium toxicity and increases chlorophyll biosynthesis in leaves.

Reduction of nutrient absorption by mint plants under fluoride and cadmium stresses is related to damage of root structure and cells. Cadmium and fluoride can reduce root growth and its absorption capacity (Dell Amico et al., 2008; Ghassemi-Golezani and Farhangi-Abriz, 2019; Shiyu et al., 2020). Cadmium can cause damage to the ion channels in the roots and ultimately reduce the absorption of nutrients by plants (Li et al., 2012). In addition, cadmium can compete directly with nutrients such as zinc in the rhizosphere and reduce their absorption by plants (Li et al., 2017). The increment of root cell lignification is another reason for reducing nutrient uptake by plants under cadmium toxicity. Lignification is a physiological process that blocks apoplastic pathways in plant roots and consequently decreases nutrient uptake by plants (Finger-Teixeira et al., 2010; Lux et al., 2011). Several reports have pointed out the reduction of the absorption of nutrients by plants under fluoride and cadmium toxicities (Ghassemi-Golezani and Farhangi-Abriz, 2019; Shiyu et al., 2020). Biochar is an organic soil amender that can act as an organic fertilizer in addition to the ability to regulate the physicochemical properties of the soil. This organic material with its high cation exchange capacity and specific surface area has a great ability to release nutrients into the rhizosphere. Typically, biochar has a high content of different macro and micronutrients, although the amount of these nutrients depends on the type of raw material from which biochar is produced. Increments of nutrients in plant tissues by biochar treatments under fluoride and cadmium toxicities (Table 3) can be related to the improvement of the physicochemical conditions of the rhizosphere and plant roots. Biochar and especially chemically modified biochars have a great cation exchange capacity (Table 1) that can improve the conditions of the rhizosphere for better absorption of nutrients by plants. In addition, these treatments can help to increase the water-holding capacity (Ghassemi-Golezani and Farhangi-Abriz, 2022) and microbial activities of the soil (Steinbeiss et al., 2009), which ultimately improves the bioavailability of the nutrients for plants.

Cadmium and fluoride stresses can cause less water absorption by the plant through the reduction of plant root growth (Ghassemi-Golezani and Farhangi-Abriz, 2019; Naeem et al., 2019). In addition, environmental stresses *via* increasing abscisic acid in the leaves and closing the leaf stomata can reduce the integrated movement of water from the rhizosphere to the plant and finally to the atmosphere, which imposes osmotic stress on plants (Kastori et al., 1992; Tao et al., 2021). Biochar is an organic material with high porosity that can increase the water-holding capacity of the soil and improve the available water for plants. The improvement of the water content of leaves

under fluoride and cadmium toxicity in response to biochar can be related to an increase in plant root growth (Ghassemi-Golezani and Farhangi-Abriz, 2019). To deal with osmotic stress, plants increase the content of osmolytes in their tissues, so that they can adjust their osmotic pressure potential to continue water absorption (Farhangi-Abriz and Ghassemi-Golezani, 2018). The reduction of osmolytes in plants due to biochar-related treatments under fluoride and cadmium stresses (Figure 2) is related to a decrease in fluoride, cadmium, and endogenous stress hormones (ABA, SA, and JA) in the plant tissues. Stress hormones have a stimulating effect on the synthesis of osmolytes, which increases the content of these organic materials in plant tissues. Reduction of fluoride and cadmium absorptions by plants under biochar-related treatments was led to a decrease in osmolytes and stress levels.

Enhancing the concentration of stress hormones in plant tissues is a known physiological reaction to the environment, that can increase plant resistance to stress. Adding solid and modified biochars to the soil reduced the stress hormones (ABA, SA, and JA), and at the same time increased the growth-promoting hormone (IAA) in leaf tissues (Figure 3). The reduction of stress hormones due to biochar treatments can be related to the reduction of fluoride and cadmium entry into the plant tissues (Figure 1). An increase in the content of IAA in plant tissues by biochar treatments could be associated with a decrease in the amount of fluoride and cadmium accumulation in plant tissues. In addition, biochar treatments increased the concentration of zinc in leaf tissues (Table 3), which has a very critical role in the synthesis of auxins (Fageria, 2016).

Increasing cadmium and fluoride in plant tissues, osmotic stress, and stress hormones caused a decrease in the growth of plants under stress (Table 2). Adding solid and modified biochars to the soil improved plant growth under fluoride and cadmium stresses. Biochar-related treatments increased plant growth by reducing the harmful effects of fluoride and cadmium in plant tissues. These treatments improved the water content of leaves by decreasing abscisic acid in plant tissues. Having enough water is necessary for the optimal growth of the plant. Many physiological reactions of plants are carried out in the presence of water, which is essential for cell growth and division (Skirycz and Inzé, 2010). On the other hand, biochar treatments enhanced the absorption of many key nutrients for plant growth, such as nitrogen (a key nutrient in the structure of proteins), phosphorus (a nutrient that plays a role in plant energy storage), potassium (a nutrient that activates many enzymes), calcium (a nutrient effective in improving cell division), magnesium (an active nutrient in improving the synthesis of sugars and forming the structure of chlorophyll), iron (an active nutrient in oxidation and reduction reactions in plants and helping to build chlorophyll) and zinc (a nutrient that controls the production of auxins in the tissues) (Fageria, 2016), leading to better growth of plants under fluoride and cadmium toxicities. In addition, biochar increased the concentration of auxin (IAA) in the leaf tissue (Figure 3), which in turn improved plant growth and biomass.

5 Conclusion

Biochar and especially chemically modified biochars have a very good potential to reduce the absorption of fluoride and cadmium in plant tissues. These organic soil amenders improved the absorption of nutrients and water by plants under fluoride and cadmium stresses, causing a higher synthesis of photosynthetic pigments, leaf expansion, and growth. In addition, biochar-related treatments affected hormonal signaling in plants by reducing the content of growth retardant hormones and enhancing a growth-promoting hormone (IAA) in plant tissues. The results of this research confirm the superiority of chemically modified biochars in reducing the harmful effects of fluoride and cadmium toxicities on plants due to their specific physicochemical properties such as a high number of functional groups, specific surface area, and adsorption capacity. Therefore, chemically modified biochars can be used as a powerful soil amender in contaminated soils.

Data availability statement

The original contributions presented in the study are included in the article/supplementary material. Further inquiries can be directed to the corresponding author.

Author contributions

SF-A: Experimental work, Data analyzing, Writing. K-GG: Supervision, Experimental design, Writing. All authors contributed to the article and approved the submitted version.

Acknowledgments

We appreciate the University of Tabriz for helping us to conduct the research.

Conflict of interest

The authors declare that the research was conducted in the absence of any commercial or financial relationships that could be construed as a potential conflict of interest.

Publisher's note

References

Abbas, T., Rizwan, M., Ali, S., Zia-ur-Rehman, M., Qayyum, M. F., Abbas, F., et al. (2017). Effect of biochar on cadmium bioavailability and uptake in wheat (Triticum aestivum l.) grown in a soil with aged contamination. *Ecotoxicol Environ. Saf* 140, 37–47. doi: 10.1016/j.ecoenv.2017.02.028

Ahanger, M. A., Qi, M., Huang, Z., Xu, X., Begum, N., Qin, C., et al. (2021). Improving growth and photosynthetic performance of drought stressed tomato by application of nano-organic fertilizer involves up-regulation of nitrogen, antioxidant and osmolyte metabolism. *Ecotoxicol Environ. Saf* 216, 112195. doi: 10.1016/j.ecoenv.2021.112195

Alam, M. Z., McGee, R., Hoque, M. A., Ahammed, G. J., and Carpenter-Boggs, L. (2019). Effect of arbuscular mycorrhizal fungi, selenium and biochar on photosynthetic pigments and antioxidant enzyme activity under arsenic stress in mung bean (Vigna radiata). *Front. Physiol.* 10. doi: 10.3389/fphys.2019.00193

Alengebawy, A., Abdelkhalek, S. T., Qureshi, S. R., and Wang, M. Q. (2021). Heavy metals and pesticides toxicity in agricultural soil and plants: Ecological risks and human health implications. *Toxics* 9 (3), 42. doi: 10.3390/toxics9030042

Ali, S., Rizwan, M., Noureen, S., Anwar, S., Ali, B., Naveed, M., et al. (2019). Combined use of biochar and zinc oxide nanoparticle foliar spray improved the plant growth and decreased the cadmium accumulation in rice (Oryza sativa l.) plant. *Environ. Sci. Pollut. Res.* 26 (11), 11288–11299. doi: 10.1007/s11356-019-04554-y

Arnon, D. I. (1949). Copper enzymes in isolated chloroplasts. polyphenoloxidase in beta vulgaris. *Plant Physiol.* 24 (1), 1. doi: 10.1104/pp.24.1.1

Bates, L. S., Waldren, R. P., and Teare, I. D. (1973). Rapid determination of free proline for water-stress studies. *Plant Soil* 39 (1), 205–207. doi: 10.1007/BF00018060

Batool, A., Taj, S., Rashid, A., Khalid, A., Qadeer, S., Saleem, A. R., et al. (2015). Potential of soil amendments (Biochar and gypsum) in increasing water use efficiency of abelmoschus esculentus l. *Moench. Front. Plant Sci.* 6. doi: 10.3389/fpls.2015.00733

Boateng, A. A., Garcia-Perez, M., Mašek, O., Brown, R., and del Campo, B. (2015). "Biochar production technology," in *Biochar for environmental management* (London, UK: Routledge), 63–87.

Bradford, M. M. (1976). A rapid and sensitive method for the quantitation of microgram quantities of protein utilizing the principle of protein-dye binding. *Anal. Biochem.* 72 (1-2), 248–254. doi: 10.1016/0003-2697(76)90527-3

Brahmi, F., Khodir, M., Mohamed, C., and Pierre, D. (2017). Chemical composition and biological activities of mentha species. *Aromatic medicinal plants-Back to nature* 10, 47–79. doi: 10.5772/67291

Chapman, H. D. (1965). Cation-exchange capacity. Methods of soil analysis: Part 2 Chemical and microbiological properties. *American Society of Agronomy, Inc. USA* 9, 891–901. doi: 10.2134/agronmonogr9.2.c6

Chintala, R., Mollinedo, J., Schumacher, T. E., Malo, D. D., and Julson, J. L. (2014). Effect of biochar on chemical properties of acidic soil. *Arch. Agron. Soil Sci.* 60 (3), 393–404. doi: 10.1080/03650340.2013.789870

Choudhary, S., Rani, M., Devika, O. S., Patra, A., Singh, R. K., and Prasad, S. K. (2019). Impact of fluoride on agriculture: A review on it's sources, toxicity in plants and mitigation strategies. *Int. J. Chem. Stud.* 7 (2), 1675–1680.

Chtouki, M., Naciri, R., Soulaimani, A., Zeroual, Y., El Gharous, M., and Oukarroum, A. (2021). Effect of cadmium and phosphorus interaction on tomato: Chlorophyll a fluorescence, plant growth, and cadmium translocation. *Water Air Soil Pollut.* 232 (3), 1–11. doi: 10.1007/s11270-021-05038-x

Cieśliński, G., Neilsen, G. H., and Hogue, E. J. (1996). Effect of soil cadmium application and pH on growth and cadmium accumulation in roots, leaves and fruit of strawberry plants (Fragaria× ananassa duch.). *Plant Soil* 180, 267–276. doi: 10.1007/BF00015310

Dell Amico, E., Cavalca, L., and Andreoni, V. (2008). Improvement of brassica napus growth under cadmium stress by cadmium-resistant rhizobacteria. *Soil Biol. Biochem.* 40 (1), 74–84. doi: 10.1016/j.soilbio.2007.06.024

El Rasafi, T., Oukarroum, A., Haddioui, A., Song, H., Kwon, E. E., Bolan, N., et al. (2022). Cadmium stress in plants: A critical review of the effects, mechanisms, and tolerance strategies. *Crit. Rev. Environ. Sci. Technol.* 52 (5), 675–726. doi: 10.1080/10643389.2020.1835435

Fageria, N. K. (2016). *The use of nutrients in crop plants* (Boca Raton, Florida, USA: CRC press).

Farhangi-Abriz, S., and Ghassemi-Golezani, K. (2018). How can salicylic acid and jasmonic acid mitigate salt toxicity in soybean plants? *Ecotoxicol Environ. Saf* 147, 1010–1016. doi: 10.1016/j.ecoenv.2017.09.070

Farhangi-Abriz, S., and Ghassemi-Golezani, K. (2021). Changes in soil properties and salt tolerance of safflower in response to biochar-based metal oxide nanocomposites of magnesium and manganese. *Ecotoxicol Environ. Saf* 211, 111904. doi: 10.1016/j.ecoenv.2021.111904

Farhangi-Abriz, S., Ghassemi-Golezani, K., Torabian, S., and Qin, R. (2022). A meta-analysis to estimate the potential of biochar in improving nitrogen fixation and plant biomass of legumes. *Biomass Convers Biorefin*, 1–11. doi: 10.1007/s13399-022-02530-0

Finger-Teixeira, A., Ferrarese, M. D. L. L., Soares, A. R., da Silva, D., and Ferrarese-Filho, O. (2010). Cadmium-induced lignification restricts soybean root growth. *Ecotoxicol Environ. Saf* 73 (8), 1959–1964. doi: 10.1016/j.ecoenv.2010.08.021

Ghassemi-Golezani, K., and Farhangi-Abriz, S. (2019). Biochar alleviates fluoride toxicity and oxidative stress in safflower (Carthamus tinctorius l.) seedlings. *Chemosphere* 223, 406–415. doi: 10.1016/j.chemosphere.2019.02.087

Ghassemi-Golezani, K., and Farhangi-Abriz, S. (2021). Biochar-based metal oxide nanocomposites of magnesium and manganese improved root development and productivity of safflower (Carthamus tinctorius l.) under salt stress. *Rhizosphere* 19, 100416. doi: 10.1016/j.rhisph.2021.100416

Ghassemi-Golezani, K., and Farhangi-Abriz, S. (2022). Improving plant available water holding capacity of soil by solid and chemically modified biochars. *Rhizosphere* 21, 100469. doi: 10.1016/j.rhisph.2021.100469

Ghassemi-Golezani, K., Farhangi-Abriz, S., and Abdoli, S. (2021). How can biochar-based metal oxide nanocomposites counter salt toxicity in plants? *Environ. Geochem Health* 43 (5), 2007–2023. doi: 10.1007/s10653-020-00780-3

Graber, E. R., Tsechansky, L., Fidel, R. B., Thompson, M. L., and Laird, D. A. (2017). "Determining acidic groups at biochar surfaces via the boehm titration," in *Biochar: A guide to analytical methods*. (Clayton, Australia: CSIRO).

Gupta, S., Gupta, S. M., Sane, A. P., and Kumar, N. (2012). Chlorophyllase in piper betle l. has a role in chlorophyll homeostasis and senescence dependent chlorophyll breakdown. *Mol. Biol. Rep.* 39 (6), 7133–7142. doi: 10.1007/s11033-012-1545-8

Haider, F. U., Liqun, C., Coulter, J. A., Cheema, S. A., Wu, J., Zhang, R., et al. (2021a). Cadmium toxicity in plants: Impacts and remediation strategies. *Ecotoxicol Environ. Saf* 211, 111887. doi: 10.1016/j.ecoenv.2020.111887

Haider, F. U., Virk, A. L., Rehmani, M. I. A., Skalicky, M., Ata-ul-Karim, S. T., Ahmad, N., et al. (2021b). Integrated application of thiourea and biochar improves maize growth, antioxidant activity and reduces cadmium bioavailability in cadmium-contaminated soil. *Front. Plant Sci.* 12. doi: 10.3389/fpls.2021.809322

Hailegnaw, N. S., Mercl, F., Pračke, K., Száková, J., and Tlustoš, P. (2019). Mutual relationships of biochar and soil pH, CEC, and exchangeable base cations in a model laboratory experiment. *J. Soils Sediments* 19 (5), 2405–2416. doi: 10.1007/s11368-019-02264-z

Hu, B., Deng, F., Chen, G., Chen, X., Gao, W., Long, L., et al. (2020). Evolution of abscisic acid signaling for stress responses to toxic metals and metalloids. *Front. Plant Sci.* 11. doi: 10.3389/fpls.2020.00909

Javeed, H. M. R., Naeem, R., Ali, M., Qamar, R., Sarwar, M. A., Nawaz, F., et al. (2022). Coupling biochar with microbial inoculants improves maize growth and nutrients acquisition under phosphorous-limited soil. *Acta Physiol. Plant* 44 (11), 1–15. doi: 10.1007/s11738-022-03440-4

Jin, H., Capareda, S., Chang, Z., Gao, J., Xu, Y., and Zhang, J. (2014). Biochar pyrolytically produced from municipal solid wastes for aqueous as (V) removal: adsorption property and its improvement with KOH activation. *Bioresour. Technol.* 169, 622–629. doi: 10.1016/j.biortech.2014.06.103

Jing, F., Chen, X., Wen, X., Liu, W., Hu, S., Yang, Z., et al. (2020). Biochar effects on soil chemical properties and mobilization of cadmium (Cd) and lead (Pb) in paddy soil. *Soil Use Manage.* 36 (2), 320–327. doi: 10.1111/sum.12557

Jones, J. B. Jr. (1991). *Kjeldahl method for nitrogen determination* (Georgia, USA: Micro-Macro Publishing, Inc).

Kastori, R., Petrović, M., and Petrović, N. (1992). Effect of excess lead, cadmium, copper, and zinc on water relations in sunflower. *J. Plant Nutr.* 15 (11), 2427–2439. doi: 10.1080/01904169209364485

Kochert, G., Hellebust, J. A., and Craigie, J. S. (1978). *Handbook of phycological methods* (London: Cambridge University Press), 455–456.

Lagriffoul, A., Mocquot, B., Mench, M., and Vangronsveld, J. (1998). Cadmium toxicity effects on growth, mineral and chlorophyll contents, and activities of stress related enzymes in young maize plants (Zea mays l.). *Plant Soil* 200 (2), 241–250. doi: 10.1023/A:1004346905592

Larsen, S., and Widdowson, A. E. (1971). Soil fluorine. *J. Soil Sci.* 22, 210–221. doi: 10.1111/j.1365-2389.1971.tb01608.x

Lateef, A., Nazir, R., Jamil, N., Alam, S., Shah, R., Khan, M. N., et al. (2019). Synthesis and characterization of environmental friendly corncob biochar based nano-composite–a potential slow release nano-fertilizer for sustainable agriculture. *Environ. Nanotechnol Monit. Manage.* 11, 100212. doi: 10.1016/j.enmm.2019.100212

Li, X. J., and Meng, F. J. (1996). Study on the photoperiodic-induced flowering in soybean: changes of plant hormones and assimilates of the first leaves. *J. China Agric. Univ* 1, 35–39.

Lindsay, W. L., and Norvell, W. A. (1978). Development of a DTPA soil test for zinc, iron, manganese, and copper. *Soil Sci. Soc Am. J.* 42, 421–428. doi: 10.2136/sssaj1978.03615995004200030009x

Li, L. Z., Tu, C., Wu, L. H., Peijnenburg, W. J., Ebbs, S., and Luo, Y. M. (2017). Pathways of root uptake and membrane transport of Cd2+ in the zinc/cadmium hyperaccumulating plant sedum plumbizincicola. *Environ. Toxicol. Chem.* 36 (4), 1038–1046. doi: 10.1002/etc.3625

Liu, Z., Xu, Z., Xu, L., Buyong, F., Chay, T. C., Li, Z., et al. (2022). Modified biochar: Synthesis and mechanism for removal of environmental heavy metals. *Carbon Res.* 1 (1), 1–21. doi: 10.1007/s44246-022-00007-3

Li, X., Wang, C., Tian, J., Liu, J., and Chen, G. (2020). Comparison of adsorption properties for cadmium removal from aqueous solution by enteromorpha prolifera biochar modified with different chemical reagents. *Environ. Res.* 186, 109502. doi: 10.1016/j.envres.2020.109502

Li, Y., Wang, S., Zhang, Q., Zang, F., Nan, Z., Sun, H., et al. (2018). Accumulation, interaction and fractionation of fluoride and cadmium in sierozem and oilseed rape (Brassica napus l.) in northwest China. *Plant Physiol. Biochem.* 127, 457–468. doi: 10.1016/j.plaphy.2018.04.017

Li, S., Yu, J., Zhu, M., Zhao, F., and Luan, S. (2012). Cadmium impairs ion homeostasis by altering k+ and Ca2+ channel activities in rice root hair cells. *Plant Cell Environ.* 35 (11), 1998–2013. doi: 10.1111/j.1365-3040.2012.02532.x

Lux, A., Martinka, M., Vaculik, M., and White, P. J. (2011). Root responses to cadmium in the rhizosphere: A review. *J. Exp. Bot.* 62 (1), 21–37. doi: 10.1093/jxb/erq281

Maclachlan, S., and Zalik, S. (1963). Plastid structure, chlorophyll concentration, and free amino acid composition of a chlorophyll mutant of barley. *Can. J. Plant Sci.* 41 (7), 1053–1062. doi: 10.1139/b63-088

Medyńska-Juraszek, A., Rivier, P. A., Rasse, D., and Joner, E. J. (2020). Biochar affects heavy metal uptake in plants through interactions in the rhizosphere. *Appl. Sci.* 10 (15), 5105. doi: 10.3390/app10155105

Mehmood, S., Saeed, D. A., Rizwan, M., Khan, M. N., Aziz, O., Bashir, S., et al. (2018). Impact of different amendments on biochemical responses of sesame (Sesamum indicum l.) plants grown in lead-cadmium contaminated soil. *Plant Physiol. Biochem.* 132, 345–355. doi: 10.1016/j.plaphy.2018.09.019

Mohan, D., Kumar, S., and Srivastava, A. (2014). Fluoride removal from ground water using magnetic and nonmagnetic corn stover biochars. *Ecol. Eng* 73, 798–808. doi: 10.1016/j.ecoleng.2014.08.017

Naeem, A., Zafar, M., Khalid, H., Zia-ur-Rehman, M., Ahmad, Z., Ayub, M. A., et al. (2019). "Cadmium-induced imbalance in nutrient and water uptake by plants," in *Cadmium toxicity and tolerance in plants* (Cambridge, Massachusetts, USA: Academic Press), 299–326.

Park, J. H., Choppala, G. K., Bolan, N. S., Chung, J. W., and Chuasavathi, T. (2011). Biochar reduces the bioavailability and phytotoxicity of heavy metals. *Plant soil* 348 (1), 439–451. doi: 10.1007/s11104-011-0948-y

Rahimzadeh, S., and Ghassemi-Golezani, K. (2022). Biochar-based nutritional nanocomposites altered nutrient uptake and vacuolar h+-pump activities of dill under salinity. *Soil Sci. Plant Nutr.* 22, 3568–3581. doi: 10.1007/s42729-022-00910-z

Rehman, M., Liu, L., Bashir, S., Saleem, M. H., Chen, C., Peng, D., et al. (2019). Influence of rice straw biochar on growth, antioxidant capacity and copper uptake in ramie (Boehmeria nivea l.) grown as forage in aged copper-contaminated soil. *Plant Physiol. Biochem.* 138, 121–129. doi: 10.1016/j.plaphy.2019.02.021

Ren, T., Chen, N., Mahari, W. A. W., Xu, C., Feng, H., Ji, X., et al. (2021). Biochar for cadmium pollution mitigation and stress resistance in tobacco growth. *Environ. Res.* 192, 110273. doi: 10.1016/j.envres.2020.110273

Rizwan, M., Ali, S., Abbas, T., Adrees, M., Zia-ur-Rehman, M., Ibrahim, M., et al. (2018). Residual effects of biochar on growth, photosynthesis and cadmium uptake in rice (Oryza sativa l.) under cd stress with different water conditions. *J. Environ. Manage.* 206, 676–683. doi: 10.1016/j.jenvman.2017.10.035

Rolon-Cardenas, G. A., Arvizu-Gómez, J. L., Soria-Guerra, R. E., Pacheco-Aguilar, J. R., Alatorre-Cobos, F., and Hernández-Morales, A. (2022). The role of auxins and auxin-producing bacteria in the tolerance and accumulation of cadmium by plants. *Environ. Geochem Health* 44, 3743–3764. doi: 10.1007/s10653-021-01179-4

Sanjoy, S., Bandopadhyay, P. K., and Nilima, K. (2011). Inhibition of cadmium on chlorophyll content and chlorophyllase activity in wheat (Triticum aestivum l.) varieties and alleviation of cadmium stress by micronutrients and organic acids. *Indian Agric.* 55 (3/4), 139–143.

Sharma, R., and Kaur, R. (2018). Insights into fluoride-induced oxidative stress and antioxidant defences in plants. *Acta Physiol. Plant* 40 (10), 1–14. doi: 10.1007/s11738-018-2754-0

Shen, C., Yang, Y. M., Sun, Y. F., Zhang, M., Chen, X. J., and Huang, Y. Y. (2022). The regulatory role of ABA cadmium uptake, accumulation and translocation in plants. *Front. Plant Sci.* 13, 953717. doi: 10.3389/fpls.2022.953717

Shiyu, Q., Hongen, L., Zhaojun, N., Rengel, Z., Wei, G., Chang, L., et al. (2020). Toxicity of cadmium and its competition with mineral nutrients for uptake by plants: A review. *Pedosphere* 30 (2), 168–180. doi: 10.1016/S1002-0160(20)60002-9

Skirycz, A., and Inzé, D. (2010). More from less: Plant growth under limited water. *Curr. Opin. Biotechnol.* 21 (2), 197–203. doi: 10.1016/j.copbio.2010.03.002

Steinbeiss, S., Gleixner, G., and Antonietti, M. (2009). Effect of biochar amendment on soil carbon balance and soil microbial activity. *Soil Biol. Biochem.* 41 (6), 1301–1310. doi: 10.1016/j.soilbio.2009.03.016

Takaya, C. A., Fletcher, L. A., Singh, S., Okwuosa, U. C., and Ross, A. B. (2016). Recovery of phosphate with chemically modified biochars. *J. Environ. Chem. Eng* 4, 1156–1165. doi: 10.1016/j.jece.2016.01.011

Tandon, H. L. S., Cescas, M. P., and Tyner, E. H. (1968). An acid-free vanadate-molybdate reagent for the determination of total phosphorus in soils. *Soil Sci. Soc. Am. J.* 32 (1), 48–51. doi: 10.2136/sssaj1968.03615995003200010012x

Tan, X. F., Liu, Y. G., Gu, Y. L., Xu, Y., Zeng, G. M., Hu, X. J., et al. (2016). Biochar-based nano-composites for the decontamination of wastewater: A review. *Bioresour. Technol.* 212, 318–333. doi: 10.1016/j.biortech.2016.04.093

Tao, Q., Jupa, R., Dong, Q., Yang, X., Liu, Y., Li, B., et al. (2021). Abscisic acid-mediated modifications in water transport continuum are involved in cadmium hyperaccumulation in sedum alfredii. *Chemosphere* 268, 129339. doi: 10.1016/j.chemosphere.2020.129339

Taqdees, Z., Khan, J., Kausar, S., Afzaal, M., and Akhtar, I. (2022). Silicon and zinc nanoparticles-enriched miscanthus biochar enhanced seed germination, antioxidant defense system, and nutrient status of radish under NaCl stress. *Crop Pasture Sci.* 73 (5), 556–572. doi: 10.1071/CP21342

Wang, S., Xu, L., Li, G., Chen, P., Xia, K., and Zhou, X. (2002). An ELISA for the determination of salicylic acid in plants using a monoclonal antibody. *Plant Sci.* 162 (4), 529–535. doi: 10.1016/S0168-9452(01)00606-9

Waqar, M., Habib-ur-Rahman, M., Hasnain, M. U., Iqbal, S., Ghaffar, A., Iqbal, R., et al. (2022). Effect of slow release nitrogenous fertilizers and biochar on growth, physiology, yield, and nitrogen use efficiency of sunflower under arid climate. *Environ. Sci. Pollut. Res.* 29, 52520–52533. doi: 10.1007/s11356-022-19289-6

Wen, E., Yang, X., Chen, H., Shaheen, S. M., Sarkar, B., Xu, S., et al. (2021). Iron-modified biochar and water management regime-induced changes in plant growth, enzyme activities, and phytoavailability of arsenic, cadmium and lead in a paddy soil. *J. Hazard Mater.* 407, 124344. doi: 10.1016/j.jhazmat.2020.124344

White, A. J. (2010). *Development of an activated carbon from anaerobic digestion byproduct to remove hydrogen sulfide from biogas* (Canada: University of Toronto).

Xue, Y., Gao, B., Yao, Y., Inyang, M., Zhang, M., Zimmerman, A. R., et al. (2012). Hydrogen peroxide modification enhances the ability of biochar (hydrochar) produced from hydrothermal carbonization of peanut hull to remove aqueous heavy metals: Batch and column tests. *Chem. Eng J.* 200, 673–680. doi: 10.1016/j.cej.2012.06.116

Xu, D., Zhao, Y., Sun, K., Gao, B., Wang, Z., Jin, J., et al. (2014). Cadmium adsorption on plant-and manure-derived biochar and biochar-amended sandy soils: Impact of bulk and surface properties. *Chemosphere* 111, 320–326. doi: 10.1016/j.chemosphere.2014.04.043

Yadu, B., Chandrakar, V., and Keshavkant, S. (2016). Responses of plants to fluoride: An overview of oxidative stress and defense mechanisms. *Fluoride* 49 (3), 293.

Yotsova, E., Dobrikova, A., Stefanov, M., Misheva, S., Bardáčová, M., Matušíková, I., et al. (2020). Effects of cadmium on two wheat cultivars depending on different nitrogen supply. *Plant Physiol. Biochem.* 155, 789–799. doi: 10.1016/j.plaphy.2020.06.042

Zhishen, J., Mengcheng, T., and Jianming, W. (1999). The determination of flavonoid contents in mulberry and their scavenging effects on superoxide radicals. *Food Chem.* 64 (4), 555–559. doi: 10.1016/S0308-8146(98)00102-2

Zhu, Y., Wang, H., Lv, X., Zhang, Y., and Wang, W. (2020). Effects of biochar and biofertilizer on cadmium-contaminated cotton growth and the antioxidative defense system. *Sci. Rep.* 10 (1), 1–12. doi: 10.1038/s41598-020-77142-7

Zong, Y., Xiao, Q., and Lu, S. (2021). Biochar derived from cadmium-contaminated rice straw at various pyrolysis temperatures: Cadmium immobilization mechanisms and environmental implication. *Bioresour. Technol.* 321, 124459. doi: 10.1016/j.biortech.2020.124459

Zulfiqar, U., Jiang, W., Xiukang, W., Hussain, S., Ahmad, M., Maqsood, M. F., et al. (2022). Cadmium phytotoxicity, tolerance, and advanced remediation approaches in agricultural soils; a comprehensive review. *Front. Plant Sci.* 13. doi: 10.3389/fpls.2022.773815

frontiers | Frontiers in Plant Science

TYPE Original Research
PUBLISHED 06 January 2023
DOI 10.3389/fpls.2022.1047268

OPEN ACCESS

EDITED BY
Muhammad Ali Raza,
Islamia University of Bahawalpur, Pakistan

REVIEWED BY
Sajad Hussain,
Islamia University of Bahawalpur, Pakistan
Muhammad Hayder Bin Khalid,
Sichuan Agricultural University, China
Atta Mohi Ud Din,
Nanjing Agricultural University, China

*CORRESPONDENCE
Rachel L. Veenstra
rveenstra@ksu.edu
Ignacio A. Ciampitti
ciampitti@ksu.edu

SPECIALTY SECTION
This article was submitted to Plant Abiotic Stress, a section of the journal Frontiers in Plant Science

RECEIVED 17 September 2022
ACCEPTED 08 December 2022
PUBLISHED 06 January 2023

CITATION
Veenstra RL, Messina CD, Berning D, Haag LA, Carter P, Hefley TJ, Prasad PVV and Ciampitti IA (2023) Corn yield components can be stabilized via tillering in sub-optimal plant densities.
Front. Plant Sci. 13:1047268.
doi: 10.3389/fpls.2022.1047268

Corn yield components can be stabilized via tillering in sub-optimal plant densities

Rachel L. Veenstra[1*], Carlos D. Messina[2], Dan Berning[3], Lucas A. Haag[4], Paul Carter[5], Trevor J. Hefley[6], P. V. Vara Prasad[1] and Ignacio A. Ciampitti[1*]

[1]Department of Agronomy, Kansas State University, Manhattan, KS, United States, [2]Horticultural Sciences Department, University of Florida, Gainesville, FL, United States, [3]Corteva Agriscience Agronomy Sciences, Johnston, IA, United States, [4]Northwest Research-Extension Center, Kansas State University, Colby, KS, United States, [5]Formerly Corteva Agriscience, Independent Agronomist, Clive, IA, United States, [6]Department of Statistics, Kansas State University, Manhattan, KS, United States

Introduction: Crop plasticity is fundamental to sustainability discussions in production agriculture. Modern corn (*Zea mays* L.) genetics can compensate yield determinants to a small degree, but plasticity mechanisms have been masked by breeder selection and plant density management preferences. While tillers are a well-known source of plasticity in cereal crops, the functional trade-offs of tiller expression to the hierarchical yield formation process in corn are unknown. This investigation aimed to further dissect the consequences of tiller expression on corn yield component determination and plasticity in a range of environments from two plant fraction perspectives – i) main stalks only, considering potential functional trade-offs due to tiller expression; and ii) comprehensive (main stalk plus tillers).

Methods: This multi-seasonal study considered a dataset of 17 site-years across Kansas, United States. Replicated field trials evaluated tiller presence (removed or intact) in two hybrids (P0657AM and P0805AM) at three target plant densities (25000, 42000, and 60000 plants ha^{-1}). Record of ears and kernels per unit area and kernel weight were collected separately for both main stalks and tillers in each plot.

Results: Indicated tiller contributions impacted the plasticity of yield components in evaluated genotypes. Ear number and kernel number per area were less dependent on plant density, but kernel number remained key to yield stability. Although ear number was less related to yield stability, ear source and type were significant yield predictors, with tiller axillary ears as stronger contributors than main stalk secondary ears in high-yielding environments.

Discussions: Certainly, managing for the most main stalk primary ears possible – that is, optimizing the plant density (which consequently reduces tiller expression), is desirable to maximize yields. However, the demonstrated escape from the

deterministic hierarchy of corn yield formation may offer avenues to reduce corn management dependence on a seasonally variable optimum plant density, which cannot be remediated mid-season.

KEYWORDS

crop plasticity, yield components, tillering, plant density, corn (maize)

1 Introduction

Corn (*Zea mays* L.) is of significant global socioeconomic importance, experiencing recent production expansion into more restrictive environments with less opportunity for intensified farming systems (Lark et al., 2020). In these regions of reduced yield potential, such as the Central High Plains of the United States (US), effective resource use is a key factor considered by farmers as they adapt to variable climatic conditions (Lobell et al., 2011). While farming systems can be acclimated to environmental conditions through management practices, such strategies often must be implemented before the crop is sown. Mid-season crop adaptation mechanisms expressed in response to stress, resource abundance, or other factors are potentially useful in regions where seasons can be quite variable. Phenotypic plasticity (herein termed as crop plasticity) refers to the ability of a genotype to adapt (e.g., express a specific trait) in response to the environment (Laitinen and Nikoloski, 2019). In sub-optimal or otherwise unpredictable growing conditions, crop plasticity mechanisms are being explored as an avenue to maintain yields (Nicotra et al., 2010).

Capitalizing on crop plasticity potential could improve the stability of production in regions with high climatic risk (Berzsenyi and Tokatlidis, 2012; Mylonas et al., 2020). The central US corn belt, where climate is relatively stable year to year, is an important hub of modern corn improvement. In this environment, breeders selected for those plasticity mechanisms conducive to high-yielding, intensively managed environments. Furthermore, as growers have intensified plant density and breeders have enhanced genetic tolerance to increased plant density over time, the expression of corn plasticity may have been constrained (Russell, 1991; Duvick et al., 2004; Assefa et al., 2018). When corn is sown at plant densities below those evaluated by breeding programs, alternative plasticity mechanisms, such as tillering, can be expressed (Lyon, 1905; Jenkins, 1941). Such plant densities (< 60000 plants ha^{-1}) are commonly targeted by producers in restrictive environments like the Central High Plains of the US, the southwestern Pampas of Argentina, as well as portions of Africa and Australia. In these restrictive environments, multiple ears (prolificacy) or greater kernels per ear (commonly "flex") are generally viewed by producers as desirable plasticity mechanisms when seasons are desirable, but only when expressed on the main shoot.

Tillers are secondary vegetative shoots common in Poacea species such as wheat (*Triticum aestivum* L.), rice (*Oryza sativa* L.), and grain sorghum (*Sorghum bicolor* L. Moench). However, tillers are less common in corn due to historic breeding selection (Major, 1977; Duvick et al., 2004). In spite of this, tiller expression potential has been conserved in modern corn germplasm (Moulia et al., 1999) and breeding program adoption of less restrictive plant densities re-introduces tillering as a plasticity mechanism (Tsaftaris et al., 2008). Tiller expression is highly dependent on genetics (Dungan et al., 1959; Tokatlidis et al., 2005; Hansey and de Leon, 2011), but also strongly influenced by environmental factors. Expressed corn tillers may remain vegetative, may abort, or may reach reproductive stages (Alofe and Schrader, 1975; Russelle et al., 1984) – developing into harvestable axillary ears or abnormal, mixed-sex apical inflorescences called "tassel ears" (Schaffner, 1930; Bonnett, 1948). Tiller development is ultimately a response to an abundance of resources, which may be triggered by nutrients, water, light, temperature, or factors resulting from a combination of these (e.g., plant density; Gardner, 1942; Downey, 1972; Stevenson and Goodman, 1972; Tetio-Kagho and Gardner, 1988). Although tiller development impacts are not well-documented in corn, yield of tillers has been proposed as respondent to factors such as plant density (light environment) and soil moisture (Thapa et al., 2018; Rotili et al., 2021; Veenstra et al., 2021).

While previous field studies have considered corn yield as a response to tiller presence (Sangoi et al., 2009; Frank et al., 2013; Veenstra et al., 2021; Massigoge et al., 2022), efforts to understand the mechanisms and flexibility of observed compensatory relationships are lacking, at least in the US. Considering trends in corn genetic selection and agronomic management in the US, plant density is a historic focal point (Duvick et al., 2004) with highly determinate, hierarchical yield components. Yield component plasticity (namely ears and kernels per area and individual kernel weight) in the idealized, single-stalked corn phenotype is marginal relative to the yield gain of additional plants per area (Fernández et al., 2022). For

example, kernel number can be adjusted through early grain-filling stages but is limited by the success of a short pollination window (R1, silking per Ritchie et al., 1997) and the number of ears on the main stalk, which is determined in vegetative stages and typically singular (Bonnett, 1948; Andrade et al., 1999). Plastic phenotypes can reduce dependency on precise plant density (Tokatlidis and Koutroubas, 2004; Berzsenyi and Tokatlidis, 2012) – for instance, by producing more than one ear per plant (Prior and Russell, 1975; Thomison and Jordan, 1995). Tillers, a demonstrated source of plasticity, may facilitate an offset in development from the deterministic, single-stalked hierarchy. Functional trade-offs in resource allocation due to tiller expression are unknown. These relationships may improve or degrade yield stability.

Exploring the impact of tiller expression on yield component plasticity is a novel avenue to understand corn environmental adaptation potential. Although trade-offs in corn yield components are well-known (Slafer, 2003; Sadras and Slafer, 2012) and the concept of tiller-conferred plasticity has been established (Downey, 1972; Yamaguchi, 1974; Rotili et al., 2021; Rotili et al., 2022), field-based research solidifying the connection between the two is inadequate. Understanding the degree to which tillers impact reproductive plasticity may provide insight for reducing plant density dependence and shed new light on environmental adaptation strategies, particularly as climatic risk intensifies. A range in favorable to negligible yield responses to tiller expression were reported for the first two seasons of this project (Veenstra et al., 2021). Authors hypothesized that tiller expression improved plasticity of yield components, thereby reducing plant density-based yield dependency. Key points to explore in the dissection of observed yield responses included which yield components were most stabilized by tiller expression, if plasticity relationships were adjusted among yield components, and if yield component source (i.e., coming from tillers or main stalk) impacted yield stability and determination. Therefore, the aim of this investigation was to explore the consequences of tiller expression on corn yield component determination and plasticity in a range of environments from two plant fraction perspectives – i) main stalks only, considering potential functional trade-offs due to tiller expression; and ii) comprehensive (main stalk plus tiller contributions as an overall view of plasticity potential).

2 Materials and methods

2.1 Field experiments

Field trials were established at 9 sites across 3 years in Kansas, US, resulting in a final field database of 17 site-year combinations. In addition to the ten site-years (2019-2020 seasons) described in previous work (Veenstra et al., 2021), seven site-years were evaluated during the 2021 growing season. These 2021 site-year characterizations are provided in Figure 1 and Supplementary Table 1. Sites ranged in seasonal normal precipitation from 330 to 550 mm and seasonal normal temperature from 19 to 22.5 °C (1991-2021 base period). Site coordinates ranged from 37.6 to 39.4 °N and 96.6 to 101.8 °W.

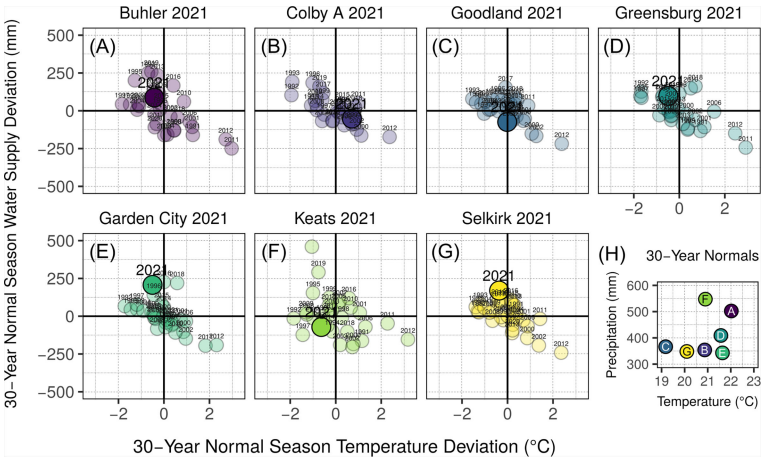

FIGURE 1
Environmental characterization of site-years added to those described previously in Veenstra et al., 2021. Annual season normal precipitation and temperature deviation for 1991-2020 are presented for each site-year **(A-G)**. Season normal precipitation and temperature characterization by site-year are shown in panel **(H)**, referring to the panel letter of described site-years. Bold vertical lines in panels **A—G** indicate normal average temperature for site-year season date ranges, while bold horizontal lines indicate normal precipitation accumulation for site-year season date ranges. Year of study for each site-year **(A-G)** is indicated with a large, opaque point and enlarged text, and considers both precipitation and irrigation in the water supply value (y-axis). All other years in panels **(A-G)** are shown with transparent points and smaller text, and water supply (y-axis) includes only precipitation. Base period for all climate normal calculations was 1991-2020.

Of the full dataset, ten site-years were implemented using a replicated three-way factorial treatment structure in a randomized complete block design (RCBD) with a split-split-plot arrangement. Plant density was the whole plot factor, with three levels selected as representative of common producer practices in limited moisture environments across Kansas (25000, 42000, and 60000 plants ha^{-1}; Roozeboom et al., 2007). Corn genotype (hybrid) was the sub-plot factor, with the two levels P0657AM and P0805AM (Corteva Agriscience, Johnston, IA, US), which were selected as suitable for the region of study and conducive to tiller. Both hybrids tillered at similar rates based on plant density, ranging from 0 (higher plant density) to 4.6 tillers $plant^{-1}$ (lower plant density), with a mean of 0.8 tillers $plant^{-1}$ for plots with tillers intact. Tiller presence was the sub-sub-plot factor, with the two levels intact or removed at development stage V10 (tenth leaf per Ritchie et al., 1997). Seven site-years were implemented with a similar RCBD design but missing either partial or total levels of the aforementioned treatment structure. Plots in all site-years were planted at least four rows wide at 0.76-m spacing, resulting in final minimum plot dimensions of 3 m by 5 m. Plant densities were seeded at double rates and thinned by hand prior to the V3 development stage to ensure accurate and even stands. Plant health was maintained as necessary with pesticides and crop nutritional needs were met with applied fertilizers.

Actual plant density, tiller density, and yield component data were collected at physiological maturity (development stage R6). Only the two central rows in each plot were included in data collection efforts. In addition, buffer zones were established on row ends to minimize edge effects. Tillers with at least one collared leaf were included in tiller density counts. Data rows were measured by carefully accounting for interplant spacing of the nearest buffer-appointed plant on row ends. Intact ears (machine-harvestable and providing > 100 collective kernels $plot^{-1}$) were counted, picked, and shelled by hand at dry maturity (< 200 g kg^{-1} moisture). Data collected were summarized by plot but separated based on plant fraction – main stalk and tillers. Harvested areas across sites were similar in size and approximately 4 m by 1.5 m. Recorded yield components included ear number per area, kernel number per area, and weight per kernel. Kernel weights were measured with a representative sample of shelled grain for each plant fraction from each plot. Two sets of 100 kernels were counted and weighed, with values averaged, and final moisture content adjusted to a 155 g kg^{-1} basis. Kernels per area were calculated based on mean kernel weights and yield values. Plot averages for yield components were calculated as weighted means of main stalk and tiller data.

2.2 Calculations

Yield environment was previously linked to corn plasticity potential and tiller productivity (Rotili et al., 2021; Veenstra et al., 2021). Therefore, yield environment clusters were identified and characterized. Site-years were clustered by mean yield using the k-means algorithm. Based on the within-cluster sums of squares generated by the k-means algorithm, the ideal number of yield clusters was visually identified as three – low, moderate, and high. Soil texture and fertility were characterized via early season soil sampling at 15-cm and 60-cm depths. Plasticity was calculated with the methods used by Dingemanse et al. (2010) previously adapted for agronomic applications (Sadras and Rebetzke, 2013). According to this method, plasticity for each variable of interest (yield, for example) was calculated by dividing the variance of each hybrid in a given site-year by the variance of all observations in the study.

2.3 Statistical analysis

2.3.1 Yield component response

All analyses were conducted using program R (R Core Team, 2022). Separate analyses were conducted for each yield component (ears per area, kernels per area, and kernel weight) considering i) main stalks only and ii) comprehensive plants. Initial treatment factor analyses were preformed first to discern if yield components responded to tiller presence. These initial analyses considered the ten site years with complete treatment structures. Ears per area, kernels per area, and kernel weight were each considered as a response to treatment factors plant density, genotype, and tiller presence for main stalks (ears and kernels harvested from main stalks only) and comprehensive plants (all ears and kernels harvested). Linear mixed effects models (Supplementary Equation 1) were fit to each yield component using the *lme4* package (Bates et al., 2015). All treatment factors and interactions were set as fixed effects. Random effects considered site-year, block, whole plot, and sub-plot. As only 10 of the 17 site years were implemented with a full split-split-plot structure and useful for initial analyses, study-wide yield environment cluster was not included in these models. The fitted models were subjected to a type III analysis of variance (ANOVA) for each treatment factor and resulting interactions with the *car* package (Fox and Weisberg, 2019).

Following analyses considered ears per area, kernels per area, and kernel weight as the response to observed plant density and observed tiller density for main stalks and comprehensive plants by yield environment, as all 17 site-years were included. Linear mixed effects models included fixed effects observed plant density, observed tiller density, yield environment cluster, and all two- and three-way interactions, in addition to random effects site-year, block, whole plot, and sub-plot (Supplementary Equation 2). The fitted models were subjected to a type III ANOVA for each factor and resulting interactions. Ears per area, kernels per area, and kernel weight predictions were generated using the significant fixed effect coefficient estimates from each of the fitted models.

Predictive limits were identified based on observed ranges (20000 to 65000 plants ha^{-1} and 0 to 80000 tillers ha^{-1}) and standardized across all environments. To maintain realistic perspective of tiller expression limits within each environment (i.e., not all environments produced similar tiller density trends), a third order polynomial regression was conducted with the 95th percentile of tiller densities for each target plant density in each yield environment. This provided a plausible maximum observed tiller density for prediction interpretation purposes. Error was quantified with the root mean squared error (RMSE).

2.3.2 Trait-yield plasticity relationships

To test correlation of yield plasticity with trait/yield component plasticity, simple linear models ($y = mx + b$) were fit using the *lm* function of the base *stats* package. Tiller number, ear number, and kernel number traits were evaluated by yield environment, as informed by prior analyses. Only plots without tiller disturbance were considered for this portion of the analyses. Appropriate models were selected separately for each yield environment with a slope parameter threshold of $p \leq 0.05$.

2.3.3 Yield response to ear type

To evaluate the relative importance of ear type (as a subset of yield component ear number) to maximizing yields, a linear mixed effects model was fit with grain yield (Mg ha^{-1}) as the response variable. Fixed effects included observed main stalk primary ears ha^{-1}, observed main stalk secondary ears ha^{-1}, observed tiller axillary ears ha^{-1}, and observed tiller apical ears ("tassel ears") ha^{-1} by yield environment. Random effects considered site-year, block, whole plot, and sub-plot. The fitted model was subjected to a type II ANOVA for each ear type × environment combination. Error was quantified via the RMSE. Resulting yield predictions were generated using the significant fixed effect coefficient estimates. Predictive limits were identified based on observed ranges of ear types for each yield environment (primary, 16000 to 65000 ears ha^{-1}; secondary, 0 to 43000 ears ha^{-1}; tiller axillary, 0 to 43000 ears ha^{-1}; and tiller apical, 0 to 31000 ears ha^{-1}). The 95% confidence intervals were generated for each coefficient to check for similarities and overlaps.

3 Results

3.1 Yield environments

The three yield environment clusters for all evaluated site-years were as follows: a) Lowest-yielding environments (LYEs) – Manhattan 2019, Colby B 2020, Colby A 2021 (mean 5.6 Mg ha^{-1}); b) Moderate-yielding environments (MYEs) – Garden City 2019 and 2021, Buhler 2020 and 2021, Colby A 2020, Greensburg 2021 (mean 9.2 Mg ha^{-1}); and c) Highest-yielding environments (HYEs) – Goodland 2019 through 2021, Garden City 2020, Greensburg 2020, Keats 2020 and 2021, Selkirk 2021 (mean 11.4 Mg ha^{-1}). Grain yields across environments by treatment factors, with relative tiller contributions, are shown in Figure 2A. Tillers averaged 25% of total yield at 25000 plants ha^{-1}.

3.2 Ears per area

The ANOVA results for models considering ears per area (ears ha^{-1}) as a response are shown in Figure 2B and Supplementary Table 2. Both ears ha^{-1} responses (main stalks and comprehensive plants) were influenced by treatment factors plant density, tiller presence, and their interaction (all significant at $p \leq 0.001$). Ears ha^{-1} ranged from 50703 to 59255 across target plant densities (25000 and 60000 plants ha^{-1}, respectively), and increased 8% overall when tillers were present. The greatest ears ha^{-1} were observed in the 60000 plants ha^{-1} density with tillers removed (59348 ears ha^{-1}), although this was not statistically different from the observed ears ha^{-1} in the 60000 or the 25000 plants ha^{-1} densities with tillers intact (59161 and 57114 ears ha^{-1}, respectively). Tiller ears averaged 40% of total ears produced at 25000 plants ha^{-1} (Figure 2B).

Additionally, both ears ha^{-1} responses were impacted by quantitative factors observed plant density and yield environment ($p \leq 0.001$), observed tiller density ($p \leq 0.001$, main; $p \leq 0.01$, comprehensive), and the interaction between yield environment and observed plant density ($p \leq 0.01$). Observation-based predictions for ears ha^{-1} are shown in Figure 3. Increased tiller densities reduced main stalk ears ha^{-1} in all yield environments, although less sharply at higher plant densities (Figure 3A). Plant density accounted for 50% of the predicted range in main stalk ears ha^{-1}. Comprehensive ears ha^{-1} were more stable than main ears ha-1 regardless of tiller or plant densities (Figure 3B). Higher tiller densities reduced the plant density-based deficit in comprehensive ears ha^{-1}. Greatest comprehensive ears ha^{-1} was predicted at both i) high observed plant densities with low observed tiller densities (all environments) and ii) low observed plant densities with high observed tiller densities (MYEs and HYEs).

3.3 Kernels per area

The ANOVA results for models considering kernels per area (kernels m^{-2}) as a response are shown in Figure 2C and Supplementary Table 3. Main stalk kernels m^{-2} were influenced by treatment factors plant density and tiller presence ($p \leq 0.001$), and their interaction ($p \leq 0.05$). Comprehensive kernels m^{-2} were only impacted by plant density ($p \leq 0.001$). Kernels m^{-2} ranged from 1950 (25000 plants ha^{-1}) to 2599 (60000 plants ha^{-1}). Tiller kernels

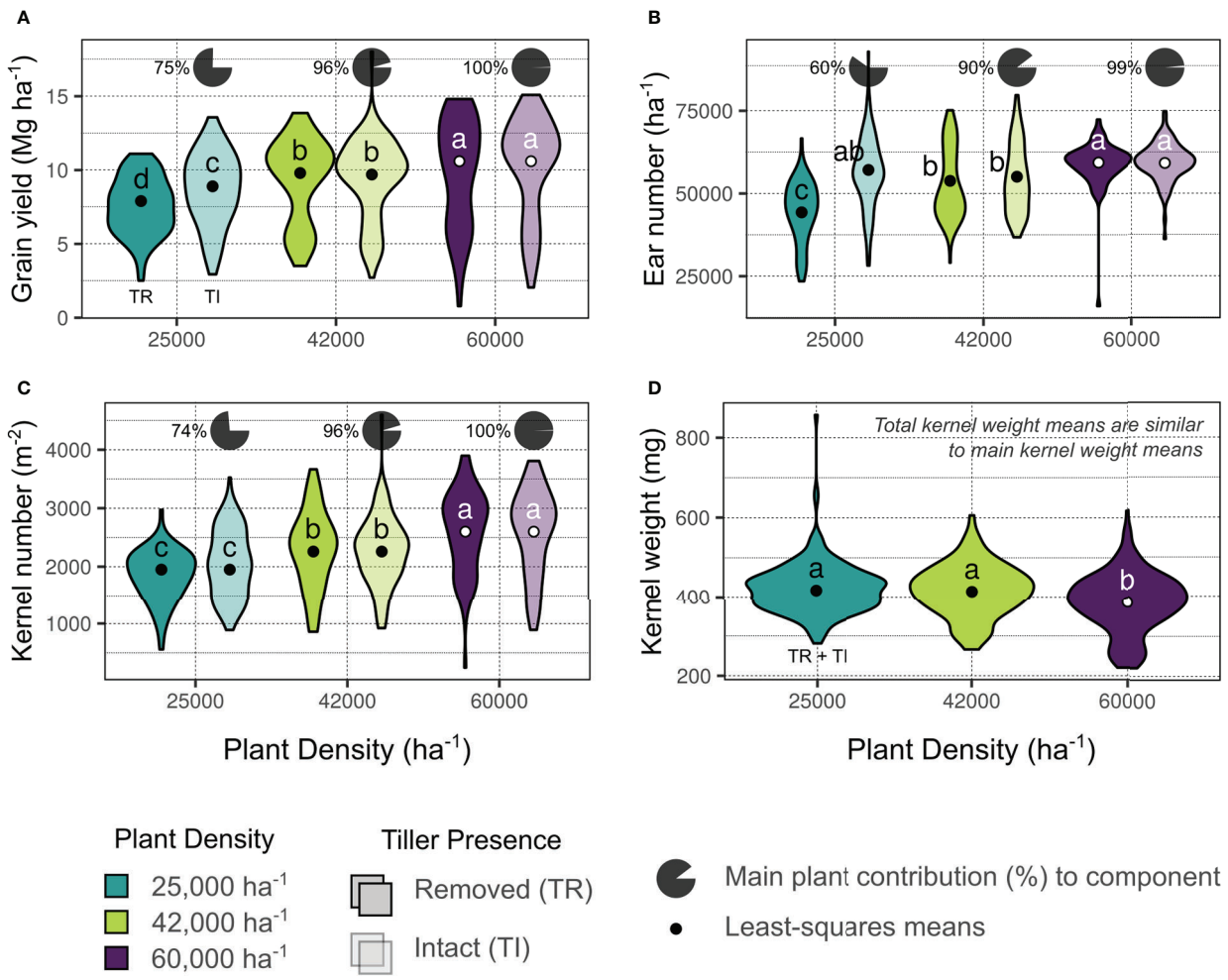

FIGURE 2
Summary of comprehensive yield **(A)**, and yield components (**(B)**, ear number; **(C)**, kernel number; **(D)**, kernel weight) based on treatment factors deemed significant by analysis of variance (Supplementary Tables 2-4). Colors indicate plant density (blue – 25000 plants ha^{-1}, green – 42000 plants ha^{-1}, purple – 60000 plants ha^{-1}) and transparency indicates tiller presence (removed, TR – opaque; intact, TI – transparent). Data distribution is shown as a a violin plot and least-squares means from fitted models are indicated with points. Different letters indicate mean differences within each panel at the 0.05 probability level. Pie charts above TI plots indicate the percent contribution of main shoots to the comprehensive components (e.g., 75% of yield was produced by main shoots in TI plants at the 25000 plants ha^{-1} density, panel A).

averaged 25% of total kernels produced at 25000 plants ha^{-1} (Figure 2C).

Main stalk kernels m^{-2} were influenced by quantitative variables tiller density, yield environment, and the interaction between yield environment and observed plant density (all significant at $p \leq 0.001$). Comprehensive kernels m^{-2} were impacted by yield environment and the interaction between yield environment and observed plant density ($p \leq 0.001$), in addition to the interaction between yield environment and observed tiller density ($p \leq 0.05$). Considering observation-based predictions, increased tiller densities consistently reduced main stalk kernels m^{-2}, regardless of plant density (Figure 4A). Plant density accounted for up to 75% of the range in predicted main stalk kernels m^{-2} when tillers were not present (Figure 4A). Comprehensive kernels m^{-2} were either not impacted by observed plant densities or tiller densities (LYEs) or independently influenced by both observed plant densities and tiller densities (MYEs and HYEs; Figure 4B). Greatest kernels per area were predicted at high observed plant densities with high observed tiller densities.

3.4 Kernel weights

The ANOVA results for models considering kernel weight (mg kernel^{-1}) as a response are shown in Figure 2D and

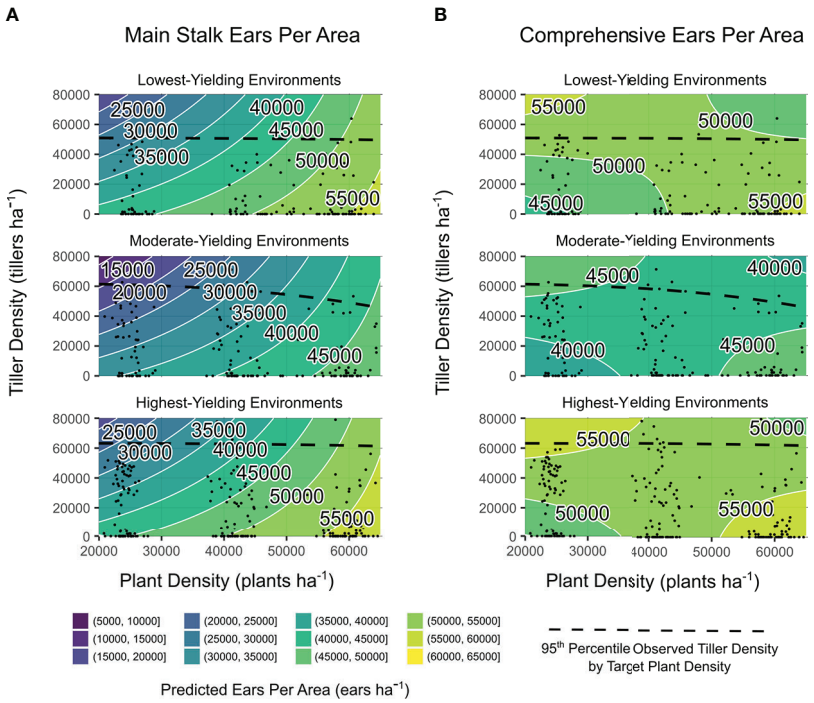

FIGURE 3
Main stalk ears per area **(A)** and comprehensive ears per area **(B)** predictions from models of observed plant density, tiller density, and yield environment as determined by analysis shown in Supplementary Table 2. Site-years are grouped by realized yield environment. Contours are shaded and labeled according to 5000 ears ha^{-1} density intervals. White lines indicate a change in ear density interval. Observed plant densities and tiller densities are indicated with black points. Black dashed lines are intended as an informal visual indicator of tiller expression potential for each yield environment. Extrapolations beyond black points and dashed black lines are shown for the purpose of comparing environments on the same density scales.

Supplementary Table 4. Main stalk kernel weight was influenced by treatment factors plant density ($p \leq 0.001$), in addition to genotype and the interaction between plant density and tiller presence ($p \leq 0.05$). Comprehensive kernel weights were impacted by treatment factors plant density ($p \leq 0.001$) and genotype ($p \leq 0.05$). Kernel weights ranged from 386 (60000 plants ha^{-1}) to 417 (25000 plants ha^{-1}) mg kernel^{-1} across plant densities. Genotypes differed in mean kernel weights by 10 mg kernel^{-1} (~2.4%; Figure 2D).

All kernel weight responses were influenced by quantitative factors observed plant density ($p \leq 0.05$) and yield environment ($p \leq 0.001$); predicted trends were similar between the two. Increased plant densities reduced both main stalk and comprehensive kernel weights in all environments, with a 25 to 50 mg kernel^{-1} discrepancy across observed plant densities. Trends were not impacted by tiller density and predictions are therefore not shown.

3.5 Trait-yield plasticity relationships

Tillered phenotype trait plasticity correlations with yield plasticity varied by yield environment (Figure 5). Tiller number plasticity (i.e., the situational nature of tiller expression in a given environment) reduced yield plasticity in LYEs and MYEs, ultimately acting to stabilize yields (Figure 5A). Greater plasticity of tiller number was associated with greater plasticity of yield in HYEs, however. Ear number plasticity reduced yield plasticity in HYEs, increased yield plasticity in MYEs, and had no impact on yield plasticity in LYEs (Figure 5B). Kernel number plasticity exhibited the strongest relationship to yield plasticity across environments, with greater plasticity of kernel number increasing yield plasticity (Figure 5C). That is, stable kernel numbers were the yield component most correlated with stable yield values in a given environment.

3.6 Ear type relationship to attainable yields

The ANOVA results for yield response to varying ear sources by yield environment are presented in Supplementary Table 5. The only ear source not significantly contributing ($p >$

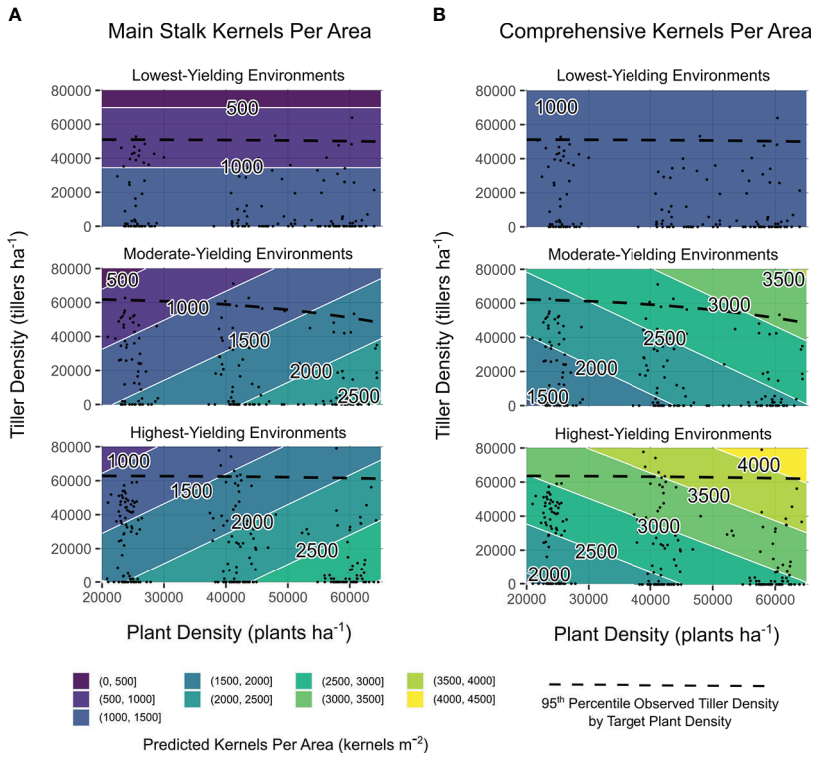

FIGURE 4
Main stalk kernels per area **(A)** and comprehensive kernels per area **(B)** predictions from models of observed plant density, tiller density, and yield environment as determined by analysis shown in Supplementary Table 3. Site-years are grouped by realized yield environment. Contours are shaded and labeled according to 500 kernels m^{-2} density intervals. White lines indicate a change in kernel density interval. Observed plant densities and tiller densities are indicated with black points. Black dashed lines are intended as an informal visual indicator of tiller expression potential for each yield environment. Extrapolations beyond black points and dashed black lines are shown for the purpose of comparing environments on the same density scales.

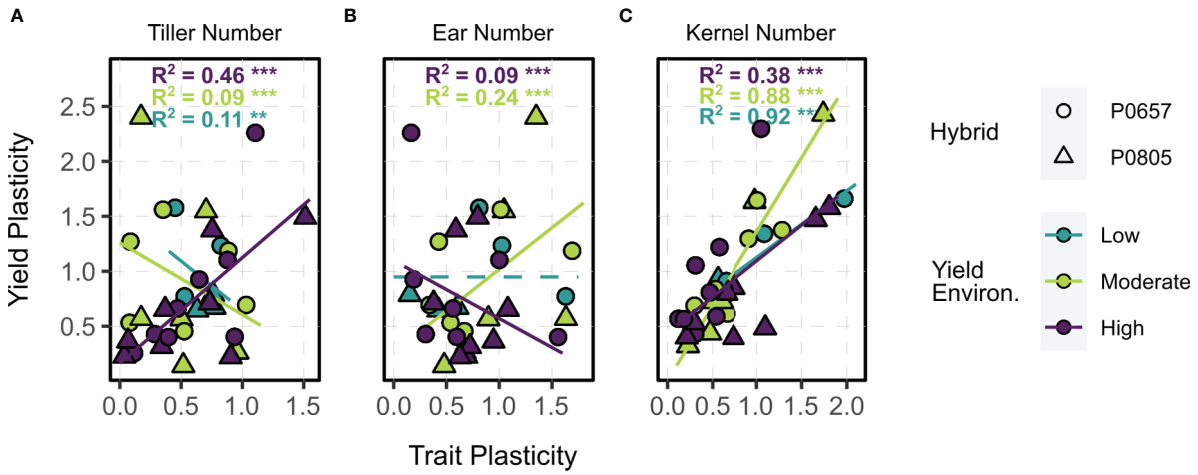

FIGURE 5
Relationships between trait plasticity (**A**, tiller number; **B**, ear number; **C**, kernel number) and yield plasticity (*y*) of tillered phenotypes. Points are colored by yield environment (blue – low, green – moderate, purple – high); and shaped by hybrid (circle – P0657AM, triangle – P0805AM). Fitted lines and model metrics, when applicable, are colored by yield environment. Dashed lines indicate intercept-only models when other candidates were not significant. Significance symbols are the following: ** $p \leq 0.01$, *** $p \leq 0.001$.

0.05) to yield determination was tiller apical ears. This coefficient estimate was therefore not included in subsequent predictions.

Yield predictions based on various combinations of ear types by yield environment are shown in Figure 4. In these ternary plots, each axis depicts the % of attainable ears ha^{-1}. The 95% confidence intervals for coefficient estimates are presented as insets. In LYEs (Figure 6A), predicted yields were greatest with 17 to 67% of attainable primary ears (11050 to 43550 ears ha^{-1}), 0 to 50% of attainable secondary ears (0 to 20500 ears ha^{-1}), and 0 to 50% of attainable tiller axillary ears (0 to 21500 ears ha^{-1}). Confidence intervals overlapped for all ear types in LYEs, indicating one ear type was not more effective in producing yields than others.

In MYEs (Figure 6B), predicted yields were greatest with 37 to 77% of attainable primary ears (24050 to 50050 ears ha^{-1}), 0 to 30% of attainable secondary ears (0 to 12300 ears ha^{-1}), and 0 to 40% of attainable tiller axillary ears (0 to 17200 ears ha^{-1}). The lowest predicted yields in MYEs were most associated with greater than 40% of attainable secondary ears. Confidence intervals indicated that primary ears exceeded other ear types in producing yield, but secondary and tiller axillary ears remained similar to each other.

In HYEs (Figure 6C), predicted yields were greatest with 37 to 77% of attainable primary ears (24050 to 50050 ears ha^{-1}), 0 to 30% of attainable secondary ears (0 to 12300 ears ha^{-1}), and 0 to 40% of attainable tiller axillary ears (0 to 17200 ears ha^{-1}). The lowest predicted yields in HYEs were most associated with > 40% of attainable secondary ears, > 50% of attainable tiller axillary ears, and > 80% of attainable primary ears ha^{-1}. Considering 95% confidence intervals, a more distinct hierarchy was evident compared to other environments (primary ears > tiller axillary ears > secondary ears) in yield formation.

4 Discussion

This study advances corn plasticity discussions by considering the unexplored extent of tiller compensatory relationships across contrasting environments and management practices (particularly plant density). Authors present data on yield component determination in tillered corn phenotypes from both main stalk and comprehensive plant perspectives in field-scale trials, thereby filling a deficit in available literature. Findings from this study apply to a considerable range of environment × management conditions, as the dataset included 17 unique site-years covering typical plant density ranges in environments similar to the semi-arid US High Plains. These 17 site-years, including the 10 site-years previously analyzed for simple yield relationships (without considering yield components) in (Veenstra et al., 2021), represent a significant, detailed corn tiller expression field study database. The tillering element of corn physiology is actively being studied at a global scale, with authors utilizing both simulation and in-field approaches to understand key mechanisms and utility (Rotili, Sadras, et al., 2021; Veenstra et al., 2021). In agreement with published literature, evaluated field trials demonstrate that tiller expression facilitates crop plasticity in response to resource availability with favorable genetics (Jenkins, 1941). Tiller appearance and development mechanisms were not explored in the current study, which limits discussion scope to reproductive outcomes (evaluated yield components). A key caveat of this study is the fact that producers will not intentionally manage corn fields to promote tillering. The results shown here consider a case in which the optimum plant density is unknown or not achieved – either due to stress, damage, or a more resourceful season than anticipated at planting (i.e., too conservative plant density selected). Tillering may have some benefits in such a scenario. This exploration of plasticity mechanisms is critical to understanding how crops (even relatively determinate ones, like corn) can cope with shifts in environment.

Flexible tiller densities were associated with more stable yield component predictions across all environments. This physiological response is of particular interest when seasonal resources are more abundant early in the growing season (Veenstra et al., 2021) to reduce dependence on plant density (Berzsenyi and Tokatlidis, 2012). Considering the density-dependent nature of yield progress in breeding and management of modern corn hybrids, this result is not surprising in tillered phenotypes (Duvick et al., 2004). An optimized plant density remained critical to maximize ear number, which supports the yield observations in previous tiller response work (Veenstra et al., 2021). However, kernel number was maximized with greater tiller development across plant densities in the present study. The modeled corn tiller expression scenarios of Rotili et al. (2021) indicated changes in kernels per area due to tillering were determined by yield environment, with marginal environments experiencing reductions in kernel number. In the present study, however, tiller density was only neutral or additive to total kernels per area. This difference is perhaps tied to the more restrictive environments evaluated by Rotili, Abeledo, et al., but it should be noted that both studies predicted/observed similar ranges of kernel set (1000 to 3000 kernels m^{-2}).

Although main stalk ears and subsequent kernels per area were reduced in lower plant densities with tiller expression, kernel weights remained relatively stable regardless of tiller expression. While these results may suggest main stalk yield reductions, work by Veenstra and Ciampitti (2021) indicated that tiller presence did not significantly reduce main stalk grain yields in the same environments considered in the present study. The lack of tiller expression impact on main stalk kernel weights also supports the hypothesis of an independent (i.e., grain-bearing tillers in lower plant densities) or nourishing (i.e., non-reproductive tillers in higher plant densities) energy and

10.3389/fpls.2022.1047268

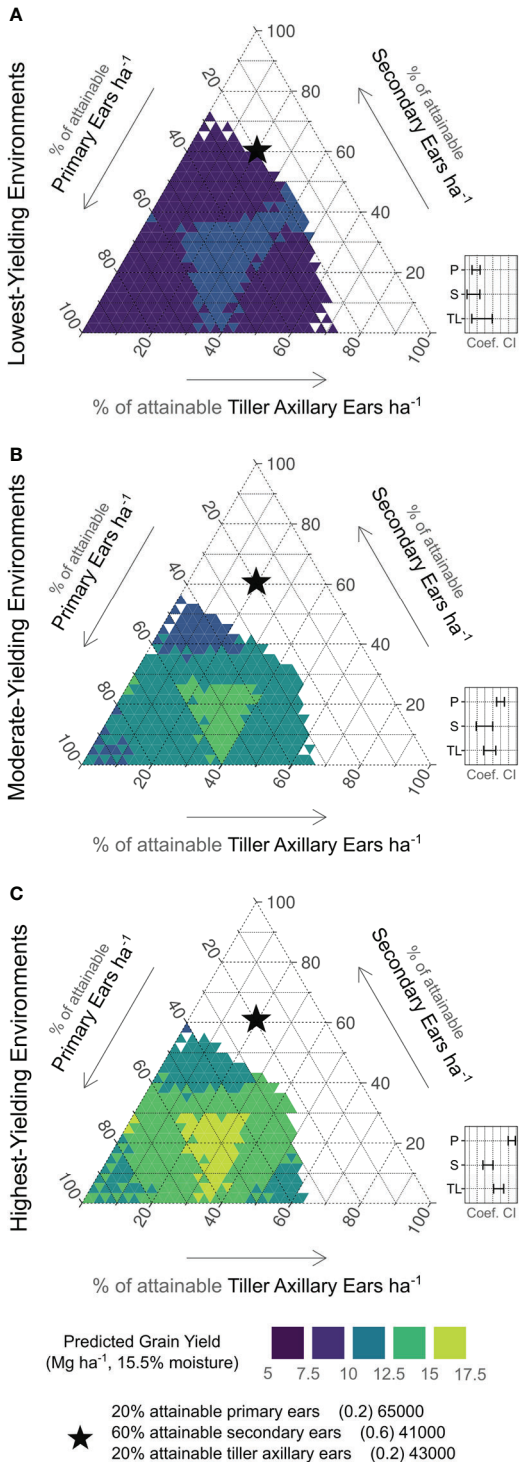

FIGURE 6
Ear type plasticity relationship to predicted yields by yield environment (**A**, low; **B**, moderate; **C**, high). Right axes indicate % of attainable primary ears observed (65000 ears ha^{-1}). Left axes indicate % of attainable secondary ears observed (41000 ear ha^{-1}). Bottom axes indicate % of attainable tiller axillary ears observed (43000 ears ha^{-1}). Contour shades indicate predicted yield level (purple < 7.5 Mg ha^{-1}; lime > 15 Mg ha^{-1}). Black star is shown for reference on each plot, indicating 20%, 60%, and 20% of attainable primary ears, secondary ears, and tiller axillary ears, respectively. Insets show relative 95% confidence intervals for each coefficient estimate (P, primary ears; S, secondary ears; TL, tiller axillary ears).

nutrient remobilization relationship for tillers and main stalk during late-season yield determination (Alofe and Schrader, 1975; Russelle et al., 1984). A key function of tillers is increasing leaf area and aboveground biomass, thus enhancing the source of energy through photosynthates and grain set potential (Lafarge and Hammer, 2002). Essentially, tillers may 1) contribute to yield directly, 2) increase the rate of light interception and growth, and/or 3) store remobilizable carbon and nitrogen. This point of source-sink relationships in tillered phenotypes requires further investigation.

Kernel number was the most significant component related to yield plasticity across all environments. This result is not surprising, as kernel number is known to be key to corn yield determination (Andrade et al., 1999). In general, situational tiller expression could be associated with non-uniform field features, which is a yield-negating factor for intensively managed corn (Hörbe et al., 2016). Tillering increased corn kernel numbers for shoots with high growth rates in field studies conducted by Rotili et al. (2022). Corn growth rates required to set kernels on primary ears appear to be lower than for tillers, and low growth rates are associated with stressed conditions (Andrade et al., 1999). In this regard, authors note that evaluated conditions in the present study may not have been harsh enough to observe such a response.

Ear number was less significantly related to yield stability than kernel number and varied by environment, which may be due to the potentially abnormal nature of tiller reproductive development (Ortez et al., 2022). A key determinant of tiller contributions to kernel number is successful reproductive development of tillers (i.e., pollination and grain fill of axillary ears). Although tiller apical ears were not found to be significant to corn yields in this study, tiller axillary ears were quite relevant, even when secondary ears were present on the main stalk. While main stalk prolificacy is commonly presented as a source of corn plasticity in environments where low plant densities are employed, secondary ears were found to be a slightly weaker source of yield than tiller axillary ears in the best-yielding environments. Similar relationships between tiller axillary and secondary ears kernel number were observed in some cases by Rotili et al. (2022). Such findings indicate value in diversifying yield determination hierarchy with tiller ears in some cases. Additionally, main stalk prolificacy has obvious limits (Tokatlidis et al., 2005; Mylonas et al., 2020), and the presented results identify tiller utility when these limits are realized. Key to note, however, are the low predicted yields when too many tiller axillary ears were present, reaffirming the importance of optimized plant densities in HYEs (Veenstra et al., 2021). Previous studies have suggested that tillering reduces yield efficiency (Kapanigowda et al., 2010; Thapa et al., 2018), but this blanket hypothesis was recently rejected (Rotili et al., 2022). Additional exploration of tiller reproductive development (i.e., vegetative, axillary ear, or apical ear) and potential impacts on efficiency metrics is needed.

While continued study is necessary, corn tillers may provide breeders and growers with plasticity trait options to achieve desirable plant density independence in certain environments (Mylonas et al., 2020). By offering additional crop reproductive plasticity when plant-available resources surpass thresholds of selected plant densities, tillers can mitigate management deficits which cannot be remediated mid-season (Rotili et al., 2021; Veenstra et al., 2021; Massigoge et al., 2022). Future work should evaluate tiller development prediction, specifically driving factors of contrasting levels of expression plasticity, in addition to parameters influencing tiller ear development and resulting reproductive efficiency.

Data availability statement

The raw data supporting the conclusions of this article will be made available by the authors, without undue reservation.

Author contributions

RV: Conceptualization, Investigation, Project Administration, Methodology, Formal Analysis, Visualization, Writing – original draft, Writing – review and editing. CM: Conceptualization, Methodology, Writing – review and editing. DB: Methodology, Writing – review and editing. LH: Resources, Investigation. PC: Conceptualization, Methodology, Writing – review and editing. TH: Writing – review and editing. PP: Writing – review and editing. IC: Conceptualization, Methodology, Supervision, Project Administration, Funding Acquisition, Writing – original draft, Writing – review and editing. All authors contributed to the article and approved the submitted version.

Acknowledgments

The authors thank Sean Wallace, Mike Legleiter, and Lisa Currie for their invaluable support in communication and care of field plots. Authors also wish to recognize all visiting scholars and interns who made field work for this study possible. Financial support provided by Corteva Agriscience, the Kansas Corn Commission, and Kansas State University to fund RV's studies and IC's research program is gratefully acknowledged. IC and his team are also members of the research network of the "Grupo de Estudio y Trabajo Red de Ultra Baja Densidad en Maíz" (Experimental Network, Study and Work Group on Ultra-Low Population Density in Maize) from Universidad de Buenos Aires. This is contribution no. 23-142-J from the Kansas Agricultural Experiment Station.

Conflict of interest

The authors declare that the research was conducted in the absence of any commercial or financial relationships that could be construed as a potential conflict of interest.

Publisher's note

All claims expressed in this article are solely those of the authors and do not necessarily represent those of their affiliated organizations, or those of the publisher, the editors and the reviewers. Any product that may be evaluated in this article, or claim that may be made by its manufacturer, is not guaranteed or endorsed by the publisher.

Supplementary material

The Supplementary Material for this article can be found online at: https://www.frontiersin.org/articles/10.3389/fpls.2022.1047268/full#supplementary-material

References

Alofe, C. O., and Schrader, L. E. (1975). Photosynthate translocation in tillered zea mays following 14 CO2 assimilation. *Can. J. Plant Sci.* 55 (2), 407–414. doi: 10.4141/cjps75-064

Andrade, F. H., Vega, C., Uhart, S., Cirilo, A., Cantarero, M., Valentinuz, O, et al. (1999). Kernel number determination in maize. *Crop Sci.* 39 (2), 453–459. doi: 10.2135/cropsci1999.0011183X0039000200026x

Assefa, Y., Carter, P., Hinds, M., Bhalla, G., Schon, R., Jeschke, M., et al. (2018). Analysis of long term study indicates both agronomic optimal plant density and increase maize yield per plant contributed to yield gain. *Sci. Rep.* 8 (1), 4937. doi: 10.1038/s41598-018-23362-x

Bates, D., Mächler, M., Bolker, B., and Walker, S. (2015). Fitting linear mixed-effects models using {lme4}. *J. Stat. Softw* 67 (1), 1–48. doi: 10.18637/jss.v067.i01

Berzsenyi, Z., and Tokatlidis, I. S. (2012). Density dependence rather than maturity determines hybrid selection in dryland maize production. *Agron. J.* 104 (2), 331–336. doi: 10.2134/agronj2011.0205

Bonnett, O. T. (1948). Ear and tassel development in maize. *Ann. Missouri Botanical Garden* 35 (4), 269–287. doi: 10.2307/2394693

Dingemanse, N. J., Kazem, A. J. N., Réale, D., and Wright, J. (2010). Behavioural reaction norms: Animal personality meets individual plasticity. *Trends Ecol. Evol.* 25 (2), 81–89. doi: 10.1016/j.tree.2009.07.013

Downey, L. A. (1972). Effect of varying plant density on a tillering variety of maize. *Exp. Agric.* 8 (1), 25–32. doi: 10.1017/S0014479700023462

Dungan, G. H., Lang, A. L., and Pendleton, J. W. (1959). Corn plant population in relation to soil productivity. *Adv. Agron.* 10, 435–473. doi: 10.1016/S0065-2113(08)60072-3

Duvick, D. N., Smith, J. S. C., and Cooper, M. (2004). "Long-term selection in a commercial hybrid maize breeding program," in *Plant breeding reviews* (Oxford, UK: John Wiley & Sons, Inc.), 109–151. doi: 10.1002/9780470650288.ch4

Fernández, J. A., Messina, C. D., Salinas, A., Prasad, P. V.V., Nippert, J. B., and Ciampitti, I. A. (2022). Kernel weight contribution to yield genetic gain of maize: A global review and US case studies. *J. Exp. Bot.* 73 (11), 3597–3609. doi: 10.1093/jxb/erac103

Fox, J., and Weisberg, S. (2019). *An {R} companion to applied regression. 3rd ed.* (Thousand Oaks {CA}: Sage). Available at: https://socialsciences.mcmaster.ca/jfox/Books/Companion/.

Frank, B. J., Schlegel, A. J., Stone, L. R., and Kirkham, M. B. (2013). Grain yield and plant characteristics of corn hybrids in the great plains. *Agron. J.* 105 (2), 383–394. doi: 10.2134/agronj2012.0330

Gardner, J. L. (1942). Studies in tillering. *Ecology* 23 (2), 162–174. doi: 10.2307/1931083

Hansey, C. N., and de Leon, N. (2011). Biomass yield and cell wall composition of corn with alternative morphologies planted at variable densities. *Crop Sci.* 51 (3), 1005–1015. doi: 10.2135/cropsci2010.08.0490

Hörbe, T. A. N., Amado, T. J. C., Reimche, G. B., Schwalbert, R. A., Santi, A. L., and Nienow, C. (2016). Optimization of within-row plant spacing increases nutritional status and corn yield: A comparative study. *Agron. J.* 108 (5), 1962–1971. doi: 10.2134/agronj2016.03.0156

Jenkins, M. T. (1941). *Influence of climate and weather on growth of corn, yearbook of agriculture* (Yearbook of Agriculture: United States Department of Agriculture).

Kapanigowda, M., Stewart, B. A., Howell, T. A., Kadasrivenkata, H., and Baumhardt, R. L. (2010). Growing maize in clumps as a strategy for marginal climatic conditions. *Field Crops Res.* 118 (2), 115–125. doi: 10.1016/j.fcr.2010.04.012

Lafarge, T. A., and Hammer, G. L. (2002). Tillering in grain sorghum over a wide range of population densities: Modelling dynamics of tiller fertility. *Ann. Bot.* 90 (1), 99–110. doi: 10.1093/aob/mcf153

Laitinen, R. A. E., and Nikoloski, Z. (2019). Genetic basis of plasticity in plants. *J. Exp. Bot.* 70 (3), 739–745. doi: 10.1093/jxb/ery404

Lark, T. J., Spawn, S. A., Bougie, M., and Gibbs, H. K. (2020). Cropland expansion in the united states produces marginal yields at high costs to wildlife. *Nat. Commun.* 11 (1), 4295. doi: 10.1038/s41467-020-18045-z

Lobell, D. B., Schlenker, W., and Costa-Roberts, J. (2011). Climate trends and global crop production since 1980. *Science* 333 (6042), 616–620. doi: 10.1126/science.1204531

Lyon, T. L. (1905). Experiments with corn. *Bull. Agric. Experiment Station Nebraska* 91 (18), 2.

Major, D. J. (1977). Seasonal dry-weight distribution of single-stalked and multi-tillered corn hybrids grown at three population densities in southern Alberta. *Can. J. Plant Sci.* 57 (4), 1041–1047. doi: 10.4141/cjps77-155

Massigoge, I., Ross, F., Fernández, J. A., Echarte, L., Ciampitti, I. A., and Cerrudo, A. (2022). Contribution of tillers to maize yield stability at low plant density. *Crop Sci* 62, 2451–2461. doi: 10.1002/csc2.20827

Moulia, B., Loup, C., Chartier, M., Allirand, J. M., and Edelin, C. (1999). Dynamics of architectural development of isolated plants of maize (*Zea mays l.*), in a non-limiting environment: The branching potential of modern maize. *Ann. Bot.* 84 (5), 645–656. doi: 10.1006/anbo.1999.0960

Mylonas, I., Sinapidou, E., Remountakis, E., Sistanis, I., Pankou, C., Ninou, E., et al. (2020). Improved plant yield efficiency alleviates the erratic optimum density in maize. *Agron. J.* 112 (3), 1690–1701. doi: 10.1002/agj2.20187

Nicotra, A. B., Atkin, O. K., Bonser, S. P., Davidson, A. M., Finnegan, E. J., Mathesius, U., et al. (2010). Plant phenotypic plasticity in a changing climate. *Trends Plant Sci.* 15 (12), 684–692. doi: 10.1016/j.tplants.2010.09.008

Ortez, O. A., McMechan, A. J., Hoegemeyer, T., Ciampitti, I. A., Nielsen, R., Thomison, P. R., et al. (2022). Abnormal ear development in corn: A review. *Agron. J.* 114 (2), 1168–1183. doi: 10.1002/agj2.20986

Prior, C. L., and Russell, W. A. (1975). Yield performance of nonprolific and prolific maize hybrids at six plant densities 1. *Crop Sci.* 15 (4), 482–486. doi: 10.2135/cropsci1975.0011183X001500040010x

R Core Team (2022). *R: a language and environment for statistical computing* (Vienna, Austria: R Foundation for Statistical Computing). Available at: https://www.r-project.org/.

Ritchie, S. W., Hanway, J. J., and Benson, G. O. (1997). How a corn plant develops', *Iowa state university coop. Ext. Serv.* (Special Report 48 Ames, IA: Iowa State University of Science and Technology Cooperate Extension Service).

Roozeboom, K., Devlin, D., Duncan, S., Janssen, K., Olson, B., and Thompson, C. (2007). "Optimum planting practices," in *Corn production handbook* (Manhattan, KS, UAS: Kansas Agricultural Experiment Station, Kansas State University), 10–14.

Rotili, D. H., Abeledo, L. G., DeVoil, P., Rodríguez, D., and Maddonni, G. Á. (2021). Exploring the effect of tillers on the water economy, plant growth and

kernel set of low-density maize crops. *Agric. Water Manage.* 243, 106424. doi: 10.1016/j.agwat.2020.106424

Rotili, D. H., Abeledo, L. G., Larrea, S. M., and Maddonni, G. Á. (2022). Grain yield and kernel setting of multiple-shoot and/or multiple-ear maize hybrids. *Field Crops Res.* 279, 108471. doi: 10.1016/j.fcr.2022.108471

Rotili, D. H., Sadras, V. O., Abeledo, L. G., Ferreyra, J. M., Micheloud, J. R., Duarte, G., et al. (2021). Impacts of vegetative and reproductive plasticity associated with tillering in maize crops in low-yielding environments: A physiological framework. *Field Crops Res*. 265, 108107. doi: 10.1016/j.fcr.2021.108107

Russell, W. A. (1991). Genetic improvement of maize yields. *Adv. Agron.* 46, 245–298. doi: 10.1016/S0065-2113(08)60582-9

Russelle, M. P., Schild, J. A., and Olson, R. A. (1984). Phosphorus translocation between small, non-reproductive tillers and the main plant of maize 1. *Agron. J.* 76 (1), 1–4. doi: 10.2134/agronj1984.00021962007600010001x

Sadras, V. O., and Rebetzke, G. J. (2013). Plasticity of wheat grain yield is associated with plasticity of ear number. *Crop Pasture Sci.* 64 (3), 234. doi: 10.1071/CP13117

Sadras, V. O., and Slafer, G. A. (2012). Environmental modulation of yield components in cereals: Heritabilities reveal a hierarchy of phenotypic plasticities. *Field Crops Res.* 127, 215–224. doi: 10.1016/j.fcr.2011.11.014

Sangoi, L., Schmitt, A., Saldanha, A., Fiorentin, C.F., Pletsch, A. J., Vieria, J., et al. (2009). Grain yield of maize hybrids at two plant densities with and without tillers removal. *Ciencia Rural* 39, 325–331. doi: 10.1590/S0103-84782008005000071

Schaffner, J. H. (1930). Sex reversal and the experimental production of neutral tassels in zea mays. *Botanical Gazette* 90 (3), 279–298. doi: 10.1086/334101

Slafer, G. A. (2003). Genetic basis of yield as viewed from a crop physiologist's perspective. *Ann. Appl. Biol.* 142 (2), 117–128. doi: 10.1111/j.1744-7348.2003.tb00237.x

Stevenson, J. C., and Goodman, M. M. (1972). Ecology of exotic races of maize. i. leaf number and tillering of 16 races under four temperatures and two photoperiods 1. *Crop Sci.* 12 (6), 864–868. doi: 10.2135/cropsci1972.0011183X001200060045x

Tetio-Kagho, F., and Gardner, F. P. (1988). Responses of maize to plant population density. i. canopy development, light relationships, and vegetative growth. *Agron. J.* 80 (6), 930–935. doi: 10.2134/agronj1988.00021962008000060018x

Thapa, S., Stewart, B. A., Xue, Q., Rhoades, M. B., Angira, B., and Reznik, J. (2018). Canopy temperature, yield, and harvest index of corn as affected by planting geometry in a semi-arid environment. *Field Crops Res.* 227, 110–118. doi: 10.1016/j.fcr.2018.08.009

Thomison, P. R., and Jordan, D. M. (1995). Plant population effects on corn hybrids differing in ear growth habit and prolificacy. *J. Production Agric.* 8 (3), 394–400. doi: 10.2134/jpa1995.0394

Tokatlidis, I., and Koutroubas, S. (2004). A review of maize hybrids' dependence on high plant populations and its implications for crop yield stability. *Field Crops Res.* 88 (2–3), 103–114. doi: 10.1016/j.fcr.2003.11.013

Tokatlidis, I., Koutsika-Sotiriou, M., and Tamoutsidis, E. (2005). Benefits from using maize density-independent hybrids. *Maydica* 50, 9–17.

Tsaftaris, A. S., Polidoros, A. N., Kapazoglou, A., Tani, E., and Kovačević, N. M. (2008). "Epigenetics and plant breeding," in *Plant breeding reviews* (Hoboken, NJ, USA: John Wiley & Sons, Inc.), 49–177. doi: 10.1002/9780470380130.ch2

Veenstra, R. L., and Ciampitti, I. A. (2021). "Corn tillers: Rethinking the "sucker" theory," in *ASA, CSSA, SSSA international annual meeting*(Salt Lake City, UT). Available at: https://scisoc.confex.com/scisoc/2021am/meetingapp.cgi/Paper/134925.

Veenstra, R. L., Messina, C. D., Berning, D., Haag, L. A., Carter, P., Hefley, T. J., et al. (2021). Effect of tillers on corn yield: Exploring trait plasticity potential in unpredictable environments. *Crop Sci.* 61 (5), 3660–3674. doi: 10.1002/csc2.20576

Yamaguchi, J. (1974). Varietal traits limiting the grain yield of tropical maize IV. plant traits and productivity of tropical varieties. *Soil Sci. Plant Nutr.* 20 (3), 287–304. doi: 10.1080/00380768.1974.10433251

frontiers | Frontiers in Plant Science

TYPE Original Research
PUBLISHED 20 January 2023
DOI 10.3389/fpls.2023.1122742

OPEN ACCESS

EDITED BY
Muhammad Ali Raza,
Islamia University of Bahawalpur, Pakistan

REVIEWED BY
Atique ur Rehman,
Bahauddin Zakariya University, Pakistan
Imran Haider,
Islamia University of Bahawalpur, Pakistan

*CORRESPONDENCE
Fulai Liu
fl@plen.ku.dk

SPECIALTY SECTION
This article was submitted to Plant Abiotic Stress, a section of the journal Frontiers in Plant Science

RECEIVED 13 December 2022
ACCEPTED 04 January 2023
PUBLISHED 20 January 2023

CITATION
Wan H, Liu X, Shi Q, Chen Y, Jiang M, Zhang J, Cui B, Hou J, Wei Z, Hossain MA and Liu F (2023) Biochar amendment alters root morphology of maize plant: Its implications in enhancing nutrient uptake and shoot growth under reduced irrigation regimes.
Front. Plant Sci. 14:1122742.
doi: 10.3389/fpls.2023.1122742

Biochar amendment alters root morphology of maize plant: Its implications in enhancing nutrient uptake and shoot growth under reduced irrigation regimes

Heng Wan[1,2], Xuezhi Liu[3], Qimiao Shi[1,2], Yiting Chen[4], Miao Jiang[1,2], Jiarui Zhang[1,2], Bingjing Cui[1,2], Jingxiang Hou[1,2,4], Zhenhua Wei[1,2], Mohammad Anwar Hossain[5] and Fulai Liu[4,6]*

[1]Key Laboratory of Agricultural Soil and Water Engineering in Arid and Semiarid Areas, Ministry of Education, Northwest A&F University, Yangling, Shaanxi, China, [2]College of Water Resources and Architectural Engineering, Northwest A&F University, Yangling, Shaanxi, China, [3]School of Civil and Hydraulic Engineering, Ningxia University, Yinchuan, China, [4]Department of Plant and Environmental Sciences, Faculty of Science, University of Copenhagen, Taastrup, Denmark, [5]Department of Genetics and Plant Breeding, Bangladesh Agricultural University, Mymensingh, Bangladesh, [6]Sino-Danish Center for Education and Research, University of Chinese Academy of Sciences, Beijing, China

Introduction: Biochar amendment provides multiple benefits in enhancing crop productivity and soil nutrient availability. However, whether biochar addition affects root morphology and alters plant nutrient uptake and shoot growth under different irrigation regimes remain largely unknown.

Methods: A split-root pot experiment with maize (*Zea mays* L.) was conducted on clay loam soil mixed with 2% (w/w) of wheat-straw (WSP) and softwood (SWP) biochar. The plants were subjected to full (FI), deficit (DI), and alternate partial root-zone drying (PRD) irrigation from the fourth leaf to the grain-filling stage.

Results and discussion: The results showed that, compared to plants grown in unamended soils, plants grown in the biochar-amended soils possessed greater total root length, area, diameter, volume, tips, forks, crossings, and root length density, which were further amplified by PRD. Despite a negative effect on soil available phosphorus (P) pool, WSP addition improved soil available nitrogen (N), potassium (K), and calcium (Ca) pool and cation exchange capacity under reduced irrigation. Even though biochar negatively affected nutrient concentrations in shoots as exemplified by lowered N, P, K (except leaf), and Ca concentration, it dramatically enhanced plant total N, P, K, Ca uptake, and biomass. Principal component analysis (PCA) revealed that the modified root morphology and increased soil available nutrient pools, and consequently, the higher plant total nutrient uptake might have facilitated the enhanced shoot growth and yield of maize plants in biochar-added soils. Biochar amendment further lowered specific

leaf area but increased leaf N concentration per area-to-root N concentration per length ratio. All these effects were evident upon WSP amendment. Moreover, PRD outperformed DI in increasing root area-to-leaf area ratio. Overall, these findings suggest that WSP combined with PRD could be a promising strategy to improve the growth and nutrient uptake of maize plants.

KEYWORDS

biochar, alternate partial root-zone drying irrigation, soil available nutrient, root morphology, biomass, nutrient uptake

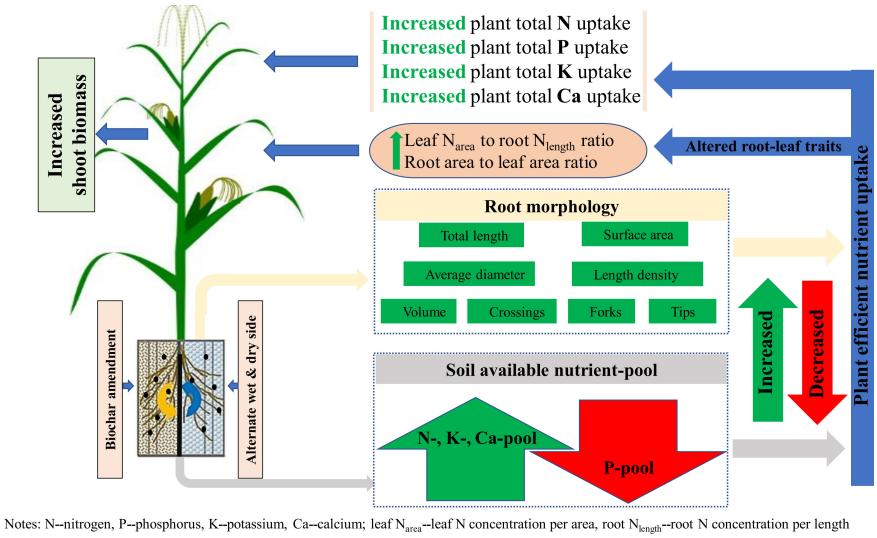

GRAPHICAL ABSTRACT

1 Introduction

Global climate change, soil degradation, and shortage of freshwater resources adversely affect agricultural productivity (Chen et al., 2013). Low soil fertility and water scarcity constrain crop yield (Reich et al., 2003). In order to improve agricultural productivity and sustainability, novel management strategies aiming at improving soil fertility and crop water-use efficiency need to be developed.

As an effective soil amendment, biochar has received widespread concerns in terms of increasing soil water holding capacity, soil carbon (C) sequestration, and nutrient bioavailability (Atkinson et al., 2010). Generally, biochar properties including pH, EC (electrical conductivity), CEC (cation exchange capacity), total ash, and nutrient content differ wildly between different feedstocks and could create multiple impacts on the rhizosphere environment (Liu et al., 2022). For instance, application of crop residue-derived biochar could increase soil total nitrogen (N) and available phosphorus (P) and potassium (K) content, contributing to nutrient uptake and growth of plants (Oladele et al., 2019). Such results concur with our previous study reporting that wheat-straw biochar yielded significant positive effects on soil nutrient availability, resulting in better K uptake and growth of tobacco (Liu et al., 2021). In contrast to these, some previous studies have noted that lignocellulose-containing wood-based biochar amendment inhibited N and ortho–P bioavailability in soil due to its anti-decomposition capacity and initial low CEC (Gul et al., 2015; Chen et al., 2021). Moreover, alteration of soil nutrient availability could be caused by adsorption/desorption processes occurring on biochar surface and precipitation/dissolution of minerals derived from biochar, thereby modulating soil nutrient pool and nutrient bioavailability (Bornø et al., 2019).

Partial root-zone drying (PRD) irrigation, an improvement on conventional deficit irrigation, employs a spatiotemporal strategy of soil wetting/drying cycles, which could positively stimulate soil microbial activity and respiration rate, thereby influencing the mineralization fixation as well as the turnover process of soil nutrients (Xiang et al., 2008; Wang et al., 2010). Furthermore, the re-wetting process in dry soil could alter soil structure properties (Rahman et al., 2018), like water absorption ability and swelling of soil aggregates, which may facilitate the decomposition of organic matter and accelerate the mineralization of mineral elements (Miller et al., 2005), hereby improving soil nutrient bioavailability (Liu et al., 2021). Such effect is known as the “Birch effect” (Birch, 1958).

Both biochar amendment and altered water dynamics under the PRD irrigation could alter the growth and physiology of plant. For instance, Liu et al. (2022) demonstrated that biochar amendment could effectively enhance root biomass density but decreased root average diameter; Xiang et al. (2017) showed that root biomass, root length, and

root tip number could be increased upon the application of biochar, strengthening the ability of plants to access resources. Similarly, PRD irrigation could increase the number of secondary root and root length (Liu et al., 2020; Qi et al., 2020). It has been demonstrated that repeated drying of the root zone could stimulate thin root growth and maximize nutrient and water availability (Comas et al., 2013). Yet, previous studies have paid less attention to the combined effects of biochar and PRD on root morphology, nutrient uptake, and their implications in altering shoot growth. Nonetheless, earlier studies have showed that biochar amendment and PRD irrigation could modulate shoot growth and leaf morphology. For instance, specific leaf area (SLA) was lowered in plants under both biochar amendment and drought conditions (Olmo et al., 2014; Liu et al., 2022). The decline in SLA was probably caused by differences in the sensitivity of photosynthesis and leaf area expansion to the change of growth environment, with leaf expansion likely to be more susceptible (Liu and Stützel, 2004; Jensen et al., 2010). It has been suggested that change of root morphology could directly influence the shoot growth as there are obvious allometric relationships between the aboveground and belowground traits that are responsive to the growth conditions of plant (Freschet et al., 2010; Silva et al., 2018). Li and Bao (2015) found that shoot height and biomass differences are closely related to the total root length. The specific root length has been described to vary considerably among soil types and negatively correlated to SLA (Liu et al., 2022). Such relationship between root morphology and leaf development may have a direct consequence on plant photosynthetic capacity, nutrient demands, and adaptability to extreme environments (Dong et al., 2020). However, to date, how PRD irrigation and biochar amendment affect root growth and its consequence on altering plant nutrient uptake and shoot development remain unclear.

The aim of the present study was to explore the combined effects of different biochar (mixed softwood and wheat-straw biochar) amendments and PRD irrigation on the root morphology, plant nutrient uptake, and shoot growth of maize plants. It was hypothesized that biochar amendment would (1) enhance soil available nutrient content, (2) alter plant morphological traits and their allometric relationships, and (3) increase plant biomass and nutrient uptake under the PRD regime.

2 Materials and methods

2.1 Soil and biochar

Two biochar materials, wheat-straw (WSP) and mixed softwood (SWP) pellet biochar, were obtained from the UK Biochar Research Centre (UKBRC), UK. Both biochars were produced *via* pyrolysis at 550°C. The pelletized biochars were crushed and passed over a 0.45-mm screen. The clay loam soil was obtained from the field in Yangling and sieved through a 5-mm sieve after air-drying. The soil water contents at full pot water-holding capacity and the permanent wilting point were 30% and 5%, respectively, and the bulk density was 1.30 g cm^{-3}. The soil and biochar properties are presented in Table 1.

TABLE 1 Soil and biochar properties.

Factor	Soil	SWP	WSP
Clay (<0.002 mm, %)	8	–	–
Silt (0.002–0.05 mm, %)	85	–	–
Sand (0.05–2 mm, %)	7	–	–
pH	7.7	7.9	9.9
EC (μS cm^{-1})	360	90	1700
CEC (cmol + kg^{-1})	2.0	3.2	6.2
Total C (%)	1.8	85.5	68.3
Total N (%)	0.1	<0.1	1.4
Total P[(c)] (%)	0.1	0.1	0.1
Total K[(c)] (%)	2.4	0.3	1.6
Total Ca[(c)] (%)	7.4	0.3	0.8
C:N	18	<855.2	49.1
$H:C_{tot}$	–	0.4	0.4
$O:C_{tot}$	–	0.1	0.1
(O + N):C		< 0.1	0.1
Surface area (m^2 g^{-1})	–	26.4	26.4
Total ash[(a)] (%)	–	1.3	21.2
C stability[(b)] (%)	–	69.6	96.5

[(a)]TGA; [(b)]Cross A, Sohi SP (2013); [(c)]Aqua Regia digestion followed by ICP.

2.2 Experimental setup

The pot experiment with maize (*Zea mays* L.) plants was carried out in a greenhouse located at the Northwest A&F University, Yangling, Shaanxi province, China (34° 15′N, 108° 04′E). The plants were grown in split-root pots (8 L) filled with 9.0 kg of clay loam soil mixed with 2% (w/w) of either WSP or SWP biochar, and pots with soil without biochar addition were set as controls. To ensure the nutrient requirement for plant growth during the experiment, 2 g N, 2 g P, and 0.22 g K were applied into all pots. The maize seeds were sown in peat on 4 March 2021 with the seedlings being transplanted into the pots at the four-leaf stage. After transplanting, the pots were daily irrigated to 90% of water-holding capacity for 30 days; thereafter, three irrigation regimes were implemented: FI (full irrigation), the whole pots were daily irrigated to 90% of water-holding capacity; DI (deficit irrigation), the whole pots were daily irrigated with 70% volume of water used in FI; and PRD (partial root-zone drying irrigation), the amount of irrigation on one compartment is the same as the DI, and the irrigation was switched while the soil water content of the other compartment decreased to 10%–12%.

The soil water content was measured by a time domain reflectometer (TDR, TRASE, Soil Moisture Equipment Crop., Goleta, CA, USA) at 4:00 p.m. each day to supplement the water consumption of the previous day. At the onset of the irrigation treatments, a 2-cm layer of perlite was placed on the soil surface to minimize soil evaporation. The experiment lasted for 9 weeks, during which each soil compartment of the PRD-treated pots was subjected to three drying/wetting cycles. Maize plants were harvested twice: one harvest before starting the irrigation treatments and the final harvest at the end of the irrigation treatment on day 63.

2.3 Leaf area, dry biomass, and nutrient accumulation in plant organs

At both harvests, leaf area (LA) was measured with a LI-3100 portable leaf area meter (LI-Cor, Inc. Lincoln, NE, USA). Specific leaf area (SLA, $cm^2\ g^{-1}$) was calculated using LA divided by leaf dry matter (LDM). The leaves, stems, fruits, and roots were harvested separately. The plant samples were dried in an oven at 105°C for 30 min, then at 75°C 48 h to constant weight, and recorded as LDM, stem dry matter ($S_{tem}DM$), fruit dry matter (FDM), shoot dry matter ($S_{hoot}DM$), and root dry matter (RDM). The root-to-shoot dry biomass ratio was also calculated. Dry plant samples were ground into fine powder and used to analyze nutrient concentration. Nitrogen concentration ([N]) in leaves, stems, and roots was determined using an Elemental Analyzer (Vario Isotope Cube, Hanau Elementar, Germany). Leaf N_{area} ([N] per leaf area)-to-root N_{length} ([N] per root length) ratio was calculated according to the method described by Liu et al. (2010). The concentrations of phosphorus ([P]), potassium ([K]), and calcium ([Ca]) in leaves, stems, and roots were determined by inductively coupled plasma mass spectrometry (ICP-MS, Agilent 7700×, Agilent Technologies, USA). Plant total nutrient accumulation, i.e., [PTN], [PTP], [PTK], and [PTCa], was calculated as:

$$PTN = [N]_{leaf} \times leaf\ dry\ matter + [N]_{stem} \times stem\ dry\ matter + [N]_{root} \times root\ \ dry\ \ matter$$

$$PTP = [P]_{leaf} \times leaf\ dry\ matter + [P]_{stem} \times stem\ dry\ matter + [P]_{root} \times root\ \ dry\ \ matter$$

$$PTK = [K]_{leaf} \times leaf\ dry\ matter + [K]_{stem} \times stem\ dry\ matter + [K]_{root} \times root\ \ dry\ \ matter$$

$$PTCa = [Ca]_{leaf} \times leaf\ dry\ matter + [Ca]_{stem} \times stem\ dry\ matter + [Ca]_{root} \times root\ \ dry\ \ matter$$

2.4 Root morphological traits

Root traits were analyzed and calculated with reference to Liu et al. (2022) and Li et al. (2009). Briefly, the cleaned root samples were placed on 20 × 25 cm transparent trays with a bottom layer covered with deionized water to avoid stacking the roots together. Subsequently, root samples were scanned at 400 dots per inch by a photo flatbed scanner (EPSON Perfection V700, Epson America, Inc.). The resulting images were analyzed by WinRHIZO Pro root analysis software (Version 2012b; Regent Instruments Inc., Québec City, QC, Canada) for root morphological traits, including total root length (RL), root surface area (RA), root average diameter (RD), root volume (RV), root tips (RT), root forks (RF), and root crossings (RC). Specific root length (SRL), specific root area (SRA), and specific root volume (SRV) were calculated by dividing RL by RDM, RA by RDM, and RV by RDM, respectively. Root length density (RLD; RL per unit soil volume), root tissue density (RTD; RL per unit RV), and RA-to-LA ratio (RLR) were also calculated.

2.5 Determination of soil nutrient contents

Soil samples collected from the rhizosphere of maize plants were air-dried, sieved through a 1-mm screen. To determine soil available nitrogen (SAN) content, 2 g of soil sample was extracted in 10.0 ml of 1.8 M NaOH solution, and the SAN was determined by the digital burette method (Brand titrette, Germany) where 2 ml of 2% H_3BO_3 was used as an indicator. For analyzing soil available phosphorus (SAP) content, 2.5 g of soil sample was extracted in 50.0 ml of 0.5 M $NaHCO_3$ solution (pH 8.5), and the SAP was determined by a UV-Visible spectrophotometer (UV-2450, Shimadzu, Japan) at 880 nm. To measure soil available potassium (SAK) content, 5 g of soil sample was digested with 50 ml of 1 M NH_4OAc solution (pH 7.0), and the SAK was determined by a flame photometer (PFP7; Jenway, UK). For soil exchange calcium (SECa) determination, 5 g of soil sample was extracted in 50 ml of NH_4Cl–70% C_2H_5OH solution (pH 8.5), and the SECa was determined by an atomic absorption spectrophotometer (Z-2000, Hitachi, Japan). Soil cation exchange capacity (CEC) was determined by the HCl-$Ca(OAc)_2$ extraction method at pH 8.2. The size of soil available nutrient pools was calculated as the sum of soil available or exchange nutrients and plant total nutrient accumulation.

2.6 Statistical analysis

Two-way analysis of variance (ANOVA) was carried out showing the effect of the biochar ([B]) and irrigation regime ([I]), as well as their interaction, i.e., [B] × [I]. Further one-way ANOVA and Tukey's multiple range tests with a 5% confidence level were applied when there was a significant interaction between the independent variables. ANOVA was conducted with IBM SPSS Statistics 23 (SPSS Inc., New York, USA) and the significance analysis of correlation was assessed using Pearson's product-moment correlation. Pearson correlation was used to evaluate the relationships between aboveground and belowground variables *via* the correlation heatmap of genescloud tool (https://www.genescloud.cn). Principal component analysis (PCA) was further performed on all the parameters by the ORIGIN-Pro 2021 software (OriginLab Inc., Northampton, Massachusetts, USA).

3 Results

3.1 Root morphological traits

Table 2 shows that total RL, RA, RD, RV, RT, RF, and RC of maize plants were significantly greater under biochar compared to non-biochar controls. RLD was solely affected by biochar treatment (Table 3), being greater for biochar-amended plants than for non-biochar plants. All these effects of biochar on root morphological traits were more evident with WSP. However, SRL, RTD, SRA, and SRV were not affected (Table 3). Interestingly, there was a clear tendency that reduced irrigation treatments increased RTD in relation to FI (Table 3).

3.2 Soil available nutrient pools and cation exchange capacity status

Table 4 showed the effects of biochar and irrigation treatment on soil available nutrients. SAN was not affected by either biochar addition or irrigation treatment. It was found that SAP was solely affected by biochar addition, where a significant reduction in SAP was found in the biochar treatments, particularly with the addition of WSP. However, there was an interaction between biochar addition and irrigation treatment on SAP. The trend for SAK and SECa to be affected by biochar addition was consistent, both having the highest values in the WSP. However, in the irrigation treatment, compared to FI, reduced irrigation significantly decreased SAP but increased SAK. In addition, there was a significant two-way interaction on SECa. SAN pool was significantly affected by two principal factors (Figure 1A), viz., biochar amendment, particularly WSP, increased SAN pool compared to unamended soils; regardless of biochar amendment, FI treatment had greater SAN pool than did reduced irrigation, and the SAN pool under PRD was slightly higher concerning DI (Figure 1A). However, compared to the unamended soils, biochar amendment, particularly WSP, remarkably decreased SAP pool (Figure 1B). Reduced irrigation especially PRD reduced SAP pool compared to FI (Figure 1B). SAK pool was significantly increased by WSP addition compared to the unamended soils (Figure 1C). Regardless of biochar amendment, FI led to greater SAK pool in relation to the reduced irrigation treatments (Figure 1C). Likewise, WSP significantly increased SACa pool than the unamended soils (Figure 1D). Compared to FI, reduced irrigation significantly increased SACa pool (Figure 1D). Moreover, there were interactive effects between biochar addition and irrigation treatment on SAP, SAK, and SACa pool (Figures 1B–D)

TABLE 2 The effects of treatments and output of two-way ANOVA for total root length (RL), area (RA), diameter (RD), volume (RV), tips (RT), forks (RF), and crossings (RC) of maize plants.

Biochar (B)	Irrigation (I)	RL (m)	RA (cm^2)	RD (mm)	RV (cm^3)	RT (k $plant^{-1}$)	RF (k $plant^{-1}$)	RC (k $plant^{-1}$)
Control	FI	48.53 ± 13.46	627.03 ± 197.56	2.37b ± 0.43	8.81d ± 2.30	14.29 ± 4.96	23.78 ± 10.88	3.18 ± 16.11
	PRD	66.06 ± 11.19	912.34 ± 105.35	3.22b ± 0.40	10.59cd ± 0.79	25.61 ± 5.12	35.36 ± 4.93	5.31 ± 10.59
	DI	73.81 ± 4.60	1,007.20 ± 72.38	3.36ab ± 0.49	11.43cd ± 0.88	26.72 ± 0.80	41.20 ± 2.76	6.54 ± 0.75
SWP	FI	71.66 ± 9.87	1,290.32 ± 131.13	4.50ab ± 0.45	19.43abc ± 1.60	27.28 ± 5.04	43.79 ± 7.93	5.28 ± 1.13
	PRD	90.24 ± 15.07	1,327.84 ± 150.09	4.05ab ± 0.46	17.21bcd ± 1.68	27.00 ± 4.80	52.12 ± 9.88	8.48 ± 2.25
	DI	57.53 ± 14.59	873.16 ± 181.53	2.47b ± 0.48	11.03cd ± 1.90	22.25 ± 1.43	35.23 ± 5.94	5.57 ± 1.20
WSP	FI	116.25 ± 22.15	1,989.28 ± 309.38	5.90a ± 1.04	28.79a ± 3.62	39.95 ± 5.68	67.86 ± 12.21	8.63 ± 2.12
	PRD	134.87 ± 17.64	1,939.19 ± 233.92	4.64ab ± 0.64	24.12ab ± 2.91	41.83 ± 5.02	81.79 ± 10.03	14.31 ± 0.02
	DI	99.10 ± 25.95	1,458.74 ± 260.55	3.58ab ± 0.32	18.71abcd ± 2.05	32.54 ± 8.16	60.04 ± 15.92	9.87 ± 3.37
Output of two-way ANOVA (*p*-value)								
Biochar (B)		***	***	**	***	**	***	**
Irrigation (I)		ns	ns	ns	ns	ns	ns	ns
B * I		ns	ns	*	*	ns	ns	ns

The treatments are different biochar (Control, SWP, and WSP) and irrigation (FI, DI, and PRD).
Values are the mean ± standard error (n = 4). *, **, and *** indicate significant levels at $p< 0.05$, $p< 0.01$, and $p< 0.001$, respectively. ns indicates no statistical significance. Different letters following the mean indicate significant differences between treatments at the $p< 0.05$ level by Tukey's test. k stands for 1000.

10.3389/fpls.2023.1122742

TABLE 3 The effects of treatments and output of two-way ANOVA for specific root length (SRL), root length density (RLD), root tissue density (RTD), specific root area (SRA), and specific root volume (SRV) of maize plants.

Biochar (B)	Irrigation (I)	SRL ($m\ g^{-1}$)	RLD ($m\ L^{-1}$)	RTD ($g\ cm^{-3}$)	SRA ($cm^2\ g^{-1}$)	SRV ($cm^3\ g^{-1}$)
Control	FI	17.82 ± 1.64	4.71 ± 1.73	0.32 ± 0.07	247.49 ± 48.28	3.50 ± 0.54
	PRD	19.70 ± 1.79	8.26 ± 1.40	0.33 ± 0.06	283.25 ± 38.16	3.43 ± 0.68
	DI	18.60 ± 2.96	9.23 ± 0.58	0.38 ± 0.07	254.48 ± 42.66	2.89 ± 0.49
SWP	FI	12.28 ± 0.33	8.96 ± 1.23	0.30 ± 0.03	224.80 ± 9.03	3.44 ± 0.29
	PRD	16.27 ± 2.13	11.28 ± 1.88	0.32 ± 0.03	242.23 ± 12.78	3.19 ± 0.30
	DI	15.42 ± 3.18	7.19 ± 1.82	0.36 ± 0.03	239.72 ± 46.28	3.08 ± 0.59
WSP	FI	14.31 ± 1.68	14.53 ± 2.77	0.28 ± 0.03	248.41 ± 21.46	3.65 ± 0.29
	PRD	17.90 ± 0.98	16.86 ± 2.20	0.31 ± 0.02	258.69 ± 16.39	3.22 ± 0.23
	DI	16.31 ± 2.91	12.39 ± 3.24	0.32 ± 0.03	247.76 ± 27.11	3.27 ± 0.36
Output of two-way ANOVA (*p*-value)						
Biochar (B)		ns	***	ns	ns	ns
Irrigation (I)		ns	ns	ns	ns	ns
B * I		ns	ns	ns	ns	ns

The treatments are different biochar (Control, SWP, and WSP) and irrigation (FI, DI, and PRD).
Values are the mean ± standard error (n = 4). *** indicates significant levels at $p < 0.001$. ns indicates no statistical significance.

Soil CEC varied among biochar treatments (Figure 2), being greater for biochar amendment than for unamended soils. Although irrigation treatment alone had no obvious effect on CEC, a significant interactive effect between the main factors on CEC was observed (Figure 2).

3.3 Nutrient acquisition in plant organs and whole plants

Nutrient concentrations for each organ of maize plants are shown in Table 5. Both $[N]_{leaf}$ and $[N]_{root}$ were significantly influenced by biochar addition and irrigation treatment; $[N]_{stem}$ was significantly affected only by biochar amendment. Interestingly, regardless of irrigation treatment, biochar amendment decreased N concentration in all organs relative to the unamended controls. Across the biochar treatments, reduced irrigation increased $[N]_{leaf}$ and $[N]_{root}$ than did FI, and PRD had greater value than that of DI treatment while the $[N]_{root}$ was the opposite.

$[P]_{leaf}$, $[P]_{stem}$, and $[P]_{root}$ were affected by biochar addition, where the biochar-added plants had greater [P] in each of the organs than the unamended plants except in root, and plants grown under SWP possessed higher $[P]_{leaf}$, $[P]_{stem}$, and $[P]_{root}$ than those grown under WSP. Irrigation treatment had a significant effect on $[P]_{leaf}$, where reduced irrigation decreased $[P]_{leaf}$, and the reduction was more evident under DI. In addition, there was a significant interactive effect between two main factors on $[P]_{stem}$.

Plants grown under biochar amendment possessed greater $[K]_{leaf}$ than those grown under unamended soils. Plants watered with reduced irrigation had considerably higher $[K]_{leaf}$ than those watered with FI, and had much higher $[K]_{leaf}$ in PRD than in DI. For $[K]_{stem}$, biochar-added plants had superior $[K]_{stem}$ compared to unamended plants, and SWP plants possessed higher $[K]_{stem}$ than WSP. When analyzed across the biochar addition, reduced irrigation especially DI increased $[K]_{stem}$ compared to FI. Moreover, biochar-added plants had higher $[K]_{root}$ compared to unamended plants, especially with WSP amendment.

Plants grown under biochar addition possessed lower $[Ca]_{leaf}$, $[Ca]_{stem}$, and $[Ca]_{root}$ compared to those grown under unamended soils, particularly with SWP amendment. Among the three irrigation treatments, both $[Ca]_{leaf}$ and $[Ca]_{stem}$ were the highest in plants grown under FI, followed by PRD, with DI being the lowest. Conversely, for $[Ca]_{root}$, PRD plants were the highest, followed by DI plants, with FI plants being the lowest.

As expected, PTN, PTP, PTK, and PTCa were significantly affected by biochar treatments (Figure 3), being greater on biochar-added plants than on non-biochar plants. Moreover, regardless of biochar amendment, reduced irrigation significantly decreased PTP in relation to FI, and a decreased trend was more pronounced with DI treatment.

3.4 Leaf area, plant biomass production, and distribution

Biochar addition especially WSP significantly increased the LA of maize plants than non-biochar controls (Table 6). Plants grown under PRD and DI possessed lower LA than those grown under FI, and LA was greater under PRD compared to DI. SLA was significantly affected by biochar treatment (Table 6), being lower on biochar-amended plants than on non-biochar plants. LDM was significantly affected by two main factors (Table 6). As expected, compared to non-

10.3389/fpls.2023.1122742

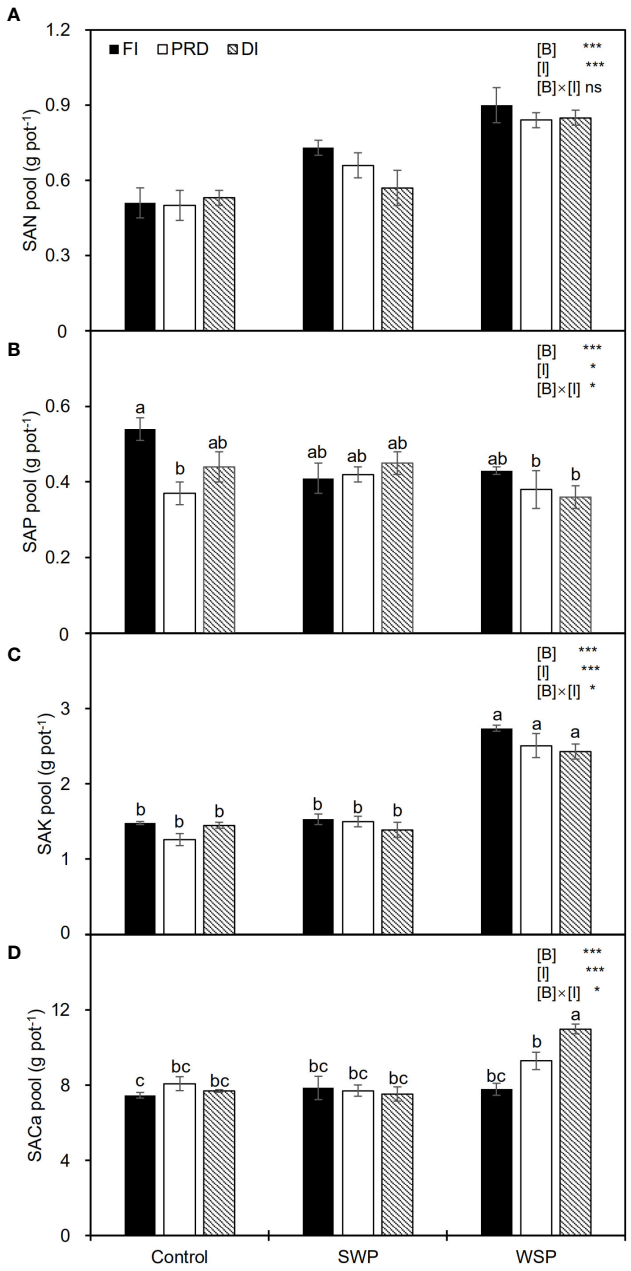

FIGURE 1
(A) Soil available N pool (SAN pool), **(B)** soil available P pool (SAP pool), **(C)** soil available K pool (SAK pool), and **(D)** soil available Ca pool (SACa pool) of maize plants exposed to different biochar (Control, SWP and WSP) and irrigation (FI, DI, and PRD) treatments. Values are the mean ± standard error (n = 4). * and *** indicate significant levels at p< 0.05 and p< 0.001, respectively. ns indicates no statistical significance. Different letters in the bars indicate significant differences between treatments at the p< 0.05 level by Tukey's test.

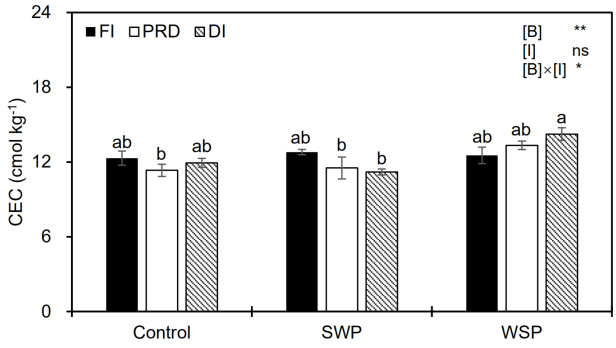

FIGURE 2
Soil cation exchange capacity (CEC) status of maize plants exposed to different biochar (Control, SWP, and WSP) and irrigation (FI, DI, and PRD) treatments. Values are the mean ± standard error (n = 4). * and ** indicate significant levels at p< 0.05 and p< 0.01, respectively. ns indicates no statistical significance. Different letters in the bars indicate significant differences between treatments at the p< 0.05 level by Tukey's test.

biochar plants, biochar-amended plants had significantly greater LDM. FI plants had higher LDM than reduced irrigation plants, which was slightly greater in PRD than in DI. S_{tem}DM, FDM, and S_{hoot}DM were affected significantly by biochar addition (Table 6), where WSP plants had the highest S_{tem}DM, FDM, and S_{hoot}DM, followed by SWP plants, with the non-biochar plants being the lowest. Also, the trend of change in RDM was the same for S_{hoot}DM (Table 6). RSR varied among biochar treatments (Table 6), being lower on biochar-amended plants than on non-biochar plants.

3.5 Relationships between different traits of soil–plant systems

The maize leaf N_{area}-to-root N_{length} ratio varied among biochar treatments (Table 7), being greater on biochar-amended plants than on non-biochar plants, especially with WSP addition. The plants grown in the reduced irrigation treatments possessed higher RLR than those grown in FI (Table 7), and RLR was greater under PRD compared to DI. RSR was significantly affected by biochar treatments (Table 7), where biochar addition particularly with WSP caused lower RSR compared to the non-biochar controls.

All data were divided into aboveground traits, belowground traits, and resource possession for analysis by correlation heatmap. The results are presented in Figure 4. RL, RA, RD, RV, RT, RF, RC, and RLD were negatively correlated to N, P, K (except leaf), and Ca concentrations in maize aboveground organs, but were positively correlated to PTN, PTP, PTK, and PTCa. Likewise, SAN pool, SAK pool, and SACa pool were positively correlated to PTN, PTP, PTK, and PTCa. SAP pool negatively affected nutrient concentrations in aboveground organs (except leaf). SRL and SRA were positively correlated to SLA but negatively correlated to leaf N_{area}. RDM and leaf N_{area}-to-root N_{length} ratio were positively correlated to LA, LDM, S_{tem}DM, and S_{hoot}DM. RSR was positively correlated to RTD and RLR but negatively correlated to LA, LDM, S_{tem}DM, and S_{hoot}DM. RLR was negatively correlated to FDM.

PCA showed that biochar treatment separated all the measured variables into distinct clusters, while irrigation treatment marginally seemed to have an impact (Figure 5). On the PCA plot, PC1 and PC2 explained 48.4% and 11.7% of the variation, respectively. PC1 isolated biochar addition on the right side of the plot; non-biochar control was isolated on the left side of the plot. Specifically, RL, RA, RD, RV, RT, RF, RC, RLD, RLR, CEC, SAN pool, SAK pool, SACa pool, PTN, PTP, PTK, PTCa, LA, leaf N_{area}, leaf N_{area}-to-root N_{length} ratio, LDM, S_{tem}DM, FDM, S_{hoot}DM, $[K]_{leaf}$, and $[K]_{root}$ contributed to biochar clustering, while the concentrations of the other nutrients in the aboveground organs, SAP pool, SLA, and RSR strongly facilitated non-biochar clustering.

TABLE 4 The effects of treatments and output of two-way ANOVA for soil available N (SAN), soil available P (SAP), soil available K (SAK), and soil exchange Ca (SECa) content.

Biochar (B)	Irrigation (I)	SAN (g pot^{-1})	SAP (g pot^{-1})	SAK (g pot^{-1})	SECa (g pot^{-1})
Control	FI	0.14 ± 0.01	0.47a ± 0.02	1.22 ± 0.04	7.34c ± 0.16
	PRD	0.13 ± 0.01	0.30b ± 0.04	0.97 ± 0.09	7.96bc ± 0.36
	DI	0.14 ± 0.01	0.37ab ± 0.04	1.13 ± 0.05	7.57bc ± 0.08
SWP	FI	0.13 ± 0.00	0.29b ± 0.03	1.06 ± 0.0 6	7.67bc ± 0.63
	PRD	0.14 ± 0.01	0.33ab ± 0.01	1.09 ± 0.06	7.56bc ± 0.30
	DI	0.13 ± 0.00	0.36ab ± 0.03	1.00 ± 0.07	7.41bc ± 0.37
WSP	FI	0.12 ± 0.01	0.28b ± 0.02	2.10 ± 0.08	7.55bc ± 0.32
	PRD	0.13 ± 0.01	0.25b ± 0.05	1.88 ± 0.14	9.10ab ± 0.47
	DI	0.14 ± 0.01	0.23b ± 0.03	1.74 ± 0.08	10.80a ± 0.26
Output of two-way ANOVA (*p*-value)					
Biochar (B)		ns	***	***	***
Irrigation (I)		ns	ns	*	**
B * I		ns	*	ns	***

The treatments are different biochar (Control, SWP, and WSP) and irrigation (FI, DI, and PRD).
Values are the mean ± standard error (n = 4). *, **, and *** indicate significant levels at p< 0.05, p< 0.01, and p< 0.001, respectively. ns indicates no statistical significance. Different letters following the mean indicate significant differences between treatments at the p< 0.05 level by Tukey's test.

4 Discussion

4.1 Biochar and reduced irrigation affected root morphology, nutrient uptake, and their implications in altering shoot growth

The roots are critical in converting and cycling nutrients in the soil–plant system. Numerous studies have demonstrated the effects of biochar on the roots firstly due to its rich microscopic pore structure and physicochemical properties. For instance, biochar addition significantly lowered the soil bulk density while increasing the total porosity, providing ample space for roots to grow and facilitating root penetration and extension (Oguntunde et al., 2008). Biochar tends to be alkaline in nature and may increase the pH of the soil, which is conducive to promoting root development, particularly in acidic soils (Yuan and Xu, 2011). In addition, the salutary effects of biochar on microbiological activities could potentially affect the rhizosphere environment and hence root growth (Warnock et al., 2007). Other researchers have found that biochar may release small molecules such as ethylene or produce hormone-like substances (Fulton et al., 2013), which might affect root secretions, thus stimulating and interfering with root physiological processes. Likewise, in this study, biochar amendment particularly WSP modified root growth with respect to root morphological traits, as indicated by the increased total RL, RA, RD, RV, RT, RF, RC, and RLD, with a consequent increase in root biomass, which was further amplified by PRD regime. As shown previously by Liu et al. (2022), PRD may stimulate root metabolic capacity and root activity by increasing the root N concentration and root C/N ratio; this response may be related to root penetration under alternating wetting/drying cycle of the soil (Chaves et al., 2003). All these effects induced by the PRD regime could contribute to root growth, especially combined with WSP amendment.

Biochar amendment has been observed to have significant effects on the rhizosphere soil nutrient availability. In our present study, compared to the unamended controls, SWP and especially WSP amendment significantly increased SAN pool and CEC. These might be correlated to biochar properties, especially in terms of N element and CEC, where WSP possessed significantly higher values than SWP. The higher CEC in soil under WSP addition could increase the inorganic N content due to the fact that biochar can adsorb more NH_4^+-N and strengthen the nitrification of NH_4^+-N into NO_3-N (Xu et al., 2016). In addition, the increased SAN pool in WSP-amended soil could potentially be interpreted as lower N leaching or higher N immobilization (Oladele et al., 2019), in which soil enzyme plays an important role (Gao and Deluca, 2018). For instance, Song et al. (2020) pointed out that wheat-straw biochar boosted the activities of β-glucosidase and leucine aminopeptidase in maize rhizosphere soil, and Gao and Deluca (2020) found that wood-based biochar improved the relative abundance of bacterial *amoA* gene in the rangeland ecosystem, which contributed to the immobilization of N. Moreover, these superior properties of biochar regarding porosity and specific surface area could enhance nutrient transport through diffusion and/or mass flow (Oladele et al., 2019).

Previous studies have found that soil P availability was connected to pH and that the high pH of biochar is generally caused by metal oxides and carbonates with high P adsorption capacity, such as oxide forms of Ca, Mg, Fe, and Al (Karunanithi et al., 2017); thus, P at neutral pH may be relatively more effective. After mixing biochar and soil, P ion precipitate with free Ca^{2+} and Mg^{2+} is released from the biochar or co-precipitate with mixed mineral complexes (Al-Si-Fe-Ca) on the biochar surface (Shepherd et al., 2017). In the present study, WSP

TABLE 5 The effects of treatments and output of two-way ANOVA for $[N]_{leaf}$, $[N]_{stem}$, $[N]_{root}$, $[P]_{leaf}$, $[P]_{stem}$, $[P]_{root}$, $[K]_{leaf}$, $[K]_{stem}$, $[K]_{root}$, $[Ca]_{leaf}$, $[Ca]_{stem}$, and $[Ca]_{root}$ of maize organs.

Biochar (B)	Irrigation (I)	$[N]_{leaf}$ (g kg^{-1})	$[N]_{stem}$ (g kg^{-1})	$[N]_{root}$ (g kg^{-1})	$[P]_{leaf}$ (g kg^{-1})	$[P]_{stem}$ (g kg^{-1})	$[P]_{root}$ (g kg^{-1})	$[K]_{leaf}$ (g kg^{-1})	$[K]_{stem}$ (g kg^{-1})	$[K]_{root}$ (g kg^{-1})	$[Ca]_{leaf}$ (g kg^{-1})	$[Ca]_{stem}$ (g kg^{-1})	$[Ca]_{root}$ (g kg^{-1})
Control	FI	25.64 ± 0.35	18.96 ± 1.43	18.88 ± 1.44	5.34 ± 0.50	4.07a ± 0.16	2.35 ± 0.17	13.50 ± 0.30	16.43 ± 0.67	10.03 ± 0.99	11.55a ± 0.60	3.38a ± 0.28	10.03b ± 0.99
	PRD	24.32 ± 0.85	16.86 ± 1.24	18.88 ± 0.40	4.32 ± 0.24	3.90a ± 0.19	2.64 ± 0.09	14.11 ± 0.70	18.44 ± 1.20	14.29 ± 0.52	9.36b ± 0.51	2.58b ± 0.21	14.29a ± 0.52
	DI	23.84 ± 0.28	17.42 ± 1.80	19.50 ± 0.92	3.35 ± 0.06	3.71ab ± 0.11	2.69 ± 0.28	14.64 ± 0.34	18.34 ± 0.54	12.69 ± 0.35	7.60bc ± 0.43	2.49b ± 0.13	12.69ab ± 0.35
SWP	FI	25.32 ± 1.34	13.48 ± 0.38	17.72 ± 0.55	4.45 ± 0.21	3.32bc ± 0.10	2.53 ± 0.06	13.59 ± 0.46	13.97 ± 0.78	11.04 ± 0.31	7.91bc ± 0.40	2.33b ± 0.09	11.04b ± 0.31
	PRD	23.45 ± 0.73	14.33 ± 0.24	20.27 ± 0.74	3.52 ± 0.21	3.21bc ± 0.05	2.81 ± 0.20	14.51 ± 0.32	15.14 ± 0.21	12.15 ± 0.20	6.90cd ± 0.43	2.06bc ± 0.05	12.15ab ± 0.20
	DI	21.41 ± 0.36	15.19 ± 0.55	20.50 ± 0.50	3.75 ± 0.40	3.67ab ± 0.07	2.60 ± 0.27	15.46 ± 0.24	16.92 ± 0.46	11.61 ± 0.67	7.82bc ± 0.46	2.48b ± 0.21	11.61ab ± 0.67
WSP	FI	23.84 ± 0.20	13.17 ± 0.31	14.13 ± 0.83	3.53 ± 0.17	3.25bc ± 0.10	2.14 ± 0.21	14.14 ± 0.65	13.38 ± 0.47	10.04 ± 0.92	6.24cd ± 0.34	1.99bc ± 0.05	10.04b ± 0.92
	PRD	21.41 ± 0.61	13.78 ± 0.25	15.35 ± 0.76	2.98 ± 0.10	2.95cd ± 0.07	2.03 ± 0.09	15.37 ± 0.67	14.84 ± 0.36	9.81 ± 0.61	6.45cd ± 0.22	1.92bc ± 0.16	9.81b ± 0.61
	DI	18.80 ± 0.73	13.22 ± 0.20	17.11 ± 0.69	2.68 ± 0.15	2.65d ± 0.08	2.38 ± 0.08	18.02 ± 0.36	13.90 ± 0.59	11.39 ± 0.99	5.16d ± 0.22	1.56c ± 0.04	11.39ab ± 0.99
Output of two-way ANOVA (*p*-value)													
Biochar (B)		***	***	***	***	***	**	***	***	**	***	***	**
Irrigation (I)		***	ns	**	***	ns	ns	***	**	ns	***	**	**
B * I		ns	ns	ns	ns	**	ns	ns	ns	ns	***	*	*

The treatments are different biochar (Control, SWP, and WSP) and irrigation (FI, DI, and PRD).
Values are the mean ± standard error (n = 4). *, **, and *** indicate significant levels at $p< 0.05$, $p< 0.01$, and $p< 0.001$, respectively. ns indicates no statistical significance. Different letters following the mean indicate significant differences between treatments at the $p< 0.05$ level by Tukey's test.

possesses greater pH and alkali metal ions, and the possible presence of carbonate and calcite might enhance P absorption capacity, hereby reducing SAP pool. Compared to WSP, SWP possessed higher C content, which may result in a potentially higher aromatic C, less crystalline mineral phases, and a more neutral pH. Our previous results reported that P sorption and release may co-occur in SWP addition (Bornø et al., 2018), consistent with the findings obtained here. Therefore, the effect of biochar on SAP depends on the feedstock of biochar.

WSP amendment caused greater SAK pool than the unamended soils, whereas there was no such effect with the addition of SWP, in good agreement with previous results reported by Liu et al. (2022). Generally, biochar possesses ash that can facilitate the electrostatic attraction of K^+ on the surface of the biochar–soil matrix, thereby reducing K^+ leaching losses (Liu et al., 2021), and most of the K incidental to biochar can usually be absorbed by plants as available K. It has been shown that biochar could enhance water-soluble and exchangeable K in the soil (Oram et al., 2014). Furthermore, biochar amendment could contribute to the dissolution of soil K-containing minerals through pH-mediated increases in soil microbial biomass and enzyme activity (Rahimzadeh et al., 2015), which consequently increased SAK content. Therefore, in the present study, the greater SAK pool generated with the added WSP than SWP was attributed to the higher ash fraction, pH, and CEC status of WSP, which would stimulate the activities of microorganisms and enzymes engaged in the mobilization and/or metabolic processes of K in soil (Gao and Deluca, 2018).

The SACa pool responded similarly to biochar application as SAK pool, in line with the result reported by Lehmann et al. (2003). The WSP-induced increase in the SACa pool could be attributed to its higher CEC. In other words, the direct cation release from biochar dominated the water-soluble Ca in the mixture, thus affecting Ca availability (Xu et al., 2013). Moreover, the large amount of Ca contained in the WSP with soluble P in the mixture may reduce the leaching and transport of available Ca, thus increasing the bioavailability of Ca in the soil (Major et al., 2009).

In addition to biochar, soil nutrient availability might also be influenced by soil water dynamics. The reduction process in soil moisture could reduce nutrient diffusion from the soil matrix to the soil solution, especially for the less mobile nutrients such as P and K (Ghosh et al., 2020). In the present study, we found that SAP appeared to be less affected by soil moisture, in agreement with the results of our previous study (Liu et al., 2022), which may be related to soil type, irrigation regimes, and drought intensity. Mayakaduwage et al. (2021) reported that this effect was modulated by the form in which P was added, and the addition of inorganic P resulted in a high

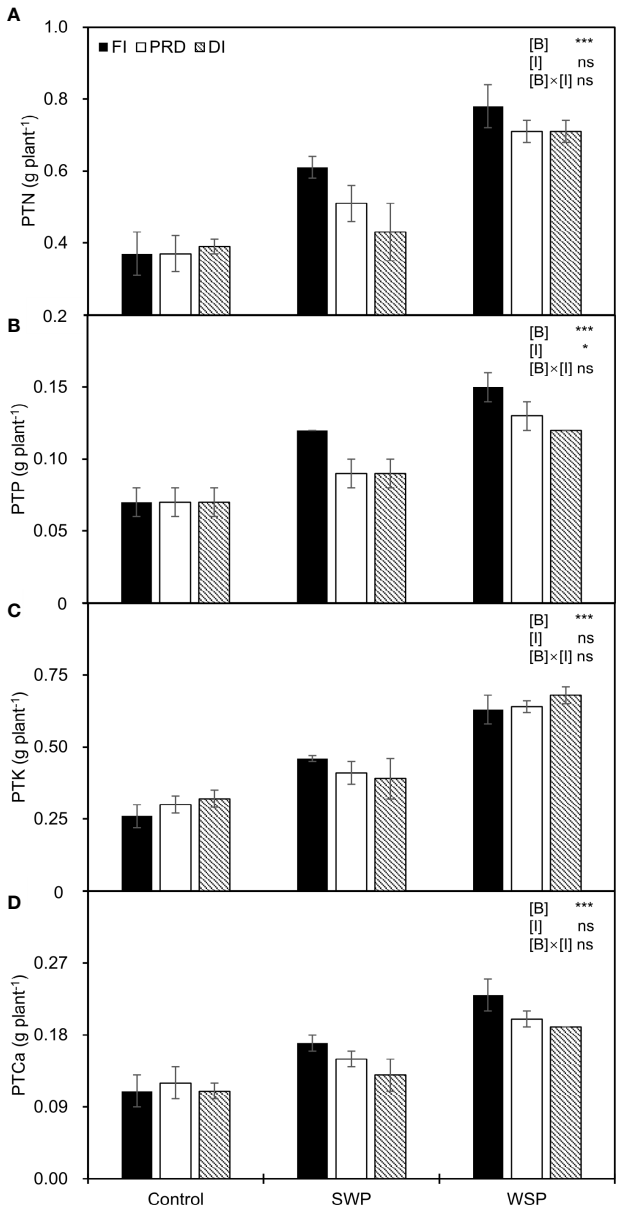

FIGURE 3
(A) Plant total N uptake (PTN), **(B)** plant total P uptake (PTP), **(C)** plant total K uptake (PTK), and **(D)** plant total Ca uptake (PTCa) of maize plants exposed to different biochar (Control, SWP, and WSP) and irrigation (FI, DI, and PRD) treatments. Values are the mean ± standard error (n = 4). * and *** indicate significant levels at p< 0.05 and p< 0.001, respectively. ns indicates no statistical significance.

concentration of labile phosphate after weeks of submergence. Therefore, our findings suggested that the soil available nutrient pools were a better representation of soil nutrient availability than single soil available nutrients, where reduced irrigation treatments significantly lowered soil available nutrient pools besides available Ca. It is known that plants grow more slowly under reduced irrigation than under well-water treatment, and this might minimize plant demand for water and nutrients, leading to a buildup of soil organic C and N with a slowdown decomposition of organic matter (Abadía et al., 2021) and, consequently, a marked decline in microbial activities. These manifestations represent a substantial suppression of soil biological activity under restricted irrigation conditions, which would negatively affect the mineralization process of soil minerals, thereby weakening soil nutrient availability (Wang et al., 2017).

Generally, improvements in soil nutrient availability especially in the case of increased root morphological parameters would facilitate plant accessibility to the available nutrients and consequently increased the accumulation of nutrients in the plant (Gahoonia and Nielsen, 2004). Echoing this, SWP and particularly WSP amendment significantly increased PTN, PTP, PTK, and PTCa uptake, which were positively correlated to root morphology (i.e., RL, RA, RD, RV, RT, RF, RC, and RLD) and soil available nutrient pools (i.e., SAN, SAK, and SACa pool), implying that the modified root morphology and increased soil nutrient availability with biochar amendment could independently and/or synergistically promote plant total nutrient uptake and that the effect of root morphology is relatively more pronounced. These changes in the roots may be a deep-seated mechanism for increased PTP despite the reduction in SAP. Interestingly, previous studies have suggested that nutrient uptake might be positively correlated to plant biomass (Chen et al., 2021). Consistent with this, here, biochar amendment especially WSP increased $S_{hoot}DM$, which was closely associated with plant total nutrient uptake. Overall, plants grown under biochar combined with PRD tended to pursue an acquisition strategy by modifying root traits. Thus, the modified root morphology and increased soil available nutrient pools, and consequently the greater plant nutrients status, might have facilitated the improved shoot growth and yield of maize in biochar-added soils compared to the unamended soils.

Furthermore, soil available nutrients appeared to have strong relationships with root morphological traits. In natural ecosystems, there was evidence confirming their connectedness, with soil nutrient availability being able to adequately nourish the dynamic performance of roots (Vogt et al., 1995). However, our experiment created relatively limited space belowground; thus, whether root traits were dominated by soil available nutrients under such conditions is unclear and needs to be further explored under field conditions.

4.2 The allometric relationships between aboveground and belowground traits under biochar and reduced irrigation regimes

Biochar amendment has been shown to modulate leaf development (Liu et al., 2022). Here, we found that the plants grown under biochar addition increased LA but depressed SLA compared to the non-biochar plants; similar findings were shown by Olmo et al. (2014). Furthermore, Niinemets (1999) reported that SLA was negatively correlated to leaf thickness, suggesting a corresponding increase in leaf thickness when SLA was reduced; this enables one to interpret that biochar addition promoted leaf thickness and facilitated plant adaptation to changing water-scarce environments (Galmes et al., 2007).

The allometric relationships of aboveground and belowground traits in response to water and fertility constraints are extremely important for deciphering the strategies of plants to cope with multiple environments (Carmona et al., 2021). For instance, here the SLA was positively correlated to SRL and SRA, which depends on plant competition for specific nutrients and/or light effectiveness (Liu et al., 2017). This may

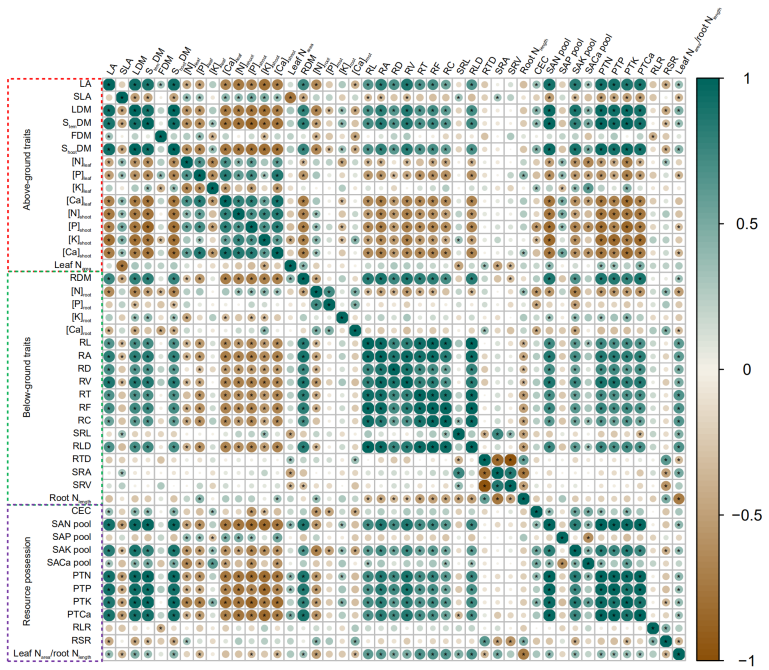

FIGURE 4
Heatmap of Pearson correlation coefficient between different traits of soil–plant systems across biochar and irrigation treatments. According to the legend, the scale of the circles and the darkness of each box color correspond to R^2 values; * indicates significant levels at $p< 0.05$. Increase and decrease in abundance are indicated in the colored bar with green and brown, respectively.

implicate that plant acquisition strategies for resources are synergistic through aboveground and belowground. Moreover, in the present study, the leaf N_{area}-to-root N_{length} ratio increased with WSP amendment, which facilitates plants to reduce fine root respiration rate under drought conditions and thereby to increase root longevity (Eissenstat et al., 2000), while maintaining strong internal CO_2 gradients to offset prolonged stomatal closure (Wright and Westoby, 2002).

The decreased RSR was observed under biochar amendment, especially under WSP. However, this result was not in accordance with our expectation, which may be due to the fact that WSP

TABLE 7 The effects of treatments and output of two-way ANOVA for $[N]_{leaf}$ per unit leaf (leaf N_{area}), $[N]_{root}$ per unit root length (root N_{length}), leaf N_{area}-to-root N_{length} ratio (leaf N_{area}/root N_{length}), root area-to-leaf area ratio (RLR), and root biomass-to-shoot biomass ratio (RSR) of maize plants.

Biochar (B)	Irrigation (I)	Leaf N_{area} (g m^{-2})	Root N_{length} (mg m^{-1})	Leaf N_{area}/Root N_{length}	RLR	RSR
Control	FI	1.03 ± 0.04	1.74 ± 0.68	0.84 ± 0.24	0.54c ± 0.04	0.14 ± 0.04
	PRD	0.91 ± 0.19	0.99 ± 0.10	0.91 ± 0.16	0.77bc ± 0.14	0.16 ± 0.02
	DI	1.03 ± 0.07	1.12 ± 0.16	0.96 ± 0.11	1.09a ± 0.14	0.20 ± 0.03
SWP	FI	1.16 ± 0.07	1.45 ± 0.08	0.81 ± 0.08	0.76bc ± 0.07	0.15 ± 0.01
	PRD	1.07 ± 0.03	1.30 ± 0.13	0.86 ± 0.11	0.82abc ± 0.05	0.17 ± 0.01
	DI	0.91 ± 0.08	1.53 ± 0.32	0.65 ± 0.08	0.65bc ± 0.10	0.14 ± 0.01
WSP	FI	1.11 ± 0.03	1.02 ± 0.10	1.12 ± 0.11	0.62bc ± 0.08	0.13 ± 0.02
	PRD	0.99 ± 0.03	1.14 ± 0.19	1.16 ± 0.09	1.11bc ± 0.23	0.13 ± 0.02
	DI	1.05 ± 0.06	0.86 ± 0.05	1.00 ± 0.18	0.61ab ± 0.09	0.10 ± 0.01
Output of two-way ANOVA (*p*-value)						
Biochar (B)		ns	ns	*	ns	*
Irrigation (I)		ns	ns	ns	*	ns
B * I		ns	ns	ns	*	ns

The treatments are different biochar (Control, SWP, and WSP) and irrigation (FI, DI, and PRD).
Values are the mean ± standard error (n = 4). * indicates significant levels at p< 0.05. ns indicates no statistical significance. Different letters following the mean indicate significant differences between treatments at the p< 0.05 level by Tukey's test.

TABLE 6 The effects of treatments and output of two-way ANOVA for leaf area (LA), specific leaf area (SLA), leaf dry matter (LDM), stem dry matter ($S_{tem}DM$), shoot dry matter ($S_{hoot}DM$), fruit dry matter (FDM), and root dry matter (RDM) of maize plants.

Biochar (B)	Irrigation (I)	LA (cm^2 $plant^{-1}$)	SLA (cm^2 g^{-1})	LDM (g $plant^{-1}$)	$S_{tem}DM$ (g $plant^{-1}$)	FDM (g $plant^{-1}$)	$S_{hoot}DM$ (g $plant^{-1}$)	RDM (g $plant^{-1}$)
Control	FI	1,124.75c ± 273.28	244.91 ± 6.41	4.59 ± 1.31	10.98 ± 1.86	4.15 ± 1.51	19.72 ± 4.65	2.60 ± 0.54
	PRD	1,294.25bc ± 222.32	170.36 ± 19.03	4.50 ± 0.90	11.43 ± 1.41	5.50 ± 1.42	21.43 ± 3.60	3.56 ± 0.85
	DI	969.50c ± 139.43	232.08 ± 4.46	4.18 ± 0.64	12.17 ± 1.00	5.55 ± 0.87	21.90 ± 2.10	0.85 ± 0.54
SWP	FI	2,032.00bc ± 93.30	219.15 ± 5.44	9.27 ± 0.56	20.15 ± 0.64	9.62 ± 1.85	39.04 ± 2.55	5.83 ± 0.78
	PRD	1,622.50bc ± 151.64	217.42 ± 12.04	7.46 ± 0.81	15.85 ± 1.32	8.70 ± 1.25	32.00 ± 3.33	5.52 ± 0.72
	DI	1,386.00bc ± 230.83	228.62 ± 20.52	6.06 ± 1.28	14.88 ± 2.50	6.72 ± 1.78	27.66 ± 5.50	3.99 ± 0.93
WSP	FI	3,148.25a ± 145.32	197.38 ± 13.42	15.95 ± 0.41	24.21 ± 2.91	23.01 ± 3.75	63.17 ± 1.06	8.07 ± 1.14
	PRD	2,476.00ab ± 109.47	207.25 ± 1.25	14.54 ± 0.97	23.58 ± 0.97	18.61 ± 2.35	56.72 ± 1.55	7.50 ± 0.80
	DI	2,377.65bc ± 136.19	179.89 ± 17.86	13.22 ± 0.63	25.46 ± 1.24	17.78 ± 1.34	56.45 ± 2.73	5.85 ± 0.66
Output of two-way ANOVA (*p*-value)								
Biochar (B)		***	***	***	***	***	***	**
Irrigation (I)		*	ns	*	ns	ns	ns	ns
B * I		*	ns	ns	ns	ns	ns	ns

The treatments are different biochar (Control, SWP, and WSP) and irrigation (FI, DI, and PRD).
Values are the mean ± standard error (n = 4). *, **, and *** indicate significant levels at $p< 0.05$, $p< 0.01$, and $p< 0.001$, respectively. ns indicates no statistical significance. Different letters following the mean indicate significant differences between treatments at the $p< 0.05$ level by Tukey's test.

increased grain yield and resulted in higher total shoot biomass and lower RSR. Therefore, RSR could not objectively represent the actual ratio of water uptake to evapotranspiration in the present study. This may also be an underlying factor in the divergent results of many studies (Turner, 1996; Liu and Stützel, 2004). Therefore, the balance between transpiration and absorption capacity can be more scientifically expressed through the ratio of root absorption area to leaf transpiration area (i.e., RLR). Here, compared to FI, RLR was significantly increased under reduced irrigation treatments, especially under PRD. The response of the RLR to drought might be triggered by the absolute growth of the root structure (Gazal and Kubiske, 2004), which provides a relationship between the surface area of water uptake and transpiration losses (Diaz-Espejo et al., 2012). This suggests a more conservative balance between aboveground and belowground in PRD plants under the same edaphic water limitation.

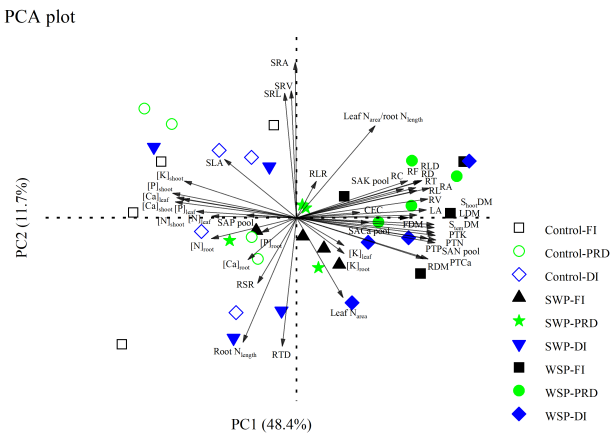

FIGURE 5
Principal component analysis (PCA) of all the measured parameters on maize plants grown under full (FI), deficit (DI), or partial root-zone drying (PRD) irrigation without (Control) and with softwood (SWP) and wheat-straw (WSP) biochar applied at 2%. The parameters are as follows: aboveground traits (LA, SLA, LDM, $S_{tem}DM$, FDM, $S_{hoot}DM$, $[N]_{leaf}$, $[N]_{stem}$, $[P]_{leaf}$, $[P]_{stem}$, $[K]_{leaf}$, $[K]_{stem}$, $[Ca]_{leaf}$, $[Ca]_{stem}$, and leaf N_{area}), belowground traits (RDM, $[N]_{root}$, $[P]_{root}$, $[K]_{root}$, $[Ca]_{root}$, RL, RA, RD, RV, RT, RF, RC, SRL, RLD, RTD, SRA, SRV, and root N_{length}), and resource possession (CEC, SAN pool, SAP pool, SAK pool, SACa pool, PTN, PTP, PTK, PTCa, RSR, RLR, and leaf N_{area}/root N_{length}). The black, blue, and green graphs represent FI, DI, and PRD, respectively. The hollow and solid graphs represent non-biochar controls and biochar additions, respectively.

5 Conclusion

Collectively, the results of this study demonstrate that biochar amendment could mitigate the partial adverse effects of reduced irrigation. Particularly, WSP amendment combined with PRD irrigation enhanced soil available N, K, and Ca pool and cation exchange capacity status, with a tendency to engage the plant in an acquisitive strategy by modifying root morphological traits, thereby promoting plant total nutrient accumulation, shoot growth, and yield. In addition, aboveground and belowground traits respond synergistically to abiotic stresses in the environment created by the co-creation of WSP and PRD, which is a considered reliable agricultural strategy from the perspective of maize productivity and soil nutrient availability in the face of both water deficit and soil degradation. However, biochar amendment was found to adversely affect soil available P pool. Accordingly, further research on P cycling in the presence of biochar is needed in the future, especially the long-term or field effects of biochar on soil available nutrients.

Data availability statement

The raw data supporting the conclusions of this article will be made available by the authors, without undue reservation.

Author contributions

HW: Experiment design and execution, conceptualization, methodology, investigation, data curation, formal analysis, and writing—original draft preparation. XL: Reviewing and editing. QS: Formal analysis. YC: Data collection. MJ: Software. JZ: Formal analysis. BC: Reviewing and editing. JH: Data analysis. ZW: Experiment execution and funding acquisition. MH: Editing. FL: Supervision, conceptualization, methodology, data curation, funding acquisition, language editing, and validation. All authors contributed to the article and approved the submitted version.

Funding

This work was funded by the Chinese Scholarship Council (No. 202206300064) and the National Natural Science Foundation of China (No. 51909220).

Acknowledgments

HW would like to thank the Chinese Scholarship Council (CSC). We would like to thank the College of Agriculture, Northwest A&F University for providing seeds in this experiment.

Conflict of interest

The authors declare that the research was conducted in the absence of any commercial or financial relationships that could be construed as a potential conflict of interest.

Publisher's note

References

Abadía, J., Bastida, F., Romero-Trigueros, C., Bayona, J., Vera, A., García, C., et al. (2021). Interactions between soil microbial communities and agronomic behavior in a mandarin crop subjected to water deficit and irrigated with reclaimed water. *Agric. Water Manage.* 247, 106749. doi: 10.1016/j.agwat.2021.106749

Atkinson, C. J., Fitzgerald, J. D., and Hipps, N. A. (2010). Potential mechanisms for achieving agricultural benefits from biochar application to temperate soils: A review. *Plant Soil* 337, 1–18. doi: 10.1007/s11104-010-0464-5

Birch, H. F. (1958). The effect of soil drying on humus decomposition and nitrogen availability. *Plant Soil* 10, 9–31. doi: 10.1007/BF01343734

Bornø, M. L., Müller-Stöver, D. S., and Liu, F. (2018). Contrasting effects of biochar on phosphorus dynamics and bioavailability in different soil types. *Sci. Total Environ.* 627, 963–974. doi: 10.1016/j.scitotenv.2018.01.283

Bornø, M. L., Müller-Stöver, D. S., and Liu, F. (2019). Biochar properties and soil type drive the uptake of macro-and micronutrients in maize (*Zea mays* l.). *J. Plant Nutr. Soil Sci.* 182, 149–158. doi: 10.1002/jpln.201800228

Carmona, C. P., Tamme, R., Partel, M., De Bello, F., Brosse, S., Capdevila, P., et al. (2021). Erosion of global functional diversity across the tree of life. *Sci. Adv.* 7, eabf2675. doi: 10.1126/sciadv.abf2675

Chaves, M. M., Maroco, J. P., and Pereira, J. S. (2003). Understanding plant responses to drought–from genes to the whole plant. *Funct. Plant Biol.* 30, 239–264. doi: 10.1071/FP02076

Chen, D., Lan, Z., Bai, X., Grace, J. B., and Bai, Y. (2013). Evidence that acidification-induced declines in plant diversity and productivity are mediated by changes in below-ground communities and soil properties in a semi-arid steppe. *J. Ecol.* 101, 1322–1334. doi: 10.1111/1365-2745.12119

Chen, X., Yang, S.-H., Jiang, Z.-W., Ding, J., and Sun, X. (2021). Biochar as a tool to reduce environmental impacts of nitrogen loss in water-saving irrigation paddy field. *J. Cleaner Product.* 290, 125811. doi: 10.1016/j.jclepro.2021.125811

Comas, L. H., Becker, S. R., Cruz, V. M. V., Byrne, P. F., and Dierig, D. A. (2013). Root traits contributing to plant productivity under drought. *Front. Plant Sci.* 4. doi: 10.3389/fpls.2013.00442

Diaz-Espejo, A., Buckley, T. N., Sperry, J. S., Cuevas, M. V., De Cires, A., Elsayed-Farag, S., et al. (2012). Steps toward an improvement in process-based models of water use by fruit trees: A case study in olive. *Agric. Water Manage.* 114, 37–49. doi: 10.1016/j.agwat.2012.06.027

Dong, N., Prentice, I. C., Wright, I. J., Evans, B. J., Togashi, H. F., Caddy-Retalic, S., et al. (2020). Components of leaf-trait variation along environmental gradients. *New Phytol.* 228, 82–94. doi: 10.1111/nph.16558

Eissenstat, D. M., Wells, C. E., Yanai, R. D., and Whitbeck, J. L. (2000). Building roots in a changing environment: Implications for root longevity. *New Phytol.* 147, 33–42. doi: 10.1046/j.1469-8137.2000.00686.x

Freschet, G. T., Cornelissen, J. H. C., Van Logtestijn, R. S. P., and Aerts, R. (2010). Evidence of the 'plant economics spectrum' in a subarctic flora. *J. Ecol.* 98, 362–373. doi: 10.1111/j.1365-2745.2009.01615.x

Fulton, W., Gray, M., Prahl, F., and Kleber, M. (2013). A simple technique to eliminate ethylene emissions from biochar amendment in agriculture. *Agron. Sustain. Dev.* 33, 469–474. doi: 10.1007/s13593-012-0118-5

Gahoonia, T. S., and Nielsen, N. E. (2004). Root traits as tools for creating phosphorus efficient crop varieties. *Plant Soil* 260, 47–57. doi: 10.1023/B:PLSO.0000030168.53340.bc

Galmes, J., Abadia, A., Cifre, J., Medrano, H., and Flexas, J. (2007). Photoprotection processes under water stress and recovery in Mediterranean plants with different growth forms and leaf habits. *Physiol. Plant.* 130, 495–510. doi: 10.1111/j.1399-3054.2007.00919.x

Gao, S., and Deluca, T. H. (2018). Wood biochar impacts soil phosphorus dynamics and microbial communities in organically-managed croplands. *Soil Biol. Biochem.* 126, 144–150. doi: 10.1016/j.soilbio.2018.09.002

Gao, S., and Deluca, T. H. (2020). Biochar alters nitrogen and phosphorus dynamics in a western rangeland ecosystem. *Soil Biol. Biochem.* 148, 107868. doi: 10.1016/j.soilbio.2020.107868

Gazal, R. M., and Kubiske, M. E. (2004). Influence of initial root length on physiological responses of cherrybark oak and shumard oak seedlings to field drought conditions. *For. Ecol. Manage.* 189, 295–305. doi: 10.1016/j.foreco.2003.08.017

Ghosh, A., Agrawal, M., and Agrawal, S. B. (2020). Effect of water deficit stress on an Indian wheat cultivar (Triticum aestivum l. HD 2967) under ambient and elevated level of ozone. *Sci. Total Environ.* 714, 136837. doi: 10.1016/j.scitotenv.2020.136837

Gul, S., Whalen, J. K., Thomas, B. W., Sachdeva, V., and Deng, H. (2015). Physico-chemical properties and microbial responses in biochar-amended soils: Mechanisms and future directions. *Agric. Ecosyst. Environ.* 206, 46–59. doi: 10.1016/j.agee.2015.03.015

Jensen, C. R., Battilani, A., Plauborg, F., Psarras, G., Chartzoulakis, K., Janowiak, F., et al. (2010). Deficit irrigation based on drought tolerance and root signalling in potatoes and tomatoes. *Agric. Water Manage.* 98, 403–413. doi: 10.1016/j.agwat.2010.10.018

Karunanithi, R., Ok, Y. S., Dharmarajan, R., Ahmad, M., Seshadri, B., Bolan, N., et al. (2017). Sorption, kinetics and thermodynamics of phosphate sorption onto soybean stover derived biochar. *Environ. Technol. Innovation* 8, 113–125. doi: 10.1016/j.eti.2017.06.002

Lehmann, J., Da Silva, J. P., Steiner, C., Nehls, T., Zech, W., and Glaser, B. (2003). Nutrient availability and leaching in an archaeological anthrosol and a ferralsol of the central Amazon basin: Fertilizer, manure and charcoal amendments. *Plant Soil* 249, 343–357. doi: 10.1023/A:1022833116184

Li, F. L., and Bao, W. K. (2015). New insights into leaf and fine-root trait relationships: Implications of resource acquisition among 23 xerophytic woody species. *Ecol. Evol.* 5, 5344–5351. doi: 10.1002/ece3.1794

Liu, G., Freschet, G. T., Pan, X., Cornelissen, J. H. C., Li, Y., and Dong, M. (2010). Coordinated variation in leaf and root traits across multiple spatial scales in Chinese semi-arid and arid ecosystems. *New Phytol.* 188, 543–553. doi: 10.1111/j.1469-8137.2010.03388.x

Liu, H., Li, Y., Ren, F., Lin, L., Zhu, W., He, J.-S., et al. (2017). Trait-abundance relation in response to nutrient addition in a Tibetan alpine meadow: The importance of species trade-off in resource conservation and acquisition. *Ecol. Evol.* 7, 10575–10581. doi: 10.1002/ece3.3439

Liu, X., Ma, Y., Manevski, K., Andersen, M. N., Li, Y., Wei, Z., et al. (2022). Biochar and alternate wetting-drying cycles improving rhizosphere soil nutrients availability and tobacco growth by altering root growth strategy in ferralsol and anthrosol. *Sci. Total Environ.* 806, 150513. doi: /10.1016/j.scitotenv.2021.150513

Liu, F., and Stützel, H. (2004). Biomass partitioning, specific leaf area, and water use efficiency of vegetable amaranth (Amaranthus spp.) in response to drought stress. *Sci. Hortic.* 102, 15–27. doi: 10.1016/j.scienta.2003.11.014

Liu, X., Wei, Z., Ma, Y., Liu, J., and Liu, F. (2021). Effects of biochar amendment and reduced irrigation on growth, physiology, water-use efficiency and nutrients uptake of tobacco (Nicotiana tabacum l.) on two different soil types. *Sci. Total Environ.* 770, 144769. doi: 10.1016/j.scitotenv.2020.144769

Liu, R., Yang, Y., Wang, Y.-S., Wang, X.-C., Rengel, Z., Zhang, W.-J., et al. (2020). Alternate partial root-zone drip irrigation with nitrogen fertigation promoted tomato growth, water and fertilizer-nitrogen use efficiency. *Agric. Water Manage.* 233, 106049. doi: 10.1016/j.agwat.2020.106049

Li, T., Yang, X., Lu, L., Islam, E., and He, Z. (2009). Effects of zinc and cadmium interactions on root morphology and metal translocation in a hyperaccumulating species under hydroponic conditions. *J. Hazard. Mater.* 169, 734–741. doi: 10.1016/j.jhazmat.2009.04.004

Major, J., Steiner, C., and Downie, A. (2009). "Biochar effects on nutrient leaching," in *Biochar for environmental management*. Eds. J. Lehmann and S. Joseph (London: Earthscan Publications Ltd), 271–287.

Mayakaduwage, S., Mosley, L. M., and Marschner, P. (2021). Phosphorus pools in acid sulfate soil are influenced by soil water content and form in which p is added. *Geoderma* 381, 114692. doi: 10.1016/j.geoderma.2020.114692

Miller, A. E., Schimel, J. P., Meixner, T., Sickman, J. O., and Melack, J. M. (2005). Episodic rewetting enhances carbon and nitrogen release from chaparral soils. *Soil Biol. Biochem.* 37, 2195–2204. doi: 10.1016/j.soilbio.2005.03.021

Niinemets, U. (1999). Components of leaf dry mass per area–thickness and density–alter photosynthetic capacity in reverse directions in woody plants. *New Phytol.* 144, 35–47. doi: 10.1046/j.1469-8137.1999.00466.x

Oguntunde, P. G., Abiodun, B. J., Ajayi, A. E., and Van De Giesen, N. (2008). Effects of charcoal production on soil physical properties in Ghana. *J. Plant Nutr. Soil Sci.* 171, 591–596. doi: 10.1002/jpln.200625185

Oladele, S., Adeyemo, A., and Awodun, M. (2019). Influence of rice husk biochar and inorganic fertilizer on soil nutrients availability and rain-fed rice yield in two contrasting soils. *Geoderma* 336, 1–11. doi: 10.1016/j.geoderma.2018.08.025

Olmo, M., Alburquerque, J. A., Barrón, V., Del Campillo, M. C., Gallardo, A., Fuentes, M., et al. (2014). Wheat growth and yield responses to biochar addition under Mediterranean climate conditions. *Biol. Fertil. Soils* 50, 1177–1187. doi: 10.1007/s00374-014-0959-y

Oram, N. J., Van De Voorde, T. F., Ouwehand, G.-J., Bezemer, T. M., Mommer, L., Jeffery, S., et al. (2014). Soil amendment with biochar increases the competitive ability of legumes *via* increased potassium availability. *Agric. Ecosyst. Environ.* 191, 92–98. doi: 10.1016/j.agee.2014.03.031

Qi, D., Hu, T., and Song, X. (2020). Effects of nitrogen supply methods on fate of nitrogen in maize under alternate partial root-zone irrigation. *Int. J. Agric. Biol. Eng.* 13, 129–135. doi: 10.25165/j.ijabe.20201303.5287

Rahimzadeh, N., Khormali, F., Olamaee, M., Amini, A., and Dordipour, E. (2015). Effect of canola rhizosphere and silicate dissolving bacteria on the weathering and K release from indigenous glauconite shale. *Biol. fertil. soils* 51, 973–981. doi: 10.1007/s00374-015-1043-y

Rahman, M., Guo, Z., Zhang, Z., Zhou, H., and Peng, X. (2018). Wetting and drying cycles improving aggregation and associated c stabilization differently after straw or biochar incorporated into a vertisol. *Soil Tillage Res.* 175, 28–36. doi: 10.1016/j.still.2017.08.007

Reich, P. B., Buschena, C., Tjoelker, M. G., Wrage, K., Knops, J., Tilman, D., et al. (2003). Variation in growth rate and ecophysiology among 34 grassland and savanna species under contrasting n supply: a test of functional group differences. *New Phytol.* 157, 617–631. doi: 10.1046/j.1469-8137.2003.00703.x

Shepherd, J. G., Joseph, S., Sohi, S. P., and Heal, K. V. (2017). Biochar and enhanced phosphate capture: Mapping mechanisms to functional properties. *Chemosphere* 179, 57–74. doi: 10.1016/j.chemosphere.2017.02.123

Silva, J. L. A., Souza, A. F., Caliman, A., Voigt, E. L., and Lichston, J. E. (2018). Weak whole-plant trait coordination in a seasonally dry south American stressful environment. *Ecol. Evol.* 8, 4–12. doi: 10.1002/ece3.3547

Song, X., Razavi, B. S., Ludwig, B., Zamanian, K., Zang, H., Kuzyakov, Y., et al. (2020). Combined biochar and nitrogen application stimulates enzyme activity and root plasticity. *Sci. Total Environ.* 735, 139393. doi: 10.1016/j.scitotenv.2020.139393

Turner, N. C. (1996). Further progress in crop water relations. *Adv. Agron.* 58, 293–338. doi: 10.1016/S0065-2113(08)60258-8

Vogt, K. A., Vogt, D. J., Asbjornsen, H., and Dahlgren, R. A. (1995). ROOTS, NUTRIENTS AND THEIR RELATIONSHIP TO SPATIAL PATTERNS. *Plant Soil* 168, 113–123. doi: 10.1007/BF00029320

Wang, Y., Jensen, C. R., and Liu, F. (2017). Nutritional responses to soil drying and rewetting cycles under partial root-zone drying irrigation. *Agric. Water Manage.* 179, 254–259. doi: 10.1016/j.agwat.2016.04.015

Wang, Y., Liu, F., De Neergaard, A., Jensen, L. S., Luxhoi, J., and Jensen, C. R. (2010). Alternate partial root-zone irrigation induced dry/wet cycles of soils stimulate n mineralization and improve n nutrition in tomatoes. *Plant Soil* 337, 167–177. doi: 10.1007/s11104-010-0513-0

Warnock, D. D., Lehmann, J., Kuyper, T. W., and Rillig, M. C. (2007). Mycorrhizal responses to biochar in soil - concepts and mechanisms. *Plant Soil* 300, 9–20. doi: 10.1007/s11104-007-9391-5

Wright, I. J., and Westoby, M. (2002). Leaves at low versus high rainfall: Coordination of structure, lifespan and physiology. *New Phytol.* 155, 403–416. doi: 10.1046/j.1469-8137.2002.00479.x

Xiang, Y., Deng, Q., Duan, H., and Guo, Y. (2017). Effects of biochar application on root traits: A meta-analysis. *Global Change Biol. Bioenergy* 9, 1563–1572. doi: 10.1111/gcbb.12449

Xiang, S.-R., Doyle, A., Holden, P. A., and Schimel, J. P. (2008). Drying and rewetting effects on c and n mineralization and microbial activity in surface and subsurface California grassland soils. *Soil Biol. Biochem.* 40, 2281–2289. doi: 10.1016/j.soilbio.2008.05.004

Xu, N., Tan, G., Wang, H., and Gai, X. (2016). Effect of biochar additions to soil on nitrogen leaching, microbial biomass and bacterial community structure. *Eur. J. Soil Biol.* 74, 1–8. doi: 10.1016/j.ejsobi.2016.02.004

Xu, G., Wei, L., Sun, J., Shao, H., and Chang, S. (2013). What is more important for enhancing nutrient bioavailability with biochar application into a sandy soil: Direct or indirect mechanism? *Ecol. Eng.* 52, 119–124. doi: 10.1016/j.ecoleng.2012.12.091

Yuan, J. H., and Xu, R. K. (2011). The amelioration effects of low temperature biochar generated from nine crop residues on an acidic ultisol. *Soil Use Manage.* 27, 110–115. doi: 10.1111/j.1475-2743.2010.00317.x

frontiers | Frontiers in Plant Science

TYPE Original Research
PUBLISHED 23 January 2023
DOI 10.3389/fpls.2023.1088285

OPEN ACCESS

EDITED BY
Oksana Sytar,
Taras Shevchenko National University of Kyiv, Ukraine

REVIEWED BY
Erna Karalija,
University of Sarajevo, Bosnia and Herzegovina
Fernando Carlos Gómez-Merino,
Colegio de Postgraduados (COLPOS), Mexico

*CORRESPONDENCE
Bin Wang
b_wang@sgu.edu.cn
Jinming He
hjm@sgu.edu.cn
Yanhui Xiao
yhxiao@sgu.edu.cn

SPECIALTY SECTION
This article was submitted to Plant Abiotic Stress, a section of the journal Frontiers in Plant Science

RECEIVED 03 November 2022
ACCEPTED 05 January 2023
PUBLISHED 23 January 2023

CITATION
Wang B, Lin l, Yuan X, Zhu Y, Wang Y, Li D, He J and Xiao Y (2023) Low-level cadmium exposure induced hormesis in peppermint young plant by constantly activating antioxidant activity based on physiological and transcriptomic analyses.
Front. Plant Sci. 14:1088285.
doi: 10.3389/fpls.2023.1088285

Low-level cadmium exposure induced hormesis in peppermint young plant by constantly activating antioxidant activity based on physiological and transcriptomic analyses

Bin Wang[1,2,3]*, Ivna Lin[2,4], Xiao Yuan[2], Yunna Zhu[1,2,3], Yukun Wang[1,2,3], Donglin Li[2,3], Jinming He[1,3]* and Yanhui Xiao[1,2,3]*

[1]Guangdong Provincial Key Laboratory of Utilization and Conservation of Food and Medicinal Resources in Northern Region, Shaoguan University, Shaoguan, China, [2]Henry Fok College of Biology and Agriculture, Shaoguan University, Shaoguan, China, [3]Shaoguan Aromatic Plant Engineering Research Center, Shaoguan University, Shaoguan, China, [4]College of Horticulture, South China Agricultural University, Guangzhou, China

As one of the most toxic environmental pollutants, cadmium (Cd) has lastingly been considered to have negative influences on plant growth and productivity. Recently, increasing studies have shown that low level of Cd exposure could induce hormetic effect which benefits to plants. However, the underlying mechanisms of Cd-triggered hormesis are poorly understood. In this study, we found that Cd stress treatment showed a hormetic effect on peppermint and Cd treatment with 1.6 mg L^{-1} concertation manifested best stimulative effects. To explore the hormesis mechanisms of Cd treatment, comparative transcriptome analysis of peppermint young plants under low (1.6 mg L^{-1}) and high (6.5 mg L^{-1}) level of Cd exposure at 0 h, 24 h and 72 h were conducted. Twelve of differentially expressed genes (DEGs) were selected for qRT-PCR validation, and the expression results confirmed the credibility of transcriptome data. KEGG analysis of DEGs showed that the phenylpropanoid biosynthesis and photosynthesis were important under both low and high level of Cd treatments. Interestingly, GO and KEGG analysis of 99 DEGs specifically induced by low level of Cd treatment at 72 h indicated that these DEGs were mainly involved in the pathway of phenylpropanoid biosynthesis and their functions were associated with antioxidant activity. The expression pattern of those genes in the phenylpropanoid biosynthesis pathway and encoding antioxidant enzymes during 72 h of Cd exposure showed that low level of Cd treatment induced a continuation in the upward trend but high level of Cd treatment caused an inverted V-shape. The changes of physiological parameters during Cd exposure were highly consistent with gene expression pattern. These results strongly demonstrate that low level of Cd exposure constantly enhanced antioxidant activity of peppermint to avoid oxidative damages caused by Cd ion, while high level of Cd stress just induced a temporary increase in antioxidant activity which was insufficient to cope with lasting Cd toxicity. Overall, the results presented in this study shed a light on the underlying mechanisms of the Cd-mediated hormesis in plant. Moreover, our

study provided a safe method for the efficient utilization of mild Cd-contaminated soil as peppermint is an important cash plant.

KEYWORDS

cadmium stress, hormesis effect, transcriptomic analysis, antioxidant system, peppermint plant

Introduction

Farmland cadmium (Cd) pollution is a universal issue in many countries especially developing countries (Yuan et al., 2021). For example, it has been reported that Cd-contaminated soil covered an area of more than 20% of the total farmland area in China (Tang et al., 2016; Xie et al., 2021). Cd is one of the most toxic environmental pollutants with a long biological half-life (Ismael et al., 2019; Yu et al., 2022), which is concurred to give rise to continuously harmful effects for farmland soil (Zhang et al., 2021). As a result, Cd ion can finally enter into the human body through a contaminated food chain, due to its high mobility from soil to plant and thus causing a Cd accumulation in plant tissues (Clabeaux et al., 2011; Zhu et al., 2018). The dietary ingestion of Cd-polluted foods causes severe Cd toxicity for the human body, including growth inhibition and some serious diseases (e.g. cardiovascular diseases, renal and gut and liver damages, and even some cancers) (Jomova and Valko, 2011; Satarug et al., 2011; Zhang and Reynolds, 2019; Lemaire et al., 2020). Therefore, the remediation and utilization of Cd-contaminated farmland soil *via* safe methods is an urgent and hard task, which is distinguished from the remediation of other Cd-polluted soils such as mine and urban soils, because it directly concerns the security and quality of agricultural products.

Peppermint (*Mentha piperita*) is an oil producing plant from the *Lamiaceae* family (Mahendran and Rahman, 2020). Previous studies have been reported that peppermint plant has the ability to adapt and/or resist Cd stress (Zheljazkov et al., 2006; Demrezen and Aksoy, 2010). Essential oil is the major products of peppermint, which has wide applications in the food and pharmaceutical and chemical industries (Tholl, 2015). The extraction of essential oil without metals including Cd from aromatic plant can be readily achieved by using some special techniques such as steam distillation (Zheljazkov et al., 2006; Gautam and Agrawal, 2017). Such reports indicate that planting aromatic plants including peppermint may be a safe method for the utilization of Cd-contaminated soils (Gautam and Agrawal, 2017). However, numerous studies reported that Cd exposure had inhibitory effects on the growth of most plants even under very low concentration, and thus resulting in a reduced biomass (Liu et al., 2018; Michelle et al., 2019; Halim et al., 2020; Zhu et al., 2021), which seriously restricts the yield of essential oil. Therefore, it is essential to know whether and how different Cd exposure levels influence the growth of peppermint plant.

The hormesis, a phenomenon improving plant life performance under low Cd dosage, has been found in an increasing number of plant species including some aromatic/medicinal plants (Carvalho et al., 2020). For example, a low level (25 mg kg^{-1}) of Cd exposure promoted the growth and essential oil yield of sweet basil, but Cd treatments with high dosage resulted in adverse effects (Prasad et al., 2011). In addition, the yield and quality of essential oil in lemongrass were improved when the seedlings were grown on a heavy-metal-contaminated soil in which Cd concentration was close to 50 mg kg^{-1}, but that was reduced when Cd concentration was exceeded 50 mg kg^{-1} (Gautam and Agrawal, 2017). Moreover, Cd exposure treatments at Cd concertation varying from 0.37 mg kg^{-1} to 7.39 mg kg^{-1} promoted the growth performance of *Polygonatum sibiricum*, a traditional Chinese medicinal herb, with elevations in tuber biomass and plant height, and Cd stress treatment under 0.37 mg kg^{-1} concertation had the best stimulative effects on plant growth (Xie et al., 2021). And therefore, the authors proposed that planting medicinal plants might be a safe way for efficient utilization of low Cd-contaminated farmland (Xie et al., 2021). Although Cd-induced hormesis is observed in many plant species, the mechanisms mediated are poorly understood.

Cd stress with high degree usually cause oxidative stress for plant cells, because Cd ion can easily trigger excessive synthesis of reactive oxygen species (ROS) or result in failure in scavenging ROS, which will inevitably cause oxidative damages for the intracellular biomacromolecules such as protein, lipid as well as nucleotide (Yuan et al., 2013). Currently, it is suggested that Cd-induced hormesis is closely related to the activation of antioxidant defense system in plant (Jia et al., 2015; Muszyńska et al., 2018; Carvalho et al., 2020; Makowski et al., 2020). For instance, the exposure of *Arabidopsis thaliana* seedlings to a short-term Cd stress significantly induced the activities of ascorbate peroxidase (APX), catalase (CAT) and glutathione reductase (GR) (Carneiro et al., 2017). The low level of Cd stress treatment induces the accumulation of responded substances, such as anthocyanins, flavonoids, phenolics, ascorbic acid and other free organic acids (Vinogradova and Glukhov, 2021), they are known non-enzymatic antioxidants in plants. These reports suggest that improving antioxidant activity to scavenge ROS is highly associated with hormetic effects in plant, and its mechanism investigation is of great significance. However, the activation mode of antioxidant system induced by Cd stress remains unclear. Firstly, which concentrations of Cd treatment are antioxidants induced: all Cd treatments? Secondly, are they activated in a transient manner or in a sustained manner? Thirdly, at what levels are different antioxidants induced: protein or gene level, or both? Fourthly, how are different antioxidants induced: all at the same time or in a specific pattern?

The objective of this study was to explore Cd-induced hormesis effects and to reveal the possible mechanisms involved in that through analyzing physiological and transcriptomic responses of peppermint young plants in response to different degrees of Cd stress. The results

presented in this work would provide helpful information for understanding the mechanisms underlying Cd-induced hormesis effects. Moreover, this study put forward a safe and efficient way for the utilization of Cd-contaminated farmland soil.

Materials and methods

Plant materials and experimental design

Peppermint (*Mentha piperita* cv hengjing gaoyou) from the variety of "Shanghai 9" is an excellent clone with strong lodging resistance and high essential oil yield, which has a huge advantage for the industrial application.

Rooted cuttings of peppermint were employed to investigate the hormesis effects induced by Cd treatment in this study. Peppermint young plants were cultured by using the method of cuttage at Shaoguan university in March 2019 in Shaoguan, China. 1-week-old rooted cuttings were moved to a vessel and incubated within 1/2 Hoagland solution for one week for acclimatization. Young plants were grown in hydroponics containing Hoagland solution supplemented with different concentrations of Cd ion ($CdCl_2$, Aladdin, China). The final concentrations of Cd ion in each treatment are as follows: 0 mg L^{-1} (control), 0.8 mg L^{-1}, 1.6 mg L^{-1}, 3 mg L^{-1} or 6.5 mg L^{-1}, respectively. During different concentrations of Cd stress treatment, peppermint leaves were collected at 0 h, 24 h and 72 h for further investigations. Each treatment was performed three times, and contained a total of 54 clones (18 clones for each biological replicate), and 6 clones from three replicates were collected at each sampling point. Harvested leaf samples were quickly frozen with liquid nitrogen and stored at -80 °C for subsequent experiments.

Determination of plant growth performance

The growth performance of peppermint young plants was assessed when the rooted cuttings were exposed in different concentrations of Cd solutions for 7 days. Before assessment, root system of fresh young plants was washed with tap water and soaked into a $CaCl_2$ solution (10 mmol L^{-1}) to remove and dissolve the residual Cd. The roots were washed for three times. Residual moisture on the surface of young plants was removed using clean tissues. The plant height was determined using a dividing rule and the number of lateral branches was recorded. The root system of peppermint young plants was scanned using a MICROTEK scanner (MRS-9600 TFU2L, China) following a standard flow. The fresh and dry weight of leaves, shoots and roots were respectively evaluated using an electronic balance. Before the measurement of dry weight, peppermint organs were dried to a constant weight in an oven (at 70 °C). Each measurement was carried out three times using different samples.

Hormetic analysis of Cd treatments

Hormetic analysis for fresh weight response variable of the whole plant of peppermint young plants was performed with the model developed by Brain and Cousens (1989).

RNA extraction, cDNA library construction and Illumina sequencing

Total RNA of peppermint samples was extracted using a RNAprep Pure Plant Plus Kit (Tiangen, China) basing on the manufactory's instructions. The concentrations of total RNA were measured with a NanoDrop 2000 spectrophotometer (Thermo, USA). The purity and integrity of RNA were checked by an Agilent Bioanalyzer 2100 system (Agilent Technologies, USA) and 1.0% denaturing agarose gels, respectively. The cDNA library construction and RNA sequencing were performed in the Biomarker Biotechnology Corporation (Beijing, China). A total of 21 cDNA libraries were constructed using an Illumina TruSeqTM RNA Sample Preparation Kit (Illumina, USA) following the manufacturer's recommendations. All libraries were sequenced using the Illumina system HiSeq2500 following the standard procedure. The detailed processes of cDNA library construction and RNA sequencing were described in our former study (Wang et al., 2021).

Transcriptome assembly and gene functional annotation

Clean reads were generated after the removal of adapter contaminations and trimming nucleotides with low quality-score. Then the clean reads were processed for assembly by Trinity software (Grabherr et al., 2011). The clean reads of each sample with high quality were mapped to unigenes using HISAT (Hierarchical indexing for spliced alignment of transcripts) method (Kim et al., 2015). The mapped reads were used in the following analysis.

Finally, all unigenes were aligned against various public databases, including NR (non-redundant protein database of the National Center for Biotechnology Information), Swiss-Prot protein (http://www.uniprot.org/), COG (Clusters of Orthologous Groups) (http://www.ncbi.nlm.nih.gov/COG/), KOG (eu-Karyotic Orthologous Groups), GO (Gene Ontology) (http://www.geneontology.org/) and KEGG (Kyoto Encyclopedia of Genes and Genomes) (http://www.genome.jp/kegg) databases, to annotate the specific gene function using BLAST program (E value < 10^{-5}) (Wang et al., 2021). The GOseq R packages were employed to perform GO enrichment analysis (Ashburner et al., 2000; Zhu et al., 2018). KEGG pathway enrichment analysis was performed using KOBAS software (Kanehisa et al., 2019). GO and KEGG analysis were performed using BMKCloud (www.biocloud.net).

Identification of differentially expressed genes (DEGs)

Gene expression values were presented with Fragments Per kilobase per Million reads (FPKM) by the RSEM software (Li and Dewey, 2011). The differences of gene expression values were compared between treatments and the control by calculating FPKM (Zhang et al., 2020). Genes with fold change (FC) of expression levels ≥1.5 and q-value (adjusted P-value) ≤0.01 were considered as significant differentially expressed genes (DEGs) (Wang et al., 2021).

Validation of transcriptomic data by qRT-PCR

Twelve DEGs involved in Cd stress response were randomly selected for qRT-PCR. Total RNA of peppermint leaves was extracted using a RNAprep Pure Plant Plus Kit (Tiangen, China). Subsequently, total RNA was treated with DNaseI to remove residual DNA, and then the cDNA synthesis was performed using a 1st Strand cDNA Synthesis Kit (Yeasen, China). qRT-PCR analysis was carried out on a CFX96 Real-Time PCR Detection System (Bio-Rad, USA) with the following program: 95°C for 1 min, followed by 40 cycles at 95°C for 15 s, 58°C for 15 s, and 72°C for 30 s.

The relative expression levels of the twelve genes were calculated with the $2^{-\Delta\Delta CT}$ method (Livak and Schmittgen, 2001; Schmittgen and Livak, 2008). The *actin* gene (GenBank: KR082011.1) was used as an internal control gene to perform normalization. The expression patterns of *actin* in different samples were shown in Supplementary Figure 1. The results indicated that the expression of this reference gene was not significantly changed among different Cd-treated samples and the control, demonstrating that the expression of this gene is stable before and after Cd treatment. The specific primers of genes for qRT-PCR were designed using the Primer-BLAST of NCBI and were listed in Supplementary Table 1.

Determination of total phenol and total flavonoid contents in peppermint

Total phenolic content (TPC) in peppermint leaves was determined using the method of Folin-Ciocalteu (Ainsworth and Gillespie, 2007). 1.0 g of fresh leaf samples and 5 mL of 1% (v/v) HCl-methanol reagent were well homogenized with a 15 mL of centrifuge tube using a handheld homogenizer. The homogenates were held at ambient temperature (25 °C) for 3 hours and then were centrifuged at 4 °C (12,000 × g) for 15 min. For the measurement of TPC, 0.5 mL of supernatants, 1.5 mL of sodium carbonate (100 mM), and 1.0 mL of Folin-Ciocalteu reagent were well mixed in a new tube and reacted at 25°C for 30 min in the dark. After 30 min of reaction, the absorbance was determined at 765 nm using an UV-visible spectrophotometer (MAPADA UV-1800, China). The TPC was calculated based on a standard curve of gallic acid (GA) and the results were expressed as milligram GA equation per kilogram of fresh weight (mg kg^{-1} FW).

For the measurement of total flavonoid content (TFC), total flavonoid in peppermint leaves was first extracted with 10 mL of acetic acid and acetone mixing solution (0.5:70, v/v) at 4 °C for 2 hours with minor revisions (Valcarcel et al., 2015). Then, 1.5 mL of supernatants, 1.0 mL of distilled water, 0.1 mL of 10% (w/v) $AlCl_3{\cdot}6H_2O$ and 0.1 mL of 5% (w/v) $NaNO_2$ and 0.3 mL of 1 M NaOH were orderly added into a new tube and were fully mixed. The absorbance was recorded at 510 nm using an UV-visible spectrophotometer. The TFC was calculated based on a standard curve of catechin and the results were expressed as milligram catechin equation per kilogram of fresh weight (mg kg^{-1} FW).

Determination of hydrogen peroxide (H_2O_2), superoxide radicals ($O_2{\cdot}-$) and malondialdehyde (MDA) contents

The H_2O_2 and MDA and $O_2{\cdot}-$ contents were respectively estimated using commercial kits (D799773, D799761 and D799771, Sangong Biotech, China) according to the manufacturer's instructions. The results of $O_2{\cdot}-$, H_2O_2 and MDA contents based on fresh weight (FW) were represented as mmol kg^{-1}, μmol kg^{-1}, and mmol kg^{-1}, respectively.

Assay of the activity of antioxidant enzymes in peppermint

The activities of superoxide dismutase (SOD), catalase (CAT), peroxidase (POD), and polyphenol oxidase (PPO) were detected by the method described previously (Wang and Zhu, 2017; Wang et al., 2022). First, crude enzyme was prepared before activity measurement. The 1.0 g of fresh leaf samples was homogenized with a 5 ml of 1 mM phosphate buffer (pH 7.0) containing 2% of polyvinylpyrrolidone under 4 °C ice bath. The homogenates were centrifuged at 12, 000× g for 15 min at 4 °C. The supernatants were collected to determine the activity of related enzymes.

One unit of SOD activity was defined as the quantity of enzyme which causes a 50% inhibition of nitro blue tetrazolium reduction at 560 nm. One unit of CAT activity was defined as the quantity of enzyme that decomposes 1 μmol of H_2O_2 per min at 240 nm. One unit of POD activity was defined as the quantity of enzyme that oxidizes 20 mM concentrated guaiacol at 470 nm. The PPO activity was measured by recording the decline of 4-methylcatechol at 398 nm. The unit of U kg^{-1} on a fresh weight basis was employed for expressing the activities of the above enzymes.

Statistical analysis

There were three biological replicates for each experiment. The Statistical Package for Social Science (SPSS) (SPSS Inc.) 20.0 software was employed to conduct statistical analysis. The results of all measurements were presented as the mean ± standard error (*SE*). Analysis of statistical differences was performed using one-way analysis of variance (ANOVA) or student's t-test in the SPSS. P values less than 0.05 were considered to represent significance.

Results

The growth performance of peppermint young plants under different concentrations of Cd treatments

As it is difficult to precisely control the concentration of Cd ion in the Cd-polluted soils, Cd stress treatment experiments were conducted with Hoagland cultivation containing different

concentrations of Cd ion to investigate the effects of different degrees of Cd stress on the growth of peppermint young plants. Under Cd stress treatment for 7 days, the biomass (fresh and dry weight) of peppermint young plants first increased and then decreased with the elevation of the concentration of Cd ion and reached the highest amount at a Cd concentration of 1.6 mg L^{-1} (Figures 1A–F). Moreover, the cutting height (Figure 1G) and number of lateral branch (Figure 1H) and projected area of root (Figure 1I) in low levels of Cd treatments (0.8 and 1.6 mg L^{-1}) were significantly higher than that in other treatments. In addition, low levels of Cd treatments (0.8 and 1.6 mg L^{-1}) obviously promoted the development of root system (Figure 1J). The root morphology of the 0 mg L^{-1} and 3.0 mg L^{-1} Cd groups was also similar in appearance.

Compared with the control (0 mg L^{-1}), the visible biomass decrease and root inhibition were not observed until the Cd concentration reached 3.0 mg L^{-1}, suggesting that peppermint young plants exhibited strong Cd resistance. 6.5 mg L^{-1} Cd treatment retarded the growth of peppermint young plants

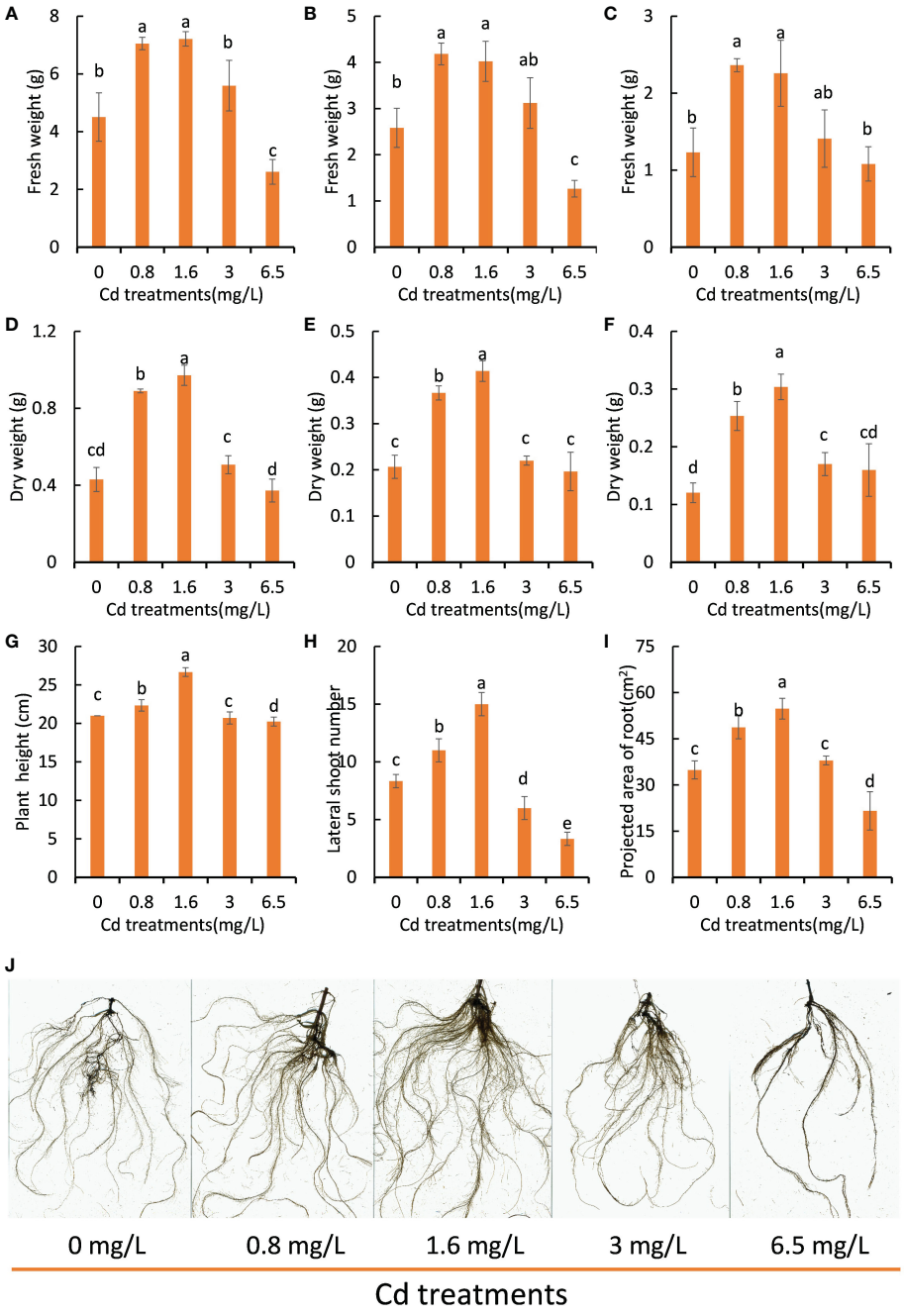

FIGURE 1
The growth performance of peppermint young plants under different concentrations of Cd treatments. **(A–C)**, fresh weight of leaves and shoots and roots, respectively; **(D–F)**, dry weight of leaves and shoots and roots, respectively; **(G)**, the height of young plants; **(H)**, the number of lateral shoots; **(I)**, projected area of root; **(J)**, root morphology. The growth performance of young plants was determined following 7 days of Cd stress treatments. Each value is presented as means ± standard error from three repeats. Statistical differences ($p \leq 0.05$) between treatments are compared in the SPSS software and indicated using different letters above the bars.

(Figures 1A–I) and the roots tended to be dark, suggesting that this Cd dosage would cause toxicities for peppermint (Figure 1J), and thus resulting in a reduced biomass.

In order to test whether the effects of Cd treatments on peppermint growth performance is hermetic, the data on fresh weight of the whole plant were adjusted to the Brain and Cousens model (Lushchak, 2014; Guzmán-Báez et al., 2021). An inverted U-shaped dose-response hormetic curve was noted, which was characterized by stimulation at low Cd concentrations but inhibition at high Cd concentrations (Supplementary Figure 2). The fresh weight of the whole plant had a maximum response at Cd concentration between 0.8 and 1.6 mg/L. The mean value of this variable decreased when the Cd concentration exceeded 3 mg/L. These results together strongly demonstrated that Cd treatment triggered hormesis on peppermint growth. However, the potential mechanisms of the Cd-induced hormesis have not been revealed to date in peppermint.

Global features and quality evaluation of RNA-seq data

Transcriptomic analysis of peppermint leaves in response to low and high degrees of Cd stress would shed light on the underlying mechanisms of the Cd-induced hormesis effects. Cd treatment at 1.6 mg L^{-1} concentration showed the best promoting effects on young plant growth (the highest biomass), but Cd treatment at 6.5 mg L^{-1} concentration significantly resulted in retrograde effects on the growth performance (Figure 1). Therefore, we analyzed the transcriptome profiles of young plants growing under low level of Cd (1.6 mg L^{-1}), high level of Cd (6.5 mg L^{-1}), and control condition (0 mg L^{-1} Cd) in this study, in order to reveal possible mechanisms of hormesis that was induced by low-level Cd exposure.

A total of 21 cDNA libraries involving 7 treatment groups (control at 0 h, 24 h and 72 h, 1.6 mg L^{-1} Cd treatment at 24 h and 72 h, 6.5 mg L^{-1} Cd treatment at 24 h and 72 h, respectively) that each group included three biological replicates were constructed. The constructed libraries were then sequenced through Illumina HiSeq platform. In total, 132.49 Gb of clean data were generated, and the size of clean data for each sample exceeded 5.70 Gb. The GC contents of the 21 libraries ranged from 48.89% to 50.17% with a mean value of 49.52%, and the minimum of Q30 percentage was 92.73% (Supplementary Table 2). After assembly, a total of 97,329 unigenes were generated, of which the lengths of 20,113 unigenes were longer than 1 Kb. The N50 length of unigenes was 1,404 bp and the mean length of unigenes was 734.16 bp (Supplementary Table 3). All unigenes were aligned against several public databases including NCBI Nr, Pfam, Swiss-Prot, KOG, KEGG, GO and COG databases (Supplementary Data 1), and the successful annotated percentage was 46.60% (Supplementary Table 4). The mapping efficiency of 21 samples based on the blast varied from 67.52% to 69.42%, as shown in Supplementary Table 5. These results indicated that the quality of transcriptome data was high and met the needs for further bioinformatics analysis.

Transcriptome analysis of peppermint leaves in response to different levels of Cd stress treatment for 24 h

The transcriptomic profiles of peppermint leaf in the (control) (0 mg/L) and low-level (1.6 mg/L) and high-level (6.5 mg/L) Cd treatments were obtained when young plants were treated for 24 h. The expression differences of genes were compared within three treatments using pairwise comparison, and the differentially expressed genes (DEGs) were divided into up- or down-regulated transcripts.

A total of 408 DEGs were identified between the comparison of control and low-level Cd treatment (Figure 2A). Among them, low-level Cd treatment induced the expression of 245 DEGs, but repressed the expression of 163 DEGs. A total of 868 DEGs were identified between the comparison of control and high-level Cd treatment (Figure 2A). In which, the expression of 552 DEGs were up-regulated but that of 316 DEGs were down-regulated by high-level Cd treatment. There were 242 DEGs in the comparison group of low- and high-level Cd treatment, and most of them were up-regulated by high-level Cd stress (Figure 2A). This result implies that high level of Cd treatment induced more extensive responses to Cd stress at the initial stage.

Compared with the control, the expression of 580 DEGs (442 plus 138) were specifically affected by high level of Cd stress treatment, and the expression of 120 DEGs (115 plus 5), by low level of Cd treatment (Figure 2B). A total of 13 DEGs were commonly detected in all three comparisons. 288 DEGs (275 plus 13) were commonly identified in the comparison groups of 0 mg L^{-1} vs 6.5 mg L^{-1} and 0 mg L^{-1} vs 1.6 mg L^{-1}, suggesting these DEGs might involve in Cd stress response. 151 DEGs (138 plus 13) were commonly found in the comparison groups of 0 mg L^{-1} vs 6.5 mg L^{-1} and 1.6 mg L^{-1} vs 6.5 mg L^{-1}. Only 18 DEGs (5 plus 13) were commonly screened in the comparison groups of 0 mg L^{-1} vs 1.6 mg L^{-1} and 1.6 mg L^{-1} vs 6.5 mg L^{-1} (Figure 2B).

KEGG enrichment analysis was employed to predict the biological functions of those DEGs. The functional annotation of DEGs would provide useful information for understanding the mechanisms how peppermint leaves respond to different levels of Cd stress. The 20 most enriched KEGG pathways were displayed in Figures 2C, D.

In the comparison group of 0 mg L^{-1} vs 1.6 mg L^{-1}, DEGs were significantly enriched in four pathways, including biosynthesis of amino acids, ubiquinone and other terpenoid-quinone biosynthesis, phenylpropanoid biosynthesis and phenylalanine, tyrosine and tryptophan biosynthesis (Figure 2C). The number of DEGs in three pathways including biosynthesis of amino acids (16 genes), phenylpropanoid biosynthesis (14 genes), and phenylalanine, tyrosine and tryptophan biosynthesis (12 genes) were more than 10 genes.

In the comparison group of 0 mg L^{-1} vs 6.5 mg L^{-1}, porphyrin and chlorophyll metabolism, and photosynthesis-antenna proteins were the two most enriched pathways, in which 18 and 11 DEGs were identified, respectively (Figure 2D). These results imply that high level of Cd stress might cause damages on the photosynthesis system of peppermint leaf, despite of undergoing short-term (24 h) Cd

10.3389/fpls.2023.1088285

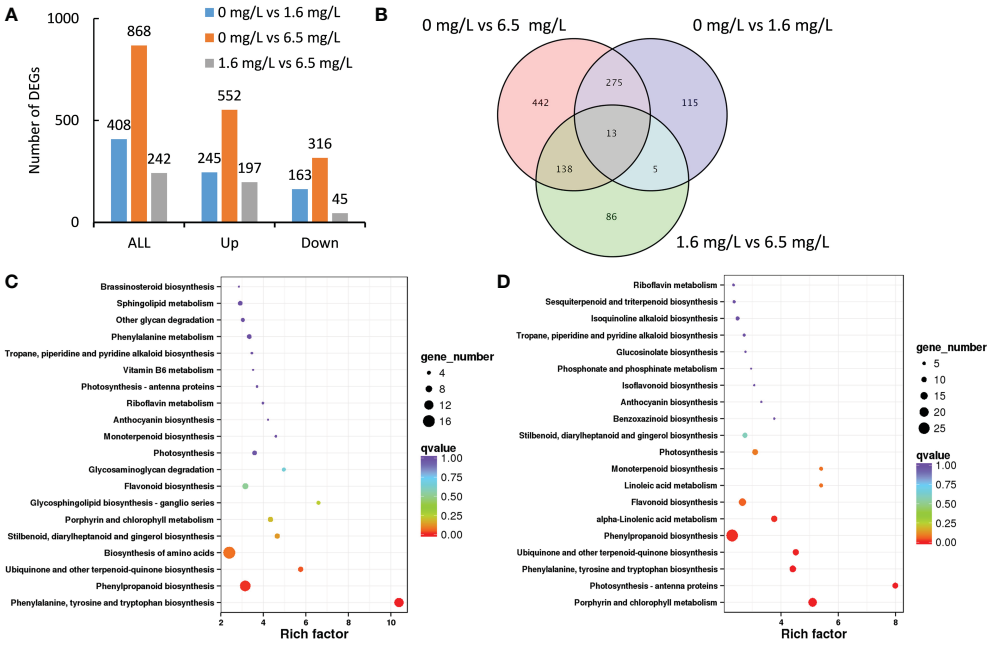

FIGURE 2
Transcriptomic profiles of peppermint leaf in response to low (1.6 mg L^{-1}) and high (6.5 mg L^{-1}) levels of Cd stress treatments at 24 h. **(A)**, the number of up- or down-regulated differentially expressed genes (DEGs); **(B)**, the venn diagram of DEGs; **(C)**, KEGG enrichment pathway of DEGs from the comparison of 0 mg L^{-1} Cd treatment vs 1.6 mg L^{-1} Cd treatment; **(D)**, KEGG enrichment pathway of DEGs from the comparison of 0 mg L^{-1} Cd treatment vs 6.5 mg L^{-1} Cd treatment.

exposure. In addition, three pathways, phenylalanine and tyrosine and tryptophan biosynthesis, ubiquinone and other terpenoid-quinone biosynthesis, and phenylpropanoid biosynthesis, were also significantly enriched. Most DEGs were enriched in the pathway of phenylpropanoid biosynthesis (26 genes) (Figure 2D).

Based on the results obtained, two levels of Cd stress treatments might influence the phenylpropanoid biosynthesis, and the increased phenylpropanoid content would provide protective effects on peppermint under Cd stress condition to reduce Cd- triggered oxidative damages.

Transcriptome analysis of peppermint leaves in response to different levels of Cd stress treatment for 72 h

A total of 539 DEGs were identified from the comparison between the control and 1.6 mgL^{-1} Cd treatment, of these DEGs, 290 DEGs were up-regulated and 249 DEGs were down-regulated by low-level Cd treatment (Figure 3A). High-level Cd treatment (6.5 mgL^{-1}) significantly affected the expression of 1054 DEGs comparing the control, in which, 382 DEGs were induced but 672 DEGs were repressed by high-level Cd treatment (Figure 3A). The number of down-regulated DEGs were far more than that of up-regulated DEGs in high-level Cd treatment (Figure 3A). Additionally, there were 865 DEGs in the comparison group of low- and high-level Cd treatment, and most of them (636 genes) were down-regulated by high-level Cd stress treatment (Figure 3A). These results suggest that long-term (72 h) Cd heavy stress might repress stress responses or heavy Cd stress had caused deadly damages on peppermint leaves, and young plants were no more "vigour" to reply to Cd stress.

Compared with the control, the expression of 787 DEGs (554 plus 233) were specifically affected by 6.5 mg L^{-1} Cd treatment, and the expression of 262 DEGs (152 plus 110), by 1.6 mg L^{-1} Cd treatment (Figure 3B). It was found that 17 DEGs were commonly detected in all three comparisons. 277 DEGs (260 plus 17) were commonly identified in the comparison groups of 0 mg L^{-1} vs 6.5 mg L^{-1} and 0 mg L^{-1} vs 1.6 mg L^{-1}. 250 DEGs (233 plus 17) were commonly detected in the comparison groups of 0 mg L^{-1} vs 6.5 mg L^{-1} and 1.6 mg L^{-1} vs 6.5 mg L^{-1}. (Figure 3B). 127 DEGs (110 plus 17) were commonly discerned in the comparison groups of 0 mg L^{-1} vs 1.6 mg L^{-1} and 1.6 mg L^{-1} vs 6.5 mg L^{-1} and 110 DEGs were overlapped in these two comparisons (Figure 3B).

In the comparison group of 0 mg L^{-1} vs 1.6 mg L^{-1}, DEGs were significantly enriched in the pathways of photosynthesis (16 genes), photosynthesis-antenna proteins (15 genes), porphyrin and chlorophyll metabolism (13 genes) and alpha-Linolenic acid metabolism (11 genes) (Figure 3C). In the comparison group of 0 mg L^{-1} vs 6.5 mg L^{-1}, DEGs were significantly enriched in the pathways of plant hormone signal transduction (33 genes), photosynthesis (17 genes), porphyrin and chlorophyll metabolism (15 genes), and hotosynthesis-antenna proteins (13 genes) (Figure 3D). These results together suggest that long-term Cd stress might injure photosynthetic system of the peppermint leaves, but the mechanisms regarding hormesis effects induced by low-level Cd exposure were unclear.

The most DEGs (33 genes) were enriched in the pathway of plant hormone signal transduction (Figure 3D), suggesting that

10.3389/fpls.2023.1088285

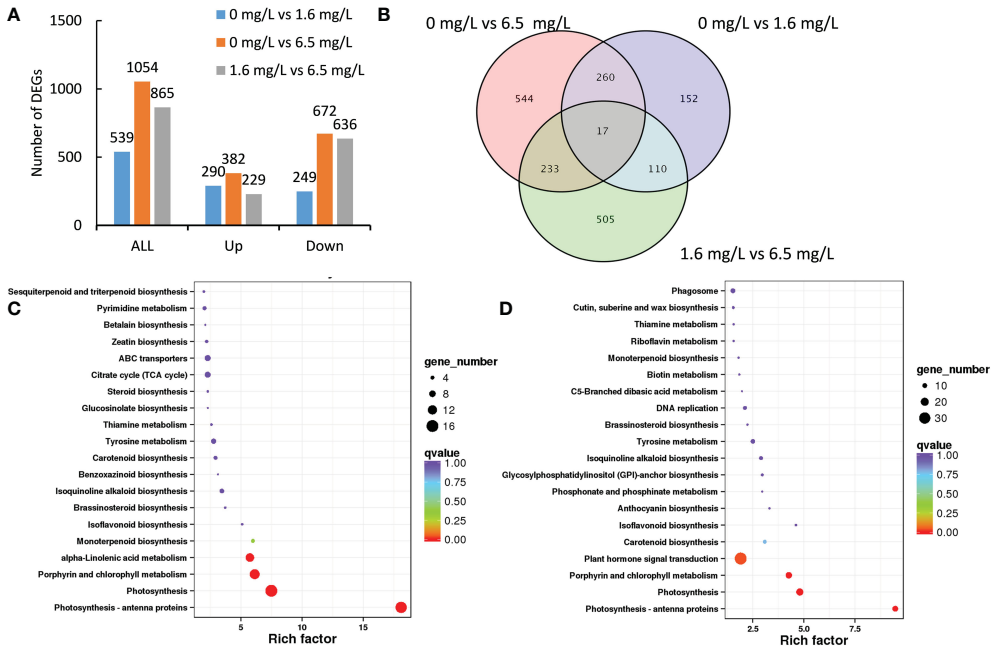

FIGURE 3
Transcriptomic profiles of peppermint leaf in response to low (1.6 mg L^{-1}) and high (6.5 mg L^{-1}) levels of Cd stress treatments at 72 h. **(A)**, the number of up- or down-regulated differentially expressed genes (DEGs); **(B)**, the venn diagram of DEGs; **(C)**, KEGG enrichment pathway of DEGs from the comparison of 0 mg L^{-1} Cd treatment vs 1.6 mg L^{-1} Cd treatment; **(D)**, KEGG enrichment pathway of DEGs from the comparison of 0 mg L^{-1} Cd treatment vs 6.5 mg L^{-1} Cd treatment.

endogenous hormones were involved in the Cd stress response under high-level Cd condition.

Functional annotation of DEGs exclusively induced by low level of Cd exposure

As low level of Cd treatment induced significant hormesis effects on peppermint growth (Figure 1), analyzing the functional roles of DEGs exclusively induced by 1.6 mg L^{-1} Cd treatment would reveal the hormesis effects mediated by that. A total of 262 DEGs were exclusively affected by low level of Cd exposure (Figure 4A). Among them, the expressions of 99 DEGs were significantly up-regulated by 1.6 mg L^{-1} Cd treatment comparing with both 0 and 6.5 mg L^{-1} Cd treatments (Figure 4A), signifying the important roles of them in Cd-induced hormesis in peppermint young plants. Therefore, we mainly analyzed the functional roles of the induced 99 DEGs through GO and KEGG enrichment analysis.

KEGG enrichment analysis showed that the two most enriched pathways were phenylpropanoid biosynthesis and alpha-Linolenic acid metabolism, which comprised of 8 and 7 DEGs, respectively (Figure 4B). 4 DEGs were also enriched in the pathway of flavonoid biosynthesis.

GO analysis showed that the induced DEGs were mainly enriched in the terms of response to oxidative stress, hydrogen peroxide catabolic process and lipid metabolic process in the biological process category (Figure 4C), integral component of membrane in cellular component category, and heme binding, oxidoreductase activity, methyltransferase activity, iron ion binding and peroxidase activity in the category of molecular function (Supplementary Figure 3).

Apart from antioxidant enzyme, many phenylpropanoids and flavonoids are known non-enzymatic antioxidants (Zhou et al., 2022). And therefore, the results of GO and KEGG analysis pointed to antioxidant system. We supposed that low-level Cd exposure might induce strong antioxidant activity under mild Cd stress condition, and thus avoiding oxidative damages for peppermint tissues and manifesting as stimulative effects on cutting growth. Therefore, the analysis was focused on the biosynthesis phenylpropanoid and flavonoid and enzymatic antioxidant activities of peppermint young plants under different degrees of Cd stress conditions.

Effects of different degrees of Cd stress treatments on the biosynthesis of phenylpropanoids and flavonoids and quinones

Total flavonoid contents (TFCs) of the control were not obviously increased during the entire period of 72 h cultivation. The TFCs of two Cd treatments were significantly increased after 24 h Cd treatment when compared with the control (Figure 5A). However, the increased TFCs in 6.5 mg L^{-1} Cd treatment was then declined to the same level as the control at 72 h. Therefore, an inverted V-shape was formed during high-level Cd exposure. But TFCs in 1.6 mg L^{-1} Cd treatment was constantly increased and which showed significantly higher levels when compared with the control and 6.5 mg L^{-1} Cd treatment (Figure 5A).

A total of 4 DEGs involving in the flavonoid biosynthesis were identified. The expression levels of all DEGs were continuously up-regulated during low-level Cd exposure (Figure 5B), while their

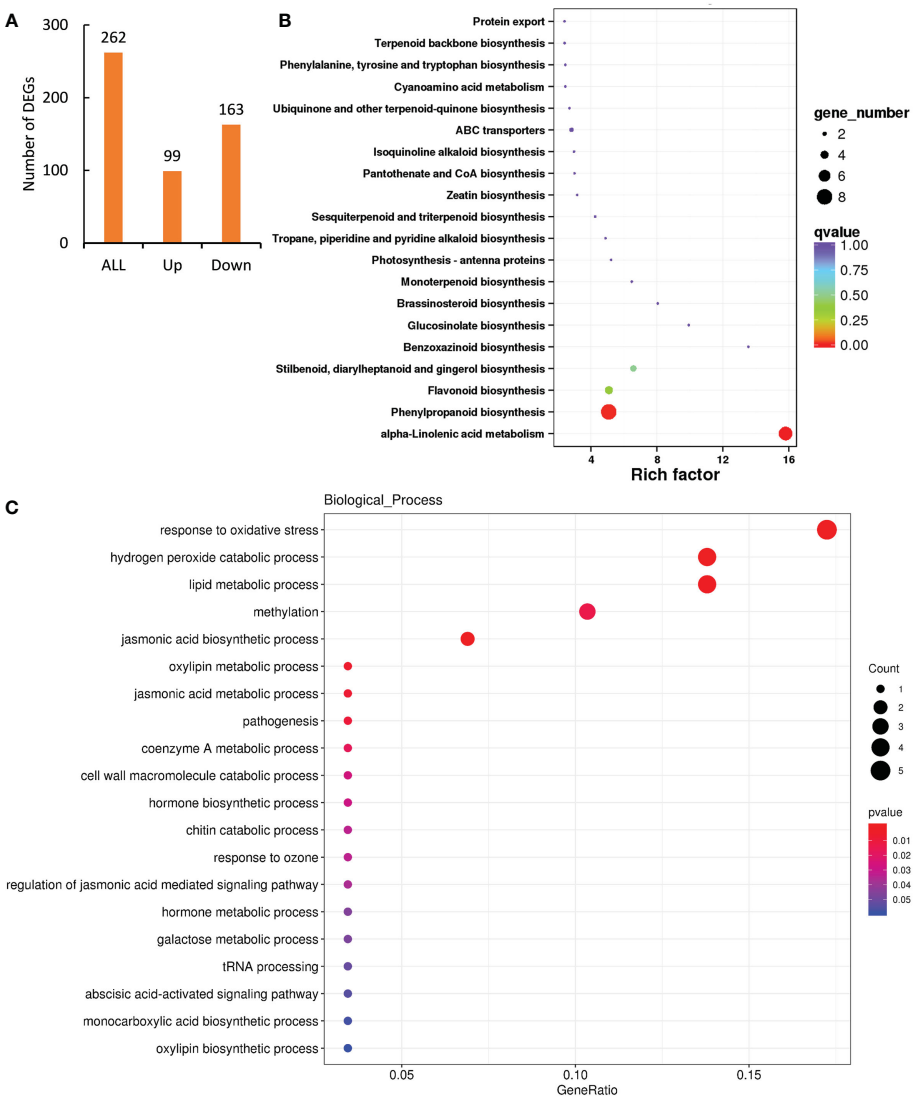

FIGURE 4
Functional annotation of DEGs exclusively induced by low level (1.6 mg L^{-1}) of Cd exposure for 72 h. **(A)**, the number of DEGs exclusively affected by 1.6 mg L^{-1} Cd exposure at 72 h; **(B)** GO and **(C)** KEGG enrichment analysis of DEGs exclusively induced by 1.6 mg L^{-1} Cd treatment.

expression levels were reached to peaks at 24 h and then declined at 72 h in high-level Cd stress treatment (Figure 5C). The overall expression pattern of 4 DEGs in flavonoid biosynthesis was highly consistent with the change trends of TFCs during Cd treatment (Figures 5A–C). One gene (c80364.graph_c0) was strongly responded to Cd treatments, implying that this gene might play a dominant role in the biosynthesis of flavonoid compounds under Cd stress condition.

The change trends of total phenolic content (TPC) in three treatments were similar with TFC during Cd stress treatment (Figure 5D). The TPCs in low level of Cd treatment were continually increased as the time goes in the course of the Cd treatment, and that was significantly higher than that in the control at any time point, whereas that in high level of Cd treatment only showed significantly higher levels than the control at 24 h (Figure 5D). Similarly, an inverted V-shape for TPC was formed during high-level Cd exposure.

A total of 8 DEGs were identified that they were involved in the phenylpropanoid biosynthesis. In low level of Cd treatment, the expression levels of all 8 DEGs were increased with the evaluation of treatment time and the expression levels of four genes (c76886.graph_c0, c70804.graph_c0, c71175.graph_c0 and c69641.graph_c0) were sharply increased after 24 h (Figure 5E). However, the expression of these four genes were merely induced by high level of Cd stress treatment at 24 h but that were reduced thereafter. The rest of 4 genes (c71270.graph_c0, c72094.graph_c0, c74544.graph_c2 and c66904.graph_c0) were not significantly induced by high-level Cd treatment at any time point (Figure 5F).

PPO is a key enzyme in the formation of quinone compounds in plant (Sullivan, 2015). The PPO activity of the control had barely risen at all during 72 h. In low level of Cd treatment, PPO activity first slightly reduced at 24 h and then sharply increased at 72 h. PPO activity of high level of Cd treatment showed an opposite trend with that of low level of Cd treatment (Figure 5G). At 72 h, PPO activity of

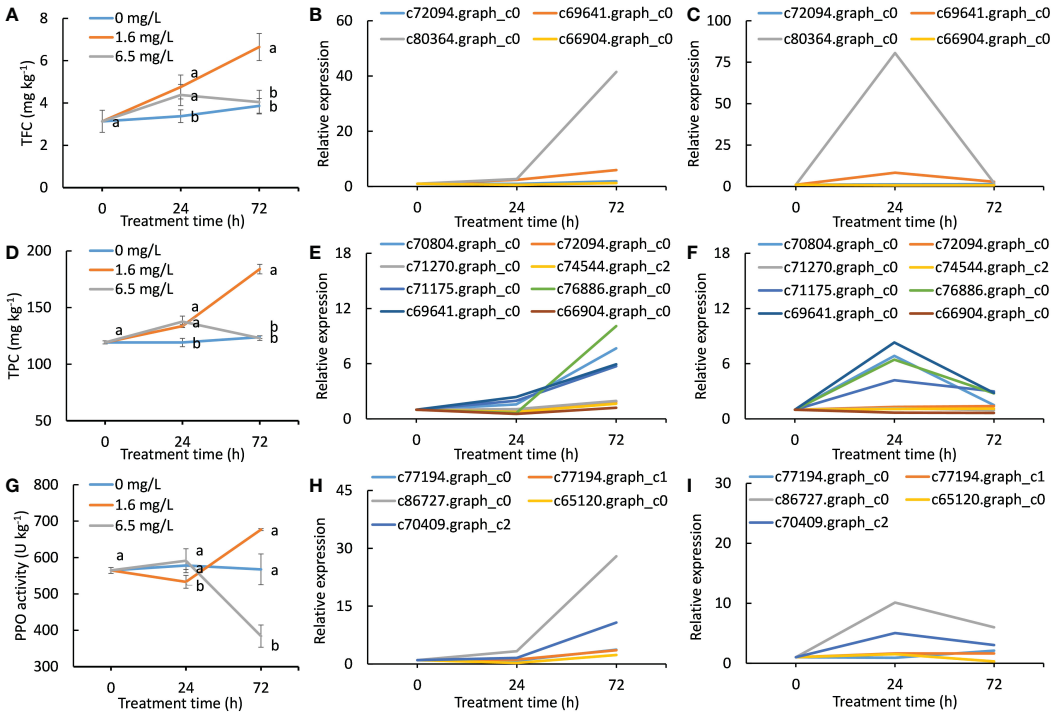

FIGURE 5
Effects of different degrees of Cd stress treatments on the biosynthesis of phenylpropanoids and flavonoids and quinones. **(A)**, total flavonoid contents of different Cd treatments in peppermint leaves; **(B, C)**, the expression patterns of DEGs involved in the biosynthesis of flavonoids during low level of Cd treatment (1.6 mg L^{-1}) and high level of Cd treatment (6.5 mg L^{-1}), respectively; **(D)**, total phenolic contents in peppermint leaves; **(E, F)**, the expression patterns of DEGs involved in the biosynthesis of phenylpropanoid during low level of Cd treatment (1.6 mg L^{-1}) and high level of Cd treatment (6.5 mg L^{-1}), respectively; **(G)**, polyphenol oxidase (PPO) activity; **(H, I)**, the expression patterns of DEGs encoding PPO during low level of Cd treatment (1.6 mg L^{-1}) and high level of Cd treatment (6.5 mg L^{-1}), respectively. Each value is presented as means from three repeats. In figures **(A, D, G)**, statistical differences ($p \leq 0.05$) between treatments are compared in the SPSS software and indicated using different letters above the bars.

low level of Cd treatment was significantly higher than that of both the control and high level of Cd treatment, and that of high level of Cd treatment was significantly lower than that of the control (Figure 5G). There were 5 DEGs encoding PPO. The expression levels of all *PPO* genes were continuously increased during Cd treatment in low level of Cd treatment (Figure 5H), while that were just induced by high-level Cd treatment at 24 h (Figure 5I). These results together demonstrate that Cd stress treatment induced the formation of quinones, and the biosynthesis ability of quinones was inhibited after long exposure to high-level Cd stress in peppermint leaves.

For the TFC, TPC, PPO activity and the expression patterns of genes in the biosynthesis of phenylpropanoids and flavonoids and quinones, inverted V-shapes were formed during high-level Cd exposure, suggesting that the induction of the biosynthesis of those antioxidants under Cd stress might be important mechanisms to adapt Cd stress, and high dosage of Cd stress just induced a temporary action on their biosynthesis and thus resulting in failure to cope with a sustained heavy Cd stress. However, low-level Cd exposure constantly induced their biosynthesis and accumulation, which would provide sufficient antioxidants to alleviate Cd toxicity. The genes responsible for the biosynthesis of phenylpropanoids and flavonoids and quinones were not activated by Cd stress at the same time, they were induced by an order manner under a yet unknown mechanism.

Effects of different degrees of Cd stress treatments on enzymatic antioxidant activity

The change trends of H_2O_2, O_2·− and MDA concentrations were similar during Cd treatment (Figures 6A–C). The 6.5 mg L^{-1} Cd treatment progressively increased in contents of H_2O_2, $O_2^{\cdot-}$ and MDA with the extended treatment, whereas those of the 0 and 1.6 mg L^{-1} Cd treatments increased much less, indicating that heavy Cd stress triggered oxidative burst. More importantly, no significant differences in contents of H_2O_2, O_2·− and MDA between the control and low-level Cd treatment were observed (Figures 6A–C), suggesting that low-level Cd exposure did not bring about severe oxidative damages on peppermint young plants. This might be one of the reasons why peppermint young plants could well grow under low levels of Cd treatment but not, under high degree of Cd stress.

POD activity of the control was changed much less during 72 h cultivation. POD activity of high-level Cd treatment was reduced with treatment time, suggesting that high-level Cd treatment inactivated POD activity *via* a yet unknown mechanism. POD activity of low-level Cd treatment was sharply increased after 24 h and was significantly higher than that of the other two treatments at 72 h (Figure 6D). Six DEGs encoding POD were exclusively induced by low-level Cd treatment. The expression levels of all genes were increased with treatment time in low-level Cd treatment (Figure 6E). In high-level

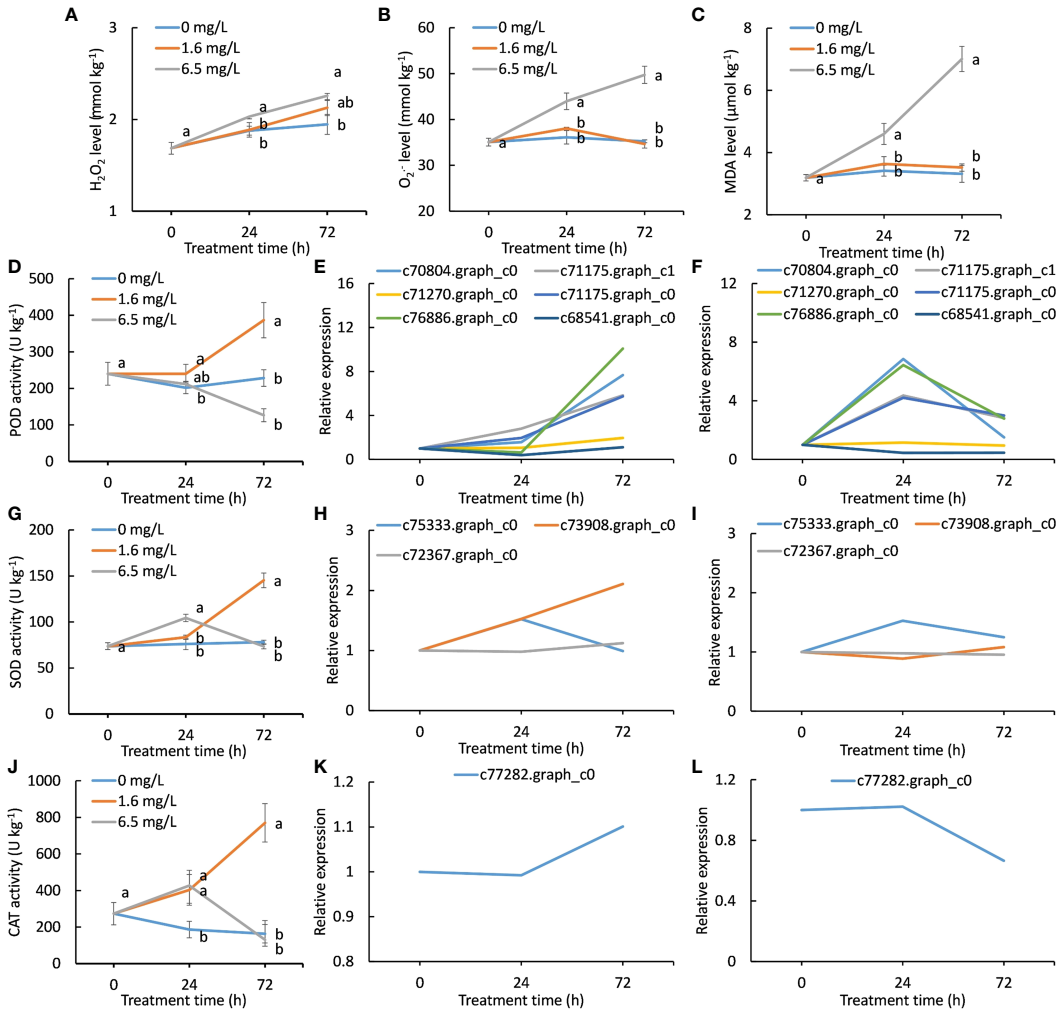

FIGURE 6
Changes of antioxidant activity and the expression patterns of DEGs encoding antioxidant enzymes during Cd exposure. **(A)**, hydrogen peroxide (H_2O_2) contents of different Cd treatments in peppermint leaves; **(B)**, superoxide anion (O_2·−) contents; **(C)**, malondialdehyde (MDA) contents; **(D)**, peroxidase (POD) activity; **(E, F)**, the expression patterns of DEGs encoding POD during low level of Cd treatment (1.6 mg L^{-1}) and high level of Cd treatment (6.5 mg L^{-1}), respectively; **(G)**, superoxide dismutase (SOD) activity; **(H, I)**, the expression patterns of DEGs encoding SOD during low level of Cd treatment (1.6 mg L^{-1}) and high level of Cd treatment (6.5 mg L^{-1}), respectively; **(J)**, catalase (CAT) activity; **(K, L)**, the expression patterns of DEG encoding CAT during low level of Cd treatment (1.6 mg L^{-1}) and high level of Cd treatment (6.5 mg L^{-1}), respectively. Each value is presented as means from three repeats. In figures **(A-D, G, J)**, statistical differences ($p \leq 0.05$) between treatments are compared in the SPSS software and indicated using different letters above the bars.

Cd treatment, the expression levels of four genes (c70804.graph_c0, c76886.graph_c0, c71175.graph_c0 and c71175.graph_c1) were first increased at 24 h and reduced thereafter (Figure 6F). Two genes (c71270.graph_c0 and c68541.graph_c0) expression were progressively reduced as treatment time increased (Figure 6F).

SOD activity of the control was almost unchanged during 72 h cultivation. SOD activity of high-level Cd treatment was reached to a peak at 24 h and then reduced to low level as same as the control at 72 h. In low-level Cd treatment, SOD activity was progressively increased during Cd treatment (Figure 6G). Low level of Cd treatment steady induced two genes (c73908.graph_c0 and c72367.graph_c0) expression during 72 h (Figure 6H), while their expression was only up-regulated at 24 h by high-level Cd treatment (Figure 6I). The expression pattern of one gene (c75333.graph_c0) during Cd treatment was similar in low- and high-level Cd treatment.

CAT activity in the control was gradually decreased in the next 72 h cultivation. Two concentrations of Cd treatments significantly enhanced CAT activity when compared with the control at 24 h (Figure 6J). CAT activity of low-level Cd treatment was continued to increase but that of high level of Cd treatment were reduced after 24 h (Figure 6J). At 72 h, CAT activity of low-level Cd treatment was significantly higher than that of the control and of high level of Cd treatment (Figure 6J). Only one *CAT* gene (c77282.graph_c0) was significantly induced by low-level Cd treatment at 72 h (Figure 6K), while high-level Cd treatment significantly inhibited its expression (Figure 6L). The expression patterns in low- and high Cd treatments were diametrically opposed during Cd treatment.

Expression verification of DEGs through qRT-PCR method

To validate the accuracy and credibility of transcriptome data, 12 DEGs were randomly selected according to the results of

transcriptomic analysis to measure the relative expression levels. The expression patterns of 12 DEGs were determined at 0 h, 24 h and 72 h following different concentrations of Cd stress treatments using specific primers based on qRT-PCR method. Among 12 DEGs selected, the expression of two genes including peppermint *ZAT10* and *AP2 like* were down-regulated by Cd stress treatment, the rest of DEGs were induced in RNA-Seq data (Figure 7). Only one gene, *AP2 like*, displayed a converse expression pattern determined by qRT-PCR and RNA-Seq during Cd stress treatment. The overall expression patterns of the rest of 11 DEGs determined by two methods were highly consistent, although the fold changes did not match exactly (Figure 7). These results indicated that the RNA-seq date were reliable and the results of transcriptomic analysis were credible.

Discussion

Peppermint traditionally grows as a cash crop in many countries (Cunningham and Ow, 1996) including China, for the production of either essential oils or herbage (Ahkami et al., 2015). In this study, we examined the effects of varying degrees of Cd stress on the growth of peppermint cuttings. The results showed that peppermint could tolerate heavy Cd stress even over 3.0 mg L^{-1} concentration (Figure 1). More importantly, low doses of Cd treatments (0.8 and 1.6 mg L^{-1}) enhanced the growth performance of peppermint young plants. These results suggest that peppermint plant had strong tolerance to Cd stress and low-level Cd exposure would be able to increase the yield of peppermint plant. Such beneficial effects offered

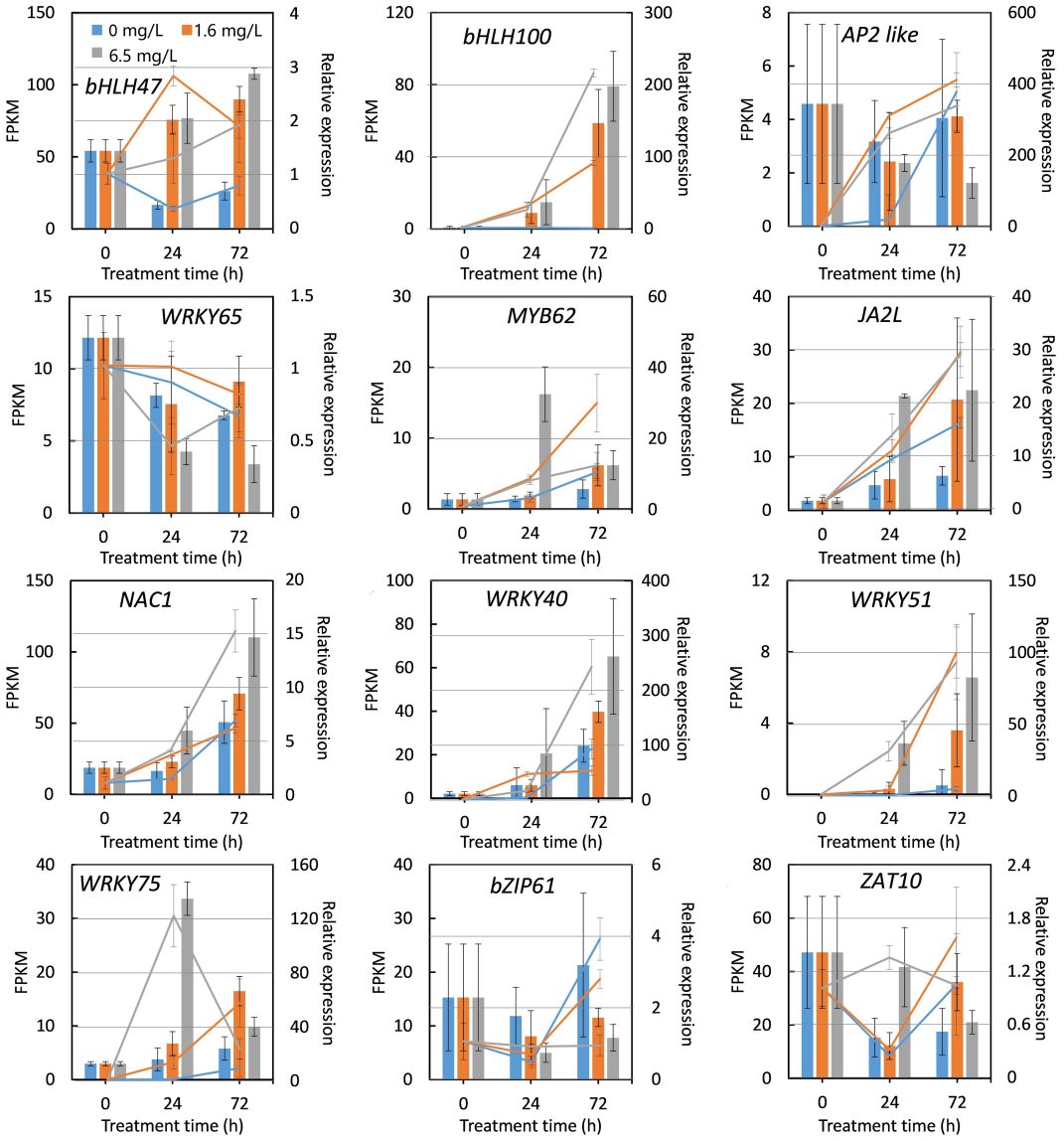

FIGURE 7
Quantitative real-time PCR (qRT-PCR) verification of the expression of 12 DEGs selected from RNA sequencing under Cd stress. The X-axis represents treatment time. The Y-axis on the left represents the expression level of specific gene obtained from RNA-seq (histogram), and on the right, from qRT-PCR analysis (line chart). Each value is presented as means ± standard error from three repeats. Standard errors are indicated in figures using the bars.

peppermint much opportunity for application in the safe utilization of mild Cd-contaminated farmland.

The chief purpose of peppermint is to extract essential oil (Ahkami et al., 2015). In another respect, the Cd accumulation in peppermint tissues must be given much attention to ensure the safety. To confirm the safety of peppermint oil, we also determined the contents of Cd ion in essential oil of peppermint planted on Cd-contaminated farmland soil, and found that Cd ions were not detected at all in essential oil (data not shown). The results from Youssef (2021) concur with our results, in which high concentrations of Cd treatments do not influence the essential oil quality of sweet basil. These results suggest that peppermint could act as an alternative cash crop to utilize the Cd-polluted soils safely and efficiently, which let the heavy metal-contaminated farmland soils be profitable for farmers. In addition, the most Cd were generally accumulated in roots, followed by shoots and leaves in plant (Xie et al., 2021). The increase in Cd concentration enhanced the yield and quality of essential oil in sweet basil (Youssef, 2021). These natural advantages of Cd effects help peppermint to be more suitable for safe soil utilization.

The growth promotion derived from low levels of Cd exposure in plant has recently aroused great interests from environmentalists regarding pollution control technology for recently (Xie et al., 2021). However, the poor understanding of Cd-induced hormesis mechanisms in plant restricts the application of this beneficial effect. It has been widely demonstrated that RNA seq combined with bioinformatic analysis is an effective method to reveal the molecular mechanisms of Cd tolerance in plant (Hu et al., 2014; Huang et al., 2019; Derakhshani et al., 2020). Analyzing the transcriptional changes of peppermint young plants in response to different concentrations of Cd treatments would provide useful information for understanding the Cd-induced hormesis. Thus, the transcriptional responses of peppermint leave to low- and high-level Cd ((1.6 and 6.5 mg L^{-1}, respectively) were compared and analyzed at a global level, to reveal the potential mechanisms of Cd-mediated hormesis effects.

In this study, a total of 21 cDNA libraries of peppermint leaf were sequenced through Illumina HiSeq platform. After sequencing, a total of 132.49 Gb of clean data with high quality were obtained (Supplementary Tables 2-5), and the credibility and reliability of transcriptome data were validated through qRT-PCR method (Figure 7). Among the assembled unigenes, 46.60% genes were successfully annotated by public databases (Supplementary Table 4). The annotated rate was higher than other plant species without genomic information, i.e., 35.92% for wild paper mulberry (Xu et al., 2019) and 40.38% for *Crossostephium chinensis* (Yang et al., 2017), indicating the high quality of RNA-seq data. After comparative analysis, the expressions of many transcripts were significantly affected by different dosages of Cd treatments (Figures 2, 3), suggesting that peppermint young plants made quick responses to varying Cd.

The affected DEGs by Cd treatments at initial stage (24 h) were mainly involved in the biosynthesis of amino acid and phenylpropanoid (Figure 2), suggesting that these biological processes were involved in the adaption to Cd stress in peppermint leaves. However, the affected DEGs at 72 h were mainly enriched in the photosynthetic system (Figure 3). Cd toxicity injures the photosynthetic apparatus, especially the light-harvesting complex and photosystems I and II (Hasan et al., 2019). The results imply that long-term exposure to high-level Cd brought about negative impacts on photosynthetic system in peppermint leaves. It has also been suggested that the improvement of photosynthetic efficiency by short-term exposure to Cd might be an important mechanism of hermetic effect in plant (Adamakis et al., 2020). The growth performance of peppermint young plants was improved after the application of low levels of Cd treatments (0.8 and 1.6 mg L^{-1}) in this study (Figure 1). The results imply that low-level Cd exposure improved the photosynthetic efficiency of peppermint leaves, which might be a reason why low-level Cd treatment increased the biomass of peppermint cuttings. However, more investigations are needed to study the effects of Cd exposure on photosynthetic system in peppermint leaves.

In order to knowing more about the mechanisms of Cd-induced hermetic effects, we mainly analyzed the roles of DEGs exclusively induced by low level of Cd exposure. The results of KEGG and GO analysis showed that the DEGs were mostly enriched in the biosynthesis pathways of phenylpropanoid and flavonoid, as well as the activity of scavenging ROS (Figure 4). These results imply that low-level Cd exposure induced hermetic effects in peppermint cuttings, probably, by activating the antioxidant system, and the ROS scavenging ability of peppermint leaves was constantly strengthened by low-level Cd exposure. To verify our findings, we analyzed the changes of antioxidant attributes of peppermint leaves in response to different Cd treatments.

Cd stress generally stimulates the generation of ROS, which will cause oxidative damages on plant tissues (Auobi Amirabad et al., 2020). Reducing ROS accumulation or enhancing detoxification may be one of the defense mechanisms of Cd toxicity in plants (Lata et al., 2019). MDA content is an indicator of membrane liquid peroxidation (Davey et al., 2005), and the increased MDA content indicates membrane lipid peroxidation. In the present study, high-level Cd treatment resulted in significant increases in H_2O_2, $O_2^{\cdot n-}$ and MDA contents, while low-level Cd exposure inhibited their increases (Figures 6A–C). These results together suggest that high level of Cd treatment caused severe oxidative damages on peppermint leaves, while low level of Cd treatment did not.

A range of natural compounds act as ROS scavengers (Haider et al., 2021). These include, but are not limited to non-enzymatic scavengers, i.e., ascorbic acid, glutathione, phenylpropanoids, flavonoids, and quinones; and enzymatic scavengers; i.e., POD, CAT and SOD (Shahid et al., 2014). Phenolic acids such as some henylpropanoids and flavonoids are the key substances for Cd tolerance in plants (Gu et al., 2021). Pretreatment with proanthocyanidins significantly alleviated Cd toxicity in industrial hemp, an annual herbaceous cash crop, and proanthocyanidins treatment induced the synthesis of secondary metabolites and antioxidant compounds (Yin et al., 2022). Flavonoid amendment enhanced Cd tolerance and had a significant stimulative effect on symplasm transport of Cd in *A. marina* roots (Li et al., 2015). In this study, low-level Cd treatment constantly induced the biosynthesis of phenylpropanoids and flavonoids, and thus resulting in an elevation of total flavonoid and phenolic contents (Figure 5). In addition, the activities and gene expressions of PPO, a key enzyme responsive for quinone formation, were incessantly enhanced by low level of Cd

treatment (Figure 5), suggesting that low-level Cd treatment also induced the quinone biosynthesis. These results suggest that the incessant biosynthesis of phenylpropanoids and flavonoids and quinones induced by low-level Cd treatment provided sufficient non-enzymatic antioxidants to protect cells from oxidative damages, and thus manifesting as beneficial effects on peppermint growth under Cd stress condition.

Antioxidant enzymes influence plant Cd tolerance as they play a crucial role in balancing the ROS level within the cell. Studies reported that antioxidant enzymes caused alternation in their activities, depending on Cd dosage and the cultivars of plants (Haider et al., 2021). Treatment with Cd had shown to enhance SOD activity in wheat (Milone et al., 2003). Cd toxicity trended to minimize the enzymatic activities of SOD and CAT in pea (Sandalio et al., 2001). Cd stress had no significant impact on the activity of POD in pea plant (Tran and Popova, 2013), but POD was increased in raddish treated with Cd (El-Beltagi et al., 2010). High CAT activity resulted to improve tolerance in cultivars of *Groenlandia densa* L. treated with Cd stress (Yilmaz and Parlak, 2011). In this study, we found that low level of Cd treatment significantly enhanced the activities and gene expression of POD, CAT and SOD during the entire 72 h Cd treatment (Figure 6). The results suggest that low-level Cd exposure could induced the activity of antioxidant enzyme at both protein and gene levels in peppermint leaves. The enhanced activity of antioxidant enzymes contributes to maintain lower ROS levels within cells.

Although high-level Cd treatment induced strong antioxidant defense response at initial stage (24 h), the induction was unsustainable and thus leading to the failure to offset Cd-triggered ROS burst. However, the antioxidant activity was continuously strengthened by low-level Cd treatment during the entire period of Cd exposure. The results strongly demonstrate that low-level Cd exposure constantly enhanced the antioxidant capacity of peppermint, which might be the possible mechanisms underlying Cd-induced hermetic effects. However, we also noticed that all the ROS scavengers were not activated by low level of Cd treatment at the same time and the induced intensity differed greatly among ROS scavengers (Figures 5, 6). These results suggest that the activated mode and the induced intensity for ROS scavengers depended on Cd concentration and treatment duration. All in all, our research provided new insights for the Cd hermetic effects in peppermint young plants.

Conclusion

Peppermint young plants showed strong Cd tolerance and low-level Cd promoted the growth performance, suggesting that planting peppermint may be a feasible strategy for the safe and efficient utilization of Cd-contaminated farmland soil. Low level of Cd exposure constantly induced the biosynthesis of phenylpropanoid and flavonoid, enhanced activities of antioxidant enzymes, while high level of Cd treatment at long period (72 h) inhibited them and caused oxidative burst, suggesting that low level of Cd exposure constantly induced the enhancement of antioxidant activity. The constant activation of antioxidant system by low-level Cd exposure suggests the possible mechanisms of hermetic effects in peppermint young plants.

Data availability statement

The data presented in the study are deposited in the NCBI Sequence Read Archive (SRA) repository, accession number PRJNA898846. The names of the repository/repositories and accession number(s) can be found in the article/SupplementaryMaterial.

Author contributions

BW: Conceptualization, Investigation, Data analysis, Visualization, Writing-review and editing; LL: Investigation; XY: Data analysis, Writing and editing; YZ, YW, and DL: Writing and editing; JH: Project administration, Review, editing and Supervision; YX: Plant material management, Cd treatment, Writing-review and editing. All authors contributed to the article and approved the submitted version.

Funding

This work was supported in part by Construction Project for Shaoguan Social Development and Collaborative Innovation of Science and Technology System (No. 220607164531948), Special Project for Soil Pollution Remediation of Shaoguan City (No. 2017sgtyfz303) and Natural Science Project of Shaoguan University (No. SY2019ZK05 and SZ2022KJ01).

Conflict of interest

The authors declare that the research was conducted in the absence of any commercial or financial relationships that could be construed as a potential conflict of interest.

Publisher's note

Supplementary material

The Supplementary Material for this article can be found online at: https://www.frontiersin.org/articles/10.3389/fpls.2023.1088285/full#supplementary-material

References

Adamakis, I. S., Sperdouli, I., Han, A., Dobrikova, A., Apostolova, E., and Moustakas, M. (2020). Rapid hormetic responses of photosystem II photochemistry to cadmium exposure. *Int. J. Mol. Sci.* 22, 41. doi: 10.20944/preprints202011.0283.v1

Ahkami, A., Johnson, S. R., Srividya, N., and Lange, B. M. (2015). Multiple levels of regulation determine monoterpenoid essential oil compositional variation in the mint family. *Mol. Plant* 8, 188–191. doi: 10.1016/j.molp.2014.11.009

Ainsworth, E. A., and Gillespie, K. M. (2007). Estimation of total phenolic content and other oxidation substrates in plant tissues using folin-ciocalteu reagent. *Nat. Protoc.* 2, 875–877. doi: 10.1038/nprot.2007.102

Ashburner, M., Ball, C. A., Blake, J. A., Botstein, D., Butler, H., Cherry, J. M., et al. (2000). Gene ontology: tool for the unification of biology. *Nature* 25, 25–29. doi: 10.1038/75556

Auobi Amirabad, S., Behtash, F., and Vafaee, Y. (2020). Selenium mitigates cadmium toxicity by preventing oxidative stress and enhancing photosynthesis and micronutrient availability on radish (*Raphanus sativus* l.) cv. cherry belle. *Environ. Sci. pollut. Res. Int.* 27, 12476–12490. doi: 10.1007/s11356-020-07751-2

Brain, P., and Cousens, R. (1989). An equation to describe dose responses where there is stimulation of growth at low doses. *Weed Res.* 29, 93–96. doi: 10.1111/j.1365-3180.1989.tb00845.x

Carneiro, J. M. T., Chacón-Madrid, K., Galazzi, R. M., Campos, B. K., Arruda, S. C. C., Azevedo, R. A., et al. (2017). Evaluation of silicon influence on the mitigation of cadmium-stress in the development of *Arabidopsis thaliana* through total metal content, proteomic and enzymatic approaches. *J. Trace Elem. Med. Biol.* 44, 50–58. doi: 10.1016/j.jtemb.2017.05.010

Carvalho, M. E. A., Castro, P. R. C., and Azevedo, R. A. (2020). Hormesis in plants under cd exposure: From toxic to beneficial element? *J. Hazard. Mater.* 384, 121434. doi: 10.1016/j.jhazmat.2019.121434

Clabeaux, B. L., Navarro, D. A. G., Aga, D. S., and Bisson, M. A. (2011). Cd tolerance and accumulation in the aquatic macrophyte, chara australis: potential use for charophytes in phytoremediation. *Environ. Sci. Technol.* 45, 5332–5338. doi: 10.1021/es200720u

Cunningham, S. D., and Ow, D. W. (1996). Promises and prospects of phytoremediation. *Plant Physiol.* 110, 715–719. doi: 10.1104/pp.110.3.715

Davey, M. W., Stals, E., Panis, B., Keulemans, J., and Swennen, R. L. (2005). High-throughput determination of malondialdehyde in plant tissues. *Anal. Biochem.* 347, 201–207. doi: 10.1016/j.ab.2005.09.041

Demrezen, D., and Aksoy, A. (2010). Heavy metal levels in vegetables in Turkey are within safe limits for Cu, zn, Ni and exceeded for cd and Pb. *J. Food Qual.* 29, 252–265. doi: 10.1111/j.1745-4557.2006.00072.x

Derakhshani, B., Jafary, H., Maleki Zanjani, B., Hasanpur, K., Mishina, K., Tanaka, T., et al. (2020). Combined QTL mapping and RNA-seq profiling reveals candidate genes associated with cadmium tolerance in barley. *PloS One* 15, e0230820. doi: 10.1371/journal.pone.0230820

El-Beltagi, H. S., Mohamed, A. A., and Rashed, M. M. (2010). Response of antioxidative enzymes to cadmium stress in leaves and roots of radish (*Raphanus sativus* l.). *Not. Sci. Biol.* 2, 76–82. doi: 10.1007/s11356-020-07751-2

Gautam, M., and Agrawal, M. (2017). Influence of metals on essential oil content and composition of lemongrass (*Cymbopogon citratus* (D.C.) stapf.) grown under different levels of red mud in sewage sludge amended soil. *Chemosphere* 175, 315–322. doi: 10.1016/j.chemosphere.2017.02.065

Grabherr, M. G., Haas, B. J., Yassour, M., Levin, J. Z., Thompson, D. A., Amit, I., et al. (2011). Full-length transcriptome assembly from RNA-seq data without a reference genome. *Nat. Biotechnol.* 29, 644–652. doi: 10.1038/nbt.1883

Gu, Q., Wang, C. Y., Xiao, Q. Q., Chen, Z. P., and Han, Y. (2021). Melatonin confers plant cadmium tolerance: An update. *Int. J. Mol. Sci.* 22, 11704. doi: 10.3390/ijms222111704

Guzmán-Báez, G. A., Trejo-Téllez, L. I., Ramírez-Olvera, S. M., Salinas-Ruíz, J., Bello-Bello, J. J., Alcántar-González, G., et al. (2021). Silver nanoparticles increase nitrogen, phosphorus, and potassium concentrations in leaves and stimulate root length and number of roots in tomato seedlings in a hormetic manner. *Dose Response* 19, 15593258211044576. doi: 10.1177/15593258211044576

Haider, F. U., Liqun, C., Coulter, J. A., Cheema, S. A., Wu, J., Zhang, R., et al. (2021). Cadmium toxicity in plants: Impacts and remediation strategies. *Ecotoxicol. Environ. Saf.* 211, 111887. doi: 10.1016/j.ecoenv.2020.111887

Halim, M. A., Rahman, M. M., Megharaj, M., and Naidu, R. (2020). Cadmium immobilization in the rhizosphere and plant cellular detoxification: Role of plant-growth-promoting rhizobacteria as a sustainable solution. *J. Agric. Food Chem.* 68, 13497–13529. doi: 10.1021/acs.jafc.0c04579

Hasan, M. K., Ahammed, G. J., Sun, S., Li, M., Yin, H., and Zhou, J. (2019). Melatonin inhibits cadmium translocation and enhances plant tolerance by regulating sulfur uptake and assimilation in *Solanum lycopersicum* l. *J. Agric. Food Chem.* 67, 10563–10576. doi: 10.1021/acs.jafc.9b02404

Huang, Y. M., Chen, H. Q., Reinfelder, J. R., Liang, X. Y., Sun, C. J., Liu, C. P., et al. (2019). A transcriptomic (RNA-seq) analysis of genes responsive to both cadmium and arsenic stress in rice root. *Sci. Total Environ.* 666, 445–460. doi: 10.1016/j.scitotenv.2019.02.281

Hu, H. Y., Lu, X., Cen, X., Chen, X. H., Li, F., and Zhong, S. (2014). RNA-Seq identifies key reproductive gene expression alterations in response to cadmium exposure. *Biomed. Res. Int.* 2014, 529271. doi: 10.1155/2014/529271

Ismael, M. A., Elyamine, A. M., Moussa, M. G., Cai, M., Zhao, X., and Hu, C. (2019). Cadmium in plants: uptake, toxicity, and its interactions with selenium fertilizers. *Metallomics* 11, 255–277. doi: 10.1039/c8mt00247a

Jia, L., Liu, Z. L., Chen, W., Ye, Y., Yu, S., and He, X. Y. (2015). Hormesis effects induced by cadmium on growth and photosynthetic performance in a hyperaccumulator, *Lonicera japonica* thunb. *J. Plant Growth Regul.* 34, 13–21. doi: 10.1007/s00344-014-9433-1

Jomova, K., and Valko, M. (2011). Advances in metal-induced oxidative stress and human disease. *Toxicology* 283, 65–87. doi: 10.1016/j.tox.2011.03.001

Kanehisa, M., Sato, Y., Furumichi, M., Morishima, K., and Tanabe, M. (2019). New approach for understanding genome variations in KEGG. *Nucleic Acids Res.* 47, D590–D595. doi: 10.1093/nar/gky962

Kim, D., Langmead, B., and Salzberg, S. L. (2015). HISAT: A fast spliced aligner with low memory requirements. *Nat. Methods* 12, 357–360. doi: 10.1038/nmeth.3317

Lata, S., Kaur, H. P., and Mishra, T. (2019). Cadmium bioremediation: A review. *Int. J. Pharm. Sci. Res.* 10, 4120–4128. doi: 10.13040/IJPSR.0975-8232.10(9).4120-28

Lemaire, J., van der Hauwaert, C., Savary, G., Dewaeles, E., Perrais, M., Lo Guidice, J. M., et al. (2020). Cadmium-induced renal cell toxicity is associated with microRNA deregulation. *Int. J. Toxicol.* 39, 103–114. doi: 10.1177/1091581819899039

Li, B., and Dewey, C. N. (2011). RSEM: accurate transcript quantification from RNA seq data with or without a reference genome. *BMC Bioinf.* 12, 323. doi: 10.1186/1471-2105-12-323

Li, J., Lu, H. L., Liu, J. C., Hong, H. L., and Yan, C. L. (2015). The influence of flavonoid amendment on the absorption of cadmium in *Avicennia marina* roots. *Ecotoxicol. Environ. Saf.* 120, 1–6. doi: 10.1016/j.ecoenv.2015.05.004

Liu, Z. L., Huang, Y. F., Zhu, Z. B., Chen, Y. H., and Cui, J. (2018). Effects of foliar feeding of melatonin on cadmium tolerance of Chinese cabbage seedlings. *Plant Physiol. J.* 54, 660–668. doi: 10.13592/j.cnki.ppj.2018.0066

Livak, K. J., and Schmittgen, T. D. (2001). Analysis of relative gene expression data using real-time quantitative PCR and the 2(-delta delta C(T)) method. *Methods* 25, 402–408. doi: 10.1006/meth.2001.1262

Lushchak, V. I. (2014). Dissection of the hormetic curve: analysis of components and mechanisms. *Dose Response* 12, 466–479. doi: 10.2203/dose-response

Mahendran, G., and Rahman, L. U. (2020). Ethnomedicinal, phytochemical and pharmacological updates on peppermint (*Mentha* × *piperita* l.)-a review. *Phytother. Res.* 34, 2088–2139. doi: 10.1002/ptr.6664

Makowski, E., Sitko, K., Szopiński, M., Gieroń, Ż., Pogrzeba, M., Kalaji, H. M., et al. (2020). Hormesis in plants: The role of oxidative stress, auxins and photosynthesis in corn treated with cd or Pb. *Int. J. Mol. Sci.* 21, 2099. doi: 10.3390/ijms21062099

Michelle, M., Mian, Z., David, R., Paul, H., and Chen, Z. H. (2019). Chloride transport at plant soil interface modulates barley cd tolerance. *Plant Soil* 441, 409–421. doi: 10.1007/s11104-019-04134-6

Milone, M. T., Sgherri, C., Clijsters, H., and Navari-Izzo, F. (2003). Antioxidative responses of wheat treated with realistic concentration of cadmium. *Environ. Exp. Bot.* 50, 265–276. doi: 10.1016/S0098-8472(03)00037-6

Muszyńska, E., Hanus-Fajerska, E., and Ciarkowska, K. (2018). Studies on lead and cadmium toxicity in *Dianthus carthusianorum* calamine ecotype cultivated *in vitro*. *Plant Biol.* 20, 474–482. doi: 10.1111/plb.12712

Prasad, A., Kumar, S., Khaliq, A., and Pandey, A. (2011). Heavy metals and arbuscular mycorrhizal (AM) fungi can alter the yield and chemical composition of volatile oil of sweet basil (*Ocimum basilicum* l.). *Biol. Fertil. Soils* 47, 853–861. doi: 10.1007/s00374-011-0590-0

Sandalio, L. M., Dalurzo, H. C., Gómez, M., Romero-Puertas, M. C., and del Río, L. A. (2001). Cadmium-induced changes in the growth and oxidative metabolism of pea plants. *J. Exp. Bot.* 52, 2115–2126. doi: 10.1093/jexbot/52.364.2115

Satarug, S. W., Garrett, S. H., Sens, M. A., and Sens, D. A. (2011). Cadmium, environmental exposure, and health outcomes. *Environ. Health Perspect.* 118, 182–190. doi: 10.1289/ehp.0901234

Schmittgen, T. D., and Livak, K. J. (2008). Analyzing real-time PCR data by the comparative C(T) method. *Nat. Protoc.* 3, 1101–1108. doi: 10.1038/nprot.2008.73

Shahid, M., Pourrut, B., Dumat, C., Nadeem, M., Aslam, M., and Pinelli, E. (2014). Heavy-metal-induced reactive oxygen species: phytotoxicity and physicochemical changes in plants. *Rev. Environ. Contam. Toxicol.* 232, 1–44. doi: 10.1007/978-3-319-06746-9_1

Sullivan, M. L. (2015). Beyond brown: Polyphenol oxidases as enzymes of plant specialized metabolism. *Front. Plant Sci.* 5. doi: 10.3389/fpls.2014.00783

Tang, X., Li, Q., Wu, M., Lin, L., and Scholz, M. (2016). Review of remediation practices regarding cadmium-enriched farmland soil with particular reference to China. *J. Environ. Manage.* 181, 646–662. doi: 10.1016/j.jenvman.2016.08.043

Tholl, D. (2015). Biosynthesis and biological functions of terpenoids in plants. *Adv. Biochem. Eng Biotechnol.* 148, 63–106. doi: 10.1007/10_2014_295

Tran, T. A., and Popova, L. P. (2013). Functions and toxicity of cadmium in plants: Recent advances and future prospects. *Turk. J. Bot.* 37, 1–13. doi: 10.3906/bot-1112-16

Valcarcel, J., Rrilly, K., and Gaffney, M. (2015). Antioxidant activity, total phenolic and total flavonoid content in sixty varieties of potato (*Solanum tuberosum* l.) grown in Ireland. *Potato Res.* 58, 221–244. doi: 10.1007/s11540-015-9299-z

Vinogradova, N. A., and Glukhov, A. Z. (2021). Ecological and phytochemical features of crataegusfallacina klokov under conditions of technogenic pollution. *Contemp. Probl. Ecol.* 14, 90–97. doi: 10.1134/S1995425521010091

Wang, B., Huang, Y. Y., Zhang, Z. M., Xiao, Y. H., and Xie, J. (2022). Ferulic acid treatment maintains the quality of fresh-cut taro (*Colocasia esculenta*) during cold storage. *Front. Nutr.* 9. doi: 10.3389/fnut.2022.884844

Wang, B., Wu, C. S., Wang, G., He, J. M., and Zhu, S. J. (2021). Transcriptomic analysis reveals a role of phenylpropanoid pathway in the enhancement of chilling tolerance by pre-storage cold acclimation in cucumber fruit. *Sci. Hortic.* 288, 110282. doi: 10.1016/j.scienta.2021.110282

Wang, B., and Zhu, S. J. (2017). Pre-storage cold acclimation maintained quality of cold-stored cucumber through differentially and orderly activating ROS scavengers. *Postharvest. Biol. Tec.* 129, 1–8. doi: 10.1016/j.postharvbio.2017.03.001

Xie, M. D., Chen, W. Q., Dai, H. B., Wang, X. Q., Li, Y., Kang, Y. C., et al. (2021). Cadmium-induced hormesis effect in medicinal herbs improves the efficiency of safe utilization for low cadmium-contaminated farmland soil. *Ecotoxicol. Environ. Saf.* 225, 112724. doi: 10.1016/j.ecoenv.2021.112724

Xu, Z. G., Dong, M., Peng, X. Y., Ku, W. Z., Zhao, Y. L., and Yang, G. Y. (2019). New insight into the molecular basis of cadmium stress responses of wild paper mulberry plant by transcriptome analysis. *Ecotoxicol. Environ. Saf.* 171, 301–312. doi: 10.1016/j.ecoenv.2018.12.084

Yang, H. Y., Sun, M., Lin, S. J., Gao, Y. H., Yang, Y. J., Zhang, T. X., et al. (2017). Transcriptome analysis of *Crossostephium chinensis* provides insight into the molecular basis of salinity stress responses. *PloS One* 12, e0187124. doi: 10.1371/journal.pone.0187124

Yilmaz, D. D., and Parlak, K. U. (2011). Changes in proline accumulation and antioxidative enzyme activities in *Groenlandia densa* under cadmium stress. *Ecol. Indic.* 11, 417–423. doi: 10.1016/j.ecolind.2010.06.012

Yin, M., Pan, L. L., Liu, J. F., Yang, X. J., Tang, H. J. , Zhou, Y. X., et al. (2022). Proanthocyanidins alleviate cadmium stress in industrial hemp (*Cannabis sativa* l.). *Plants* 11, 2364. doi: 10.3390/plants11182364

Youssef, N. A. (2021). Changes in the morphological traits and the essential oil content of sweet basil (*Ocimum basilicum* l.) as induced by cadmium and lead treatments. *Int. J. Phytoremediation* 23, 291–299. doi: 10.1080/15226514.2020.1812508

Yuan, H. M., Liu, W. C., Jin, Y., and Lu, Y. T. (2013). Role of ROS and auxin in plant response to metal-mediated stress. *Plant Signal. Behav.* 8, e24671. doi: 10.4161/psb.24671

Yuan, X. H., Xue, N. D., and Han, Z. G. (2021). A meta-analysis of heavy metals pollution in farmland and urban soils in China over the past 20 years. *J. Environ. Sci.* 101, 217–226. doi: 10.1016/j.jes.2020.08.013

Yu, E., Wang, W. G., Yamaji, N., Fukuoka, S., Che, J., Ueno, D., et al. (2022). Duplication of a manganese/cadmium transporter gene reduces cadmium accumulation in rice grain. *Nat. Food* 3, 597–607. doi: 10.1038/s43016-022-00569-w

Zhang, J. W., Cao, X. R., Yao, Z. Y., Lin, Q., Yan, B. B., Cui, X. Q., et al. (2021). Phytoremediation of cd-contaminated farmland soil *via* various sedum alfredii-oilseed rape cropping systems: Efficiency comparison and cost-benefit analysis. *J. Hazard. Mater.* 419, 126489. doi: 10.1016/j.jhazmat.2021.126489

Zhang, M., Hong, L. Z., Gu, M. F., Wu, C. D., and Zhang, G. (2020). Transcriptome analyses revealed molecular responses of *Cynanchum auriculatum* leaves to saline stress. *Sci. Rep.* 10, 499. doi: 10.1038/s41598-019-57219-8

Zhang, H., and Reynolds, M. (2019). Cadmium exposure in living organisms: A short review. *Sci. Total Environ.* 678, 761–767. doi: 10.1016/j.scitotenv.2019.04.395

Zheljazkov, V. D., Craker, L. E., and Xing, B. (2006). Effects of cd, Pb, and Cu on growth and essential oil contents in dill, peppermint, and basil. *Environ. Exp. Bot.* 58, 9–16. doi: 10.1016/j.envexpbot.2005.06.008

Zhou, L. H., Li, K. N., Duan, X. Y., Hill, D., Barrow, C., Dunshea, F., et al. (2022). Bioactive compounds in microalgae and their potential health benefits. *Food Biosci.* 49, 101932. doi: 10.1016/j.fbio.2022.101932

Zhu, H. H., Ai, H. L., Cao, L. W., Sui, R., Ye, H. P., Du, D. Y., et al. (2018). Transcriptome analysis providing novel insights for cd-resistant tall fescue responses to cd stress. *Ecotoxicol. Environ. Saf.* 160, 349–356. doi: 10.1016/j.ecoenv.2018.05.066

Zhu, T. T., Li, L. Y., Duan, Q. X., Liu, X. L., and Chen, M. (2021). Progress in our understanding of plant responses to the stress of heavy metal cadmium. *Plant Signal. Behav.* 16, 1836884. doi: 10.1080/15592324.2020.1836884

frontiers | Frontiers in Plant Science

TYPE Original Research
PUBLISHED 02 February 2023
DOI 10.3389/fpls.2022.1035836

OPEN ACCESS

EDITED BY
Oksana Sytar,
Taras Shevchenko National University of Kyiv, Ukraine

REVIEWED BY
Mohammad Sohidul Islam,
Hajee Mohammad Danesh Science &Technology University, Bangladesh
Meilin Wu,
South China Sea Institute of Oceanology (CAS), China

*CORRESPONDENCE
Shan Chen
chenshan@tio.org.cn

SPECIALTY SECTION
This article was submitted to Plant Abiotic Stress, a section of the journal Frontiers in Plant Science

RECEIVED 03 September 2022
ACCEPTED 09 December 2022
PUBLISHED 02 February 2023

CITATION
Chen S (2023) Mechanism of Zn alleviates Cd toxicity in mangrove plants (*Kandelia obovata*). *Front. Plant Sci.* 13:1035836. doi: 10.3389/fpls.2022.1035836

Mechanism of Zn alleviates Cd toxicity in mangrove plants (*Kandelia obovata*)

Shan Chen*

Third Institute of Oceanography, Ministry of Natural Resources, Xiamen, China

Cadmium (Cd) pollution is very common and serious in mangrove ecosystems in China. Zinc (Zn) has been used to reduce Cd accumulation in plants, and phenolic acid metabolism plays an important role in plant response to stress. In present study, in order to clarify whether Zn alleviates Cd toxicity in mangrove plants through phenolic acid metabolism, the Cd-contaminated *Kandelia obovata* plants were treated with different concentrations of (0, 80,300, and 400 $mg{\cdot}kg^{-1}$) $ZnSO_4$ in a set of pot experiments and the biomass, the contents of Cd, Zn, soluble sugar, chlorophyll and the activities of 1,1-diphenyl-2-picrylhydrazyl (DPPH), ferric-reducing antioxidant power (FRAP), L-phenylalanine ammonia-lyase (PAL), shikimic acid dehydrogenase (SKDH), cinnamyl alcohol dehydrogenase (CAD) and polyphenol oxidase (PPO) in the leaves were analyzed. The results showed that Cd contents in the leaves of *Kandelia obovata* ranged from 0.077 to 0.197 $mg{\cdot}kg^{-1}$ under different treatments, and Zn contents ranged from 90.260 to 114.447 $mg{\cdot}kg^{-1}$. Low-dose $ZnSO_4$ treatment (80 $mg{\cdot}kg^{-1}$) performed significant positive effects on the biomass, phenolic acid metabolism-related enzyme activities, antioxidant capacity, and chlorophyll and soluble sugar contents in the leaves of Cd-contaminated mangrove plants. At the meantime, the addition of low-dose $ZnSO_4$ promoted the biosynthesis of hydroxycinnamic acid, hydroxybenzoic acid, and enhanced the plant antioxidant capacity, thus alleviated Cd toxicity in mangrove plants.

KEYWORDS

zinc, cadmium, *Kandelia obovata*, phenolic acid metabolism, reactive oxygen species

Introduction

Mangroves are located in the interlaced zone of coastal areas in tropical regions, and constitute a high-yield ecosystem that supports a variety of plants and animals through the food chain (Bharathkumar et al., 2007). Some common and widely distributed mangrove species, such as *Aegiceras corniculatum*, *Sonneratia caseolaris* and *Kandelia obovata*, have useful metabolite extracts with great medicinal value (Chen et al., 2012). The economic

value of mangroves brings much wealth to human beings; however, various interferences of human activities, such as mining wastes, metal smelting waste residues, and untreated domestic sewage causes mangroves to suffer from serious heavy metal pollution, and their habitats are decreasing in size (Das et al., 2016). Previous research showed that mangroves suffer from serious cadmium (Cd) and zinc (Zn) pollution, and are tolerant to various metal pollution in their environment (Sundaramanickam et al., 2016; Analuddin et al., 2017). Cd is a widely existing nonessential element that is classified as a harmful heavy metal to human health (Chao et al., 2009; Shang et al., 2020). Cd can be absorbed and accumulated by some plants and flows into higher nutrient level organisms through the intricate food chain (Adamczyk-Szabela et al., 2020), threatening human health (Bodin et al., 2013; Chen et al., 2021). Zn is a familiar essential element of plants and animals, and plays a fundamental role in stabilizing and protecting biofilms from oxidative and peroxidative damage (Zhang et al., 2022). However, high levels of Zn can also cause heavy metal pollution in mangrove ecosystems, leading to restricted plant germination, reduced root development and induced plant aging (Lefevre et al., 2014; Chen et al., 2019). Cd and Zn are in the same group with similar physical and chemical properties and always exist together in nature (Zha et al., 2004; Mongkhonsin et al., 2016). Mongkhonsin et al. (2016) proved that Zn can reduce Cd toxicity under Cd and Zn treatments in *Gynura pseudochina*. Our previous studies also found that 100 $mg{\cdot}kg^{-1}$ Zn treatment can ease Cd toxicity in *K. obovata* (Chen et al., 2019). Many researchers have speculated that this phenomenon is caused by phenolic acid metabolism, but no one has specified what the mechanism is or tested any hypothesis.

Phenolic compounds are secondary metabolites consisting of hydroxylated aromatic compounds and carbon-based compounds, which are only found in plants and microorganisms (Tato et al., 2013). Phenolic compounds can protect plant tissues from wounds, oxidative damage, insects and pathogen infections (Ali et al., 2005). For example, *K. obovata* contains various common phenols, such as cinnamic acids, flavonoids and phenylpropanoid derivatives, and their ecological functions have been tested *in vitro* antioxidant and heavy metal bioavailability assays (Lu et al., 2007; Li et al., 2016; Jiang et al., 2017). Phenolic compounds play a variety of important chemical and biological functions in plants to adapt to various changing environments. These physiological processes are metabolic plasticity because plants can respond to external pressures by rapidly inducing phenolic compound synthesis in a reversible way (Tanveer et al., 2022). For instance, the addition of Cd significantly increased the total content of phenol in mangrove species such as *K. obovata* (Kováčik et al., 2009). Numerous studies have also reported that the increase in phenolic compounds in plant tissues and root secretions is a special response to different biological and abiotic stresses (Tato et al., 2013). $ZnSO_4$-treated *K. obovata* plant showed higher biomass and stronger antioxidative capacity as compared to only $CdCl_2$ treated *K. obovata* plant due to the enhancement of its phenolic biosynthesis (Zhao and Zheng, 2015; Chen et al., 2019). Phenolic acids are mainly synthesized by the shikimic acid and phenylpropanoid pathways (Ali et al., 2005; Barros et al., 2019). The precursors of shikimic acid-mediated phenolic acid synthesis are mainly aromatic amino acids, phenylpropyl amino acids, and tryptophan produced by simple carbohydrate glycolysis and the pentose phosphate pathway (Abdulrazzak et al., 2006). The shikimic acid pathway is a common pathway that provides precursors for subsequent secondary metabolites. It also shows how primary and secondary aromatic metabolism are related. It has been estimated that 60% of the total plant biomass consists of molecules passing through the shikimic acid pathway (Tato et al., 2013). According to the above analysis, the soluble sugar content in plant leaves directly influences the amount of phenolic compound synthesis, and the synthesis of soluble sugar is formed by the photosynthesis of plants, while plant photosynthetic ability is closely related to leaf chlorophyll content. Therefore, this experiment measured the soluble sugar content and chlorophyll content of plants to assess their phenolic acid metabolism. Phenolic compound metabolism-related enzymes include L-phenylalanine ammonia-lyase (PAL), which can catalyze phenylalanine to cinnamate; shikimic acid dehydrogenase (SKDH), which can provide substrate for PAL; cinnamyl alcohol dehydrogenase (CAD), which can provide precursors for the synthesis of lignin; and polyphenol oxidase (PPO), which can catalyze the oxidation of catechol to catechol diquinone and act on the substrate monophenol monooxygenase (Kováčik et al., 2009). These phenolic acids are considered to be effective substances protecting plants against oxidative damage caused by heavy metal stress. The structure of phenolic acids endows them with a strong ability to scavenge free radicals and chelate heavy metals, which prevents Fenton reactions. In particular, phenolic acids such as caffeic acid, chlorogenic acid, ferulic acid, and *p*-coumaric acid have been shown to have greater antioxidant capacity than hydroxyl derivatives of benzoic acid such as *p*-hydroxybenzoic acid, vanillic acid, and syringic acid (Sgherri et al., 2003). Phenolic acids not only function in free radical scavenging but also inhibits lipid peroxidation and electron donors (Shi et al., 2010; Maqsood et al., 2014). Therefore, they can be used as excellent reaction substrates for some antioxidant enzymes (peroxidases) to reduce oxidative stress (Oh et al., 2009; Posmyk et al., 2009). In addition, phenolic acids can protect photosynthetic organs from light damage under heavy metal stress (Burchard and Weissenbock, 2000; MacFarlane and Burchett, 2000). Recently, it has been reported that phenolic acid content is related to the heavy metal tolerance process of mangroves, particularly which can prevent mangrove plants against oxidative damage caused by heavy metal stress (Michalak, 2006; Das et al., 2016; Rui et al., 2016; Jiang et al., 2017). 1,1-Diphenyl-2-picrylhydrazyl (DPPH) is a free radical that can remain stable at room temperature and produces a violet

solution in ethanol. However, it can be reduced in the presence of an antioxidant molecule, giving rise to uncolored ethanol solutions. The use of DPPH provides a simple and rapid method for evaluating antioxidants (Mensor et al., 2001; Adjimani and Asare, 2015). Ferric-reducing antioxidant power (FRAP) is another method to estimate the antioxidant capacity of phenolic acids (Afroz et al., 2016).

To date, nutrient supply has been an effective method to induce tolerance responses to different heavy metals in plants, such as selenium (Se), phosphorus (P) and silicon (Si) (Xie et al., 2014; Cui et al., 2017), or organic acid supplies, such as salicylic acid (SA) and jasmonic acid (JA). They act against stress by enhancing antioxidant activity or chelating with heavy metals that stimulate plant growth (Irtelli and Navari-Izzo, 2006; Khan et al., 2016; Liu et al., 2016). However, there are few studies on the effects of heavy metal interactions on phenolic acid metabolism in plants. Therefore, the purpose of this study was to explore the following questions: whether the addition of $ZnSO_4$ could alleviate the toxicity of Cd on plants, and whether its resistance could be attributed to heavy metal interaction effects of phenolic acid metabolism in *K. obovata*.

Materials and methods

Plant material collection and treatments

In this study, mature *K. obovata* hypocotyls were obtained from Jiulongjiang Estuary, Fujian Province, China. The hypocotyls of *K. obovata* were soaked in mass concentration of 1 % $KMnO_4$ solution for 24 h, and then rinsed with distilled water. Hypocotyls with strong vitality were selected for sand culture until four-leaf seedlings were obtained, and then seedlings of the same size were transplanted to 2L plastic buckets in soil culture.

The soil was collected from the Cd-contaminated mangrove wetland, Jiulongjiang Estuary. Sampling points were located at 24°28′ N, 117°24′ E. The background values of Cd and Zn in sediments were 3.99 and 367.54 $mg{\cdot}kg^{-1}$, respectively. The collected soil was treated with $ZnSO_4$ ($ZnSO_4{\cdot}7H_2O$) after debris removal. The addition of $ZnSO_4$ were 0, 80, 300, and 400 $mg{\cdot}kg^{-1}$ for Zn0, Zn80, Zn300 and Zn400 treatments, respectively. The treatment without $ZnSO_4$ addition (Zn0) was used as the control, then the soils were stirred well for 30 days before the seedlings were transplanted into cultivation for 60 days. Each treatment was repeated three times.

Determination of chlorophyll content in leaves

The mature leaves with no middle veins were cut into small pieces, and 0.2 g of the fresh leaves was weighed in a mortar containing a small amount of calcium carbonate and quartz sand. Then, 5 ml of 95% ethanol was added to the mortar, and homogenized until the tissues turned white. The mixture was filtered through a funnel, and distilled water was added to the filtrate to equal 25 ml. The absorbance of the filtrate was measured at wavelengths of 645 and 663 nm. The chlorophyll content was calculated by the equation of Sae-Lee et al. (2012).

Determination of soluble sugar in leaves

Soluble sugar was extracted from freeze-dried powder (0.1 g) of leaves with 1.5 mL sodium phosphate buffer (pH 6.8). The samples were centrifuged for 20 min at 12,000 × g, and 0.5 mL supernatant was measured and mixed with 0.5 mL phenol (5 %) and 2.5 mL concentrated sulfuric acid. The mixture was shaken well, and left at room temperature for 30 min to color. Then, the absorbance was measured with distilled water as the blank at the wavelength of 485 nm. The standard curve was drawn with sucrose (100 $\mu g{\cdot}L^{-1}$) as the standard solution (Falahi et al., 2018).

Determination of Cd and Zn content

In order to determine the content of Cd^{2+} and Zn^{2+} in the leaves, 0.05 g of dried *K. obovata* leaves were digested with 5 ml nitric acid and 1 ml H_2O_2 for 4 h, and then diluted with 50 ml distilled water. The total content of Cd^{2+} and Zn^{2+} in the leaves was measured directly by inductively coupled plasma mass spectrometry (ICP-MS) (Agilent 7500 ICP-MS, USA) (Chen et al., 2019).

Detection of phenolic acids by high-performance liquid chromatography coupled to triple-quadrupole mass spectrometry (HPLC-QQQ-MS)

For the qualitative and quantitative determination of phenolic acids 0.1 g of ground lyophilized plant leaves were leached with 3 ml of water by oscillating at 300 rpm at 4°C for 4 h, followed by overnight maceration. The resulting extract was centrifuged at 7,500 rpm at 4°C for 10 min, and filtered with through a 0.45 μm polyvinylidene fluoride (PVDF) membrane. The Agilent 1290 LC 6490 QQQ was used for HPLC-MS analysis. Chromatographic column specifications were as follows: 00D-4462-YD, Kinetex 2.6 μ C18 100A, and New Column 100 × 3.0 mm high-performance chromatographic column. The mobile phase consisted of two solvents: (A) 2% glacial acetic acid, and (B) methanol; the gradient program started with 75% of mobile phase A at 1 min, which decreased to 73 % in 8 min and then to 50 % in 3 min and after that increased to 75 % in 2 min. The velocity of the mobile phase was

0.3 ml min^{-1}, and the injection sample volume was 0.5 µl. The column temperature was 30°C, and the pressure was 500 bar. The mass spectrometer was operated in a multiple reaction monitoring mode (MRM). Mass spectrometric detection was operated in a negative ion mode after electrospray ionization. The following parameters were used for the mass spectrometer: capillary voltage, 3,371 V; drying gas (nitrogen) temperature, 350°C; flow, 11.0 L min^{-1}; and collision gas, nitrogen (99.999%) (Chen et al., 2020). The *m/z* ratios for precursor and product ions of target analytes, as well as collision energies and retention times, are presented in Figures 1, S1 (Supplementary Materials), and Table 1, respectively.

Phenolic acid metabolism-related enzyme assay

To determine the PAL activities, 0.2 g of fresh leaves were homogenized in liquid nitrogen, and then extracted with 4 ml buffer solution (50 mM Tris pH 8.5, 14.4 mM 2-meryl ethanol, 5% w/v insoluble polyvinyl polypyrrolidone). The homogenate was centrifuged at 12,000 × g for 15 min at 4°C. Then, 0.5 mM, pH 8.0 Tris-HCl buffer and 10 µM L-phenylalanine solution were added to the obtained supernatant, and the mixture was incubated at 35 °C for 2 h. The reaction was terminated with 50 µl of 5 M hydrochloric acid. The content of reacted L-phenylalanine in the presence of PAL was determined by UV-spectrophotometry at 290 nm. The total protein concentration in the extract was measured by the Bradford (1976) method. PAL activity was expressed as nmol·min^{-1}·mg^{-1} protein (Ali et al., 2006).

To determine the SKDH, CAD and PPO activities, fresh leaves were homogenized in a mortar with 50 mM potassium phosphate buffer (pH 7.0) at 4°C. The obtained homogenates were stored in an ice bath and centrifuged successively at a speed of 15,000 g for 15 min at 4°C (Kováčik et al., 2009; Blasco et al., 2013). The obtained supernatant was the crude enzyme extract. To determine SKDH activity, 0.1 M Tris-HCl buffer (pH 9), 1.45 ml of 2 mM shikimic acid, and 1.45 ml of 0.5 mM NADP was gradually added to the 0.1 mL crude enzyme solution. The absorbance was read at 340 nm over 1 min, and the molar absorbance of 6.22 mM^{-1} cm^{-1} was used to calculate its activity. CAD activity was measured by using 0.1 M Tris-HCl buffer (pH 8.8). The reaction tube contained 1.45 ml of 1 mM coniferyl alcohol, 1.45 ml of 1 mM NADP and 0.1 ml of supernatant. Measurement and calculation of CAD activity were calculated the same way as SKDH activity. PPO detection experiment was carried out in a reaction centrifuge tube containing 2.85 ml of 50 mM (pH 7.0) potassium phosphate buffer, 50 µl of 60 mM catechol and 0.1 ml of crude enzyme extract. The absorbance was read at 420 nm after 2 min. Activity was expressed as units of activity (UA) in which one unit of PPO was defined as the change in one unit of absorbance min^{-1} protein content (UA $mg^{-1}g^{-1}$ FW and recalculated with the known protein) (Kováčik et al., 2009).

DPPH (1,1-diphenyl-2-picrylhydrazyl) free radical-scavenging activity and ferric-reducing antioxidant power (FRAP) of phenolic acids in leaves assay

A total of 3 ml of distilled water was added to 0.1 g of ground freeze-dried leaves. Then, the homogenate was shaken at 300 rpm at 4°C for 4 h, and subsequently centrifuged at 7,500 rpm at 4°C for 10 min. The supernatant was filtered with a 0.22 µm membrane to obtain the phenolic acid crude extract of the leaves.

A 0.1 g·L^{-1} DPPH solution was made by dissolving in a small amount of toluene and then diluting with 60% ethanol. Two milliliters of phenolic acid crude extract was transferred to 2 ml of 0.1 g·L^{-1} DPPH solution, and then rapidly mixed and stored at room temperature for 20 min without light. The absorbance was measured at 517 nm with 60% ethanol as a blank. The DPPH

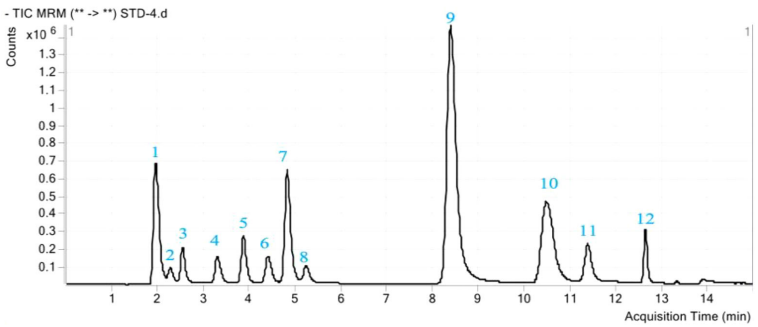

FIGURE 1
A total ion chromatogram (TIC) of phenolic acid mixture standards. The peak number represents the twelve phenolic acids as follows: 1, Pyrogallic acid; 2, Coumaric acid; 3, Protocatechuic acid; 4, Chlorogenic acid; 5, 4-Hydroxy benzoic acid; 6, Caffeic acid; 7, Syringic acid; 8, Vanillin; 9, Ferulic acid; 10, Benzoic acid; 11, Salicylic acid; 12, Cinnamic acid.

TABLE 1 LC-ESI-QQQ-MS/MS analysis of these phenolic acids.

Compound	Molecular formula	Retention time (min)	Collision energy		ESI-MS *m/z*	
			E1 (V)	E2 (V)	[M-H]	MS/MS fragment
Pyrogallic acid	$C_6H_6O_3$	1.954	20	10	124.9	79.1, 97
Coumaric acid	$C_6H_4O_4$	2.264	0	0	139.09	139.1, 95
Protocatechuic acid	$C_7H_6O_4$	2.519	10	5	153	109.1, 153
Chlorogenic acid	$C_{16}H_{18}O_9$	3.259	15	5	353	190.8, 352.9
4-Hydroxybenzoic acid	$C_7H_6O_3$	3.844	10	0	137.1	93.1, 137.1
Caffeic acid	$C_9H_8O_4$	4.418	30	30	179	134, 88.9
Syringic acid	$C_9H_{10}O_5$	4.858	15	30	197.17	123, 95
Vanillin	$C_8H_8O_3$	5.246	5	5	150.9	136.1, 151
Ferulic acid	$C_{10}H_{10}O_4$	8.283	5	5	192.9	177.8, 134
Benzoic acid	$C_7H_6O_2$	10.374	0	10	121	121, 77.1
Salicylic acid	$C_7H_6O_3$	11.308	15	5	137.1	93.1, 137.1
Cinnamic acid	$C_9H_8O_2$	12.592	5	5	147.1	103, 147

radical scavenging activity was then calculated (Afroz et al., 2016). The preparation method of the FRAP reagent was the same methods as described by Afroz et al. (2016). The above phenolic acid crude extract of 200 µl was mixed with 1.5 ml of FRAP reagent and reacted at 37°C for 4 min. The absorbance of the mixture was measured at 593 nm using distilled water as the blank. Then, the FRAP of phenolic acids in the leaves was calculated.

Statistical analysis

All data related to biomass, Cd, Zn and phenolic acid content and enzyme activity of the *K. obovata* leaves were submitted to SPSS 25 software for variance analysis (ANOVA), the results were expressed as the Mean ± SD, Pearson correlation analysis was used for detecting relationship among the index of biomass, Cd content, Zn content, soluble sugar content, chlorophyll content, DPPH, FRAP, PAL ability, SKDH ability, CAD ability and PPO ability. Duncan multi-range test was conducted at the significance level ($P \leq 0.05$) of 5 % to compare the differences among them.

Results

Effects of $ZnSO_4$ treatments on the biomass and heavy metal content of Cd-contaminated *K. obovata* leaves

As shown in Table 2, the addition of $ZnSO_4$ treatments significantly affected the leaves biomass, Cd content and Zn content of Cd-contaminated *K. obovata*. In contrast to the control (Zn0 treatment), the leaves biomass increased 13.7 % under Zn80 treatment, but the results significantly decreased by 15.1 and 33.4 % under Zn300 and Zn400 treatments, respectively. At the meantime, the Cd content in the leaves significantly reduced by 31.9 % under Zn80 treatment, but the results significantly increased by 74.3 and 72.5 % under Zn300

TABLE 2 Effects of $ZnSO_4$ treatments on biomass, cadmium content and zinc content in the leaves of cadmium contaminated *K. obovata*.

Treatments	Biomass (g·plant^{-1})	Cd content (mg·kg^{-1})	Zn content (mg·kg^{-1})
Zn0	1.820 ± 0.170 c	0.113 ± 0.015 b	90.260 ± 4.860 a
Zn80	2.070 ± 0.163 c	0.077 ± 0.006 a	100.450 ± 2.234 ab
Zn300	1.545 ± 0.105 b	0.197 ± 0.003 c	109.339 ± 3.638 bc
Zn400	1.213 ± 0.094 a	0.195 ± 0.005 c	114.447 ± 10.229 c
p-value	***	***	**

Values are the mean ± SD (n = 3). Means followed by the same letter do not differ significantly. Levels of significance: **p < 0.01; ***p < 0.001.

and Zn400 treatments, respectively (Table 2). Zn content in the leaves increased by 11.3 % under Zn80 treatment, but the results significantly increased by 21.3 and 26.7 % under Zn300 and Zn400 treatments, respectively (Table 2).

Effects of $ZnSO_4$ treatments on the contents of total chlorophyll (ChlT) and soluble sugar in the leaves of Cd-contaminated *K. obovata*

As shown in Figure 2A, the highest total chlorophyll content in the leaves (1.825 $mg{\cdot}g^{-1}$ FW) was observed at Zn80 treatment, which was higher than that of Zn300 or Zn400 treatments, but no significant difference was found between Zn80 and Zn0, Zn300 and Zn400 treatments. By comparing with the control (64.80 $mg{\cdot}g^{-1}$), the soluble sugar contents under Zn300 and Zn400 treatments significantly increased by 13.5 and 22.2 %, respectively, but it significantly decreased by 6.7 % under Zn80 treatment (Figure 2B).

Effects of $ZnSO_4$ treatments on phenolic compounds content in the leaves of Cd-contaminated *K. obovata*

As shown in Table 3, the contents of phenolic compounds (not including Sal) obviously increased under Zn300 and Zn400 treatments, but no significant differences were found between Zn80 and Zn0 treatments. The maximum contents of Gal, Pro, Sal, Ben, Fer, Cou and Chl were found in Zn300 treatment, and the contents of Gal, Pro, Ben, Fer, Cou and Chl were significantly higher than that of Zn400 treatment. The maximum contents of Hyd and Cin were found in Zn400 treatment, but there were no significant differences between Zn300 and Zn400 treatments (Table 3). It is worth noting that, among all detected phenolic acids, Hyd, Cin and Chl were the main phenolic compounds in the levels of treated plants (Table 3 and Figure S2).

Effects of $ZnSO_4$ treatments on phenolic acid metabolism related enzyme activities in the leaves of Cd-contaminated *K. obovata*

The activities of phenolic acid metabolism related enzymes were obviously impacted by the addition of $ZnSO_4$ treatments (Table 4). Compared with the control, PAL activity in leaves of the plants significantly increased by 22.4% and 43.4%, under Zn300 and Zn400 treatments. However, it declined by 27.7 % under Zn80 treatment (Table 4). The activities of SKDH, CAD and PPO in leaves of the plant totally increased with the levels of $ZnSO_4$ treatments, and the strongest activity were detected under Zn400 treatment, which were by 86.2, 38.8 and 97.2 % higher than those of the control, respectively. But there were no differences in the activities of SKDH, CAD and PPO between Zn80 treatment and the control (Table 4).

Effects of $ZnSO_4$ treatment on antioxidant activity of Cd-contaminated *K. obovata* leaves

As shown in Figure 3, the DPPH free radical scavenging activity and FRAP values remarkably increased by Zn300 and Zn400 treatments. However, there were no significant differences were observed between Zn80 treatment and the control (Figures 3A, B). With respect to the control, the DPPH free radical scavenging activity increased by 115.6~127.3 %, and the FRAP values increased by 31.1~38.7 % under Zn300 and Zn400 treatments (Figure 3A, B).

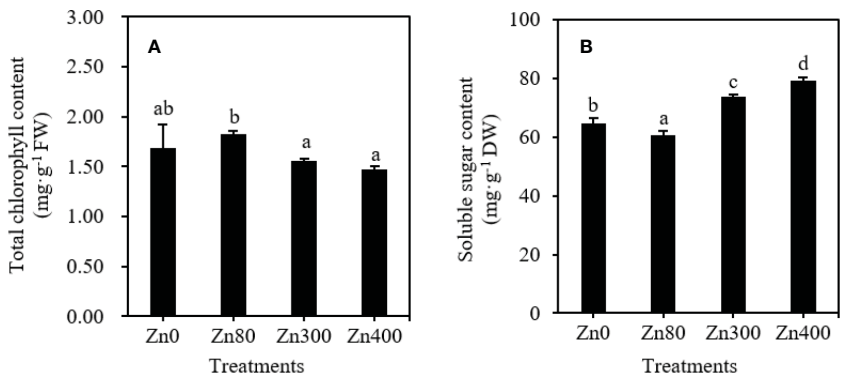

FIGURE 2
The contents of total chlorophyll **(A)**, soluble sugar **(B)** in leaves of Cd-contaminated K. obovata under different concentration of Zn treatments. The data are shown as the means ± SD (n=3).

TABLE 3 Effects of $ZnSO_4$ treatments on phenolic compounds (PCs) in Cd-contaminated *K. obovata*.

PCs ($\mu g \cdot g^{-1}$)	Treatment				*p*-value
	Zn0	Zn80	Zn300	Zn400	
Pyrogallic acid	0.015 ± 0.003 a	0.013 ± 0.002 a	0.151 ± 0.027 b	0.038 ± 0.010 a	***
4-Hydroxybenzoic acid	1.359 ± 0.130 a	0.988 ± 0.291a	3.633 ± 1.392 b	4.180 ± 0.727 b	***
Protocatechuic acid	0.033 ± 0.006 a	0.030 ± 0.002 a	0.076 ± 0.008 b	0.035 ± 0.016 a	*
Salicylic acid	0.027 ± 0.010 a	0.022 ± 0.003 a	0.079 ± 0.030 b	0.054 ± 0.032 ab	ns
Benzoic acid	0.068 ± 0.005 a	0.073 ± 0.004 a	0.222 ± 0.037 c	0.118 ± 0.016 b	***
Ferulic acid	0.089 ± 0.017 a	0.108 ± 0.025 a	0.204 ± 0.025 b	0.134 ± 0.050 a	***
Couramic acid	0.022 ± 0.009 a	0.016 ± 0.001 a	0.415 ± 0.008 c	0.158 ± 0.074 b	*
Chlorogenic acid	2.007 ± 0.072 a	1.847 ± 0.133 a	6.228 ± 1.854 b	1.696 ± 1.974 a	***
Cinnamic acid	0.601 ± 0.045 a	0.668 ± 0.223 a	2.589 ± 0.455 b	2.785 ± 0.374 b	***

Values are the mean ± SD (n = 3). Means followed by the same letter do not differ significantly. Levels of significance: *, P < 0.05; ***, P < 0.001; ns, not significant. Gal, pyrogallic acid; Hyd, 4-hydroxy benzoic acid; Pro, protocatechuic acid; Sal, salicylic acid; Ben, benzoic acid; Fer, ferulic acid; Cou, coumaric acid; Chl, chlorogenic acid; Cin, cinnamic acid.

Correlations among the physiological index in the leaves

As shown in Table 5, the leaves biomass had a positive correlation with chlorophyll content (r = 0.74), but showed a negative correlation with soluble sugar content (r = –0.90), Cd content (r = –0.89) Zn content (r = –0.61), SKDH activity (r = –0.88), CAD activity (r = –0.83) and PPO activity (r = –0.87). The positive correlations were found between Zn content and soluble sugar content (r = 0.94), the activities of SKDH (r = 0.78), CAD (r = 0.80), PPO (r = 0.80), DPPH (r = 0.79) and FRAP (r = 0.64) in leaves. Cd contents in leaves were highly positively correlated to Zn content (r = 0.66), soluble sugar content (r = 0.94), the activities of DPPH (r = 0.95), FRAP (r = 0.86), PAL (r = 0.90), SKDH (r = 0.87), CAD (r = 0.91), and PPO (r = 0.92) in leaves, whereas Cd contents in leaves had a negative correlation with chlorophylls content (r = -0.74) in leaves (Table 5). Thus, we can see that Cd treatments inhibited the growth of *K. obovata*, while Zn application improved the free radical-scavenging ability of *K. obovata*.

Discussion

Biomass, Cd and Zn content of *K. obovata* leaves

Biomass is one of the important indicators that reflect whether the growth of a plant is restrained (Kováčik and Bačkor, 2007; Wang et al., 2016). The addition of 300 or 400 $mg \cdot kg^{-1}$ $ZnSO_4$ inhibited the growth of *K. obovata*, while 80 $mg \cdot kg^{-1}$ $ZnSO_4$ promoted the growth of *K. obovata* (Table 2). These results suggest that treatment with this concentration of Zn^{2+} (≤ 80 $mg \cdot kg^{-1}$ $ZnSO_4$) may initiate a special heavy metal tolerance mechanism to alleviate the Cd toxicity in *Kandelia obovata* plants to some extent.

The toxicity of heavy metal stress to plants not only causes plant growth to slow down, but also leads to the accumulation of heavy metals in plant leaves (Armas et al., 2014). The accumulation of Cd^{2+} and Zn^{2+} ions in plant leaves can trigger membrane lipid peroxidation (Jia et al., 2017), causing the production of reactive oxygen species (ROS)

TABLE 4 Effects of $ZnSO_4$Effects of ZnSO4 treatments on phenolic compounds metabolism related enzymes activity in the leaves of Cd-contaminated *K. obovata*.

Activity	Treatments				*p*-value
	Zn0	Zn80	Zn300	Zn400	
PAL ($nmol \cdot min^{-1} \cdot mg^{-1}$)	20.30 ± 3.16 b	14.67 ± 0.47 a	24.84 ± 0.71 c	29.11 ± 1.33 d	***
SKDH ($nmol \cdot min^{-1} \cdot mg^{-1}$)	215.24 ± 4.333a	226.79 ± 4.60 a	325.24 ± 13.29 b	400.79 ± 18.44 c	***
CAD ($nmol \cdot min^{-1} \cdot mg^{-1}$)	223.82 ± 6.14 a	230.55 ± 16.39 a	294.49 ± 13.82 b	310.69 ± 9.29 b	***
PPO ($UA \cdot mg^{-1}$)	1.44 ± 0.06 a	1.50 ± 0.05 a	2.44 ± 0.12 b	2.84 ± 0.09 c	***

Values are the mean ± SD (n = 3). Means followed by the same letter do not differ significantly. Levels of significance: ***, P < 0.001. PAL, L- phenylalanine ammonia-lyase; SKDH, shikimic acid dehydrogenase; CAD, cinnamyl alcohol dehydrogenase; PPO, polyphenol oxidase.

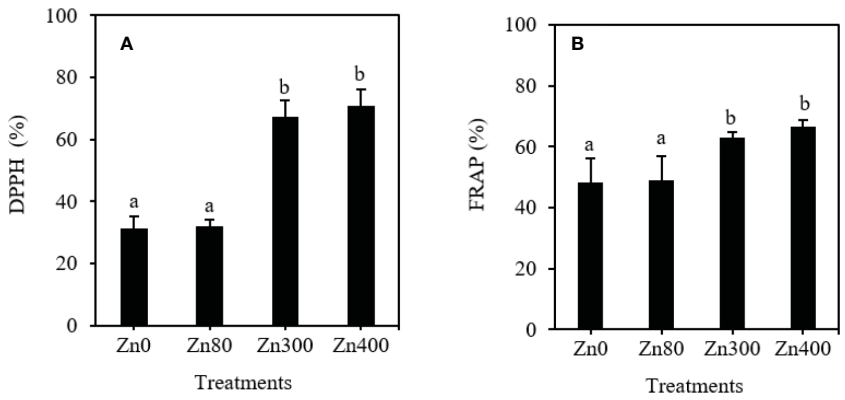

FIGURE 3
The scavenging ability of DPPH **(A)** and FRAP **(B)** of phenolic acids in leaves of Cdcontaminated *K. obovata* under different concentration of Zn treatments. The data are shown as the means ± SD (n=3). DPPH, 1,1-diphenyl-2-picrylhydrazyl; FRAP, ferric-reducing antioxidant power.

(Weng et al., 2012). In this study, the control plants showed lower ion concentrations of Cd^{2+} and Zn^{2+} than those in plants treated with 300 or 400 mg·kg^{-1} $ZnSO_4$ (Table 2). The contents of Cd^{2+} and Zn^{2+} in leaves treated with high concentrations of $ZnSO_4$ could account for the depress *K. obovata* leaf biomass found in these treatments (Table 2). In addition, 300 or 400 mg·kg^{-1} $ZnSO_4$ caused an increase in the Cd^{2+} and Zn^{2+} concentrations compared to the control treatment (Table 2), probably because of the synergism between the Cd^{2+} and Zn^{2+}. However, 80 mg·kg^{-1} $ZnSO_4$ treatment inhibited the Cd^{2+} absorption in leaves (Table 2), likely due to the antagonism between the Cd^{2+} and Zn^{2+}. Therefore, it can be seen that Cd and Zn have antagonistic effects under low concentration Zn treatment and synergistic effects under high concentration Zn treatment. The past report also confirmed these findings (Wang et al., 2016). This phenomenon could be explained by the competition between Zn and Cd because of their similar chemical properties (Wang et al., 2016). Zn is an essential element for plant growth at low concentrations, whereas Cd is a non-essential metal for plants with a low toxicity threshold (5–10 mg·kg^{-1}) (Wang et al., 2016). To counteract the toxicity of Cd, plants must increase the transport of Zn from roots to shoots. Another group of authors have suggested that the interaction between Cd and Zn is synergistic. In heavy metal hyper accumulative plants, the

TABLE 5 Pearson correlation coefficients among biomass, the contents of Cd, Zn, soluble sugar, chlorophyll and the activities of DPPH, FRAP, PAL, SKDH, CAD and PPO in the leaves of Cd-contaminated *Kandelia obovata*.

Physiological index	Cd content	Zn content	Soluble sugar content	Chlorophyll content	DPPH	FRAP	PAL activity	SKDH activity	CAD activity	PPO activity
Biomass	−0.89**	−0.61*	−0.90**	0.74**	−0.86**	−0.76**	−0.88**	−0.88**	−0.83**	−0.87**
Cd content	1	0.66*	0.94**	−0.74**	0.95**	0.86**	0.90**	0.87**	0.91**	0.92**
Zn content		1	0.70*	−0.56	0.79**	0.64*	0.57	0.78**	0.80**	0.80**
Soluble sugar content			1	−0.72**	0.93**	0.87**	0.96**	0.95**	0.91**	0.95**
Chlorophyll content				1	−0.71*	−0.55	−0.67*	−0.72**	−0.74**	−0.76**
DPPH					1	0.90**	0.84**	0.94**	0.96**	0.97**
FRAP						1	0.73**	0.84**	0.89**	0.87**
PAL activity							1	0.88**	0.82**	0.87**
SKDH activity								1	0.93**	0.98**
CAD activity									1	0.97**

*Correlation is less than or equal to 0.05 level (2-tailed); **Correlation is less than or equal to 0.01 level (2-tailed).

accumulation of Zn in the stems was positively correlated with the Cd levels in plants, and the author believes that the stimulation of Cd accumulation in stems was related to the increased xylem transport of Cd from roots to shoots (Wang et al., 2016). Additionally, it was reported that most accumulated Zn could be bonding to polygalacturonic acids and carbohydrates in the cell wall (Xing et al., 2008). It has been reported that another possible mechanism for *A. marina* with excessive Zn accumulation is to secrete excess Zn through leaf glands (MacFarlane and Burchett, 2000). Under Cd and Zn pollution conditions, the growth of *K. obovata* was only slightly affected by Zn300 treatment, but an obvious reduction of foliar biomass of *K. obovata* was observed in Zn400 treatment. These results imply that low concentration Zn^{2+} treatment could alleviate Cd toxicity, but high concentration Zn^{2+} treatment could increase the toxicity of heavy metals to *K. obovata*. The main mechanism of Zn^{2+} treatment alleviate the stress by Cd pollution in *K. obovata* can be explained by the improvement of antioxidant capacity induced by Zn^{2+}. This can be further confirmed by the metabolism of phenolic acids and their oxidation abilities (Lavid et al., 2001; Sgherri et al., 2003; Kováčik et al., 2009).

Chlorophyll content, soluble carbohydrate content, and their relationships with phenolic acid metabolism

Phenolic acids are synthesized from the amino acids produced by glycolysis, which is closely related to the photosynthesis of plants (Cocetta et al., 2015). Chlorophyll consists the foundation of plant photosynthesis (Li et al., 2022). The reduction of total chlorophyll content was often found in biologically stressed plants which under nutrient imbalance or oxidative stress induced by heavy metal stress (Wang et al., 2011). In present study, we found that the total chlorophyll content in leaves decreased under Zn300 and Zn400 treatments, however, increased under Zn80 treatment (Figure 2A). The above results showed that adding 80 $mg{\cdot}kg^{-1}$ $ZnSO_4$ under high concentration of Cd pollution could enhance the photosynthesis of plants, and increase the biomass, while adding 300 or 400 $mg{\cdot}kg^{-1}$ $ZnSO_4$ treaments weaken the photosynthesis of plants. Soluble sugar is one of the products of photosynthesis, the levels of soluble sugar directly influenced the biosynthesis of phenolic acids, and the accumulation of flavonoid compounds (Cocetta et al., 2015). In our study, the change trend of soluble sugar content in leaves of *K. obovata* under Zn stress was contrary to that of total chlorophyll content (Figure 2B). This can be comfirmed by the significant negative correlationship between total chlorophyll content and soluble sugar content, and the significant positive correlationship between soluble sugar content and phenolic acids (Table 5). Therefore, the soluble sugar content can indirectly reflect the amount of phenolic acid synthesis. However, we only know that the synthesis of phenolic acid is based on sugar metabolism. So, it is necessary to further explore whether the high sugar content does necessarily lead to the high metabolism of phenolic acids.

Effects of heavy metal stress on phenolic acid metabolism

Phenolic acids are often produced when animals and plants are subjected to abiotic and biotic stresses. In previous studies, Loponen et al. (2001) found that birch leaves from contaminated areas had higher levels of several low-molecular weight phenols than birch leaves from control areas. Blasco et al. (2013) found that phenolic acids are powerful antioxidants that can scavenge free radicals and other oxidizing substances. However, little work has been done on the response of phenolic acids to heavy metals in mangrove plants. Some studies have suggested that high concentrations of Zn and/or Cd promote phenolic acid synthesis in herbal plants (Mongkhonsin et al., 2016). Higher levels of phenolic compounds were found in both young and old leaves of *Matricaria chamomilla* following long-term exposure to 60 and 120 μM $CdCl_2$ (Kováčik et al., 2009). Similar results were found in blueberry plantlets in response to Cd pollution (Manquian-Cerda et al., 2016). Whereas, whether low concentration of Zn treatment alleviating Cd toxicity is due to the upregulated metabolism of some phenolic compounds, it needed to be uncovered. This study found that long-term exposure to Zn300 or Zn400 treatments obviously increased the content of some phenolic acid metabolites (Table 3), but the effects of 80 $mg{\cdot}kg^{-1}$ $ZnSO_4$ treatment was not as significant as those treated with 300 or 400 $mg{\cdot}kg^{-1}$ $ZnSO_4$. This discrepancy in findings may be due to the heavy metal endurance of plant (Sgherri et al., 2003) and the higher concentrations of Cd (3.99 $mg{\cdot}kg^{-1}$), and Zn (367.54 $mg{\cdot}kg^{-1}$) in soil sediments of this experiment. Additionally, previous results have shown that inhibiting phenolic acid metabolism would result in early death of leaves of transgenic tobacco plant and change its cell morphology (Lodovico et al., 1998). Therefore, most of the studies have shown that phenolic acid metabolism is closely related to the normal growth of plants. Indeed, soluble sugar is formed by the photosynthesis of plants, which is closely linked to shikimic acid pathway and directly influences the amount of phenolic compound synthesis (Tato et al., 2013). So the same change trends of phenolic acid content and soluble sugar content in the leaves of Cd-contaminated *K. obovata* under different $ZnSO_4$ treatments. It can be concluded that the higher the soluble sugar content in the leaves, the more phenolic acid synthesis occurs.

Mechanism of heavy metal tolerance involved in phenolic acid metabolism

In our work, the application of $ZnSO_4$ treatment in Cd-contaminated sediment, especially 300 and 400 $mg{\cdot}kg^{-1}$ $ZnSO_4$

treatments, raised the content of phenolic acids in leaves of *K. obovata* (Table 3). The enhancement of phenolic acid content caused by $ZnSO_4$ addition allowed plants to survive high concentrations of Cd stress (Tables 2, 3). These phenolic acids are considered to play an important role in protecting the *K. obovata* from oxidative damage caused by Cd stress. Because phenolic acids are strong antioxidants, they can scavenge free radicals and ROS (Kim et al., 2006). The properties of phenolic acids are determined by their structures, which mainly depend on the number and position of the hydroxyl groups on the aromatic ring (Kim et al., 2006). The phenolic acids in *K. obovata* plants are usually divided into two groups: benzoic and cinnamic acid derivatives. The antioxidant activity of cinnamic acid derivatives such as ferulic acid, caffeic acid and *p*-coumaric acid was higher than that of hydroxybenzoic acid derivatives such as *p*-hydroxybenzoic acid vanillic acid and salicylic acid (Kim et al., 2006). That is because that the presence of the CH=CH–COOH group in the hydroxycinnamic acids is considered to be key for the significantly higher antioxidative efficiency compared to the COOH in the hydroxybenzoic acids (Kim et al., 2006). In addition, phenolic acids can mitigate the effects of oxidative stress due to its electron donor functions and can be used as an excellent substrate for some antioxidant enzymes (Blasco et al., 2013). Table 3 shows that the application of $ZnSO_4$ significantly induces the biosynthesis of cinnamic acid and benzoic acid, which can scavenge free radicals efficiently and stimulate antioxidant activity under different types of adverse stress in plants (Blasco et al., 2013), and the 300 and 400 $mg{\cdot}kg^{-1}$ $ZnSO_4$ treatments can stimulate the synthesis of benzoic and cinnamic acid derivatives more effectively than the 80 $mg{\cdot}kg^{-1}$ $ZnSO_4$ treatment. Therefore, under the same concentration of Cd stress, plants treated with $ZnSO_4$ at low concentration are more resistant to Cd than those without $ZnSO_4$. This is because zinc ion can enhance the plant's tolerance to heavy metals by stimulating the metabolism of phenolic acid. The Zn supplementation could not only be inhibitory for Cd-induced oxidative stress (Garg and Kaur, 2013) by inducing the biosynthesis of phenolic compounds (Mongkhonsin et al., 2016), but also be used as a remediation agent for heavy metals (Rai et al., 2019). The plant phytoavailability of Cd (≥ 54.13%) was significantly reduced in the soil mixed with single superphosphate, triple superphosphate, and calcium magnesium phosphate sepiolite in conjunction with $ZnSO_4$ (Guo et al., 2017). All of these studies indicated that $ZnSO_4$ can alleviate Cd stress and $ZnSO_4$ is an effective remediation agent for Cd pollution soil.

It was reported that the activities of PAL, SKDH, CAD and PPO were enhanced for plants to better resist Cd pollution (Irtelli and Navari-Izzo, 2006; Kováčik et al., 2009). Similar results can be found in our work (Table 4). PAL mediates phenylalanine to produce cinnamic acid, which is a key branching point in primary and secondary metabolism, and it is also the first and most important regulatory step in the formation of many phenolic acids (Cocetta et al., 2015). SKDH is a member of shikimate pathway which can convert simple carbohydrates into aromatic amino acids including phenylalanine (Kováčik et al., 2009). It is one of the enzymes that controls the reaction of carbohydrates toward to phenolic acids and provides a substrate for PAL (Blasco et al., 2013; Chen et al., 2019). Plants can generate gallic acid and 4-hydroxybenzoate through shikimate pathways (Zhou et al., 2019). The 4-hydroxybenzoate and 3,4-dihydroxybenzoic acid are produced by general phenylpropanoid pathway with cinnamic acid precursor. Cinnamic acid is also a precursor for the synthesis of benzoic acid, salicylic acid, caffeic acid, ferulic acid, coumaric acid and vanillin (Renault et al., 2017; Barros et al., 2019). Cinnamic acid and *p*-coumaric acid are substrates of CAD (Barros et al., 2019), which provide precursors for the biosynthesis of lignin (Chen et al., 2019). In fact, phenolic compounds are the substrates of enzymatic browning reactions, which can form colored quinones under the enzymatic oxidation by PPO (Léchaudel et al., 2018). However, the high level of PPO activity reduces the free oxygen level available for ROS production, which may be one of the reason for the reduced ROS level of cellular under stress conditions (Léchaudel et al., 2018). As can be seen from Table 4, the lowest activities of the SKDH, CAD, and PPO found in the control plants (Table 4), corresponding to the minimum concentrations of phenolic acids in *K. obovata* plants. On the contrary, the application of 300 or 400 $mg{\cdot}kg^{-1}$ $ZnSO_4$ treatment increased the activity of PAL, SKDH, CAD and PPO compared with the 80 $mg{\cdot}kg^{-1}$ $ZnSO_4$ treatment (Table 4). These findings could explain why the concentration of phenolic acids increased (Table 3), why phenolic acids can protect plants against heavy metal stress, and why the leaf biomass of the 80 $mg{\cdot}kg^{-1}$ $ZnSO_4$ treatment group was higher than that of the 300 and 400 $mg{\cdot}kg^{-1}$ $ZnSO_4$ treatments groups. It has been reported that stronger phenolic acid metabolism related enzyme activities and the content of phenolic acids are linked to the resistance of plants to abiotic stress (Blasco et al., 2013). Zn^{2+} treatment contributed to the increase in SKDH enzyme activity, which may be due to the promoting influence of Zn on photosynthesis and carbohydrate synthesis. And the additional carbohydrates can be provided to meet the increased synthesis of phenolic acids under Cd stress. PPO activity is correlated with the production of quinine and ROS, so the increase in PPO activity will aggravate oxidative stress (Blasco et al., 2013). The results showed that *K. obovata* had the lowest foliar biomass under the 400 $mg{\cdot}kg^{-1}$ $ZnSO_4$ treatment (Table 2), but its PPO activity was the highest (Table 4), which is related to the greater oxidative stress and the formation of more ROS in these plants. While, the application of 80 $mg{\cdot}kg^{-1}$ $ZnSO_4$ inhibited PPO activity (Table 4), the reduced PPO activity would decrease the concentration of H_2O_2 in the plant, and thus, enhance the plant's ability to resist stress (Thipyapong et al., 2004).

Free radical scavenging ability of phenolic acids

DPPH and FRAP are important indexes to measure the antioxidant potential of phenolic acid effectively (Cocetta et al.,

2015). The DPPH and FRAP values in plant leaves increased under $ZnSO_4$ treatment; adding 300 or 400 $mg{\cdot}kg^{-1}$ $ZnSO_4$ increased the antioxidant capacity of phenolic acid extracts from leaves. In addition, some phenolic acid content of plants under high concentration $ZnSO_4$ treatment was also higher than that of under low concentration $ZnSO_4$ treatment (Table 3). Therefore, the higher the content of some phenolic acids in leaves, the stronger the antioxidant capacity of leaves and the stronger the resistance to Cd oxidative damage. It can also be seen from the Pearson correlation values in Table 5 that the content of Cd and Zn in leaves is highly positively correlated with the activity of enzymes related to phenolic acid metabolism and the content of chlorophyll is highly negatively correlated with the activity of those enzymes; however, the soluble sugar content and the antioxidant capacity were highly positively correlated with the activity of those enzymes. These results indicated that under the pollution of Cd and Zn, *K. obovata* can stimulate the metabolism of phenolic compounds, sugar metabolism, and photosynthesis related to phenolic acid metabolism to improve the antioxidant capacity of plants to resist the oxidative damage caused by heavy metal stress; 80 $mg{\cdot}kg^{-1}$ $ZnSO_4$ can alleviate Cd toxicity by improving the ability of phenolic acid metabolism of plants.

Conclusion

Our findings showed that the application of $ZnSO_4$ to Cd-contaminated sediment increased phenolic acid contents and related enzyme activities in leaves of *K. obovata*. These increases also led to an increase of the biosynthesis of hydroxycinnamic acids, and hydroxybenzoic acid and their derivatives, which have a strong ROS scavenging ability in plant leaves, and can be used as protective compounds for mangrove plants under Cd stress conditions. Overall, this work revealed that the application of repair agents containing low concentrations of $ZnSO_4$ is an effective strategy to raise the resistance of Cd contaminated mangrove plants. This is not only beneficial to improve the growth and reduce Cd accumulation of mangrove plants, but also increase the nutritional value of animal diets, including phenolic compounds the trace element of Zn, in the food chains of mangrove ecosystems.

Data availability statement

The original contributions presented in the study are included in the article/Supplementary Material. Further inquiries can be directed to the corresponding author.

Author contributions

The author confirms being the sole contributor of this work and has approved it for publication.

Funding

This project was supported by the Fujian Provincial Science and Technology (Project, No. 2021Y0066), the Scientific Research Foundation of Third Institute of Oceanography, MNR (No. 2019017 and No. 2020013), and a key technology research and development project based on "Research on ecological restoration technology of land-sea ecotone".

Acknowledgments

The author would like to acknowledge of Professor Chongling Yan of Xiamen University and Professor Ruiyu Lin of Fujian Agricultural and Forest University for their help in revising the article.

Conflict of interest

The author declares that the research was conducted in the absence of any commercial or financial relationships that could be construed as a potential conflict of interest.

Publisher's note

Supplementary material

The Supplementary Material for this article can be found online at: https://www.frontiersin.org/articles/10.3389/fpls.2022.1035836/full#supplementary-material

References

Abdulrazzak, N., Pollet, B., Ehlting, J., Larsen, K., Asnaghi, C., Ronseau, S., et al. (2006). A coumaroyl-ester-3-hydroxylase insertion mutant reveals the existence of nonredundant meta-hydroxylation pathways and essential roles for phenolic precursors in cell expansion and plant growth. *Plant Physiol.* 140 (1), 30–48. doi: 10.1104/pp.105.069690

Adamczyk-Szabela, D., Lisowska, K., Romanowska-Duda, Z., and Wolf, W. M. (2020). Combined cadmium-zinc interactions alter manganese, lead, copper uptake by *Melissa officinalis*. *Sci. Rep.* 10 (1), 1675. doi: 10.1038/s41598-020-58491-9

Adjimani, J. P., and Asare, P. (2015). Antioxidant and free radical scavenging activity of iron chelators. *Toxicol. Rep.* 2, 721–728. doi: 10.1016/j.toxrep.2015.04.005

Afroz, R., Tanvir, E. M., Paul, S., Bhoumik, N. C., Gan, S. H., and Khalil, M. D. I. (2016). DNA Damage inhibition properties of sundarban honey and its phenolic composition. *J. Food Biochem.* 40 (4), 436–445. doi: 10.1111/jfbc.12240

Ali, M. B., Hahn, E. J., and Paek, K. Y. (2005). CO_2-induced total phenolics in suspension cultures of *Panax ginseng* c. a. Mayer roots: role of antioxidants and enzymes. *Plant Physiol. Biochem.* 43 (5), 449–457. doi: 10.1016/j.plaphy.2005.03.005

Ali, M. B., Singh, N., Shohael, A. M., Hahn, E. J., and Paek, K. Y. (2006). Phenolics metabolism and lignin synthesis in root suspension cultures of *Panax ginseng* in response to copper stress. *Plant Sci.* 171 (1), 147–154. doi: 10.1016/j.plantsci.2006.03.005

Analuddin, K., Sharma, S., Jamili,, Septiana, A., Sahidin, I., Rianse, U., et al. (2017). Heavy metal bioaccumulation in mangrove ecosystem at the coral triangle ecoregion, southeast sulawesi, Indonesia. *Mar. pollut. Bull.* 125, 472–480. doi: 10.1016/j.marpolbul.2017.07.065

Armas, T., Pinto, A. P., de Varennes, A., Mourato, M. P., Martins, L. L., Gonçalves, M. L. S., et al. (2014). Comparison of cadmium-induced oxidative stress in *Brassica juncea* in soil and hydroponic cultures. *Plant Soil* 388, 297–305. doi: 10.1007/s11104-014-2330-3

Barros, J., Escamilla-Trevino, L., Song, L., Rao, X., Serrani-Yarce, J. C., Palacios, M. D., et al. (2019). 4-coumarate 3-hydroxylase in the lignin biosynthesis pathway is a cytosolic ascorbate peroxidase. *Nat. Commun.* 10 (1), 1994. doi: 10.1038/s41467-019-10082-7

Bharathkumar, S., RameshKumar, N., Paul, D., Prabavathy, V. R., and Nair, S. (2007). Characterization of the predominant bacterial population of different mangrove rhizosphere soils using 16S rRNA gene-based single-strand conformation polymorphism (SSCP). *World J. Microbiol. Biotechnol.* 24 (3), 387–394. doi: 10.1007/s11274-007-9487-3

Blasco, B., Leyva, R., Romero, L., and Ruiz, J. M. (2013). Iodine effects on phenolic metabolism in lettuce plants under salt stress. *J. Agric. Food Chem.* 61 (11), 2591–2596. doi: 10.1021/jf303917n

Bodin, N., N'Gom-Ka, R., Ka, S., Thiaw, O. T., Tito de Morais, L., Le Loc'h, F., et al. (2013). Assessment of trace metal contamination in mangrove ecosystems from Senegal, West Africa. *Chemosphere* 90 (2), 150–157. doi: 10.1016/j.chemosphere.2012.06.019

Bradford, M. M. (1976). A rapid and sensitive method for the quantitation of microgram quantities of protein utilizing the principle of protein-dye binding. *Analytical Biochem.* 72, 248–254. doi: 10.1016/0003-2697(76)90527-3

Burchard, P., and Weissenbock, G. (2000). Contribution of hydroxycinnamates and flavonoids to epidermal shielding of UV-a and UV-b radiation in developing rye primary leaves as assessed by ultraviolet- induced chlorophyll fluorescence measurements. *Plant Cell Environ.* 23, 1373–1380. doi: 10.1046/j.1365-3040.2000.00633.x

Chao, Y. Y., Chen, C. Y., Huang, W. D., and Kao, C. H. (2009). Salicylic acid-mediated hydrogen peroxide accumulation and protection against cd toxicity in rice leaves. *Plant Soil* 329, 327–337. doi: 10.1007/s11104-009-0161-4

Chen, S., Lin, R. Y., Lu, H. L., Wang, Q., Yang, J. J., Liu, J. C., et al. (2020). Effects of phenolic acids on free radical scavenging and heavy metal bioavailability in *Kandelia obovata* under cadmium and zinc stress. *Chemosphere* 249, 126341. doi: 10.1016/j.chemosphere.2020.126341

Chen, S., Wang, Q., Lu, H., Li, J., Yang, D., Liu, J., et al. (2019). Phenolic metabolism and related heavy metal tolerance mechanism in *Kandelia obovata* under cd and zn stress. *Ecotoxicol. Environ. Saf.* 169, 134–143. doi: 10.1016/j.ecoenv.2018.11.004

Chen, J., Xing, X. K., Zhang, L. C., Xing, Y. M., and Guo, S. X. (2012). Identification of *Hortaea werneckii* isolated from mangrove plant *Aegiceras comiculatum* based on morphology and rDNA sequences. *Mycopathologia* 174 (5-6), 457–466. doi: 10.1007/s11046-012-9568-1

Chen, H., Yang, R., Zhang, X., Chen, Y., Xia, Y., and Xu, X. (2021). Foliar application of gibberellin inhibits the cadmium uptake and xylem transport in lettuce (*Lactuca sativa* l.). *Scientia Hortic.* 288, 1–8. doi: 10.1016/j.scienta.2021.110410

Cocetta, G., Rossoni, M., Gardana, C., Mignani, I., Ferrante, A., and Spinardi, A. (2015). Methyl jasmonate affects phenolic metabolism and gene expression in blueberry (*Vaccinium corymbosum*). *Physiol. Plant* 153 (2), 269–283. doi: 10.1111/ppl.12243

Cui, J., Liu, T., Li, F., Yi, J., Liu, C., and Yu, H. (2017). Silica nanoparticles alleviate cadmium toxicity in rice cells: Mechanisms and size effects. *Environ. pollut.* 228, 363–369. doi: 10.1016/j.envpol.2017.05.014

Das, S. K., Patra, J. K., and Thatoi, H. (2016). Antioxidative response to abiotic and biotic stresses in mangrove plants: A review. *Int. Rev. Hydrobiol.* 101 (1-2), 3–19. doi: 10.1002/iroh.201401744

Falahi, H., Sharifi, M., Maivan, H. Z., and Chashmi, N. A. (2018). Phenylethanoid glycosides accumulation in roots of *Scrophularia striata* as a response to water stress. *Environ. Exp. Bot.* 147, 13–21. doi: 10.1016/j.envexpbot.2017.11.003

Garg, N., and Kaur, H. (2013). Response of antioxidant enzymes, phytochelatins and glutathione production towards cd and zn stresses in *Cajanus cajan* (L.) millsp. genotypes colonized by *Arbuscular mycorrhizal* fungi. *J. Agron. Crop Sci.* 199 (2), 118–133. doi: 10.1111/j.1439-037X.2012.00533.x

Guo, G. H., Lei, M., Chen, T. B., and Yang, J. X. (2017). Evaluation of different amendments and foliar fertilizer for immobilization of heavy metals in contaminated soils. *J. Soils Sediments* 18 (1), 239–247. doi: 10.1007/s11368-017-1752-y

Irtelli, B., and Navari-Izzo, F. (2006). Influence of sodium nitrilotriacetate (NTA) and citric acid on phenolic and organic acids in *Brassica juncea* grown in excess of cadmium. *Chemosphere* 65 (8), 1348–1354. doi: 10.1016/j.chemosphere.2006.04.014

Jiang, S., Weng, B., Liu, T., Su, Y., Liu, J., Lu, H., et al. (2017). Response of phenolic metabolism to cadmium and phenanthrene and its influence on pollutant translocations in the mangrove plant *Aegiceras corniculatum* (L.) blanco (Ac). *Ecotoxicol. Environ. Saf.* 141, 290–297. doi: 10.1016/j.ecoenv.2017.03.041

Jia, X., Zhao, Y. H., Liu, T., and He, Y. H. (2017). Leaf defense system of *Robinia pseudoacacia* l. seedlings exposed to 3 years of elevated atmospheric CO_2 and cd-contaminated soils. *Sci. Total Environ.* 605-606, 48–57. doi: 10.1016/j.scitotenv.2017.06.172

Khan, I., Iqbal, M., Ashraf, M. Y., Ashraf, M. A., and Ali, S. (2016). Organic chelants-mediated enhanced lead (Pb) uptake and accumulation is associated with higher activity of enzymatic antioxidants in spinach (*Spinacea oleracea* l.). *J. Hazard Mater.* 317, 352–361. doi: 10.1016/j.jhazmat.2016.06.007

Kim, K., Tsao, R., Yang, R., and Cui, S. (2006). Phenolic acid profiles and antioxidant activities of wheat bran extracts and the effect of hydrolysis conditions. *Food Chem.* 95 (3), 466–473. doi: 10.1016/j.foodchem.2005.01.032

Kováčik, J., and Bačkor, M. (2007). Changes of phenolic metabolism and oxidative status in nitrogen-deficient *Matricaria chamomilla* plants. *Plant Soil* 297 (1-2), 255–265. doi: 10.1007/s11104-007-9346-x

Kováčik, J., Klejdus, B., Hedbavny, J., Štork, F., and Bačkor, M. (2009). Comparison of cadmium and copper effect on phenolic metabolism, mineral nutrients and stress-related parameters in *Matricaria chamomilla* plants. *Plant Soil* 320 (1-2), 231–242. doi: 10.1007/s11104-009-9889-0

Lavid, N., Schwartz, A., Lewinsohn, E., and Tel-Or, E. (2001). Phenols and phenol oxidases are involved in cadmium accumulation in the water plants *Nymphoides peltata* (Menyanthaceae) and *Nymphaeae* (Nymphaeaceae). *Planta* 214 (2), 189–195. doi: 10.1007/s004250100610

Léchaudel, M., Darnaudery, M., Joët, T., Fournier, P., and Joas, J. (2018). Genotypic and environmental effects on the level of ascorbic acid, phenolic compounds and related gene expression during pineapple fruit development and ripening. *Plant Physiol. Biochem.* 130, 127–138. doi: 10.1016/j.plaphy.2018.06.041

Lefevre, I., Vogel-Mikus, K., Jeromel, L., Vavpetic, P., Planchon, S., Arcon, I., et al. (2014). Differential cadmium and zinc distribution in relation to their physiological impact in the leaves of the accumulating *Zygophyllum fabago* l. *Plant Cell Environ.* 37 (6), 1299–1320. doi: 10.1111/pce.12234

Li, J., Liu, J. C., Lu, H. L., Jia, H., Yu, J. Y., Hong, H. L., et al. (2016). Influence of the phenols on the biogeochemical behavior of cadmium in the mangrove sediment. *Chemosphere* 144, 2206–2213. doi: 10.1016/j.chemosphere.2015.10.128

Liu, Z., Ding, Y., Wang, F., Ye, Y., and Zhu, C. (2016). Role of salicylic acid in resistance to cadmium stress in plants. *Plant Cell Rep.* 35 (4), 719–731. doi: 10.1007/s00299-015-1925-3

Li, Y., Xin, J., Ge, W., and Tian, R. (2022). Tolerance mechanism and phytoremediation potential of *Pistia stratiotes* to zinc and cadmium co-contamination. *Int. J. Phytoremediation.* 1-8. doi: 10.1080/15226514.2021.2025201

Lodovico, T., Angel, M., Nicola, S., Kitty, P., Adrian, P., Chi, F. C., et al. (1998). Inhibition of phenolic acid metabolism results in precocious cell death and altered cell morphology in leaves of transgenic tobacco plants. *Plant Cell* 10, 1801–1816. doi: 10.1105/tpc.10.11.1801

Loponen, J., Lempa, K., Ossipov, V., Kozlov, M. V., Girs, A., Hangasmaa, K., et al. (2001). Patterns in content of phenolic compounds in leaves of mountain birches along a strong pollution gradient. *Chemosphere* 45, 291–301. doi: 10.1016/S0045-6535(00)00545-2

Lu, H. L., Yan, C. L., and Liu, J. C. (2007). Low-molecular-weight organic acids exuded by mangrove (*Kandelia candel* (L.) druce) roots and their effect on cadmium species change in the rhizosphere. *Environ. Exp. Bot.* 61 (2), 159–166. doi: 10.1016/j.envexpbot.2007.05.007

MacFarlane, G. R., and Burchett, M. D. (2000). Cellular distribution of copper, lead and zinc in the grey mangrove, *Avicennia marina* (Forsk.) vierh. *Aquat. Bot.* 68, 45–59. doi: 10.1016/S0304-3770(00)00105-4

Manquian-Cerda, K., Escudey, M., Zuniga, G., Arancibia-Miranda, N., Molina, M., and Cruces, E. (2016). Effect of cadmium on phenolic compounds, antioxidant enzyme activity and oxidative stress in blueberry (*Vaccinium corymbosum* l.) plantlets grown *in vitro*. *Ecotoxicol. Environ. Saf.* 133, 316–326. doi: 10.1016/j.ecoenv.2016.07.029

Maqsood, S., Benjakul, S., Abushelaibi, A., and Alam, A. (2014). Phenolic compounds and plant phenolic extracts as natural antioxidants in prevention of lipid oxidation in seafood: A detailed review. *Compr. Rev. Food Sci. Food Saf.* 13 (6), 1125–1140. doi: 10.1111/1541-4337.12106

Mensor, L. L., Menezes, F. S., Leitão, G. G., Reis, A. S., Santos, T. C. D., Coube, C. S., et al. (2001). Screening of Brazilian plant extracts for antioxidant activity by the use of DPPH free radical method. *Phytother. Res.* 15 (2), 127–130. doi: 10.1002/ptr.687

Michalak, A. (2006). Phenolic compounds and their antioxidant activity in plants growing under heavy metal stress. *Polish J. @ Environ. Stud.* 15, 523–530.

Mongkhonsin, B., Nakbanpote, W., Hokura, A., Nuengchamnong, N., and Maneechai, S. (2016). Phenolic compounds responding to zinc and/or cadmium treatments in *Gynura pseudochina* (L.) DC. extracts and biomass. *Plant Physiol. Biochem.* 109, 549–560. doi: 10.1016/j.plaphy.2016.10.027

Oh, M. M., Trick, H. N., and Rajashekar, C. B. (2009). Secondary metabolism and antioxidants are involved in environmental adaptation and stress tolerance in lettuce. *J. Plant Physiol.* 166 (2), 180–191. doi: 10.1016/j.jplph.2008.04.015

Posmyk, M. M., Kontek, R., and Janas, K. M. (2009). Antioxidant enzymes activity and phenolic compounds content in red cabbage seedlings exposed to copper stress. *Ecotoxicol. Environ. Saf.* 72 (2), 596–602. doi: 10.1016/j.ecoenv.2008.04.024

Rai, P. K., Lee, S. S., Zhang, M., Tsang, Y. F., and Kim, K. H. (2019). Heavy metals in food crops: Health risks, fate, mechanisms, and management. *Environ. Int.* 125, 365–385. doi: 10.1016/j.envint.2019.01.067

Renault, H., Alber, A., Horst, N. A., Basilio Lopes, A., Fich, E. A., Kriegshauser, L., et al. (2017). A phenol-enriched cuticle is ancestral to lignin evolution in land plants. *Nat. Commun.* 8, 14713. doi: 10.1038/ncomms14713

Rui, H., Chen, C., Zhang, X., Shen, Z., and Zhang, F. (2016). Cd-induced oxidative stress and lignification in the roots of two *Vicia sativa* l. varieties with different cd tolerances. *J. Hazard Mater.* 301, 304–313. doi: 10.1016/j.jhazmat.2015.08.052

Sae-Lee, N., Kerdchoechuen, O., and Laohakunjit, N. (2012). Chemical qualities and phenolic compounds of Assam tea after soil drench application of selenium and aluminium. *Plant Soil.* 356, 381–393. doi: 10.1007/s11104-012-1139-1

Sgherri, C., Cosi, E., and Navari-Izzo, F. (2003). Phenols and antioxidative status of *Raphanus sativus* grown in copper excess. *Physiologia Plantarum* 118, 21–28. doi: 10.1034/j.1399-3054.2003.00068.x

Shang, X., Xue, W., Jiang, Y., and Zou, J. (2020). Effects of calcium on the alleviation of cadmium toxicity in *Salix matsudana* and its effects on other minerals. *Polish J. @ Environ. Stud.* 29 (2), 2001–2010. doi: 10.15244/pjoes/109720

Shi, C., Xu, M. J., Bayer, M., Deng, Z. W., Kubbutat, M. H., Watjen, W., et al. (2010). Phenolic compounds and their anti-oxidative properties and protein kinase inhibition from the Chinese mangrove plant *Laguncularia racemosa*. *Phytochemistry* 71 (4), 435–442. doi: 10.1016/j.phytochem.2009.11.008

Sundaramanickam, A., Shanmugam, N., Cholan, S., Kumaresan, S., Madeswaran, P., and Balasubramanian, T. (2016). Spatial variability of heavy metals in estuarine, mangrove and coastal ecosystems along parangipettai, southeast coast of India. *Environ. pollut.* 218, 186–195. doi: 10.1016/j.envpol.2016.07.048

Tanveer, Y., Yasmin, H., Nosheen, A., Ali, S., and Ahmad, A. (2022). Ameliorative effects of plant growth promoting bacteria, zinc oxide nanoparticles and oxalic acid on *Luffa acutangula* grown on arsenic enriched soil. *Environ. pollut.* 300, 118889. doi: 10.1016/j.envpol.2022.118889

Tato, L., De, N. P., Donnini, S., and Zocchi, G. (2013). Low iron availability and phenolic metabolism in a wild plant species (*Parietaria judaica* l.). *Plant Physiol. Biochem.* 72, 145–153. doi: 10.1016/j.plaphy.2013.05.017

Thipyapong, P., Melkonian, J., Wolfe, D. W., and Steffens, J. C. (2004). Suppression of polyphenol oxidases increases stress tolerance in tomato. *Plant Sci.* 167 (4), 693–703. doi: 10.1016/j.plantsci.2004.04.008

Wang, C., Zhang, S., Wang, P., Hou, J., Qian, J., Ao, Y., et al. (2011). Salicylic acid involved in the regulation of nutrient elements uptake and oxidative stress in *Vallisneria natans* (Lour.) hara under Pb stress. *Chemosphere* 84 (1), 136–142. doi: 10.1016/j.chemosphere.2011.02.026

Wang, S. F., Zhao, Y., Guo, J. H., and Zhou, L. Y. (2016). Effects of cd, Cu and zn on *Ricinus communis* l. growth in single element or co-contaminated soils: Pot experiments. *Ecol. Eng.* 90, 347–351. doi: 10.1016/j.ecoleng.2015.11.044

Weng, Z. X., Wang, L. X., Tan, F. L., Huang, L., Xing, J. H., Chen, S. P., et al. (2012). Proteomic and physiological analyses reveal detoxification and antioxidation induced by cd stress in *Kandelia candel* roots. *Trees* 27 (3), 583–595. doi: 10.1007/s00468-012-0811-7

Xie, X. Y., Weng, B., Cai, B. P., Dong, Y. R., and Yan, C. L. (2014). Effects of arbuscular mycorrhizal inoculation and phosphorus supply on the growth and nutrient uptake of *Kandelia obovata* (Sheue, liu & yong) seedlings in autoclaved soil. *Appl. Soil Ecol.* 75, 162–171. doi: 10.1016/j.apsoil.2013.11.009

Xing, J. P., Jiang, R. F., Ueno, D., Ma, J. F., Schat, H., McGrath, S. P., et al. (2008). Variation in root-to-shoot translocation of cadmium and zinc among different accessions of the hyperaccumulators *Thlaspi caerulescens* and *Thlaspi praecox*. *New Phytol.* 178 (2), 315–325. doi: 10.1111/j.1469-8137.2008.02376.x

Zha, H. G., Jiang, R. F., Zhao, F. J., Vooijs, R., Schat, H., Barker, J. H. A., et al. (2004). Co-Segregation analysis of cadmium and zinc accumulation in *Thlaspi caerulescens* interecotypic crosses. *New Phytol.* 163, 299–312. doi: 10.1011/j.1469-8137.2004.01113.x

Zhang, H., Zhang, W., Huang, S., Xu, P., Cao, Z., Chen, M., et al. (2022). The potential role of plasma membrane proteins in response to zn stress in rice roots based on iTRAQ and PRM under low cd condition. *J. Hazard Mater.* 429, 128324. doi: 10.1016/j.jhazmat.2022.128324

Zhao, H., and Zheng, W. J. (2015). Effects of zinc stress on growth and antioxidant enzyme responses of *Kandelia obovata* seedlings. *Toxicol. Environ. Chem.* 97 (9), 1190–1201. doi: 10.1080/02772248.2015.1094476

Zhou, K., Hu, L. Y., Li, Y. T. S., Chen, X. F., Zhang, Z. J., Liu, B. B., et al. (2019). MdUGT88F1-mediated phloridzin biosynthesis regulates apple development and valsa canker resistance. *Plant Physiol.* 180 (4), 2290–2305. doi: 10.1104/pp.19.00494

frontiers | Frontiers in Plant Science

TYPE Original Research
PUBLISHED 23 February 2023
DOI 10.3389/fpls.2023.1086098

OPEN ACCESS

EDITED BY
Walid Soufan,
King Saud University, Saudi Arabia

REVIEWED BY
Kotb Attia,
King Saud University, Saudi Arabia
Hai-Ming Zhao,
Jinan University, China

*CORRESPONDENCE
Xiao-Zhang Yu
xzyu@glut.edu.cn

†These authors have contributed equally to this work

SPECIALTY SECTION
This article was submitted to Plant Abiotic Stress, a section of the journal Frontiers in Plant Science

RECEIVED 01 November 2022
ACCEPTED 06 February 2023
PUBLISHED 23 February 2023

CITATION
Feng Y-X, Yang L, Lin Y-J, Song Y and Yu X-Z (2023) Merging the occurrence possibility into gene co-expression network deciphers the importance of exogenous 2-oxoglutarate in improving the growth of rice seedlings under thiocyanate stress.
Front. Plant Sci. 14:1086098.
doi: 10.3389/fpls.2023.1086098

Merging the occurrence possibility into gene co-expression network deciphers the importance of exogenous 2-oxoglutarate in improving the growth of rice seedlings under thiocyanate stress

Yu-Xi Feng†, Li Yang†, Yu-Juan Lin, Ying Song and Xiao-Zhang Yu*

College of Environmental Science and Engineering, Guilin University of Technology, Guilin, China

Thiocyanate (SCN^-) can find its way into cultivated fields, which might hamper the harmony in carbon and nitrogen metabolism (CNM) of plants, ebbing their quality and productivity. In the current study, we investigated the role of the exogenous application of 2-oxoglutarate (2-OG) in maintaining homeostasis of CNM in rice seedlings under SCN^- stress. Results showed that SCN^- exposure significantly repressed the gene expression and activities of CNM-related enzymes (e.g., phosphoenolpyruvate carboxylase, NADP-dependent isocitrate dehydrogenases, and isocitrate dehydrogenases) in rice seedlings, thereby reducing their relative growth rate (RGR). Exogenous application of 2-OG effectively mitigated the toxic effects of SCN^- on rice seedlings, judged by the aforementioned parameters. The co-expression network analysis showed that genes activated in CNM pathways were categorized into four modules (Modules 1–4). In order to identify the key module activated in CNM in rice seedlings exposed to SCN^-, the results from real-time quantitative PCR (RT-qPCR) tests were used to calculate the possibility of the occurrence of genes grouped in four different modules. Notably, Module 3 showed the highest occurrence probability, which is mainly related to N metabolism and 2-OG synthesis. We can conclude that exogenous application of 2-OG can modify the imbalance of CNM caused by SCN^- exposure through regulating N metabolism and 2-OG synthesis in rice seedlings.

KEYWORDS

rice, thiocyanate, 2-OG, carbon metabolism, nitrogen metabolism

1 Introduction

Carbon (C) and nitrogen (N) are the two primary nutrient species, and their adequate supply and dynamic balance of both elements should be essential for regulating cellular functions during plant growth and development (Zheng, 2009; Naseeruddin et al., 2018). It is well known that C-rich biomolecules (e.g., sucrose, glucose, and fructose) provide the majority of energy and C-skeletons for ammonium (NH_4^+) assimilation, while N-containing compounds are parts of organic (e.g., amino acids and proteins) and simple inorganic compounds (e.g., nitrate [NO_3^-] and NH_4^+), which can be synthesized through the incorporation of NH_4^+ into the C-skeletons (Zheng, 2009). At the enzymatic level, nitrate reductase (NR), glutamine synthetase (GS), sucrose-phosphate synthase (SPS), trehalose-6-phosphate synthase (TPS), and glutamyl tRNA synthetase (ERS) play a dominant role in regulating the carbon and nitrogen metabolism (CNM) in plants (Coruzzi and Zhou, 2001). However, various environmental stimuli, such as pollutants, drought, salinity, fertilization, and extreme temperature, can influence and destabilize CNM-associated enzymes, thereby weakening the yield and quality of crops (Xin et al., 2019; Alves et al., 2021; Guo et al., 2021).

Thiocyanate (SCN^-), being part and parcel of many industrial activities (e.g., manufacturing of chemical insecticide and herbicide, production of thiourea, metal separation, and gold mining), is continuously marking its imprint in a clean environment (Yu and Zhang, 2013). Notably, gold ore processing generates a large amount of SCN^- because of the lixiviant cyanide complexed with the reduced sulfur species in the gold-bearing ore (Gao et al., 2022). Even mine waste is treated before being discharged, with the aim to convert cyanide into SCN^- (Gould et al., 2012). Different governing bodies have issued standards regarding the discharge of cyanide-rich effluent in the environment considering its environmental risk and health hazard (Mudder and Botz, 2004); however, discharge of SCN^- in effluent has not been restricted by standards, ultimately raising SCN^- level in the effluent (Gould et al., 2012). Indeed, the levels of SCN^- at 1,000 mg SCN/L were detected in gold tailings wastewaters (Gao et al., 2022). Persistence of higher levels of SCN^- in soils, sediments, rivers, and aquatic biota in nearby areas of gold mines has been observed, which eventually makes its entry into the food chain and poses a threat to all living organisms (Bhunia et al., 2000; Yu and Zhang, 2013; Sun et al., 2018; Lin et al., 2020). Indeed, accumulation of SCN^- in plants can cause serious damage to plant growth and development by decreasing nutrient balance and transpiration, degrading photosynthetic pigments, changing the free amino acid composition, and inhibiting the activities of antioxidant enzymes (Hansson et al., 2008; Yu and Zhang, 2013). Our previous studies at the physio-biochemical and molecular levels also indicated that SCN^- exposure is able to result in the dysfunction of chloroplast (Yang et al., 2021). These studies suggested that the negative effects of SCN^- exposure on the CNM in rice seedlings are detectable.

In recent years, the application of plant growth regulators has been suggested to curtail the negative impact imposed by various abiotic factors (Yang et al., 2021). It is evident that 2-oxoglutarate (2-OG) is a key organic acid involved in the processes of CNM in plants (Yue et al., 2018; Ji et al., 2020). Specifically, the GS initially converts NH_4^+ into glutamine in an ATP-dependent reaction; afterward, the glutamate synthase (GOGAT) catalyzes the conversion of glutamine and 2-OG into two molecules of glutamate. Clearly, there is a mandatory interaction between N metabolism and C metabolism (Gálvez et al., 1999). In addition, exogenous application of 2-OG can enhance the activities of phosphoenolpyruvate carboxylase (PEPC), GS, and NADP-dependent isocitrate dehydrogenases (NADP-ICDH) in roots of rice (Yuan et al., 2007). Feeding of exogenous 2-OG can also improve the transcripts of N metabolism-related genes in plants (Araújo et al., 2014). These studies suggested the positive feedback of exogenous 2-OG on the CNM in plants. To date, little is known about the role of exogenous 2-OG in regulating the imbalance of CNM induced by SCN^- in plants.

Rice (*Oryza sativa* L.) is one of the most important staple food crops worldwide, especially in eastern Asia countries (Mostofa et al., 2014). Nowadays, agricultural crops suffer from various environmental issues. The SCN^- is a typical N-containing pollutant that can be assimilated by rice plants. Therefore, in the present study, we hypothesized that SCN^- can disturb the CNM in rice plants during the detoxification of exogenous SCN^-, while the application of exogenous 2-OG can maintain homeostasis of CNM in rice seedlings in response to SCN^- exposure. To prove this hypothesis, the following works were performed: 1) we estimated the relative growth rate and percentage of carbon/nitrogen of rice seedlings under SCN^- exposure with or without exogenous 2-OG, 2) we analyzed the effects of exogenous 2-OG on CNM-related genes and enzymes under SCN^- stress, and 3) we clarified the strategies of exogenous 2-OG to regulate the imbalance of CNM in rice plants under SCN^- exposure by merging the occurrence possibility into a co-expression module analysis. Overall, this study provides new evidence to expand our understanding of exogenous 2-OG to regulate the imbalance of CNM in rice plants during SCN^- exposure.

2 Methods and materials

2.1 Plant growth and experiment design

The seeds of a regular medium-maturing indica rice (*O. sativa* L. XZX 45) were sowed in river sand after being soaked in distilled water for 24 h and then moved inside an artificial climate chamber with a controlled temperature of 25°C ± 0.5°C at a relative humidity of 60% ± 2% Zhang et al., 2022. The rice seedlings were irrigated daily with a modified 8692 nutrient solution, which was described in our previous work (Yang et al., 2021). The modified 8692 nutrient solution with KNO_3 (39.5 mg N/L) was used. After 16-day growth, rice seedlings of similar size were collected and incubated in a MES-Tris solution (pH = 6.0) for 4 h to remove additional ions from the root surface and the apparent free space. These pretreated seedlings were transferred into a nutrient solution spiked with SCN^- and utilized in subsequent experiments. Two treatment series were conducted:

(1) SCN^- treatments: SCN^- spiked solutions at concentrations of 0 (control 1), 24.0, 96.0, and 300.0 mg SCN/L. Control 1 refers to the nutrient solution without SCN^- and exogenous 2-OG.

(2) "SCN^- + 2-OG" treatments: seedlings were pretreated with a 2-OG solution at a concentration of 4 mmol/L for 4 h (Fritz et al., 2006), and then seedlings were exposed to SCN^- solution at 0 (control 2), 24.0, 96.0, and 300.0 mg SCN/L. Control 2 refers to the nutrient solution without SCN^-, but with exogenous 2-OG.

Exposure concentrations of SCN^- used were based on three different effective concentrations (ECs), i.e., EC_{20}, EC_{50}, and EC_{75}, referring to the 20%, 50%, and 75% inhibition of relative growth rates of rice seedlings, respectively (Lin et al., 2020). All seedlings were placed in the plant growth chamber for a 3-day exposure. Potassium thiocyanate (KSCN) of analytical grade purity with 98.5% purity was purchased from Sinopharm Chemical Reagent Co., Ltd. (Shanghai, China). α-Ketoglutaric acid (2-OG) of analytical grade purity with 98.0% purity was obtained from Shanghai Macklin Biochemical Co., Ltd. (Shanghai, China). To minimize water loss and prevent algae growth, each flask was covered with aluminum foil. Each treatment concentration was performed with four independent replicates.

2.2 Analysis of growth parameter

The relative growth rate (RGR) is one of the most crucial parameters to reflect the performance of plants under various stresses (Lin et al., 2020). The RGR (%) was calculated using the biomass change of young seedlings during SCN^- exposure, as follows:

$$RGR = \frac{W_{(F)} - W_{(I)}}{W_{(I)}} \times 100\,\% \quad , \quad (1)$$

where $W_{(I)}$ and $W_{(F)}$ are the initial and final fresh weights of rice seedlings, respectively.

2.3 Measurement of total C and N contents in rice tissues

After exposure to the SCN^- solution for 3 days, rice seedlings were harvested and separated into roots and shoots. After being washed with double-distilled water, plant materials were oven dried at 90°C for 48 h and weighed. Then, 0.010 g of oven-dried plant materials was grained into fine powder. Total C and N (%) were measured by a vario elemental analyzer (vario EL) (Brown et al., 2007).

2.4 Measurements of activities of CNM-related enzymes in rice tissues

Activities of enzymes related to C metabolism, including PEPC (Osuna et al., 1996),ERS (Ratinaud et al., 1983), TPS (Goddijn et al., 1997), and SPS (Feng et al., 2019) in rice tissues were assayed (detailed information is shown in Supplementary material M1).

Activities of enzymes activated in N metabolism, namely, NR (Ahanger et al., 2021), nitrite reductase (NiR) (Lin et al., 2022a), and GS (Hou et al., 2019) in rice tissues were determined (detailed information is shown in Supplementary material M1).

Activities of enzymes involved in 2-OG biosynthesis, i.e., NADP-ICDH (Gálvez et al., 1994), isocitrate dehydrogenases (NAD-IDH) (Gálvez et al., 1994), and glutamate dehydrogenases (GDH) (Turano et al., 1996), were also measured (detailed information is shown in Supplementary material M1).

2.5 RNA extraction and RT-qPCR analysis

Real-time quantitative PCR (RT-qPCR) was used to quantify the expression levels of CNM-related enzymes in rice seedlings after SCN^- exposure. Total RNA was extracted from both the root and shoot of all rice samples by using an Ultrapure RNA Kit (CWBio, Taizhou, China). DNase I (CWBio, Taizhou, China) was used to remove genomic DNA contamination, if any, from RNA extract. Then, the total RNA was purified by an RNeasy MinElute Cleanup Kit (Qiagen, Hilden, Germany). Each sample was prepared in four independent biological replicates.

A total of 40 genes encoding enzymes or proteins activated in the CNM pathways were searched from the databases, including RGAP (http://rice.plantbiology.msu.edu/analyses_search_blast.shtml), NCBI (https://www.ncbi.nlm.nih.gov/), and RAPDB (http://rapdb.dna.affrc.go.jp/). Expression of genes was assayed after SCN^- exposure by RT-qPCR analysis, including PEPC (*Osppc1*, *Osppc2a*, *Osppc3*, and *Osppc4*), ERS (*OsERS1*, *OsERS2*, and *OsERS3*), TPS (*OsTPS1*, *OsTPS4*, *OsTPS5*, *OsTPS8*, and *OsTPS9*), SPS (*OsSPS1*, *OsSPS2*, *OsSPS4*, *OsSPS5*, and *OsSPS6*), NR (*OsNIA1*, *OsNIA2*, and *OsNR1*), NiR (*OsNiR1*, *OsNiR2*, and *OsNiR3*), GS (*OsGS1;1*, *OsGS1;2*, *OsGS1;3*, and *OsGS2*), NADP-ICDH (*OsICDH1*, *OsICDH2*, *OsICDH3*, and *OsICDH4*), NAD-IDH (*OsIDHc;2*, *OsIDHc;1*, *OsIDHa*, and *OsIDH1*), and GDH (*OsGDH1*, *OsGDH2*, *OsGDH3*, and *OsGDH4*). All genes primer sequences are listed in Table S1. RT-qPCR cycling conditions were as follows: 1) denaturation at 95°C for 10 s, 2) annealing at 58°C for 30 s, and 3) extension at 72°C for 32 s. This cycle was imitated 40 times. The RT-qPCR analysis was executed using the 7500 Fast Real-Time PCR system (Applied Biosystems, Foster City, CA, USA) and SYBR green chemistry. Rice GAPDH (glyceraldehyde-3-phosphate dehydrogenase, LOC_Os08g03290.1) was selected as the housekeeping gene (Yang et al., 2021). The standard $2^{-\Delta\Delta CT}$ method was used to calculate the relative expression of each of the targeted genes (Schmittgen and Livak, 2008). All values were represented as cumulative means ± standard deviation of four independent replicates.

2.6 Identification of key regulatory genes in the CNM regulatory module

2.6.1 Co-expression network analysis

In order to establish the CNM regulatory module with statistical significance, all CNM-related genes were uploaded to the STRING

(https://version-10-5.string-db.org/) software, and the protein–protein interaction (PPI) networks (combined score >0.4) were constructed. Then, the modules (resolution = 0.8) with higher visualization were performed by the program Gephi 0.9.2 (Lin et al., 2022b).

2.6.2 Estimation of the normcdf of CNM-related genes

In order to identify the key module activated in CNM in rice seedlings exposed to SCN^-, the results from PCR tests were used to calculate the possibility of the occurrence of genes grouped in four different modules. We first converted the data through the functions of "COMPUTE x_new=SQRT(X)" or "COMPUTE x_new = LN(x)" in the SPSS software since they were non-normally distributed. Then, the normcdf was calculated statistically.

2.7 Data analysis

Tukey's multiple range tests were used to assess the statistical significance at the level of 0.01 or 0.05. Different letters refer to the significant difference between the treatments and control ($p< 0.05$). The asterisk symbol refers to the significant difference between SCN^--treated and "SCN^- + 2-OG"-treated seedlings ($p< 0.05$).

3 Results

3.1 Relative growth rate of rice seedlings

A remarkable ($p< 0.05$) reduction in RGR of rice seedlings was observed at all SCN^- treatments after 3-day exposure in comparison to the control (Figure 1A). Similarly, in the case of "SCN^- + 2-OG" treatments in rice seedlings, a decrease in RGR that was visible in all treated plants reversed to that of control ($p< 0.05$). However, the RGR of rice seedlings under "SCN^- + 2-OG" treatments was significantly ($p< 0.05$) higher than that of SCN^- treatments, suggesting that the inoculation of 2-OG could mitigate the negative effect of SCN^- on plant biomass growth.

3.2 The total amount of C and N in rice seedlings

The C% in rice roots (shoots) was 36.99%, 36.94%, 36.58%, and 37.04% (40.31%, 40.15%, 39.35%, and 39.93%, respectively) under 0, 24, 96, and 300 mg SCN/L treatments, respectively. The application of exogenous 2-OG caused a negligible effect on the C % in rice tissues compared with their respective SCN^- treatments (Figures 1B, C). The N% in rice roots (shoots) was 2.0%, 2.26%, 3.16%, and 5.28% (2.79%, 3.44%, 3.43%, and 3.61%, respectively) under 0, 24, 96, and 300 mg SCN/L treatments, respectively, while application of exogenous 2-OG significantly decreased the N% in rice tissues compared with their respective SCN^- treatments (Figures 1D, E).

3.3 Response of CNM-related genes in rice plants

Mostly, more than one isogene was encoded with the specific enzyme in plants, in which the activity of the enzyme was regulated and/or governed by these isogenes together. However, each specific isogene does not carry the same weight during the regulation process, wherein there is always a master regulator gene (Yang et al., 2021), which chiefly controls the enzyme activity. Here, the upregulated master regulator genes in rice seedlings were described, while downregulated genes are not described in the following sections.

3.3.1 Response of C metabolism-related genes

As shown in Figure 2A, PEPC, upregulated genes in roots were *Osppc4*, *Osppc2a*, and *Osppc2b*, at all SCN^- treatments, while *Osppc1*, *Osppc2a*, and *Osppc2b* were upregulated in shoots. In roots of rice seedlings from the "SCN^- + 2-OG" treatments, *Osppc4* and *Osppc3* were upregulated, while *Osppc4*, *Osppc1*, and *Osppc2a* showed remarkable expression in shoots.

Expression of ERS-related genes is shown in Figure 2A, ERS, wherein *OsERS1*, *OsERS2*, and *OsERS3* were generally upregulated in SCN^--exposed rice parts, i.e., in roots and shoots. However, the expression levels of *OsERS1*, *OsERS2*, and *OsERS3* showed raised pattern in shoots of rice plants from the "SCN^- + 2-OG" treatments.

Figure 2A, TPS, depicts that higher expression levels of TPS-related genes of *OSTPS5* and *OSTPS1* were prominent in roots in SCN^- treatments, while *OSTPS5* and *OSTPS8* had greater expression in shoots. Interestingly, when rice seedlings were pretreated with 2-OG, *OSTPS5*, *OSTPS8*, and *OSTPS9* were upregulated in roots. However, the expression levels of five TPS isogenes in shoots conferred a variance tendency, which reinforced at 0 mg SCN/L and then declined at 24 mg SCN/L.

Upregulation of three SPS isogenes (*OsSPS1*, *OsSPS3*, and *OsSPS5*) was observed in roots in all SCN^- treatments (Figure 2A, SPS), while only *OsSPS2* was upregulated in shoots. Differential expression patterns were found in SPS-related genes of roots in "SCN^- + 2-OG" treatments. The expression levels of *OsSPS1*, *OsSPS3*, and *OsSPS5* in roots from the "SCN^- + 2-OG" treatments were higher than those of SCN^- treatments. *OsSPS1* and *OsSPS5* were upregulated in shoots of "SCN^- + 2-OG" treatments, which differed from SCN^- treatments.

3.3.2 Response of N metabolism relative genes

Positive expressions of NR genes, i.e., *OsNIA1*, *OsNIA2*, and *OsNR1*, were observed in roots after SCN^- exposure (Figure 2B, NR). However, the expression levels of *OsNIA1*, *OsNIA2*, and *OsNR1* in shoots showed a disparate trend with an initial escalation from 24 mg SCN/L and then dropped at 96 mg SCN/L. In the case of rice seedlings from the "SCN^- + 2-OG" treatments, higher expression levels of *OsNIA1*, *OsNIA2*, and *OsNR1* were observed in rice shoots.

Within NiR genes, only *OsNiR-1* was upregulated in roots at all SCN^- treatments (Figure 2B, NiR), while upregulation of *OsNiR-1* and *OsNiR-3* was detected in shoots. Interestingly, the expression

10.3389/fpls.2023.1086098

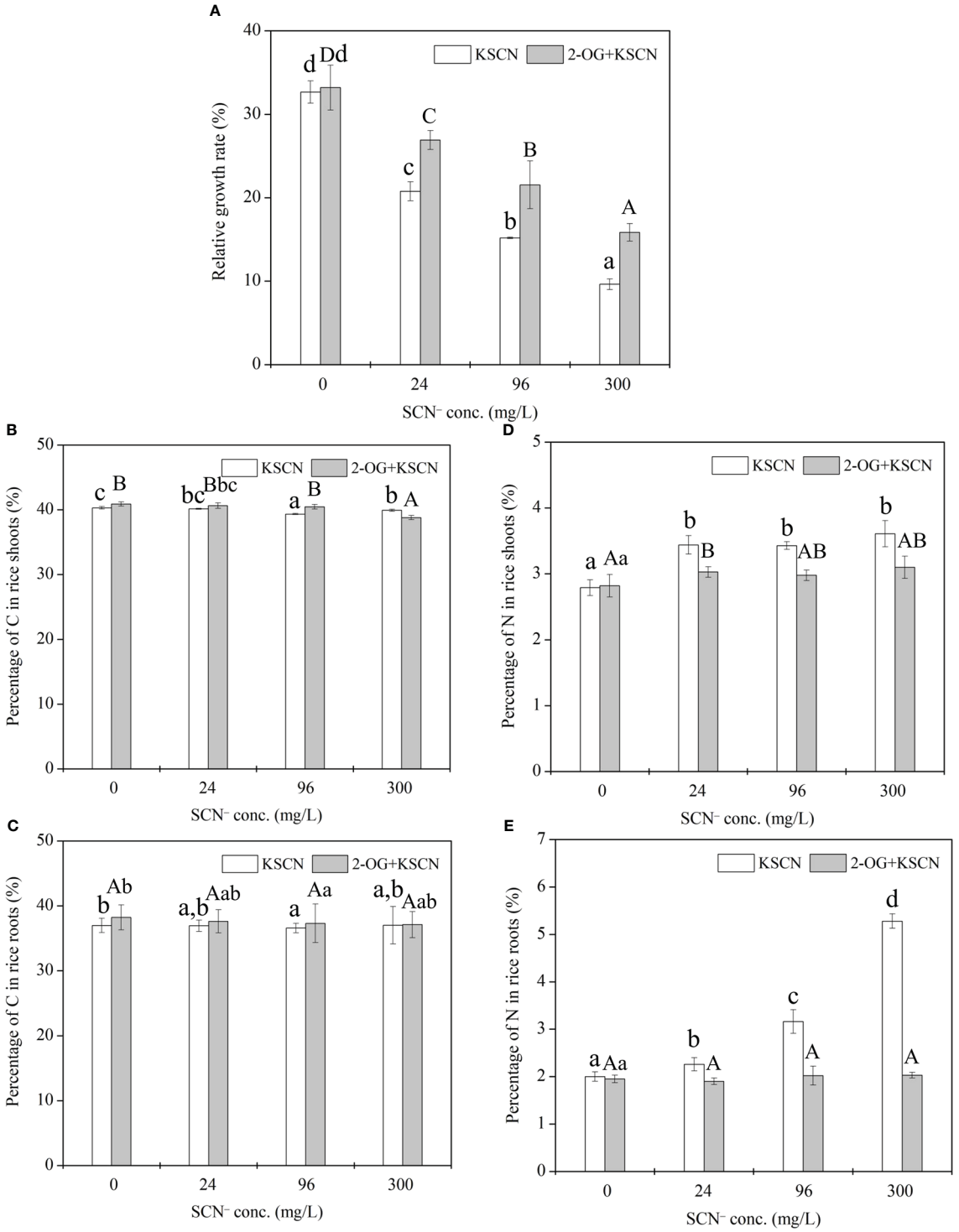

FIGURE 1
(A) Relative growth rate of rice seedlings under SCN^- exposure in the presence or absence of 2-OG. **(B)** The percentage of C in rice shoots. **(C)** The percentage of C in rice roots. **(D)** The percentage of N in rice shoots. **(E)** The percentage of N in rice roots. Values are the mean of four independent biological replicates ± standard deviation. Different letters refer to the significant difference between treatment and control ($p < 0.05$). 2-OG, 2-oxoglutarate.

levels of *OsNiR-1*, *OsNiR-2*, and *OsNiR-3* conferred an accelerating pattern in both roots and shoots of the "SCN^- + 2-OG" treatments.

Differential expression of GS-related genes was observed between roots and shoots, with significant upregulation of *OsGS2*, *OsGS1;2*, and *OsGS1;3* in roots and shoots (*OsGS2* and *OsGS1;3*) (Figure 2B, GS). However, the expression levels of *OsGS2*, *OsGS1;2*, *OsGS1;1*, and *OsGS1;3* showed linear inclination with increasing SCN^- concentrations in both rice tissues by inoculation of 2-OG.

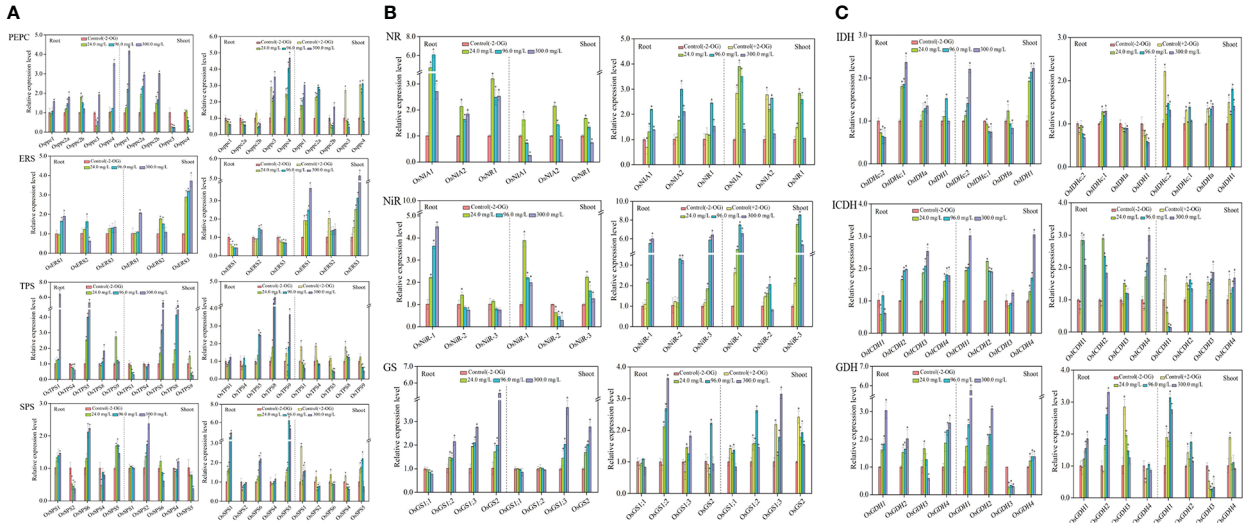

FIGURE 2
Response of CNM-related genes in rice roots and shoots under SCN^- stress in the presence or absence of 2-OG. **(A)** Response of C metabolism-related genes. **(B)** Response of N metabolism-related genes. **(C)** 2-OG synthesis-related genes. The asterisk symbol refers to the significant difference between SCN^--treated (24.0, 96.0, and 300.0 mg SCN/L) and SCN−+2-OG-treated (0, 24.0, 96.0, and 300.0 mg SCN/L) seedlings and control 1 ($p< 0.05$). CNM, carbon and nitrogen metabolism; 2-OG, 2-oxoglutarate.

3.3.3 Genes involved in the biosynthesis of 2-OG

Transcriptional changes of NAD-IDH genes are shown in Figure 2C, IDH. As apparent from the figures, *OsIDHa* and *OsIDHc;1* were upregulated in roots, while *OsIDHc;2* and *OsIDH1* were overexpressed in shoots. When rice seedlings were pretreated with 2-OG, upregulation of *OsIDHc;1* was observed in roots, and *OsIDHa*, *OsIDHc;2*, and *OsIDH1* were upregulated in shoots.

As presented in Figure 2C, ICDH, *OsICDH2*, *OsICDH3*, and *OSICDH4* were significantly ($p< 0.05$) upregulated in roots after SCN^- exposure, while positive expressions ($p< 0.05$) of *OsICDH1*, *OsICDH2*, and *OsICDH4* were observed in shoots. Interestingly, *OsICDH1*, *OsICDH2*, and *OsICDH4* in roots presented an upregulated pattern in the "SCN^- + 2-OG" treatments and the expression levels of *OsICDH2*, *OsICDH3*, and *OsICDH4* were remarkable in shoots.

Upregulation of *OsGDH1*, *OsGDH2*, and *OsGDH4* was observed in both rice tissues after SCN^- exposure (Figure 2C, GDH), while significantly ($p< 0.05$) higher expressions of *OsGDH1*, *OsGDH2*, and *OsGDH3* were observed in roots, and significant upregulation of *OsGDH1*, *OsGDH2*, and *OsGDH4* was detected in shoots of the "SCN^- + 2-OG" treatments.

3.4 Response of CNM-related enzyme activities

3.4.1 Response of C metabolism-related enzyme activities

The activities of CNM-related enzymes were assayed in SCN^- and "SCN^- + 2-OG" treatment plants (Figure 3). The activity of PEPC in roots was affirmatively increased ($p< 0.05$) after SCN^- exposure compared with the control, while the activity of PEPC in shoots presented a downward tendency. The activity of ERS in roots was significantly inhibited ($p< 0.05$) after SCN^- exposure in comparison with the control, while the activity of ERS was increased in shoots. Activities of TSP and SPS presented significant increasing patterns in both roots and shoots in the presence of SCN^- stress ($p< 0.05$). Under "SCN^- + 2-OG" treatments, activities of PEPC, ERS, TSP, and SPS intensified in roots compared to control ($p > 0.05$), while activities of ERS, TSP, and SPS showed a decrement in shoots unlike control ($p > 0.05$).

3.4.2 Response of N metabolism-related enzyme activities

Activities of NR and NiR in roots presented an exponential emulate compared with the control ($p< 0.05$), while activities of NR and NiR in shoots illustrated an inverted "U" shape curve under SCN^- stress (Figure 3). The analogous activity of GS was noticed in both roots and shoots of SCN^- stress ($p< 0.05$), following linearity with stress concentration. Under "SCN^- + 2-OG" treatments, activities of NR, NiR, and GS showed a similar pattern of increment in both roots and shoots ($p< 0.05$).

Overall, the activities of all selected enzymes in "SCN^- + 2-OG" treatments were generally higher than those of SCN^- treatments. Exogenous 2-OG had a pronounced impact on enzyme activities in shoots, unlike its counterpart. To reveal the regulation mechanism of exogenous 2-OG on the CNM in rice plants under SCN^- exposure, we distinguished the effects of exogenous 2-OG on C and N metabolism in rice tissues.

3.4.3 Response of 2-OG biosynthesis-related enzyme activities

The activity of NAD-IDH was inhibited significantly ($p< 0.05$) in both roots and shoots under SCN^- exposure compared with the control (Figure 3). The activity of NADP-ICDH in SCN^--exposed

10.3389/fpls.2023.1086098

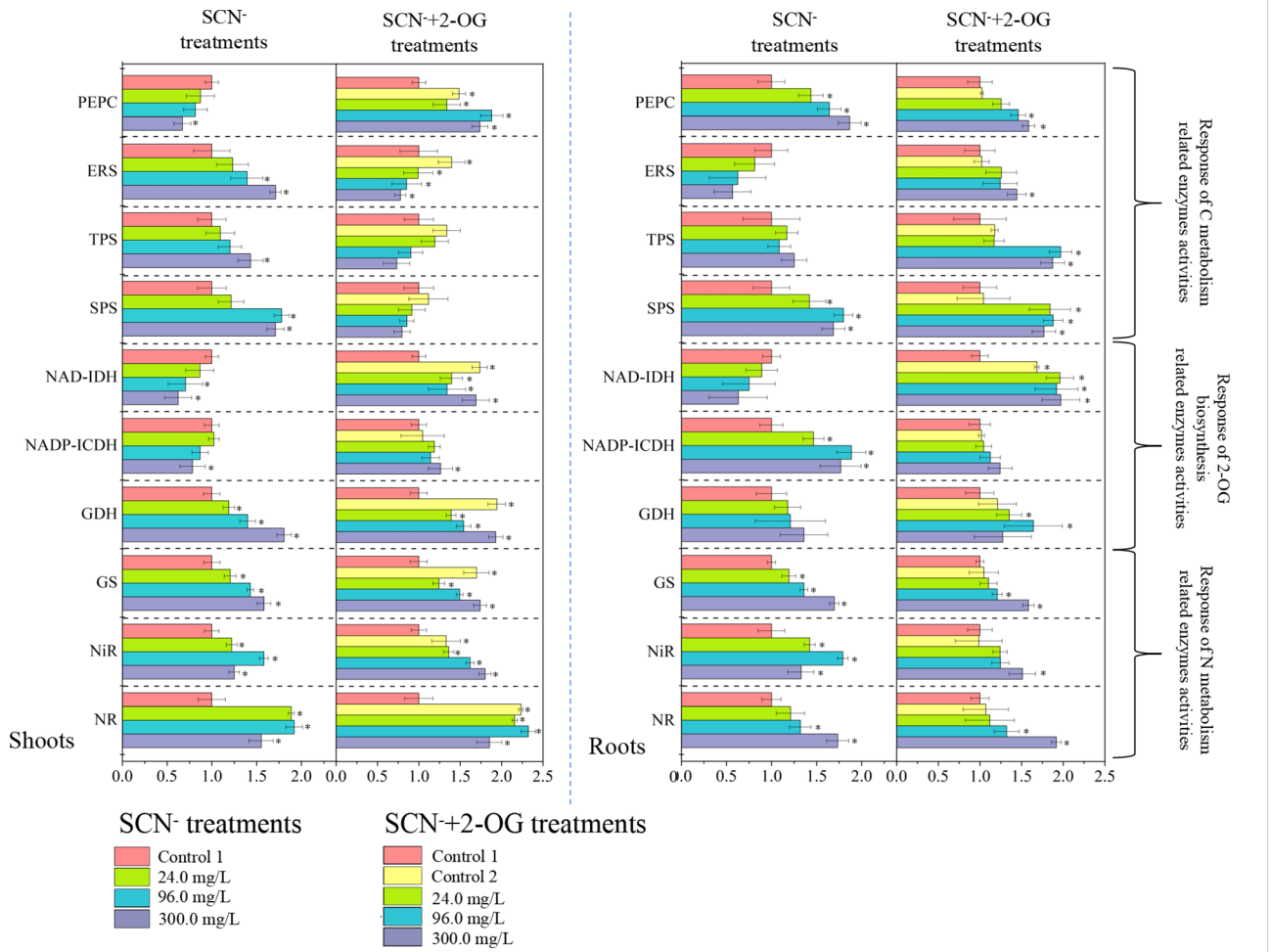

FIGURE 3
Response of CNM-related enzyme activities in rice roots and shoots under SCN^- stress in the presence or absence of 2-OG. The asterisk symbol refers to the significant difference between SCN^--treated (24.0, 96.0, and 300.0 mg SCN/L) and SCN−+2-OG-treated (0, 24.0, 96.0, and 300.0 mg SCN/L) seedlings and control 1 ($p< 0.05$). CNM, carbon and nitrogen metabolism; 2-OG, 2-oxoglutarate.

roots was prominently enhanced; nevertheless, the scenario was reversed in the case of shoots ($p< 0.05$). Elevated activity of GDH was observed in both roots and shoots in the presence of SCN^- ($p< 0.05$). Under "SCN^- + 2-OG" treatments, the activities of NAD-IDH, NADP-ICDH, and GDH were generally increased in rice tissues, except for GDH in shoots of rice seedlings. These results indicated that the modification mechanism of exogenous 2-OG on CNM-related enzymes in rice seedlings under SCN^- exposure varied greatly.

3.5 Identification of key regulatory genes in the CNM regulatory module

3.5.1 Co-expression analysis of CNM-related genes

Plants have evolved the coordinated actions responsible for their diverse physiological processes *via* either direct or indirect gene connections. In order to elucidate the functional module of genes activated in the CNM process, a co-expression network was performed by the STRING program, and four modules were obtained. Detailed information on gene interaction strengths in these four modules is given in Table S2. Interestingly, all modules had similar interaction contributions, namely Module 1 (25.0%), Module 2 (25.0%), Module 3 (27.5%), and Module 4 (22.5%) (Figure 4A). We also noticed that the genes grouped in Modules 1 and 2 were involved in C metabolism (11 genes) and biosynthesis of 2-OG (10 genes), respectively; genes categorized in Module 3 were responsible for N metabolism (five genes) and biosynthesis of 2-OG (five genes). In addition, genes grouped in Module 4 were activated in C metabolism (one gene) and N metabolism (five genes) and biosynthesis of 2-OG (three genes) (Figure 4B).

3.5.2 The occurrence probability of CNM-related genes

The normcdf of rice shoots was quite different between under SCN^- and SCN−+2-OG treatments, based on the non-linear regression (Figure 5). Herein, the threshold for the highest occurrence probability was set, $p > 0.75$. Therefore, Module 3 showed the highest occurrence probability, suggesting that the

exogenous application of 2-OG mainly regulated the expression of genes activated in the N metabolism and 2-OG synthesis to modify the imbalance of CNM in rice plants imposed by SCN^- exposure. In fact, a similar conclusion was also reached in the analysis of C and N fractions in rice tissues. We noticed that the change of C fraction in rice shoots was almost constant (Figures 1B, C), while the change of N in rice shoots was evident between SCN^- treatments and "SCN^- + 2-OG" treatments (Figures 1D, E).

4 Discussion

4.1 Exogenous 2-OG promotes plant growth *via* regulating CNM during SCN^- exposure

The growth and development of plants are tightly coordinated with the balance of cellular CNM (Zheng, 2009). Once plants suffer from environmental stresses, the CNM in plants could be disrupted, thereby causing an imbalance of CNM and eventually resulting in a reduction in plant growth (Reddy et al., 2004). In this current study, the imbalance of CNM in rice seedlings due to SCN^- exposure was judged by the relative growth rate (Figure 1A), in which SCN^- exposure led to a significant reduction in RGR of rice seedlings ($p< 0.05$), indicating a severe impact on the balance of CNM in rice seedlings under SCN^- stress. Also, we found that SCN^- exposure significantly affected the percentage of N in rice seedlings (Figures 1D, E). This is because SCN^- exposure can result in the dysfunction of chloroplast (Yang et al., 2021) and repress the activities of NR, GS, and glutamate synthase (GOGAT) in rice seedlings (Lin et al., 2022a). In addition, SCN^--treated rice seedlings with 2-OG supplied had significantly ($p< 0.05$) higher RGR than those without exogenous 2-OG, suggesting a positive effect of exogenous 2-OG on the RGR of rice seedlings corresponding to SCN^- exposure. It is known that 2-OG is a decisive chemical involved in the homeostasis of CNM in higher plants (Yuan et al., 2007). Also, exogenous 2-OG enhances photosynthesis and increases the levels of C-skeletons in rice plants, thus affecting the N metabolism (Yuan et al., 2007; Zheng, 2009). Therefore, the imbalance of CNM in rice seedlings due to SCN^- exposure could be positively modified by exogenous 2-OG.

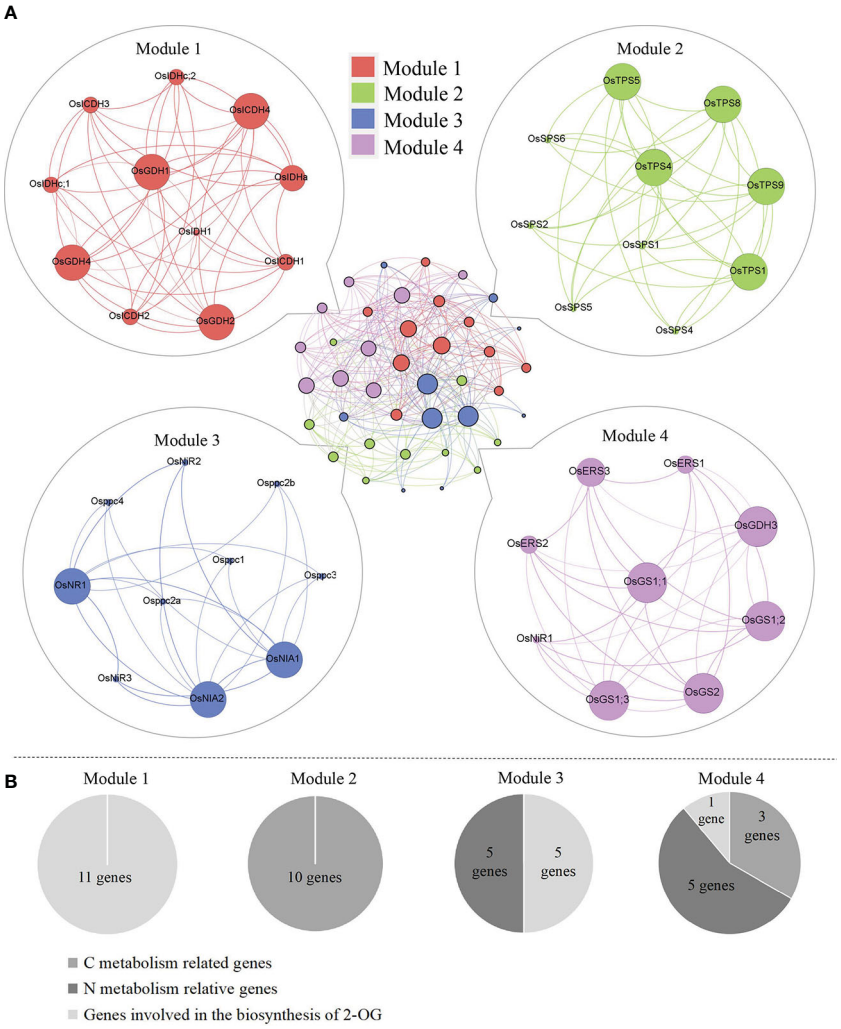

FIGURE 4
(A) Genetic matrix integrative analysis of CNM-related genes. **(B)** The number of CNM genes in each matrix. CNM, carbon, and nitrogen metabolism.

10.3389/fpls.2023.1086098

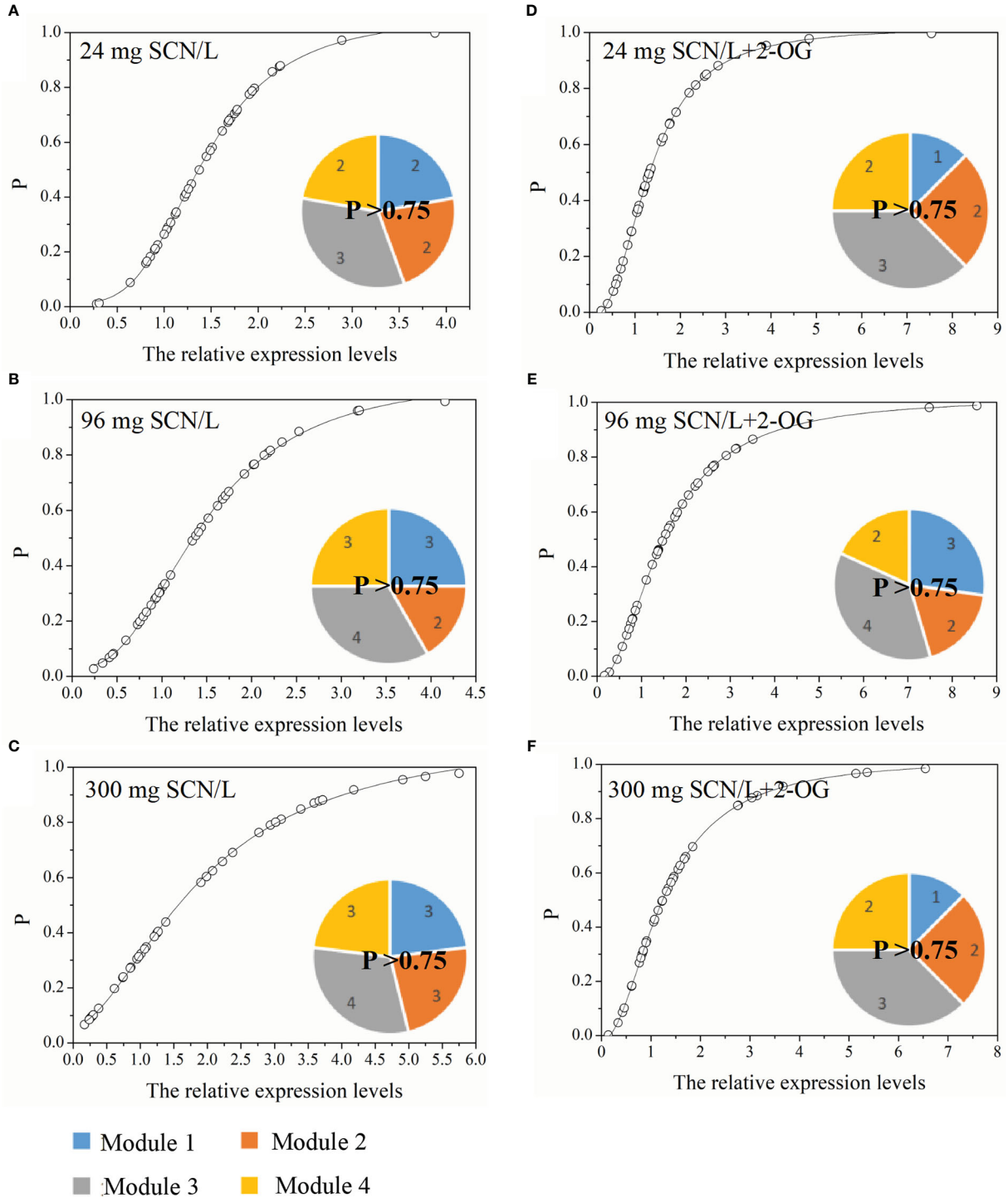

FIGURE 5
Occurrence P (p > 0.75) of CNM-related genetic expression in rice shoots under **(A)** 24 mg SCN/L, **(B)** 96 mg SCN/L, and **(C)** 300 mg SCN/L treatments and under **(D)** 24 mg SCN/L + 2-OG, **(E)** 96 mg SCN/L + 2-OG, and **(F)** 300 mg SCN/L + 2-OG treatments. CNM, carbon and nitrogen metabolism; 2-OG, 2-oxoglutarate.

4.2 Modification of 2-OG in balancing CNM in SCN^--treated rice plants

Herein, the main N source present in the nutrient solution to support plant growth is NO_3^-. In plants, only a small fraction of NO_3^- is assimilated in roots after uptake, and a greater part is translocated into shoots and assimilated into NH_4^+ and amino acids. Photosynthesis in the chloroplast is a major process for C metabolism in plants during their entire period of life (Lemaitre et al., 2007). Therefore, modification of 2-OG on CNM-related genes and enzyme activities in rice shoots will be discussed accordingly.

4.2.1 Effects of SCN^- on innate 2-OG synthesis

It is known that there are three innate routines for the biosynthesis of 2-OG in plants, in which the PEPC pathway and the NADP-ICDH/NAD-IDH pathway belong to C metabolism, and the GDH pathway is mainly involved in N metabolism. In this study, we focused on correlating and perceiving the most competent pathway in controlling the generation of 2-OG and regulating the imbalance of CNM in rice seedlings caused by SCN^- exposure.

The PEPC pathway in plants is an anaplerotic reaction to replenish the tricarboxylic acid (TCA) cycle with intermediates that are withdrawn for different biosynthesis pathways and N metabolism (Lemaitre et al., 2007). For example, PEPC is able to catalyze phosphoenolpyruvic acid (PEP) into 2-OG, and 2-OG synthesis from malate can be suppressed by the knockdown of *Osppc4*, therefore causing a decrease in plant growth and leaf area (Masumoto et al., 2010), suggesting that *Osppc4* is crucial for the growth of rice plants. In the present study, significant downregulation of *Osppc4* was observed in shoots of rice seedlings after SCN^- exposure (Figure 2C). The activity of PEPC was decreased in shoots after SCN^- treatments (Figure 3), suggesting that the synthesis of 2-OG in shoots from the PEPC pathway was repressed by SCN^- exposure.

The second pathway of 2-OG generation is the NADP-ICDH/NAD-IDH pathway (Ferrario-Mery et al., 2001), in which citrate can be either exported from mitochondria to cytosol for 2-OG synthesis by cytosolic enzymes aconitase NADP-ICDH or transformed into 2-OG in mitochondria by TCA cycle enzyme aconitase NAD-IDH (Yuan et al., 2007). Indeed, NAD-IDH is often regarded as a major governing point in plants (Lemaitre et al., 2007), which is encoded with one single gene *OsIDHa* in rice plants (Lancien et al., 1998). Herein, significant downregulation of *OsIDHa* was detected in shoots after SCN^- exposure (Figure 2C), suggesting that SCN^- exposure could inhibit the expression of *OsIDHa* in shoots. A significant correlation was obtained in the enzymatic assay of NAD-IDH, wherein a decrease in the activity of NAD-IDH was observed in shoots of rice seedlings exposed to SCN^- (Figure 3). Results from both C-related pathways indicated that SCN^- exposure significantly repressed both pathways to produce 2-OG, thereby causing a severe impact on the C metabolism and breaking the balance of CNM.

The third source to produce 2-OG is from the GDH pathway, in which the oxidative deamination of glutamate (Glu) into 2-OG is catalyzed by GDH. It has been reported that exogenous 2-OG increased the activities of GDH in wheat seedlings and promoted yield productivity under drought stress (Lancien et al., 1998). Additionally, GDH plays a unique role in the formation of NH_4^+ and 2-OG during the assimilation of Glu (Lodwig et al., 2003). We found that the expression levels of *OsGDH1* and *OsGDH2* were significantly upregulated in shoots after SCN^- treatments (Figure 2C). The change of GDH activity in shoots was constructive against SCN^- exposure (Figure 3). These results indicated that SCN^- exposure does not disturb the conversion of Glu into 2-OG through the activation of GDH. Combined with the results from C-related pathways of 2-OG, we have sufficient reasons to conclude that the imbalance of CNM in rice seedlings was evident due to SCN^- exposure through repressing the two C-related pathways.

4.2.2 Effects of SCN^- on innate 2-OG synthesis in the presence of exogenous 2-OG

Compared with SCN^- treatments (Figure 2C), the expression levels of *Osppc4* in shoots of rice seedlings under "SCN^- + 2-OG" treatments were significantly upregulated, and the activity of PEPC in shoots was also positively responsive, suggesting that the application of 2-OG enhances the enzyme activity of PEPC and might stimulate the generation of 2-OG. A similar conclusion was also predicted in the second pathway of 2-OG generation due to the application of exogenous 2-OG, wherein a correlation between upregulated expression of *OsIDHa* and increases in NAD-IDH activity was obtained. Additionally, the expression levels of *OsGDH1* and *OsGDH2* in shoots of rice seedlings fed with 2-OG were significantly upregulated, and an increase of GDH activity in shoots was also detected (Figure 3), suggesting that the conversion of Glu into 2-OG was independent of the application of 2-OG. Co-expression network analysis showed that the GDH-related genes in Module 1 had a higher connection degree with others (Figure 4A). Apparently, these results indicated that the two C-related pathways were significantly activated due to the application of 2-OG, in which sufficient 2-OG in plant cells was able to modify the imbalance of CNM in rice seedlings caused by SCN^- exposure, subsequently decreasing the negative impact on rice seedlings, which was judged by a measurable increase in biomass growth of rice seedlings from the SCN^--treated rice seedlings with 2-OG, compared with the SCN^--treated rice seedlings without 2-OG.

4.3 Responses of other CNM-related enzymes and genes in rice plants after SCN^- exposure

4.3.1 Effects of SCN^- on C metabolism in rice plants

The TPS and SPS are primary targeted cytosolic enzymes involved in the C metabolism (Coruzzi and Zhou, 2001). Previous studies indicated that the expressions of *OsTPS2*, *OsTPS5*, and *OsTPS6* in rice were negatively correlated with sucrose starvation (Wang et al., 2007). The expression of *SPS* genes was positively correlated with non-structure carbohydrate content in the leaf, wherein *OsSPS1* expression and SPS activity were affirmatively corresponding to spike number and grain yield (Li and Cui, 2018). However, another study showed that mRNA levels of *OsSPS1* and *OsSPS6* were negatively correlated with sucrose concentrations (Yonekura et al., 2013). In the present study, upregulation of *OsTPS5* was detected in both rice tissues under SCN^- stress (Figure 2). In addition, upregulated *OsSPS1* was also evident in both roots and shoots. Meanwhile, increases in TPS and SPS activities in rice tissues were detectable (Figure 3). These results indicated that SCN^- exposure stimulated the expression of C metabolism-related master regulation genes, thus regulating the enzyme activities. Enzyme ERS has an important role in

maintaining the physiological homeostasis of amino acids and C metabolism as well as redox status (Yang et al., 2018). Like TPS and SPS, upregulation of *OsERS1* was distinguished in both rice tissues after SCN^- stress (Figure 2). Also, we observed that responses of *OsERS1* to SCN^- exposure were identical to the enzyme activity of ERS in rice tissues (Figure 2).

4.3.2 Effects of SCN^- on N metabolism in rice plants

NR, NiR, and GS are three key enzymes involved in N assimilation. The conversion of NO_3^- into NH_4^+ is catalyzed by the enzymes NR and NiR, which is a rate-limiting step in NO_3^- assimilation. In the present study, three isogenes of NR (*OsNIA1*, *OsNIA12*, and *OsNR1*) and NiR (*OsNiR-1*, *OsNiR-2*, and *OsNiR-3*) showed a declining expression pattern in shoots after SCN^- exposure, of which SCN^- treatments at 24.0 and 96.0 mg/L positively regulated transcriptional changes in *OsNR1*, and 300.0 mg SCN/L treatment demonstrated a negative response (Figure 2). Enzymatic assay showed that activities of NR and NiR had a positive correlation with gene expression (Figure 3), suggesting that low-to-moderate concentrations of SCN^- exposure might stimulate the conversion of NO_3^-, and higher SCN^- concentrations had a negative effect on this process, whereas a similar conclusion was also reached by Lin et al. (2022a). Another crucial enzyme in N metabolism is GS, which is responsible for converting NH_4^+ into glutamine. In this study, almost all GS genes were upregulated in the SCN^- treatments (Figure 2). It is established that GS in most plants occurs as GS2 in plastids and GS1 in the cytosol. The role of GS1 is to assimilate NH_4^+ in roots and reassimilate NH_4^+ in leaves, whereas GS2 is mainly responsible for assimilating NH_4^+ derived from NO_3^- reduction in plastids (Lin et al., 2022a). The enzymatic assay also showed that activities of GS had a positive correlation to gene expression (Figure 3), suggesting that SCN^- treatments do not inhibit the activity of GS and subsequently increase the conversion of NH_4^+.

4.3.3 Effects of exogenous 2-OG on CNM in rice plants under SCN^- stress

Compared with SCN^- treatments (Figure 2), exogenous 2-OG decreased the expression of *OsTPS5* in shoots of rice seedlings after SCN^- exposure. Similarly, the downregulation of *OsSPS6* and *OsERS1* was also detectable. Enzymatic assays indicated that the application of 2-OG decreased the activities of TPS, SPS, and ERS in shoots of rice seedlings (Figure 3). A co-expression network analysis showed that the C metabolism-related genes in Module 2 and Module 4 had a lower connection degree with others (Figure 4A). However, we noticed that NR and NiR genes were upregulated in

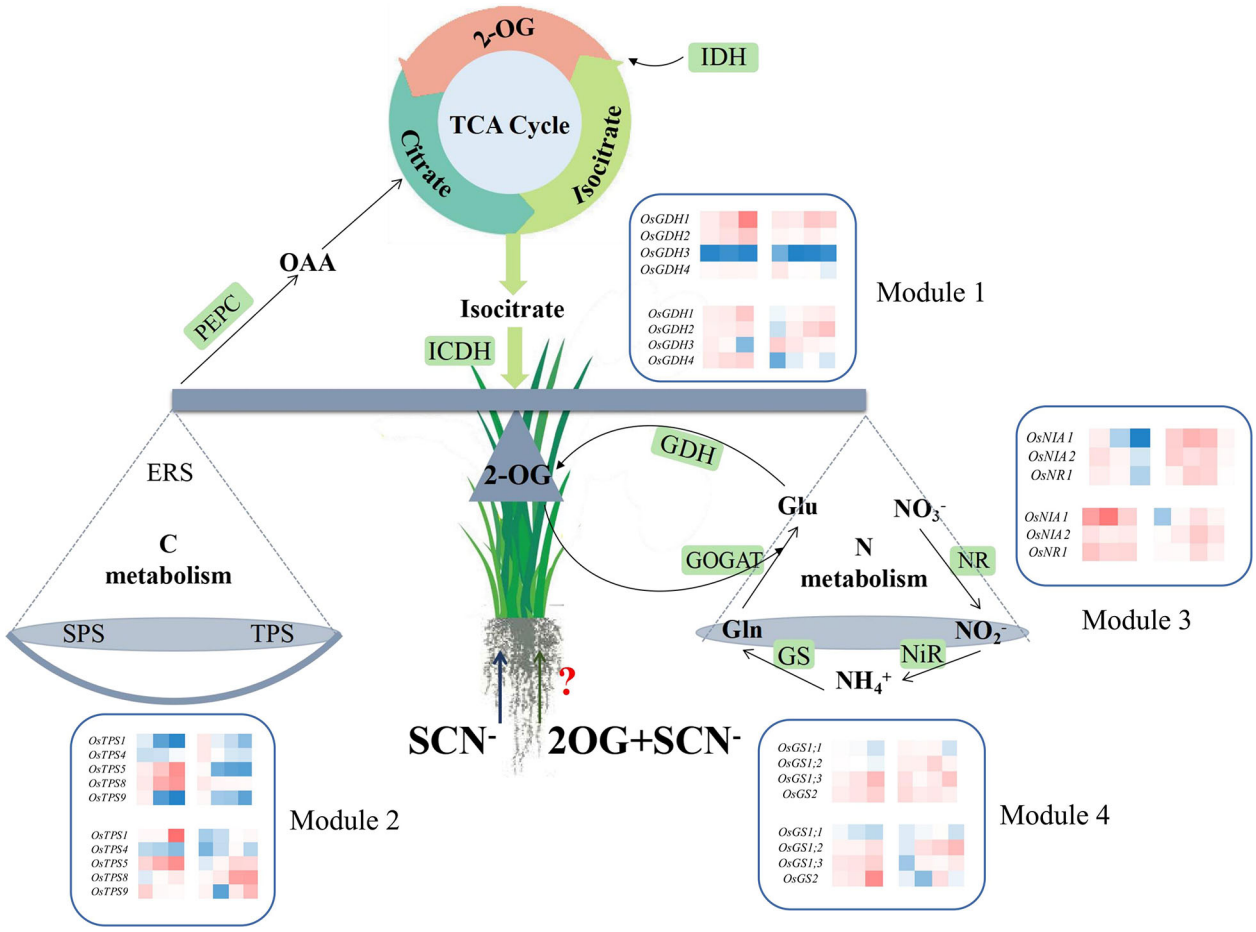

FIGURE 6
Overview of exogenous 2-OG-mediated CNM in rice tissues under SCN^- stress. 2-OG, 2-oxoglutarate; CNM, carbon and nitrogen metabolism.

SCN^--treated rice seedlings inoculated with 2-OG, wherein enzymes of NR and NiR were positively responsive to 2-OG application, indicating that the application of 2-OG had a positive impact on the conversion of NO_3^-. A previous study also reported that feeding of 2-OG increased transcripts of the NR gene in tobacco leaf (Ferrario-Mery et al., 2001). Additionally, under "SCN^- + 2-OG" treatments, the expression levels of *OsGS1;2* were significantly higher than those under SCN^- treatments, suggesting that the application of 2-OG also increases the conversion of NH_4^+ derived from the main N source of NO_3^- supplied. A co-expression network analysis showed that the N metabolism-related genes in Module 3 and Module 4 had a higher connection degree with others (Figure 4A). These results indicated that sufficient 2-OG in plant cells can modify the imbalance of N metabolism-related genes in rice seedlings caused by SCN^- exposure.

5 Conclusion

The balance of CNM in rice seedlings can be broken by SCN^- exposure, resulting in a significant reduction in the biomass growth of rice seedlings. The application of exogenous 2-OG showed a positive regulatory effect on the imbalance of CNM in rice seedlings under SCN^- stress. Higher connection degrees of genes in each module in rice plants under SCN^- and "SCN^- + 2-OG" treatments are marked in Figure 6. Although our findings provide new insight into the role of exogenous 2-OG in minimizing the negative effect of SCN^- exposure on rice plants through regulating the pathways involved in CNM, the global molecular map of regulatory genes involved in CNM remains unclear. Further comprehensive studies are needed to experimentally prove the influence of exogenous 2-OG as a chemical regulator on the quality and quantity of agricultural crops through the "omics" technology, such as transcriptome, proteome, and metabolome.

Data availability statement

The original contributions presented in the study are included in the article/Supplementary Materials. Further inquiries can be directed to the corresponding author/s.

Author contributions

X-ZY: conceptualization, methodology, supervision, writing-reviewing and editing, and funding acquisition. Y-XF: writing-original draft preparation and visualization. LY: investigation. Y-JL: investigation, data analysis, visualization, and software. YS: data analysis, visualization, and software. All authors contributed to the article and approved the submitted version.

Funding

This work was financially supported by the National Natural Science Foundation of China (No. 41761094) and the Postdoctoral Research Foundation of China (2021MD703821).

Conflict of interest

The authors declare that the research was conducted in the absence of any commercial or financial relationships that could be construed as a potential conflict of interest.

Publisher's note

Supplementary material

The Supplementary Material for this article can be found online at: https://www.frontiersin.org/articles/10.3389/fpls.2023.1086098/full#supplementary-material

References

Ahanger, M. A., Qi, M., Huang, Z., Xu, X., Begum, N., Qin, C., et al. (2021). Improving growth and photosynthetic performance of drought stressed tomato by application of nano-organic fertilizer involves up-regulation of nitrogen, antioxidant and osmolyte metabolism. *Ecotoxicol. Environ. Saf.* 216, 112195. doi: 10.1016/j.ecoenv.2021.112195

Alves, H., Matiolli, C. C., Soares, R. C., Almadanim, M. C., Oliveira, M. M., and Abreu, I. A. (2021). Carbon/nitrogen metabolism and stress response networks-calcium-dependent protein kinases as the missing link? *J. Exp. Bot.* 72, 4190–4201. doi: 10.1093/jxb/erab136

Araújo, W. L., Martins, A. O., Fernie, A. R., and Tohge., T. (2014). 2-oxoglutarate: linking TCA cycle function with amino acid, glucosinolate, flavonoid, alkaloid, and gibberellin biosynthesis. *Front. Plant Sci.* 5, 552. doi: 10.3389/fpls.2014.00552

Bhunia, F., Saha, N. C., and Kaviraj, A. (2000). Toxicity of thiocyanate to fish, plankton, worm and aquatic system. *Bull. Environ. Contam. Toxicol.* 64, 197–204. doi: 10.1007/s001289910030

Brown, S., Devolder, P. S., Compton, H., and Henry, C. (2007). Effect of amendment C:N ratio on plant richness, cover and metal content for acidic Pb and zn mine tailings in leadville, Colorado. *Environ. Pollut.* 149, 165–172. doi: 10.1016/j.envpol.2007.01.008

Coruzzi, G. M., and Zhou, L. (2001). Carbon and nitrogen sensing and signaling in plants: emerging 'matrix effects'. *Curr. Opin. Plant Biol.* 4, 247–253. doi: 10.1016/S1369-5266(00)00168-0

Feng, Y. X., Yu, X. Z., Mo, C. H., and Lu, C. J. (2019). Regulation network of sucrose metabolism in response to trivalent and hexavalent chromium in *Oryza sativa*. *J. Agric. Food Chem.* 67, 9738–9748. doi: 10.1021/acs.jafc.9b01720

Ferrario-Mery, S., Masclaux, C., Suzuki, A., Valadier, M. H., Hirel, B., and Foyer, C. H. (2001). Glutamine and a-ketoglutarate are metabolite signals involved in nitrate reductase gene transcription in untransformed and transformed tobacco plants deficient in ferredoxin-glutamine-a-ketoglutarate aminotransferase. *Planta* 213, 265–271. doi: 10.1007/s004250000504

Fritz, C., Mueller, C., Matt, P., Feil, R., and Stitt, M. (2006). Impact of the c-n status on the amino acid profile in tobacco source leaves. *Plant Cell Environ.* 29, 2055–2076. doi: 10.1111/j.1365-3040.2006.01580.x

Gálvez, S., Bismuth, E., Sarda, C., and Gadal, P. (1994). Purification and characterization of chloroplastic NADP-isocitrate dehydrogenase from mixotrophic tobacco cells. comparison with the cytosolic isoenzyme. *Plant Physiol.* 105, 593–600. doi: 10.1104/pp.105.2.593

Gálvez, S., Lancien, M., and Hodges, M. (1999). Are isocitrate dehydrogenases and 2-oxoglutarate involved in the regulation of glutamate synthesis? *Trends Plant Sci.* 4, 484–490. doi: 10.1016/s1360-1385(99)01500-9

Gao, J. J., Wang, B., Li, Z. J., Xu, J., Fu, X. Y., Han, H. J., et al. (2022). Metabolic engineering of *Oryza sativa* for complete biodegradation of thiocyanate. *Sci. Total Environ.* 820, 153283. doi: 10.1016/j.scitotenv.2022.153283

Goddijn, O. J., Verwoerd, T. C., Voogd, E., Krutwagen, R. W., De Graff, P. T. H. M., Poels, J., et al. (1997). Inhibition of trehalase activity enhances trehalose accumulation in transgenic plants. *Plant Physiol.* 113, 181–190. doi: 10.1104/pp.113.1.181

Gould, W. D., King, M., Mohapatra, B. R., Cameron, R., Kapoor, A., and Koren, D. W. (2012). A critical review on destruction of thiocyanate in mining effluents. *Miner. Eng.* 34, 38–47. doi: 10.1016/j.mineng.2012.04.009

Guo, L. Y., Lu, Y. Y., Bao, S. Y., Zhang, Q., Geng, Y. Q., and Shao, X. W. (2021). Carbon and nitrogen metabolism in rice cultivars affected by salt-alkaline stress. *Crop Pasture Sci.* 72, 372–382. doi: 10.1071/CP20445

Hansson, D., Morra, M. J., Borek, V., Snyder, A. J., Johnsonmaynard, J. L., and Thill, D. C. (2008). Ionic thiocyanate (SCN^-) production, fate, and phytotoxicity in soil amended with *Brassicaceae* seed meals. *J. Agric. Food Chem.* 56, 3912–3917. doi: 10.1021/jf800104x

Hou, W. F., Xue, X. X., Li, X. K., Khan, M. R., Yan, J. Y., Ren, T., et al. (2019). Interactive effects of nitrogen and potassium on: Grain yield, nitrogen uptake and nitrogen use efficiency of rice in low potassium fertility soil in China. *Field Crop Res.* 236, 14–23. doi: 10.1016/j.fcr.2019.03.006

Ji, J., Shi, Z., Xie, T., Zhang, X., Chen, W., Du, C., et al. (2020). Responses of gaba shunt coupled with carbon and nitrogen metabolism in poplar under NaCl and $CdCl_2$ stresses. *Ecotoxicol. Environ. Saf.* 193, 110322. doi: 10.1016/j.ecoenv.2020.110322

Lancien, M., Gadal, P., and Hodges, M. (1998). Molecular characterization of higher plant NAD-dependent isocitrate dehydrogenase: Evidence for a heteromeric structure by the complementation of yeast mutants. *Plant J.* 16, 325–333. doi: 10.1046/j.1365-313x.1998.00305.x

Lemaitre, T., Urbanczyk-Wochniak, E., Flesch, V., Bismuth, E., Fernie, A. R., and Hodges, M. (2007). NAD-dependent isocitrate dehydrogenase mutants of *Arabidopsis* suggest the enzyme is not limiting for nitrogen assimilation. *Plant Physiol.* 144, 1546–1558. doi: 10.1104/pp.107.100677

Li, G. H., and Cui, K. H. (2018). The effect of nitrogen on leaf sucrose phosphate synthase and its relationships with assimilate accumulation and yield in rice. *Plant Physiol. J.* 54, 1195–1204. doi: 10.13592/j.cnki.ppj.2018.0257

Lin, Y. J., Feng, Y. X., and Yu, X. Z. (2022a). The importance of utilizing nitrate (NO_3^-) over ammonium (NH_4^+) as nitrogen source during detoxification of exogenous thiocyanate (SCN^-) in *Oryza sativa*. *Environ. Sci. Pollut. Res.* 29, 5622–5633. doi: 10.1007/s11356-021-15959-z

Lin, Y. J., Feng, Y. X., Zhang, Q., and Yu, X. Z. (2022b). Proline-mediated modulation on DNA repair pathway in rice seedlings under chromium stress by integrating gene chip and co-expression network analysis. *Ecotoxicology* 31, 1266–1275. doi: 10.1007/s10646-022-02586-8

Lin, Y. J., Yu, X. Z., Li, Y. H., and Yang, L. (2020). Inhibition of the mitochondrial respiratory components (Complex I and complex III) as stimuli to induce oxidative damage in *Oryza sativa* L. under thiocyanate exposure. *Chemosphere* 243, 125472. doi: 10.1016/j.chemosphere.2019.125472

Lodwig, E. M., Hosie, A. H., Bourdès, A., Findlay, K., Allaway, D., Karunakaran, R., et al. (2003). Amino-acid cycling drives nitrogen fixation in the legume–rhizobium symbiosis. *Nature* 422, 722. doi: 10.1038/nature01527

Masumoto, C., Miyazawa, S. I., Ohkawa, H., Fukuda, T., Taniguchi, Y., Murayama, S., et al. (2010). Phosphoenolpyruvate carboxylase intrinsically located in the chloroplast of rice plays a crucial role in ammonium assimilation. *Proc. Natl. Acad. Sci. U.S.A.* 107, 5226–5231. doi: 10.1073/pnas.0913127107

Mostofa, M. G., Seraj, Z. I., and Fujita, M. (2014). Exogenous sodium nitroprusside and glutathione alleviate copper toxicity by reducing copper uptake and oxidative damage in rice (*Oryza sativa* L.) seedlings. *Protoplasma* 25, 1373–1386. doi: 10.1007/s00709-014-0639-7

Mudder, T. I., and Botz, M. (2004). Cyanide and society: a critical review. *Eur. J. Miner. Process. Environ. Prot.* 4, 62–74.

Naseeruddin, R., Sumathi, V., Prasad, T.N.V.K.V., Sudhakar, P., Chandrika, V., and Reddy, B. R. (2018). Unprecedented synergistic effects of nanoscale nutrients on growth, productivity of sweet sorghum [*Sorghum bicolor* (L.) moench] and nutrient biofortification. *J. Agric. Food Chem.* 66, 1075–1084. doi: 10.1021/acs.jafc.7b04467

Osuna, L., Gonzalez, M. C., Cejudo, F. J., Vidal, J., and Echevarria, C. (1996). *In vivo* and *in vitro* phosphorylation of the phosphoenolpyruvate carboxylase from wheat seeds during germination. *Plant Physiol.* 111, 551–558. doi: 10.1104/pp.111.2.551

Ratinaud, M. H., Thomes, J. C., and Julien, R. (1983). Glutamyl-tRNA synthetases from wheat. isolation and characterization of three dimeric enzymes. *Eur. J. Biochem.* 135, 471–477. doi: 10.1111/j.1432-1033.1983.tb07675.x

Reddy, A. R., Chaitanya, K. V., and Vivekanandan, M. (2004). Drought-induced responses of photosynthesis and antioxidant metabolism in higher plants. *J. Plant Physiol.* 161, 1189–1202. doi: 10.1016/j.jplph.2004.01.013

Schmittgen, T. D., and Livak, K. J. (2008). Analyzing real-time PCR data by the comparative $C_{(T)}$ method. *Nat. Protoc.* 3, 1101–1108. doi: 10.1038/nprot.2008.73

Sun, Z., Xie, X., Wang, P., Hu, Y., and Cheng, H. (2018). Heavy metal pollution caused by small-scale metal ore mining activities: A case study from a polymetallic mine in south China. *Sci. Total. Environ.* 639:217–227 doi: 10.1016/j.scitotenv.2018.05.176.

Turano, F. J., Dashner, R., Upadhyaya, A., and Caldwell, C. R. (1996). Purification of mitochondrial glutamate dehydrogenase from darkgrown seedlings. *Plant Physiol.* 112, 1357–1364. doi: 10.1104/pp.112.3.1357

Wang, H. J., Wan, A. R., Hsu, C. M., Lee, K. W., Yu, S. M., and Jauh, G. Y. (2007). Transcriptomic adaptations in rice suspension cells under sucrose starvation. *Plant Mol. Biol.* 63, 441–463. doi: 10.1007/s11103-006-9100-4

Xin, W., Zhang, L., Zhang, W., Gao, J., Yi, J., Zhen, X., et al. (2019). An integrated analysis of the rice transcriptome and metabolome reveals root growth regulation mechanisms in response to nitrogen availability. *Int. J. Mol. Sci.* 20, 5893. doi: 10.3390/ijms20235893

Yang, L., Feng, Y. X., Lin, Y. J., and Yu, X. Z. (2021). Comparative effects of sodium hydrosulfide and proline on functional repair in rice chloroplast through the D1 protein and thioredoxin system under simulated thiocyanate pollution. *Chemosphere* 284, 131389. doi: 10.1016/j.chemosphere.2021.131389

Yang, X., Li, G., Tian, Y., Song, Y., Liang, W., and Zhang, D. A. (2018). Rice glutamyl-tRNA synthetase modulates early anther cell division and patterning. *Plant Physiol.* 177, 728–744. doi: 10.1104/pp.18.00110

Yonekura, M., Aoki, N., Hirose, T., Onai, K., Ishiura, M., Okamura, M., et al. (2013). The promoter activities of sucrose phosphate synthase genes in rice, *OsSPS1* and *OsSPS11*, are controlled by light and circadian clock, but not by sucrose. *Front. Plant Sci.* 4, 31. doi: 10.3389/fpls.2013.00031

Yu, X. Z., and Zhang, F. Z. (2013). Effects of exogenous thiocyanate on mineral nutrients, antioxidative responses and free amino acids in rice seedlings. *Ecotoxicology* 22, 752–760. doi: 10.1007/s10646-013-1069-6

Yuan, Y., Ou, J., Wang, Z., Zhang, C., Zhou, Z., and Lin, Q. (2007). Regulation of carbon and nitrogen metabolisms in rice roots by 2-oxoglutarate at the level of hexokinase. *Physiol. Plantarum* 129, 296–306. doi: 10.1111/j.1399-3054.2006.00806.x

Yue, J., Du, C., Ji, J., Xie, T., Chen, W., Chang, E., Chen, L., Jiang, Z., and Shi, S. (2018). Inhibition of α-ketoglutarate dehydrogenase activity affects adventitious root growth in poplar via changes in GABA shunt. *Planta* 248, 963–979. doi: 10.1007/s00425-018-2929-3

Zhang, Q., Feng, Y. X., Lin, Y. J., Tian, P., and Yu, X. Z. (2022). Proline-mediated regulation on jasmonate signals repressed anthocyanin accumulation through the MYB-bHLH-WDR complex in rice under chromium exposure. *Front. Plant Sci* 13, 13953398. doi: 10.3389/fpls.2022.953398

Zheng, Z. L. (2009). Carbon and nitrogen nutrient balance signaling in plants. *Plant Signal Behav.* 4, 584–591. doi: 10.4161/psb.4.7.8540

frontiers | Frontiers in Plant Science

TYPE Original Research
PUBLISHED 03 April 2023
DOI 10.3389/fpls.2023.1049824

OPEN ACCESS

EDITED BY
Walid Soufan,
King Saud University, Saudi Arabia

REVIEWED BY
Liaqat Shah,
Mir Chakar Khan Rind University, Pakistan
Xiping Wang,
Hebei Normal University, China

*CORRESPONDENCE
Youhong Song
uqysong@163.com

†These authors have contributed equally to this work

‡PRESENT ADDRESS
Najeeb Ullah,
Agricultural Research Station, Office of VP for Research & Graduate Studies, Qatar University, Doha, Qatar

SPECIALTY SECTION
This article was submitted to Plant Abiotic Stress, a section of the journal Frontiers in Plant Science

RECEIVED 21 September 2022
ACCEPTED 16 March 2023
PUBLISHED 03 April 2023

CITATION
Fang D, Huang J, Sun W, Ullah N, Jin S and Song Y (2023) Characteristics of historical precipitation for winter wheat cropping in the semi-arid and semi-humid area. *Front. Plant Sci.* 14:1049824. doi: 10.3389/fpls.2023.1049824

Characteristics of historical precipitation for winter wheat cropping in the semi-arid and semi-humid area

Dan Fang[1†], Jingyao Huang[1†], Weiwei Sun[1], Najeeb Ullah[2‡], Suwen Jin[3] and Youhong Song[1*]

[1]School of Agronomy, Anhui Agricultural University, Hefei, Anhui, China, [2]Faculty of Science, Universiti Brunei Darussalam, Gadong, Brunei, [3]Anhui Provincial Meteorological Information Center, Anhui, Meteorological Service, Hefei, Anhui, China

Winter wheat (*Triticum aestivum* L.) is one of major crops in the area along Huai river, China where it is a semi-arid and semi-humid region with sufficient precipitation for an entire season, but with uneven distribution within various growth stages. The instability of precipitation is an important factor in limiting wheat production potential under climate change. Therefore, it is essential to characterise the precipitation associated with different crop developmental stages. Based on climate data from 1999 to 2020 in six representative meteorological stations, we characterised the historical precipitation relating to seven key growth stages in winter wheat. There is no clear trend of interannual variation of precipitation for wheat season, with an average of precipitation of 414.4 $\pm$ 121.2 mm. In terms of the distribution of precipitation grade within a season, light rain was dominant. Continuous rain occurred frequently during the pre-winter seedling and overwintering stages. The critical period of water demand, such as jointing and booting, has less precipitation. The fluctuation range of precipitation in sowing, heading-filling and maturation stages is large, which means that there is flood and drought at times. In conclusion, these findings provide a foundation for instructing winter wheat cropping in confronting with waterlogging and drought risk due to uneven precipitation in 'Yanhuai' region, China.

KEYWORDS

winter wheat, waterlogging, drought, phenological development, precipitation grade, continuous rainfall

Introduction

The both sides along the Huai River in Anhui Province, China are named as 'Yanhuai', which is a large, low-lying Plain located adjacent to the river and some of its tributaries. This region is an important commodity grain supplier, both regionally and nationally. The cultivation system is dominated by an annual relay double cropping system, including

wheat-rice, wheat-maize and wheat-soybean. The winter wheat in this area is with a relatively fixed growing window i.e. from mid-October to early June, next year (Wang et al., 2011). The 'Yanhuai' area is located at the southern part of the Huaibei Plain and to the northern part of the middle and lower reaches of the Yangtze River, which is classified as a semi-arid and semi-humid area. The spatiotemporal distribution of precipitation resources within crop growing season is quite uneven due to monsoonal climate. In particular, great variability in intensity and frequency of precipitation often causes frequent waterlogging and drought, resulting in huge risk for wheat cropping.

Spatiotemporal variation in precipitation across Anhui Province has been reported (Ding et al., 2016; Jiang and Sun, 2012; Du et al., 2021). A study from over 50-year data suggests an increasing trend in annual precipitation of Anhui Province with a highly interdecadal variability in the summer rainfall. In space, precipitation in the whole Province shows a decreasing trend from Southeast to Northwest (Nie et al., 2017). Spatiotemporal distribution analysis for different magnitudes of precipitation in the 'Yanhuai' region suggests that the precipitation mainly occurred in the form of middle, large, and torrential rain events (Zhu et al., 2019). Uncertain and erratic distribution of precipitation is the major limitation to crop growth in the 'Yanhuai' basin (Nie et al., 2019). The distribution of precipitation among various growth stages of winter wheat crop is uneven, which may compromise the potential of crop yield (Yao et al., 2017). Hence, it is necessary to characterise the features of precipitation with regards to winter wheat season in the 'Yanhuai' region, China.

Previous studies are primarily focused on the spatiotemporal distribution of precipitation (Ye and Li, 2017; Yu et al., 2017; Sun et al., 2019) and characteristics of precipitation intensity in this region (Liu et al., 2021; Yin et al., 2021). However, the pattern of precipitation with regards to wheat growth and development has seldom been reported. As such, the existing information is inadequate in advising wheat sustainable farming under this particular climate scenario. Therefore, the objective of this study is to investigate the spatiotemporal distribution of precipitation in relating to wheat developmental stages, and quantify the characteristics of the precipitation amount and days, distribution of different grades, and continuous rain events based on climate data from 1999 to 2020 at six meteorological stations.

Materials and methods

Study area

The Huai River runs through from West to East in North Anhui Province, China, which is located in Anhui Province with a total length of 430 kilometers. It has a drainage area of 21,434 km^2, accounting for 15.3% of the Anhui provincial territory. Six meteorological stations i.e. Yingshang, Huoqiu, Fengtai, Shouxian, Huaiyuan, and Fengyang along the 'Yanhuai' in Anhui Province (Figure 1), located at the latitude of 32° 22'–32 °59'N and the longitude of 116°14'–117°33'E (Table 1), were chosen in this study. The 'Yanhuai' region is located at the transition zone between the warm temperate zone and subtropical zone, which has many low-lying, flood diversion and retention areas. The majority of precipitation occurs from May to October, with an annual average of 846.5 mm (Yu et al., 2007).

Growth stages of winter wheat

Based on local practice, the life cycle of winter wheat along the Huai River in Anhui Province was divided into seven growth stages (Table 2).

Data source and analysis

The meteorological data obtained from the Anhui Provincial Meteorological Information Center, including daily precipitation, precipitation days, and sunlit hours, during the wheat growing seasons from 1999 to 2020 at the six meteorological stations (Figure 1), were obtained. These data were analyzed for

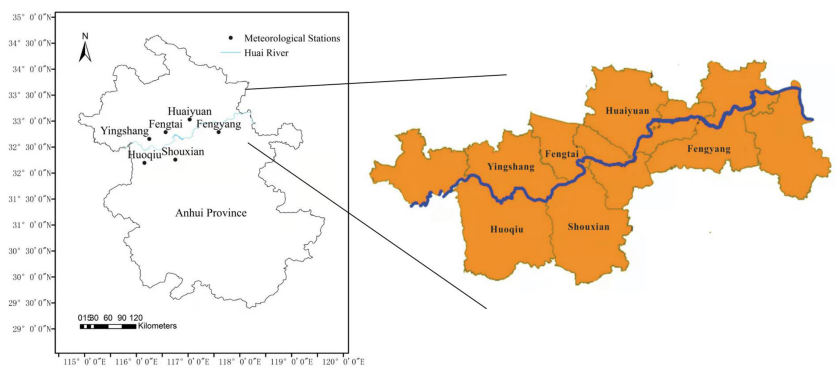

FIGURE 1
Locations of the six meteorological stations i.e. Yingshang, Huoqiu, Fengtai, Shouxian, Huaiyuan, and Fengyang in 'Yanhuai' region.

TABLE 1 Basic information of the six meteorological stations i.e. Yingshang, Huoqiu, Fengtai, Shouxian, Huaiyuan, and Fengyang in 'Yanhuai' region.

Station Name	Latitude	Longitude	Altitude (m)
Yingshang	32.39	116.14	25.2
Huoqiu	32.22	116.18	27.9
Fengtai	32.43	116.46	23.0
Shouxian	32.26	116.47	25.7
Huaiyuan	32.59	117.04	24.5
Fengyang	32.51	117.33	24.6

TABLE 2 Growth stages of winter wheat and associated calendar in Huaibei Plain, Anhui Province, China.

Growth stage	S1	S2	S3	S4	S5	S6	S7
	Sowing	Pre-winter Seed-ling	Overwintering	Jointing	Booting	Heading-Filling	Maturation
Time	Mid to late Oct	Nov to Dec	Jan to Feb	Mar	Early to mid-Apr	Late Apr to mid-May	Late May to early Jun

characterising the precipitation distribution during wheat growing season in 'Yanhuai' region.

Grade of precipitation

According to the "Grade of precipitation standard" National GB/T28592-2012 (AQSIQ, 2012), precipitation can be divided into seven grades, based on the amount of precipitation over a 24-hour period (Table 3). If daily precipitation including fog, dew, and frost is ≥ 0.1 mm, it is counted as a precipitation day.

Analysis of continuous rain features

When precipitation occurs for 3 consecutive days or more (daily precipitation ≥ 0.1 mm), it is regarded as continuous rain. A break in precipitation for 1 day is allowed in the middle of continuous rainfall events of more than 3 days, but the sunlit time of that day is considered to be less than 2 h. During continuous rain, a trace of precipitation is allowed, but the sunlit time on that day is considered to be less than 4 h (Anhui Meteorological Bureau Data Room, 1983). Based on the difference in the number of rainy days, continuous rainy days are divided into 3–6 days and ≥ 7 days (Chen et al., 2009; Liu et al., 2012).

TABLE 3 Grade of precipitation over a 24-hour period.

	Grade	24-hour precipitation (mm)
G0	Scattered rain	<0.1
G1	Light rain	0.1–9.9
G2	Moderate rain	10.0–24.9
G3	Heavy rain	25.0–49.9
G4	Rainstorm	50.0–99.9
G5	Torrential rain	100.0–249.9
G6	Extraordinary rainstorm	≥250.0

Data analysis

Microsoft Office Excel (Microsoft Excel 2016, Microsoft, USA) was used to analyze the data of winter wheat during each specific growth stage. Coefficient of variation (CV) was used to indicate the fluctuation of historical data.

Results

Distribution of precipitation during wheat growing season

Precipitation characteristics from 1999 to 2020 at six sites (Figure 1) are shown in Table 4. Precipitation during wheat growing season varied with years, with an average of six stations ranging from 141.4 to 709.2 mm over the 22 years. The highest precipitation occurred in 2017 at Huoqiu and other five stations in 2016; the lowest precipitation in all six meteorological stations was observed in 2010. The maximum precipitation was 808.5 mm (Huoqiu), while the minimum precipitation was 127.0 mm (Shouxian), and the range is 681.5 mm. The overall CV ranged from 0.27 to 0.34, indicating that variability of precipitation over wheat season was moderate.

Distribution of precipitation during different wheat growth stages

The precipitation distribution during different wheat growth stages was fluctuant, and the variability for each meteorological station was similar (Figure 2). The average precipitation during the pre-winter seedling (S2), overwintering (S3), heading-filling (S6), and maturation stages (S7) were relatively large with a value over 60 mm; during the sowing (S1), jointing (S4), and booting stages

10.3389/fpls.2023.1049824

TABLE 4 Precipitation characteristics during wheat growing season from 1999 to 2020 at six meteorological stations.

	Maximum (mm)	Minimum (mm)	Mean (mm)	CV
Yingshang	771.2	137.8	425.0	0.31
Huoqiu	808.5	166.6	455.5	0.29
Fengtai	706.3	134.1	414.0	0.28
Shouxian	780.8	127.0	416.3	0.34
Huaiyuan	589.1	153.4	374.7	0.27
Fengyang	708.3	129.5	401.1	0.32

(S5) were relatively small. The precipitation fluctuated greatly during the maturation (S7) and sowing stages (S1) but remained relatively stable during the overwintering stage (S3).

Precipitation amount distribution during seven wheat growth stages across the 22 years is presented in the heatmap (Figure 3). Where, 0% indicates no precipitation, and 100% represents the proportion of the current year's precipitation to the maximum precipitation from 1999 to 2020 at this stage. The 'Yanhuai' region is subjected to alternation of waterlogging and drought, in addition, the frequencies of waterlogging were relatively high during the pre-winter seedling, overwintering and heading-filling stages.

Drought that persists for years was observed during the sowing and booting stage. The minimum value for the precipitation and the number of precipitation days of the six stations all appeared in 2010. Both were the fewest since 1961. The continuous lack of precipitation led to severe drought in autumn, winter and spring. During the sowing stage for wheat in 2016, the soil was so wet after more than 12 consecutive days of rain that the wheat could not be planted as scheduled. The number of days for precipitation were significantly

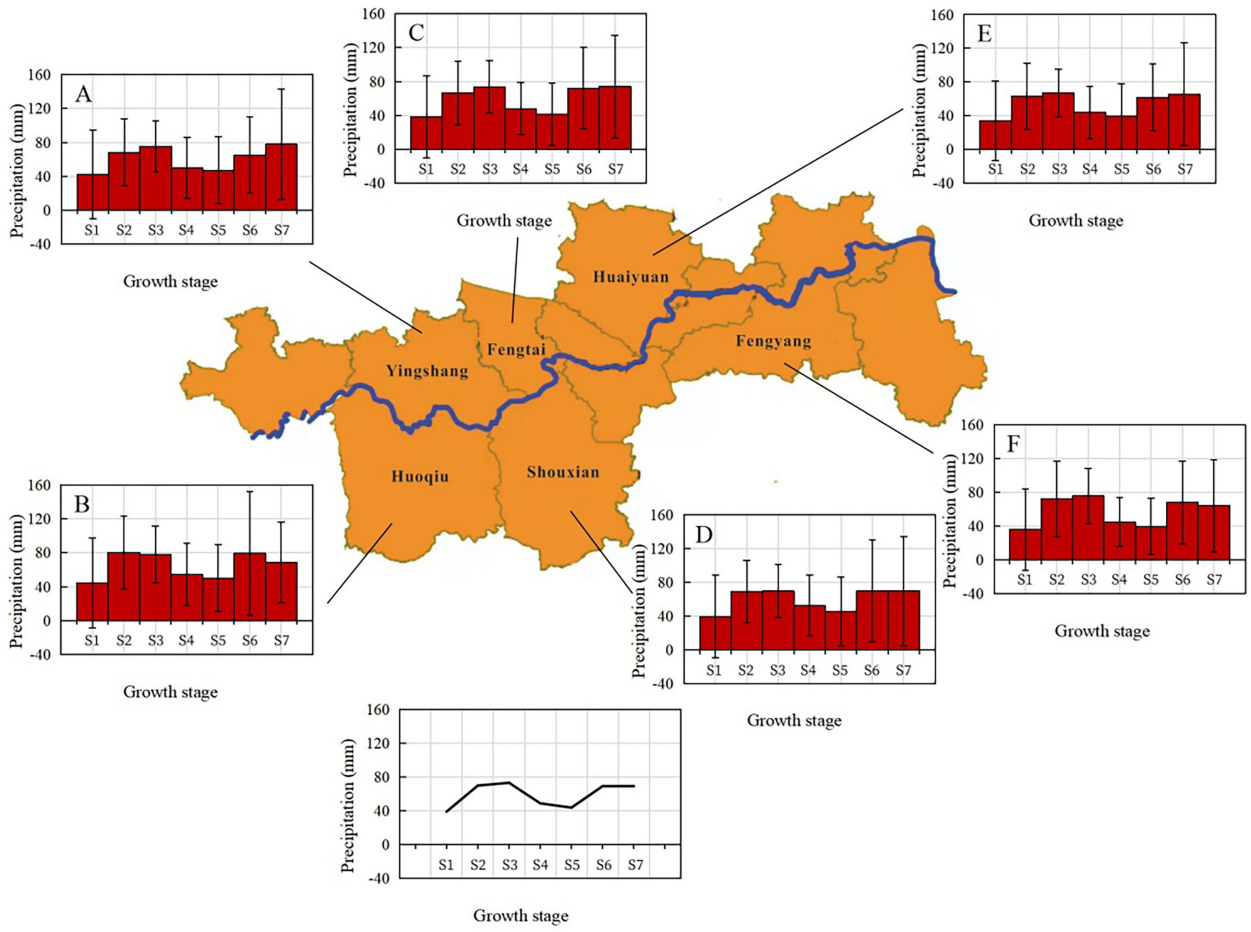

FIGURE 2
Average precipitation during wheat growth stages in 'Yanhuai' region i.e. **(A)** Yingshang, **(B)** Huoqiu, **(C)** Fengtai, **(D)** Shouxian, **(E)** Huaiyuan, and **(F)** Fengyang from 1999 to 2020.

greater than usual, while the sunshine duration was significantly lesser. In the early and middle of May in 2018, there was a lot of precipitation, especially concentrated heavy precipitation, resulting in extreme wet soil, for winter wheat in the head-filling stage. Serious waterlogging occurred during the maturation stage for wheat in 2000. Such extreme weather processes can be seen in Figure 3.

Distribution of precipitation days during wheat growing season

Distribution of annual precipitation days from 1999 to 2020 at six sites i.e., Yingshang, Huoqiu, Fengtai, Shouxian, Huaiyuan, and Fengyang is shown in Table 5. Precipitation days of wheat growing season varied across the years, and the average precipitation days of six stations ranged from 38 days to 78 days over the 22 years. The year with the maximum precipitation days during wheat season greatly differed, while the minimum precipitation days occurred in 2010. The CV of precipitation days ranged from 0.16 to 0.17, and the randomicity of growing season precipitation days was determined as the mild variability.

Different grades of precipitation during various wheat growth stages

Frequency in Precipitation days in different precipitation grades

The frequencies of precipitation days in different grades during various wheat growth stages across six sites i.e., Yingshang, Huoqiu, Fengtai, Shouxian, Huaiyuan, and Fengyang are shown in Figure 4. Light rain, moderate rain, and heavy rain occurred during seven wheat growth stages. During each wheat growth stage, for the different-grade rain, the light rain occurs the most frequently, followed by the moderate rain, and the heavy rain and rainstorm occur less frequently than the moderate rain, while torrential rain is rare. Rainstorm occurred during the sowing (0.2-0.4%), booting (0.2-0.7%), heading-filling (0.2-0.6%), and maturation (0.9-1.5%) stages but did not occur during the overwintering stage. Torrential rain only occurred during the heading-filling (0-0.2%) and maturation (0.4-1.1%) stages. It is noted that extraordinary rainstorms were not observed in none of the six meteorological stations.

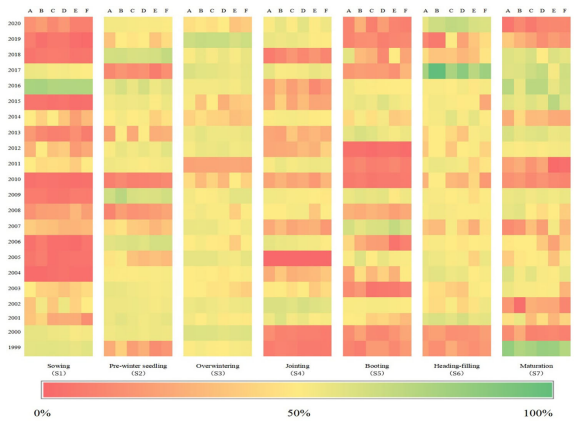

FIGURE 3
Precipitation during various wheat growth stages including Sowing (S1), Pre-winter seedling (S2), Overwintering (S3), Jointing (S4), Booting (S5), Head-filling (S6) and Maturation (S7) in 'Yanhuai' region i.e. **(A)** Yingshang, **(B)** Huoqiu, **(C)** Fengtai, **(D)** Shouxian, **(E)** Huaiyuan, and **(F)** Fengyang from 1999 to 2020. The greater greenness indicates more precipitation and wetter, while the greater redness indicates less precipitation and drier.

TABLE 5 Annual precipitation days with regards to the whole wheat growing season from 1999 to 2020 at six meteorological stations i.e. Yingshang, Huoqiu, Fengtai, Shouxian, Huaiyuan, and Fengyang, located in Yanhuai region.

	Maximum	Minimum	Mean	CV
Yingshang	78	35	63	0.16
Huoqiu	85	41	67	0.17
Fengtai	81	37	64	0.17
Shouxian	77	36	63	0.17
Huaiyuan	72	35	60	0.17
Fengyang	78	43	62	0.16

10.3389/fpls.2023.1049824

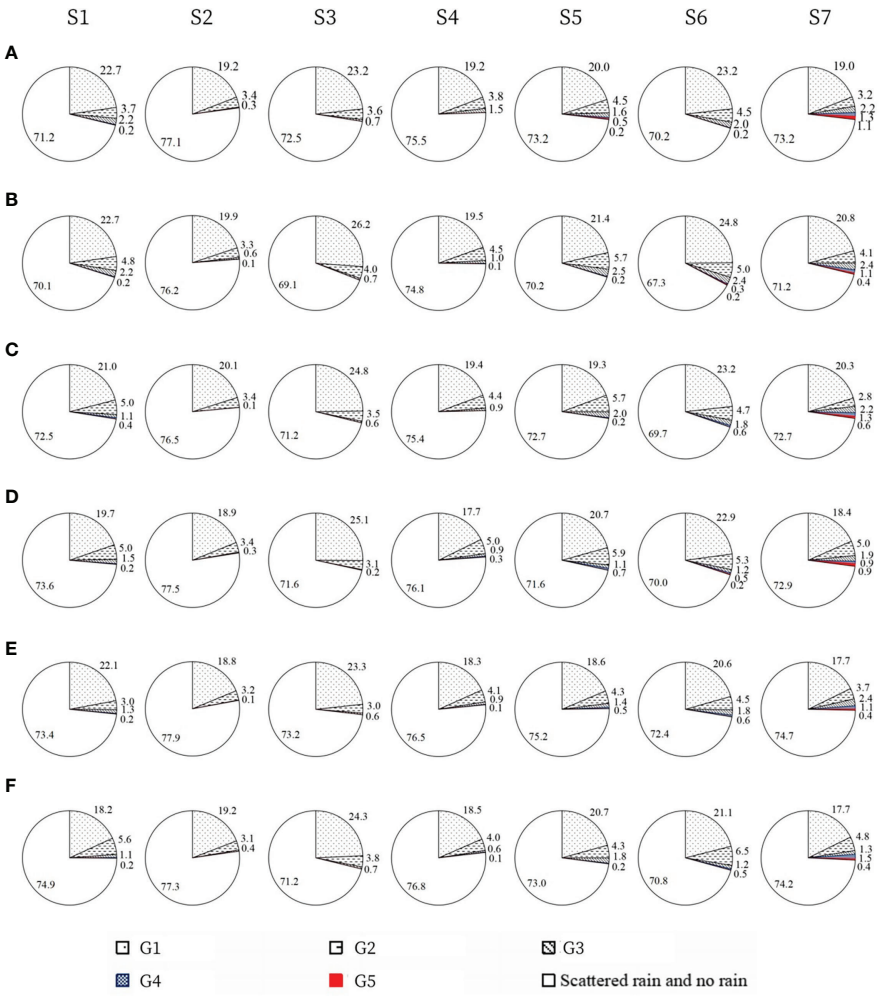

FIGURE 4
Frequencies of precipitation days in precipitation grades during wheat growth stages in Yanhuai region i.e. **(A)** Yingshang, **(B)** Huoqiu, **(C)** Fengtai, **(D)** Shouxian, **(E)** Huaiyuan, and **(F)** Fengyang from 1999 to 2020.

Precipitation percentage in different precipitation grades

The percentages of precipitation from various grades at different wheat growth stages at six sites i.e. Yingshang, Huoqiu, Fengtai, Shouxian, Huaiyuan, and Fengyang are shown in Figure 5. The percentages of rainfall in different grades and a significant difference during seven wheat growth stages is shown (Figure 5). Light rain and moderate rain were dominant during the pre-winter seedling and overwintering stages, while light, moderate, and heavy rain were dominant during the sowing, jointing, and booting stages. Torrential rain only occurred during the maturation stage at six sites.

Distribution of continuous rain during different wheat growth stages

Frequency of continuous rain during different wheat growth stages

The frequencies of continuous rain during each wheat growth stage at six sites i.e. Yingshang, Huoqiu, Fengtai, Shouxian, Huaiyuan, and Fengyang are shown in Figure 6. The frequencies of continuous rain varied among different growth stages. Continuous rain lasting more than 7 days occurred more frequently during the sowing (4.5-7.4%), overwintering (2.4-5.5%), pre-winter seedling (3.6-5.1%) stages, and rarely occurred during the other growth stages. It can be seen from the figure that continuous rain is more likely to occur during the early growth stages of winter wheat. The longest continuous rainy days occurred during the sowing stage were 12 days (Yingshang, Huoqiu, Shouxian, and Huaiyuan) and 14 days (Fengtai and Fengyang), respectively.

Precipitation percentage of continuous rain during different wheat growth stages

The precipitation percentage of continuous rain during each growth stage at six sites i.e. Yingshang, Huoqiu, Fengtai, Shouxian, Huaiyuan, and Fengyang is shown (Figure 7). The precipitation percentage of continuous rain lasting 3–6 days was highest during the overwintering stage (50.3-71.8%), followed by the pre-winter seedling stage (42.9-55.6%). The precipitation percentage of

10.3389/fpls.2023.1049824

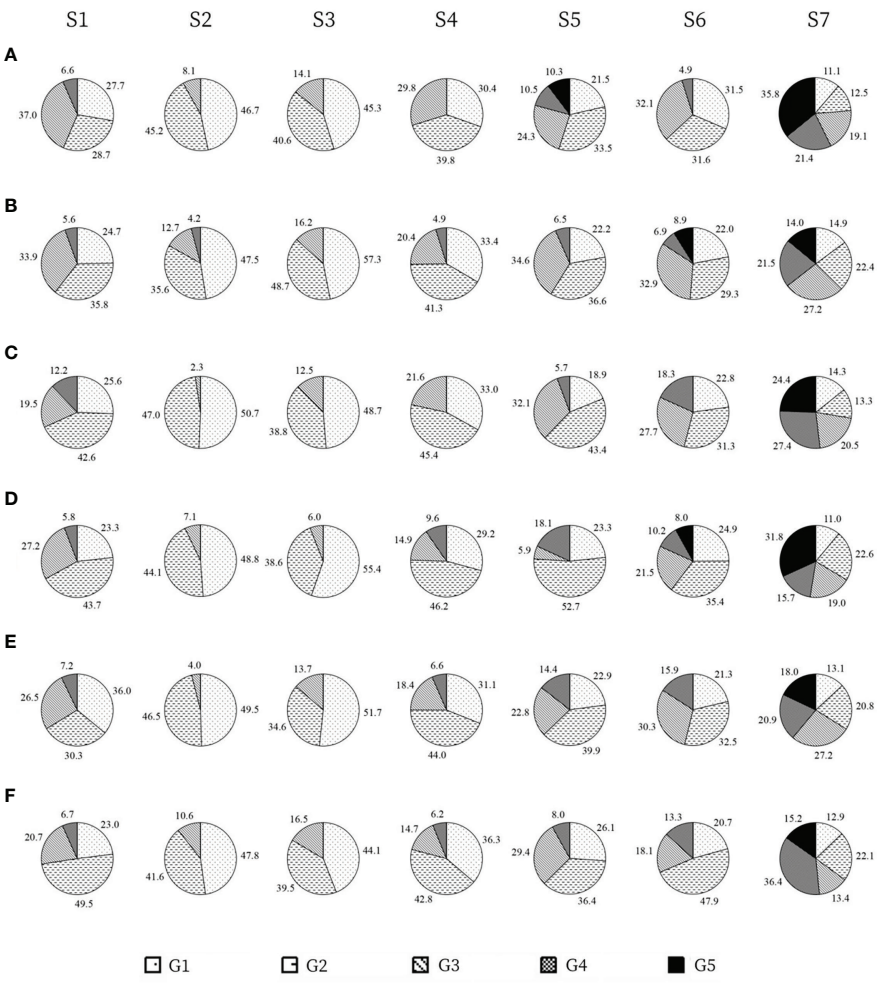

FIGURE 5
Precipitation amount percentage at different precipitation grades during wheat growth stages in 'Yanhuai' region i.e. **(A)** Yingshang, **(B)** Huoqiu, **(C)** Fengtai, **(D)** Shouxian, **(E)** Huaiyuan, and **(F)** Fengyang from 1999 to 2020.

continuous rain lasting more than 7 days was highest during the sowing stage (29.3-38.7%), followed by the pre-winter seedling (10.1-25.9%) and overwintering (16.8-20.5%) stages. The data reveals that the precipitation type during the early growth stages (S1-S3) is mainly dominated by continuous rain. The maximum precipitation occurred during the sowing stage (Huoqiu and Fengyang) and the maturation stage (Yingshang, Fengtai, Shouxian, and Huaiyuan).

Discussion

Characteristics of waterlogging and drought

The climatic productivity potential of winter wheat in the Huai River Basin is restricted by precipitation episode in the growing season (Yuan et al., 2016). Precipitation appears sufficient during the growing season of winter wheat in the region, nevertheless the distribution of precipitation is fairly uneven, causing high risk of drought or waterlogging events. The impacts are also influenced by meteorological condition e.g. sunshine, soil environment e.g. soil texture and crops themselves e.g. water demand, root characteristics (Dickin and Wright, 2008; Licausi and Perata, 2009; Katerji et al., 2010; Zhang et al., 2010; Araki et al., 2012b; Zhang et al., 2021). This study mainly considered the influence of precipitation and sunshine, and thus focused on characterising the precipitation during winter wheat growing season.

The representative soil types in 'Yanhuai' region, include sand ginger black soil, tidal soil and silty soil. The soil is short of organic matter and hard to keep soil water. Root growth has a close relationship with soil water content (Lv et al., 2010). Either too much or insufficient soil water are adverse conditions for root growth. The soil moisture refers to the soil water status in the main root system activity layer of crops (Inoue et al., 2004). In this study, soil moisture was used as an index to determine whether the soil is too dry or too wet. And soil moisture measured is normally at the depth of 0-20 cm, 20-40cm in the particular region due to shallow soil layers. Soil moisture less than 60% is considered drought, while more than 80% is waterlogging.

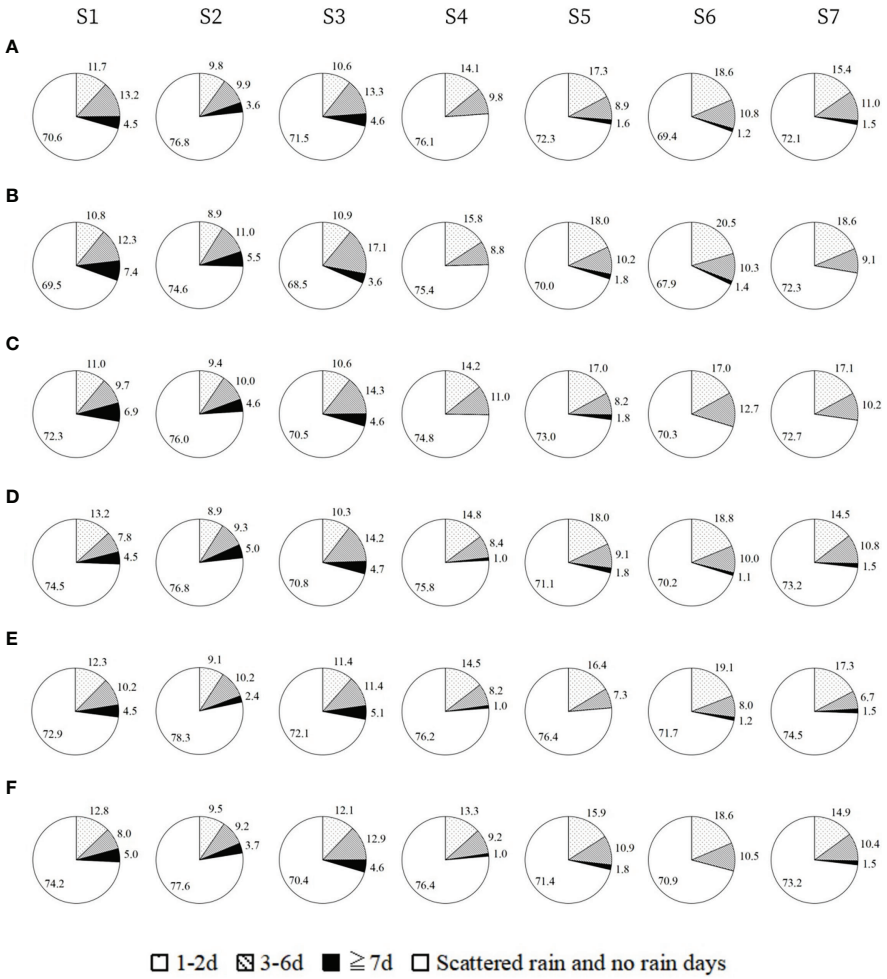

FIGURE 6
Frequencies of continuous rain during different winter wheat growth stages in Yanhuai region i.e. **(A)** Yingshang, **(B)** Huoqiu, **(C)** Fengtai, **(D)** Shouxian, **(E)** Huaiyuan, and **(F)** Fengyang from 1999 to 2020.

Therefore, in the growing season of wheat, the influence of soil moisture profile and soil texture on available soil water holding capacity and wheat root will be considered in future. Due to the differences in drainage and irrigation conditions and the cost, many farmers did not take irrigation measures, so irrigation and drainage methods were not investigated in this study. The losses caused by drought and waterlogging with the same intensity to areas with good drainage and irrigation conditions are less than those with poor conditions, which is the manifestation of regional vulnerability differences (Zhang et al., 2007). Drought and flood indicators should take more account of the impact on agriculture. On the basis of collecting crop growth information of wheat growing season, combined with some meteorological, phenological and soil observation data, the disaster monitoring, diagnosis and analysis model will be established (Ge et al., 2016; Ge et al., 2017).

The water requirement of winter wheat of the whole growing period and different growth stages during 1961-2010 in China were estimated (Sun et al., 2013). Combined with the spatial distribution characteristics of precipitation, the water-meeting situation of winter wheat during the growing season was analyzed. Results revealed that water requirement of winter wheat in Anhui Province is 300-400 mm. By comparing the water deficit of the most serious areas, the growth stage of the water deficit of the least seriously is from sowing to over-wintering and the growth stage of the water deficit of the most severe is from flowering to ripening. However, the results of this study showed that winter wheat was always dry during sowing stage and waterlogging occasionally occurred during heading-filling stage. The metrological data from the 22 years indicated that 'Yanhuai' region was subjected to alternation of waterlogging and drought. The frequencies of waterlogging were relatively high during the pre-winter seedling, overwintering and heading-filling stages. Drought that persists for years was observed during the sowing and booting stage. The continuous lack of precipitation led to severe autumn, winter and spring drought in 2010. Waterlogging and drought that persists for years or the alternating occurrence of waterlogging and drought (from drought to waterlogging and from waterlogging to drought) in the same year are often observed.

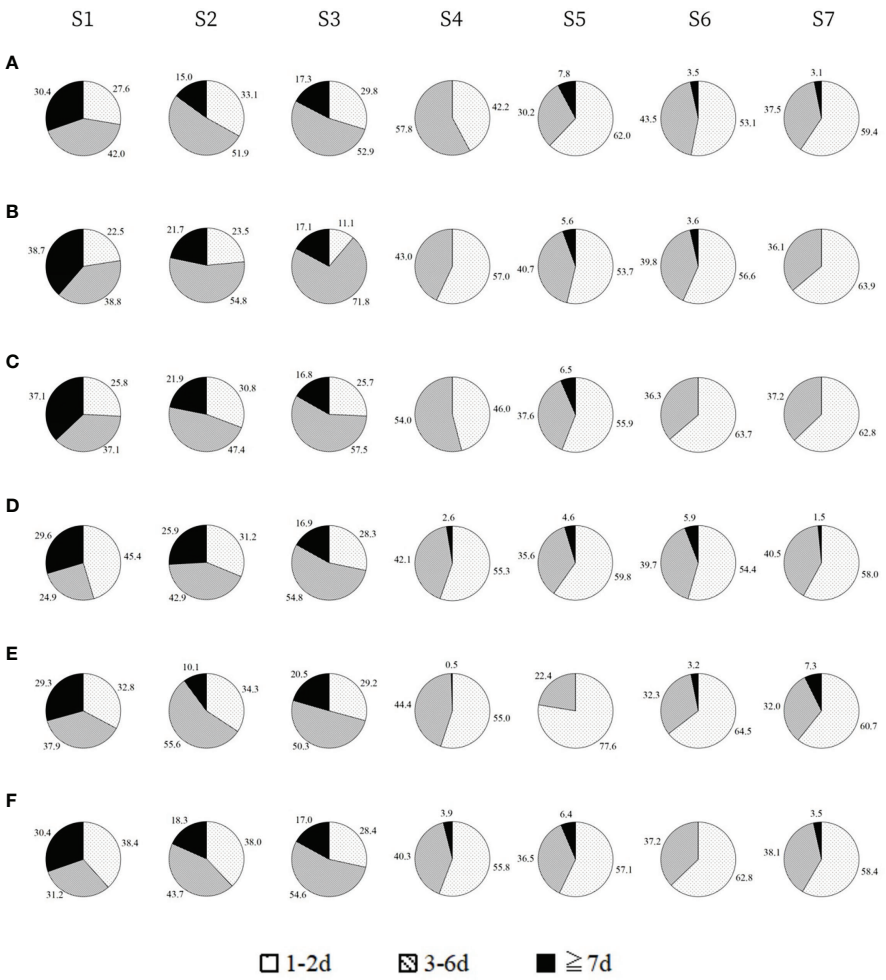

FIGURE 7
Precipitation amount percentages of continuous rain during different wheat growth stages in Yanhuai region i.e. **(A)** Yingshang, **(B)** Huoqiu, **(C)** Fengtai, **(D)** Shouxian, **(E)** Huaiyuan, and **(F)** Fengyang from 1999 to 2020.

Cropping risk and cultivation practices of wheat production in 'Yanhuai' region

The 'Yanhuai' region is an important commodity grain production base. Good knowledge of waterlogging and drought behaviors is of great importance in the planning and management of agricultural activities in this region. The interannual fluctuation of precipitation is large, and the interannual relative variability of precipitation is the largest in autumn. Maintaining the balance of groundwater exploitation and replenishment, combining drainage and storage, aiming at improving the efficiency of water resources utilization, vigorously developing efficient water-saving irrigation technology is the key measure to deal with the adverse effects of frequent meteorological droughts on crop production, and also an important measure to ensure water resources and food security.

As observed in this study, continuous rains may occur at each stage in winter wheat growing season. In the mechanized agriculture, these continuous rains may delay crop sowing and impact the harvesting activities (Chen et al., 2009). Further, frequent rains and low temperature during the pre-winter seedling and overwintering stages, and sudden temperature increases during jointing stage, could cause severe aphid outbreaks. After heading and flowering, aphids will erupt again in high temperature and humidity (Zhao et al., 2016). The booting stage is the sensitive stage of wheat waterlogging injury (Li et al., 2001). The number of rainy days during the heading-filling stage is the most important factor for the occurrence of scab (Zhao et al., 2016). Waterlogging during booting to maturation stage which are the key periods of yield formation can lead to reduced production (Li et al., 2001). Continuous rain during maturation stage, may induce pre-harvest sprouting in winter wheat (Zhao et al., 2016). To minimize this damage, it is necessary to plow the soil on sunny days after rice harvest. After rainfall in spring, timely dredge furrows can ensure the smooth drainage of the field, to prevent waterlogging, and reduce disease, insect and grass damage. Selecting suitable fertilizer and growth regulator during different growth stages can alleviate waterlogging damage to a certain extent (Gao et al., 2020). Considering the water and heat resources and the actual situation of agriculture, it is of great significance to modify the tillage system in minimise impacts of likely waterlogging and drought.

Conclusion

Precipitation during wheat growing season varied greatly with years in the wheat producing regions of Huai river in Anhui Province, China. Precipitation is unevenly distributed across winter wheat developmental phases. Continuous rain occurred frequently during the pre-winter seedling and overwintering stages, and timely drainage measure is needed at this time. There is less precipitation in key water demand periods such as jointing and booting, so irrigation should be timely. The precipitation fluctuated greatly in sowing, heading, filling and maturity, and drought and flood occurred from time to time. Our work guides to take effective measures for irrigation or drainage management based on the precipitation characteristics of winter wheat at different growth stages. Our findings provide a scientific basis for disaster prevention and mitigation in wheat sustainable production in the 'Yanhuai' region or similar climate zones.

Data availability statement

The original contributions presented in the study are included in the article/supplementary material. Further inquiries can be directed to the corresponding authors.

Author contributions

DF did data collection and analysis, as well as drafted and finalized the manuscript; JH contributed to data analysis and the manuscript drafting; WS contributed to data analysis and figure presentation; NU contributed to manuscript revision; SJ contributed to data collection and analysis, and manuscript revision. YS supervised the work and finalized the writing. All authors contributed to the article and approved the submitted version.

Funding

This study was financially supported by the National Key R&D Program of China (No. 2017YFD0301307).

Conflict of interest

The authors declare that the research was conducted in the absence of any commercial or financial relationships that could be construed as a potential conflict of interest.

Publisher's note

References

Anhui Meteorological Bureau Data Room (1983). *Anhui climate* (Hefei, China: Anhui Science and Technology Press), 75–79.

AQSIQ (2012). *Grade of precipitation (GB/T 28592–2012)* (Beijing, China: China Standards Press).

Araki, H., Hossain, M., and Takahashi, T. (2012b). Waterlogging and hypoxia have permanent effects on wheat root growth and respiration. *J. Agron. Crop Sci.* 198 (4), 264–275. doi: 10.1111/j.1439-037X.2012.00510.x

Chen, X. Y., Ma, X. Q., and Yao, Y. (2009). Law of autumn continuous precipitation occurrence and its influence on autumn harvesting and planting in anhui province. *Chin. J. Agrometeorol.* 30 (supplement 2), 210–214. doi: CNKI:SUN:ZGNY.0.2009-S2-007

Dickin, E., and Wright, D. (2008). The effects of winter waterlogging and summer drought on the growth and yield of winter wheat (*Triticum aestivum* l.). *Eur. J. Agron.* 28 (3), 234–244. doi: 10.1016/j.eja.2007.07.010

Ding, J. L., Wang, H. O., Dong, Z. R., and Wang, F. W. (2016). Characteristics of extreme precipitation events in anhui province during 1960-2013. *J. Arid Meteorol.* 34 (2), 252–260. doi: 10.11755/j.issn.1006-7639(2016)-02-0252

Du, M. C., Zhang, J. Y., Yang, Q. L., Wang, Z. L., Bao, Z. X., Liu, Y. L., et al. (2021). Spatial and temporal variation of rainfall extremes for the north anhui province plain of China over 1976-2018. *Natural Hazards* 105, 2777–2797. doi: 10.1007/s11069-020-04423-9

Gao, J. W., Su, Y., and Shen, A. L. (2020). Research progress of the response mechanism of wheat growth to waterlogging stress and the related regulating managements. *Chin. J. Appl. Ecol.* 31 (12), 4321–4330. doi: 10.13287/j.1001-9332.202012.028

Ge, D. K., Cao, H. X., Ma, X. Q., Zhang, W. Y., and Zhang, W. X. (2016). Sensitivity analysis and damage assessment for wheat drought and waterlogged based on crop growth model. *Jiangsu J. @ Agr. Sci.* 32 (6), 1302–1309. doi: 10.3969/j.issn.1000-4440.201.06.017

Ge, D. K., Cao, H. X., Yang, Y. W., Ma, X. Q., Zhang, W. Y., and Zhang, W. X. (2017). Regional monitoring and refined assessment for damage from wheat drought and waterlogging based on WCSODS. *Jiangsu J. @ Agr. Sci.* 33 (5), 1062–1068. doi: 10.3969/j.issn.1000-4440.2017.05.016

Inoue, T., Inanaga, S., Sugimoto, Y., and El Siddig, K. (2004). Contribution of pre-anthesis assimilates and current photosynthesis to grain yield, and their relationships to drought resistance in wheat cultivars grown under different soil moisture. *Photosynthetica* 42, 99–104. doi: 10.1023/B:PHOT

Jiang, J. J., and Sun, W. G. (2012). Analysis of spatial-temporal precipitation variation in anhui province during 1959-2007. *Chin. J. Agrometeorol.* 33 (1), 27–33. doi: 10.3969/j.issn.1000-6362.2012.01.00

Katerji, N., Mastrorilli, M., and Cherni, H. E. (2010). Effects of corn deficit irrigation and soil properties on water use efficiency. a 25-year analysis of a Mediterranean environment using the STICS model. *Eur. J. Agron.* 32, 177–185. doi: 10.1016/j.eja.2009.11.001

Li, J. C., Dong, Q., and Yu, S. L. (2001). Effect of waterlogging at different growth stages on photosynthesis and yield of different wheat cultivars. *Acta Agronomica Sin.* 27 (4), 434–441. doi: 10.1136/bmj.2.6096.1220

Licausi, F., and Perata, P. (2009). Low oxygen signaling and tolerance in plants. *Adv. Botanical Res.* 50, 139–198. doi: 10.1016/S0065-2296(08)00804-5

Liu, R. N., Yang, T. M., Chen, J. H., Chen, P., and Wang, X. D. (2012). Study on the distribution characteristics of spring continuous precipitation and assessment of rape yield losses in anhui province. *Chin. Agric. Sci. Bull.* 28 (34), 252–256. doi: 10.3969/j.issn.1000-6850.2012.34.043

Liu, Y. B., Zhang, C., Tang, Q. H., Hosseini-Moghari, S. M., Haile, G. G., Li, L. F., et al. (2021). Moisture source variations for summer rainfall in different intensity classes over huaihe river valley, China. *Climate Dynam.* 57, 1121–1133. doi: 10.1007/s00382-021-05762-4

Lv, G. H., Kang, Y. H., Li, L., and Wan, S. Q. (2010). Effect of irrigation methods on root development and profile soil water uptake in winter wheat. *Irrigation Sci.* 28, 387–398. doi: 10.1007/s00271-009-0200-1

Nie, H., Qin, T. L., Li, C. Z., Tang, Y., Weng, B. S., and Wang, Y. (2019). Trend analysis of effective precipitation in different growth stages of winter wheat in huaihe river plain. *Theor. Appl. Climatol.* 138, 2043–2056. doi: 10.1007/s00704-019-02949-y

Nie, B., Shen, F., Xu, G. L., and Huang, Y. P. (2017). Analysis of temporal-spatial change in anhui province in recent 50 years. *J. Anhui Normal Univ. (Natural Science)* 40 (6), 574–579. doi: 10.14182/J.cnki.1001-2443.2017.06.011

Sun, S., Yang, X. G., Li, K. N., Zhao, J., Ye, Q., Xie, W. J., et al. (2013). Analysis of spatial and temporal characteristics of water requirement of winter wheat in China. *Trans. Chin. Soc. Agric. Eng.* 29 (15), 72–82. doi: 10.3969/j.issn.1002-6819.2013.15.010

Sun, Y., Zhu, W. J., Liu, D. Y., Huang, W. Y., and Chen, S. J. (2019). Precipitation climatically features over the huai river basin, China. *Dynam. Atmospheres Oceans* 86, 104–115. doi: 10.1016/j.dynatmoce.2019.03.006

Wang, J. L., Zhao, L., and He, X. F. (2011). SWOT analysis on wheat production in the huai river region in anhui province. *J. Anhui Agric. Sci.* 39 (22), 13309–13310, 13313. doi: 10.13989/j.cnki.0517-6611.2011.22.183

Yao, Y., Xu, Y., and Ma, X. Q. (2017). Influence of precipitation change on climatic potential productivity of major crops in the huaihe river basin. *Resour. Sci.* 39 (3), 490–500. doi: 10.18402/resci.2017.03.11

Ye, Z. W., and Li, Z. H. (2017). Spatiotemporal variability and trends of extreme precipitation in the huaihe river basin, a climatic transitional zone in East China. *Adv. Meteorol.*, 1–15.2017. doi: 10.1155/2017/3197435

Yin, Y. X., Chen, H. S., Wang, G. J., Xu, W. C., Wang, S. M., and Yu, W. J. (2021). Characteristics of the precipitation concentration and their relationship with the precipitation structure: A case study in the huai river basin, China. *Atmospheric Res.* 253, 105484. doi: 10.1016/j.atmosres.2021.105484

Yu, J. C., Huang, X. Y., Yu, Y., Chen, X. H., and Wang, H. (2007). Characteristics of agricultural flood disaster phase and the cultivating models for avoiding flood disaster along huai river of anhui province. *J. China Agric. Univ.* 12 (6), 24–30. doi: 10.3321/j.issn:1007-4333.2007.06.005

Yu, Z. L., Yan, D. H., Ni, G. H., Do, P., Yan, D. M., Cai, S. Y., et al. (2017). Variability of spatially grid-distributed precipitation over the huaihe river basin in China. *Water* 9 (7), 489. doi: 10.3390/w9070489

Yuan, Z., Yan, D. H., Yang, Z. Y., Yin, J., Breach, P., and Wang, D. Y. (2016). Impacts of climate change on winter wheat water requirement in haihe river basin. *Mitigation Adaptation Strategies Global Change* 21, 677–697. doi: 10.1007/s11027-014-9612-1

Zhang, X. Y., Chen, S. Y., Sun, H. Y., Wang, Y. M., and Shao, L. W. (2010). Water use efficiency and associated traits in winter wheat cultivars in the north China plain. *Agric. Water Manage.* 97, 1117–1125. doi: 10.1016/j.agwat.2009.06.003

Zhang, L., Chu, Q. Q., Jiang, Y. L., Chen, F., and Lei, Y. D. (2021). Impacts of climate change on drought risk of winter wheat in the north China plain. *J. Integr. Agric.* 20 (10), 2601–2612. doi: 10.1016/S2095-3119(20)63273-7

Zhang, A. M., Ma, X. Q., Yang, T. M., Sheng, S. X., and Huang, Y. (2007). The influence of drought and waterlogging disasters on crop yields in anhui province. *J. Appl. Meteorol. Sci.* 18 (5), 619–626. doi: 10.11898/1001-7313.20070517

Zhao, Z. H., Wang, Q., and Zhu, X. M. (2016). New occurrence characteristics and control measures of wheat disease and insect pests in 2015. *China Plant Prot.* 36 (08), 33–36, 45. doi: 10.3969/j.issn.1672-6820.2016.08.006

Zhu, J. Q., Han, M., Xu, Z. H., Zhang, X., and Tian, L. X. (2019). Temporal-spatial distribution characteristics and factors of different magnitude rainfall in huai river basin. *Res. Soil Water Conserv.* 26 (4), 87–95. doi: CNKI:SUN:STBY.0.2019-04-016

frontiers | Frontiers in Plant Science

TYPE Original Research
PUBLISHED 21 April 2023
DOI 10.3389/fpls.2022.1000877

OPEN ACCESS

EDITED BY
Vicent Arbona,
University of Jaume I, Spain

REVIEWED BY
Sajad Hussain,
Islamia University of Bahawalpur, Pakistan
Stefania Toscano,
University of Catania, Italy
Muhammad Mehood Iqbal,
Central Cotton Research Institute (CCRI), Pakistan

*CORRESPONDENCE
Allah Wasaya
wasayauaf@gmail.com
Marian Brestic
marian.brestic@uniag.sk
Ayman El Sabagh
ayman.elsabagh@agr.kfs.edu

SPECIALTY SECTION
This article was submitted to Plant Abiotic Stress, a section of the journal Frontiers in Plant Science

RECEIVED 22 July 2022
ACCEPTED 29 December 2022
PUBLISHED 21 April 2023

CITATION
Wasaya A, Rehman I, Mohi Ud Din A, Hayder Bin Khalid M, Ahmad Yasir T, Mansoor Javaid M, El-Hefnawy M, Brestic M, Rahman MA and El Sabagh A (2023) Foliar application of putrescine alleviates terminal drought stress by modulating water status, membrane stability, and yield- related traits in wheat (*Triticum aestivum* L.). *Front. Plant Sci.* 13:1000877. doi: 10.3389/fpls.2022.1000877

Foliar application of putrescine alleviates terminal drought stress by modulating water status, membrane stability, and yield- related traits in wheat (*Triticum aestivum* L.)

Allah Wasaya[1,2]*, Iqra Rehman[1,2], Atta Mohi Ud Din[3], Muhammad Hayder Bin Khalid[3], Tauqeer Ahmad Yasir[2], Muhammad Mansoor Javaid[4], Mohamed El-Hefnawy[5], Marian Brestic[6]*, Md Atikur Rahman[7] and Ayman El Sabagh[8,9]*

[1]Department of Agronomy, Bahauddin Zakariya University Multan, Multan, Pakistan, [2]College of Agriculture, University of Layyah, Layyah, Pakistan, [3]National Research Center of Intercropping, The Islamia University of Bahawalpur, Multan, Pakistan, [4]Department of Agronomy, College of Agriculture, University of Sargodha, Sargodha, Pakistan, [5]Department of Chemistry, Rabigh College of Sciences and Arts, King Abdulaziz University, Jeddah, Saudi Arabia, [6]Department of Plant Physiology, Slovak University of Agriculture, Nitra, Slovakia, [7]Grassland and Forage Division, National Institute of Animal Science, Rural Development Administration, Cheonan, Republic of Korea, [8]Department of Agronomy, Faculty of Agriculture, Kafrelsheikh University, Kafr al-Sheik, Egypt, [9]Department of Field Crops, Faculty of Agriculture, Siirt University, Siirt, Türkiye

Drought stress is one of the major limitations to the growth and yield productivity of cereal crops. It severely impairs the early growing and grain -filling stages of wheat. Therefore, cost- effective and eco-friendly approaches for alleviating drought stress in cereal crops are in high demand. Polyamines, such as putrescine, have a significant effect on improving crop yield under drought-stress conditions. Therefore, the current study was executed with the aim of exploring the significance of putrescine in alleviating drought stress and improving yield- related traits in wheat. Two distinct wheat cultivars (Fakhar-e-Bhakkar and Anaj-2017) were treated with the foliar application of different concentrations (control, 0.5, 1.0, and 1.5 PPM) of putrescine (put) under two moisture conditions (well- watered and terminal drought stress). The results demonstrate that the imposition of terminal drought stress significantly reduces different physiological and yield- related traits of both wheat cultivars. The reduction of relative water content (RWC%), membrane stability index (MSI), leaf area, tillers per plant, biomass yield, number of spikelets per spike, 100-grain weight, grain yield per plant, and straw yield was greater in Anaj-2017 than in Fakhar-e-Bhakkar cultivar. The results further explain that the foliar application of increased concentrations of putrescine from 0.0 to 1.0 PPM gradually improved physiological and yield traits, whereas these traits declined with the application of putrescine at the highest dose (1.5 PPM). The exogenous application of 1.0 PPM putrescine improved the relative water content (19.76%), specific leaf area (41.47%), and leaf area ratio (35.84%) compared with the controlled treatment. A higher grain yield (28.0 g plant^{-1}) and 100-grain weight (3.8 g) were obtained with the foliar application of 1.0 PPM

putrescine compared with controlled treatments. The findings of this study confirm the protective role of putrescine against terminal drought stress. It is therefore recommended to use putrescine at a concentration of 1.0 PPM, which could help alleviate terminal drought stress and attain better wheat yield.

KEYWORDS

bread wheat, yield, terminal drought, putrescine, leaf area ratio, membrane stability index

Introduction

Drought stress is a serious threat to cereal crop growth, development, and productivity (Toulotte et al., 2022). The early growth and grain- filling phases of cereal crops are significantly affected by drought (Vijayaraghavareddy et al., 2021). Low water levels reduce vegetative growth, post-anthesis photosynthetic capacity, and grain yield in wheat (Cui et al., 2015). Drought occurs frequently in fields that alter the physiological and molecular characteristics of plants (Rahman et al., 2022; Islam et al., 2023). Drought stress reduces cell division, cell proliferation, and stem elongation, which leads to severe impairments to plant growth and productivity (Azooz and Youssef, 2010; Farooq et al., 2013; Wasaya et al., 2018). Plant morphology and physiology are adversely affected by environmental stresses, including drought, which ultimately reduce crop growth and agricultural yield (Sabagh et al., 2020). Drought stress leads to regulating several oxidative stress indicators, including the generation of reactive oxygen species (ROS), cellular injury, peroxidation of lipids, and membrane stability in plants (Kar, 2011; Rahman et al., 2015; Sabagh et al., 2021). Therefore, affordable and eco-friendly approaches are highly desirable for the improvement of economically important cereal crops under drought- stress conditions. Several eco-friendly approaches have been documented for abiotic stress tolerance and plant improvements (Sabagh et al., 2021; Khan et al., 2022; Raza et al., 2022a; Raza et al., 2022b). A numerical group of signaling molecules and growth regulators has been reported to alleviate drought stress in economically important crop plants, including cereals (Abd Elbar et al., 2019; Rahman et al., 2021; Islam et al.,2022).

Wheat (*Triticum aestivum*) is one of the most widely cultivated cereal crops across the globe, from subtropical to temperate climates, predominantly in the Mediterranean and semi-arid regions (Ahmed et al., 2019). It directly contributes to food security as it is considered the second-most significant staple food crop in the world (Zaheer et al., 2021). However, global plant production is at risk due to environmental changes, a decline in water levels, and irregular rain patterns, which severely influence crop growth stages (Nielsen et al., 2010; Rahman et al., 2018; Schmidt et al., 2020; Ahmed et al., 2022; Chauhan et al., 2022). For instance, the flowering and grain- filling stages of wheat are highly critical for yield protection, whereas the onset of terminal drought stress during these phases may cause a reduction in the number of kernels/ears and kernel weight and may be responsible for huge yield loss (Liu et al., 2015; Liu et al., 2016; Ebeed et al., 2017; Dong et al., 2017; Habib-ur-Rahman et al., 2022). Similarly, drought stress at anthesis can inflict a more profound impact on grain filling, leading to a shortened period of grain filling and altered enzymatic activities (Ahmadi and Baker, 2001; Shah and Paulsen, 2003; Pireivatlou, 2010; Farooq et al., 2014). Drought causes tissue dehydration, leading to metabolic impairment at critical growth stages of wheat crops (Farooq et al., 2009b; Hasan et al., 2021). Moreover, terminal drought disturbs stomatal oscillations, reduces transpiration and water- use efficiency (WUE), and decreases chlorophyll content and nutrient uptake, collectively resulting in yield reduction (Farooq et al., 2009a; Dawood et al., 2019; Yasir et al., 2019). It also imposes adverse effects on the physio-morphological responses of plants, resulting in significant yield reduction (Iqbal et al., 2019; Ejaz et al., 2022). For instance, drought stress induces the excessive production of ROS and inhibits antioxidant enzyme activity, which impairs photosynthesis, increases lipid peroxidation, and destroys cell membrane structure (Farooq et al., 2009a; Miller et al., 2010; Ju et al., 2020). Since crop genotype is an important determinant of drought response, different cultivars within crop species may differ strongly in their response and adaptation to drought stress (Abid et al., 2018; Mohammadi et al., 2018). Therefore, the response of wheat genotypes against drought stress, combined with their stress mitigation potential, must be studied to improve the drought tolerance of wheat genotypes in Pakistan.

Nowadays, different strategies are being employed to mitigate drought stress in crop plants. One such strategy is the exogenous application of polyamines (PAs) (Phornvillay et al., 2019; Seifikalhor et al., 2020; Zhang et al., 2020; Çığ et al., 2021; Irshad et al., 2021). PAs, such as putrescine, are responsible for accumulating osmolytes and endogenous PAs in stressful environments, which help crop plants to protect themselves against stressful conditions (Ebeed et al., 2017). Putrescine (Put) is a type of PA found in all living organisms (Abd Elbar et al., 2019). The exogenous application of putrescine alleviated drought stress by regulating physio-biochemical traits in sugar beet (Islam et al.,2022), regulating protein and fatty acids in thylakoid membrane under several abiotic stresses, including drought in plants (Rahman et al., 2014; Shu et al., 2015), and improving shoot/root dry matter ratio, morph-anatomical changes in roots, stems, and leaves to avoid tissue dehydration in *Thymus vulgaris* (Abd Elbar et al., 2019). Additionally, putrescine helps enhance the stability of cell membranes by preventing excessive water loss, ultimately retaining photosynthetic efficiency under adverse environmental conditions (Grigorova et al., 2012). The foliar spray of putrescine can trigger different physiological processes and induce osmotic adjustment in

plants (Chen et al., 2019). It was also reported that putrescine foliar spray might slow aging and protect cell membranes from oxidative damage by removing free radicals in plants under drought-stress conditions (Hussein et al., 2019). These studies justify the beneficial effect of Put in plant abiotic stress. Under the current climate change scenario, there is a high demand for eco-friendly strategies for abiotic stress alleviation in crop plants in arid and semi-arid regions. Therefore, this study was undertaken to explore the insights of Put-mediated drought stress alleviation in wheat, along with how Put regulates agricultural and physiological yield attributes under water-deficient conditions. These studies open a new avenue of drought-stress alleviation in field crop research that might be useful to the plant breeder and farmer for improving drought stress tolerance in plants through breeding programs.

Materials and methods

Experimental sites, plant material, and treatments

The present experiment was conducted under Lath House at the College of Agriculture, Bahauddin Zakariya University, Bahadur Sub-Campus Layyah, Punjab, Pakistan. Viable seeds of two different wheat varieties, Fakhar-e-Bhakkar (V1) and Anaj-2017 (V2), arranged by the Arid Zone Research Institute (AZRI) Bhakkar, Punjab, Pakistan, were used as experimental material. The pots were filled with soil and farmyard manure at a ratio of 2:1. Earthen pots (14 cm in diameter and 70 cm in height) were filled with 11 kg of well- pulverized sieved soil. The pots were irrigated uniformly and then, upon reaching optimum moisture conditions, eight seeds per pot were sown at a depth of 2 cm on 20th November 2020. The pots were irrigated regularly, and thinning was performed at the three-leaf stage of the seedlings to keep three plants per pot for observations. Commercial fertilizers were applied according to the recommended doses as follows: 0.66 g pot^{-1} nitrogen (as urea), 0.55 g pot^{-1} phosphorus as DAP (di-ammonium phosphate), 0.44 g pot^{-1} potassium as SOP (sulfate of potash) respectively. The crop was grown until the heading stage without drought imposition by watering the pots as and when required. At the heading stage, the pots were divided into two groups: well-watered (normal or control) and terminal drought (40% water holding capacity (WHC)). To maintain WHC, the pots were weighed regularly after every alternative day of drought imposition, and a difference in weight was achieved by adding water to attain the required weight. After one week of drought imposition at the heading stage, the wheat plants were sprayed with four different concentrations (PPM) of putrescine *viz.* putrescine 0 (control, put1), 0.5 (put 2), 1.0 (put 3), and 1.5 PPM (put 4). In the control treatment, plants were sprayed with distilled water, while the rest of the treatment groups were sprayed with different concentrations of putrescine, as per the treatment doses. The experiment containing three replications of each treatment under the factorial arrangement was laid out as a Completely Randomized Design (CRD). The experiment consisted of 48 experimental pots in total. Wheat plants were harvested on 14th April 2021 at physiological maturity. The harvested plants were sundried for a week and yield-related traits were collected.

Measurement of leaf area, specific leaf area, and leaf area ratio

Leaf area (LA), specific leaf area (SLA), and leaf area ratio (LAR) were determined after 7 days of putrescine treatment. The LA, SLA, and LAR were calculated from destructive flag leaf samples by following a distinct formula. The following Quarrie and Jones LA equation was used for measuring leaf area (Aldesuquy et al., 2014).

$$\text{Leaf area } (cm^2) = \text{Length} \times \text{Width} \times 0.75$$

The SLA and LAR were calculated using following formula (Amanullah et al., 2007).

$$\text{Specific Leaf Area} = \text{Leaf area} \div \text{leaf dry weight plant}^{-1} (cm^2 g^{-1})$$

$$\textit{Leaf Area Ratio} = \textit{Leaf area plant}^{-1} \div \textit{total dry weight plant}^{-1} (cm^2 g^{-1})$$

The plant height (cm), number of tillers per plant, and plant biomass were measured for non-treated and treated plants. Plant samples were kept at 71°C in a hot air oven for 48 hours, then total biomass yields (dry weight basis) were recorded for two distinct wheat varieties, respectively.

Determination of membrane stability index

After 7 days of foliar application of putrescine, fully matured leaves were detached from each treated plant. Two pieces of fresh flag leaves, each of 0.2 g, were taken and divided into small strips then put in glass test tubes containing 10 ml of distilled water. Two sets of test tubes were prepared. One set of test tubes was put in a water bath for approximately 30 minutes with the temperature set at 40°C, then the EC (electrical conductivity) of each test tube sample was recorded using an EC meter and was designated C_1. Meanwhile, the second set of test tubes was put in a water bath for about 15 minutes at 100°C; its EC (electrical conductivity) was noted and represented as C_2. The MSI was estimated according to the given formula presented by Sairam et al. (1997).

$$\text{MSI} = \left[1 - \left[\frac{C_1}{C_2}\right]\right] \times 100$$

Determination of relative water content

Fresh, fully emerged flag leaves were collected from each experimental pot after 7 days of putrescine application and kept in a polythene bag, which was quickly shifted in the laboratory to estimate the relative water content (RWC). After moving the plant samples to the laboratory, the fresh weight (FW) of the detached leaves was recorded. Afterward, these leaves were dipped in distilled water and kept in dark conditions at room temperature for 24 hrs to record the turgid weight (TW). After recording the TW, leaf samples were air -dried in a hot air oven at a temperature of 70°C. The leaf samples were completely dried until a constant weight was achieved,

then the dry weight (DW) was recorded using an electronic digital balance. The RWC was estimated according to the formula presented by Barrs and Weatherley (1962).

$$RWC = [FW - DW/TW - DW] \times 100$$

Determination of yield -related traits

Yield and related traits, like spike length (cm) per plant, spike weight (g) per plant, number of spikelets per spike, 100-grain weight (g), grain yield per plant, harvest index (HI), and straw yield were recorded for the wheat varieties, respectively, after plant harvesting. Three plants from each pot were randomly selected and the productive tillers per plant were counted manually. Moreover, the height (from the stem base to the apex of the ear) of three plants at maturity was recorded *via* a meter scale and was later averaged. Similarly, ten spikes per pot were selected randomly, and the length of each spike was measured using a scale then averaged to determine the spike length per plant. T hese selected spikes were then used for the calculation of the number of spikelets per spike and averaged. Three plants were harvested manually after reaching physiological maturity and sundried for a week, and biological yield was recorded using an electrical balance. The spikes were then separated from these three plants and threshed to record grain yield and the number of grains per spike. After threshing, 100 grains were counted from the seed lot of each pot to record the 100-grain weight. The harvest index (HI) was calculated considering the ratio of grain and biological yield as a percentage (%).

Statistical analysis

Data regarding all the traits were analyzed statistically by performing an analysis of a variance (ANOVA) test using the software, Statistix 8.1. Tukey's test was applied in order to draw data means and the significant difference at $P<0.05$ (Steel et al., 1997). Bar graphs for the mean and interactive study were generated on graphing and analysis software, OriginPro Version 9.8.0.200.

Results

Effect of putrescine on the leaf area of wheat genotypes under drought stress

Drought stress significantly reduced the LA, LAR, and SLA of both wheat genotypes. Moreover, these indices were considerably reduced in the Anaj-2017 (V2) wheat variety compared to the Fakhar-e-Bhakkar (V1) variety (Figure 1). However, the putrescine application mitigated the impact of drought stress in both the genotypes, and the foliar application of 1.0 PPM seemed most suitable against drought stress. Maximum LA and LAR were recorded in Fakhar-e-Bhakkar with the foliar application of 1.0 PPM putrescine, while the minimum LA and LAR were recorded under controlled conditions. The foliar application of 1.0 PPM putrescine produced 39% more LA, 30% SLA, and 26% more LAR compared with controlled treatments (Figure 1).

Effect of putrescine on plant height, tillers per plant, and biomass accumulation of wheat genotypes under drought stress

The plant height of both genotypes was significantly affected under both normal and drought conditions (Figure 2). Among wheat cultivars, V1 attained significantly greater plant height, tillers per plant, and biomass accumulation than cultivar V2, under both normal and terminal stress conditions. Although putrescine improved the performance of both genotypes, especially under drought conditions, genotype V1 was more responsive to Putrescine than V2. Regarding plant height, putrescine application under all levels produced greater plant height than controlled treatments. Regarding the biomass per plant under all putrescine treatments, the 1.0 PPM was statistically superior to other concentrations, especially under drought conditions.

Effect of putrescine on spike length, spike weight, and spikelet per spike of wheat genotypes under drought stress

Wheat genotype Fakhar-e-Bhakkar (V1) showed a larger and heavier spike than the Anaj-2017 (V2), particularly under drought conditions (Figure 3), which suggests that V2 is more sensitive to terminal drought. The application of putrescine, particularly at 1.00 PPM, significantly reduced drought impact, which was more obvious in V1. The interaction between drought stress, genotypes, and putrescine application showed an insignificant effect on spike length and spikelets per spike (Figure 3), while it was found to significantly affect spike weight per plant. Under terminal drought stress, significantly, the spike weight per plant was observed with the foliar application of 1.0 PPM putrescine compared with other treatments (Figure 3).

Effect of putrescine on MSI and RWC of wheat genotypes under drought stress

The figure shows that higher RWC and MSI were recorded in Fakhar-e-Bhakkar under well-watered conditions with the foliar application of 1.0 PPM putrescine compared with other treatments. However, considering the drought treatments, the foliar application of 1.0 PPM putrescine maintained higher RWC and MSI in Fakhar-e-Bhakkar compared with other combinations, while less RWC and MSI was observed in Anaj2017 with water spray under terminal drought stress (Figure 4).

Effect of putrescine on grain yield of wheat genotypes under drought stress

Drought stress significantly reduced the grain yield and 100-grain weight in both genotypes (Figure 5). Statistically, a higher 100-grain weight was recorded in Fakhar-e-Bhakkar under both well-watered and terminal drought stress with the foliar application of putrescine. However, a higher grain yield was recorded under well-watered conditions with putrescine application. Regarding terminal drought

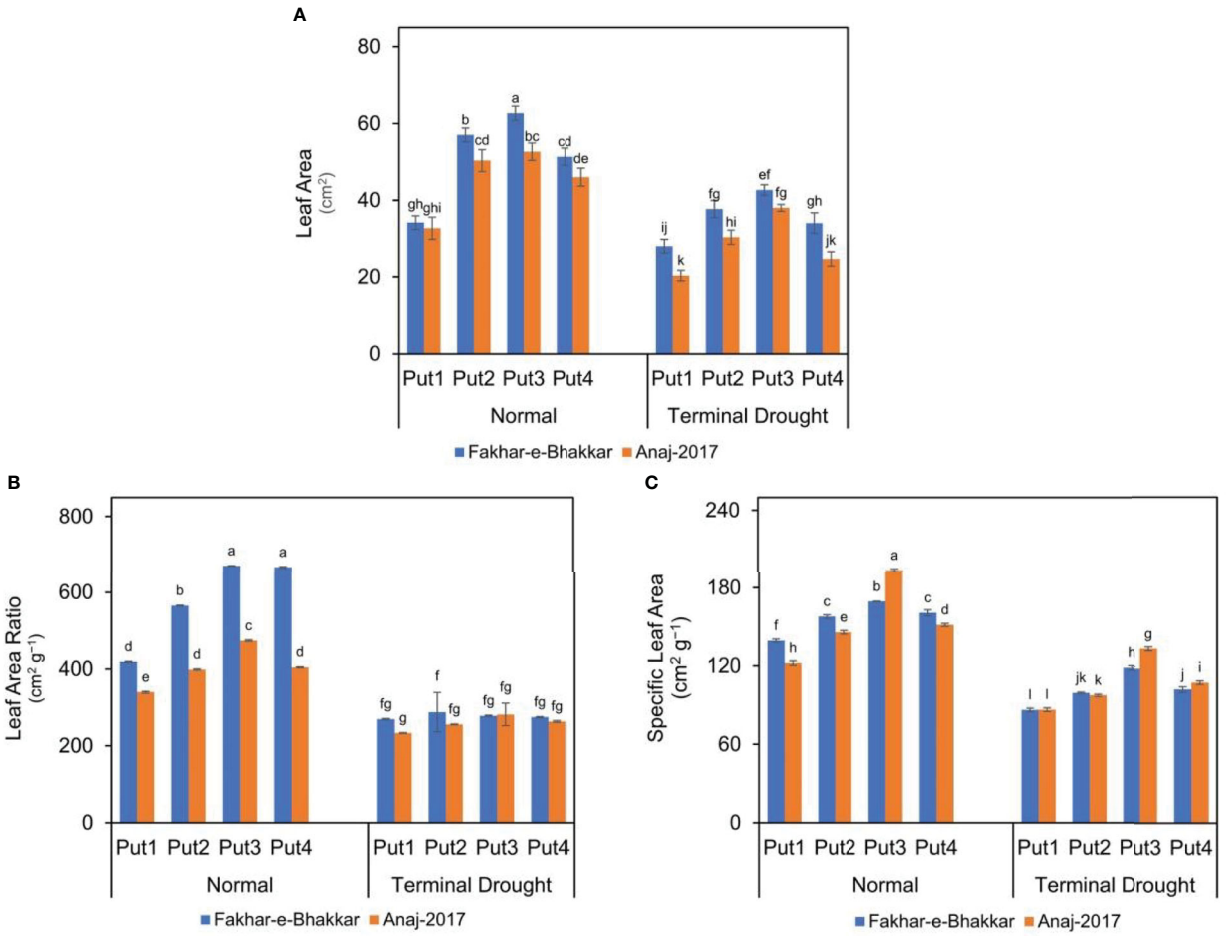

FIGURE 1
Effect of putrescine on the leaf area **(A)**, leaf area ratio **(B)**, and specific leaf area **(C)** of two wheat cultivars under normal and terminal drought conditions. Abbreviation: PPM, parts per million, Put1, putrescine 0 PPM (untreated control); Put2, putrescine 0.5 PPM; Put3, putrescine 1.0 PPM; Put4, putrescine 1.5 PPM. The different letters above the bar columns indicate significant differences in mean ± SE at $p < 0.05$. At least three independent biological replications were considered for each treatment.

stress, Fakhar-e-Bhakkar produced a higher grain yield per plant with the foliar application of 1.0 PPM putrescine compared with other treatments. Similarly, a higher straw yield was recorded in Fakhar-e-Bhakkar with the foliar application of 1.0 PPM putrescine compared with other combinations. A higher harvest index was observed in Fakhar-e-Bhakkar under well-watered conditions, which was statistically on par with all other combinations (Figure 5).

Discussion

Climate change has worsened the outbreak of drought stress, particularly in the later reproductive stages of wheat. Therefore, the evaluation of different strategies to mitigate drought stress is necessary to enable wheat genotypes to perform well under drought conditions. This study investigates the drought tolerance and response of two wheat cultivars against putrescine application. The overall results of our study show that the wheat cultivar Fakhar-e-Bhakkar performed better against drought stress than Anaj-2017. In addition, in both genotypes, among four treatments of putrescine; the application of 1.0 PPM was found most effective against drought stress (Figure 1).

Putrescine application improved the leaf area and leaf area ratio in wheat

Under drought stress, plants experience numerous morphological changes, such as reduced leaf size, leaf rolling, leaf senescence, and limited leaf extension, which could be the reason for lower LAR (leaf area ratio), LA (leaf area), and SLA in drought conditions. As Basu et al. (2016) reported drought stress could be the silent cause of leaf area reduction due to leaf rolling that minimizes water loss and decreases the activity of photosynthesis and the accumulation of dry matter. Reduced leaf area under drought stress might be due to reduced cell turgidity leading to a reduction in cell elongation, an imbalanced antioxidant defense system, and a higher number of reactive oxygen species (ROS) (Alishah et al., 2006; DaCosta and Huang, 2007; Zahoor et al., 2020). Similarly, Put improved leaf area,

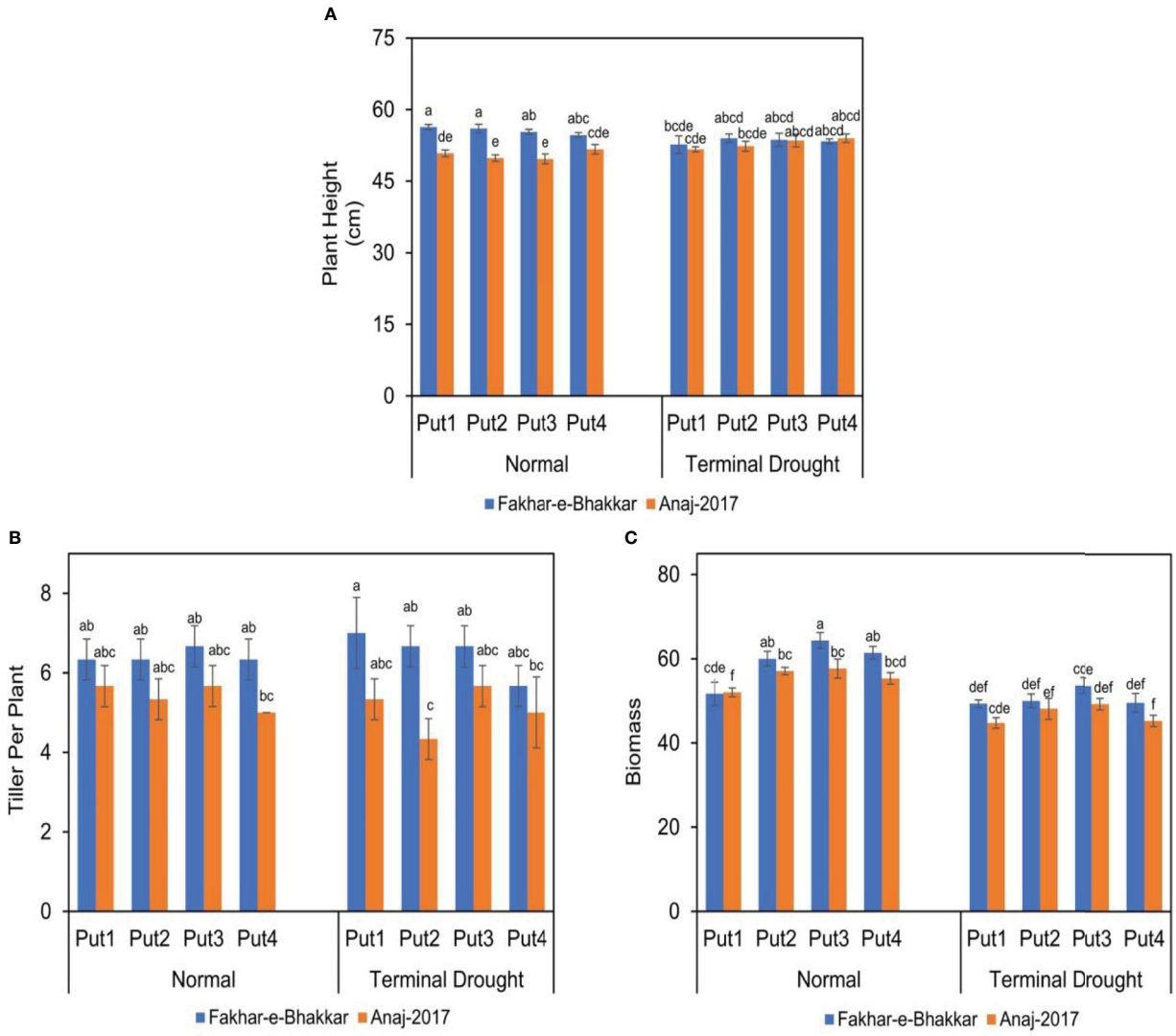

FIGURE 2
The effect of putrescine on the plant height **(A)**, tiller per plant **(B)**, and biomass (g plant-1) **(C)** of two wheat cultivars under normal and terminal drought conditions. Abbreviation: PPM, parts per million, Put1, putrescine 0 PPM (untreated control); Put2, putrescine 0.5 PPM; Put3, putrescine 1.0 PPM; Put4, putrescine 1.5 PPM. The different letters above the bar columns indicate significant differences in mean ± SE at $p< 0.05$. At least three independent biological replications were considered for each treatment.

LAR, and SLA in the present study due to the regulation of LAI, turgidity, and photosynthetic activity (Farooq et al., 2009b).

Putrescine application helped the wheat to retain higher biomass under drought stress

The current study shows that drought stress had no significant effect on plant height and the number of tillers per plant in wheat, as the timing and length of drought stress execution are important factors affecting plant height and tiller number. Drought stress at the heading stage had little influence on plant height due to the cessation of stem elongation and vegetative growth. Wheat tillers cease to grow between the commencement of stem elongation and anthesis. Drought stress during the grain- filling stage in wheat reduces plant height by up to 7% (Caverzan et al., 2016a). Many researchers have found that water stress causes a considerable reduction in plant growth, which can be reflected in leaf area, dry weight, and other important growth parameters and functions (Kilic and Yağbasanlar, 2010; Budak et al., 2013; El Sabagh et al., 2019). Similarly, drought stress significantly reduced the biomass and tillers in wheat genotypes in this study, but the 0.5-1.0 PPM application of putrescine mitigated the drought effects. In addition, the higher number of tillers in the Fakhr-e-Bhakkar genotype suggests that it has higher drought tolerance (Figure 2).

Putrescine application improved the spike length and number of spikelets under drought stress

Data analysis unveiled that drought and putrescine both considerably affect grain yield. Drought execution in wheat genotypes at the heading stage reduced the number of spikelets per

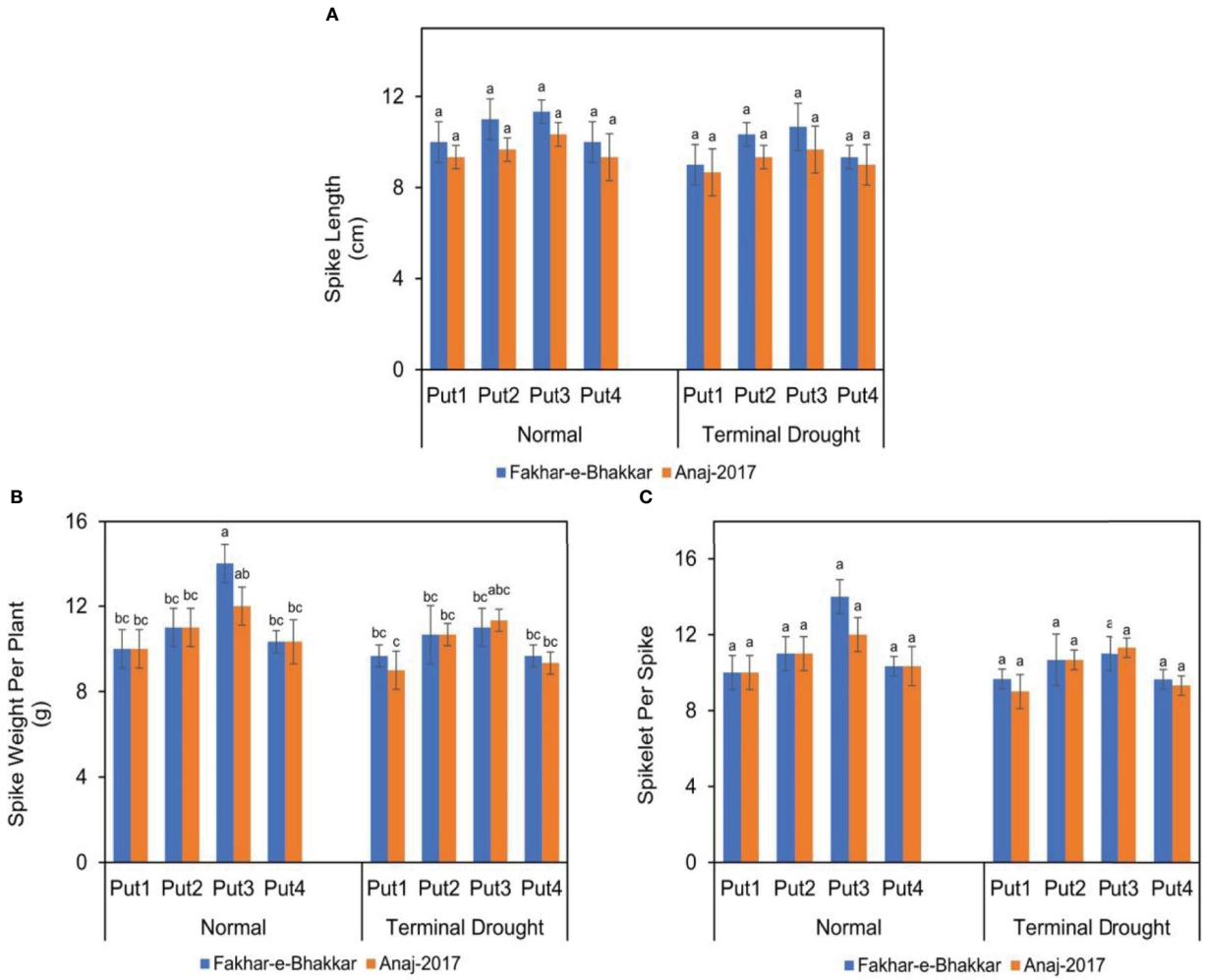

FIGURE 3
The effect of putrescine on the spike length **(A)**, spike weight **(B)**, and spikelets per spike **(C)** of two wheat cultivars under normal and terminal drought conditions. Abbreviation: PPM, parts per million, Put1, putrescine 0 PPM (untreated control); Put2, putrescine 0.5 PPM; Put3, putrescine 1.0 PPM; Put4, putrescine 1.5 PPM. The different letters above the bar columns indicate significant differences in mean ± SE at $p < 0.05$. At least three independent biological replications were considered for each treatment.

plant, causing a reduction in yield. Exogenous putrescine application of 1.0 PPM recorded a positive effect on spikelets per spike and the spike weight when compared with the control treatment (Figure 3) because of improved and higher RWC, MSI, and spikelet numbers. Scientists declared that grain yield was boosted due to increased spikelet numbers per spike (Philipp et al., 2018; Sakuma and Schnurbusch, 2020). Similarly, increased grain yield under putrescine application might be due to an improvement in growth and yield components as putrescine is involved in the production of abscisic acid (ABA) as well as osmotic adjustment and free radicals under abiotic stress (Velikova et al., 2000; Al-Kandari et al., 2009; Alcázar et al., 2010).

Putrescine application reduced the oxidative damage caused by drought stress in wheat genotypes

Data analysis of RWC and MSI revealed that drought-stressed plants have a lower water content than well-watered plants. Drought stress enforces physiological changes in the integrity of plant cell membranes. Consistent with Awasthi et al. (2014), drought stress boosts electrolyte leakage and enhances the instability of the membrane, together with lessening the chlorophyll content, having a huge impact on RWC. According to Reddy et al. (2004), drought stress has an inverse relationship with the water content of plant tissue; an increase in the severity and duration of drought stress results in reduced water content. Our investigation results of RWC and MSI also show that prolonged drought conditions diminish the membrane stability index and RWC. Alternatively, the exogenous putrescine application at the heading stage under terminal drought stress helped to retain the RWC inside the plant and reduced electrolyte leakage and ROS in contrast with no putrescine application. Putrescine, being a scavenger of "free radicals" or ROS detoxifiers, protected the membrane from oxidative injury. There is strong evidence to suggest that polyamines (PAs), like putrescine, have the ability to eliminate ROS by binding the conjugates directly (Hussain et al., 2011). Putrescine application within the 0.5-1.0 PPM range under drought stress alleviated the cell membrane injury in both wheat genotypes (Figure 4).

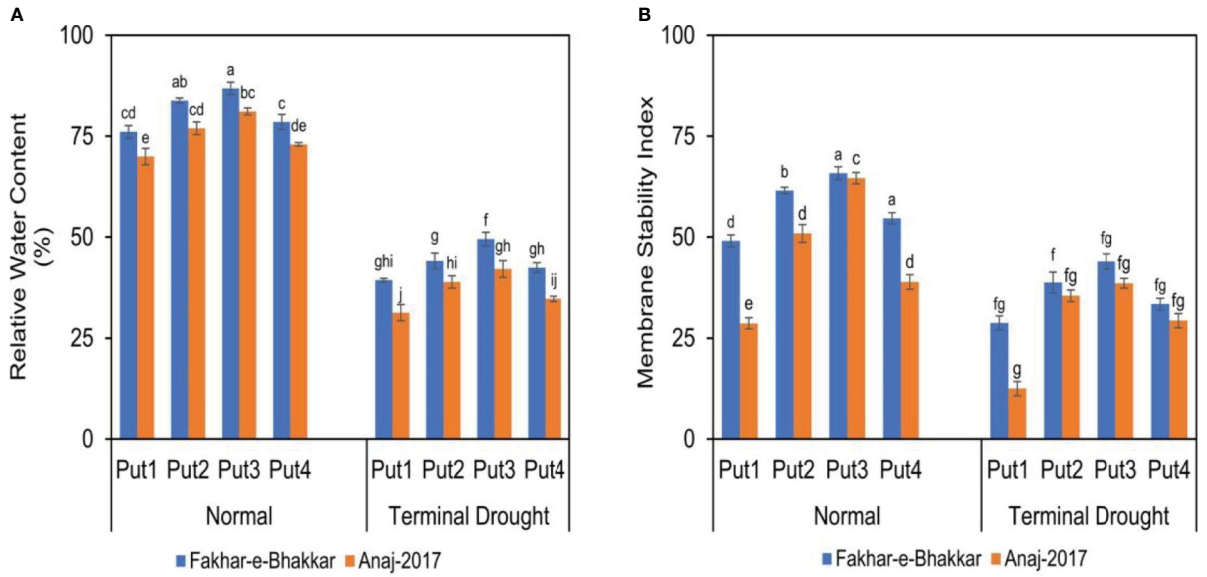

FIGURE 4
The effect of putrescine on the relative water content **(A)** and membrane stability index (%) **(B)** of two wheat cultivars under normal and terminal drought conditions. Abbreviation: PPM, parts per million, Put1, putrescine 0 PPM (untreated control); Put2, putrescine 0.5 PPM; Put3, putrescine 1.0 PPM; Put4, putrescine 1.5 PPM. The different letters above the bar columns indicate significant differences in mean ± SE at $p< 0.05$. At least three independent biological replications were considered for each treatment.

Foliar putrescine application upgraded the status of RWC (relative water content) under drought stress in wheat. It enhanced the organic compatible solute accretion that helps to avoid water loss in plants by increasing solute potential (Alcázar et al., 2010). The improvement in RWC through the foliar application of putrescine might be due to ROS's scavenging role and ability to regulate osmotic balance (Al-Kandari et al., 2009; Alcázar et al., 2010). Exogenous application of putrescine improved MSI under drought stress. This might be due to the regulation of membrane integrity and antioxidant activity mediated by the translation of specific genes, which helps plants to resist ROS produced under drought stress (Bajguz, 2000; Takahashi and Kakehi, 2009).

Putrescine application helps to retain the yield and harvest index of wheat under drought stress

Data analysis demonstrated that water stress imposes the most prominent adverse effects in the Anaj-2017 genotype. Drought stress at the heading stage influenced the yield of terminal stress-sensitive wheat genotype and attributed to the severe reduction in yield components, namely biological yield, spikelet number, and grain weight. It was observed that drought stress reduced the yield of drought-sensitive wheat genotypes as a result of a decrease in photosynthetic parameters and chlorophyll content (Wasaya et al., 2021). Thus, it is obvious that stomata behavior, water status, and photosynthesis response to drought stress distinguish between sensitive genotypes and drought-tolerant genotypes (Munns et al., 2010). In relative terms, the foliar application of putrescine at the heading stage not only improves the yield of wheat genotypes but also assists in mitigating drought stress (Figure 5).

Data analysis showed that Fakhar-e-Bhakkar produced higher biological and grain yields than Anaj-2017 under drought stress, which could be attributed to the higher number of spikelets per spike, spike weight per plant relative to water content, and 100-grain weight. It was observed that some genotypes are able to complete the life cycle under moisture stress and maintain their yield compared with drought-susceptible genotypes due to their genetic makeup (Ahmad et al., 2009). Grain weight and spikelet number are the most effective and essential variables that could influence the grain yield of the wheat genotype (Leilah and Alkhateeb, 2005). Drought stress execution in the reproductive phase affects the traits contributing to yield parameters (Bayoumi et al., 2008). Fakhar-e-Bhakkar is a drought- resistant wheat genotype and attained the highest plant height, biomass, number of tillers, spike weight, number of spikelets per spike, grain weight per spike, 100-grain weight, and grain yield under drought stress and well-watered conditions. Because of its prodigious genetic makeup and its enzymatic defense system and osmolyte accumulation, the adverse effects of drought stress in the Fakhar-e-Bhakkar genotype are mitigated. Meanwhile, the wheat genotype Anaj-2017 recorded the lowest grain yield, being drought-sensitive, because sink capacity for dry matter accumulation is susceptible to drought conditions; nonetheless, this may be responsible for its low yield (Bayoumi et al., 2008).

Conclusion

The current study recommends that the foliar application of polyamine, such as putrescine, is the best approach to tackle and mitigate undesirable drought effects in wheat. A higher grain yield was achieved under the putrescine application, probably due to improved spike weight, spikelet numbers, and 100-grain weight,

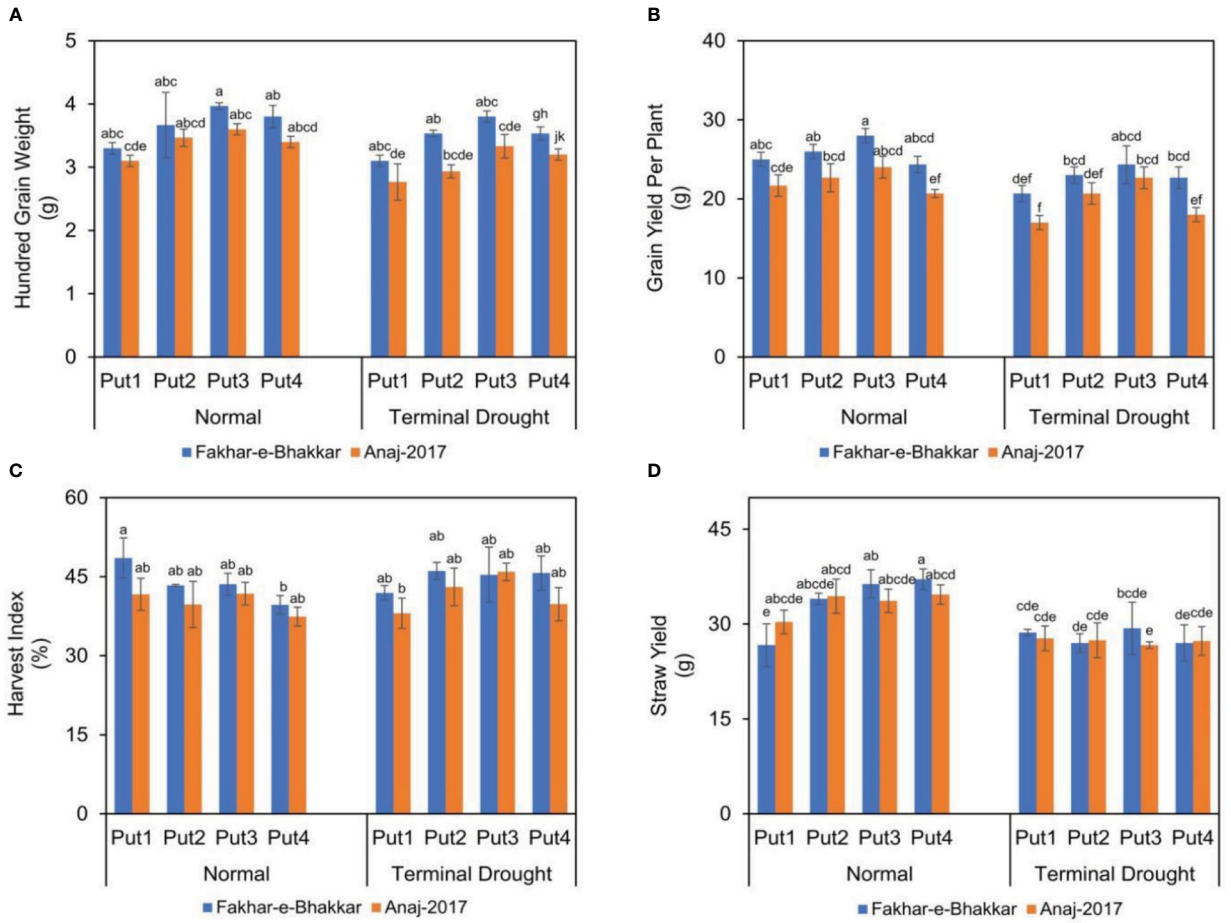

FIGURE 5
The effect of putrescine on the 100-grain weight **(A)**, grain yield **(B)**, harvest index **(C)**, and straw yield **(D)** of two wheat cultivars under normal and terminal drought conditions. Abbreviation: PPM, parts per million, Put1, putrescine 0 PPM (untreated control); Put2, putrescine 0.5 PPM; Put3, putrescine 1.0 PPM; Put4, putrescine 1.5 PPM. The different letters above the bar columns indicate significant differences in mean ± SE at $p< 0.05$. At least three independent biological replications were considered for each treatment.

particularly in the stress-tolerant genotype (Fakhar-e-Bhakkar). According to the research findings, the foliar application of putrescine improved the membrane stability index and relative water content, which results in enhanced 100-grain weight and spike weight. Wheat cultivar Fakhar-e-Bhakkar showed more tolerance against terminal drought than Anaj-2017. Similarly, Fakhar-e-Bhakkar was most responsive to the putrescine application, and the foliar application of putrescine (1.0 PPM) has the potential to stabilize wheat against terminal drought stress. Our study suggests that Fakhar-e-Bhakkar has the potential to grow and survive in low- water and well-watered conditions, so farmers can grow this wheat genotype for longer with better outcomes.

Data availability statement

The datasets presented in this study can be found in online repositories. The names of the repository/repositories and accession number(s) can be found in the article/supplementary material.

Author contributions

AW and TY: conceptualization. IR: data collection. AW, IR and TY: writing the original draft. AD, MK, MJ, GR, IA, ME-H, MB, MR, and AS: review and editing. All authors contributed to the article and approved the submitted version.

Funding

This research work was funded for publication purpose by Institutional Fund Projects under grant no (IFPIP:1166-662-1443) provided the Ministry of Education and King Abdulaziz University, DSR, Jeddah, Saudi Arabia.

Acknowledgments

The authors gratefully acknowledge the technical and financial support provided by the Ministry of Education and King Abdulaziz

University, DSR, Jeddah, Saudi Arabia, to this research work through project number IFPIP: 1166-662-1443.

Conflict of interest

The authors declare that the research was conducted in the absence of any commercial or financial relationships that could be construed as a potential conflict of interest.

Publisher's note

All claims expressed in this article are solely those of the authors and do not necessarily represent those of their affiliated organizations, or those of the publisher, the editors and the reviewers. Any product that may be evaluated in this article, or claim that may be made by its manufacturer, is not guaranteed or endorsed by the publisher.

References

Abd Elbar, O. H., Farag, R. E., and Shehata, S. A. (2019). Effect of putrescine application on some growth, biochemical and anatomical characteristics of thymus vulgaris l. under drought stress. *Ann. Agric. Sci.* 64 (2), 129–137. doi: 10.1016/j.aoas.2019.10.001

Abid, M., Ali, S., Qi, L. K., Zahoor, R., Tian, Z., Jiang, D., et al. (2018). Physiological and biochemical changes during drought and recovery periods at tillering and jointing stages in wheat (*Triticum aestivum* l.). *Sci. Rep.* 4615 (8), 1–15. doi: 10.1038/s41598-018-21441-7

Ahmad, S., Ahmad, R., Ashraf, M. Y., Ashraf, M., and Waraich, E. A. (2009). Sunflower (*Helianthus annuus* l.) response to drought stress at germination and seedling growth stages. *Pak. J. Bot.* 41 (2), 647–654.

Ahmadi, A., and Baker, D. A. (2001). The effect of water stress on the activities of key regulatory enzymes of the sucrose to starch pathway in wheat. *Plant Growth Regul.* 35, 81–91. doi: 10.1023/A:1013827600528

Ahmed, H. G. M. D., Sajjad, M., Li, M., Azmat, M. A., Rizwan, M., Maqsood, R. H., et al. (2019). Selection criteria for drought-tolerant bread wheat genotypes at seedling stage. *Sustainability* 11 (9), 2584. doi: 10.3390/su11092584

Ahmed, H., Zeng, Y., Raza, H., Muhammad, D., Iqbal, M., Uzair, M., et al. (2022). Characterization of wheat accessions under salinity stress. *Front. Plant Sci.* 2583. doi: 10.3389/fpls.2022.953670

Alcázar, R., Altabella, T., Marco, F., Bortolotti, C., Reymond, M., Koncz, C., et al. (2010). Polyamines: molecules with regulatory functions in plant abiotic stress tolerance. *Planta* 231 (6), 1237–1249. doi: 10.1007/s00425-010-1130-0

Aldesuquy, H., Baka, Z., and Mickky, B. (2014). Kinetin and spermine mediated induction of salt tolerance in wheat plants: Leaf area, photosynthesis and chloroplast ultrastructure of flag leaf at ear emergence. *Egyp. J. Basic Appl. Sci.* 1, 77–87. doi: 10.1016/j.ejbas.2014.03.002

Alishah, H. M., Heidari, R., Hassani, A., and Dizaji, A. (2006). Efect of water stress on some morphological and biochemical characteristics of purple basil (*Ocimum basilicum*). *Res. J. Biol. Sci.* 6 (4), 763–767. doi: 10.3923/jbs.2006.763.767

Al-Kandari, M., Redha, A., and Suleman, P. (2009). Polyamine accumulation and osmotic adjustment as adaptive responses to water and salinity stress in *Conocarpus lancifolius*. *Func. Plant Sci. Biotech.* 3 (1), 42–48. doi: 10.3390/plants10071313

Amanullah, M. J. H., Nawab, K., and Ali, A. (2007). Response of specific leaf area (SLA), leaf area index (LAI) and leaf area ratio (LAR) of maize (*Zea mays* l.) to plant density, rate and timing of nitrogen application. *World Appl. Sci. J.* 2 (3), 235–243.

Awasthi, R., Kaushal, N., Vadez, V., Turner, N. C., Berger, J., Siddique, K. H., et al. (2014). Individual and combined effects of transient drought and heat stress on carbon assimilation and seed filling in chickpea. *Funct. Plant Biol.* 41, 1148–1167. doi: 10.1071/FP13340

Azooz, M., and Youssef, M. (2010). Evaluation of heat shock and salicylic acid treatments as inducers of drought stress tolerance in hassawi wheat. *Amer. J. Plant Physiol.* 5 (2), 56–70. doi: 10.3923/ajpp.2010.56.70

Bajguz, A. (2000). Efect of brassinosteroids on nucleic acid and protein content in cultured cell of *Chlorella vulgaris*. *Plant Physiol. Biochem.* 38, 209–215. doi: 10.1016/S0981-9428(00)00733-6

Barrs, H. D., and Weatherley, P. E. (1962). A re-examination of the relative turgidity technique for estimating water deficits in leaves. *Aust. J. Biol. Sci.* 15, 413–428. doi: 10.1071/BI9620413

Basu, S., Ramegowda, V., Kumar, A., and Pereira, A. (2016). Plant adaptation to drought stress. *F1000Res. 5 F1000 Faculty*, Rev–1554. doi: 10.12688/f1000research.7678.1

Bayoumi, T. Y., Eid, M. H., and Metwali, E. M. (2008). Application of physiological and biochemical indices as a screening technique for drought tolerance in wheat genotypes. *Afr. J. Biotechnol.* 7, 2341–2352.

Budak, H., Kantar, M., and Kurtoglu, K. Y. (2013). Drought tolerance in modern and wild wheat. *Sci. C World J.*

Caverzan, A., Casassola, A., and Brammer, S. P. (2016a). Antioxidant responses of wheat plants under stress. *Gene. Mol. Biol.* 39 (1), 1–6. doi: 10.1590/1678-4685-GMB-2015-0109

Chauhan, J., Srivastava, J. P., Singhal, R. K., Soufan, W., Dadarwal, B. K., Mishra, U. N., et al. (2022). Alterations of oxidative stress indicators, antioxidant enzymes, soluble sugars, and amino acids in mustard [*Brassica juncea* (L.) czern and coss.] in response to varying sowing time, and field temperature 13. doi: 10.3389/fpls.2022.875009

Chen, D., Shao, Q., Yin, L., Younis, A., and Zheng, B. (2019). Polyamine function in plants: metabolism, regulation on development, and roles in abiotic stress responses. *Front. Plant Sci.* 9, 1945. doi: 10.3389/fpls.2018.01945

Çığ, F., Sönmez, F., Nadeem, M. A., and El Sabagh, A. (2021).). effect of biochar and pgpr on the growth and nutrients content of einkorn wheat *(Triticum monococcum l.)* and post-harvest soil properties. *Agronomy* 11 (12), 2418. doi: 10.3390/agronomy11122418

Cui, Y., Tian, Z., Zhang, X., Muhammad, A., Han, H., Jiang, D., et al. (2015). Effect of water deficit during vegetative growth periods on post-anthesis photosynthetic capacity and grain yield in winter wheat (*Triticum aestivum* l.). *Acta Physiol. Plant* 37 (10), 1–10. doi: 10.1007/s11738-015-1944-2

DaCosta, M., and Huang, B. (2007). Changes in antioxidant enzyme activities and lipid peroxidation for bent grass species in response to drought stress. *J. Am. Soc Hortic. Sci.* 132, 319–326. doi: 10.21273/JASHS.132.3.319

Dawood, M. F. A., Abeed, A. H. A., and Aldaby, E. E. S. (2019). Titanium dioxide nanoparticles model growth kinetic traits of some wheat cultivars under different water regimes. *Indian J. Plant Physiol.* 24, 129–140. doi: 10.1007/s40502-019-0437-5

Dong, B., Zheng, X., Liu, H., Able, J. A., Yang, H., and Zhao, H. (2017). Effects of drought stress on pollen sterility, grain yield, abscisic acid and protective enzymes in two winter wheat cultivars. *Front. Plant Sci.* 8, 1008. doi: 10.3389/fpls.2017.01008

Ebeed, H. T., Hassan, N. M., and Aljarani, A. M. (2017). Exogenous applications of polyamines modulate drought responses in wheat through osmolytes accumulation, increasing free polyamine levels and regulation of polyamine biosynthetic genes. *Plant Physiol. Biochem.* 118, 438–448. doi: 10.1016/j.plaphy.2017.07.014

Ejaz, M. K., Aurangzaib, M., Iqbal, R., Shahzaman, M., Habib-ur-Rahman, M., El-Sharnouby, M., et al. (2022). The use of soil conditioners to ensure a sustainable wheat yield under water deficit conditions by enhancing the physiological and antioxidant potentials. *Land* 11 (3), 368. doi: 10.3390/land11030368

El Sabagh, A., Hossain, A., Barutcular, C., Islam, M. S., Awan, S. I., Galal, A., et al. (2019). Wheat *(Triticum aestivum l.)* production under drought and heat stress–adverse effects, mechanisms and mitigation: A review. *Appl. Ecol. Environ. Res.* 17 (4), 8307–8332. doi: 10.15666/aeer/1704_83078332

Farooq, M., Hussain, M., and Siddique, K. H. M. (2014). Drought stress in wheat during flowering and grain-filling periods. *CRC Crit. Rev. Plant Sci.* 33, 331–349. doi: 10.1080/07352689.2014.875291

Farooq, M., Irfan, M., Aziz, T., Ahmad, I., and Alam, S. (2013). Seed priming with ascorbic acid improves drought resistance of wheat. *J. Agron. Crop Sci.* 199, 12–22. doi: 10.1111/j.1439-037X.2012.00521.x

Farooq, M., Wahid, A., Kobayashi, N., Fujita, D., and Basra, S. M. A. (2009a). Plant drought stress: effects, mechanisms and management. *Agron. Sustain. Dev.* 29, 185–212. doi: 10.1051/agro:2008021

Farooq, M., Wahid, A., and Lee, D. J. (2009b). Exogenously applied polyamines increase drought tolerance of rice by improving leaf water status, photosynthesis, and membrane properties. *Acta Physiol. Plant* 31, 937–945. doi: 10.1007/s11738-009-0307-2

Grigorova, B., Vassileva, V., Klimchuk, D., Vaseva, I., Demirevska, K., and Feller, U. (2012). Drought, high temperature, and their combination affect ultrastructure of chloroplasts and mitochondria in wheat (*Triticum aestivum* l.) leaves. *J. Plant Interact.* 7, 204–213. doi: 10.1080/17429145.2011.654134

Habib-ur-Rahman, M., Raza, A., Ahrends, H. E., Hüging, H., and Gaiser, T. (2022). Impact of in-field soil heterogeneity on biomass and yield of winter triticale in an intensively cropped hummocky landscape under temperate climate conditions. *Precis. Agric.* 23, 912–938. doi: 10.1007/s11119-021-09868-x

Hasan, M. M., Skalicky, M., Jahan, M. S., Hossain, M. N., Anwar, Z., Zhengfei, N., et al. (2021). Spermine: Its emerging role in regulating drought stress responses in plants. *Cells* 10, 261. doi: 10.3390/cells10020261

Hussain, S. S., Ali, M., Ahmad, M., and Siddique, K. H. M. (2011). Polyamines: natural and engineered abiotic and biotic stress tolerance in plants. *Biotechnol. Adv.* 29, 300–311. doi: 10.1016/j.biotechadv.2011.01.003

Hussein, H. A. A., Mekki, B. B., El-Sadek, M. E. A., and El-Lateef, E. E. (2019). Effect of l-ornithine application on improving drought tolerance in sugar beet plants. *Heliyon* 5, e02631. doi: 10.1016/j.heliyon

Iqbal, N., Hussain, S., Raza, M. A., Yang, C. Q., Safdar, M. E., Brestic, M., et al. (2019). Drought tolerance of soybean (*Glycine max* l. merr.) by improved photosynthetic characteristics and an efficient antioxidant enzyme activities under a split-root system. *Front. Physiol.* 10. doi: 10.3389/fphys.2019.00786

Irshad, M., Ullah, F., Fahad, S., Mehmood, S., Khan, A. U., Brtnicky, M., et al. (2021). Evaluation of *Jatropha curcas* l. leaves mulching on wheat growth and biochemical attributes under water stress. *BMC Plant Biol.* 21 (1), 1–12. doi: 10.1186/s12870-021-03097-0

Islam, M.-R., Kamal, M.-M., Hossain, M.-F., Hossain, J., Azam, M.-G., Akhter, M.-M., et al. (2022). Drought tolerance in mung bean is associated with the genotypic divergence, regulation of proline, photosynthetic pigment and water relation. *Phyton*. doi: 10.32604/phyton.2023.025138

Islam, M.-R., Kamal, M. -M., Hossain, M. -F., Hossain, J., Azam, M. G., Akhter, M. -M., et al. (2023). Drought tolerance in mung bean is associated with the genotypic divergence, regulation of proline, photosynthetic pigment and water relation). *Phyton* 92 (3), 955–981. doi: 10.32604/ phyton.2023.025138

Ju, Y. L., Yue, X. F., Min, Z., Wang, X. H., Fang, Y. L., and Zhang, J. X. (2020). VvNAC17, a novel stress-responsive grapevine (*Vitis vinifera* l.) NAC transcription factor, increases sensitivity to abscisic acid and enhances salinity, freezing, and drought tolerance in transgenic arabidopsis. *Plant Physiol. Biochem.* 146, 98–111. doi: 10.1016/j.plaphy.2019.11.002

Kar, R. K. (2011). Plant responses to water stress: Role of reactive oxygen species . *Plant Signal. Behav* 6, 1741–1745.

Khan, I., Muhammad, A., Chattha, M. U., Skalicky, M., Chattha, M. B., Ayub, M. A., et al. (2022). Mitigation of salinity-induced oxidative damage, growth, and yield reduction in fine rice by sugarcane press mud application. *Front. Plant Sci.* 13. doi: 10.3389/fpls.2022.840900

Kilic, H., and Yağbasanlar, T. (2010). The effect of drought stress on grain yield, yield components and some quality traits of durum wheat (*Triticum turgidum*) cultivars. *Not. Bot. Horti. Agrobot.* 38, 164. doi: 10.15835/nbha3814274

Leilah, A. A., and Alkhateeb, S. A. (2005). Statistical analysis of wheat yield under drought conditions. *J. Arid. Environ.* 61, 483–496. doi: 10.1016/j.jaridenv.2004.10.011

Liu, Y., Liang, H., Lv, X., Liu, D., Wen, X., and Liao, Y. (2016). Effect of polyamines on the grain filling of wheat under drought stress. *Plant Physiol. Biochem.* 100, 113–129. doi: 10.1016/j.plaphy.2016.01.003

Liu, H., Searle, I. R., Mather, D. E., Able, A. J., and Able, J. A. (2015). Morphological, physiological and yield responses of durum wheat to pre-anthesis water-deficit stress are genotype-dependent. *Crop Pasture Sci.* 66, 1024–1038. doi: 10.1071/CP15013

Miller, G., Suzuki, N., Ciftci-yilmaz, S., and Mittler, R. (2010). Reactive oxygen species homeostasis and signalling during drought and salinity stresses. *Plant Cell Environ.* 33, 453–467. doi: 10.1111/j.1365-3040.2009.02041.x

Mohammadi, H., Ghorbanpour, M., and Brestic, M. (2018). Exogenous putrescine changes redox regulations and essential oil constituents in field-grown thymus vulgaris l. under well-watered and drought stress conditions *Ind. Crops Prod.* 122, 119–132. doi: 10.1016/j.indcrop.2018.05.064

Munns, R., James, R. A., Sirault, X. R. R., Furbank, R. T., and Jones, H. G. (2010). New phenotyping methods for screening wheat and barley for beneficial responses to water deficit. *J. Exp. Bot.* 61 (13), 3499–3507. doi: 10.1093/jxb/erq199

Nielsen, D. C., Halvorson, A. D., and Vigil, M. F. (2010). Critical precipitation period for dryland maize production. *Field Crops Res.* 118, 259–263. doi: 10.1016/j.fcr.2010.06.004

Nishizawa-Yokoi, A., Yabuta, Y., and Shigeoka, S. (2008). The contribution of carbohydrates including raffinose family oligosaccharides and sugar alcohols to protection of plant cells from oxidative damage. *Plant Signal. Behav.* 3, 1016–1018. doi: 10.4161/psb.6738

Philipp, N., Weichert, H., Bohra, U., Weschke, W., Schulthess, A. W., and Weber, H. (2018). Grain number and grain yield distribution along the spike remain stable despite breeding for high yield in winter wheat. *PloS One* 13, e0205452. doi: 10.1371/journal.pone.0205452

Phornvillay, S., Pongprasert, N., Wongs-Aree, C., Uthairatanakij, A., and Srilaong, V. (2019). Exogenous putrescine treatment delays chilling injury in okra pod (*Abelmoschus esculentus*) stored at low storage temperature. *Sci. Hortic. Amsterdam* 256, 1–7. doi: 10.1016/j.scienta.2019.108550

Pireivatlou, A. S. (2010). Evaluation of wheat (*Triticum aestivum* l.) genotypes under pre-and post-anthesis drought stress conditions. *J. Agric.* 10, 109–121.

Rahman, M. A., Alam, I. , Kim, Y. G., Ahn, N.-Y, Ahn, N.-Y, Heo, S.-Y, and Lee, D.-Y (2015). Screening for salt-responsive proteins in two contrasting alfalfa cultivars using a comparative proteome approach . *Plant Physiol. Biochem.* 89, 112–122.

Rahman, M. H. U., Ahmad, A., Wang, X., Wajid, A., Nasim, W., Hussain, M., et al. (2018). Multi-model projections of future climate and climate change impacts uncertainty assessment for cotton production in Pakistan. *Agric. For. Meteorol.* 253, 94–113. doi: 10.1016/j.agrformet.2018.02.008

Rahman, M. A., Alam, I., Sharmin, S. A., Kabir, A. H., Kim, Y.-G., Liu, G., et al. (2021). Physiological and proteomic analyses reveal the protective roles of exogenous hydrogen peroxide in alleviating drought stress in soybean plants. *Plant Biotechnol. Rep.* 15 (6), 805–818. doi: 10.1007/s11816-021-00719-9

Rahman, M. A., Kim, Y.-G., and Lee, B.-H. (2014). Proteomic response of alfalfa subjected to aluminum (Al) stress at low pH soil. *J. Korean Soc. Grassl. Forage Sci.* 34 (4), 262–268. doi: 10.5333/KGFS.2014.34.4.262

Rahman, M. A., Woo, J. H., Song, Y., Lee, S.-H., Hasan, M. M., Azad, M. A. K., et al. (2022). Heat shock proteins and antioxidant genes involved in heat combined with drought stress responses in perennial rye grass. *Life* 12 (9), 1426. doi: 10.3390/life12091426

Raza, A., Charagh, S., García-Caparrós, P., Rahman, M. A., Ogwugwa, V. H., Saeed, F., et al. (2022a). Melatonin-mediated temperature stress tolerance in plants. *GM Crops Food* . 13 (1), 196–217. doi: 10.1080/21645698.2022.2106111

Raza, A., Salehi, H., Rahman, M. A., Zahid, Z., Haghjou, M. M., Najafi-Kakavand, S., et al. (2022b). Plant hormones and neurotransmitter interactions mediate antioxidant defenses under induced oxidative stress in plants. *Front. Plant Sci.* 13. doi: 10.3389/fpls.2022.961872

Reddy, A. R., Chaitanya, K. V., and Vivekanandan, M. (2004). Drought-induced responses of photosynthesis and antioxidant metabolism in higher plants. *J. Plant Physiol.* 161, 1189–1202. doi: 10.1016/j.jplph.2004.01.013

Sabagh, A. E., Hossain, A., Islam, M. S., Iqbal, M. A., Raza, A., Karademir, Ç., et al. (2020). Elevated CO_2 concentration improves heat-tolerant ability in crops. *In Abiotic Stress Plants IntechOpen*, 1–17. doi: 10.5772/intechopen.94128

Sabagh, A. E., Mbarki, S., Hossain, A., Iqbal, M. A., Islam, M. S., Raza, A., et al. (2021). Potential role of plant growth regulators in administering crucial processes against abiotic stresses. *Front. Agron.* 3. doi: 10.3389/fagro.2021.648694

Sairam, R. K., Deshmukh, P. S., and Shukla, D. S. (1997). Tolerance to drought and temperature stress in relation to increased antioxidant enzyme activity in wheat. *J. Agron. Crop Sci.* 178, 171–177. doi: 10.1111/j.1439-037X.1997.tb00486.x

Sakuma, S., and Schnurbusch, T. (2020). Of floral fortune: tinkering with the grain yield potential of cereal crops. *New Phytol.* 225, 1873–1882. doi: 10.1111/nph.16189

Schmidt, J., Claussen, J., Worlein, N., Eggert, A., Fleury, D., Garnett, T., et al. (2020). Drought and heat stress tolerance screening in wheat using computed tomography. *Plant Methods* 16, 1–12. doi: 10.1186/s13007-020-00565-w

Seifikalhor, M., Aliniaeifard, S., Bernard, F., Seif, M., and Li, T. (2020). γ-aminobutyric acid confers cadmium tolerance in maize plants by concerted regulation of polyamine metabolism and antioxidant defense systems. *Sci. Rep.* 10, 3356. doi: 10.1038/s41598-020-59592-1

Shah, N. H., and Paulsen, G. M. (2003). Interaction of drought and high temperature on photosynthesis and grain-filling of wheat. *Plant Soil* 257, 219–226. doi: 10.1023/A:1026237816578

Shu, S., Yuan, Y., Chen, J., Sun, J., Zhang, W., Tang, Y., et al. (2015). The role of putrescine in the regulation of proteins and fatty acids of thylakoid membranes under salt stress. *Sci. Rep.* 5 (1), 14390. doi: 10.1038/srep14390

Steel, R. G. D., Torrie, J. H., and Dicky, D. A. (1997). "Principles and procedures of statistics," in *A biometrical approach, 3rd edition* (New York: McGraw Hill Book Int. Co.), 172–177.

Takahashi, T., and Kakehi, J. I. (2009). Polyamines: ubiquitous polycations with unique roles in growth and stress responses. *Ann. Bot.* 105, 1–6. doi: 10.1093/aob/mcp259

Toulotte, J. M., Pantazopoulou, C. K., Sanclemente, M. A., Voesenek, L., and Sasidharan, R. (2022). Water stress resilient cereal crops: lessons from wild relatives. *J. Integr. Plant Biol.* 64 (2), 412–430. doi: 10.1111/jipb.13222

Velikova, V., Yordanov, I., and Edreva, A. (2000). Oxidative stress and some antioxidant systems in acid rain-treated bean plants: protective role of exogenous polyamines. *Plant Sci.* 151 (1), 59–66. doi: 10.1016/S0168-9452(99)00197-1

Vijayaraghavareddy, P., Akula, N. N., Vemanna, R. S., Math, R. G. H., Shinde, D. D., Yin, X., et al. (2021). Metabolome profiling reveals impact of water limitation on grain filling in contrasting rice genotypes. *Plant Physiol. Biochem.* 162, 690–698. doi: 10.1016/j.plaphy.2021.02.030

Wasaya, A., Manzoor, S., Yasir, T. A., Sarwar, N., Mubeen, K., Ismail, I. A., et al. (2021). Evaluation of fourteen bread wheat (*Triticum aestivum* l.) genotypes by observing gas exchange parameters, relative water and chlorophyll content, and yield attributes under drought stress. *Sustainability* 13 (9), 4799. doi: 10.3390/su13094799

Wasaya, A., Zhang, X., Fang, Q., and Yan, Z. (2018). Root phenotyping for drought tolerance: a review. *Agronomy* 8 (11), 241. doi: 10.3390/agronomy8110241

Yasir, T. A., Wasaya, A., Hussain, M., Ijaz, M., Farooq, M., Farooq, O., et al. (2019). Evaluation of physiological markers for assessing drought tolerance and yield potential in bread wheat. *Physiol. Molec. Bio. Plants.* 25, 1163–1174. doi: 10.1007/s12298-019-00694-0

Zaheer, M. S., Ali, H. H., Soufan, W., Iqbal, R., Habib-ur-Rahman, M., Iqbal, J., et al. (2021). Potential effects of biochar application for improving wheat *(Triticum aestivum l.)* growth and soil biochemical properties under drought stress conditions. *Land* 10 (11), 1125. doi: 10.3390/land10111125

Zahoor, A., Waraich, E. A., Barutcular, C., Hossain, A., Erman, M., Çig, F., et al. (2020). Enhancing drought tolerance in wheat through improving morphophysiological and antioxidants activities of plants by the supplementation of foliar silicon. *Phyton* 89, 52. doi: 10.32604/phyton.2020.09143

Zhang, F., Zou, Y. N., Wu, Q. S., and Kuca, K. (2020). Arbuscular mycorrhizas modulate root polyamine metabolism to enhance drought tolerance of trifoliate orange. *Environ. Exp. Bot.* 171, 103926. doi: 10.1016/j.envexpbot.2019.103926

frontiers | Frontiers in Plant Science

TYPE Correction
PUBLISHED 27 June 2023
DOI 10.3389/fpls.2023.1231723

OPEN ACCESS

APPROVED BY
Frontiers Editorial Office,
Frontiers Media SA, Switzerland

*CORRESPONDENCE
Allah Wasaya
wasayauaf@gmail.com
Marian Brestic
marian.brestic@uniag.sk
Ayman El Sabagh
ayman.elsabagh@agr.kfs.edu

RECEIVED 30 May 2023
ACCEPTED 31 May 2023
PUBLISHED 27 June 2023

CITATION
Wasaya A, Rehman I, Mohi Ud Din A, Hayder Bin Khalid M, Ahmad Yasir T, Mansoor Javaid M, El-Hefnawy M, Brestic M, Rahman MA and El Sabagh A (2023) Corrigendum: Foliar application of putrescine alleviates terminal drought stress by modulating water status, membrane stability, and yield- related traits in wheat (*Triticum aestivum* L.). *Front. Plant Sci.* 14:1231723. doi: 10.3389/fpls.2023.1231723

Corrigendum: Foliar application of putrescine alleviates terminal drought stress by modulating water status, membrane stability, and yield- related traits in wheat (*Triticum aestivum* L.)

Allah Wasaya[1,2]*, Iqra Rehman[1,2], Atta Mohi Ud Din[3], Muhammad Hayder Bin Khalid[3], Tauqeer Ahmad Yasir[2], Muhammad Mansoor Javaid[4], Mohamed El-Hefnawy[5], Marian Brestic[6]*, Md Atikur Rahman[7] and Ayman El Sabagh[8,9]*

[1]Department of Agronomy, Bahauddin Zakariya University Multan, Multan, Pakistan, [2]College of Agriculture, University of Layyah, Layyah, Pakistan, [3]National Research Center of Intercropping, The Islamia University of Bahawalpur, Multan, Pakistan, [4]Department of Agronomy, College of Agriculture, University of Sargodha, Sargodha, Pakistan, [5]Department of Chemistry, Rabigh College of Sciences and Arts, King Abdulaziz University, Jeddah, Saudi Arabia, [6]Department of Plant Physiology, Slovak University of Agriculture, Nitra, Slovakia, [7]Grassland and Forage Division, National Institute of Animal Science, Rural Development Administration, Cheonan, Republic of Korea, [8]Department of Agronomy, Faculty of Agriculture, Kafrelsheikh University, Kafr al-Sheik, Egypt, [9]Department of Field Crops, Faculty of Agriculture, Siirt University, Siirt, Türkiye

KEYWORDS

bread wheat, yield, terminal drought, putrescine, leaf area ratio, membrane stability index

A Corrigendum on

Foliar application of putrescine alleviates terminal drought stress by modulating water status, membrane stability, and yield- related traits in wheat (*Triticum aestivum* L.)

by Wasaya A, Rehman I, Mohi Ud Din A, Hayder Bin Khalid M, Ahmad Yasir T, Mansoor Javaid M, El-Hefnawy M, Brestic M, Rahman MA and El Sabagh A (2023) *Front. Plant Sci.* 13:1000877. doi: 10.3389/fpls.2022.1000877

Incorrect Acknowledgments

In the published article, there was an error in the Acknowledgments statement.

The authors gratefully acknowledge technical and financial support provided the Ministry of Education and King Abdulaziz University, DSR, Jeddah, Saudi Arabia for funding this research work to publish through the project number (IFPIP:1166-662-1443). The authors extend their appreciation to VEGA1/0664/22 Mitigation of the effects of environmental stresses in photosynthesis and plant production.

The correct Acknowledgments statement appears as follows.

Acknowledgments

The authors gratefully acknowledge the technical and financial support provided by the Ministry of Education and King Abdulaziz University, DSR, Jeddah, Saudi Arabia, to this research work through project number IFPIP: 1166-662-1443.

The authors apologize for this error and state that this does not change the scientific conclusions of the article in any way. The original article has been updated.

Publisher's note

Frontiers in
Plant Science

Cultivates the science of plant biology and its applications

The most cited plant science journal, which advances our understanding of plant biology for sustainable food security, functional ecosystems and human health.

Discover the latest Research Topics

See more →

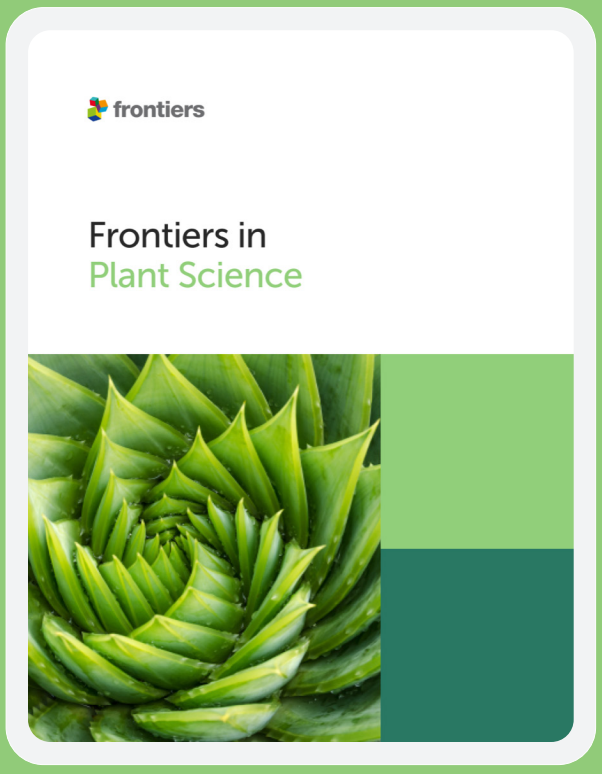

Frontiers

Avenue du Tribunal-Fédéral 34
1005 Lausanne, Switzerland
frontiersin.org

Contact us

+41 (0)21 510 17 00
frontiersin.org/about/contact